DISCLAIMER NOTICE

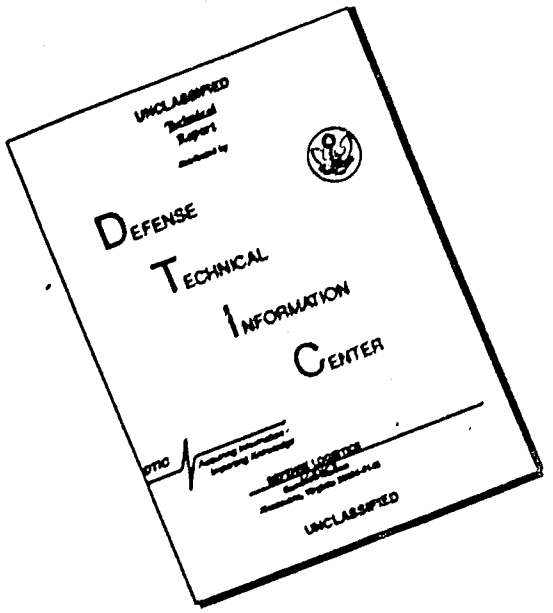

THIS DOCUMENT IS BEST QUALITY AVAILABLE. THE COPY FURNISHED TO DTIC CONTAINED A SIGNIFICANT NUMBER OF PAGES WHICH DO NOT REPRODUCE LEGIBLY.

THE FRANKLIN INSTITUTE

Laboratories for Research and Development

PROCEEDINGS OF SECOND HERO CONGRESS - 1963

on Hazards of Electromagnetic Radiation to Ordnance

Sponsored by
U.S. NAVAL WEAPONS LABORATORY
DAHLGREN, VIRGINIA
Contract N178-8063

For
U.S. Bureau
of
NAVAL WEAPONS

Held at
THE FRANKLIN INSTITUTE
PHILADELPHIA, PENNSYLVANIA
APRIL 29, MAY 1, 1963

THE FRANKLIN INSTITUTE

Laboratories for Research and Development

F-B1982

PROCEEDINGS
OF
SECOND HERO CONGRESS · 1963
on Hazards of Electromagnetic Radiation to Ordnance

Sponsored by
U.S. NAVAL WEAPONS LABORATORY
DAHLGREN, VIRGINIA
Contract N178-8083

For
U.S. BUREAU
of
NAVAL WEAPONS

Held at
THE FRANKLIN INSTITUTE,
PHILADELPHIA 3, PENNSYLVANIA,
APRIL 30, MAY 1, 2, 1963

PREFACE

The Second Hero Congress was attended by 393 people from 64 government agencies and 120 industrial organizations. The Congress was sponsored by the U. S. Naval Weapons Laboratory, Dahlgren, Virginia for the U. S. Bureau of Naval Weapons. It was the purpose of this Congress to bring together for mutual benefit the various people working with, or interested in, the hazards of radio frequency electromagnetic radiation to ordnance systems and components.

The success of the Congress was due in large measure to the authors and to the chairmen of the several sessions who kept matters going smoothly and on schedule. Not to be forgotten are those who, in a less conspicuous role, increased the value of formal presentations by participating in discussions. Their comments together with the formal papers are recorded in these Proceedings. We hope that our editorial condensation has left the meaning of the discussions intact.

Forty papers were presented ~~to the assembled~~ and 12 additional papers are included ~~in the Proceedings~~, although shortage of time prevented verbal presentations.

Please note that the Proceedings are issued this time under two covers, this being the general volume. Ten classified papers are contained in the supplement.

For additional copies of these Proceedings, the request should be sent to the Defense Documentation Center, Arlington Hall Station, Arlington 12, Virginia. Copies of the Proceedings of the first HERO Congress may also be obtained from DDC (AD 326 263).

It would not be practical to list individually all those staff members of The Franklin Institute who contributed to organizing and arranging the Congress. Mr. E. E. Hannum, Manager of The Applied Physics Laboratory, served as general manager. Sharing the responsibility for the technical program and arrangement details were Paul F. Mohrbach and Gunther Cohn.

TABLE OF CONTENTS

TABLE OF CONTENTS (Cont.)

TABLE OF CONTENTS (Cont.)

TABLE OF CONTENTS (Cont.)

TABLE OF CONTENTS (Concl.)


WELCOME
TO THE
1963
NERO
CONGRESS

ABSTRACTS - SESSION I

Welcome — J. G. R. Heckscher

Introduction of Keynote Speaker — Capt. R. F. Sellars

1. Keynote Address (U) — R. Adm. Kleber S. Masterson

2. The Navy HERO Program — C. M. Cormack, Jr.

This paper describes significant changes and accomplishments of the BuWeps HERO Program since the first HERO Congress in 1961. The basic policy documents are cited and a brief explanation of their application is included.

3. AFSWC Approach to the EMR Hazard Problem — 2/Lt. Raymond J. Hengel

The AFSWC is a late entry into the study of EMR problems. Thus, a great deal of data is available for use in making a preliminary evaluation. Full use of data and corollary situations are used in making an EMR determination of a new system to cut to a minimum the actual test requirements.

4. The Army's Nuclear Munitions RF Vulnerability Program (U) — G. M. Rosenberg

The vulnerability program has advanced greatly since the last HERO Congress. Consideration is given to the various stages of assembly of munitions of which EED's are components, and also the probable worst RF environments to which the stages are subjected. New facilities, well organized, have been put into operation. A Radio Frequency Radiation Effects Committee, established within Army Materiel Command, aids in information exchange and in planning.

5. The Achilles' Heel of Modern Weapons (U) — Film

Missile failures may be due to the reaction of electromagnetic radiation on electroexplosive devices. Research carried on and sponsored by Picatinny Arsenal offers one solution to the problem in the form of solid state attenuators. Having the capability of broad band RF protection, the attenuators replace insulator plugs in electric initiators.

Welcoming Remarks

J. G. Richard Heckscher
Executive Vice President, The Franklin Institute

On behalf of Dr. LePage, President, I extend to all of you a cordial welcome to The Franklin Institute. It is a source of considerable satisfaction to us that, under the sponsorship of the Naval Weapons Laboratory, you have selected this institution for the HERO Congress. We are honored that so many of you have traveled from every section of the United States, from Canada, from Australia, from the United Kingdom, and from other parts of the world to attend these proceedings in Philadelphia.

Let me in a few words tell you what is going on right around you in The Franklin Institute. In this building is the Franklin Memorial and the great Science Museum; adjacent to the lobby is the most up-to-date Planetarium in the world; on the second floor an unusually fine Library specializing in the physical sciences at the graduate level; on the ground floor a fully equipped Univac data center; on the third floor the editorial offices of the Journal of The Franklin Institute, published continuously for 137 years. I extend you a cordial invitation to visit any of these whenever you wish.

In this building and in several locations in the immediate neighborhood is The Franklin Institute Laboratories for Research and Development, host to the Second HERO Congress. Growing from Ordnance work done by the Institute during World War II, The Franklin Institute Laboratories were established in 1946 to serve industry and government in a rapidly developing technological era. With a staff of more than 330 top caliber professionals, the Laboratories continues the Institute's proud tradition established nearly 150 years ago; here was conducted the first U. S. Government-sponsored research contract in 1832. Today, under the direction of Francis L. Jackson, comprehensive scientific and engineering services are provided in many areas: solid state physics, chemistry, nuclear

engineering, applied mechanics, instrumentation and controls, data processing, communication, power equipment, operations research and, of course, the very special problem area which brings you together this morning. Our Applied Physics Laboratory is one of the most active in studies of hazards of electromagnetic radiation to ordnance.

Over 100,000 square feet of floor space house is complex of research activities. Next year will see a new Laboratories building rise across the street with 150,000 square feet to accommodate our expanding activities here in one of the most accessible locations in Philadelphia, and with all-weather access to the excellent library and computing facilities in this building. But the principal asset of a research organization is its staff, and in this The Franklin Institute Laboratories is unusually well endowed. Laboratories' scientists enjoy stature both as individual investigators and as members of interdisciplinary project teams. This is exemplified in the team that is participating with you in an effort to solve the problems connected with the hazards of electromagnetic radiation.

Another activity of The Franklin Institute is the Bartol Foundation, a leader in cosmic radiation, and low energy nuclear physics research, located on the campus of Swarthmore College in suburban Philadelphia.

You will find it well worth your time to visit some of these research activities, for I feel certain that we have here kindred spirits who are probing some of the same areas as each of you.

We hope you enjoy your visit, and that you will return soon and often. Toward this end we have tried to plan for your comfort and convenience, as well as for free exchange of technical information. If we have overlooked something, please bring it to our attention. Gunther Cohn of our Applied Physics Laboratory is on hand for this purpose. The Franklin Institute staff members are wearing white badges so you may spot them easily if you need their help.

Again, we bid you welcome and wish you a pleasant and rewarding meeting.

Introduction of Keynote Speaker
Capt. R. F. Sellars, USN
Commander, U. S. Naval Weapons Laboratory

I am very happy to be here and to see so many people concerned with the HERO problem. As you know, The U. S. Naval Weapons Laboratory has been assigned the direction of the HERO project and I think that we are succeeding well in coordinating the research efforts. However, I will be the first to admit that we don't as yet know all there is to know about electromagnetic radiation and particularly we don't know the effects of outer space environment but we are working hard on the problem.

To keep pace with the ever increasing problems, we have to speed our work considerably. We hope to obtain two additional ground planes, more RF anechoic rooms, and more laboratories located either at our facility or at the Naval Air Test Center in Patuxent. This increase will probably start next year. We now have a staff of about a hundred at Dahlgren working on the HERO program. This effort is complemented at other organizations such as NOTS, NASA, BuWeps itself, the other Armed Services, The Franklin Institute, and many of you in Industry. In this connection, I might also mention the contribution of the British Royal Air Force in the person of Wing Cmdr. Gray, stationed at Dahlgren, who has given substantial assistance to our efforts.

The U. S. Naval Weapons Laboratory has been concerned with HERO for a number of years, but it was not until about a year ago that our influence in this area became markedly significant. The operating forces are, of course, the ones most vitally concerned with the solution to this problem. The areas of safety, possible dudding, and radio frequency compatibility have assumed such proportions that our Naval fighting forces have been handicapped in the performance of their mission. I am sure that you are fairly familiar with these problems.

If not, you certainly will be by the time this Congress is completed. Exchange of ideas is the purpose of this Congress. If we can maintain adequate communications with each other, I'm sure we'll make great strides in finding the necessary fixes.

Our keynote speaker today is a Naval Officer and a gentleman whose friendship I have valued over the many years I have known him. He is most familiar with the HERO problems, he is a missile expert, and he has contributed in the field of ordnance. As a foundation for his qualifications in technical management, he has served in aircraft carriers, destroyers, and battleships; and after receiving a valuable post-graduate degree in ordnance, he served his apprenticeship in the former Bureau of Ordnance. With these years of experience behind him, he enjoyed such tours as Destroyer Division Commander, Deep Draft Command during the Korean War, Commanding Officer of the USS Boston, our second guided missile firing ship, and after becoming Admiral, Commander of Cruiser Division ONE. Then, with further experience gained at the Naval War College, in the Armed Forces Special Weapons Project, and in the Office of Naval Operations on shore duty, he was a most appropriate choice for the Chief of the Bureau of Naval Weapons.

It is my great pleasure to introduce to you as our keynote speaker today Rear Admiral Kleber S. Masterson, U. S. Navy, Chief of the Bureau of Naval Weapons.

Keynote Address is in Supplement, Section 1.

2. THE NAVY HERO PROGRAM

by
Charles M. Cormack, Jr.
U.S. Bureau of Naval Weapons

The first HERO Congress served to point up the growing importance of the service generated electromagnetic environment and the need for its consideration in the design of modern weapons. The Bureau of Naval Weapons, having recognized the potential problems which can be generated by this environment, provided for a significant effort in both dollars and man-power to determine its effect on all in-service weapons and to devise means for minimizing these effects.

A large backlog of testing developed when it was established that all in-service weapons and related equipments utilizing EED's be certified for use in the service generated EMR fields. To expedite the effort testing was placed on a three shift schedule. While this was successful to an extent the difficulties of testing at night, particularly out of doors and in the winter months, clearly indicated that a better approach was needed. The additional facilities mentioned by the Keynote Speaker were conceived for this purpose and essentially consist of laboratory spaces including shielded rooms and two additional ground plane test facilities. Completion of these facilities is anticipated in the late fall of 1963. Transmitting equipment is being obtained and mounted in trailers for transfer from one facility to another as needed.

The new test facilities will expedite the test program in several ways, first, the present capacity will be tripled, second, one of the new facilities will be located at an air station where high performance jet aircraft will be readily available. The present need for these aircraft can only be met by barging them to and from the test facility. Occasionally an aircraft is "stricken" or removed from service for any of a number of reasons, and it has been possible to obtain

permanent custody of it for use in HERO tests. Unfortunately for the HERO program this occurs all too seldom, for to date the HERO "Air Force" consists of only four aircraft; an A4B (A4D), F-8 (F4D), A-1 (AD4) and EA1E (AD5W). Three of these are operational type aircraft at the present time, however, one is phasing out, and another is an early warning aircraft with no armament capability. The latter is used as a signal generator since it contains high powered radar equipment.

In addition to the above aircraft eight different types have been employed in testing various weapons; F8(F8U), A2A (A3D), S2 (S2F), SH34H (HSS-1), F3B (F3H), UH2A (Hu2K), E2A (W2F), and E1B (WF2). Three of these aircraft (underlined) required barging and of these three two have required second or third test periods.

Although the majority of our test effort is directed towards air launched weapon systems we have many surface launched weapons and their complex mobile launching platforms, namely the cruisers and destroyers. HERO tests have been conducted on at least one ship of each of the major types such as Destroyers (DD's), Escort Vessels (DE's), Guided Missile Destroyers (DDG's), Frigates (DL's), Guided Missile Frigates (DLG's), Guided Missile Heavy Cruisers (CAG's), Guided Missile Cruisers (CG), Guided Missile Light Cruisers (CLG). Within these types are a number of classes involving different weapon systems and electronic equipments. As technology advances and as systems dictate, weapons are improved; new versions are introduced into ships and the fire control and search radars replaced with more efficient and higher powered models. Communications equipment and their antennas are also being improved and antennas relocated aboard ship for more efficient use, hence the requirement for reevaluating a system which has been previously tested. (The Bureau policy regarding requirements for the testing of weapon systems is described in BuWeps Instruction 5101.2A of April 1962; see attachment).

When an in-service weapon is tested and found to be susceptible to EMR, operational restrictions are issued to the Fleet and the development of a fix is undertaken. While the "fix" is being developed rf tests are conducted to determine its effects on adjacent circuits and components. This is necessary because any of several mechanisms may be involved in the coupling of rf energy into a weapon and most often more than one EED is utilized in a weapon.

For all new weapons the designer must make certain that premature actuation of any EED will result only in a reliability type failure and further that adequate precautions are taken to minimize the probability of this occurrence.

Naval Weapons Requirement, WR-27, a "Design Guide to Preclude the Hazards from Environmental Electromagnetic Fields" has been issued with the above objectives in mind. This document is our first approach to provide information and techniques for minimizing the effects of rf on weapons containing EED's but can only be used effectively if it is taken into consideration early enough in the design phase of a weapon.

A Handbook is under preparation which will describe in detail such techniques as proper rf shield termination, the advantages and trade-offs of some rf insensitive devices and methods for their employment in advanced weapon designs.

The general terms "service generated EMR fields" or "Shipboard Electromagnetic Radiation Environment" used above defies a simple definition since the equipments which generate this environment vary from ship to ship within a given class and beyond this from ship type to ship type depending on mission, armament, etc.

It should be recognized that the Navy must be quite flexible in the use of radio frequencies. Figure (1) shows the frequency bands to which the Navy has access. This frequency spectrum is required to provide for any changes in a ship's mission and any changes in a ship's electronic suit. Therefore we must be prepared to encounter any frequency within this spectrum on any ship. Along with the changes in frequency assignments our weapons must also be prepared to accept limits in field strengths which are representative of the present state-of-the-art for transmitters. Considering these facts along with the confining dimensions of a ship's deck it should be apparent that the Navy HERO problem is quite complex and severe. For emphasis I would like to point out that our largest ship's deck is smaller than the average single airfield landing strip.

The values in Figure (2) were predicted from a study of the maximum field intensities anticipated is a given frequency band.

While Figures (1) and (2) indicate the magnitude of the rf fields one can anticipate aboard ship they do not correlate this data with weapon susceptibility data. We define a potentially hazardous field intensity to ordnance as an rf field which exceeds the values shown in Figures (3) and (4). These values apply primarily to disassembled electrically initiated ordnance, exposure of internal wires, testing involving additional electrical connections to weapons, handling bare squibs, primers, blasting caps or other EED's having lead wires.

Similarly Figures (5) and (6) show numerical definitions of the rf fields considered hazardous to fully assembled weapons.

The need for more effort on the theoretical aspects of the HERO problem has long been recognized but, as stated above, we have been faced with the urgent requirement of proving out weapons in their anticipated shipboard EMR environments and providing interim guide lines for Fleet Operation. However, some studies have been initiated, and much useful information has been obtained in the areas of predicting the EMR environment adjacent to deck edge antennas, determining aircraft armament circuits response in high intensity EMR fields and the coupling of rf energy into weapon circuits. The latter has been the most difficult area because of the numerous system variables encountered in handling weapons aboard ship and the statistical probabilities involved in both EED sensitivity and EMR environment.

A significant effort has also been directed towards the development of "generic fixes", (items or techniques which will be generally applicable in reducing the effects of EMR on ordnance).

Another phase of the HERO Program involves a study of the effects of the rapidly changing electromagnetic fields encountered by weapons and associated equipment in ships during deperming operations. These operations occur after and occasionally between each yard period depending on the permanent magnetism built up in the ship. This "Perm" is measured on a degaussing range and when it exceeds a given level the deperming operation is required. This operation consists of creating a giant solenoid by wrapping the entire ship in a coil of wire then applying approximately 3000 amperes dc to this coil for short periods of time. The polarity of the current is reversed during successive applications. This results in removing or satisfactorily reducing the permanent longitudinal and athwartship magnetization.

A requirement to off load electrically initiated ordnance prior to deperming was established because of anticipated hazards from the deperming fields.

The magnitude of the fields and the rates of change of these fields during deperming "shots" have been measured on several types of ships and at various locations such as missile ready service magazines and checkout areas, inside above deck launchers, etc.

Fields of similar or greater magnitudes have been generated in a laboratory facility with instrumented weapons and the effects measured.

To date none of the weapons tested revealed any deleterious effects due to deperming and they have been removed from the list of weapons requiring off loading. This is gratifying since the impact has been to remove existing restrictions at a considerable saving in labor costs and time.

The overall level of effort of the HERO Program has doubled since the first HERO Congress and, in addition to the in-house effort contracts have been issued to various research and development establishments.

FIGURE 1. Maximum Shipboard Electromagnetic Environment on CVA and CVS Aircraft Carriers

I. Communication Equipments

Frequency/ Megacycles/Sec	Distance from Antenna (ft)	Field Strength: Electric "E" Field Volts/Meter	Magnetic "H" Field Amp Turns/Meter	Power Density Micro Watts/cm²
.25-.35	10	300	.9	
2-32	10	100	.5	
100-[illegible]	100	-		10
225-400	100	-		10

II. Radar (Search and Fire Control)

Frequency Megacycles/Sec	Power Density Milliwatts/cm²: During Loading	Post Load
200-225	1.0	10.0
400-450	0.1	1.0
1,000-1,300	0.1	1.0
2700-3600	10.0	10.0
5400-5900	10.0	10.0
8,500-10,300	100.0	100.0

FIGURE 2 Maximum Shipboard Environment

I. Communication Equipments

Frequency Range Megacycles/Sec	"E" Field Volts/Meter	"H" Field Amp Turns/Meter	Power Density "E" mw/cm²
0.3 - 6	500	.7	
6 - 30	150	.6	
30 - 300			80
690 - 1215			80

II. Radar (Search and Fire Control)

Frequency Range * Megacycles/Sec	Power Density Milliwatts/cm²: Integration Time 1 Millisecond	1 Second
200-225	8.0	200
410-450	500	200
890-942	1000	300
1215-1365	2000	600
2700-3600	1800	350
5400-5900 **	60,000	60,000
8,500-10,300	350	350
10,300-16,500	200	200

* Power density for the radar bands assume the worst possible conditions, i.e. within the main antenna beam at the point of maximum power density.

** This value results from consideration of the proposed AF/SPG-59. If this radar is not used to establish the criteria in this frequency band, the values are: 400 mw/cm² for 1 millisecond and 250 mw/cm² for 1 second integration time.

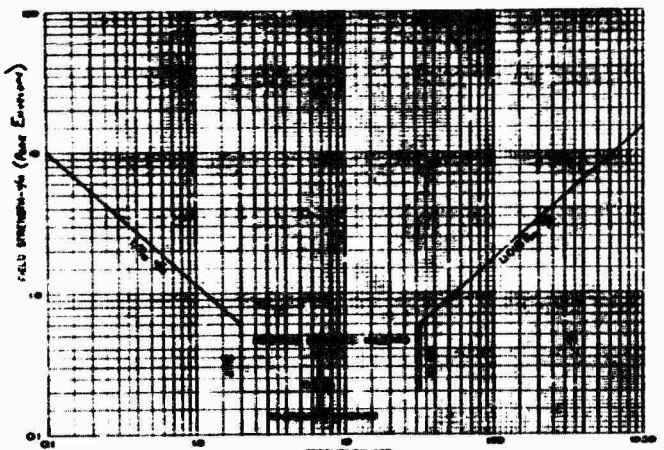

FIGURE 3 - HAZARDOUS FIELD INTENSITY TO ORDNANCE - RADIO TRANSMITTERS

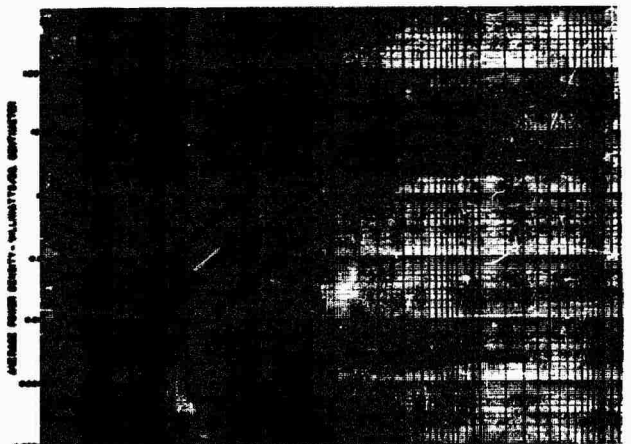

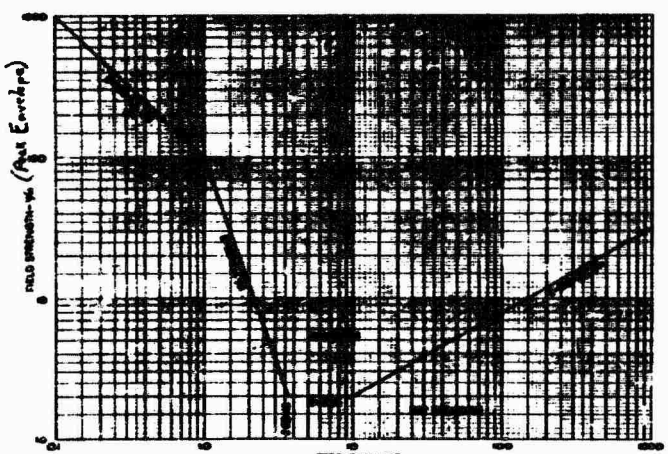

FIGURE 5 - MAXIMUM SAFE FIELDS FOR WEAPONS - RADIO TRANSMITTERS

DEPARTMENT OF THE NAVY
BUREAU OF NAVAL WEAPONS
WASHINGTON 25, D.C.

IN REPLY REFER TO

BUWEPS 5101.2A
RREN-3
26 Apr 1962

BUWEPS INSTRUCTION 5101.2A

From: Chief, Bureau of Naval Weapons

To: Assistant Chiefs, Directors of Divisions, and Heads of Offices, Branches, and Sections, Bureau of Naval Weapons

Subj: Hazards of Electromagnetic Radiation to Ordnance (HERO); policy for conduct of program to alleviate

Ref: (a) OPNAV INSTRUCTION 5101.1A of 15 Sep 1959
(b) BUWEPS INSTRUCTION 5430.6 of 1 Dec 1960
(c) BUWEPS INSTRUCTION 5200.2 of 30 Dec 1959
(d) Weapons Requirement WR-27 - Naval Weapons Design Guide to Preclude Hazards from Environmental Electromagnetic Fields of 12 Feb 1962

1. Purpose. This Instruction establishes policy within the Bureau of Naval Weapons for the conduct of a program to determine and rectify any deleterious effects of electromagnetic radiation (EMR) on air, surface, and underwater weapons and other devices which have been accepted or are proposed for Naval use and are under the design cognisance of, or are recommended for naval use by the Bureau of Naval Weapons. This Instruction is applicable to all tests and other efforts conducted to assess and alleviate the hazards of electromagnetic radiation to material, as well as tests conducted aboard ship for the purpose of determining shipboard radio frequency (RF) environmental conditions.

2. Cancellation. This Instruction cancels and supersedes BUWEPS Instruction 5101.2 of 11 January 1962.

3. Background

a. Weapon system and other components contain numerous electro-explosive devices (EED's) which are susceptible to initiation by electromagnetic radiation, as from radar or communication equipment. Initiation of an EED by radio frequency radiation may result in a premature firing, a dud, or a faulty operation (hang-fire, low-order burst, unwanted parachute ejection, etc.).

b. Reference (a) established policy for attacking the general radio frequency radiation hazards problem within the Department of the Navy. The general problem includes, in addition to the hazards associated with ordnance material, hazards involving ignition of inflammable material and injurious effects of radio frequency energy on personnel.

c. Reference (b) established responsibilities for the Bureau of Naval Weapons Explosive Safety Program. The HERO program implemented by this Instruction is considered to be a part of the over-all Bureau Explosive Safety Program described in reference (b).

4. Policy

a. General

(1) HED's shall not be used in weapon systems and other devices where the requirement can be met by other reasonable means. (See reference (d))

(2) Weapon systems and devices shall be designed to preclude spurious functioning of any HED or degradation of any HED with respect to reliability or performance characteristics by environmental, radio frequency (RF) electromagnetic fields. (See reference (d))

(3) Weapon systems and devices containing HED's shall not be produced, procured, or issued to the Fleet until a positive certification, as a result of HERO tests, has been made that they can be handled with impunity in the maximum predicted shipboard electromagnetic environment. Any exceptions to this mandatory requirement will be determined by the Chief of the Bureau on the basis of over-riding Fleet readiness or operational necessity.

(4) A supporting research and test program in the Bureau of Naval Weapons entitled HERO, under the direction of the Research and Engineering Division, has been established to pursue a systematic attack on the hazards of electromagnetic radiation to ordnance.

b. Weapon Susceptibility Tests

(1) Instrumented HERO tests as described below are required on all weapons and devices containing HED's currently in use.

(2) Instrumented HERO tests are required on all new weapons and devices during their development, and as necessary on production weapons.

(3) Instrumented HERO tests as described below are required on each new weapon installation, and shall be made prior to tests of explosive-loaded components aboard ship or aircraft in the development test phase or early shipboard trials prior to shipboard training. "Installation" as stated herein includes each new construction and each conversion or modification which tends to affect the electromagnetic radiation aspects significantly. For example:

(a) Major ship alterations involving the ships' electronic suit as it pertains to the ships' superstructure and antenna radiation patterns, including weapons guidance systems.

(b) Addition of new weapon systems

(c) Major modification of existing weapons

(d) Major modification of HED's or explosive circuitry in existing weapons.

c. Instrumented HERO Tests

(1) Simulated HED's Assembled Into Weapons. In this test the HED's will be replaced, wherever possible, with simulators consisting of current sensing, voltage sensing, or temperature measuring devices coupled with suitably designed, internally mounted recording equipment having self-contained power supplies. Weapons configured with simulators will be run through normal handling procedures from magazines to launching vehicles, including all electrical plug-in and circuit-checking operations, over as wide a frequency range as possible and with maximum power available.

(2) Explosively Loaded HED's Assembled Into Weapons. In this test the HED as used in the operational weapon will be utilized as a threshold gauge, but the main propellant and high explosive charges will be omitted. Test weapons will be handled as in 4c(1) above. These tests shall be run concurrently with the instrumented HERO tests. The test specified in this section is designed as a back-up for the simulator assembled weapons since the present state of the art does not permit positive correlation of the two types in the microwave region. This test is more commonly known as a GO/NO-GO type test. Reliance on GO/NO-GO tests solely is to be avoided, since adequate numbers of these items cannot be tested to achieve the desired degree of confidence for either safety or reliability.

5. Responsibilities

a. The Assistant Chief for Research, Development, Test and Evaluation is responsible for administering and executing that portion of the HERO program that parallels his responsibilities set forth in enclosure (1) to reference (c) concerning the safe design, development, and testing of weapons, weapon systems, and explosive materials throughout the Naval Establishment, specifically by Division:

(1) RR Division. As coordinator of the HERO program the Engineering Branch (RREN) of the Research and Engineering Division is responsible for the following:

(a) Determining, in collaboration with the Bureau of Ships, the electromagnetic environment aboard ships and forwarding this information to the Weapon System Division Directors for their use in the design of weapon systems.

(b) Scheduling and conducting weapon susceptibility tests on current stockpile weapons and devices containing EED's.

(c) Scheduling and conducting weapon susceptibility tests on newly developed weapons and devices upon completion of development, and, at the request of Division Directors, during development.

(d) Advising cognizant Division Directors of the results of the tests. When items are found susceptible, details of the investigation as well as recommended fixes or approaches to the fix problem shall be furnished.

(e) Scheduling and conducting weapon susceptibility proof tests after completion of fixes.

(f) Planning and conducting HERO tests on the first ship of a class as well as subsequent modifications or conversions.

(g) Maintaining summary lists of all shipborne and airborne sources of RF radiation for the purpose of ready identification of ship and aircraft profile by equipment nomenclature and characteristics.

(h) Compiling and maintaining a detailed listing of all weapons and devices which utilize EED's and which are maintained in the Navy stockpile as well as those undergoing various phases of RDT&E. This listing shall tabulate the various EED's used in each component of each weapon, and describe the status of HERO testing and, where indicated, the status of fixes or modification programs which have been established to overcome demonstrated susceptibility. Periodically this listing will be updated and distributed to all concerned.

(i) Recommending release of weapons and devices for production, procurement, or Fleet issue when found to be not susceptible to spurious initiation or degradation in the maximum predicted RF environment. RREN will assign the designation "-6", to be appended to the Model designations of assembled weapons and ordnance which either do not contain EED's or have been specifically cleared by HERO tests. This action will be included in the listing in 5a(1)(h) above.

(j) Coordinating or advising on any restrictions required to obviate hazards due to electromagnetic radiations, maintaining and promulgating the official compendium of restrictions released and their status.

(k) Under the supporting research program, investigating generic fixes as well as components having less inherent RF susceptibility and recommending their applicability to Division Directors.

(2) RA, RM and RU Divisions are responsible for the following:

(a) Design evaluations

1. Submission of new weapon and/or component designs for HERO review to the HERO technical director at NWL Dahlgren.

2. Provision of representative hardware as part of the Prototype Production for Evaluation (PPE) or equivalent programs for specific use in HERO type tests.

(b) Taking corrective action to provide fixes for weapons, launchers, and aircraft armament circuits, found to be susceptible to electromagnetic radiation, and providing the associated new and revised documentation (drawings, specifications, manuals, etc.).

(c) After coordination by RR, authorizing any restrictions required to obviate hazards due to electromagnetic radiation and subsequent modifications or cancellations.

(d) Conducting tests during the fix period, or supporting RR in such tests.

(e) Providing hardware as required for all HERO type tests except as noted in paragraph 5b.

(f) Providing information copies of all correspondence pertaining to the above responsibilities to the HERO program coordinator, RREN, and to other interested Bureau activities.

(g) In order to facilitate the compilation described in 5a(1)(h) and (i), providing to RREN the detailed information required for each weapon or device undergoing RDT&E and updating on a continual basis as the information becomes available.

(3) RE Division is responsible for coordinating the scheduling of ships with CB, CNO, BUSHIPS, and others as may be necessary to accomplish the HERO tests required and for providing information and data on ship and airborne installations.

b. The Assistant Chief for Fleet Readiness and Training is responsible for that portion of the HERO program which parallels his responsibilities set forth in enclosure (1) to reference (c) concerning maintenance, usage, and disposal of weapons, weapon systems and explosive material throughout the Naval Establishment; specifically:

(1) Providing resources and hardware for HERO tests on Fleet issue weapons and devices.

(2) Providing the information required for the compilation of 5a(1)(h) and (i) above for all in-service weapons and devices.

(3) Providing RHEO and Division Directors concerned with failure and casualty reports or other information involving HERO problems, including results of inspections to detect spurious actuations of HED's.

c. The Assistant Chief for Plans and Programs is responsible for the program management aspects of the HERO program including the assignment of resources for the accomplishment thereof.

CB is responsible for introduction of HERO considerations in the formulation of Ship Characteristics and Class Improvement Plans by the Ships Characteristics Board and CNO.

d. The Assistant Chief for Surface Missile Systems is responsible for the program management aspects of the HERO program including the assignment of resources for the accomplishment thereof in connection with TERRIER, TARTAR, TALOS, and TYPHON.

6. Technical Support Activities

a. Under Bureau of Naval Weapons WEPTASK, the Naval Weapons Laboratory, Dahlgren, Virginia provides support technical direction for the Bulweps HERO program, and has a suitable staff to accomplish the tests, evaluations and documentation outlined in subparagraphs 5a(1) above.

b. To the extent feasible beyond the scope of subparagraph 5a(1), the resources of the Naval Weapons Laboratory will be made available to BUWEPS Division Directors for direct assistance in areas of design review and weapon modifications.

R. S. MASTERSON
Deputy

Copy to:
(W activities, estab. quantity; others 4 except as shown) SNDL: 21, 26F (all), 29F (2 copies), 29H (2 copies), 29L (2 copies), 29O (2 copies), K26(FBMC-CL only),A3(12 copies),A5(BUSHIPS (12 copies),BUWEPS: DD3-251 (5 copies), DDS-111 (1 copy), DDS-321 (2 copies), DDS-512 (2 copies),MA(25 copies), RMSM-3 (50copies): L1, W7C, W7F, W7G, W7J, W7K, W7P, W7Q, W7R, W7S, W7V, W7W, W7X, W7Y, W9B (Louisville (Code 1000) (1 Copy), W9E (Code 1000) (1 copy), W11A (Crane (Code 1000) (1 copy)) FRC, OSA, Alexandria (2 copies); MAT;

Stocked at NAVWPNPLI

3. THE AFSWC APPROACH TO THE EMR HAZARD PROBLEM

Lt Raymond J. Hengel
AFSWC, Kirtland AFB, Albuquerque, N.M.

Since AFSWC is a late entry into the study of EMR problems, a great deal of data is available for making a preliminary survey. Full use is made of existing data and corollary situations in making an EMR evaluation of a new system, in order to minimize the actual test requirements. We presently have no facility and must therefore draw on other agencies, such as NWL for some test support, to run complete tests. However, we have conducted tests associated with the on-board radiators for the B-52 and B-58.

One technique for analyzing the EMR hazard problem of an existing location is to use a layout of the area of interest, listing of associated weapons, and a knowledge of the power, frequency and antenna characteristics and location of the radiating equipment. When aircraft are involved, knowledge of the on-board RF equipment, to include: frequency, power, mode of operation and antenna details, such as type, location and gain, is used in making the analysis. This information is then applied to the weapons in their various configurations. From this we determine if:

A. No hazard exists

B. The expected levels fall in a region where the expected response is uncertain.

C. A hazard is a likelihood.

The action to A. is obvious. Based on the particular situation associated with B & C, you can either establish restrictions on use of the offending equipment, or conduct tests to answer the uncertainties.

A report that has been of considerable use to us is "EMR Environmental Measurement Requirements for Nuclear Weapons". This is the result of a study conducted under the auspices of the "Ad Hoc Group on Weapon Susceptibility to EMR". We have repeatedly used the "upper limit" values of electromagnetic field for safe assembly and dis-assembly operations as our conservative estimate to evaluate a given situation. (Fig. 1) In many cases, even assuming the worst possible conditions, the field strength values fall well below even this conservative curve, which is based on matched dipole conditions connected to unprotected squibs. This has proved most valuable, however, this approach cannot be either the final or most accurate method of determining EMR hazards. This is an extremely conservative criteria, and if these levels could not be met, we have to request that the environmental conditions be better defined. Where no directly related data is available, as in the case of the MK-4 RV, and exposure was a reality we established test requirements, which, in this instance, were run for us by NWL.

As an example of a situation involving an external environment, the Sandia Corporation assisted us in conducting an analysis of the EMR hazard at two overseas locations. All of the RF data from the sites was compared with the RF field levels that are considered "non damaging levels" for performing bomb assembly, dis-assembly and test operations, as well as loading and unloading. In all cases the existing RF field never exceeded the allowable level. Since all frequencies were found to be non-damaging by this "worst condition" method, it was reasonable to assume that no hazard existed, and the situation could be certified without the necessity of conducting tests.

All on-base RF equipment having a power of 50 watts or greater were considered as being a potential hazard. The locations where field strengths were calculated were selected to be points in the loading, storage and transportation routes where the highest field strength would likely be experienced. Certain assumptions were made as follows:

(1) For communication systems, antennas were assumed to be of the half-wave dipole type, vertically oriented.

(2) The gain used was assumed to be with reference to an isotropic radiator.

(3) Existing structures between the RF emitters and the weapon storage or loading areas were assumed to not shadow or reduce the field strength at all.

(4) The far zone of the radiated field was assumed to begin one wave length from the antenna.

(5) Since the thermal time constants of the weapon's EED's are considerably longer than radar pulses, the average radiated power from radars is used.

(6) For positions having more than one transmitter, (i.e. control towers) that can radiate simultaneously, the combined power output of all transmitters operating simultaneously is used in calculating the effective field strength. We realize this is a highly improbable situation, but yet this is the worst possible condition that could occur.

(7) The calculated field strengths are compared to non-damaging levels for EED's, having 100% no fire current of 100 ma.

The resultant calculated field strengths were plotted on the curve of field strength limits during assembly - dis-assembly of weapon systems, and it was found that all fell well below the allowable values, as a function of frequency.

The previous example was one entirely concerned with the external environment. We also have situations involving the on-board RF equipment. The RF-101 aircraft and its associated armament is an example of this situation.

In response to a query concerning the adequacy of safety in the RF-101 system, AFSWC requested identification to include power, frequencies, antenna type and location for all RF sources of the RF-101 system.

The following list was furnished:

(a) RT-263/ARC-34 frequency range is 225.0 to 399.9 MC, one blade antenna on split vertical camera door and one fin cap on the tall section, 9 to 20 watts output.

(b) RT-220/ARN-21 range 962 to 1213 MC, blade antenna center fuselage door 106, 2.5 KW output.

(c) RT-279/APX-25 range 1030 to 1090 MC, blade antenna nose section door 102L and R, 60 watts maximum output.

(d) RT-160/APN-22 frequency 400 MC, 115 volts, AC and 28 volts DC, flush mounted antenna nose section door 101, 1.5 watts output.

(e) RT-395/APN-102 8800 MC, flush mounted antenna forward fuselage peak 500 watts average, 10 watts output.

Based on this information, in the manner detailed earlier, we were able to state that there should be no weapon EMR hazard associated with the listed on-board equipment, even if the equipment should be operated during the loading process. This is readily apparent, using our previous curve, (Fig. #1) as the high powered transmitters are all in the 1000 MC range, high on the curve and the lower frequency transmitters, in the susceptible region, are low power.

In many instances, sufficient data has been gathered so that we can draw correlations between systems. However, there are certain precautions that must be taken. For example, we must make sure that we are correlating between similar systems: e.g. fighter systems and their

on-board equipment cannot be used in determining hazardous conditions involving bomber systems with entirely different on-board equipment and locations. It is well established that the particular geometry of a system is important.

Thus, in the two cases cited, both for on-board equipment and for external environment, without performing any tests, but using only readily available data, determinations of the EMR hazard problems were made. It was established, in both cases cited, that no hazard existed, therefore, saving the time and expense of running tests. We do not mean to imply that tests are not meaningful, but this method as a preliminary evaluation can determine if they are necessary.

We plan to have at the Air Force Weapons Laboratory an EMR mobile facility designed to be used to evaluate the effect of EMR environments on components, sub-systems and complete systems in use or planned for use by the USAF. This will be used either when our method of preliminary analysis determines that testing is necessary, or when no directly related data is available.

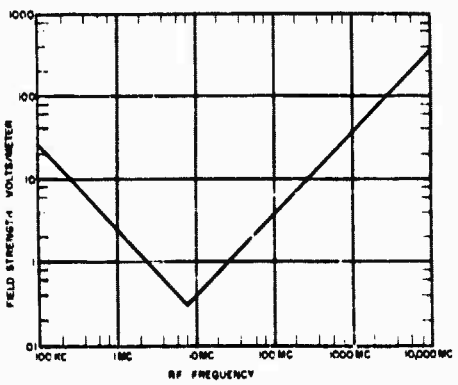

FIGURE 1 FIELD STRENGTH LIMITS DURING ASSEMBLY-DISASSEMBLY OF WEAPON SYSTEMS

6. Variables Involved in HERO Testing — L. J. Lysher

The amount of energy transferred from a transmitting antenna to an electro-explosive device in a weapon is dependent upon many variables. This paper discusses some of the known variables that must be considered in evaluating the electromagnetic radiation susceptability of a weapon. The variables are considered to exist in three major areas; weapon configuration, environment and handling operations.

7. RF Susceptibility Tests of Type 19 Spotting Device (U) — Richard J. Aaron

Tests were conducted to determine the RF susceptibility of the Type 19 Spotting Device to dudding and/or initiation under field conditions. The sensitivity of the detonator used in this device to RF and DC was determined in the laboratory while instrumented devices capable of detecting the relative temperature of the bridgewire were constructed. These were subjected to various RF environments after assembly to the missile. Test results are given.

8. Vulnerability of the M6 Electric Blasting Cap to Missile System Radars (U) — Theodore Warshall

Laboratory and field tests are described which were conducted to determine if the M6 Electric Blasting Cap is vulnerable to the radars of a missile system. The results of the tests are summarized.

9. Picatinny Arsenal Theoretical Analysis of RF Vulnerability of Weapon Systems (U) — Richard G. Sats

A theoretical analysis of typical missile antenna configurations will be discussed with respect to: antenna characteristics, extracted power, skin effect, loads, etc., including formulas, definitions of terms, references and assumptions. An RF safety probability analysis of warheads will be discussed. Philosophy of these analyses will be discussed with respect to usefulness, present and future, in evaluating the susceptibility of a weapon to EMR.

10. Missile with Attached Umbilical Cable as a Receiving Antenna — Charles W. Harrison, Jr.

In this paper principles of antenna analysis are applied to estimate the magnitude of undesired radio-frequency current along the skin of a rocket on the launching pad, with umbilical cable attached, due to a plane wave incident field. In the ready state, such systems are only partially shielded from the electromagnetic field environment, and form effective receiving antennas. Radio-frequency energy may be fed to sensitive electroexplosive initiating devices, resulting in spurious operation, or malfunctioning.

11. Radio-Frequency Leakage Into Missiles — Charles W. Harrison, Jr.

Summary: This paper treats the idealized problem of RF energy leakage through a slot in an infinite cylinder as a perturbation on the scattering problem for the same object with no slot. It is shown that interior response depends on three factors: the exterior skin current density from the scattering problem, the transmitting admittance of the slot, and an eigenfunction expansion of the interior field when unit voltage is impressed across the slot. It is then proposed that the form of this solution may be applicable and conceptually useful in treating other problems either theoretically or experimentally.

13. Analysis of Response of Thermocouple Instrumented Devices to Short-Pulse Transients — Richard K. Fry, D. Boyd Barker

With the assumption that the bridgewire, thermocouple and recording instrument behave as successively-coupled, linear systems, their response to short pulses of energy into the bridgewire was determined. This model and its verification make possible the calibration of instrumented devices to recover pulse energies and/or bridgewire temperatures from the output of the recorder.

14. Methods of Measuring RF Power at a Given Point in a High Loss System — Norman P. Faunce, Paul F. Mohrbach, George H. McKay, Robert W. Wood

When losses in an RF transmission line are high, and especially when impedances are widely mismatched, it is difficult to determine power at a particular point. Three methods are outlined, to do this. (A) Voltage-Impedance: RF voltage and complex impedance are determined at the desired point; from these, power can be computed. (B) Differential Power: Directional couplers are used in measuring power toward and away from the load; the difference is the net power transmitted. (C) Voltage Max-Min: Standing voltage waves are measured; knowing load resistance, power can be computed.

15. Determination of Response of RF Insensitive Devices — Norman P. Faunce, Paul F. Mohrbach, George H. McKay, Robert W. Wood

Usually, each class of RF "fix" requires a new testing procedure, and new evaluation techniques. This paper discusses some of the special problems. One problem, in particular, is the determination of true attenuation, by dissipation of power, as distinguished from insertion loss, or reflection of power.

6. HERO Variables and Test Facilities

L. J. Lysher

U. S. Naval Weapons Laboratory
Dahlgren, Virginia

INTRODUCTION

The amount of energy transferred from a transmitting antenna to an electroexplosive device (EED) in a weapon is dependent upon many variables. These variables must be identified, examined and weighed in the evaluation of weapon system susceptibility to electromagnetic radiation. The number of variables is quite large; only those considered most important will be discussed here. The variables may be divided into three major groups; (1) weapon configuration, (2) handling operations and (3) environment.

WEAPON CONFIGURATION

The amount of energy transferred to an EED is dependent upon the characteristics of the weapon in which it is employed; the effect of this energy is dependent upon the firing energy requirements of the EED. The pertinent weapon characteristics include circuitry, coupling factors between circuits, external (to the weapon) cables, ports, openings, etc. In most cases it is not practical to extrapolate from one weapon type to another because small differences may cause large changes in the rf response of the weapon. In fact, care must be taken in extrapolation of results from one weapon to another of the same type because of production differences between units (i.e., location of wires in a bundle with respect to each other). Included as a part

of the weapon system is the launching vehicle; i.e., aircraft, launcher, etc.

The effect of a given level of energy in an EED circuit is obviously dependent upon the firing energy requirements of the particular EED. While it is true that a high energy EED may not be affected as much as a low energy one by a specified amount of energy, impedance changes must be considered. The energy induced in the high energy EED may be greater than in the low energy one because of an impedance change.

HANDLING OPERATIONS

There are many variables which are not associated with either the weapon configuration (as defined), or the environment, but are concerned with operations which are performed upon the weapon. These include transport, handling, testing, loading aboard aircraft, etc. All possible operations cannot be investigated; however, those which are likely to occur must be investigated. The more important of these will now be considered individually.

Handling

When testing, all operations that are normally performed under operational conditions when the weapon is in an electromagnetic field should be performed or simulated. Also, operations that are not normally performed but which are possible (for example, connecting an umbilical cable before racking, if the normal procedure is to rack before connecting) should be performed during tests. The maximum allowable energy for abnormal operations depends upon the probability that the operation in question might be performed.

Variation of Induced Current Under Identical Test Conditions

It has been found that if an operation such as connecting an umbilical cable is repeated under identical conditions of rf source frequency and power, distance, weapon orientation, etc., a set of data, rather than a single value of induced current is obtained. This characteristic is present in all cases wherein the induced current is of short time duration and where contact is made or broken somewhere in the weapon system. In some cases a graph of the distribution of the induced current approaches that of a normal distribution curve; however, in other cases the distributions range from slightly skewed to multimodal.

Transmitter to weapon/aircraft Distance

The transmitter to weapon distance affects the induced current, but not in a simple relationship. In the "far field" the field, and hence the induced current, varies inversely as the distance from the antenna; in the "near field", and near discontinuities such as a deck edge, this rule does not hold true; as large a field may be found 100 ft from the antenna as ten ft from the antenna. If a uniform field exists around the test object, the test results may be extrapolated to any given field strength, and any convenient "far" distance can be used for the tests (within the limits of detection sensitivity). This extrapolation is not correct in the case of weapons very near communications antennas. Under this condition the test object is not immersed in a uniform field; in fact, the effect of the radiated field may be secondary to that of the induction field. In order to make statements regarding the susceptibility of a weapon located very near an antenna actual tests must therefore be conducted at such distances.

Weapon/aircraft Orientation

The orientation of the weapon/aircraft combination with respect to the transmitting antenna is very important, particularly at wave lengths comparable to or smaller than the maximum dimensions of the aircraft. This orientation sensitivity is discussed in NWL Report No. 1787, The Antenna Characteristics of an A4D-2 Aircraft (U) by Harry P. Bird. It is therefore essential when conducting tests adequately to investigate sufficient orientations to assure that no maximum points have been omitted. At frequencies below 26 Mc, increments of 90° rotation, and above 200 Mc increments of 15°, are ordinarily adequate to determine trends in the induced current versus orientation function; much smaller increments are required unless only trend information rather than magnitude of maxima is required.

Grounding

It is not possible to ground an object at rf frequencies in the same sense as a ground can be provided at dc; however, it is possible to provide a low impedance path for rf current at some frequencies. For convenience, however, I will speak of grounding in the sense of simply joining two points with a metallic conductor.

Grounding the aircraft and grounding the weapon must be considered separately. Grounding of the aircraft to the deck normally does not increase the hazard; however, it may cause a shift in the frequency at which current is induced in an EED, thereby reducing the hazard at some frequencies and increasing it at others. In the case of the weapon this is not necessarily true; in many instances one side of the firing

circuit is connected to the weapon skin, and when the weapon is grounded a convenient path is provided for the return of the rf current to the deck. In loading the weapon on an aircraft it is possible that the weapon may be grounded to the deck either intentionally or inadvertently, for example, by a bomb truck or personnel touching the weapon; hence, it is necessary to conduct tests with the weapon grounded and ungrounded.

Auxiliary power supply

Auxiliary power sources (external to the aircraft) are used for aircraft starting and check-out functions. With the power source connected to the aircraft, the rf configuration of the aircraft is changed; consequently, the rf susceptibility of a weapon loaded or being loaded on the aircraft is changed.

ENVIRONMENT

The test environments must be either the actual environment to which the weapon will be exposed, or one that can be extrapolated to that environment, since it is the weapon's performance in the actual environment that must be evaluated. The important environmental variables will now be considered individually.

Transmitter Power

The current induced in an EED is proportional to the square root of the antenna power if all other variables are constant. Any convenient power level can be used and the results extrapolated to any other power. A critical factor is the threshold of detection of the device used to measure the induced current. The instrumentation presently being used by NWL has a threshold of approximately 5 percent of the EED maximum

no-fire current; if the transmitter power used does not produce a current greater than this amount, extrapolation is not possible. In practical usage, it is best to use rf powers that keep the maximum induced current just below the upper limit of the detection system. To determine if the weapon can be handled with impunity aboard ship, the test results must be extrapolated to powers or fields expected aboard ship. If field strength values are to be extrapolated, the unperturbed test site field, (that is the field without the weapon and aircraft) should be measured. With the test site fields and the fields existing on board ship available, the magnitude of induced currents to be expected in ordnance aboard ship can be readily scaled for a given set of test conditions.

Transmitter Frequency

There are several variables that are functions of frequency; these include weapon impedance, antenna characteristics of the aircraft and weapon, and coupling between (wiring) circuits of weapon and aircraft. For this reason the optimum test would be to scan the complete frequency spectrum. Since tests at the higher rf powers must be conducted at discrete frequencies, the weapon can be evaluated at only a finite number of frequencies. Because of the frequency dependance of many of the weapon/aircraft variables, current may be induced only over a certain frequency band or bands. The susceptibility bandwidth or Q of a weapon system will dictate the size of test frequency increments. When frequency allocations prohibit selection of optimumly spaced test frequencies, the test results must be corrected by weighing the data relative to the weapon Q. It may also be necessary to supplement an assumed Q by tests to determine where response peaks lie in the frequency spectrum.

Reflections

Electromagnetic energy is reflected by metallic objects; hence reflections must be considered when conducting tests and establishing acceptable induced current levels. Reflections should be avoided or at least not permitted to become one of the unknown variables. Should destructive interference between the incident and reflected waves occur, the resultant field at the site of the device under test could be much lower than the unperturbed field. When establishing acceptable induced current levels, the opposite condition (i.e., enhancement of the field) must be considered since it is quite possible to find areas aboard ship where interference has doubled the unperturbed field.

NWL GROUND PLANE TEST FACILITY

The ground plane facility provides a means of conducting tests under controlled conditions and provides flexibility that cannot be achieved in field or shipboard testing. It lends itself to the simulation of a wide range of service conditions for the accomplishment of preliminary evaluations and for various EMR research projects. It also provides a laboratory for research on antenna theory and field strength measurements and distribution. The turntable incorporated in the ground plane makes it possible to readily examine the effects of azimuth changes in the weapon during illumination by the rf sources.

The ground plane deck is constructed of 1/4 inch steel plate, welded into a continuous sheet (240 ft by 100 ft) simulating the deck structure of a naval vessel. It is capable of supporting loads of up to 10 tons per square foot. All ground plane power cables and coaxial cables are

located underground. Tiedowns and grounds are provided for aircraft. The ground plane is grounded around the periphery to 6 ft ground rods located at 20 ft intervals.

The turntable is a steel disc 15 ft in diameter located 50 ft from one end of the ground plane. It was constructed by inverting a 5"/54 gun mount and has a load capacity of 15 tons. It can rotate continuously about an axis perpendicular to the ground plane in either direction at speeds from 0 to 4 rpm. The turntable is electrically driven, and may be operated from controls located in a pit near the ground plane or similar controls located in an adjacent hangar.

Transmitting equipment ordinarily employed in HERO testing at NWL includes equipments operating in frequency bands from 100 kc to 10,000 Mc.

These equipments are operated at spot frequencies assigned to the Naval Weapons Laboratory by the Chief of Naval Operations for HERO testing at full power.

MEASUREMENT EQUIPMENT

RF power density and field intensity measurements are conducted during tests on the ground plane facility to determine the magnitude of the electromagnetic fields. Antenna impedance measurements are made prior to testing and are used in determining the radiated power of the transmitter. The field information is used in conjunction with test records of the instrumented HEDs within the weapon in evaluating the test results. Measuring equipment is available for field intensity and impedance measurements throughout the complete frequency range to 10,000 Mc.

The experimental determination of the effects of the various test variables requires that the amount of rf energy induced in the EED be measured. When installing the instrumentation to measure induced energy, every effort is made to avoid perturbing the rf response of the weapon; particular care is taken to avoid creating new paths of entry for rf energy. It is not possible to install instrumentation without making some changes in the weapon; this fact must be considered when analyzing test results.

Several types of EED simulators have been or are being used to measure the current induced in the EEDs. The simulator used most in HERO tests at Dahlgren is the thermocouple developed by the Denver Research Institute. This instrumentation uses an actual EED base and bridge wire assembly without explosives. The thermocouple element is located near, but not touching the bridgewire. This unit is compact and can be mounted in almost all places in a weapon occupied by real EEDs. The output from the squib simulators are fed via shielded leads into recorders or direct reading meters which are calibrated before and after tests.

The recorders which are used with the squib simulators include conventional oscillograph galvanometer type recorders, miniature, self-contained tape recorders developed by Edwards Engineering Co., and also a small cylindrical oscillograph recorder developed at the Naval Weapons Laboratory. The NWL recorder is an eight channel recorder, cylindrically shaped 4 1/2 inches in diameter by 19 inches long. With battery pack it measures 5 inches x 41 inches long. Using 150 ft of recording paper

(at 0.33 inch per second), a recording time of about 90 minutes is obtained. In those weapons which are too small to accomodate recording equipment, a shielded dc chopper-amplifier developed by NWL, Dahlgren for use in amplifying thermocouple output from squib simulators is employed. The amplifier measures 1 1/2 inches in diameter by 4 inches long. The output of the amplifier may be monitored by conventional dc meters.

CONCLUSION

We have now discussed some of the variables that influence the susceptibility of a weapon, and briefly, the methods and facility used at Dahlgren to determine the effects of these variables. The object of testing is to identify those combinations of variables which result in a hazard. Upon identification of those combinations, the probability of exceeding any stated value of current can be determined by tests. It should be noted, however, that a prohibitively large amount of data may be required to adequately determine this probability. When the extent of the hazard has been found under the determined set of conditions, as a separate problem, it is necessary to obtain the probability of occurrence of such conditions. This probability can be estimated from operational experience or from actual observation in the field where the weapon will be handled. One approach is to assume that those worst conditions have a probability of one of occurrence, and to determine the time interval in which these conditions are virtually certain to occur. NWL is presently engaged in an intensive program to establish procedures to provide a sound mathematical probability statement about the susceptibility of a weapon under operational usage. Until the time when a mathematical statement can be made after a practical amount testing, good engineering judgement will still play an important part in determining if a weapon can be employed without undue fear of accidents or serious degradation of reliability.

10 MISSILE WITH ATTACHED UMBILICAL CABLE AS A RECEIVING ANTENNA

by

Charles W. Harrison, Jr.
Member of the Technical Staff,
Sandia Corporation, Albuquerque, N. M.

Introduction

In this age of space exploration it has become necessary to assess the receiving characteristics of rockets to unwanted radio signals because they are fired by electroexplosive devices (EEDs). If the rocket on its launching pad, with umbilical cable attached, is unduly sensitive to the electromagnetic field environment, a premature launching might occur, or a degradation in performance result. The unwanted radio-frequency field environment may be caused by the operation of one or more radio transmitters in the vicinity of the launching pad, by local thunderstorm activity, or by a nuclear detonation in the neighborhood.[1-5]

A similar problem exists in the general field of ordnance. Potter[6] has written a good summary of the problem of radio-frequency hazards to ordnance. He says,

> "The recent trend in radar and communications equipment toward greater effective radiated power has resulted in growing concern about RF hazards .... The most serious hazards stem from the use of sensitive electrically-initiated explosive elements, known as electro-explosive devices (EEDs), which can be spuriously initiated by induced radio frequency energy. EEDs are used extensively ... to activate control and arming devices and to initiate explosive trains. Hazards include both spurious functioning of the EED and degradation of the EED reliability or performance characteristics."

Radio-frequency energy is fed to the EEDs by the internal circuitry in the rocket. The wiring is activated by radio-frequency leaks through access doors (slots), anodized peripheral butts between sections, etc., and by direct connection (by way of the umbilical cable) to improperly shielded external circuitry.

The basic problem of radio-frequency hazards to ordnance consists in evaluating the response of a dipole receiving antenna within an imperfectly conducting cylinder of modest wall thickness and of finite length. Harrison and King[7] have demonstrated that for any conceivable field amplitude there is no hazards problem at low frequencies, where the length of the cylinder and radius are small in terms of the wavelength. At higher frequencies skin effect affords sufficient protection. The theory presupposes no breaks in the rocket skin and no attached umbilical cable. However, King and Harrison[8] have shown that the pickup of a coaxial cable of sufficient length to approach resonance at low frequencies is surprisingly large.

Harrison has discussed radio-frequency shielding of cables in a qualitative way,[9] evaluated approximately the response of a loop antenna in a large imperfectly conducting cylinder,[10] and determined the shielding properties of a circular grating of finite length.[11] Work is currently under way at

the Sandia Laboratory to evaluate theoretically the transmission of radio energy through access doors. Dickinson[12] has considered electromagnetic coupling to ordnance devices, and some 30 years ago King[13] obtained the shielding effect of imperfectly conducting spherical and infinite cylindrical shells at low frequencies. This work is now the classic in the field of electromagnetic shielding.

Radio-frequency hazards to ordnance problems relate to partially shielded receiving antennas of very general configuration. The solutions of these problems are often obtained by combining methods of antenna analysis with suitable arranged experiments. Thus theory complements experiment. If a correlation has been obtained in the Laboratory between some easily measured current in the rocket and EED current, and the former current can be estimated theoretically for a new radio-frequency field environment, the problem is solved.

In the present paper it is assumed that the relation between rocket EED current and total current in the shield of the umbilical cable at the point of attachment near the nose is known. The theoretical problem is that of estimating the umbilical cable current for a specified electromagnetic field in the vicinity. The physical configuration of the rocket on its launching pad, and the umbilical cable, resembles a folded monopole for reception. This paper lays the foundations of a very general theory of reception by folded dipoles.[14] The analysis has many points in common with the earlier work of Harrison and King in which relations for mutual and self-impedance for identical folded antennas were determined,[15] as well as the driving point impedance of folded dipoles and loops containing series impedances and reactive interconnections.[16]

An area of electromagnetics research is unfolding where the objective is not the enhancement of the transmitting or receiving qualities of a given antenna but the evolvment of ways and means of reducing the signal pickup of extended circuits. In future rocket and ordnance design, as much attention must be paid to the radio-frequency environmental problem as is now given the effects of altitude, shock, temperature, humidity, etc.

Theoretical Considerations

The receiving characteristics of a symmetrically loaded dipole excited by plane waves may be deduced as follows: The antenna is driven by a generator at its center, and the current distribution I(z) found at all points along the dipole by solving the integral equation for the current. The current at the driving point I(o) determines the input admittance Y_a. The reciprocal of Y_a is the driving point impedance Z_a. Knowledge of the current distribution also permits calculation of the radiation field pattern $F\left(\theta, \beta h, \frac{a}{h}\right)$. As a consequence of the Rayleigh-Carson reciprocity theorem, $\beta h_e\left(\theta, \beta h, \frac{a}{h}\right) = \left(F\ \theta, \beta h, \frac{a}{h}\right)$ for a two-terminal radiator. Here, $h_e\left(\theta, \beta h, \frac{a}{h}\right)$ is the effective half-length, β is the radian wave number, h is the half-length of the structure, a is its radius, and θ is the usual spherical coordinate angle measured from the axis of the dipole. If E is the incident electric field strength in the plane of the receiving dipole, the open-circuit voltage at $z = 0$ is $V_{oc} = 2h_eE$. The current in the load impedance Z_L is $I_L = 2h_eE/(Z_a + Z_L)$, and the current with load terminals short-circuited is $I_{sc}(o) = 2h_eE/Z_a$.

It is apparent that if the receiving properties of an asymmetrically loaded dipole are desired, it is necessary to obtain a completely general expression for the current distribution for arbitrary generator position, so that the impedance and effective length of the structure may be obtained, referred to the terminal location. Evidentally, moving the generator alters both the current distribution and field pattern. While in principle the receiving properties of an antenna may be deduced from an accurate knowledge of the current distribution when the antenna is used for transmission, the writer is of the opinion that in some cases, especially for asymmetrically loaded folded dipoles, it is easier to work directly with the integral equations that apply to the structure when excited by an incident plane wave, than to determine the impedance and the effective length from the radiation field pattern utilizing the reciprocity theorem.

A folded receiving antenna consisting of two conductors of radii, a_1 and a_2, and total length $2h$, connected to equal impedances Z_L at the ends, is shown in Figure 1. The structure lies in the yz plane, and the wires are parallel to the z-axis. The axis of conductor 1 (of radius a_1) is located at $x = o$, $y = \frac{b}{2}$, and $-h \leq z \leq h$. The axis of conductor 2 (of radius a_2) is located at $x = o$, $y = -\frac{b}{2}$, and $-h \leq z \leq h$. For simplicity it is assumed that the incident electric field is linearly polarized parallel to the z-axis and arrives from the distant source at the azimuth angle Φ, measured from the positive x-axis. It is further assumed that the structure is so proportioned that the following inequalities apply: $a_1 << h$, $a_2 << h$, $(a_1 + a_2) < b$, $(\beta b)^2 << 1$.

The circuit of Figure 1 approximates a rocket of height h and radius a_1, with umbilical cable of length h and radius a_2 attached, over a large perfectly conducting plane. It is assumed that there is a gap in the shield of the umbilical cable at the point of attachment to the rocket. The voltage developed across this gap by action of the incident field excites currents in the wires surrounded by the shield. The "equivalent impedance" of the internal circuitry is represented by the lumped loading impedance Z_L.

The analysis begins with the equations[17]*

$$J_d(z) + I_1(z)r_{s1} + I_2(z)r_b = -j\frac{4\pi}{\zeta}\left\{C_1 \cos \beta z + U_1\right\} \tag{1}$$

$$J_d(z) + I_1(z)r_b + I_2(z)r_{s2} = -j\frac{4\pi}{\zeta}\left\{C_2 \cos \beta z + U_2\right\} \tag{2}$$

where (1) and (2) apply to conductors 1 and 2, respectively. The definitions of terms follow.

$$J_d(z) = \int_{-h}^{h} I_T(z')K_d(z, z')\,dz' \tag{3}$$

$$I_T(z) = I_1(z) + I_2(z)\,;\ I_T(\pm h) = 0 \tag{4}$$

$I_1(z)$ and $I_2(z)$ are the currents along conductors 1 and 2, respectively.

$$K_d(z, z') = \exp(-j\beta R_d)/R_d \tag{5}$$

---

*Reference 16, Equation 18, p. 174.

$$R_d = \sqrt{(z - z')^2 + d^2} \tag{6}$$

$$r_{a1} = 2 \ln \frac{d}{a_1} \tag{7}$$

$$r_{a2} = 2 \ln \frac{d}{a_2} \tag{8}$$

$$r_b = 2 \ln \frac{d}{b} \tag{9}$$

$\zeta = 120\pi$ ohms

C_1 and C_2 are constants of integration

$$U_1 = Ue^{j \frac{\beta h}{2} \sin \phi} \tag{10}$$

$$U_2 = Ue^{-j \frac{\beta h}{2} \sin \phi} \tag{11}$$

$$U = -\frac{V}{\beta} \tag{12}$$

Multiplying (2) by a parameter m, and adding it to (1) gives

$$J_d(z) + I_1(z)\left[\frac{r_{a1} + mr_b}{m+1}\right] + I_2(z)\left[\frac{r_b - r_{a1} + m(r_{a2} - r_b)}{m+1}\right] =$$

$$-j \frac{4\pi}{\zeta}\left[\frac{(C_1 + mC_2)}{m+1} \cos \beta z + \frac{(U_1 + mU_2)}{m+1}\right] \tag{13}$$

This expression may be reduced to the integral equation for the current along an unloaded solid conductor receiving dipole of length 2h and radius d by setting the coefficients of $I_1(z)$ and $I_2(z)$ equal to zero.

Thus,

$$r_{a1} + mr_b = 0 \tag{14}$$

$$r_b - r_{a1} + m(r_{a2} - r_b) = 0 \tag{15}$$

It follows that that

$$d = b^{\frac{1}{2}}(a_1 a_2)^{\frac{1}{2}} e^{\frac{1}{2}p} \tag{16}$$

where

$$p = \frac{\left(\ln \frac{a_1}{a_2}\right)^2}{4 \ln \frac{b^2}{a_1 a_2}} \tag{17}$$

and

$$m = \frac{\ln \frac{b}{a_1}}{\ln \frac{b}{a_2}} \tag{18}$$

The antenna equation (13) now takes the form

$$J_d(z) = -j\frac{4\pi}{\zeta}\left[C_d \cos \beta z + U_d\right] \tag{19}$$

where C_d is evaluated from the boundary condition $I_T(\pm h) = 0$, and the source function U_d is given by

$$U_d = \frac{U_1 + mU_2}{m+1} = -\frac{E}{\beta}\left[\frac{\ln \frac{b}{a_2} e^{j\frac{\beta b}{2}\sin\phi} + \ln \frac{b}{a_1} e^{-j\frac{\beta b}{2}\sin\phi}}{\ln \frac{b^2}{a_1 a_2}}\right] \tag{20}$$

Because $(\beta b)^2 << 1$, it is clear that $U_d \approx U = -\frac{E}{\beta}$.

Note that (19) is valid only for an electric field directed tangential to the wires.

$I_T(z)$ is available from the work of King,[10] and is considered known for the purposes of this paper. If only the current $I_T(0)$ is of interest, it may be obtained from the formula

$$I_T(0) = \frac{2h_e E}{Z_e} \tag{21}$$

where the effective length $2h_e$ is obtained (by application of the reciprocity theorem) from the radiation field pattern of a dipole of length 2h and radius d, and Z_e is the impedance of the same dipole.

The transmission line equation

$$I_1(z) = I_T(z)\left[\frac{\ln \frac{b}{a_2}}{\ln \frac{b^2}{a_1 a_2}}\right] - \frac{1}{Z_c}\left[(C_1 - C_2)\cos \beta z + j2U \sin\left(\frac{\beta b}{2}\sin\phi\right)\right] \tag{22}$$

is obtained, fundamentally, by subtracting (2) from (1). Here Z_c is the characteristic impedance of the structure, given by

$$Z_c = 60 \ln \frac{b^2}{a_1 a_2} \tag{23}$$

Alternative forms of (30) are

$$I_1(h) = 2U \sin\left(\frac{\beta b}{2} \sin\Phi\right) \left\{ \frac{\sin \beta h}{Z_c \sin \beta h - jZ_L \cos \beta h} \right\} \tag{32}$$

and

$$I_1(h) = j2U \sin\left(\frac{\beta b}{2} \sin\Phi\right) \left\{ \frac{\tan \beta h}{R_L + jX_L + jZ_e \tan \beta h} \right\} \tag{33}$$

Clearly from (32) $I_1(h) = 0$ when $\beta h = \pi$, $Z_L \neq 0$. Also, when $\beta h = \frac{\pi}{2}$,

$$I_1(h) = \frac{2U}{Z_e} \sin\left(\frac{\beta b}{2} \sin\Phi\right) \approx - \frac{Eb \sin\Phi}{Z_e} \tag{34}$$

From (33) it is seen that whenever

$$Z_e \tan \beta h >> \left| R_L + jX_L \right| \tag{35}$$

(34) holds.

Readers are reminded that in the development of these equations radiation from the structure (in the transmission line mode) is ignored, transmission line losses are neglected, and no account is taken of proximity effect.

As a numerical illustration, let the current input to the nose of a rocket from a shielded umbilical cable be estimated under the conditions stated below. The structural dimensions are:

$a_1 = 1.219$ m
$a_2 = 0.743$ m
$b = 3.639$ m
$h = 16.76$ m

The incident plane wave E is vertically polarized and has a magnitude of 3 volts/m. The frequency is $f = 1.85$ mc/sec, or $\lambda = 162.2$ m. The shield is continuous, so that $Z_L \approx 0$. It is assumed that this system can be represented satisfactorily by a two-conductor folded monopole over a perfectly conducting earth.

The characteristic impedance is

$$Z_e = 60 \ln \frac{b^2}{a_1 a_2} = 160.9 \text{ ohms}$$

Since $\beta h = \frac{2\pi}{\lambda} h = 0.6492$, $\tan \beta h = 0.7566$. It follows that $Z_e \tan \beta h >> \left| Z_L \right|$ since Z_L is assumed to be small. Hence the formula

$$\left| I_1(h) \right| = \frac{Eb \sin\Phi}{Z_e}$$

is applicable. Substituting numbers in this formula gives

$$\left|I_1(h)\right| = \frac{3 \times 3.639}{160.9} = 67.85 \text{ ma}$$

if $\Phi = \frac{\pi}{2}$ radians.

If laboratory experiments reveal that considerably more than 100-ma nose current is required at 1.85 mc/sec before the most sensitive EED current exceeds the safe level, one may conclude in this instance that no hazards problem exists. As mentioned before, the firing circuits are energized by radio-frequency leaks in the umbilical cable shield and in the rocket skin when $Z_L \simeq 0$.

It is to be emphasized that the solution of this problem is only approximate. The radius of the "equivalent" dipole is d = 1.904 m, so that $\Omega = 2 \ln\left(\frac{2h}{d}\right) = 5.736$. Accuracy may be obtained from existing methods of cylindrical antenna analysis for $\Omega \geq 7$.

If a break exists in the umbilical cable shield at the point it enters the missile, $Z_L \neq 0$. This impedance, which appears across the gap in the shields, is a manifestation of the loading effect of the wires entering the missile from the umbilical cable. Z_L may be determined as follows: Measure the gap impedance Z_G (shield-to-shield). This impedance is the parallel combination of Z_L and Z_T. Z_T is the impedance of a transmission line of length h and characteristic impedance Z_e (given by (23)) terminated in a short circuit (the ground plane). Then,

$$Z_L = \frac{Z_G Z_T}{Z_T - Z_G}. \tag{36}$$

The true current on the shield of the umbilical cable at the point of attachment to the missile is then computed from (30) using (36).

It is important to observe that a laboratory-determined relation between nose-cone input current and EED current (when the umbilical cable is disconnected) is no longer valid when $Z_L \neq 0$, because the circuits in the missile are excited by the gap voltage. Ordinarily the currents flowing in the internal wiring induce larger currents in the firing circuits than the missile skin current, even when there are open access doors and anodized peripheral butts between sections. Indeed, it is possible that more correct results may be obtained by disregarding the shields and treating the internal wiring as a lits cable, in the form of a folded monopole. The total cable current is obtained theoretically for the specified RF environment. The RF hazards to ordnance problem is solved if the relation between the most sensitive EED current and total cable current has been obtained experimentally.

Discussion

A few remarks might be made relating to the use of (31) in solving conventional two-conductor folded receiving antenna problems. If conductor 1 is broken at point $z = \ell$, a voltage $V_{oc} = I_{se}(\ell) Z(\ell)$ will appear across the break. Here $I_{se}(\ell)$ is the short circuit current, and may be obtained from (31)

with $z = \ell$ and $Z_L = 0$. $Z(\ell)$ is the driving point impedance of the structure, looking in at the break. For a two-conductor antenna, $Z(\ell)$ may be obtained easily by superposition,[19] if the number of conductors $N>2$, more advanced techniques must be employed, as a general rule. $Z(\ell)$ depends on the impedance of an asymmetrical dipole and of two transmission-line sections in series with short-circuited terminations. The sections of the equivalent dipole are of radius d, and the transmission lines are of length $h + \ell$ and $h - \ell$.

The equivalent circuit of the receiving antenna consists of V_{oe} driving $Z(\ell)$ connected in series with the load impedance Z_L used.

When the electric field is directed tangential to the wires of the folded antenna only currents of even symmetry are excited. When the field is tilted with respect to the axes of the conductors, currents of even and odd symmetry flow. If the load is located in the middle of one of the conductors, the voltage drop across the load impedance is due only to current of even symmetry. (Note that this current is a function of the angle of wave tilt.) For a displaced load, i.e., an asymmetrically loaded structure (assuming nonparallel incidence of the field), currents of both symmetries flow in the load. These currents may be found individually by applying the integral equation technique. The total currents is then obtained by superposition.

Conclusions

Antenna theory is useful for solving problems relating to radio-frequency hazards to ordnance. In this paper a theory of folded conductor structures, as receiving antennas, is developed and applied to estimate the current in the shield of an umbilical cable at the point of attachment to a rocket on the launching pad. An experimentally obtained correlation between input current to the rocket and electroexplosive current permits solution of this RF hazards problem.

REFERENCES

1. Lippman, B. A., Electromagnetic Signal from Nuclear Explosions, presented at URSI Spring 1962 Meeting at Georgetown University, Washington, D.C.

2. Suydam, B. R., Electromagnetic Signal from a Bomb Burst in Vacuo, Los Alamos Scientific Laboratory Report LAMS-2624 of November 3, 1961.

3. Kompaneets, A. S., "Radio Emission from an Atomic Explosion," Soviet Physics JETP, June 1959, Vol. 35(8), pp 1076-1080.

4. Karzas, W. J., and Latter, R., Electromagnetic Radiation from a Nuclear Explosion in Space, Rand-RM-2849-AFT, October 1961.

5. Karzas, W. J., The Electromagnetic Signal Due to the Exclusion of the Earth's Magnetic Field by Nuclear Explosions, Rand-RM-2890-PR, December 1961.

6. Potter, R. R., Weapon Design Requirements to Preclude Hazards from Environmental Electromagnetic Fields, U. S. Naval Weapons Laboratory (Dahlgren, Va.), Technical Memorandum No. W/2-61 of January 1961.

7. Harriaon, C. W., Jr., and King, R. W. P., "Response of a Loaded Electric Dipole in an Imperfectly Conducting Cylinder of Finite Length," Journal of Research of the National Bureau of Standards - D, Radio Propagation, May-June 1960, Vol. 64D, No. 3, pp 289-293.

8. King, R. W. P., and Harrison, C. W., Jr., "Cylindrical Shields," IRE Transactions on Antennas and Propagation, March 1961, Vol. AP-9, No. 2, pp 186-170.

9. Harrison, C. W., Jr., "Radio Frequency Shielding of Cables," Journal of the American Society of Naval Engineers, August 1961, Vol. 73, No. 3, pp 529-533.

10. Harrison, C. W., Jr., and Denton, D. H., Jr., Receiving Characteristics of Quasi-Shielded Antennas, Sandia Corporation Technical Memorandum 396-58(14) October 15, 1958.

11. Harrison, C. W., Jr., Radio Frequency Hazards to Ordnance Materials--Shielding Effect of a Circular Grating of Finite Length, Sandia Corporation Internal Memorandum, July 21, 1961.

12. Dickinson, W. T., A Method to Determine Electromagnetic Coupling to Ordnance Devices Aboard Ships, Technical Report No. 5456, June 15, 1961, Jansky & Bailey, Inc., Alexandria, Va. See also Dickinson, W. T. de Pian, Louis, and Glock, R., Jr., Electromagnetic Coupling to Ordnance Systems, Technical Report covering Phase I, June 15, 1960, Jansky & Bailey, Inc.

13. King, L. V., "Electromagnetic Shielding at Radio Frequencies," Philosophical Magazine and Journal of Science, February 1933, Vol. 15, No. 97, pp 201-223. See also H. Kaden, "Die Elektromagnetische Schirmung in der Fernmelde and Hockfrequenztechnik," (Springer-Verlag, 1950).

14. Harrison, C. W., Jr., Folded Wire Structures as Receiving Antennas, Sandia Corporation Technical Memorandum 253-58(14), June 18, 1958.

15. Harrison, C. W., Jr., and King, R. W. P., "Theory of Coupled Folded Antennas," IRE Transactions on Antennas and Propagation, March 1960, Vol. AP-8, No. 2, pp 131-135.

16. Harrison, C. W., Jr., and King, R. W. P., "Folded Dipoles and Loops," IRE Transactions on Antennas and Propagation, March 1961, Vol. AP-9, No. 2, pp 171-187.

17. Harrison, C. W., Jr., "Antenna Coupling Error in Direction Finders," Journal of Research of the National Bureau of Standards - D. Radio Propagation, July-August 1961, Vol. 65D, No. 4, pp 363-369, Equations (1)-(2).

18. King, R. W. P., Theory of Linear Antennas, Chapter 4, Harvard University Press, 1956.

19. King, R. W. P., Mimno, H. R., and Wing, A. H., Transmission Lines, Antennas, and Wave Guides, Section 45, Chapter 2, p. 224, McGraw-Hill Book Co., Inc., 1945.

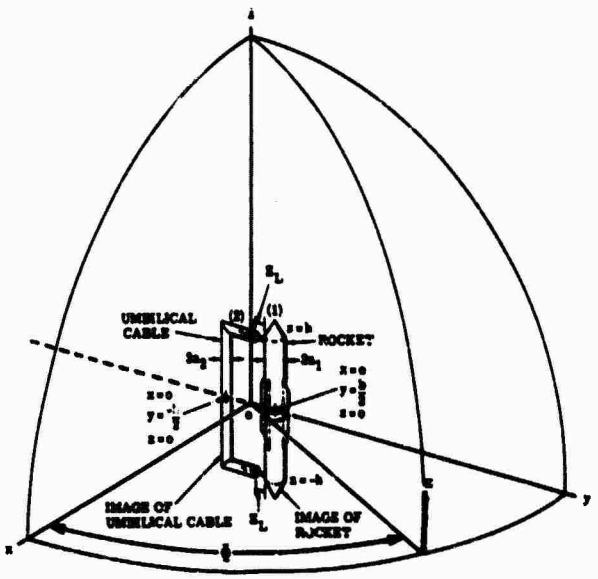

Figure 1. Rocket with attached umbilical cable, and image

11 RADIO-FREQUENCY LEAKAGE INTO MISSILES

by

R. H. Duncan
Research Center, New Mexico State University
University Park, New Mexico

and

C. W. Harrison, Jr.
Member of the Technical Staff
Sandia Corporation
Albuquerque, New Mexico

1. Introduction

There are at least three mechanisms by which electromagnetic radiation can leak into regions surrounded by metallic shields. At low frequencies an imperfectly conducting shield may fail to isolate the shielded region from an externally applied field. King and Harrison (1961) have considered this case in some detail. A second possibility is that the shield may be incomplete. For example, there is a functional requirement for openings (such as access doors) in the outer shell of a missile. If the missile is exposed to the field of a nearby radar or communications antenna, the resulting level of interference with missile circuitry may be objectionable. The circuitry may be that associated with sensitive electroexplosive devices used to initiate missile responses upon command. It is obvious that inadvertent interference with these circuits may affect ordnance reliability. However, many of our comments are applicable to other problems in radio-frequency interference and to equipment other than missiles. A third possibility is that radio-frequency energy will be carried into the missile along umbilical cables. This case is not being considered in this paper.

It must be taken for granted that efforts toward better design of potentially unreliable circuits will continue. Radio-frequency filters, sealed components, coded input schemes, and other techniques will all undoubtedly play a larger role in future design. However, at any given time it will be necessary to adequately assess the level of interference and to know the margin of safety. Designs which are presently adequate may become inadequate if radar power continues to increase.

It is also important to make the point that the art of predicting induced currents must be refined and made accurate. Underestimation of danger leads to a false sense of security. Overestimation may lead to ridiculous precautionary procedures. One occasionally observes "Turn Off Two-Way Radio" signs in the vicinity of highway or industrial projects in which explosives are used. If the same policy were invoked at Cape Canaveral, the countdown procedure for launching a rocket could not begin until all nearby sources of radio frequency were turned off. Excessive caution can be a source of petty annoyance, or it can interfere with the operation of a complicated system.

At first glance the complexity of the problem seems overwhelming. Exact analysis of the environment and internal details of a missile from the point of view of electromagnetic theory is certainly impossible. If one shuns analysis and electrical measurements entirely, the only kind of testing possible is to illuminate the missile with electromagnetic energy and simply observe whether or not the electroexplosive devices (hereafter referred to by the short and popular name, squibs) are affected. The test should be performed in a realistic environment with the illumination being provided by the actual sources which may be suspect. (Of course, one must alter internal details in such a way that an exploding squib does not actually initiate action by the missile.) This test is simple and meaningful if a few squibs are actually exploded. Then one knows that certain circuits must be redesigned, or that the use of less

sensitive squibs is indicated. The problem is considerably magnified if the firing of a squib is a rare event. The probability of the type of accident being considered here may be small but nevertheless intolerable. To clearly establish a probability, p, by experimental means requires more than p^{-1} tests. We are lead to reject the purely probabilistic model because it requires an excessive amount of testing which should be repeated for a large variety of missile environments. A last point against this approach is that it provides no knowledge regarding the margin of safety. It may be practically impossible to accidentally fire the squibs in a presently existing design which will be quite unacceptable in the near future.

The next step in evolving a model is to consider the measurement of the currents induced in the squib circuits. Separate bench tests of the squibs can be made. It is a simple matter now to guarantee that all squibs in a given sample are fired and to estimate the mean, variance, and probability distribution of the required firing current. Conclusions are then reached by comparing these data with the currents induced in the missile circuits with the missile in a realistic environment.

We shall not dwell on the details of setting confidence limits and the somewhat subjective problem of safety recommendations as we intend to concentrate on deterministic models for describing the induced currents. The reader should be warned that another important aspect of the problem will not be treated here. We have not made any distinction between transient and steady-state situations. It is well known that a squib can be subjected to a large current for a short period of time without firing. However, the construction of a theoretical model for the steady-state case is a necessary prelude to the transient solution. Finally, it may seem that we have relegated statistical aspects of the problem to consideration of quality-control data on squibs. We are not ruling out error and variance analysis of the field measurements of induced currents. It should be obvious that these measurements can be carried out on a sample of several missiles and it would be prolix to dwell on this point.

Leaving experimental refinements aside, further development of a meaningful test program must lead toward an understanding of the induced currents in terms of the interaction of the missile with its electromagnetic environment. This part of the problem is the most difficult because of the infinite variety of possible complicated situations. However, in spite of the complications, a great deal of conceptually useful information can be gleaned from careful application of physical principles. The next section of this paper provides a brief review and critique of various attempts to organize induced squib current data. Then we turn attention to the solution of a representative idealized boundary value problem. Idealized problems have certain features which would survive in complicated problems if they could be explicitly solved. Realizing this, we propose a rather general semiempirical approach to the problem in the final part of the paper.

2. Review of Previous Work

In this section we shall attempt to present a brief review of those ideas and experiments which have been used in attempts to obtain a satisfactory model for explaining induced squib currents. Many technical details are omitted. In some cases, variations or refinements of the methods exist and we have taken the liberty of giving only bare essentials. We have included a few general statements regarding experimental data. Actual data have been omitted since most of it is too particular to be relevant to a general discussion.

The approach which we recommend in a later section of this paper has not yet been subjected to experimental tests. The names of the methods in the following outline were coined by the authors for their own convenience.

a. Mutual Impedance Method. This method is based on the well-known fact that the electromagnetic field equations for linear homogeneous media can be manipulated to provide an equivalent circuit description of the interaction between sources and sinks of electromagnetic energy. As a simple example, let the current and voltage at the terminals of an antenna be I_1, V_1, respectively. Denote similar quantities at a pair of squib terminals inside a nearby missile by I_2, V_2. Then,

$$\begin{pmatrix} I_1 \\ I_2 \end{pmatrix} = \begin{pmatrix} Y_{11} & Y_{12} \\ Y_{12} & Y_{22} \end{pmatrix} \begin{pmatrix} V_1 \\ V_2 \end{pmatrix}. \tag{2.1}$$

If the squib impedance is Z_L,

$$I_2 = \frac{Y_{12} V_1}{1 - Y_{22} Z_L}. \tag{2.2}$$

The attractive simplicity of (2.2) leads to the deception that progress can be made by measuring the admittance coefficient Y_{12}. (The diagonal elements, Y_{11} and Y_{22}, are not difficult to measure.) Admittances are dependent on position and environmental details. Off diagonal terms in an admittance matrix are notoriously difficult to estimate theoretically in all but the simplest problems. One would be just as well off to move the missile about and directly catalog squib current as a function of position and orientation of the missile. Either procedure is likely to generate coffers of unexplained data. There may be special situations or aspects of the problem in which mutual impedance concepts can be used to advantage. However, we do not favor this method as the basis for an over-all attack.

b. Transfer Function Method. The method consists of taking data on squib current and field intensity to define a transfer function

$$Y(f) = \left(\frac{I_s}{\bar{E}}\right)_{\text{measured}}, \tag{2.3}$$

where f is the frequency of the illuminating field, and E is the field intensity for a given polarization. Measurements of $\bar{E}$ are usually made at a single point in the field with the missile removed. It is then supposed that if the missile is immersed in a field of different magnitude the squib current will be $I_s = Y(f)E$. The method has both a fallacy and a correct limit. The fallacy is that a point measurement of $\bar{E}$ is not always adequate. Rather, the distribution of $\bar{E}$ determines the interior response of an object placed in the field. However, except in the immediate vicinity of sharp points and edges in the environment, an electromagnetic field $(\bar{E}, \bar{H})$ does not vary much over distances short compared to a wavelength. Heuristically, the method should provide an adequate description of the interior response of objects which are uniformly illuminated. If sharp points and edges are an appreciable fraction of a wavelength away from the object, $Y(f)$ should be insensitive to environmental details.

c. Radiation Pattern Method.* This method is based on the realization that if radiation can leak into a missile it can also certainly leak out. The squib is removed and a transmitter is attached to the circuit terminals. The resulting radiation pattern, $G(\theta, \phi)$, is then measured. (Absolute field intensity measurements must be made; the usual relative pattern will not serve.) Now the reciprocity theorem can be invoked to calculate squib current for the case of plane-wave illumination. Omitting impedance mismatch factors which are required in practice and assuming an incident plane wave of intensity S, the absorbed power is given by

$$P_s = SA(\theta, \phi),$$

where

$$A(\theta, \phi) = \frac{\lambda^2}{4\pi} G(\theta, \phi). \qquad (2.4)$$

The relation between $A(\theta, \phi)$ and $G(\theta, \phi)$ shown in (2.4) is established in many texts for efficient antennas. It can also be shown to hold for inefficient antennas (Appendix A). It is necessary to make this point since much of the energy injected into the squib circuit in the transmitting mode may be absorbed inside the missile.

Difficulties with the model can be attributed to the fact that in a complicated environment, the external transmitted field can not be interpreted as a radiation far field and the illuminating field will rarely be a plane wave. From a fundamental point of view, improvement of the approach will have to involve a study of the interaction of antennas with near fields and surface waves, the latter because many of the measurements must, of necessity, be carried out over a partially conducting ground. Finally, the model is undoubtedly valid for application to inflight interference with circuits inside missiles and aircraft.

d. Antenna Equivalent Circuit Method.† This method is distinct from those discussed above in that it is entirely theoretical; no measurements are involved. It is also the most difficult to discuss briefly, involving, as it does, several intricate papers dealing with explicit problems. Basically, the approach is to find the parameters for the Thévenin equivalent circuit for a receiving antenna, namely: V_{oc}, the open circuit voltage, and Z_T, the transmitting impedance. If these parameters are known and a load impedance is presumed to be part of a simple circuit connected across the leak (antenna terminals), the load current can be readily calculated. The procedure is likely to overestimate the current delivered to squibs in practical situations. Practical circuits are often located at a considerable distance from the actual leak; interfering energy propagates in some complicated way from the leak to the circuit location. This process inevitably involves some attenuation. Focusing effects in the interior are not anticipated in the wavelength region of interest.

Theory of this type has been successful in order-of-magnitude calculations. It provides nominal agreement with the slope of some experimental curves of squib current versus frequency. Both linear antenna theory and slot antenna theory have been used in particular situations. In one application folded

*G. E. Gaios (Ordnance Mission, White Sands Missile Range), unpublished information.

†C. W. Harrison, Jr., (Sandia Corporation) unpublished information.

dipole theory is used to estimate the change in the squib current caused by attaching a control cable to a missile, assuming that the interior response of the missile without the cable is known.

This approach can be shown to be an approximation to the more general method to be described later in the paper.

3. Scattering by Slotted Cylinders

It has been pointed out that radio-frequency interference problems are too complicated to allow detailed theoretical solutions. The role of theory in this case is to provide organizing concepts as a basis for economical and meaningful experimentation.

The main problem we wish to present is that of scattering of a cylindrical wave by an infinite slotted cylinder of infinite conductivity. Coordinates for the problem are the conventional (ρ, ϕ, z) circular cylinder coordinates. The slot is totally circumferential in the region $|z| < w$ at $\rho = a$, the radius of the cylinder. The choice of an infinite cylinder need not be a source of concern since it can be shown that the effective length and, hence, the open circuit voltage, of an infinite cylindrical receiving antenna is finite (Appendix B). Also, we will discuss modification of the treatment to obtain an approximate solution for a finite cylinder. Cylindrical wave excitation enables us to avoid the complications of asymmetry in the azimuthal coordinate during a preliminary investigation of the problem. This feature of the idealized problem can also be revised. In what follows, those symbols which are used without explicit definition are conventional in the literature of electromagnetic theory.

We assume, for simplicity, that the electric vector of the incoming field is parallel to the cylinder axis. Time dependence of $\exp(j\omega t)$ is assumed, but suppressed. Consistant with this latter assumption, $H_0^{(1)}(k\rho)$ and $H_0^{(2)}(k\rho)$ are chosen to represent the incoming and reflected waves, respectively. In addition to these waves, there will be a diffracted wave because of the slot. The electric field in the slot will be an unknown function, $f(z)$. It is convenient to redefine this function as $Vf_0(z)$ where $f_0(z)$ is normalized to unity on the interval $|z| < w$. The electric field vanishes at the surface of the cylinder everywhere outside the slot. We also normalize the incident field to E_0 volts per meter at the surface of the cylinder. If $F_0(\alpha)$ is the Fourier transform of $f_0(z)$,

$$E_s^0(\rho, z) = E_0\left[\frac{H_0^{(1)}(k\rho)}{H_0^{(1)}(ka)} - \frac{H_0^{(2)}(k\rho)}{H_0^{(2)}(ka)}\right] + \frac{V}{2\pi}\int_{-\infty}^{+\infty} \frac{H_0^{(2)}(\beta\rho)}{H_0^{(2)}(\beta a)} F_0(\alpha) e^{-j\alpha z}\, d\alpha \qquad (3.1)$$

represents the field outside the cylinder and satisfies the boundary conditions at $\rho = a$ (Stratton, 1941). Similarly

$$E_s^i(\rho, z) = \frac{V}{2\pi}\int_{-\infty}^{+\infty} \frac{J_0(\beta\rho)}{J_0(\beta a)} F_0(\alpha) e^{-j\alpha z}\, d\alpha \qquad (3.2)$$

represents the field inside the cylinder and satisfies the boundary conditions at $\rho = a$.

In the above expressions we have defined β as follows:

$$\beta^2 = k^2 - \alpha^2;$$

$$\text{ph}\beta = 0, \ |\alpha| < k; \tag{3.3}$$

$$\text{ph}\beta = -\pi/2, \ |\alpha| > k.$$

The contour of integration is along the real α axis with downward and upward indentations at $\alpha = -k$ and $\alpha = +k$, respectively.

Expressions (3.1) and (3.2) are tautologically equal at $\rho = a$. A second condition is required if the solution is to yield any information. We require continuity of H_ϕ through the slot. Modes of the magnetic field can be found by applying the operator

$$-\frac{jk^2}{\mu\omega(k^2 - \alpha^2)} \frac{\partial}{\partial \rho} \tag{3.4}$$

to each mode of E_z with the understanding that $\alpha = 0$ for the incident and reflected Hankel functions. The continuity condition on H_ϕ results in

$$\frac{4E_0}{\pi Z_0 K D(K)} - \frac{V}{2\pi a} I_w^0(z) = \frac{V}{2\pi a} I_w^i(z), \tag{3.5}$$

where we have abbreviated by letting

$$ka = K, \ Z_0 = \sqrt{\mu/\epsilon},$$

$$D(K) = J_0^2(K) + Y_0^2(K),$$

$$I_w^0(z) = \frac{K}{Z_0} \int_{-\infty}^{+\infty} \frac{H_1^{(2)}(\beta a)}{j\beta H_0(\beta a)} F_0(\alpha) e^{-j\alpha z} \, d\alpha, \tag{3.6}$$

$$I_w^i(z) = \frac{K}{Z_0} \int_{-\infty}^{+\infty} \frac{jJ_1(\beta a)}{\beta J_0(\beta a)} F_0(\alpha) e^{-j\alpha z} \, d\alpha. \tag{3.7}$$

Equation (3.5) is an integral equation on the interval $|z| < w$ for the function $f_0(z)$. The first term is the surface current density on a cylinder in a scattering problem for a cylinder with no slot. $I_w^0(z)$ and $I_w^i(z)$ are the total outer and inner currents on a transmitting antenna with unit voltage impressed across the slot (Duncan, 1962)* by means of an idealized generator. In the slot these quantities are not actually currents but no ambiguity results from using the same functional notation on the entire z domain.

---

* A reference manual of data for the infinite cylindrical antenna is in preparation.

We shall not attempt a rigorous solution of the integral equation. A convenient procedure is to assume a form for $f_0(z)$, require that (3.5) be satisfied at $z = 0$, and solve for the parameter V. We obtain

$$V = \frac{8E_0 a}{Z_0 KD(K)} \frac{1}{I_w^0(0) + I_w^1(0)} . \tag{3.8}$$

A convenient choice for $f_0(z)$ is

$$f_0(z) = \frac{1}{2W}, \quad |z| < w,$$
$$= 0, \text{ otherwise;} \tag{3.9}$$

with

$$F_0(\alpha) = \sin \alpha w / \alpha w .$$

A somewhat better choice (Wait, 1959) which satisfies appropriate edge conditions near $z = \pm w$ is

$$f_0(z) = \frac{1}{\pi \sqrt{w^2 - z^2}}, \quad |z| < w$$
$$= 0, \text{ otherwise;} \tag{3.10}$$

with

$$F_0(\alpha) = J_0(\alpha w) .$$

Final numerical results are not very sensitive to the choice of $f_0(z)$; we use (3.9) in the analysis.

We now turn attention to the evaluation of $I_w^0(0)$. If we set $F_0(\alpha) = 1$ in (3.6) we obtain

$$I_\delta^0(z) = \frac{\chi}{Z_0} \int_{-\infty}^{+\infty} \frac{H_1(\beta a)}{j\beta H_0(\beta a)} e^{-j\alpha z} d\alpha, \tag{3.11}$$

the outer current on a δ-gap transmitting antenna for which the boundary value of E_z is given by $Ez = -\delta(z)$. From the form of (3.6),

$$I_w^0(z) = \int_{-\infty}^{+\infty} I_\delta^0(z_0) f(z - z_0) dz_0 . \tag{3.12}$$

Since all of the functions involved are even and $f_0(z)$ vanishes for $z > w$,

$$I_w^0(0) = 2 \int_0^w I_\delta^0(z_0) f(z_0) dz_0 . \tag{3.13}$$

Thus, the net effect of the window function is to require a smoothed version of the current distribution for a δ-gap model. The latter has a short-range logarithmic singularity at the origin. If w exceeds the range of the singularity, z_s, and is not too large, the value of $I_w^0(z)$ is not very sensitive to the choice

of $f_0(z)$, it being understood, of course, that $f_0(z)$ must be an integrable function. Since $f_0(z)$ is not actually known in the present problem we shall obtain $I_w^0(0)$ by the graphical smoothing procedure which also serves to define z_s. Letting Y_s represent the admittance corresponding to the smoothed δ-gap current function,

$$V \simeq \frac{8E_0 a}{Z_0 KD(K)} \left[\frac{1}{Y_s + I_w^i(0)} \right], \quad z_s < w << \lambda. \tag{3.14}$$

This approximation is incorrect in the limit of very narrow slots. If $w < z_s$, the logarithmic nature of $I_\delta(z)$ must be taken into account explicitly. It is known that for small z

$$I_\delta^0(z) + I_\delta^i(z) \approx -j \frac{4K}{Z_0} \ln kz. \tag{3.15}$$

When this is averaged over the window function,

$$I_w^0(0) + I_w^i(0) \approx -j \frac{4K}{Z_0} \ln kw, \quad w < z_s. \tag{3.16}$$

Preliminary to evaluating $I_w^i(0)$ consider the interior current for the δ-gap model,

$$I_\delta^i(z) = \frac{K}{Z_0} \int_{-\infty}^{+\infty} \frac{jJ_1(\beta a)}{\beta J_0(\beta a)} e^{-j\alpha z} d\alpha. \tag{3.17}$$

The integrand of (3.17) is continuous across the branch cut. Poles of the integrand are at $\beta_n a = \xi_n$, where (ξ_n) are the ordered zeros of $J_0(\chi)$. If the tube is below cutoff, all poles are on the imaginary axis at

$$\alpha_n = \pm \frac{j}{a} \sqrt{\xi_n^2 - K^2} = \pm \frac{j\gamma_n}{a}. \tag{3.18}$$

If K is greater than some ξ_n, there will be propagating modes corresponding to poles along the real axis in the interval $-k < \alpha < +k$. We define downward indentations at the poles in the interval $-k < \alpha < 0$, upward indentations for those in the interval $0 < \alpha < k$. The contour may be closed in the lower or upper half-planes corresponding to $z > 0$ and $z < 0$, respectively. The result is

$$I_\delta^i(z) = j \frac{2\pi K}{Z_0} \sum_{n=1}^{n=\infty} \frac{\exp\left(-\frac{\gamma_n |z|}{a}\right)}{\sqrt{\xi_n^2 - K^2}}. \tag{3.19}$$

From (3.7) and (3.11) we have

$$I_w^i(0) = 2 \int_0^w I_\delta^i(z_0) f(z_0) dz_0. \tag{3.20}$$

From (3.19) and (3.20), $I_w^i(0)$ is given by

$$I_w^i(0) = j\frac{2\pi Ka}{Z_0 w}\sum_{n=0}^{n=\infty}\frac{1-e^{-\frac{\gamma_n w}{a}}}{\left(\xi_n^2-K^2\right)}. \tag{3.21}$$

The rate of convergence of (3.21) can be improved. First use the Fourier inversion theorem to obtain

$$\frac{K}{Z_0}\frac{jJ_1(\beta a)}{\beta J_0(\beta a)} = \frac{1}{2\pi}\int_{-\infty}^{+\infty} I_0^i(z)e^{j\alpha z}dz. \tag{3.22}$$

Then set $\alpha = 0$ in (3.22) to obtain

$$\frac{jKJ_1(K)}{Z_0 kJ_0(K)} = \frac{1}{\pi}\int_0^{\infty} I_0^i(z)dz \tag{3.23}$$

and use (3.19) to calculate the right-hand side of (3.23). The result is the useful identity

$$\frac{J_1(K)}{KJ_0(K)} = \sum_{n=0}^{n=\infty}\frac{2}{\left(\xi_n^2-K^2\right)}. \tag{3.24}$$

This may be combined with (3.21) to give

$$I_w^0(0) = \frac{j\pi Ka}{Z_0 w}\left[\frac{J_1(K)}{KJ_0(K)} - \sum_{n=0}^{n=\infty}\frac{2e^{-\frac{\gamma_n w}{a}}}{\left(\xi_n^2-K^2\right)}\right]. \tag{3.25}$$

The series in (3.25) is now rapidly convergent and convenient for computational purposes except near resonance. If K is nearly equal to some ξ_n, it is only necessary to keep the dominant term in (3.21). The exponential can also be expanded to low order to give

$$I_w^i(0) \approx j\frac{2\pi k}{Z_0}\frac{1}{\sqrt{\xi_t^2-K^2}}. \tag{3.26}$$

Components of the interior field can be computed by the residue theorem from (3.2). The presence of $F_0(\alpha)$ will cause the integral to diverge on the infinite arc used to close the contour unless $|z| > w$ no matter which window function is used. If field components are desired in the region $|z| < w$, they can be computed by convolution of the window function and the residue series for field components in the δ-gap problem just as in the above treatment of $I_w^i(0)$. The results for $|z| > w$ are:

$$E_\rho^i(\rho, z) = \frac{V}{a}\sum_{n=1}^{n=\infty}\frac{\xi_n J_0\left(\xi_n\frac{\rho}{a}\right)F_0(\alpha_n)}{J_1(\xi_n)\sqrt{\xi_n^2-K^2}}e^{-\frac{\gamma_n|z|}{a}}, \tag{3.27}$$

$$H_\phi^i(\rho, z) = j \frac{kV}{Z_0} \sum_{n=1}^{n=\infty} \frac{J_1\left(\xi_n \frac{\rho}{a}\right) F_0(\alpha_n)}{J_1(\xi_n) \sqrt{\xi_n^2 - K^2}} e^{-\frac{\gamma_n |z|}{a}}, \tag{3.28}$$

$$E_\rho^i(\rho, z) = (\pm) \frac{V}{a} \sum_{n=1}^{n=\infty} \frac{J_1\left(\xi_n \frac{\rho}{a}\right) F_0(\alpha_n)}{J_1(\xi_n)} e^{-\frac{\gamma_n |z|}{a}}. \tag{3.29}$$

As a criterion of interior response we calculate the interior skin current density, $\mathcal{J}(z)$, from (3.28) by evaluating $H_\phi(a, z)$. Then,

$$\mathcal{J}(z) = j \frac{kV}{Z_0} \sum_{n=1}^{n=\infty} \frac{F_0(\alpha_n)}{\sqrt{\xi_n^2 - K^2}} e^{-\frac{\gamma_n |z|}{a}}. \tag{3.30}$$

The interior response is finite at resonance in spite of the appearance of (3.30). At resonance, $I_w^i(0)$, as given by (3.26), is much larger than Y_s. The result is that V approaches zero in just the right way to maintain finite fields in the interior. With either window function, $F_0(\alpha_n)$ becomes unity for the resonant term. Keeping only the dominant resonant terms in the expressions for V and $\mathcal{J}(z)$ gives

$$\mathcal{J}_r(z) \simeq \frac{4E_0}{\pi Z_0 KD(K)}, \quad K = \xi_r. \tag{3.31}$$

Note that $\mathcal{J}_r(z)$ does not contain z since $\exp\left(-\frac{\gamma_n |z|}{a}\right)$ becomes unity at resonance. At low frequency the damping factors insure that the field does not penetrate far into the tube. If the frequency is above the first resonant frequency, there will be at least one mode which propagates unattenuated in the z direction. Combination of these notions leads to the suggestive sketch shown in Figure 1 in which the envelope of resonant responses is given by (3.31). Comparison with (3.5) shows that (3.31) is just the outer skin current density in the scattering problem for an object with no slot.

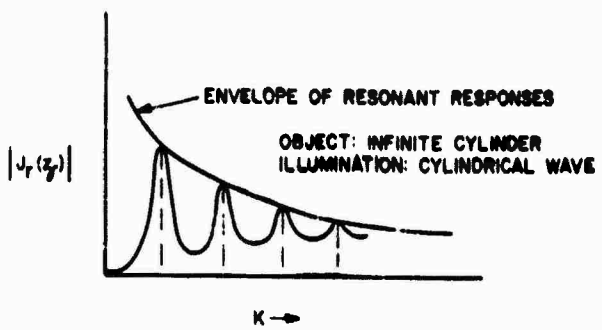

Fig. 1 -- Sketch of interior response versus K

The intimate connection between interior response and the scattering problem for an object with no leaks is a quite general result. Consider the solution of any problem similar to the one above in which an object with a leak is illuminated by a field in which $\overline{E}$ is parallel to the longitudinal axis of the object. Let the distribution of the incident field be entirely arbitrary. Introduce the interior and exterior diffracted fields as perturbations on the scattering problem for the object with no leak, as we have done above. If the leak is small with respect to a wavelength, the phase of the window field is not expected to change appreciably over the window. Introduce an approximate window function, $Vf_0(z, \phi)$. Choose a reasonable form for $f_0(z, \phi)$ and solve for the parameter V, obtaining the analog of (3.14) which contains a factor depending on the scattering problem and a second factor which depends on the interior and exterior admittances when the leak is driven by unit voltage in the transmitting mode. The interior admittance is just the interior skin current density function evaluated at the slot position. Hence, these quantities depend on the interior eigenfunctions and resonant frequencies in precisely the same way. If the problem is not azimuthally symmetric and the object is of finite length, three parameters, one for each dimension, will be required to label the interior eigenfunctions. If the interior is complicated it will not be feasible to find these eigenfunctions explicitly. However, it is sufficient for our purposes to know that they exist in principle. Whatever the nature of the complications, near resonance the terms with resonant denominators dominate the equations analogous to (3.21) and (3.28). If only dominant terms are retained, the resonant denominators cancel, leaving the factor which depends only on the incident and reflected fields evaluated at the slot position,

$$\left|\mathcal{J}_z\right| \simeq \left(H_\phi^{inc} + H_\phi^{ref}\right)_{slot}. \tag{3.32}$$

Using these ideas we can now sketch the kind of behaviour to be expected of the interior response of a missile. For the infinite cylinder, (3.31) is monotonic. However, for a finite object, we can expect that (3.32) will exhibit resonances associated with the length of the object, as shown in Figure 2. The internal resonances exist in principle; in practice they would have to be located experimentally. An interesting possibility is that of accidental coincidence of internal and external resonances leading to an unusually large interior response. Heretofore, unexplained peaks have occurred in experimental data taken on missiles.

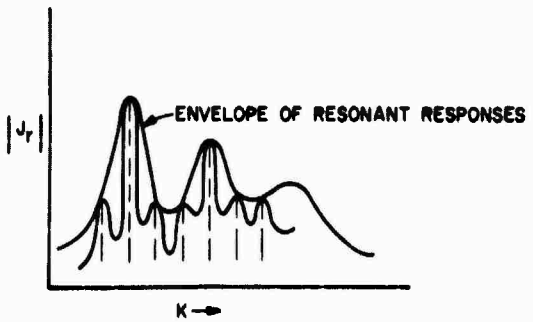

Fig. 2 -- Sketch of interior response of a finite object

An approximate formula accounting for the coupling to a simple circuit inside a cylinder is not difficult to derive. Consider the simple circuit of Figure 3.

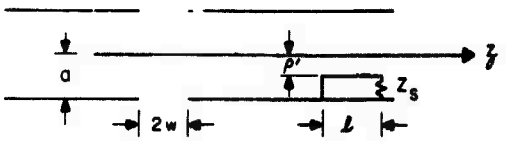

Fig. 3 -- Simple circuit inside alotted cylinder

It will be assumed that the voltage induced in the circuit is given simply by

$$V_i = \oint E \cdot ds = -j\omega\mu \int \bar{H} \cdot \bar{n} da, \tag{3.33}$$

and that the unperturbed fields (for the cylinder with no circuit) can be used in the computation. At resonance, (3.14), (3.26), (3.28), (3.33), and Ohm's law for the circuit combine to give, for the current in the circuit,

$$|I_s| = \left[\frac{4E_0}{\pi Z_0 KD(K)}\right] \frac{J_0\left(\xi_r \frac{\rho'}{a}\right) Z_0 \ell}{J_1(\xi_r) Z_c}. \tag{3.34}$$

Away from resonance, Y_s must be retained in (3.14) and the integration must include all the modes of (3.28). At high frequencies, ξ_r will be one of the large roots of $J_0(x)$, and $J_0\left(\xi_r \frac{\rho'}{a}\right)$ will contain several nodes. One can choose ρ' such that (3.34) is identically zero and then obtain an appreciable nonzero result by changing ρ' only slightly. This rather unphysical ambiguity is the price one pays for the simplification achieved by neglecting the higher order interactions between the circuit and the field and treating the circuit as a wire of zero diameter. The formula may, however, be useful at low frequency.

In all of the theory derived so far we have assumed a lossless interior. Under this assumption resonant terms dominate in various expressions so that a great deal of simplification is possible at the resonant frequencies. In problems involving complicated lossy interiors, arbitrary illumination, and finite objects we postulate that

$$|I_s| \simeq \left[H_\phi^{inc} + H_\phi^{ref}\right]_P \left[\frac{1}{Y_s + Y_i}\right] F(P', Z_c, f, L, a). \tag{3.35}$$

In (3.35) P is the leak location, P' is the circuit location, L and a are the length and radius of the object, and f is the applied frequency. F(P', Z_c, f, L, a) is some complicated (and underivable) function characteristic of the interior of the object. In a truly complicated situation all that is left is a way of thinking about the problem which may be useful to the experimentalist. An obvious objection to (3.35) is that it is suggested by a particular case in which there is only a TM field. However, it is known experimentally that the component of the illumination which is polarized in the direction of the longitudinal axis of a missile is the most effective in producing unwanted currents in circuits inside the missile. Also, gross approximations are permissible. Any describing function which proved to be useful and reliable to within, say, +5 db would represent an improvement over other attempts to construct a theoretical model.

It should be clear by now that this approach is a generalization of the earlier approach by Harrison which was discussed briefly in the introduction. The factor $\left[H_\phi^{inc} + H_\phi^{ref}\right]$ (times $2\pi a$) can be regarded as a constant current generator feeding admittances associated with the slot and the interior of the object. Return to the earlier theory involves regarding the illumination as a plane wave and the object as a linear antenna, connecting the load circuit across the slot, neglect of the interior fields, and, finally, the transformation from an equivalent circuit representation involving a constant current generator to one involving a voltage generator whose open circuit voltage is given by linear antenna theory.

4. Conclusions

We have demonstrated the intimate connection between the interior response of a leaky object illuminated by electromagnetic energy and the scattering solution for a congruent object with no leaks. This part of the paper will be devoted to pointing out some implications of the results for those concerned with electromagnetic interference with ordnance or other industrial problems of radio-frequency interference. The work is applicable in those situations where the location of the leak is known. Access ports on rockets and missiles provide an example.

It has been shown that interior response breaks rather neatly into three factors: the current density for a scattering problem, a factor depending on the slot admittance in the transmitting mode, and the interior response-per-unit voltage. The theory suggests an alternative to present experimental techniques which involve radiating the object and measuring the interior response. Instead it may be advantageous to study the interior response directly by attaching a feeding transmission line to the leak and normalizing the results to unit applied voltage. Measurements of this type can be carefully performed in a laboratory. Slot admittance could be measured in a realistic environment. No other measurements would be required in any situation which allowed even an approximate treatment of the scattering factor. Linear antenna theory may serve well in this regard at low frequency.

Factorization of the interior response is conceptually useful in another way. Suppose that empirical changes are made in the internal layout of a missile which reduce the levels of currents in hazardous circuits. Factorization allows the conclusion that a design improvement for one type of illumination is, in fact, an improvement for any assumed distribution of illumination.

Although we have emphasized the importance of the scattering solution, not much help can be obtained from the literature of scattering theory. Most of existing theory is concerned with far field expressions; current density on the scattering object is the quantity needed here. Although linear antenna theory may be used at low frequencies much of the scattering theory relevant to the hazards-to-ordnance problem is yet to be developed. Thick cylinder theory, both in the transmitting and scattering modes, could make a considerable contribution to the hazards problem. Another fruitful field of research would be the interaction of classical objects with illuminating fields other than plane wave. In particular, the interaction of realistic antennas with surface waves is a much-needed study. It is hoped that these remarks will help ordnance engineers to identify relevant literature should it become available in the future.

In closing, we should not leave the impression that the problem of electromagnetic leakage into missiles can be "solved" in the same sense that a well-defined problem can be solved. One only needs to glance at the complicated interior of a missile and then to imagine an exterior problem containing an electromagnetic jungle called a gantry crane to be convinced of the difficulties. Fortunately, not all situations are that complicated. In any case, the most that can be achieved is an engineering solution involving an intuitive synthesis of theory, experience, and engineering judgment.

ACKNOWLEDGMENT

The writers are indebted to K. S. Kunz, Research Professor, New Mexico State University, for many helpful suggestions.

REFERENCES

Brown, G. H. and King, R. W. P., "High-Frequency Models in Antenna Investigations," Proc. IRE, 22, pp 457-460, April 1934.

Duncan, R. H., "Theory of the Infinite Cylindrical Antenna Including the Feed-Point Singularity in Antenna Current," J. Research NBS 66D (Radio Prop.) No. 2, pp 181-188, March-April 1962.

King, R. W. P. and Harrison, C. W., Jr., "Cylindrical Shields," IRE Transactions on Antennas and Propagation, AP-9, No. 2, pp 166-170, March 1961.

Scheikunoff, S. A. and Friis, H. T., Antennas Theory and Practice, John Wiley and Sons, Inc., p 301, 1952.

Silver, S., Microwave Antenna Theory and Design, McGraw-Hill Book Company, Inc., p 45, 1949.

Stratton, J. A., Electromagnetic Theory, McGraw-Hill Book Company, Inc., p 360, 1941.

Wait, J. R., Electromagnetic Radiation From Cylindrical Structures, Pergammon Press, 1959.

APPENDIX A

RECEIVING CROSS SECTION OF INEFFICIENT ANTENNAS

Several texts establish the formula

$$A(\theta, \phi) = \frac{\lambda^2}{4\pi} G(\theta, \phi) \tag{A-1}$$

relating the receiving cross section and gain function of an efficient antenna. Slight modification of a typical derivation (Silver, 1949) suffices to demonstrate that (A-1) is also true for lossy antennas. We define the gain function as

$$G(\theta, \phi) = \frac{P(\theta, \phi)}{P_T/4\pi}, \tag{A-2}$$

where $P(\theta, \phi)$ is the actual radiated power per unit solid angle and P_T is the total power injected into the antenna terminals. The ratio of $\int P(\theta, \phi)\, d\Omega$ to P_T is the transmitting efficiency, α. The receiving cross section is defined by

$$p(\theta, \phi) = A(\theta, \phi)S, \tag{A-3}$$

where S is the intensity of an incident plane wave and $p(\theta, \phi)$ is the power delivered to a load. From the reciprocity theorem for antenna patterns,

$$\frac{A(\theta, \phi)}{A_M} = \frac{G(\theta, \phi)}{G_M}. \tag{A-4}$$

In (A-4) the factors A_M and G_M serve to normalize the receiving and gain patterns. Denoting the average of $A(\theta, \phi)$ by $\overline{A}$, it is now easy to show that

$$A(\theta, \phi) = \frac{\overline{A}}{\alpha} G(\theta, \phi). \tag{A-5}$$

Now consider two antennas, a and b, with a transmitting energy to b. Under matched conditions,

$$\frac{G_a G_b \overline{A}_b}{\alpha_b} = \frac{16\pi r^2 R_a R_b |i_a|^2}{|V_a|^2}, \tag{A-6}$$

where r is the distance between a and b, R_a and R_b are the antenna resistances, i_a and V_a are the terminal current and voltage, respectively, of antenna a. Reversing the roles of the antennas as transmitter and receiver provides another equation which is derivable from (A-6) merely by interchanging the indices a and b. The ratio of these expressions, together with the relation $i_a V_b = i_b V_b$ from the reciprocity theorem, gives

$$\frac{\overline{A}_a}{\alpha_a} = \frac{\overline{A}_b}{\alpha_b}. \tag{A-7}$$

Average receiving cross section divided by transmitting efficiency is a universal constant for all antennas. Choose the constant as $\lambda^2/4\pi$ in the usual way by considering an efficient short dipole. It is now apparent that (A-1) is true for lossy antennas.

APPENDIX B

EFFECTIVE LENGTH OF AN INFINITE CYLINDRICAL ANTENNA

The basic definition of the effective length (Schelkunoff, Friis, 1952) of an antenna of length 2h is

$$\ell_{eff} = \frac{\int_{-h}^{+h} I(z)dz}{I(0)}, \tag{B-1}$$

where I(z) is the transmitting current distribution along the antenna and I(0) is the input current at the antenna terminals. It is customary in antenna theory to introduce an idealized driving generator such that the electric field in a narrow gap in the antenna surface at $z = 0$ is given by $-V\delta(z)$. The result of this idealization is a short-range singularity in I(z). Strictly speaking, (B-1) is identically zero for the δ-gap theoretical model. The significance of the singularity and means for removing it have been discussed previously (Duncan, 1962). We shall replace (B-1) by

$$\ell_{eff} = \frac{1}{Y_g}\int_{-\infty}^{+\infty} I(z)dz, \tag{B-2}$$

where Y_g is defined by a procedure which smooths out the singularity inherent in the δ-gap model. Values of Y_g corresponding to several values of K are given in the reference. With (3, 11) and the Fourier inversion theorem one obtains

$$\frac{K}{Z_0}\,\frac{H_1(\beta a)}{j\beta H_0(\beta a)} = \frac{1}{2\pi}\int_{-\infty}^{+\infty} I(z)\,e^{j\alpha z}\,dz. \tag{B-3}$$

From (B-3) it follows by setting $\alpha = 0$ that

$$\int_{-\infty}^{+\infty} I(z)dz = \frac{2\pi K}{Z_0}\,\frac{H_1(K)}{jkH_0(K)}. \tag{B-4}$$

Now (B-4) can be combined with numerical data for Y_g according to (B-2) to give the effective length of an infinite cylindrical antenna. Curiously, it turns out that $|\ell_{eff}| \simeq \lambda/4$.

13. ANALYSIS OF RESPONSE OF THERMOCOUPLE INSTRUMENTED DEVICES TO SHORT-PULSE TRANSIENT[1]

Richard K. Fry
D. Boyd Barker

University of Denver
Denver, Colorado

With the assumption that the bridgewire, thermocouple and recording instrument behave as successively-coupled, linear systems, an analysis was performed to determine the response of the several components of the system to short pulses of electrical energy into the bridgewire. Both qualitatively and quantitatively the mathematical model so devised agrees with the experimentally determined behavior of the physicel system. This model and its verification make possible the celibration of instrumented devices to recover pulse energies and/ or bridgewire temperature from the output of the recorder. Table 1 lists all the symbols used.

TABLE - 1

T_1 - temperature of bridgewire above ambient, °C

T_2 - temperature of thermocouple above ambient, °C

β_1 - dissipation constant of bridgewire, watts/ °C

τ_1 - time constant of bridgewire, msec

τ_2 - time constant of thermocouple in instrumented EED, msec

τ_3 - rise time of thermocouple for short pulse into bridgewire, msec

τ_4 - time constant of recorder, msec

1. This work was supported by Sandia Corporation. The complete analysis and experimental results may be found in reference 6.

C_1 - heat capacity of bridgewire, joules/ °C

P - power delivered to bridgewire, mwatts

v - voltage output of thermocouple, μ volts

θ - deflection of recorder, cm

C - steady-state ratio of P to v, mwetts/μ volts

C' - steady-state ratio of P to θ, mwatts/cm

D - steady-stete ratio of T to v, °C/ μ volt

D' - steady-state ratio of T to θ, °C/cm

E - energy of short pulse, μ joules

RESPONSE OF THE SYSTEM TO SHORT-PULSES OF ENERGY

The analysis of the effect of short pulses of power upon bridgewire temperature has shown that for a pulse whose duration is short compared to the bridgewire time constant,[2] the temperature approximates a step discontinuity which is proportional to the pulse energy and inversely proportional to the heat capacity of the bridgewire, i.e., $T = E/C_1$. After the step discontinuity at the time of the pulse, the bridgewire's temperature decays exponentially with the bridgewire's characteristic time constant (Figure 2).

$$T_1(t) = \frac{E}{C_1} \exp(-t/\tau_1) \qquad (1)$$

---

2. A short pulse as used here is one whose duration is on the order of 1% or less of the bridgewire's time constant although the conclusions hold to a fair approximation for pulses whose duration is as high as 10% of the bridgewire's time constant.

The analysis has also shown that for short pulses of power into the bridgewire, the output of the thermocouple exhibits a step discontinuity in its time derivative at the time of the pulse. The discontinuity in the time derivative is proportional to the pulse energy (Figures 1 and 2).

$$\dot{v}(t+) = \dot{v}(t-) + \frac{E}{C\tau_1\tau_2} \tag{2}$$

After a characteristic time which depends upon the thermocouple and bridgewire

$$\tau_3 = \frac{\tau_1\tau_2}{\tau_2 - \tau_1} \ln\left(\frac{\tau_2}{\tau_1}\right) \tag{3}$$

the difference between the thermocouple output and what it would have been were there no pulse, achieves a maximum. The maximum difference is proportional to the energy of the pulse (Figures 1 and 2.)

$$v_{max} = \frac{E}{\tau_1 C}\left(\frac{\tau_1}{\tau_2}\right)^{\frac{1}{1-\tau_1/\tau_2}} \tag{4}$$

Figure 1 is a graph of thermocouple output for a short pulse of energy into the bridgewire as calculated from

$$v = \frac{E}{C(\tau_2-\tau_1)}\left\{\exp\left(-t/\tau_2\right) - \exp\left(-t/\tau_1\right)\right\} \tag{5}$$

by assuming a ten millisecond bridgewire time constant and a 40 millisecond thermocouple time constant. (Figure 5 is a typical experimental record.) It is worth noting that the area under the curve is also proportional to the pulse energy.

$$\int_0^\infty v\,dt = E/C \tag{6}$$

To illustrate the theory, Figure 2 is a graph of bridgewire temperature and thermocouple output as a function of time as predicted by this analysis when the power input into the bridgewire is short pulses. Calculations for this graph were made from the appropriate equations. The two time constants τ_1 and τ_2 were chosen to be 10 milliseconds and 20 milliseconds respectively. This gives the characteristic time (τ_3) of 13.9 milliseconds after a pulse that the thermocouple output achieves a maximum over what it would have been were there no pulse. (Note that the shape of the curves would be different for a different pair of time constants.) Calculations for the graph were based upon the initial conditions of ambient temperature and zero thermocouple output. Pulses of energy, E_1, E_2 and E_3, whose durations are 100 μseconds or less, strike the bridgewire at t=0, t=20 and t=50 milliseconds respectively. The relative ratios of the 3 pulse energies, E_1: E_2: E_3, are 4: 1: 2. Since the pulse duration is 100 μseconds or less, it is justifiable to graph the bridgewire temperature as a step discontinuity at the time of the pulse when actually the bridgewire's temperature rises continuously during the pulse duration. The same argument holds for the discontinuity in the slope of the thermocouple voltage.

On the graph, J is the proportionality constant between the maximum effect of a given pulse on thermocouple voltage and the pulse energy,

$$J = \frac{1}{\tau_1 C} \left(\frac{\tau_1}{\tau_2}\right)^{\frac{1}{1-\tau_1/\tau_2}} \tag{7}$$

and τ_3 is the 13.9 millisecond characteristic rise time for the system of a 10 millisecond bridgewire and a 20 millisecond thermocouple. Notice that this rise time is the time after the pulse that the thermocouple voltage achieves a maximum above what it would have been were there no pulse. This does not mean that the <u>voltage</u> itself necessarily achieves

a maximum value 13.Ø9 milliseconds after the time of the pulee. (Inspection of the graph indicates this.) Also notice that the peak voltage when multiplied by the steady state calibration gives the temperature of the bridgewire at the time when the peak voltage occurred but this temperature is markedly less than the peak bridgewire temperature which occurred previous to the recording of a maximum voltage. In fact, the higheet peaks of voltage do not necessarily correspond to the highest temperatures achieved by the bridgewire: the voltage peaks due to pulese 1 and 2 are about the same height, yet the temperature achieved by the bridgewire is three timee as high for pulse 1 as for pulse 2. For the voltage peaks due to pulse 2 and 3, the higher voltage corresponds to the lower maximum temperature. These considerations indicate that some care must be used in interpreting the voltage output of a thermocouple which is instrumenting an EED.

Another conclusion can be drawn from the analysis concerning the thermocouple; if the thermocouple's heat capacity is decreased, e. g., by using a thinner substrate, thereby decreasing the thermocouple time constant, then the voltage of the thermocouple will achieve a higher maximum above what it would have been were there no pulse (eq. 4). Figure 3 is a graph of the voltage output, for thermocouples with various time constants (in milliseconds), all other conditions being identical, and for a bridgewire time constant of ten milliseconds, for short pulse inputs into the bridgewire. An instantly responding thermocouple's output replicates the bridgewire temperature. For slower responding thermocouples (with the same dc sensitivity) the peak is delayed and lowered. It is interesting to note that the area under each of these curves is the same, and that the ratio of pulse energy to area under the curve depends upon the steady state ratio of voltage output of thermocouple to input power into bridgewire (eq. 6).

When the voltage of the thermocouple is used to drive a recording instrument, the recorder's time response, unless instantaneous, distorts the transient response to short pulses in three significant ways; although the voltage of the themocouple suffers a step discontinuity in its time derivative at the time of the pulse, the output of the recorder is continuous in its time derivative. The other two distortions caused by the recorder are that the recorded peak is both lowered and delayed in time from that of an instantly responding recorder (which replicates the thermocouple voltage). Figure 4 is a graph calculated to show the affect of the recorder's time constant upon the response to short pulses.

$$\theta(t) = \frac{\mathcal{E}}{C(\tau_1 - \tau_0)} \left\{ \frac{\tau_1}{\tau_1 - \tau_0} \exp\left(\frac{-t}{\tau_1}\right) - \frac{\tau_0}{\tau_1 - \tau_0} \exp\left(\frac{-t}{\tau_0}\right) + \frac{\tau_0(\tau_1 - \tau_0)}{(\tau_1 - \tau_0)(\tau_1 - \tau_0)} \exp\left(\frac{-t}{\tau_0}\right) \right\} \qquad (8)$$

The recorders are assumed to have the same dc calibration. An instantly responding recorder and thermocouple replicates the bridgewire temperature. An instantly responding recorder replicates the thermocouple output. For other than instant response the effects mentioned above are evident. It will be noted that the areas under these curves, too, are the same and depend only on the pulse energy and the steady state ratio of recorder output to power into the bridgewire. The maximum recorder indication is proportional to the pulse energy. However, an expression for the peak height is not as easily obtained as for an instantly responding recorder (eq. 4). The maximum value of equation 8 as a function of the time constants must be evaluated by numerical methods.

METHODS FOR RECOVERING PULSE ENERGY AND BRIDGEWIRE TEMPERATURE

The theoretical analysis suggests two methods for recovering the pulse energies from the recorder's output, and two methods for recovering bridgewire transient temperatures.

Since the peak of the recorder output is proportional to the pulse energy (eq. 8), the pulse energy can be inferred from the peak height and a knowledge of the proportionality constant. A direct calibration seems most easily achieved and accurate. Pulses of known energy can be introduced into the bridgewire by discharging a capacitor. The capacitor value is chosen to give the pulse a sufficiently short duration. The ratio between this known energy and the measured peak recorder indication provide a means of determining unknown pulse energies from the height of the recorder indication.

Since the area under the galvonometer record is also proportional to energy, the pulse energy can be calculated from the area under the curve and a knowledge of the proportionality constant C'.

$$E = C' \int \theta \, dt \tag{9}$$

This method is applicable for other than pulse inputs into the bridgewire and such an integral will result in the total energy supplied to the bridgewire for a given period of time if the limits of integration are between quiescent values of recorder output.

One method of temperature recovery is applicable only to short pulse inputs. It is based upon the fact that the bridgewire peak temperature due to a short pulse is proportional to the pulse energy and inversely proportional to the heat capacity of the bridgewire. This result is independent of whether the squib is loaded or instrumented provided the

pulse duration is short compared to the bridgewire's time constant in the given thermal environment. Thus for short pulses of energy

$$T_{max} = E/C_1 \tag{10}$$

The pulse energy, E, can be found from either of the two described methods and a knowledge of C_1, the bridgewire heat capacity, can be deduced from the product of the bridgewire's time constant, τ_1, and the bridgewire's dissipation constant, β_1, both of which can be measured.

A second method of temperature recovery is of more general applicability: the equation relating recorder output to bridgewire temperature is:

$$T_r(t) = D' \left\{ \theta + (\tau_2 + \tau_4)\dot{\theta} + \tau_2 \tau_4 \ddot{\theta} \right\} \tag{11}$$

where D' is the steady state ratio between bridgewire temperature and recorder indication. If the time constant of the recorder, τ_4, is negligible compared to the time constant of the thermocouple, τ_2, then

$$T_r(t) = D' \left\{ \theta + \tau_2 \dot{\theta} \right\} \tag{12}$$

It has been suggested (refs. 2,3) that a computer be used to recover the bridgewire temperature from the thermocouple output through equation 12. An analysis of the computer requirements for stability and drift has been carried out (ref. 4). Because of these requirements, it was suggested that a laboratory computer with adjustable parameters D' and τ_2 would be the most feasible for data reduction. The expense and complexity of computers for each instrumented EED would be prohibitive. (See reference 2, 3 and 4 for a more complete discussion.)

It should be noted here that the recorder of the thermocouple output should have a response time much faster than the thermocouple and should have an output easily transformed into a voltage in order that such a data reduction system be meaningfully utilized. If a computer is not used, the data could be manually reduced for selected points by a measure of v and dv/dt from a graph and using the constants to calcultate the temperature of the bridgewire. With only a little experience the person reducing the date would be able to recognize the points corresponding to high bridgewire temperature and calculate only these.

REFERENCES

1. Denver Research Institute of the University of Denver, Supplementary Final Report, Contract N123(60530) 10049A, Test Equipment for and Evaluation of Electromagnetic Radiation, March 1961, pp. 1 - 16.
2. Denver Research Institute of the University of Denver, Final Report, Contract N123(60530) 10049A, Test Equipment for and Evaluation of Electromagnetic Radiation, Vol. VII, "Methods of Detecting R F Power in Bridgewires of Electroexplosive Devices and Instrumentation Problems", November 1960, pp. 74 - 79.
3. op. cit. ref. 1, pp. 41 - 43.
4. Denver Research Institute of the University of Denver, Quarterly Report Number 2, Contract N178-7818, Research and Development Leading to Perfection of Instrumentation of Electroexplosive Devices, September 1961, pp. 89 - 95.
5. op. cit. ref. 1, p. 3 and p. 9.
6. Denver Research Institute of the University of Denver, Sandia Corp. P. O. No. 73-2582, Task 1 Report, Transient Response of Thermocouple Instrumented EED's, September 1962.

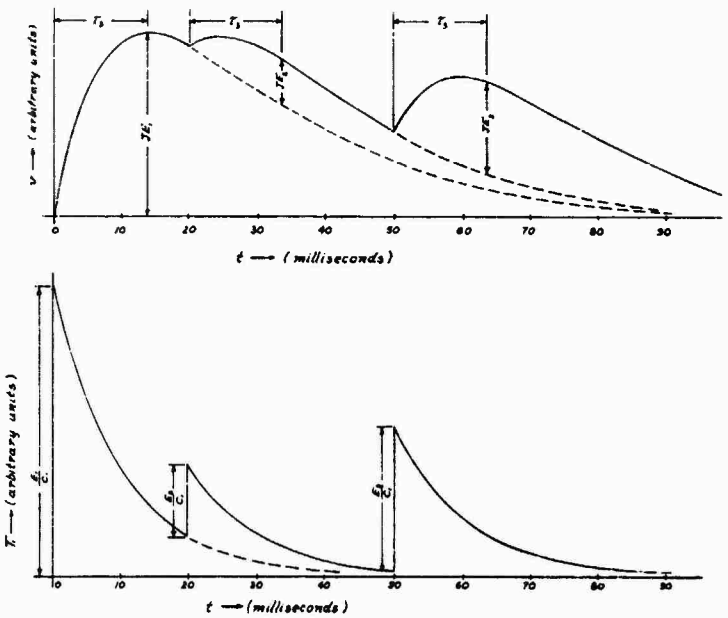

Figure 2. Bridgewire temperature and thermocouple voltage as a function of time for short pulses of energy into bridgewire.

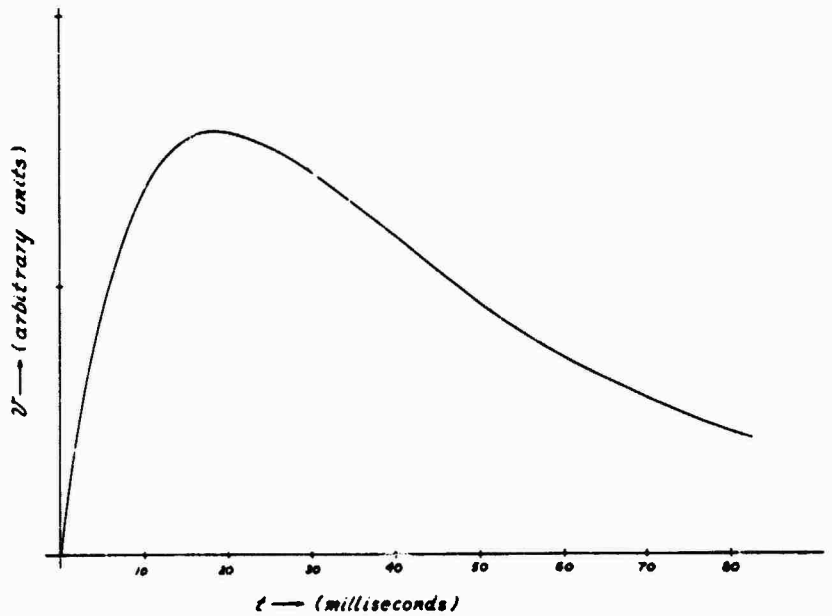

Figure 1. Thermocouple voltage due to a short pulse of energy into the bridgewire.

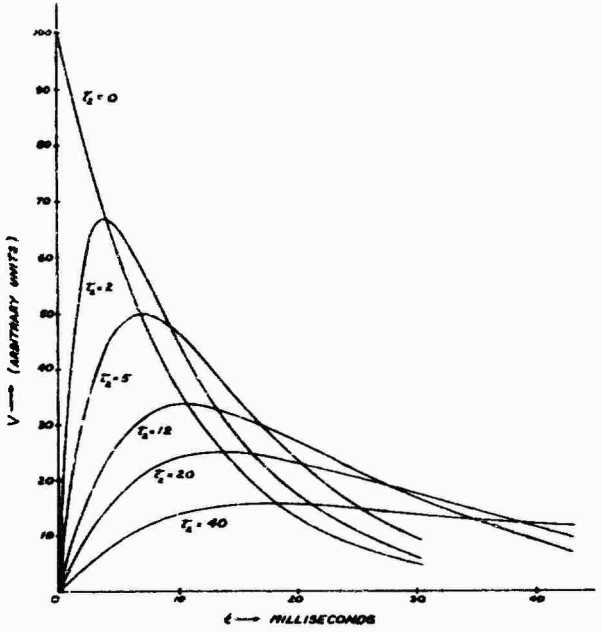

Figure 3. Thermocouple voltage as a function of time for a 10 msec. bridgewire and various thermocouple time constants in sensing bridgewire temperature due to a short pulse of energy.

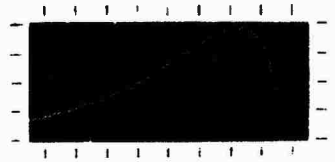

Figure 5 Response of thermocouple to energy pulse into bridgewire. Time increases to the left - 20 msec/div. Vertical scale - 50 μv/div.

Figure 4. The recording instrument's indication as a function of time for various instrumentation time constants in sensing bridgewire temperature due to a short pulse of energy.
A - instantaneous response of thermocouple and galvanometer;
B - 20 msec thermocouple and instantaneous galvanometer;
C - 20 msec thermocouple and 5 msec galvanometer;
D - 20 msec thermocouple and 25 msec galvanometer.

13. DISCUSSION

Mr. Davey of The Franklin Institute commented that one can conduct a DC Bruceton sensitivity test of the explosive device, and the instrumented device can be calibrated under the same input conditions. Good agreement has been found between instrumented EED readings and firing sensitivity. This has been done primarily for relatively long-duration (10 second) pulses.

A representative of NWL commented that in his experience a correction was found necessary for this to be accomplished.

Another person commented that his organization experimented with platinum wire thermometers as a means of measuring bridgewire temperature. This technique can permit the device to remain loaded with some inert material or with the explosive itself.

A comment was made that measuring bridgewire resistance using conventional means of doing this (Wheatstone Bridges and similar devices) would cause an entirely different RF picture by creating different impedances and coupling.

14. METHODS OF MEASURING RADIO FREQUENCY POWER AT A GIVEN POINT IN A HIGH LOSS SYSTEM

By

G. H. McKay, N. P. Faunce, R. F. Wood, P. F. Mohrbach
The Franklin Institute

1. INTRODUCTION

One of the major problems that has always existed in the field of radio frequency measurements has been the accurate determination of RF power. In recent years, measuring equipment has been refined so that accurate measurements of this power can be made at any point where it is possible to introduce measuring equipment. If the system being used can be assumed lossless, then the power determination one might make from the port of a directional coupler placed in the system can be expected to be a reasonable representation of the power passing some other point in the system. Today, standard line components placed in a system with a very low voltage standing wave are good approximations of lossless systems.

In the evaluation of the behavior of electroexplosive devices when exposed to RF we rarely are fortunate enough to have small standing waves. Most standard laboratory equipment has a characteristic impedance of 50 ohms and most EED's have an impedance differing greatly from this. When it is necessary to couple the power from a 50-ohm system into an EED by an impedance matching device, the resulting standing waves between the matching device and the EED may become quite large, so that the system components begin to cause losses comparable to the losses in the EED itself. Under such conditions it is obviously inaccurate to assume that all of the power matched from the generator into the system is arriving at the EED. While it would be advantageous to have RF systems in which the system impedance was the same as the termination, at the

present time this would be too vast a problem for the large variety of impedances represented by the many kinds of EED's. The alternative, then, is to determine either the losses in the measuring system or the amount of power actually arriving at the EED.

While there are probably many ingenious ways of approaching this problem, we are at present investigating three, and two of these are actually in operation. We will refer to these techniques as the differential power technique, the voltage-impedance technique, and the voltage-min-max technique.

2. THE DIFFERENTIAL POWER TECHNIQUE

Figure 1 shows a block diagram of the components necessary for the differential power measuring system. Superficially, the concept is relatively simple. Using directional couplers, we are able to measure the incident and the reflected powers in a transmission line. The difference between these quantities is the net power flow, and if the couplers can be located close to the load one has a good approximation of the power arriving at the load. If most of the power is being reflected from the load then the difference between the incident power and the reflected power becomes very small and the errors can be such that the method can become practically useless. The cumulative errors involved in this approach can be somewhat minimized by using one meter for both the incident and the reflected power determination. In this case, the meter can be adjusted for zero reading when the line is terminated in a short circuit, that is when the incident power equals the reflected power. If the detectors are properly selected and carefully calibrated, the major errors of this technique are related to the reflection coefficient of the termination, and the directivity of the couplers used.

The error equations are:

$$\% \text{ error} = 100\left[\frac{\pm 4\rho_d \rho_e}{1 - \rho_e^2} - \rho_d^2\right] \qquad (1)$$

$$\text{where } \rho_d = \frac{1}{\text{antilog } (D/20)}$$

D = directivity of couplers (db)

ρ_e = reflection coefficient.

The curve of these results is plotted in Figure 2. From it, one can see that the possible error becomes quite large as the reflection coefficient approaches 1. The greater the directivity of the couplers, the more reliable the results become, but even then the maximum error approaches one per cent for a reflection coefficient of 0.55 and 10 per cent for reflection coefficients of approximately 0.92. It should be noted that this analysis is based on maximum error. Directivity error occurs because directional separation is not perfect, so that part of the reflected power is measured with the incident power and vice versa; the error may be reduced by use of phase shifting techniques. In the development of the error equation it was assumed that the desired and undesired voltages add at the coupler auxiliary ports, in the phase relationship that produces maximum error. Adjustment of this phase relationship could greatly minimize the directivity error.

This technique would seem to be capable of good precision with suitable refinements. However, for our specific needs at the moment it was decided that other techniques could be brought to a usable stage more quickly. Additional refinement was therefore temporarily suspended.

3. THE VOLTAGE-IMPEDANCE TECHNIQUE

The net power passing a point on an arbitrarily terminated transmission line can be calculated by measuring the RMS voltage and the input impedance of the line at the same point. Figure 3 shows a diagram of the transmission line and its equivalent circuit. The input impedance, Z_s, is measured looking into the load from a point at a distance s from the load. Since the voltmeter input impedance parallels Z_s, it will not affect the measurement of load power, although to the generator it appears as an additional load. The power dissipated beyond the voltmeter junction can be expressed by

$$P_{net} = V_s^2 \, Re(Y_s) = V_s^2 G_s \text{ (watt)} \tag{2}$$

where

P_{net} = power dissipated beyond point s

V_s = magnitude of RMS voltage measured at point s

Y_s = input admittance of transmission line at point s

Re = real part of

Im = imaginary part of

G_s = real part of Y_s.

This can be reduced to

$$P_{net} = \frac{V_s^2 R}{R^2 + X^2} \text{ watt} \tag{3}$$

where

R = real part of Z_s the input impedance

X = imaginary part of Z_s.

If the section of transmission line between the voltmeter and load is lossless then the net power is equal to the power dissipated by the load.

The accuracy of the power determination depends on the accuracies of the voltage and impedance measurements. The voltage measurement accuracy is generally good ($\pm 5\%$ or better) at frequencies up to about 500 Mc. Above this, special calibrating methods must be used. One such method involving a calorimetric power meter is shown in Figure 4. The power meter terminates the transmission line in a matched impedance (50 ohms); hence the magnitude of the rms voltage (V) at any point on the line equals the incident voltage to the calorimeter. This voltage is

$$V = \sqrt{PR_o}$$

where

P = power measured by calorimeter

R_o = characteristic impedance of the transmission line.

The voltmeter is connected at any point on the line and calibrated against the calorimeter reading, which is accurate to better than $\pm 5\%$. Since our calorimeters are good up to 100 watts, a maximum of about 70 volts rms can be calibrated directly.

Impedance measurements are made with several instruments, the choice depending on the frequency. Accuracy generally falls off for low impedance measurements, however, which is unfortunate since most of our terminations have impedances of about one ohm.

The overall accuracy of the voltage impedance method of measuring net power can be computed for various magnitudes of load impedance and frequencies, given the individual accuracies of the system components.

4. THE VOLTAGE MIN-MAX TECHNIQUE

The net power through an arbitrarily terminated transmission line can be expressed in terms of the voltage standing wave maximum and minimum by

$$P_n = \frac{V_{max} V_{min}}{R_o} \text{ (watts)} \tag{4}$$

where

P_n = net power (watts)

V_{max} = RMS magnitude of line voltage at a voltage maximum (volts)

V_{min} = RMS magnitude of line voltage at a voltage minimum (volts)

R_o = characteristic impedance of transmission line (ohms)

In actual practice, if one places a slotted line with a probe between the matching section and the termination, the proper readings can be taken to show the power passing this point.

While in principle this is simple, there are several special questions which one must consider. First, is it possible to use the concept with waveguide, since it is difficult to define characteristic impedance with waveguide? Fortunately, the answer appears to be yes, if we make use of a quantity, D_x, the scale indication in arbitrary units of the galvanometer used with the probe.

Then,
$$\frac{V_x^2}{R_o} = f(D_x) \text{ (watts)} \tag{5}$$

V_x in this expression is the voltage appearing at the probe when the line is terminated in a power meter with a characteristic impedance equal to that of the system. V_x is also given by

$$V_x = \sqrt{P_L R_o} \quad \text{(volts)} \tag{6}$$

where

P_L is the power measured by the power meter as a load.

This being accepted, we can calibrate the crystal detectors of the probe in terms of D_x. If this calibration and all subsequent calibrations are carried out within the square law response of the crystal detectors then it can be shown that

$$P_n = K\left[D_{max} D_{min}\right]^{\frac{1}{2}} \quad \text{(watts)} \tag{7}$$

where

$$K = \frac{P_L}{D_x} \text{ (watt/volt)}$$

This expression can be used directly with waveguide systems and waveguide slotted sections.

Since the measurement requires two voltage readings physically separated by a quarter wave length, one might also raise the question at which point in the line is the power really being determined. An analysis of the problem with the assumption that the losses per unit length of line are very small leads to the expression

$$q \pm \frac{\lambda/4}{(S^2 - 1)} \tag{8}$$

This gives the distance, expressed in wavelengths, from the position at which S, the standing wave ratio is strictly correct, to the position where V_{min} is measured. It is apparent from this expression that S need not become very large before the point of power measurement is located very close to the V_{min} position. Figure 5 is a plot of equation 8. It can be seen from this that by the time the VSWR has reached a value of 7 the distance from the V_{min} position is extremely small. As S becomes small, the location of S moves away from V_{min}, but likewise the line losses become very small.

One other point should be made regarding this approach. When the wave length is short enough, several $V_{max} - V_{min}$ values can be found, and determination of the actual losses along the line can be made. The data can then be extrapolated down to the base of the test device. We are presently making use of this system in the 1 Gc to 10 Gc frequency range.

5. CONCLUSIONS

Three methods for determining the actual RF power passing a given point in a lossy system have been described. All three of these systems have been actually assembled and used and two, the voltage-impedance and voltage min-max techniques, are in common use in our firing systems at the present time. In general, we have found the voltage-impedance system effective and the more easily used system at frequencies up to 500 Mc, and the voltage min-max system more effective from 1 Gc to 10 Gc. From 500 Mc to 1 Gc either system is used. These techniques have gone a long way toward solving the problem of determining the actual RF power dissipated in electroexplosive devices. However, considerable refinement is still necessary. Furthermore, alternative solutions must be kept in mind, for the field of RF measurements is surely not a static one at the present time. While little is certain in this field, the regions of doubt are growing ever smaller.

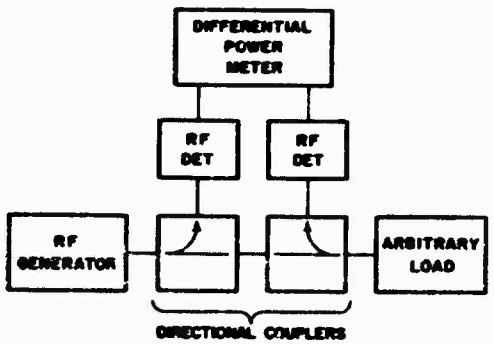

FIG. 1 SYSTEM FOR MEASUREMENT OF DIFFERENTIAL DIRECTIONAL COUPLERS

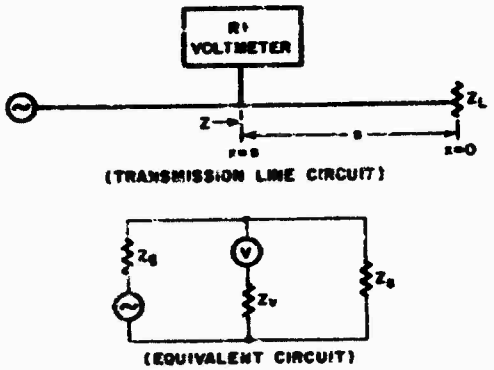

FIG. 3. VOLTAGE-IMPEDANCE CIRCUIT FOR NET POWER DETERMINATION

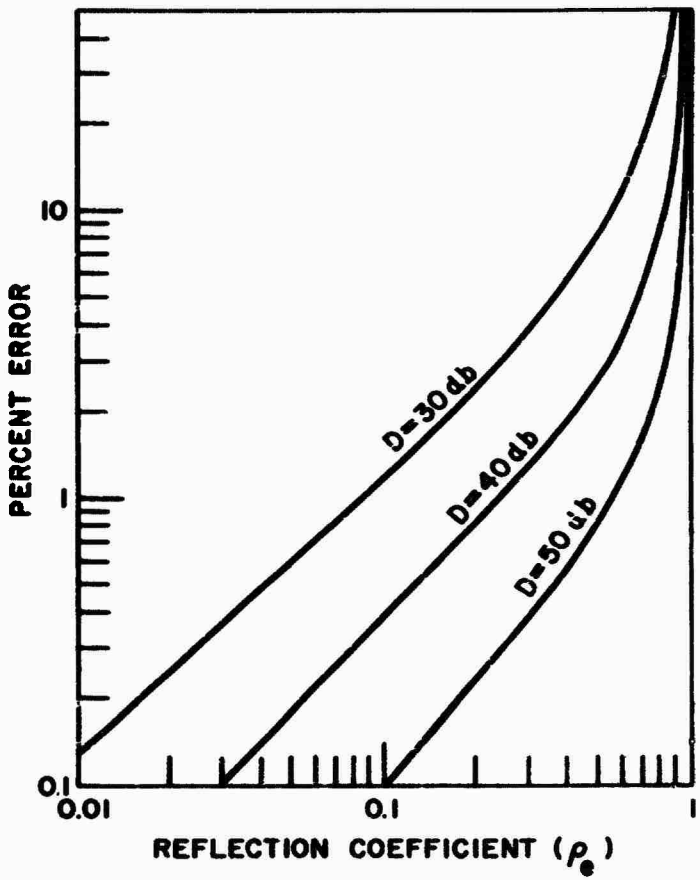

FIG. 2. MAXIMUM MEASUREMENT ERROR DUE TO DIRECTIONAL COUPLER DIRECTIVITY

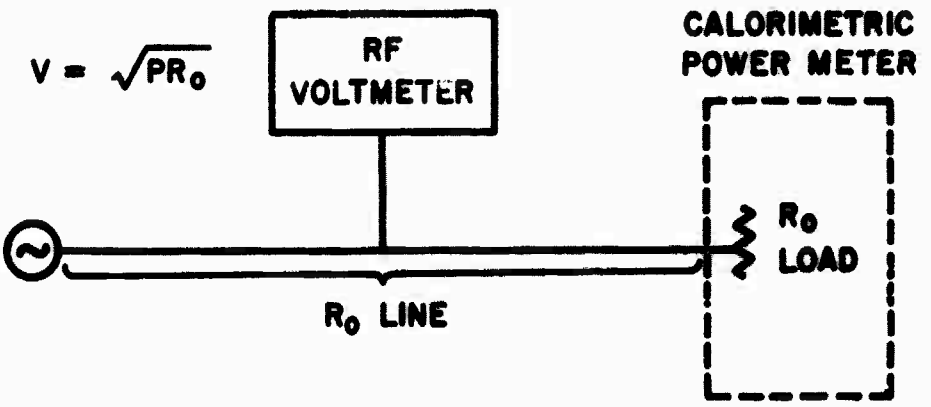

FIG. 4. RF VOLTMETER CALIBRATION
USING CALORIMETER

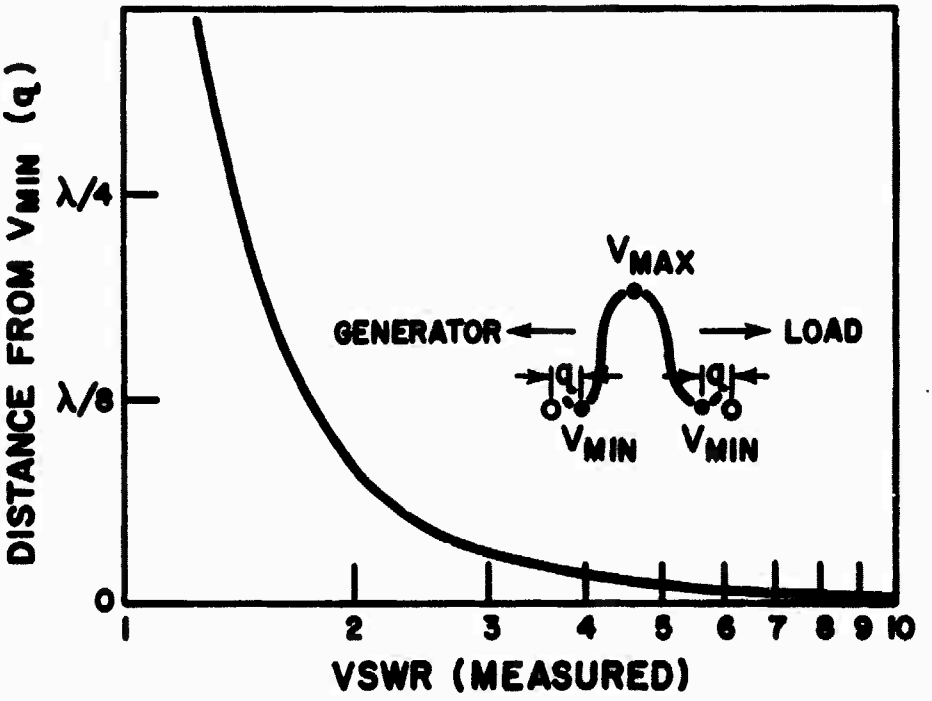

FIG. 5. LOCATION OF MEASURED VSWR

15. DETERMINATION OF RESPONSE OF RF INSENSITIVE DEVICES

by
N. P. Faunce, G. H. McKay, R. R. Raksnis, R. F. Wood, P. F. Mohrbach
The Franklin Institute

I. INTRODUCTION

All radio frequency fixes are compromises. Some choice of balance must be made between producing minimum effect on the normal firing signals and maximum effect on any other electrical signal. Fixes must be particularly effective in high intensity RF environments. Within this area there are a great number of possible approaches to the problem, and each one poses its own special set of obstacles when it is necessary to evaluate their effectiveness.

In the general class of RF-insensitive devices one could include dissipative filters, inherently insensitive electroexplosive devices EED's containing integral attenuators, lossy transmission lines, shielded transformers, special relays, and many others. In evaluating the many types, it is useful to break them into two broad categories: First, those that are integral parts of the EED so that they are virtually inseparable; and second, those that can either be easily separated from the EED or are already separated and are to be added as circuit components at the discretion of the designer. While each of these has special problems of its own, there are certain general requirements for tests that can be set down for all types. A brief list of such requirements might include the following:

a. Determine the sensitivity of the devices to dc stimuli, or the degree of alteration of dc stimuli by the device under test.

b. Determine the degree of RF rejection over the frequency range of 20 Kc to 10 Gc. This should be determined under worst-case conditions whenever possible.

c. Determine the ability to withstand substantial power absorption without marked degradation.

d. Determine the degree of temperature rise produced in the test device by absorbed power.

e. Determine the behavior of the device at temperature and humidity extremes.

Having set forth these general requirements, we can now turn our attention to some of the specific evaluation problems.

2. INSERTION UNIT EVALUATIONS

The devices in this category represent a wide variety of types. They are characterized by the fact that attachments can be made both to their input and to their output, although the design can call for a specific output impedance. The fixes in this group include electric wave filters which depend primarily on reflections from discontinuities and are characterized by the classical L-C filter, dissipative filters such as the solid state attenuating materials, which actually convert electromagnetic energy into other forms (usually heat), arming systems such as the solenoid relay, which depend on shielding of the electro-explosive device, and composite filters which make use of combinations of all these techniques, such as the RIG (radiation interference guard).

The most important consideration is the amount of RF protection provided. For devices which are not designed for a specific terminating impedance, the characteristic of prime interest is its worst-case attenuation. This is the least attenuation afforded under

any conditions of source and terminating impedances. At the present state of the art in the laboratory we determine this attenuation by two methods.

Figure 1 is a block diagram of a measurement system using matching networks. In this system a lossless piece of transmission line is inserted between the supposedly lossless matching systems, and the systems are adjusted until maximum power is indicated on the power indicating termination, and recorded. At this point the reflected power indicator will read zero. The device to be tested is now placed between the matching systems, which are adjusted so that again the reflected power reads zero and the power indicator reads a maximum. The attenuation in decibels is ten times the logarithm of the ratio of the two powers. To the extent that the lossless matching systems are perfect (i.e., are capable of transforming any impedance into any other impedance) this procedure gives the worst-case attenuation. This is so, because the matching process eliminates reflection of power, and the remaining attenuation is inherent, being true dissipation of energy. At the present time, one can obtain relatively efficient and lossless matching devices in the frequency range from approximately 40 Mc to 10 Gc and conceivably to even higher frequencies if desired.

At the present time, however, the lower frequencies are, in general, taken care of by lumped component matching systems which tend to be inherently lossy and limited in their range of matching ability. Because of the problems inherent in this approach at low frequencies another system has been worked out which makes use of a unique dissymmetrical-T network model determined from impedance measurements of the test device. A full discussion of this procedure is presented in a separate paper in the minutes of this meeting.

This measurement is shown diagrammatically in Figure 2. Briefly, the real network is first described as an equivalent dissymmetrical-T. This is done by operating on input/output impedance measurements made on the network. From the knowledge of the model's components we next calculate the termination (Z_{wc}) which will absorb maximum power. Finally, we evaluate the ratio of the input power to the power dissipated in the worst-case termination. The attenuation in decibels, db_{wc}, is ten times the logarithm of this ratio. Because of the complexity of these calculations we avail ourselves of a digital computer. The system is limited primarily by the accuracy of the impedance measurements and at the present time we are limited to a maximum of 30 db for accurate results. The technique is effective over the frequency range of 20 Kc to 100 Mc.

Figure 3 presents data for two typical devices subjected to these measurements.

While there are special evaluation problems (for example, devices with very low impedances make matching and accurate impedance measurements very difficult), these attenuation measurement techniques are applicable to just about every insertion type device. However, there are some devices, that have been designed to operate with specific terminations. In this case, the worst-case attenuation value would not be entirely fair. For this type of device we evaluate the "terminated power loss" (TPL).

Many different arrangements are used to make this determination, but basically the method consists of mounting a bridgewire of the proper terminating impedance at the output of the device. Power dissipated in this bridgewire is then determined. In one method of doing this, an infrared detector, situated over the bridgewire, is calibrated in terms of bridgewire heating for a given power dissipation.

On the input end of the device it is necessary to determine the amount of power entering the unit. One commonly used system particularly at the lower frequencies is to determine the voltage and the impedance at a point close to the input interface of the device. With this information, the power passing this point can be determined. The terminated power loss in db is then computed from the ratio of the input power and the power dissipated in the termination. Figure 4 shows a block diagram of such a system, with a plot of the data from a shielded transformer device terminated in a one-ohm load.

If the device successfully passes these tests then we can proceed to investigate its effect upon dc firing pulses, its ability to dissipate adequate amounts of input power, and the amount and effect of temperature rise on the device when exposed to large input powers. These tests are either straightforward or depend on the same techniques already developed for the attenuation measurements.

3. EVALUATION OF RF PROTECTED EED's

When the RF protection is an integral part of an electro-explosive device, the problem facing the evaluator is considerably different. In the case where the explosive material can be removed and the investigator can get to the bridgewire or even remove the bridgewire he has essentially reduced the problem to the same as that of the insertion unit type just discussed and he can treat it accordingly. When this is not possible or when one wants only a final proof test on the complete item without removing any effects of the explosive charges, then the investigator has no control over the output end of the device insofar as the amount of power arriving there. It is necessary, therefore, to devise systems which can tell one precisely how much power is passing through the interface on the input side of the device. Once this is accomplished, one can devise statistical

programs based on the percentage of fires or non-fires for a given power input which will accurately define the sensitivity of the electroexplosive devices to whatever input stimulus is being applied. These techniques are the same as those already developed for evaluation with dc inputs and add no complication beyond the standard statistical evaluation of the sensitivity of explosive components.

Figure 5 shows a block diagram of a typical firing system. In theory, all of the power from the generator is transferred into the system beyond the matching section. The magnitude of the power is measured at the directional coupler. If the system beyond the matching system was relatively lossless, as is often assumed, one could then state that this measured power was delivered to the EED. Unfortunately, because of the mismatch between the impedance of the line and that of the termination much power is reflected, so that the portion of the system between the matching arrangement and the termination absorbs much of the power. It is therefore necessary to determine either the losses in the system or the amount of power delivered directly to the EED, and this must be done for each and every type of device. Several techniques are available for determining power passing specific points in the line, and while none are without their complications they can be used under certain circumstances. These techniques are fully discussed in another paper. The firing techniques are applicable to both protected and standard electroexplosive devices.

Figure 6 shows a plot of data obtained on two devices, the MARK 1 MOD 0 squib and the MARK 2 MOD 0 Ignition Element. It can be seen from the data that after correcting for system losses a substantically flat curve was obtained for firing sensitivity versus frequency up to 1000 Mc. Furthermore, calculations indicate that the level obtained is about the same as the sensitivity to long-time dc constant current pulses. Many hot wire devices show this behavior. However, one cannot

state this as an absolute rule and separate consideration must be given each device. Above 1000 Mc large variations in behavior have been observed; and while instrumentation problems become increasingly difficult at these higher frequencies there is considerable evidence that these variations are a function of the electroexplosive devices themselves.

Figure 7 shows a plot of the data obtained for another hot-wire device. In this particular case the item appeared to become less sensitive as the frequency increased up to about 3 Gc. Beyond this point there was evidence that the sensitivity increased until at 10 Gc it was the same as at the very low frequencies.

All of the data shown on the last two figures were for CW sources. When the stimulus is delivered in repetitive pulses, severe changes in sensitivity are often noted. However, the problem of predicting behavior for any pulse width or repetition rate has not yet been completely solved.

Numerous problems still exist. The wide variation in types of EED's continually present new problems. For example, exploding bridgewire types which make use of a series gap present very large reactive impedances while matching, but if the gap is broken down during the test the impedance suddenly becomes very small. Interpretation of such conditions can be very difficult. Many kinds of devices tend to arc at the higher frequencies and under pulsed power input, and occasionally the arc occurs at places other than between the leads. Some devices appear more sensitive when the power is applied between leads and case. The design of mounts strong enough to withstand many detonations and yet properly designed from an RF standpoint is sometimes very difficult. But while many problems still remain, enormous strides have been made.

4. CONCLUSION

We have attempted to give a very brief idea of the techniques now being employed to evaluate RF fixes. In theory and, to a large extent, in practice, techniques are now available to evaluate properly the RF characteristics of any RF fix over the frequency range from 20 Kc to 10 Gc and conceivably to even higher frequencies. It must be kept in mind, however, that each device may present new problems and may demand some modification of the basic testing procedures. Furthermore, each technique has its limits either in frequency, magnitude, or impedance-handling abilities; further refinement and study is required before completely routine procedures can be specified. At the present time, interpretation is difficult in some special cases and an investigator must continually question his procedures and his results to be absolutely certain that he has determined that parameter at which he originally aimed. However the basic concepts have been laid out and the path along which one can proceed is much clearer than it was three years ago. While there is still much to be done it is now possible to establish relatively precise relationship between RF stimuli and the fixes and electroexplosive devices, and through calculation to relate this to actual behavior under field conditions.

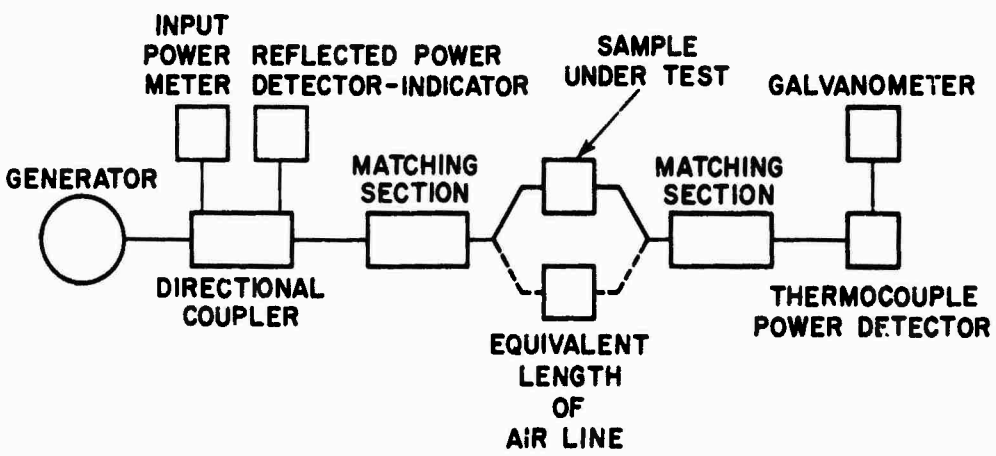

FIG. I. ATTENUATION MEASURING SYSTEM

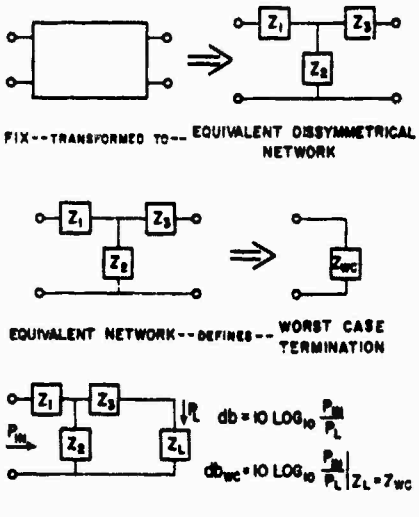

FIG. 2. DETERMINATION OF WORST CASE LOSS

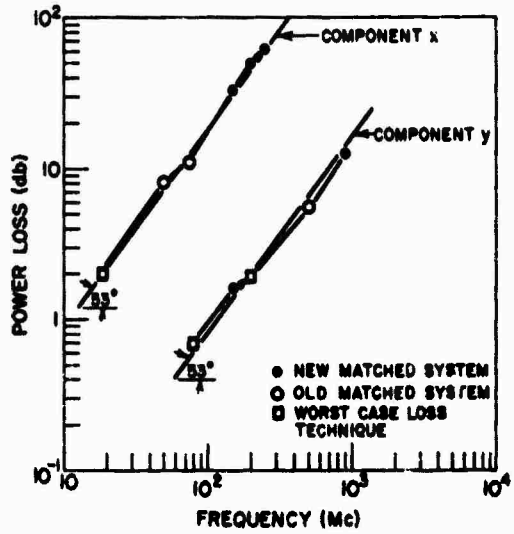

FIG. 3. TYPICAL LOSS MEASUREMENTS

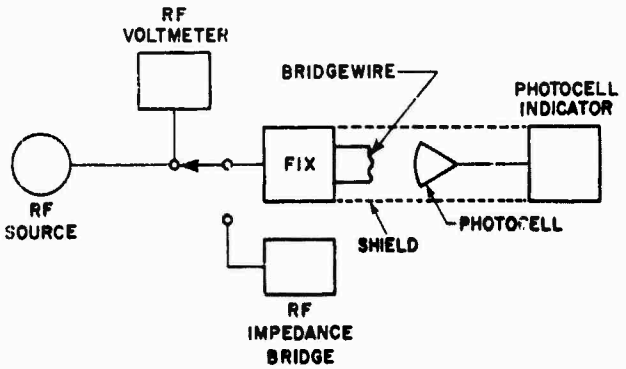

FIG. 4 (a) TERMINATED POWER LOSS SYSTEM

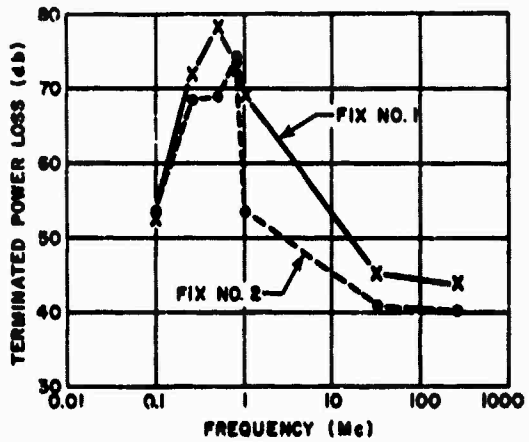

FIG. 4 (b) TERMINATED POWER LOSS MEASUREMENTS

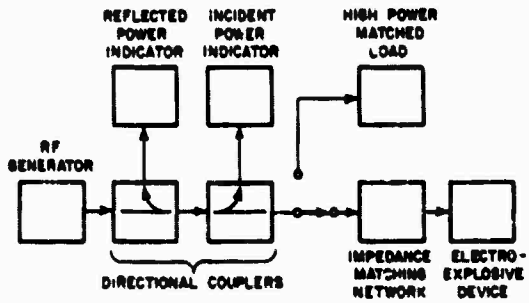

FIG. 5 BLOCK DIAGRAM OF RF FIRING SYSTEM

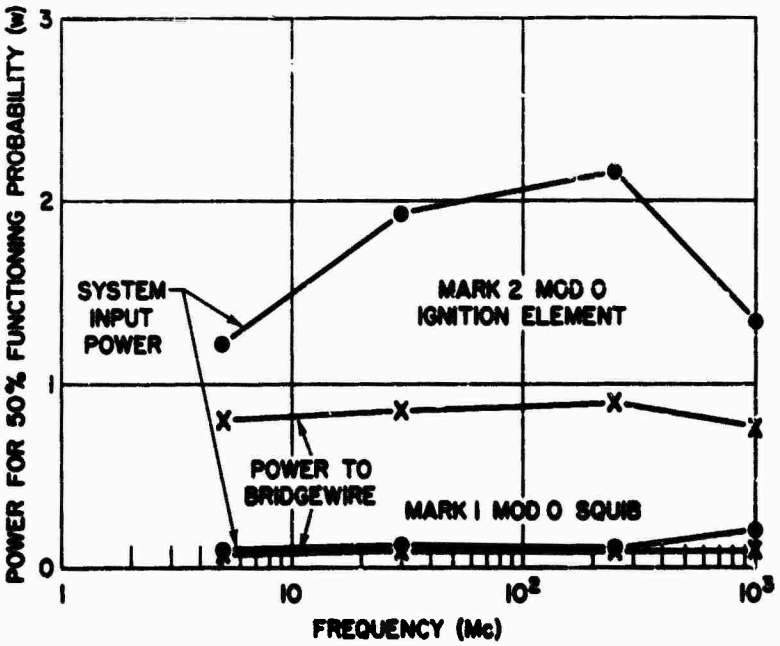

FIG. 6. TYPICAL RF FIRING RESPONSE

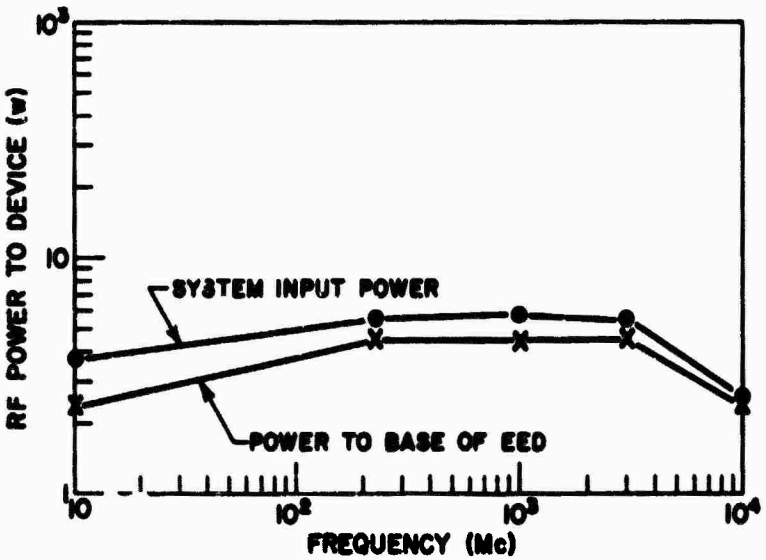

FIG.7. RESPONSE OF HOT WIRE BRIDGED EED

ABSTRACTS - SESSION III

16. Recent HERO Research Progress — P. S. Altman

New techniques for initiator bridgewire instrumentation, including a variation of the Golay cell and an infrared sensing head, are discussed briefly. Three new devices utilizing a metallic shielding effect for the prevention of electromagnetic hazards are described. A method for non-destructive testing of initiators for determination of sensitivity is presented.

17. Some Design Considerations for RF Insensitive Electroexplosive Devices — D.A. Schlachter

An RF insensitive device is defined and considerations for applying RF attenuating materials in the design of such devices are given. Emphasis is given to the nature and amount of compromise which must be made with conflicting requirements. Results of current work on special ferrites are also presented.

18. Low Pass Coaxial Relay — Raymond W. Heidorn, George V. Zimmerman

A low pass coaxial relay has been designed and prototyped which provides virtually complete RF isolation for an electroexplosive device without interfering with the efficiency of the firing circuit. It employs novel and unusual features to provide fast operation, small size, and high temperature accommodations.

19. Low Band Pass Transformer — Amnon Gordon

Radio frequency electromagnetic radiation from communication and radar transmitters has been shown to cause accidental firing of electrically initiated explosive devices. An effective solution to protect such devices has been conceived and developed in a form of a small transformer. The transformer utilizes a non-ferrous shield between the primary and secondary windings causing a reduction of the power transmitted in the stop band of frequencies and yet permits the operation of the transformer in the pass band.

20. Radio Frequency Interference Guard — Karl Kraus

The paper describes the radio interference guard, DC and AC operation, the novel design, the analytical approach of DC parameters, the DC and RF test evaluation and the power dissipation measurements. The radio interference guard is a new approach to protecting electroexplosive devices against radio frequency interferences. Attenuation of radio interference guard is accomplished by propagation through solid metal.

21. RADHAZ Proof Magnetic Coupling — Edward A. White, Jr.

The RADHAZ problem with aircraft delivered weapons is attacked by completely shielding the weapon with a conducting material. A method of communication between the plane and weapon is proposed in which low frequency magnetic fields are propagated through the shield. It is shown both theoretically and experimentally that electromagnetic radiation above 10 KC will be attenuated to a negligible value for reasonable shield thicknesses and for adequate communication bit rates.

22. A Mechanical Pulse Transformer — Roland W. Schlie

Prevention of RF inputs to a bomb fuze could be accomplished by using a shielded transformer. With the primary excited by the aircraft "intent-to-drop" signal, mechanical-electrical energy transformation produces a secondary output when the transformer is partitioned during the drop. Thus, neither electrical energy or bomb release occurring separately could cause fuze initiation.

23. RF Sensitivity of Controlled Rectifiers — Richard J. Sanford

The RF sensitivity of the silicon controlled rectifier is described, as are ways of decreasing this sensitivity. These principles are applied in a circuit which protects electroexplosive devices against low frequency radio signals but presents negligible resistance to the DC firing signal.

16. RECENT RESEARCH PROGRESS

Peter Altman

U. S. Naval Weapons Laboratory

INTRODUCTION

This paper presents some of the developments we have observed in the HERO research program. Thermal parameters of wire bridge initiators were described by the Naval Ordnance Laboratory, White Oak, Maryland, at the last HERO Congress, and continued study of these effects has yielded some new guides for the prediction of firing sensitivity. A pneumatic system for rf hazards measurement using the initiator bridgewire as a heat source will be illustrated, and an infrared detector contained within a squib envelope will also be shown. New HERO fixes which are completely adequate for the prevention of rf hazards, when used in conjunction with suitably designed, conventional initiators will be described briefly.

THERMAL PARAMETERS FOR FIRING SENSITIVITY PREDICTION

The equation $P(t) = C_p \frac{d\theta}{dt} + \gamma\theta$ describes approximately the thermal relationship that exist in a conventional bridgewire initiator. Here C_p is the heat capacity of the wire bridge, γ is the thermal energy loss "constant", θ is the temperature rise above ambient, and $P(t)$ is the time dependent power function. An additional function $\tau = C_p/\gamma$ can be specified as the cooling time constant in conjunction with the equation $\theta = \theta_o \epsilon^{-(\gamma/C_p)t}$. The time constant τ is the time interval in which the temperature falls from its maximum value θ_o, to θ_o/ϵ during cooling.

So we have:

Thermal equation with power input.

$$P(t) = C_p \frac{d\Theta}{dt} + \gamma\Theta;$$

Cooling equation with power off

$$\Theta = \Theta_o \epsilon^{-(\gamma/C_p)t}$$

yielding for the time to $\Theta = \frac{\Theta_o}{\epsilon}$

$$\tau = C_p/\gamma$$

Typical values of these parameters for the Mk 1 Mod 0 squib are:

C_p = 2.4 microwatt seconds/°C

γ = 600 microwatts/°C

τ = 4000 microseconds

Short stimulus times with $t \ll \tau$ are associated with a firing sensitivity which is primarily energy dependent. With a firing temperature of 470°C above ambient the amount of energy required for firing is then (470) $(2.4 \times 10^{-6}) = 1130 \times 10^{-6}$ watt seconds or approximately 11,000 ergs. This value agrees well with values obtained experimentally.

By an extension of this technique a number of new non-destructive tests on wire bridge initiators should be possible. For example, initiator assembly procedures could be checked. The correct application of the primary explosive, or of the bridgewire to the base plug, could be verified. Also, safe current levels for initiator testing can be predicted.

Taking a conservative value for maximum temperature, say the 165°F specified in Military Standard 304, and a low value for thermal energy loss "constant", say 200 microwatts per degree C, we have $50 \times 200 \times 10^{-6} =$ 10 milliwatts, or the power produced by 0.1 ampere flowing in a 1.0 ohm bridgewire.

A third application of thermal paremeters is for predicting the response of initiators to pulses of different lengths. The parameters C_p and γ vary from one initiator to another. The Naval Ordnance Laboratory, White Oak, Maryland, has found C_p to vary from 3.1 to 4.8 microwatt seconds per degree centigrade and γ to vary from 250 to 560 microwatts per degree centigrade in a single lot of 200 Mk 1 squibs. We expect that it will be possible through non-destructive testing to isolate from a production lot of initiators some which are sensitive to short pulses with lower than average energy, and others which will require more than the average current level of "constant current" power for firing. These groups would consist of initiators with low values of C_p and high values of γ respectively.

A study program to verify this postulate is now underway at NOL/WO. The general applicability of these concepts to initiators has not yet been shown. Thermal parameters would not, of course, be expected to apply directly to carbon bridge, conductive mix or exploding wire initiators because their mechanism of firing is different from the conventional wire bridge initiator. We anticipate that thermal parameters will furnish a powerful tool for better understanding and improved quality control of conventional wire bridge electric initiators.

INSTRUMENTATION

The Marcel Golay cell (Figure 1.) is a thermal radiation sensor which uses a gas thermometer optically coupled to an electronic readout. A flexible reflective diaphragm responds to the pneumatic pressure by physical displacement and so changes the light path in an optical system. The particular configuration developed by Randolph Macon College, Ashland, Virginia, (see Figure 2.) for HERO instrumentation uses optical fibers

for the optical-electronic coupling. Through a suitable arrangement of the glass fiber input and output bundles, the photoelectric system produces an output signal when the bridgewire is heated by electrical energy. This technique makes it possible to place the thermal sensing head (built into a Mk 1 squib case) some distance from the electronic readout system. It also eliminates the perturbation of the rf fields around the instrumented squib which would ordinarily result from the presence of lead wires. This system is capable of measuring the heating produced by 100 microwatts in the Mk 1 squib.

A second technqiue for rf hazards measurement consists of a complete infrared sensing system using optical chopping and a photoconductive detector all contained within a Mk 1 squib case (Figure 3). This system was developed to provide fast response to bridgewire heating through the use of a 1600 cycle per second optical chopping rate. It is presently undergoing evaluation tests at Dahlgren.

FIXES

Here is shown a solution to the HERO problem (Figure 4.). It consists of a metallic case which completely surrounds the initiator while also shunting the firing leads. As an electromagnetic shield it is successful, but it introduces a new problem. The initiator is greatly desensitized because the firing current flows around the initiator and through the shield. This problem can be alleviated by changing the physical configuration of the shielding enclosure so as to increase the resistance shunting the firing

signal. The resulting increase in dc shield resistance makes it possible to fire the initiator with a reasonable firing current. (See Figure 5.) Wing Commander Gray of the R.A.F. has developed an adaptation of this approach which converts the shielded volume into a small coaxial line with an iron or steel shell. This device is called the radio interference guard or RIG. It will be described in more detail after the coffee break by Mr. Kraus of Bendix-Scintilla.

A second device developed by Wing Commander Gray and using the "total shielding" approach is the low-band pass transformer. (Figure 6.) This device works by coupling low-frequency firing signals through the rf shield in a transformer coupling mode, while inhibiting higher frequency coupling. These transformers are now being made with firing signal insertion loss of less than 5 decibels. They will be described in detail later this morning by a representative of Daystrom, Incorporated.

These "total rf shield" studies at Dahlgren have also produced a third device of this kind, a "normally shielded" coaxial relay system, which will be described by an Elgin National Watch Company representative in a few minutes.

SUMMARY

This paper has presented some of the recent developments of the HERO research program. These developments include three new fixes; the low pass coaxial relay, the low band-pass transformer, and the radio interference guard, or RIG, all invented by Wing Commander R. I. Gray of the R.A.F. and developed at Dahlgren. Two new types of HERO instrumentation which are presently being developed were also described, the pneumatic fiber optic system, and the miniaturized infrared detection system. Also, applications of conventional wire bridge thermal parameters to ordnance development were discussed briefly.

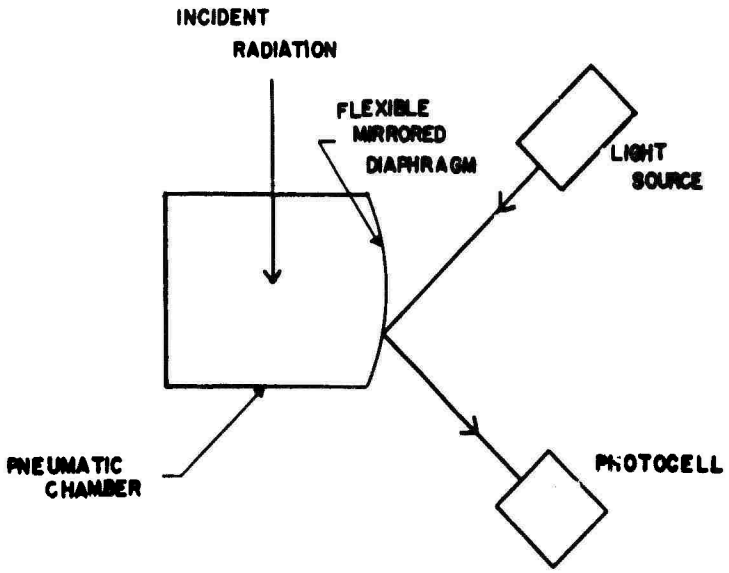

Figure 1

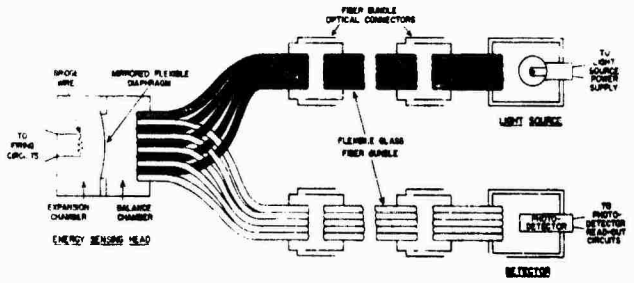

Figure 2

PNEUMATIC FIBER OPTIC INSTRUMENTATION SYSTEM

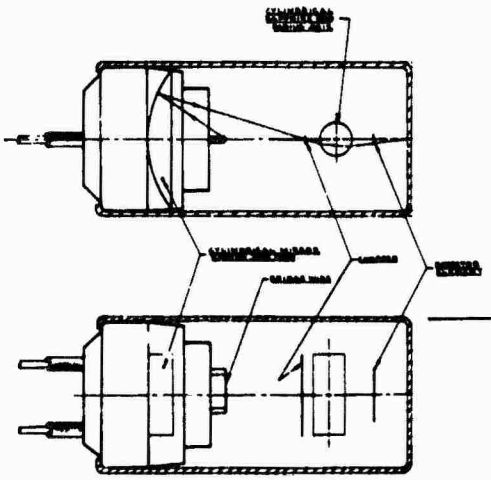

Figure 3

MINIATURIZED INFRARED DETECTOR

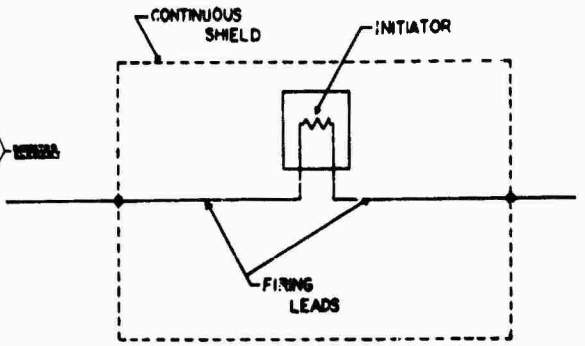

RF-PROOF INITIATOR

Figure 4

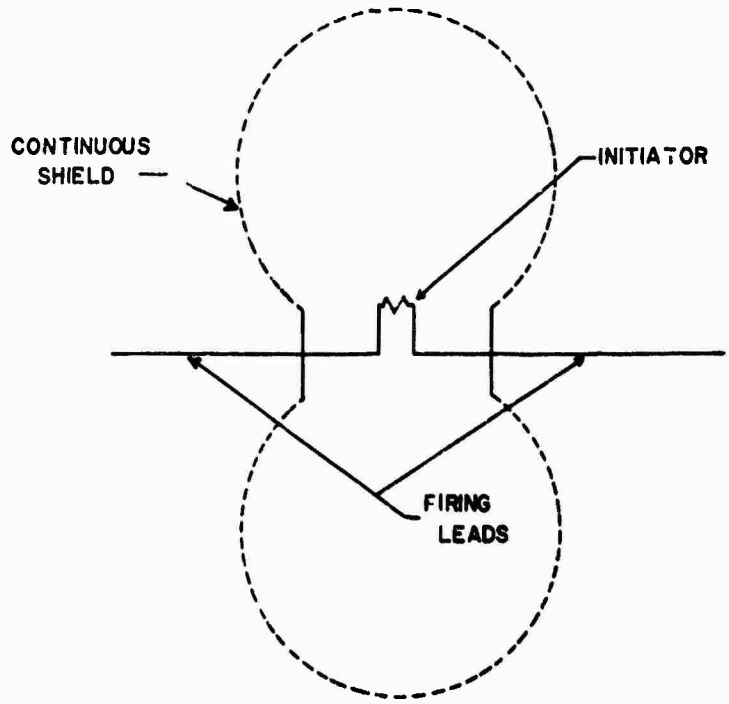

IMPROVED RF PROOF INITIATOR

Figure 5

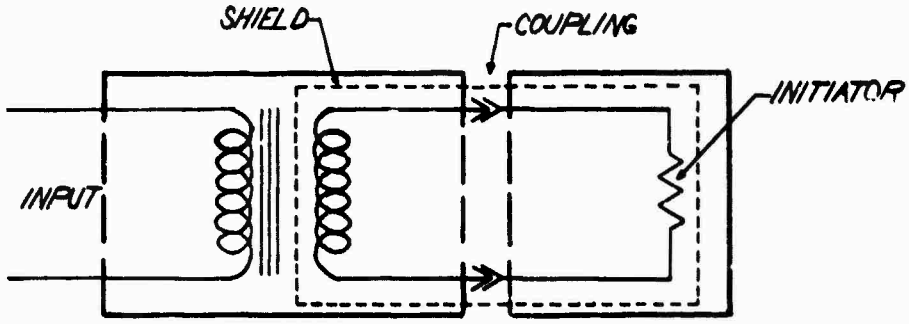

LOW BAND PASS TRANSFORMER

Figure 6

16. DISCUSSION

Mr. Kelly of The Franklin Institute asked if the heat capacity and thermal time constant were also determined non-destructively. Mr. Altman answered that these were determined by the application of low-energy pulses by a technique that was prssented at the last NERO Congress.

A Beckman and Whitley representative asked to what extent the miniature infrared dstector was dsvelcped. Mr. Altman answered that they have an operating unit with amplifiers, choppsr, oscillator and power supplies. Two sensors are built into the case. Some preliminary chscking has been completed on this system but mors is required.

It was asked if this unit will be available to industry. Mr. Altman, mentioned that Measurement Systems Inc. manufactured the unit.

Mr. Amicone, of Ths Franklin Institute commented that this non-dsstructive test method was not only feasible but also practicable. He said that The Franklin Institute has been able to apply this technique to individual initiators. Not all types have been examined at this time, but it appears that it can be applied to many different types.

A person asked what the pressure equivalent of 100 microwatts was behind the diaphragm in the Golay sensor. Mr. Altman replied that Golay found it had two properties (1) a very high sensitivity and (2) a good frequency response. He had further details for interssted persons.

17. SOME DESIGN CONSIDERATIONS FOR RF INSENSITIVE ELECTROEXPLOSIVE DEVICES

D. A. Schlachter

U. S. Naval Weapons Laboratory

INTRODUCTION

The term "rf insensitive device", for the purposes of this paper, will define an explosive device initiated by the passage of electrical current through a resistance wire, and having a bias against rf current. This bias will be accomplished by an attenuator designed to dissipate rf energy at some place other than the resistance wire. Further we will confine the discussion to attenuators which lend themselves to transmission line analysis, that is having two good conductors, such as copper wire, separated and surrounded by material specified in terms of ϵ (permittivity), μ (permeability) and σ (conductivity). These three parameters will be confined to real numbers so that the problem can be formulated in the simplest possible terms. Another simplification we can make requires some caution; it amounts to assuming perfect conductivity in the conductors. More will be said of this later, but for now we make this assumption so that we can use the plane wave solution for electromagnetic waves propagating in the attenuating material. Thus the conductors serve only as guides for the wave, and do not enter into the solution provided they are reasonably straight. Without going into the details of this solution (see for instance J. A. Stratton, Electromagnetic Theory) we note that, for a medium in which the conduction current greatly exceeds the displacement current, the propagation function reduces to:

$$\gamma = \alpha + j\beta = (1 + j)\sqrt{\frac{\omega\mu\sigma}{2}} \qquad \text{Equation (1)}$$

where ω is the angular frequency. In the commonly used engineering terminology, the real part, α, measures the attenuation of the wave. Since this is a function of frequency, we can use it to bias the explosive device against rf power.

To make this bias large, we obviously need high permeability and high conductivity, for the attenuation varies as the square root of both these quantities. But with a conducting material we will reduce even the dc power reaching the resistance wire. This forces us to an important conclusion: to bias an electroexplosive device against rf power with this type of attenuator, we must sacrifice some of the available dc firing power. This is a bitter pill to swallow but it offers a cure for some of our rf ailments.

THE BITTER PILL

The first question is: how much of our dc power must we sacrifice? The answer is of course another question: how much rf attenuation do we want? To know this we need to be able to assess the extent of the rf hazard, a big problem in itself, so let's set that question aside and consider some numerical examples.

Suppose we have a length of two centimeters in which to install an attenuator, and further that we have available a ferrite material recently developed for the Naval Weapons Laboratory by the Krystinel Corporation.[1] This material has a relative permeability of around 2000 and a conductivity variable in the range from 0.05 to 0.5 mho per centimeter. Using

[1]Krystinel Corporation, Port Chester, N. Y. with Metavac Incorporated, Flushing, N. Y.; U. S. Naval Weapons Laboratory, Contract N178-8108

equation (1) we find that this stuff can have an attenuation as high as 54 decibels per centimeter at 1 megacycle per second, or 5.4 db at 10 kilocycles, or 0 db at dc. Does this mean that we have no attenuation at dc? No, equation (1) gives this ridiculous result because we have assumed perfect conductors. The easiest way to find dc attenuation is to use ordinary circuit analysis; we just have to be careful about the range of validity of the result. Also we have to specify the resistance wire; let's say it is one ohm, since that is a fairly representative value.

So, we have two resistors in parallel, the one ohm resistance wire and the ferrite attenuator with a resistance that we can control to some extent. The dc attenuation is

$$\Sigma = 10 \log \frac{P_r}{P_r + P_a} \qquad \text{Equation (2)}$$

where P_r is the power in the resistance wire, P_a is the power in the attenuator, and Σ is the sacrifice in decibels. This formula actually defines the attenuation at any frequency but is difficult to apply when the electrical length of the attenuator becomes a significant part of one wavelength of the applied frequency; for the case at hand, 1000 cycles per second is a borderline situation. Also, now that we have specified a definite resistance wire, equation (1) has limitations, which will be deferred so that we can present Table 1.

Table 1

Attenuation at dc and at 1 Mc for a Two Centimeter Ferrite Attenuator

Σ(dc)	σ	α (1 Mc)
1/2 db	.06 mho/cm	38 db
1 db	.12 mho/cm	54 db
2 db	.3 mho/cm	83 db
3 db	.5 mho/cm	106 db

Note that by sacrificing a mere 3 db (one-half the firing power) we can get over 100 db attenuation at one megacycle. Perhaps we should stop for a minute to consider what 100 db means. It means that, to get one microwatt in the resistance wire, we must apply 10 kilowatts to the attenuator. The first explosion we hear will be the attenuator, not the black powder. This is an unrealistic example, but it emphasizes that 100 db is more than ample rf protection for all ordinary electroexplosive devices. Table I also shows the conductivity that is required in the ferrite to give the indicated attenuation. Up to the present time, .5 mho/cm is as high as we have been able to go in a high permeability ferrite, but work is continuing since higher conductivity is desirable in cases where we must have the shortest feasible attenuator. How short we can make it is the subject of the next section.

THE EFFECT OF LENGTH ON ATTENUATION

It goes without saying that, for a given attenuating material, greater length means correspondingly greater attenuation. However, suppose we have decided that we can afford to sacrifice 1 db of the firing power, for this given sacrifice, does it make any difference how long the attenuator is? That's right, it certainly does. We note that in equation (1) the parameters μ and σ must be expressed <u>per unit length</u>, whereas, for computing dc attenuation, it is the <u>total</u> conductivity that counts. So the longer unit of length we use, the greater permeability per unit length can be had with a given material, and the greater the rf attenuation. Since rf attenuation varies as the square root of these parameters, we can double the attenuation by increasing the length four times. In other

words, once we have decided how much dc we can sacrifice, we make the attenuator as long as possible. The only restrictions, besides the space available, are the range of conductivity of the attenuating material and the nature of the firing signal. This last restriction is difficult to handle analytically since it is determined by the frequency response of the attenuator-resistance wire network near the edge of the pass band where response is a complicated function of frequency. It appears that the best procedure is to define the pass band arbitrarily as the band from dc to that frequency at which the attenuation computed from equation (1) equals the dc attenuation.

For example, suppose the firing signal is a rectangular pulse one millisecond in duration, then the pass band should extend to at least one kilocycle. The attenuation of frequency components above 1 kc will round off the corners of the pulse and introduce some time delay in the explosive response. The extent and acceptability of this time delay are best determined experimentally since, as we said before, the analytical problems are all but insurmountable. A good rule of thumb is to take the reciprocal of the desired response time as the upper frequency limit of the pass band.

Table 2 shows how attenuation varies with length for the ferrite having relative permeability of 2000. We have taken the dc attenuation as fixed at 1.8 db and varied the length of the attenuator.

Table 2

Effect of Attenuator Length for a Given dc Attenuation

Length	σ	α (1 Mc)
1 cm	0.5 mho/cm	54 db
2 cm	0.25 mho/cm	76.4 db
3 cm	0.166 mho/cm	93.5 db
4 cm	0.125 mho/cm	108 db

The rf attenuation α is again computed at one megacycle and the conductivity is determined by the given dc attenuation (1.8 db).

Now let's look at the question of length in a slightly different way. Suppose that we have decided that we want the rf attenuation to be 108 db at one megacycle. Table 3 shows some of the many combinations that will yield this figure for a material with relative permeability of 2000.

Table 3

Some Parameter Combinations that Will Yield 108 db at 1 Mc

Length	σ	Σ (dc)
4 cm	0.125 mho/cm	1.8 db
2 cm	0.5 mho/cm	3 db
1 cm	2.0 mho/cm	4.8 db
0.005 cm	100,000 mho/cm	26.5 db

The first two entries in Table 3 were presented before in Tables 1 and 2. The third entry describes a material that we have not as yet been able to fabricate, as we said before, 0.5 mho/cm is as high as we've been able to go with the high permeability ferrites. The fourth and final entry represents pure iron. We see that it is very thin, and that it sacrifices a very large proportion of the firing power. The iron also puts us on shaky ground in regard to the approximation we made that our conductors

were essentially perfect conductors. The conductivity of iron is uncomfortably close to that of copper, so it is no longer valid to say that the wave is guided by the copper wires. However, this is of no consequence, since it is doubtful that we will be required to confine the attenuator to such small dimensions as 50 microns. Unless we can find a way to control the conductivity of iron, we have no choice but to use ferrites.

THE QUESTION OF FIRING TIME

Any chemical reaction, including an explosion, requires a finite time for its consummation, so there is a time delay inherent in any explosive device. But we are concerned here with electrical delay which will certainly be significant if we insist on high levels of attenuation at the low radio frequencies. For instance our 108 db attenuator will have 34 db at 100 kilocycles and 3.4 db at 1000 cycles. The effect of all this attenuation on the firing signal is best illustrated by experimental measurements. Figure (1) shows oscillograms of a 1 millisecond pulse applied to a 108 db attenuator that we constructed in the laboratory. The first trace shows the input pulse, the second the output pulse, and the third the difference between the two. Note that the output pulse is rounded off at its leading edge and, from the difference trace, that there is a delay of about 50 microseconds.

Firing time is intimately connected with the problem that we skipped over in the previous section. When we specify the resistance wire, we also specify the response of the device to the high frequency components

of the firing signal. If there is a serious impedance mismatch between the resistance wire and the attenuator, most of the higher frequency power will be reflected and lost, resulting in a greater time delay. When we speak of the impedance of the attenuator we mean of course its characteristic impedance, which is a function of frequency, permeability, and conductivity. More precisely:

$$Z = \sqrt{\frac{j\omega\mu}{\sigma}} \qquad \text{Equation (3)}$$

In some cases it may be necessary to strike a compromise between matching the resistance wire to the attenuator and matching the attenuator to the source of firing power. For instance, if the source is a discharging capacitor, a condition of series resonance could be produced at any given frequency.

ODDS AND ENDS

The discussion of matching the impedance of the attenuator to the source of firing power leads to an interesting question, that is, can we be making the situation worse for ourselves by unknowingly matching to the source of unwanted rf power? I say yes and I'll tell you why. If we assume that it makes no difference what impedance the attenuator presents to the rf source, then we must conclude that all rf source impedance are equally probable. This conclusion may be sensible for a universe of randomly oriented substances with random electromagnetic properties, but we are concerned with a fairly definite arrangement of specific matter: steel ships with antennas in air, rf generators with known output impedances, all floating (hopefully) in a sea of salt water.

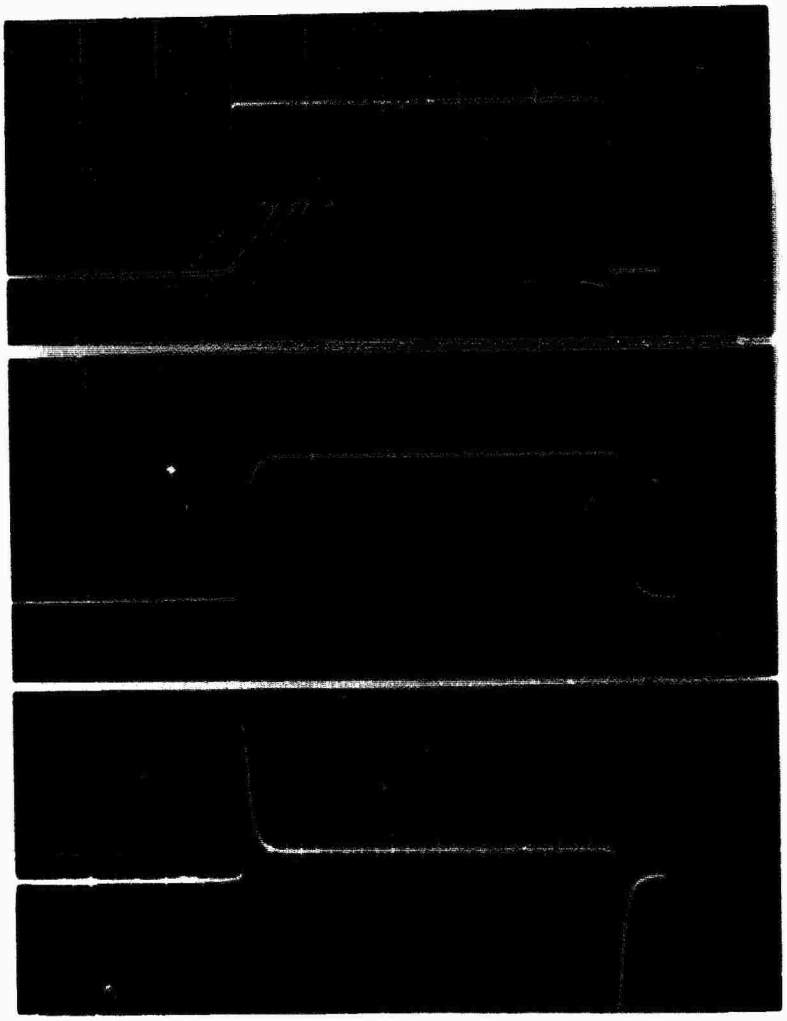

Scale: 1 centimeter = 0.2 millisecond

FIGURE 1

Input Pulse, Output Pulse, and Difference between Input and Output for an Attenuator with 108 db at 1 Megacycle

In other words, we have taken a biased sampling of the universe, and a series of impedance measurements for this sample should likewise be biased. All we need now is an enterprising genius to figure out which impedances are least probable so that we can design our attenuators to reflect as well as absorb the dangerous rf energy. Reflection is much to be preferred over absorption, since there is then no problem with heat dissipation. But so far we have had to insist on absorption in the absence of any knowledge about rf source impedances. The attenuators described in this paper are of course absorbers and are in the final analysis limited in their protective ability by the amount of thermal energy that they are able to divert from the resistance wire. This means that a heat sink is required and that the thermal conductivity of the attenuator is an important factor. However, our primary concern here is the electrical conductivity and its relation to the dielectric coefficient.

In the beginning we justified equation (1) by saying that the conduction current in the attenuator greatly exceeds the displacement (capacitive) current. This is not true of all ferrites, but is reasonably accurate for the highly conductive types we have used in our examples, notwithstanding the remarkably high dielectric coefficients normally encountered in these materials. However, as the frequency is increased indefinitely, the situation reverses and displacement current exceeds conduction current. In this situation the attenuation becomes independent of frequency and, in the cases cited here, is extremely high.

There are other, perhaps more important, difficulties with ferrites. They are hard and brittle, and lose their high permeability above certain temperatures and frequencies. Making good electrical contact to them has been another problem, but the electroplating process appears to be a good solution. Ferrites plated with copper will take solder nicely so that conductors can be installed in and around them. It is, by the way, imperative that intimate contact be made between the conductors and the attenuator, if there is not an intimate contact, much of the rf attenuation will be lost. What happens if an insulating layer is interposed between the conductors and the attenuator is discussed by others here at the Congress.

There may be some question about the interchangeability of the conductivity parameter and the conductance actually measured between the wires or conductors of the device. This is determined by the geometry. In a parallel wire system for instance, they are interchangeable if the distance between the wires is about ten times their diameter. As a general rule, however, we want to keep the contact surface area between conductors and attenuator at a minimum so as to minimize dc attenuation.

Finally, it has been assumed throughout that the only path for rf to the resistance wire is through the attenuator. This is not the case for "open" systems such as parallel wires, and provisions must be made to shield the output from the input. The shield must necessarily be metal, and can serve also as a heat sink or radiator for the attenuator. Coaxial systems are of course self shielding.

CONCLUSION

To conclude we will enumerate the design guides that we have discussed for the hot wire type electroexplosive devices.

1. For the attenuator select a material with high permeability and conductivity controllable in the range from about 10 mho/cm to 10 millimho/cm. Ferrites are in this category.

2. Sacrifice as much of the firing power as the system will allow.

3. Make the attenuator as long as possible.

4. Check to see if firing time is short enough. If it is not, compromises must be made with length, or firing power, or rf attenuation.

5. Make certain that all conductors are in electrically intimate contact with the attenuator and, for electrically "open" arrangements such as parallel wires, isolate the input side of the device from the resistance wire side with a metal shield which can also serve as a heat sink.

17. DISCUSSION

A person asked for a qualitative curve of attenuation vs. frequency for this material. Mr. Schlacter replied that The Franklin Institute has such a curve. He explained that attenuation increases with frequency until a couple of hundred megacycles is reached and then flattens.

A questioner expressed surprise at the magnitude of attenuation available. Mr. Schlacter explained that contact problems had earlier plagued the measurements. Electroplating seems to work better than silver-loaded epoxies for obtaining good contact.

A questioner asked concerning what was available for commercial firms to use. The answer was that a small firm named Meadow-Vac developed them for NWL.

A question arose concerning the frequency at which permeability drops off. It was explained that this was not measured directly. Attenuation was measured, but loss of permeability is the suspected reason for flattening of the attenuation curve.

A comment was made that as permeability drops off, the loss tangent increases. Therefore at higher frequencies there is little need to worry about permeability decreasing. The increased loss tangent compensates for this. Mr. Schlachter expressed agreement.

A questioner from Douglas Aircraft asked if there is a problem with continued application of high frequency voltage and also if there was a voltage breakdown phenomenon to be considered.

Mr. Schlacter confirmed that with all the attenuation there is going to be heat generated that must be dissipated. The material would otherwise crack or be adversely affected by accumulated heat. He said that voltage breakdown is hard to visualize in this situation because the material is shunted by a bridgewire with a resistance of around 1 ohm. The same questioner asked about the impedance of the device. Mr. Schlacter

said that characteristic impedance will be low at low frequencies and as frequency increases the material begins to look like a metal.

Mr. Steinmark of Picatinny Arsenal asked if powdered iron or ferrites offered an advantage from a technical point of view and in manufacturing. In addition he asked if all research and development is pointed to metallurgical techniques. In answer, it was etated that iron experiences great attenuation in the microwave bands and not much in the communication band where current Navy interest exists. Ferritee offer a reaeonable chance of success in the 1 to 30 Mc region. Ferrite developments are in early stagee and no squibs or detonatore have been built containing them. Powdered iron, or the other hand, has been incorporated into the Army's T24E1. This material is available right now.

In the matter of non-metals, we are faced with the problem of obtaining high permeability, which limits the choice. Iron, properly controlled, would be easier to fabricate and much better than ferrites many respecte.

Mr. Steirmark asked about polymers as attenuators. Mr. Schlacter answered that an attenuating cable study is being conducted and that considerable attenuation can be had with a cable of these materials, but considerable length and volume are required.

Mr. Sowlakis questioned the use of solder to bond these materials to a conductor. Mr. Schlacter answered that the ferrites were first electroplated with copper and then soldering is relatively easy. Mr. Sowlakis asked if the soldering technique did not dislodge the bridgewire. Mr. Schlacter said that operations are sequenced so that the ferrites are soldered first, followed by bridgewire operations. He added that no EED has been built using this technique to the best of his knowledge.

A person from NOL White Oak commented that some real systems problems that required retrofit fixes were studied about two years ago. He asked if we have fixes available now. Mr. Schlacter answered no.

18. LOW PASS COAXIAL RELAY

Raymond W. Heidorn and George V. Zimmerman
ELGIN NATIONAL WATCH COMPANY
Research and Development Division
1200 Hicks Road
Rolling Meadows, Illinois

INTRODUCTION

As a result of studies made under the HERO Program, a coaxial relay of novel design has been conceived. This coaxial relay will provide virtually complete Radio Frequency isolation up to the instant of operation. It will also prevent premature functioning by Radio Frequency energy above its pass band characteristics. This novel design is the invention of Reginald Gray, Wing Commander of the RAF. Figure 1 shows his coaxial relay.

Figure 2 shows the construction of this coaxial relay. The operation is essentially that of a solenoid. It consists of an operating coil wound on a brass bobbin. Inside the bobbin is the contact system which comprises a small iron poppet valve, the moving contact, similar in shape to those used in combustion engines. The valve seat is a brass block which is an integral part of the ID of the bobbin. The moving contact is retained in contact with the seat by a spring which also serves as a conductor between the moving contact and the coaxial input lead. The valve stem and spring are insulated from the valve housing. The fixed contact is a soft iron rod which is positioned near the valve. It is also insulated from the bobbin.

The operation is as follows (See Figure 3, Schematic): The relay is effectively a single pole double throw action. The relay is placed in the line

between the power source and the load, which in this case is the electro-explosive device (EED) and would be located as near to the EED as practical for maximum effectiveness. When the contacts are in the normally closed position, the EED is isolated mechanically by the plunger or moving contact being held against the concave seat or barrier. This then has the positive effect of shorting the terminals of the EED.

If the line to the relay acquires spurious high frequency energies above the pass band, this energy will be dissipated by the reactance of the relay at low frequencies and by the skin effect of the brass bobbin at the higher frequencies. The attenuation of the higher frequencies therefore increases by the square root of the frequency or $R = K\sqrt{f}$.

When a pulse of direct current is passed through the coil with sufficient magnitude and duration to cause the plunger to move toward the fixed contact, the short across the EED is removed and direct contact from the EED to the power source is then made.

The main effort of Elgin was to carry the development of the original relay as left by Wing Commander Gray to a point where it is a practical production device.

This would necessarily include a study of the theory and limitations of the existing device. Other considerations and areas of investigation were as follows:

1. Material characteristics to attenuate radio frequencies.
2. Optimize size relationships.
3. Coil winding methods.
4. Plating and deposited coatings.
5. Contact materials.
6. Spring materials.

The specifications in general were as follows:

1. Operate Time:

The operate time should be one (1) millisecond so as to be compatible with most current weapons.

2. Sensitivity:

This requirement was necessary so that the firing circuits would not "see" the additional component and would not effect the firing of the weapon.

3. Size:

The relay had to be as small as practical since there are installations where space is at a premium.

4. Attenuation:

The relay has to attenuate and dissipate at least 10 watts of energy in the radio communications and radar frequency range.

5. Switching:

The relay has to be able to deliver to the HED 100 watts for one (1) millisecond. (Contact current range will be from 1.5 to 20.0 Amperes D.C.)

6. Voltage:

Normal aircraft power operation of 28 V DC.

7. Environment:

The general and applicable requirements of MIL-E-5272.

8. Duty Cycle:

The relay is expected to make a reliable electrical contact for one operation at its maximum contact rating.

9. Construction:

The relay will be hermetically sealed with a four (4) pin input connector and a two (2) pin output connector. The four pin connector is to be used rather than a three (3) pin so that there will be flexibility in wiring the fix into the circuit.

DESIGN APPROACH

From our past experience, we have found that relays using a permanent magnet for biasing have a much faster operate time than those using a spring for biasing. There are two main reasons for this faster operate time. One reason is the principle that like poles repel. The second is that the restraining force is removed as you move away from the permanent magnet. Because of these principles, our first design concept was a permanent magnet biased coaxial relay. Figure 4 shows this basic design. With the relay in the unenergized position, the magnet is held against the seat by the permanent magnet. When the coil is energized, its magnetic field opposes the field of the permanent magnet driving the plunger forward as is shown in Figure 5. There is an additional electromagnetic attraction at the contact face. Figure 6 shows the coaxial relay in the energized position. It operated satisfactorily except that the plunger would stick in the energized position even when the coil was de-energized. Examining the magnetic circuit, we found that we had a low reluctance magnetic path around the coil through the tip and back to the other side of the magnet as shown in Figure 7. With this path there was too little permanent magnet attractive force at the seat to return the plunger to its original position. To eliminate this it was decided to use two independent magnetic circuits as shown in Figure 8. This would have less repelling force

than the first design when the unit is energized, but the effect of the unimpeded movement of the plunger will still enhance the operate time. Figure 9 shows the separate magnetic circuits in the energized position.

Concurrently, we carried a parallel development of a spring biased relay which was more similar in design to the original invention. These were both to be brought up through the final testing so that in the event that the unusual high frequency test requirements caused a failure, we would have a back-up. If both relays fared equally in a technical sense, other considerations such as relative cost, material availability, and ease of production will be evaluated.

With these design principles in mind, it was necessary to determine how big the relay should be; type of magnetic materials to use; type of insulation needed; and contact material necessary.

DESIGN DETAILS

Size:

To determine the size of the coaxial relay, we had to consider two (2) important facts: 1 - The relay must be small enough to be used in somewhat limitied space; 2 - It also must be large enough so that it can dissipate ten (10) watts of RF power. Because of available connectors, it was decided to make the relay one-half ($\frac{1}{2}$) inch in diameter. This, we felt, would handle the ten (10) watts of RF Power. The proportions of the coil, that is, the ratio of coil length to mean coil diameter will affect to some extent the efficiency of the electromagnet. For a short electromagnet such as the coaxial relay, the optimum proportion is obtained with a length of about one and one-half ($1\frac{1}{2}$)

times the mean diameter. Thus, it was decided that the coil length should be one-half ($\frac{1}{2}$) inch.

Magnetic Material:

In the past, we have conducted extensive studies into different types of magnetic materials. We have found that Allegheny Relay Five Iron which is a silicon steel is one of the best materials to be used in this type of application. Relay Five Iron has very low residual magnetism and a very high saturation point. A nickel iron material such as 4750 has a low saturation point and would tend to give a slower operate time. Tests were conducted on the relay to compare 4750 iron and Relay Five Iron. The results of these tests indicated that of the two, Relay Five Iron is the appropriate magnetic material to use.

Contact Material:

The contacts on the Coaxial Relay must be capable of carrying high current and also must maintain low resistance. Some contact materials develop high resistance because of the formation of inorganic films such as oxides, sulfides and carbonates. Noble metals in the platinum group develop high resistance from organic films. Silver is subject to inorganic films but not to organic films. Gold is not subject to organic or inorganic films but has poor wear characteristics. A contact of silver with a gold protective coating will give the relay high current capacity and also maintain low resistance.

Insulation:

Dielectric requirements for the relay are such that it will withstand 1000 volts between the coil and the bobbin and 500 volts between the contacts (plunger and stop) and bobbin. From our experience, we have found that a coating of Teflon on the wall of the bobbin will withstand a 1000 volt breakdown test. As Teflon is also a good bearing surface because of its low coef-

ficient of friction, we felt that it would be an excellent material to use on the plunger to insulate it from the bobbin. Because the plunger had to have some areas which had to be insulated and some plated for good contact a better method of insulating had to be found. The small size of the bobbin made it impractical to try to insulate its ID with Teflon. It was felt that an aluminum bobbin instead of the brass bobbin would not change the attenuating characteristics of the relay. Aluminum bobbins can be insulated by anodizing.

It was found that standard anodizing procedures would not produce an insulation that would meet our dielectric requirements. A special hard coat anodized as done by Sanford Aluminum Processing Company of Chicago gave us the dielectric requirements necessary on the ID of the bobbin but this was only after we changed materials. We started our investigation using a series 20 aluminum which contains a high content of copper. This copper causes voids in anodizing giving it a poor insulating quality. A pure aluminum such as 1100 does not have these voids and will give excellent results but is very poor for machining. 6061 aluminum which does not contain any copper and is not difficult to machine can also be used. This gave us the 500 volt breakdown requirement between the plunger and the bobbin but not the 1000 volt between the coil and the bobbin, so it was decided to maintain a Teflon coating in the coil area of the bobbin.

P. M. Biased Coaxial Relay:

Figure 10 is our original design for the permanent magnet coaxial relay. It has the barrier across the output end and the open contact inside the coil. The permanent magnet material for biasing the relay is Alnico 6. Alnico 6 was picked because its field strength can be adjusted easily and thereby adjusting the holding force on the plunger. Reviewing the demagnetizing curve for Alnico 6, it can be noted that its field strength can be reduced gradually as

relay with the brass bobbin cuts off at the lowest frequency. With an aluminum bobbin, it cuts off at a slightly higher frequency, but the spring type with a brass bobbin cuts off at a still higher frequency. In all three cases, this cutoff point is well within the audio frequency range and will not decrease the effectiveness of the relay.

High Temperature:

Temperature checks were made on the relays with 4 KC impressed across the coil and it was found that with 10 watts the relay temperature was approaching 500° F. This led to an investigation of high temperature magnet wire.

Ceramic insulated magnet wires were investigated. They have temperature rating of 650° to 1000° F. One disadvantage is that the ceramic has poor moisture resistance and the coils would have to be encapsulated. Another disadvantage is its cost. Even in large quantities the cost for the magnet wire alone would be $5.00 per relay.

We also investigated the use of anodized aluminum magnet wire. It has a temperature rating of 1000° F. Disadvantages of anodized aluminum wire are that it requires special soldering techniques, breaks easily and has high resistance. Its cost per relay would be approximately $1.00.

Teflon insulated magnet wire has a temperature rating of only 400° F and its cost per relay would be approximately $.20. This could be used if the temperature of the relay is decreased when the case and connectors are added but most magnet wire manufacturers do not recommend its use. They recommend using ML insulated magnet wire. ML insulation is a polyimid resin that has the highest thermal capabilites and chemical stability of any available organic film insulation. Its temperature rating is 465° F and its cost per relay would be less than $.05. Unless the final temperature of the relay is higher than anticipated, ML insulated magnet wire will be used on the relay.

As the relay's maximum temperature is approaching the upper limit of Teflon, it was necessary to investigate other types of insulating materials. One promising insulating material was Doryl. This is a new thermosetting resin made by Westinghouse. While it is considered a Class "H" material, the tests have proven that it is mechanically stable up to 575° F range. Other advantages of Doryl are its high bonding strength and low cost. Tests are being conducted to decide whether Doryl is equal or superior to Teflon.

Spring:

For the spring biased coaxial relay it is necessary that the spring material maintain its force for extended intervals even at high temperatures. Elgiloy, a cobalt nickel alloy manufactured by Elgin National Watch Company, can satisfy these requirements. Elgiloy was developed by Elgin to solve the problem of mainspring breakage that plagued the watch industry. After years of testing, Elgiloy was used for the original "unbreakable mainspring". Tests have proven that Elgiloy retains its power over 275% longer than carbon steel and even retains it at temperatures up to 1000°F. It is also non-magnetic and has excellent corrosion resistance. Due to these excellent properties, Elgiloy will be used as the spring material.

Hermetically Sealing:

The coaxial relay is expected to operate satisfactorily in atmospheres of Salt Spray, High Humidity and Dust. Therefore, the relay contacts should be protected from this environment by hermetically sealing. Two methods are being considered for sealing the coaxial relay. They are soldering and a heatless seal method.

The soldering or brazing method of sealing the relay is quite common. It's disadvantage is the fact that gases are created by the heating and will cause contamination of the contacts. This lowers production yield and also

reduces the quality of the relay. In addition, such processing methods involve extensive fixturing and time consuming operations to produce a good seal.

The heatless seal is a crimping method of sealing the unit which has been developed by Standard Steel Company for the use on transistors. This seal will meet and exceed Federal Specifications MIL-STD-202B, Method 107a. Figure 14 shows this method of sealing. The important element in the heatless seal is the unique configuration of the caps seal rings that first bottoms in the annular groove in the mounting base and then curled up under applied mechanical pressure as displaced base metal is pressed in over it. The seal is enhanced by the spring-like seal ring's attempt under residual stress to return to its original form. This method of sealing will require extensive testing before we will consider using it on the relay. While the first coaxial relay will be sealed by brazing, we feel confident that this seal can be developed and will be later incorporated into the design of the coaxial relay.

CONCLUSION

Figure 15 shows the latest design of the magnetic biased coaxial relay. You will note this design carries two independent magnetic circuits as discussed previously. So as not to load the plunger and increase operate time a spring was used to connect the plunger to the connector. It has been so designed as to put minimum tension on the plunger and still be capable of carrying the current necessary to detonate the weapon.

Figure 16 shows the latest design of the spring biased coaxial relay. The spring used on this relay is similar to the one used on the magnetic relay except that it is under tension to hold the plunger against the seat.

Relays of both designs have been sent to Franklin Institute for testing to insure that the relay will attenuate the RF as so intended. Figure 17 shows a completed Coaxial Relay. In conclusion I would like to say we believe we have a coaxial relay which will provide you complete RF isolation up to the instant of operation. It will also prevent premature functioning by RF energy above the band pass characteristics. It is small size and should be easy to insert in any existing weapons or any new design. It is a sensitive unit and requires comparatively little current so that if it is inserted into the firing line of an existing weapon, it will not effect its operation. Also it will not effect the operation because of its fast operate time.

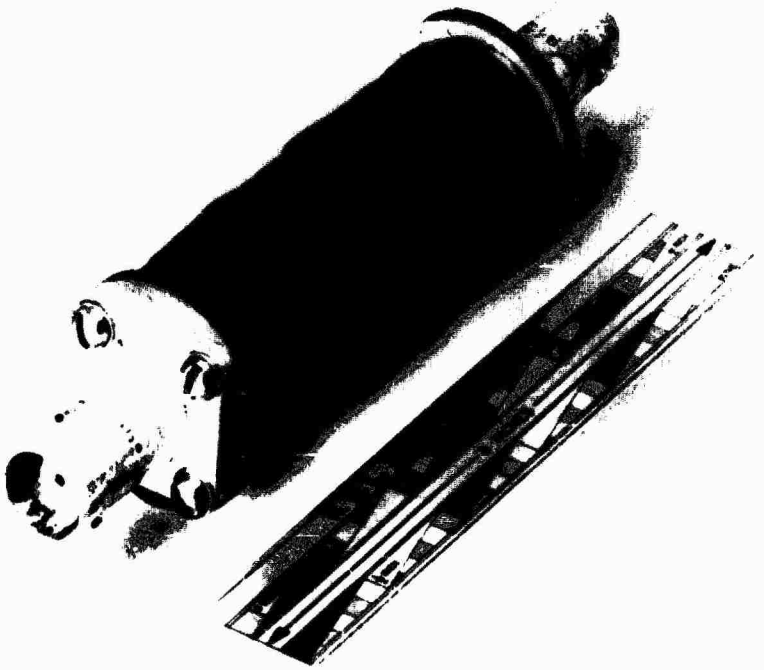

Figure 1. Original Coaxial Relay

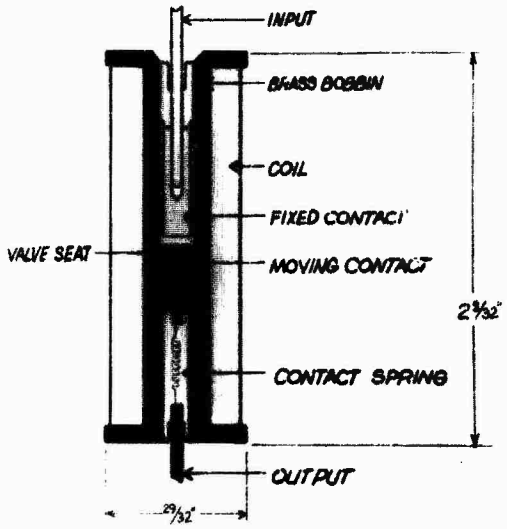

Cross Section of Original Coaxial Relay

Figure 2

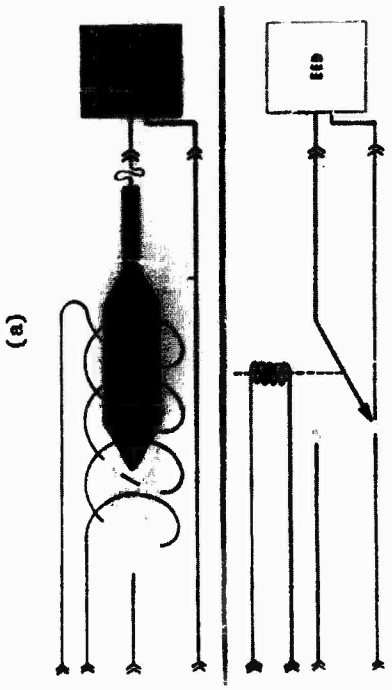

Schematic

Figure 3

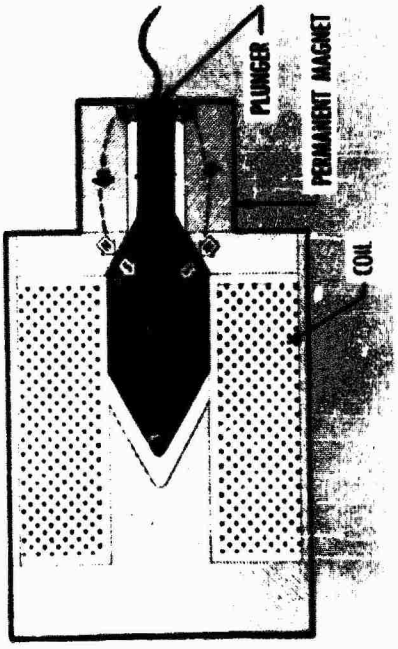

Unenergized Condition

Figure 4

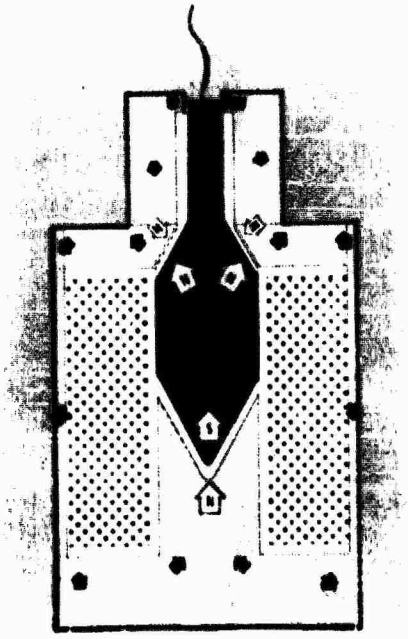

Energized transient condition

Figure 5

Energized Condition

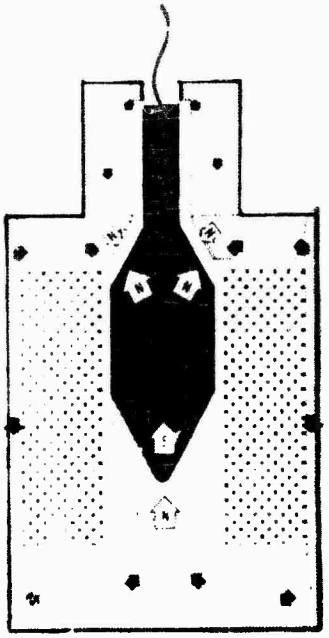

Figure 6

Parallel magnetic path

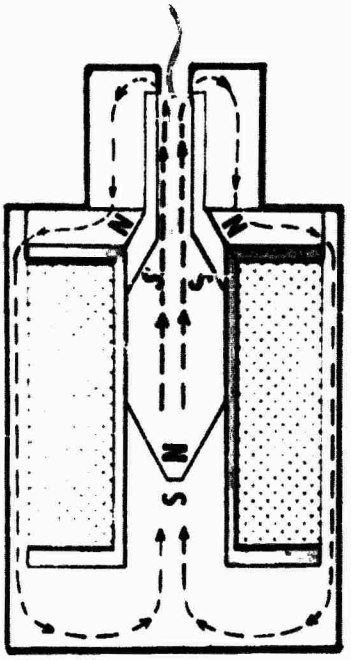

Figure 7

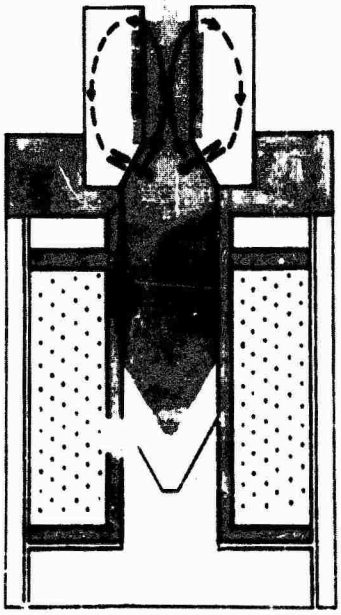

Unenergized relay with separate magnetic circuits

Figure 8

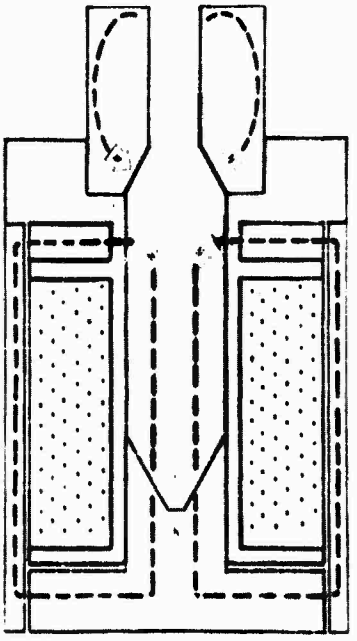

Energized relay with separate magnetic circuits

Figure 9

Magnetic Biased Coaxial Relay

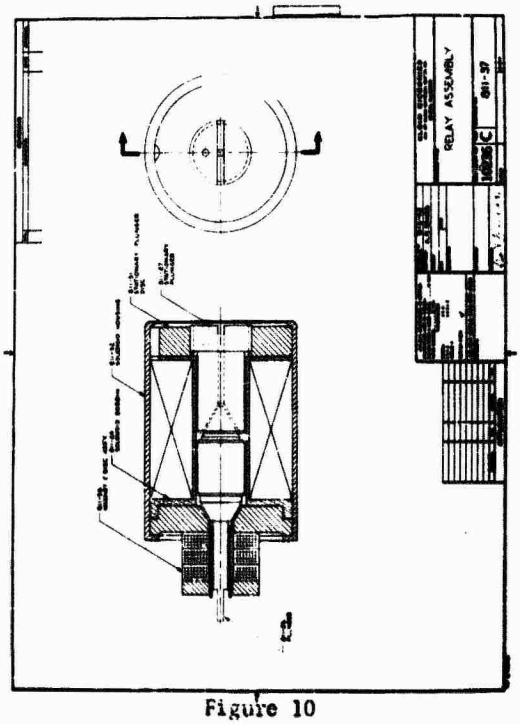

Figure 10

Spring Biased Coaxial Relay

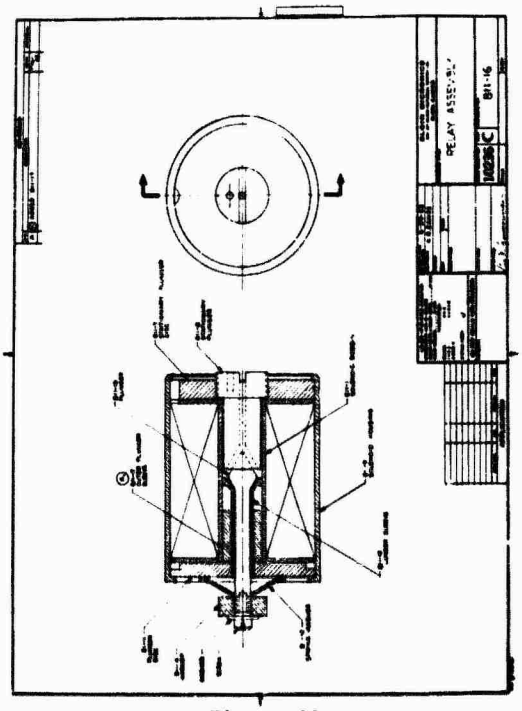

Figure 11

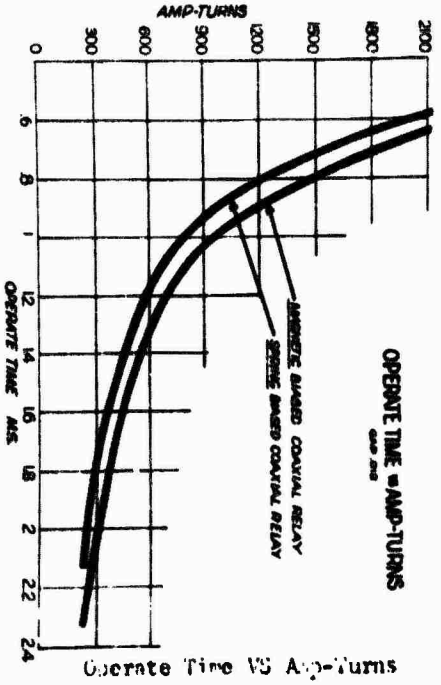

Operate Time VS Amp-Turns

Figure 12

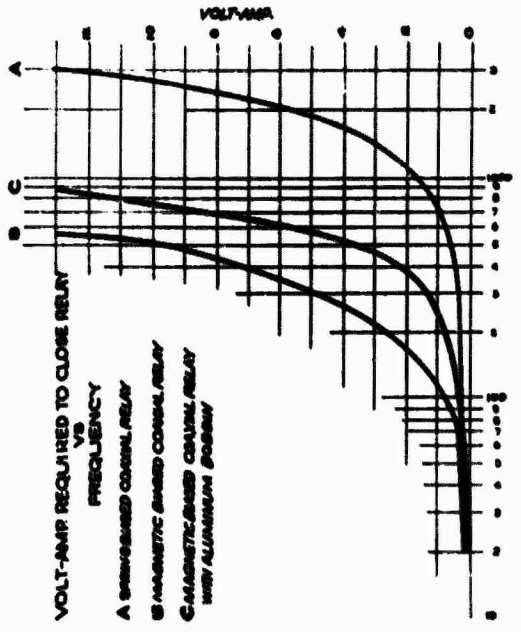

Volt.-Amp. Required to Close Relay VS Frequency

Figure 13

Heatless Hermetic Sealing

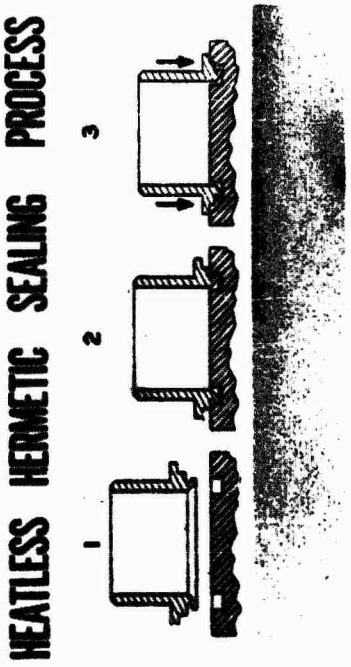

Figure 14

Magnetic Biased Coaxial Relay

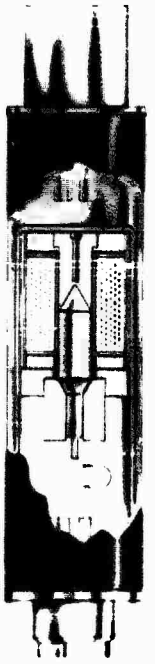

Figure 15

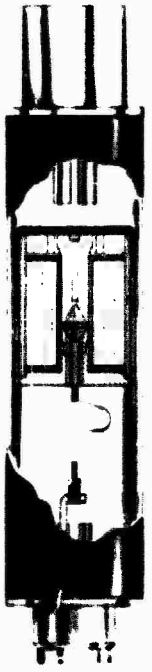

Spring Biased Coaxial Relay

Figure 16

Coaxial Relay

Figure 17

19. LOW BAND PASS TRANSFORMER

Amnon Gordon

Weston Instruments and Electronics

Division of Daystrom Incorporated

Newark, New Jersey

SUMMARY

Radio frequency electromagnetic radiation from communication and radar transmitters has been shown to cause accidental firing of electrically initiated explosive devices. An effective solution to protect such devices and other systems has been conceived and developed in a form of a small transformer.

The transformer utilizes a non-ferrous metal shield between primary and secondary windings which causes a reduction of the power transmitted in the stop band of frequencies. The operation of the transformer in the pass band of frequencies, however, is not impeded.

INTRODUCTION

Systems utilizing high power r-f generating equipment are being used in ever increasing numbers. The power generating equipments present a difficult problem to the weapons designer. It has been established that unintentional radiation from radio frequency transmitters can cause the

actual firing of electrically initiated explosive devices or damage their mechanism. Protecting ordnance devices from these and other spurious energies is therefore of paramount importance. The simplest and most direct solution to the r-f hazard problem is to shield the entire system. In most cases, however, this is highly impractical if not virtually impossible. Another solution is to apply restriction at the source of the spurious energy. This is undesirable because it might curtail the operation of the power source.

Most electrically initiated explosive devices (EED) and other "loads" are contained in metal cases, and, except for the r-f leak where the leads enter, provide their own shielding. These leaks may be stopped by the use of suitable r-f rejection devices which can be inserted into the line just before the EED and which will reflect or absorb most of the r-f energy. Existing devices of similar functions are limited to specific conditions only. An ultimate device is one that can be used for general applications and, hence, becomes a standard item for the weapon designer. A device of this nature is the Low Band Pass Transformer, which has been conceived, developed and successfully tested for the specific purpose of protecting electrically initiated explosive devices.

Under the U.S. Navy Hazard of Electromagnetic Radiation to Ordnance Program, the Low Band Pass Transformer was conceived by Wing Commander Reginald I. Gray of the Royal Air Force. The invention of Com-

mander Gray, as stated in U.S Navy Case No. 33459, pertains to a small power transformer designed to attenuate r-f power without affecting the operation of the transformer in the pass band of frequencies.

"The primary object for which it has been designed is to provide adequate protection in a-c firing circuits of weapon electroexplosive devices (EED) against spurious induced energies from electromagnetic and electrostatic fields".

LIMITATION OF EXISTING DEVICES

The general solution to the Hazard of Electromagnetic Radiation to Ordnance requires protection at all frequencies above a nominal frequency in the region of 10 to 100 kc/s. It is also realized that the impedances of the spurious electromagnetic generators may have any value from a few tenths of an ohm to megohms and will generally be complex. Existing devices that may exhibit characteristics for the protection of systems against spurious energies do not satisfy the above requirements. Some of the devices and their limitations are listed below:

Low Pass Non-Dissipative Electric Filters:

These filters generally comprise a combination of coils and capacitors, the performance of which depends upon their ability to cause appreciable, impedance mismatch between generators and loads of specified impedances, thereby resulting in purely reflective attenuation. They are useless in this application because the generator impedances cannot be specified. At some particular frequencies, input impedance of the filter can be matched by its

conjugate impedance and the filter becomes a matching section. In this case, all the power will be dissipated in the load. Commercial practice is to use 50 ohms impedances in the measuring system for insertion loss. Hence, a filter with a high insertion loss in a 50 ohm system might have practically no loss in a system of higher or lower impedance.

Low Pass Dissipative Electric Filters:

These filters are a combination of low pass non-dissipative electric filters and attenuators. They may be used under closely controlled conditions. At some frequencies, the filter may exhibit band pass characteristics and may yield a net insertion gain if the reflective insertion gain is greater than the dissipative insertion loss. Other band pass characteristics may result from changes in component impedance with variation of frequency. Capacitors may become inductive, inductances may be reduced by self-capacitance, and resistors may become reactive. Furthermore, a filter that provides real attenuation at a particular frequency, when using a low impedance load, may give a significant gain when a high impedance load is used.

Electro-mechanical Filters:

(e. g. Piezo-electric, mechanical vibration devices, etc.). These filters usually have good low frequency band pass characteristics, however, they do not provide the required stop band characteristics.

Broad Band Attenuators:

These devices are useless for this application because they lack the re-

quired low pass characteristics.

Conventional Transformers:

Conventional transformers deliver power over a wide range of frequencies. Their efficiency falls off rapidly at high frequency because of iron and copper losses. Unfortunately, capacitive coupling between windings causes power transfer at the higher frequencies, particularly in the symmetric, co-axial mode in which the driving voltage appears between line and shield.

DESCRIPTION OF THE LOW BAND PASS TRANSFORMER

The low band pass transformer which was developed for the Naval Weapons Laboratory has been found to be an effective component to protect electrically initiated explosive devices from spurious energies.

During the pass band mode of operation, the transformer functions in a conventional manner with reduced efficiency due to the proximity of the windings and size and composition of the ferromagnetic parts. At higher frequencies, the shield attenuates the magnetic flux produced by the stop band signals, preventing any coupling between primary and secondary windings. The attenuation increases with frequency in accordance with the law of induction described below.

The attenuation of the field of the primary winding in passing through a non-magnetic shield follows the well known law of propagation in metals. The general theory deals with the propagation of the electro-magnetic wave in

a continuous medium.

The electro-magnetic characteristics of the shield with various frequencies follows the law of induction of current passing through a medium at depth z. This can be expressed as:

$$i = i_o e^{-\sqrt{\frac{wuc}{2}}\, z} \quad e^{j\left(wt - \sqrt{\frac{wuc}{2}}\, z\right)}$$

Equation 1

Where:

i_o = the current just inside the boundary

u = permeability of the medium (henry/meter)

$w = 2\pi f$ (f=cps)

c = conductivity of the medium (mho/meter)

The second exponential term represents the periodic variation of the current, the second term in the bracket is the phase angle of the current at a depth z with respect to the surface current i_o.

The first exponential term indicates the damping or decrease in current amplitude with an increased depth z. The damping will also increase with the frequency. Since magnetic flux obeys the same equations as the current, the induction inside a non-magnetic medium will also decrease as the frequency increases.

The analysis above well demonstrates the theory behind the Low Band Pass

Transformer that is, for a certain shield thickness, the attenuation at low frequencies may be nil, but as the frequency increases, the attenuation will increase rapidly.

Figure 1 illustrates the detail construction of the low band pass transformer. It is rated for continuous operation at 10 watts in the stop band of frequencies. The transformer is hermetically sealed and measures 1.38 inches in diameter by 2.0 inches long.

The device comprises the following parts:

Ferromagnetic Core:

The material and construction of the core must produce minimum eddy current losses during the pass band mode of operation. A laminated construction would have resulted in high efficiency, but because of the laminations, shielding the primary and secondary windings is not possible. A study of different core materials, such as Mu-metal, Supermalloy, Alnico, Silicone Steel, Hiperco, Cold-Rolled Steel, Iron, etc., indicated that the more ductile metals exhibit the best characteristics. The size of the core has some affect on the performance of the transformer. A shorter core provides a shorter path for the magnetic flux, thereby decreasing the amount of losses due to eddy currents. Slotting the core also reduces eddy current losses, however, the reduction was only slight, and did not warrant the increased expense involved. In addition, at some point along the core length, the slots will have to be discontinued to pro-

vide complete shielding between the windings.

Non-ferromagnetic Metal Shield:

The transformer core must not permit any flux established by the r-f stop band signals from leaking the secondary winding because of the attenuation and losses produced by eddy currents and magnetic hysteresis. The non-ferromagnetic shield must protect the secondary winding from the magnetic flux established by the stop band excitation. The shield performs this function by attenuating the flux thus avoiding any coupling with the secondary coil. While protecting the secondary winding from r-f signals, the shield must permit the maximum magnetic flux to circulate between the windings in the pass band of frequencies. It is of utmost importance that the shield be mechanically secured to the case and the core in order to provide complete shielding between the input and the output signals. A non-ferromagnetic material must be used to avoid shortening the magnetic circuit between the windings. From Equation 1, it is evident that the attenuation is a function of the permeability, conductivity, and thickness of the shield. Different shield materials will require different thicknesses in order to yield the same attenuation. The final selection of the shield depends largely on the feasibility from a metallurgical and metal-working point of view.

The importance of the non-ferrous shield in the construction of the transformer is well demonstrated by comparing the two curves in Figure 2. The transformer containing the non-ferrous shield exhibits similar characteristics in the pass band to the transformer constructed without the shield.

In the stop band, the attenuation of the transformer without the shield increases slightly and then starts to fall off, due to capacitive coupling. The attenuation of the transformer containing the shield, however, increases steadily. Figure 3 demonstrates the variation in the performance of the transformer for various shield materials having the same thicknesses. The material having the lowest conductivity exhibited the highest attenuation. This is expected since the conductivity is inversely proportional to the depth of penetration, as shown by Equation 1. For all practical purposes, the permeability of these metals is 1.0.

Case and Covers:

The case and covers of the transformer provide r-f shielding for the secondary winding in the stop band of frequencies. They also furnish a magnetic path for the flux produced by the primary winding in the pass band. Although ductile metals, which were mentioned in the discussion of the core, provides the necessary charactsristics, the final selection of the material depends on how easily it can be assembled, formed, brazed, etc. The same material was selected for the construction of the core case and covers, in order to provide a homogenous path for the magnetic flux.

The surface of the transformer must be sufficiently large to conduct the heat produced by the losses. The overall size was also a function of the coils dimensions.

Primary and Secondary Coils:

The design of the coils is mainly a function of the input and output requirements. The impedance of the primary windings determines the amount of power received from a fixed voltage source. To obtain the maximum efficiency, the impedance of the secondary winding must match the load resistance. The turns ratio between the primary and secondary coils must yield the maximum transformation of power in the pass band. The wire used to wind the coils was of a size to withstand the continuous current in the stop band, and contained the proper insulation to withstand continuously the temperature resulting from the losses as well as the ambient temperature. The efficiency of the transformer in the pass band depends largely upon the flux linkage between the windings. Unfortunately, it is impractical to wind the coils concentrically and still maintain shielding between the windings. The minimum clearance between windings will produce the greatest resultant efficiency. Within physical limitations thinner coils having larger diameters produced better coupling and higher efficiency at the pass band of frequencies.

Connectors:

The device cannot be useable unless provisions are made to permit it to be easily connected to the system. To accomplish these requirements, the transformer is terminated by two hermetically sealed glass connectors. The input connector is a standard type which mates a standard cable jack. The output connector is a special r-f type which also mates a standard r-f cable jack. The r-f connector insures the complete shielding of the system from r-f energy, providing proper shielded cables and connectors are used to

deliver the output signal to the load.

Characteristics and Properties:

Some characteristics of the transformer are demonstrated in Figure 4 and 5. The power frequency characteristics of the low band pass transformer for 45 watts of input power are shown in Figure 4. The solid line curves represents the total power loss and the input and output power, while the dotted line curves represent the core losses and the copper (i^2R) loss. The copper loss is high at low frequencies, due to the high input current. At high frequencies, the current is reduced considerably and with it the copper loss. The core losses exhibit the opposite characteristics since they are a function of the frequency rather than the current. It can be seen that the minimum losses occur at 400 cps approximately; the frequency at which minimum attenuation is required.

Referring to Figure 5, it may be of interest to note that this type of transformer has the inherent characteristics shown in the pass band. The frequency of minimum attenuation may be varied slightly between 200 and 1000 cps, but the general shape of the curve will remain the same.

Density vs core loss characteristics and frequency vs core loss characteristics are shown in Figure 6 and 7. These characteristics demonstrate the magnetic properties of the device. At 50 kilolines/in^2, while the frequency increased five times, the core loss increased by a factor of ten.

Another important aspect of the performance is the temperature variation.

The two curves in Figure 8 demonstrate the variation of temperature rise and the maximum temperature with ambient temperature. With an increase in ambient temperature, the temperature rise decreases and the maximum temperature increases. The maximum temperature as a function of time is shown in Figure 9. This temperature is well within the temperature limitation of all the individual parts.

Performances:

The Low Pass Band Transformer had been designed to have the following characteristics:

1. With an input power of 45 watts at 28 volts 400 cps, the transformer will deliver, to a one ohm resistive load, a minimum of 11.3 watts (6 db) for a period of 1.0 millisecond minimum.
2. The transformer will withstand 100 watts of input power for a minimum of 1.0 millisecond over the frequency range of 100 cps to 10 kc/s (pass band).
3. The transformer will dissipate continuously 10 watts of incident power over the frequency range of 100 kc/s to 10 kmc/s. The attenuation at these frequencies will be 40 db minimum.

ENVIRONMENTAL PERFORMANCE

To determine the environmental performance of the low band pass transformer, a group of prototype units were subjected to tests in accordance with applicable portions of specification MIL-STD-202B.

These tests included: visual and mechanical examination, a dielectric withstanding voltage of 1000 V rms from terminals to case at 25°C, insulation resistance, hermetic seal test, electrical performance, attenuation, vibration, shock, salt spray, temperature cycling, immersion cycling, moisture resistance and life.

None of the units subjected to above tests failed electrically or mechanically. It is safe to assume that the device can provide high reliability performance.

CONCLUSION

Protection of weapons and other systems from spurious r-f energy may now be accomplished by using the low band pass transformer. It has been demonstrated that this device will deliver the signals applied to it in the pass band of frequencies, while attenuating any r-f energy as the frequency increases. As the impedance of the generator is not a function in the design of the transformer, it can be used indescriminately with different power sources. The reliability of performance has been established in addition to the fact that all parts used are "state of the art" material, which have been used in the past under similar conditions.

ACKNOWLEDGMENTS

The development of the Low Band Pass Transformer has been supported by the Naval Weapons Laboratory.

Appreciation is extended to Wing Commander Reginald I. Gray for the use of his patent detail and his helpful comments, and to Messrs. L. S. Pruett and N. Chlosta of the Naval Weapons Laboratory for their cooperation.

The assistance of Messrs. G. Stolar and C. B. Stegner is gratefully acknowledged.

REFERENCES

1. R. I. Gray, "Disclosure of Invention", - Navy Case No. 33459.
2. E. E. Hannum, "RF Sensitivity Specifications for Electroexplosive Devices", AIEE - CP 62-1141.
3. G. P. Harnwell, "Principles of Electricity and Electromagnetism", McGraw-Hill Book Company, New York.

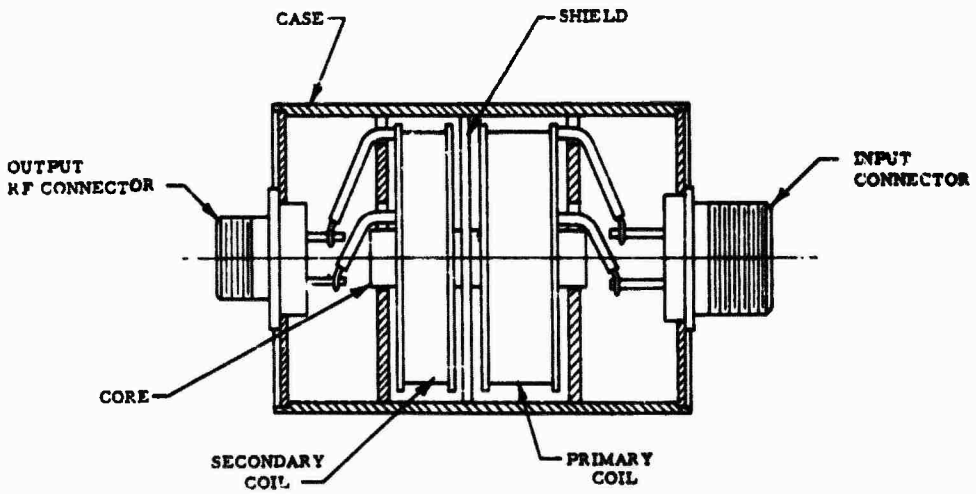

LOW BAND PASS TRANSFORMER

FIGURE 1

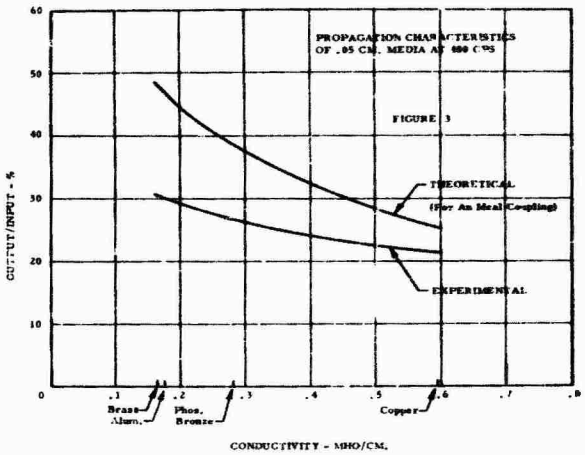
PROPAGATION CHARACTERISTICS
OF .05 CM. MEDIA AT 600 CPS
FIGURE 3
THEORETICAL
(For An Ideal Coupling)
EXPERIMENTAL
OUTPUT/INPUT - %
Brass-
Alum.
Phos.
Bronze
Copper
CONDUCTIVITY - MHO/CM.

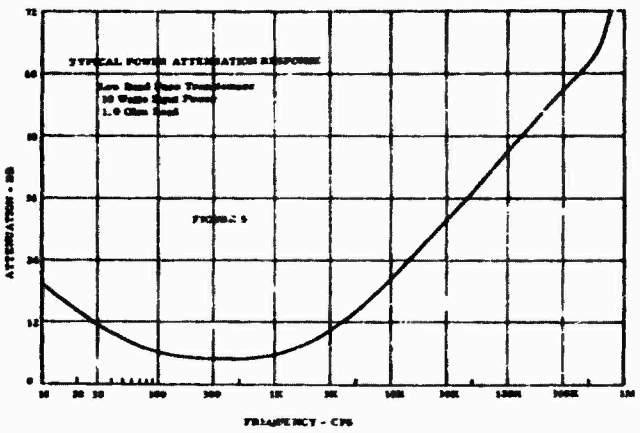
TYPICAL POWER ATTENUATION RESPONSE
Low Band Pass Transformer
10 Watts Input Power
1.0 Ohm Load
FIGURE 5
ATTENUATION - DB
FREQUENCY - CPS

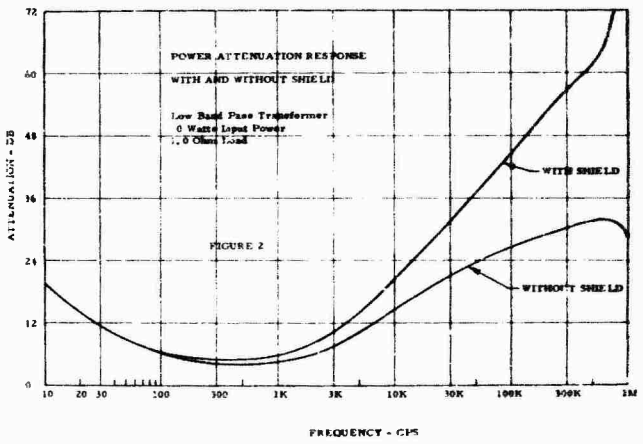
POWER ATTENUATION RESPONSE
WITH AND WITHOUT SHIELD
Low Band Pass Transformer
0 Watts Input Power
1.0 Ohm Load
WITH SHIELD
WITHOUT SHIELD
FIGURE 2
ATTENUATION - DB
FREQUENCY - CPS

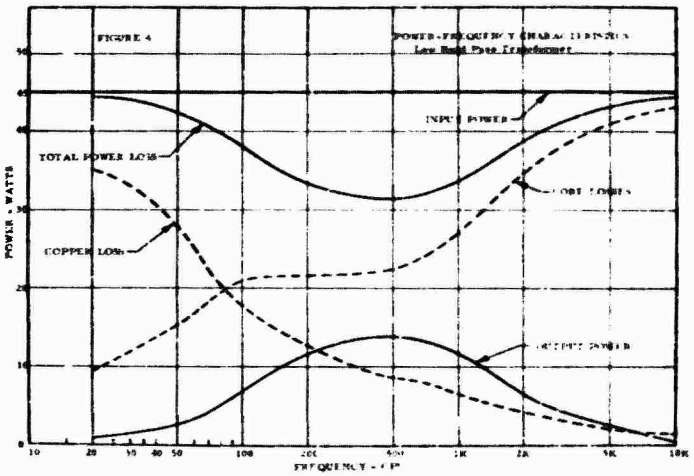
FIGURE 4
INPUT POWER
TOTAL POWER LOSS
COPPER LOSS
POWER - WATTS

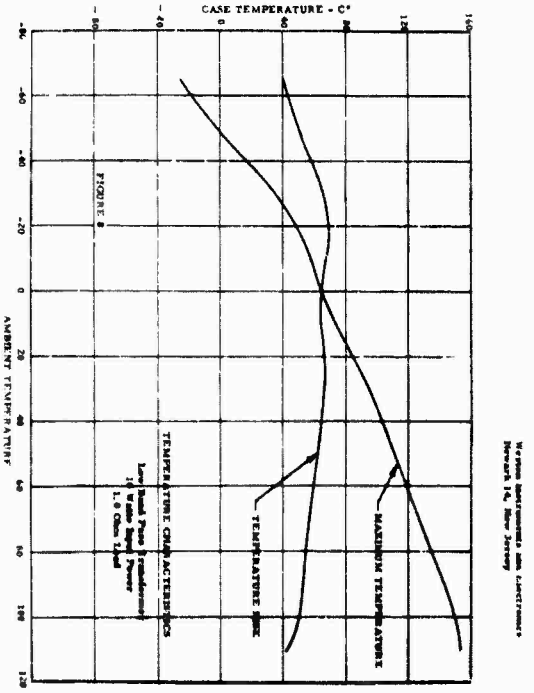
CASE TEMPERATURE - C°
AMBIENT TEMPERATURE
TEMPERATURE CHARACTERISTICS
Low Band Pass Transformer
10 Watts Input Power
1.0 Ohm Load
TEMPERATURE RISE
MAXIMUM TEMPERATURE
FIGURE 8
Weston Instruments and Electronics
Newark 14, New Jersey

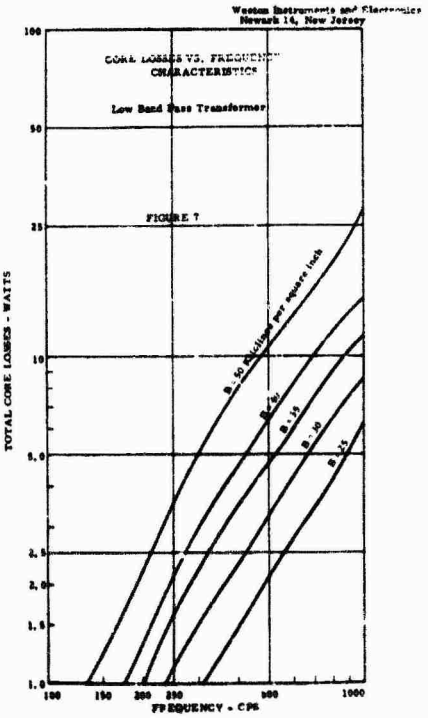
Weston Instruments and Electronics
Newark 14, New Jersey
CORE LOSSES VS. FREQUENCY CHARACTERISTICS
Low Band Pass Transformer
FIGURE 7
TOTAL CORE LOSSES - WATTS
FREQUENCY - CPS
B = 50 Kilolines per square inch
B = 40
B = 35
B = 30
B = 25

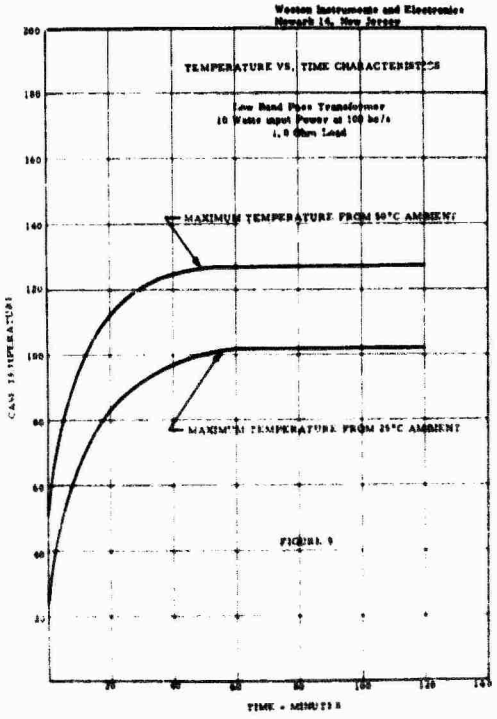
Weston Instruments and Electronics
Newark 14, New Jersey
TEMPERATURE VS. TIME CHARACTERISTICS
Low Band Pass Transformer
10 Watts input Power at 100 cps
1.0 Ohm Load
MAXIMUM TEMPERATURE FROM 50°C AMBIENT
MAXIMUM TEMPERATURE FROM 25°C AMBIENT
FIGURE 9
CASE TEMPERATURE
TIME - MINUTES

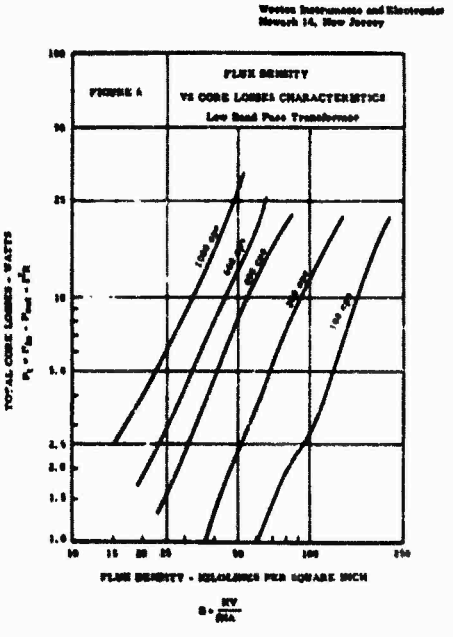
Weston Instruments and Electronics
Newark 14, New Jersey
FIGURE 6
FLUX DENSITY
VS CORE LOSSES CHARACTERISTICS
Low Band Pass Transformer
TOTAL CORE LOSSES - WATTS
FLUX DENSITY - KILOLINES PER SQUARE INCH
B = EV / 4fNA

19. DISCUSSION

Mr. Brown asked how far the transformer could be mounted from the EED and how these black boxes imposed between the firing switch and the EED would affect system checkout. Mr. Stegner said that the transformer was checked out against specifications and not against field conditions per se. As far as system checkout is concerned, he has no answer.

Mr. Meyer of Bjorkstm Research commented that credit for this device should go to Bjorksen and specifically to Dale Holinbeck who conceived the idea in 1961. This comment was made for the record. Commander Gray, for the record, apologized for having conceived this in England in 1957.

A question was then asked concerning dimensions of the device. Mr. Stegner said it was 1.28 inches in diameter by 2 inches long. There is no estimate of what it would cost to mass produce this item at this time. It was said that the cost would be dependent upon the cost of the relays and connectors. The device could conceivably be put into the fuze without connectors to save space.

Mr. C. Blank asked if these units were subjected to vibration, drop or shock tests. The reply was that the unit was subjected to 40 G of vibration at 2000 or 3000 cycles. No drop test to date; some are planned. Mr. Blank commented that he had a solenoid failure from a 2 foot drop test.

Wing Cmdr. Gray commented that the EED should be removed from any secondary heat source because of the danger of cook-off.

Mr. Salisbury of Lawrence Radiation Laboratory asked if a magnetic material had been used for the shielded transformer. The answer was that the material served to short out some of the flux. Comdr. Gray added that of many materials tried, the non-ferrous ones are the best compromise. The RF attenuation can be obtained by increasing permeability or decreasing the thickness or vice versa. A comment was made that an efficient device had been developed using thin magnetic films.

Mr. Blank asked if any thought had been given to protecting the EED during servicing or replacement. The answer was that there was not but

there is obviously a point to designing the EED lead with proper shielding to obviate RF pick up.

It was stated that the most vulnerable time in many missile applications occurs when the EED is taken from its safe container, the shunt removed and it is installed in the firing system while the missile is on the launching pad.

It was agreed that this is a major problem and Cmdr. Gray commented that not all of the problems would be solved today.

A question was asked concerning the power requirements of the solenoid and the EED. The answer was that direct current is used but the magnitude is determined for each specific application. The power sources for the solenoid and the squib could be different ones. The choice of the firing source is left to the user. It may oe a capacitor, battery or transformer. The main action here is in arming.

20. RADIO FREQUENCY INTERFERENCE GUARD

by Karl Kraus, Chief Engineer of RF Connectors and Allied Products

Scintilla Division, The Bendix Corporation

Introduction

The need to develop a miniature low-pass Radio Frequency Attenuator or RIG (Radio Interference Guard) stems from the necessity of adequately protecting EED (electro-explosive devices) against spurious energies induced into their associated circuits by electromagnetic fields. Generally, shipboard radar and communications equipment are the sources of these spurious energies. At the present time, to prevent misfiring of these EED, the use of equipment endangering ordnance operations must be restricted or the ordnance operations must be accomplished at a point remote from transmitting antennas. As a result of studies under the U. S. Navy's HERO (Hazards of Electromagnetic Radiation to Ordnance) program, this RIG of novel design and capabilities has been conceived. Patent application has been filed at the U. S. Patent Office under Navy Case No. 33,460, Patent Serial No. 163162 by Wing Commander R. I. Gray.

Basic Concept

The design of the RIG device is based on the concept of enclosing an electrical load within a continuous electromagnetic shield of suitable metal and thickness, thereby providing adequate protection for the load against all radio frequency and electrostatic fields. This concept is illustrated very simply in Figure 1.

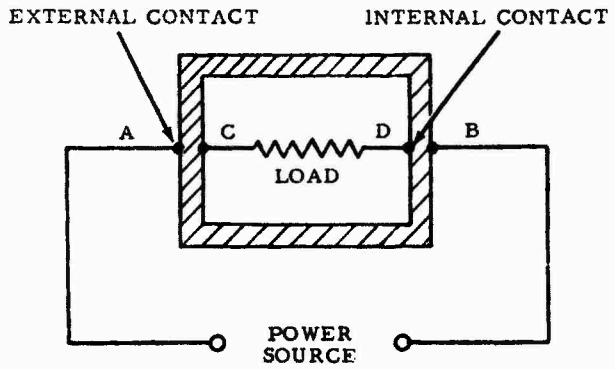

BASIC CONCEPT OF A RADIO INTERFERENCE GUARD
Figure 1

The load is intentionally energized by application of a potential difference between points A and B on the exterior of the metal box. When steady state DC is used, an internal potential difference is set up between points C and D, which is almost equal to the external potential difference. Low frequency excitation may also be used, and thus a DC step function will pass all except its high frequency components with only little power attenuation. Furthermore, frequencies such as 60 c/s and 400 c/s can be used without serious power loss.

Design

The RIG which Scintilla Division is developing consists of a coaxial transmission line the length of which can vary from 3 to 10 feet. This line requires an outer conductor of high permeability and an inner conductor of low resistivity. The inner conductor is soldered to the outer conductor on both ends of the coaxial line. The mid-point of the outer conductor is soldered to a metallic wall as shown in Figure 2. Figure 3 represents the DC equivalent circuit of the RIG.

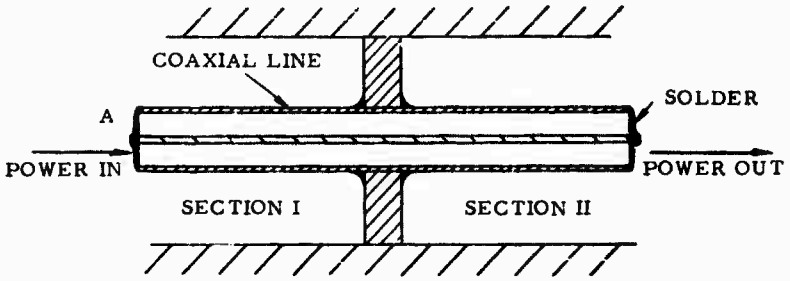

DC PROPAGATION

Figure 2

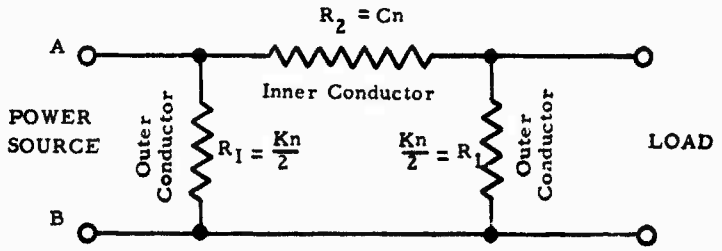

Figure 3

Operation

If a DC source is connected between terminals A and B, current flows through the inner conductor. The only attenuation which occurs results from the shunt losses in the outer conductor, which in Figure 3 is represented by the two resistors R_1, and from the series loss of the inner conductor, represented by R_2. The mode of operation changes at higher frequencies. The electromagnetic wave, because it is restricted to the outer conductor surface, propagates along the outer surface of that conductor. When the wave has built up a sufficient electromotive potential, it propagates from the outside surface

through the wall toward the center of the coaxial line. (See Figure 4.) In passin through the wall, the wave is attenuated according to the skin depth equation:

$$\delta = \frac{1}{a} + \frac{1}{j\beta} \simeq (1+j)\sqrt{\frac{2}{\omega\mu\sigma}} \quad \text{meter/neper or radian}$$

a = attenuation function (nepers/meter)

β = phase function (radian/meter)

μ = initial permeability (henry/meter)

σ = conductivity (mho/meter)

ω = 2π x frequency in cycles per second

This expression describes the distance at which both the electric field (E) and the magnetic field (H) are attenuated to e^{-1} of their respective magnitudes. This is also the distance at which the phase is retarded by one radian.

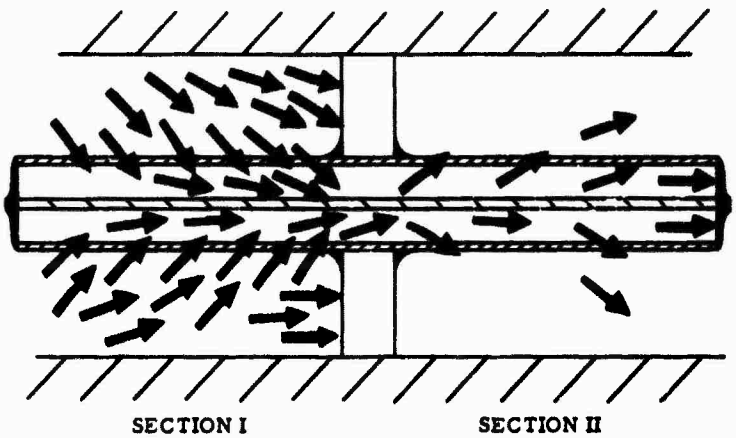

AC PROPAGATION
Figure 4

A new wave phenomenon is then excited along the inner surface of the outer conductor by the attenuated wave. This new wave propagates toward the second section of the RIG where, upon penetration of the wall of the outer conductor from the inside, this wave also undergoes very strong attenuation.

The attenuation which takes place as the wave passes through the metallic barrier is governed by the real part α in accordance with this propagation function equation:

$$\gamma = \alpha + j\beta \simeq (1+j)\sqrt{\frac{\omega\mu\sigma}{2}}$$

It can be seen that the material which gives the highest $\mu\sigma$ product will give the maximum attenuation per unit volume.

The operation of the RIG may be described more simply as "attenuation is accomplished by propagation through solid metal".

Advantages

Unlike conventional dissipationless filters, the RIG does not rely on reflective attenuation for its low-pass performance characteristic and because it is a dissipative device, it cannot be rendered ineffective by inadvertent matching to a radio frequency generating source. However, the RIG employs reflective attenuation in the dissipative attenuation band with the result of increasing the probability of protecting itself against overheating by the radio frequency generating source.

DC Analysis

As was previously mentioned, the DC performance and attenuation is dependent on the resistance of the outer conductor (K= ohms/ft), the resistance of the inner conductor (C= ohms/ft), and the length of the conductors (n= ft).

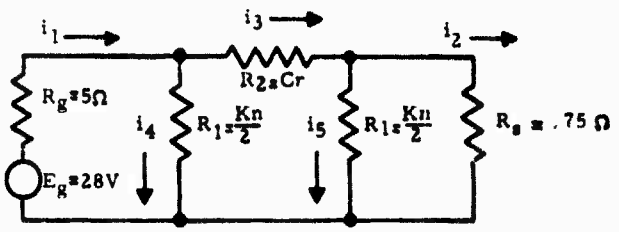

Figure 5

Expressions were derived by solving the DC network for the input current (i_1 = amps) and output current (i_2 = amps):

$$(A) \qquad i_1 = \frac{\left(\frac{R_2(R_1+R_s)}{R_1} + 2R_s + R_1\right) E_g}{\left(R_sR_1 + 2R_sR_g + \frac{R_gR_2R_s}{R_1} + R_sR_2 + R_gR_2 + R_gR_1 + R_2R_1\right)}$$

$$(B) \qquad i_2 = \frac{R_1E_g}{\left(R_sR_1 + 2R_sR_g + \frac{R_gR_2R_s}{R_1} + R_sR_2 + R_gR_2 + R_gR_1 + R_2R_1\right)}$$

The analysis showed that all expressions for current are independent of each other and that each contain the variables of n, K, and C. Thus expressions (A) and (B) may be written in terms of these variables and rearranged to give the following expressions:

$$(C) \qquad \left[\frac{K}{C}\right] = \frac{-(R'\left[nC\right] + 2T') + \sqrt{(R'\left[nC\right] + 2T')^2 - 4\left[nC\right](\left[nC\right] + R')T'}}{\left[nC\right](\left[nC\right] + R')}$$

$$(D) \qquad \left[\frac{K}{C}\right] = \frac{-(S\left[nC\right] + 2T) - \sqrt{(S\left[nC\right] + 2T)^2 - 4\left[nC\right](\left[nC\right] + R)T}}{\left[nC\right](\left[nC\right] + R)}$$

For convenience and facility in obtaining maximum information, the quotient of the outer conductor K over the inner conductor C and the product of the length n times the inner conductor C were plotted on a single set of co-ordinate axes by assignment of a specific value of 0.75 ohm for the load resistance R_s. (0.75 ohm is the approximate DC resistance of the Mark I squib.) The generator voltage E_g is 28 volts and the generator resistance R_g is 5 ohms. Data obtained from computer runs were used to arrive at the two families of

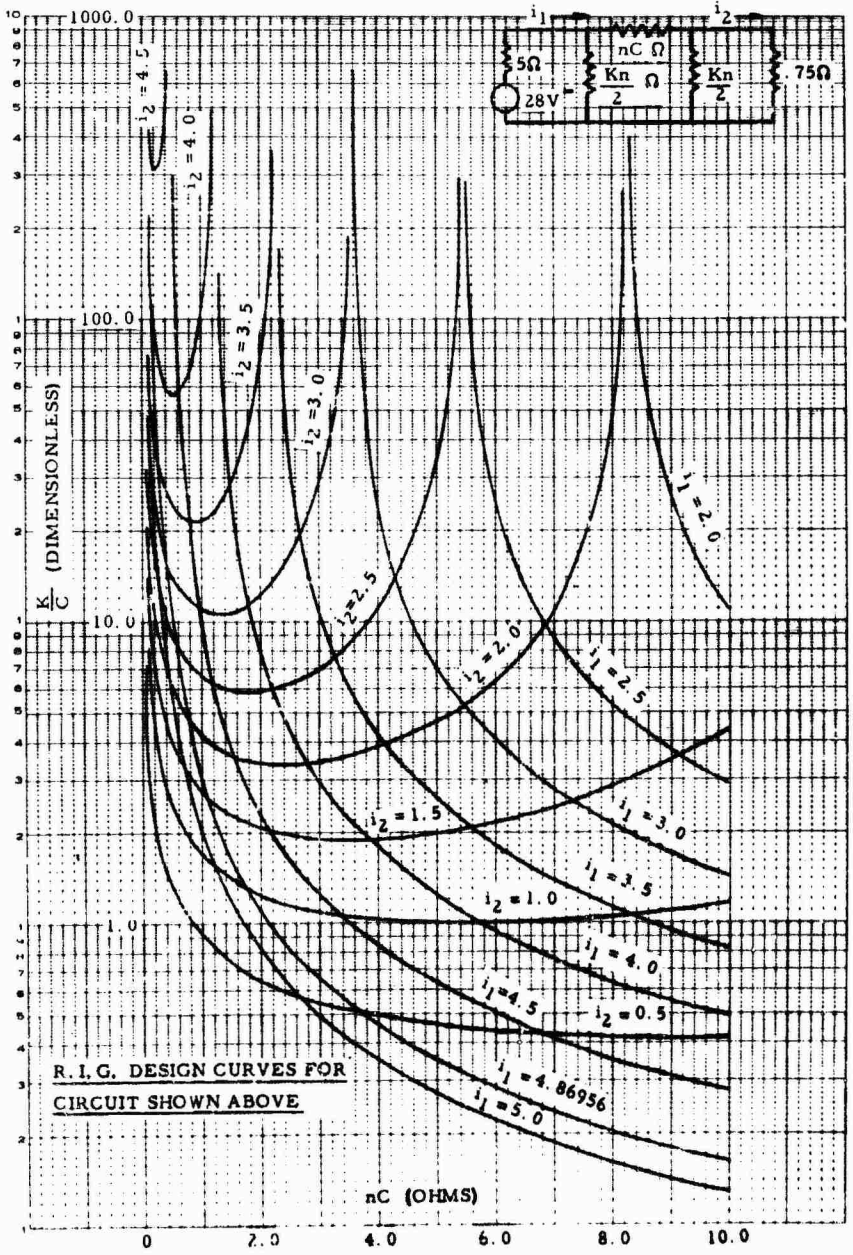
1000.0
100.0
10.0
1.0
K/C (DIMENSIONLESS)
nC (OHMS)
0
2.0
4.0
6.0
8.0
10.0
i1
i2
5Ω
28V
nC Ω
Kn/2 Ω
Kn/2
75Ω
i2 = 4.5
i2 = 4.0
i2 = 3.5
i2 = 3.0
i2 = 2.5
i2 = 2.0
i2 = 1.5
i2 = 1.0
i2 = 0.5
i1 = 2.0
i1 = 2.5
i1 = 3.0
i1 = 3.5
i1 = 4.0
i1 = 4.5
i1 = 4.86956
i1 = 5.0
R. I. G. DESIGN CURVES FOR
CIRCUIT SHOWN ABOVE

Figure 6

curves for a broad range of values for the input and output currents. (See Figure 6.)

Because intermediate intersection points can always be interpolated, these curves give all possible solutions to the circuit. However, additional conditions were imposed on the analysis in order to determine which portions of the curves were most suitable.

One condition imposed was that of cable geometry. Because RF attenuation is a function of outer conductor thickness (t_K = inches), a relationship was derived between the lumped parameters $\frac{K}{C}$, the resistance per foot of the inner conductor C, and the thickness of the outer conductor t_K.

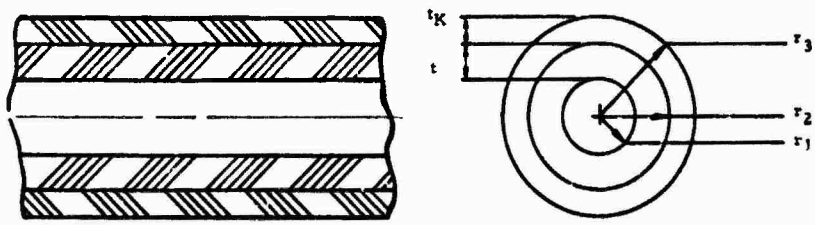

Figure 7

$$(E) \qquad \left[\frac{K}{C}\right] = \frac{\rho_K}{[C]}\left(\frac{1}{M + \sqrt{N}}\right)$$

a) $M = \pi\ t_K\ (2t + t_K)$ b) $N = 4\pi\ \rho_C\ t_K^2$

The units of resistivity ρ are ohms-inches^2/ft. with the result that the insulation thickness t and the thickness of the outer conductor t_K are thicknesses in inches and C in ohms/ft. Expression (E) makes it possible to plot $\frac{K}{C}$ as a function of C when the insulation t, the resistivity of the outer conductor ρ_K and resistivity of the inner conductor ρ_C are fixed. Several curves, each

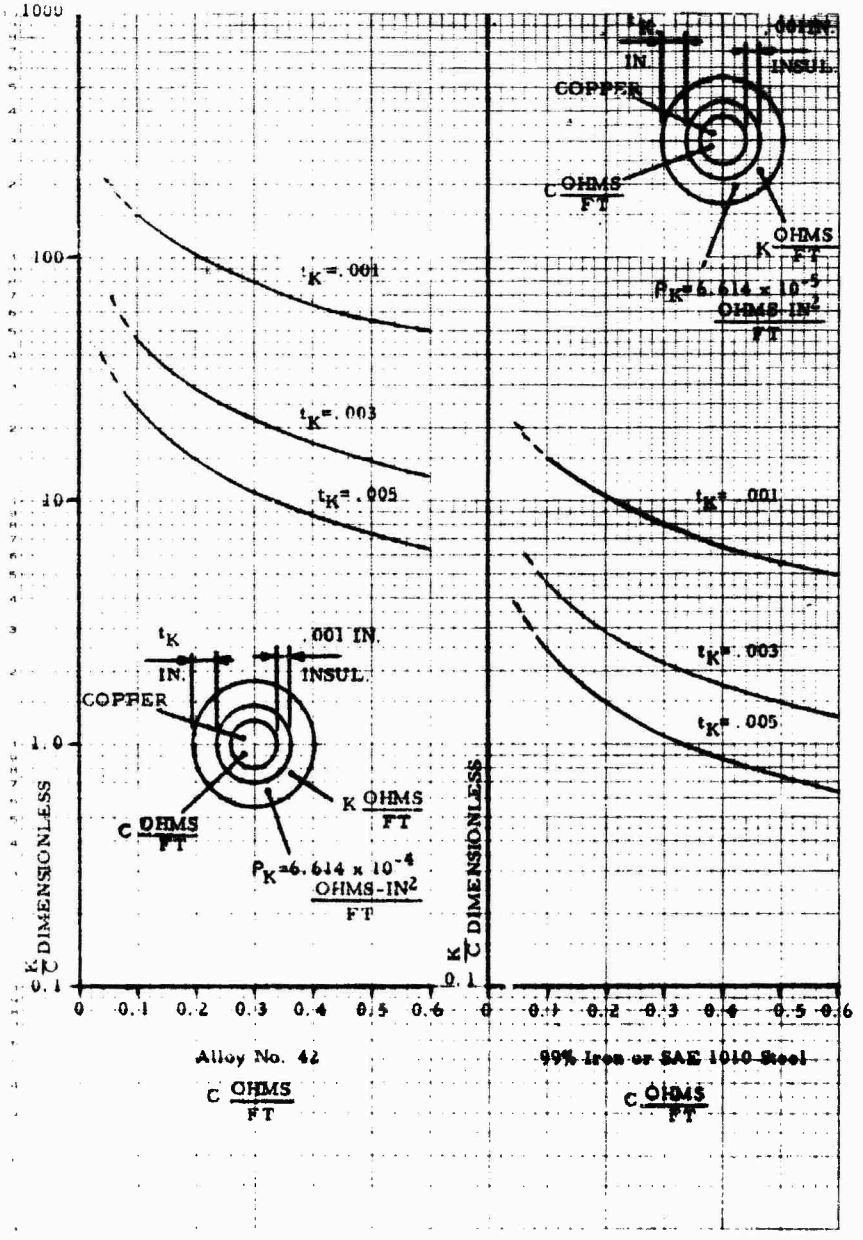
1000
100
10
1.0
0.1
t_K = .001
t_K = .003
t_K = .005
t_K
IN.
.001 IN.
INSUL.
COPPER
C OHMS/FT
K OHMS/FT
P_K = 6.614 x 10^{-4} OHMS-IN²/FT
K/C DIMENSIONLESS
0 0.1 0.2 0.3 0.4 0.5 0.6
Alloy No. 42
C OHMS/FT
t_K = .001
t_K = .003
t_K = .005
P_K = 6.614 x 10^{-5} OHMS-IN²/FT
99% Iron or SAE 1010 Steel
C OHMS/FT

Figure 8

for a different material, of this function were plotted. (See Figure 8.)

The information obtained from these curves shows that, for increased RF attenuation, it is better to work in the lower regions of the curve. (See Figure 6.)

DESIGN PARAMETERS FOR RIG

Selection of Coaxial Cables

The coaxial cable must have a sufficiently high shunt DC resistance to enable firing of an EED (electro-explosive device) with reasonable low currents. This can be achieved only by making the box (Figure 1) in the form of a thin tube. Because attenuation is proportional to the square root of the conductivity, use of a higher resistivity material to increase resistance would defeat the prime requirements for high attenuation and therefore is not permissible . Furthermore, because direct current resistance is inversely proportional to wall thickness, whereas RF attenuation is an exponential function of the thickness (e^{-kt}), it is not permissible to obtain high resistance in a short length by decreasing the wall thickness. The DC analysis permits the selection of coaxial cables according to information given by extreme points which appeared to be limits on the curves (Figures 6 and 8). The analysis showed that the thickest possible wall of the outer conductor will give the maximum RF attenuation and the longest possible length of the coaxial cable will give the least DC attenuation.

Because of design limitations of size, DC attenuation, and RF attenuation, compromise was necessary. Six designs were selected which made it possible to investigate the affect of attenuation on the RIG device based on:

a. material

b. cable size

c. inner conductor size

d. cable length

e. DC resistance of the outer conductor

f. wall thickness of the outer conductor

g. permeability of the outer conductor

Three materials, 99% pure iron, 1010 steel, and Driver Co. 42 alloy, were chosen to compare the $\mu\sigma$ product resulting from variation in conductivity and initial permeability. Four coaxial cables with diameter sizes varying from 0.012 to 0.025 inches, three inner conductors with diameter sizes varying from 0.008 to 0.015 inches, five coaxial cables with lengths varying from 3 to 10 ft., outer conductors with thickness varying from 0.0015 to 0.005 inches, and initial permeability varying from 200 to 30,000 were chosen.

Construction and Size

An analytical study of heat dissipation for the RIG was conducted in order to gain information necessary for selection of a proper size. The analysis was approximate and contained three variables: the heat dissipated at the surfaces of the housing, by the connectors, and by the leads. No attempt was made to study the temperature gradients inside the RIG itself.

As a result of this study a small unit, 1.500 inches long and 0.550 inches in diameter, and a large unit, 2.100 inches long and 0.750 inches in diameter, were selected. The small unit had power dissipation capabilities of 7 watts and the large unit, of 10 watts. Under the conditions of the analytical study these devices had surface temperatures of approximately 300°F.

The construction of the coaxial version of the RIG is depicted in Figure 9. This version of the RIG employs a 6 foot long coaxial cable. This cable has a nominal outside diameter of 0.018 inch, a nominal 0.003 inch wall, and uses

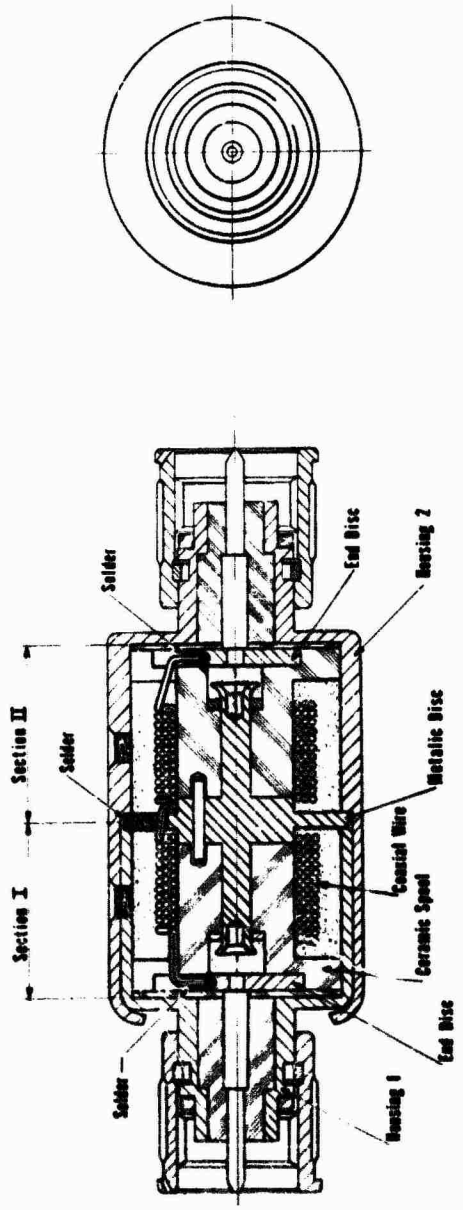
Solder
End Disc
Housing 2
Section II
Solder
Metallic Disc
Coaxial Wire
Section I
Ceramic Spool
End Disc
Solder
Housing 1

Figure 4

a 0.010 inch copper wire insulated with Silotex. The exterior of this coaxial cable is coated with DuPont ML high temperature polyemide lacquer in order to provide the cable with insulation. Half of the cable is wound in three layers onto a ceramic spool. The two sections of this spool and a metallic disc at the mid-point of the spool are held together by a metallic rivet. The mid-point of the outer conductor of the coaxial cable is soldered to the disc. The remaining three feet of coaxial cable is wound in three layers onto the second section of the spool. The line is short-circuited at both ends and soldered to the end discs. Section I is placed into housing 1 and sealed with solder. This operation ensures an electromagnetic shield between the two sections. Housing 2 is placed over housing 1 and formed over at the end. To ensure environmental sealing, the entire unit is impregnated with a potting compound. In turn, the filling holes are sealed with solder in order to ensure proper shielding.

RF Attenuation

The value μ, or incremental permeability, is a function of the frequency and the applied field intensity. The formula for the propagation constant shows that the values for μ directly establish the magnitude for both the attenuation constant α and the phase constant β. No accurate figures for μ versus frequency and field intensity, which would allow calculation of the attenuation, are available for the materials used in the RIG . Therefore, it was necessary to determine the attenuation versus frequency of the RIG experimentally.

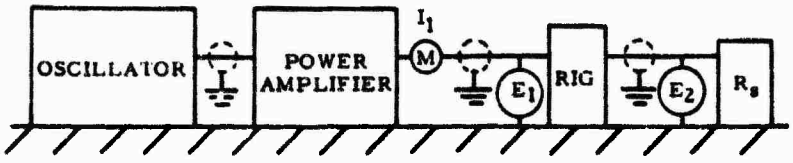

GROUND POTENTIAL

Attenuation = $10 \log 10 \frac{P_1}{P_2}$

BLOCK DIAGRAM OF ATTENUATION TEST
Figure 10

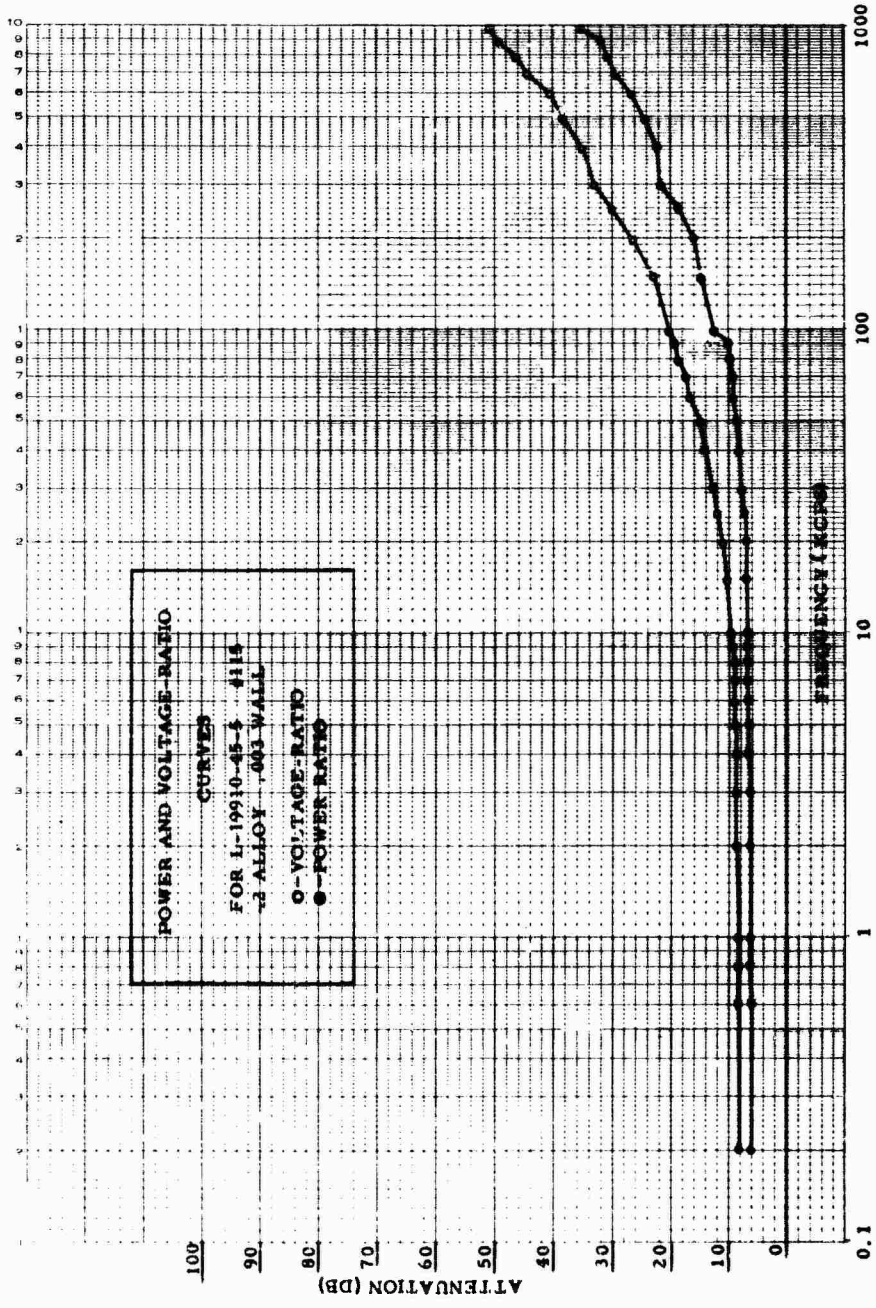
POWER AND VOLTAGE-RATIO
CURVES
FOR L-19910-45-4 4114
2 ALLOY .003 WALL
O-VOLTAGE-RATIO
●-POWER RATIO
ATTENUATION (DB)
FREQUENCY (KCPS)
100
90
80
70
60
50
40
30
20
10
0
0.1
1
10
100
1000

Figure 11

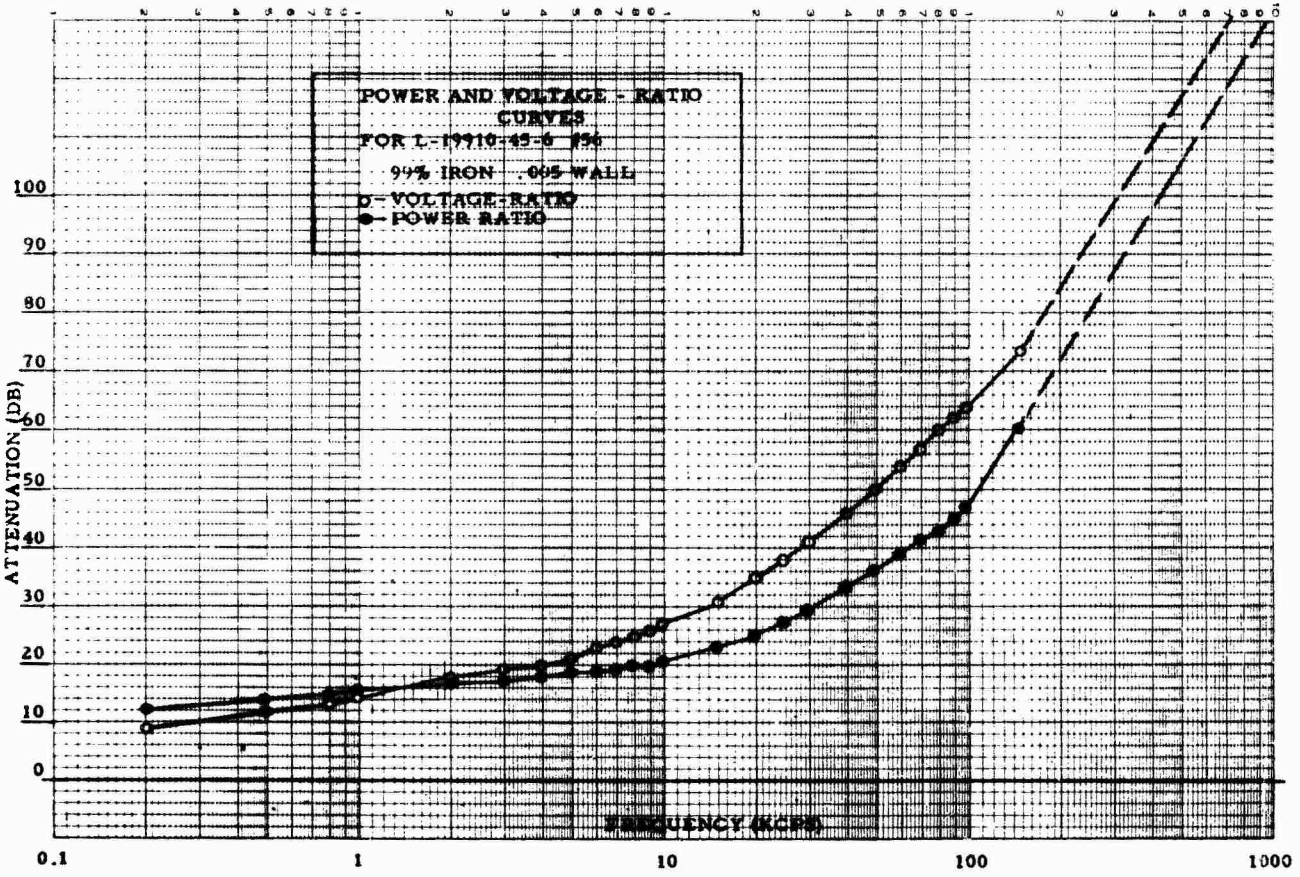
POWER AND VOLTAGE - RATIO
CURVES
FOR L-19910-45-6 #36
99% IRON .005 WALL
O- VOLTAGE-RATIO
●- POWER RATIO
ATTENUATION (DB)
100
90
80
70
60
50
40
30
20
10
0
FREQUENCY (KCPS)
0.1
1
10
100
1000

Figure 12

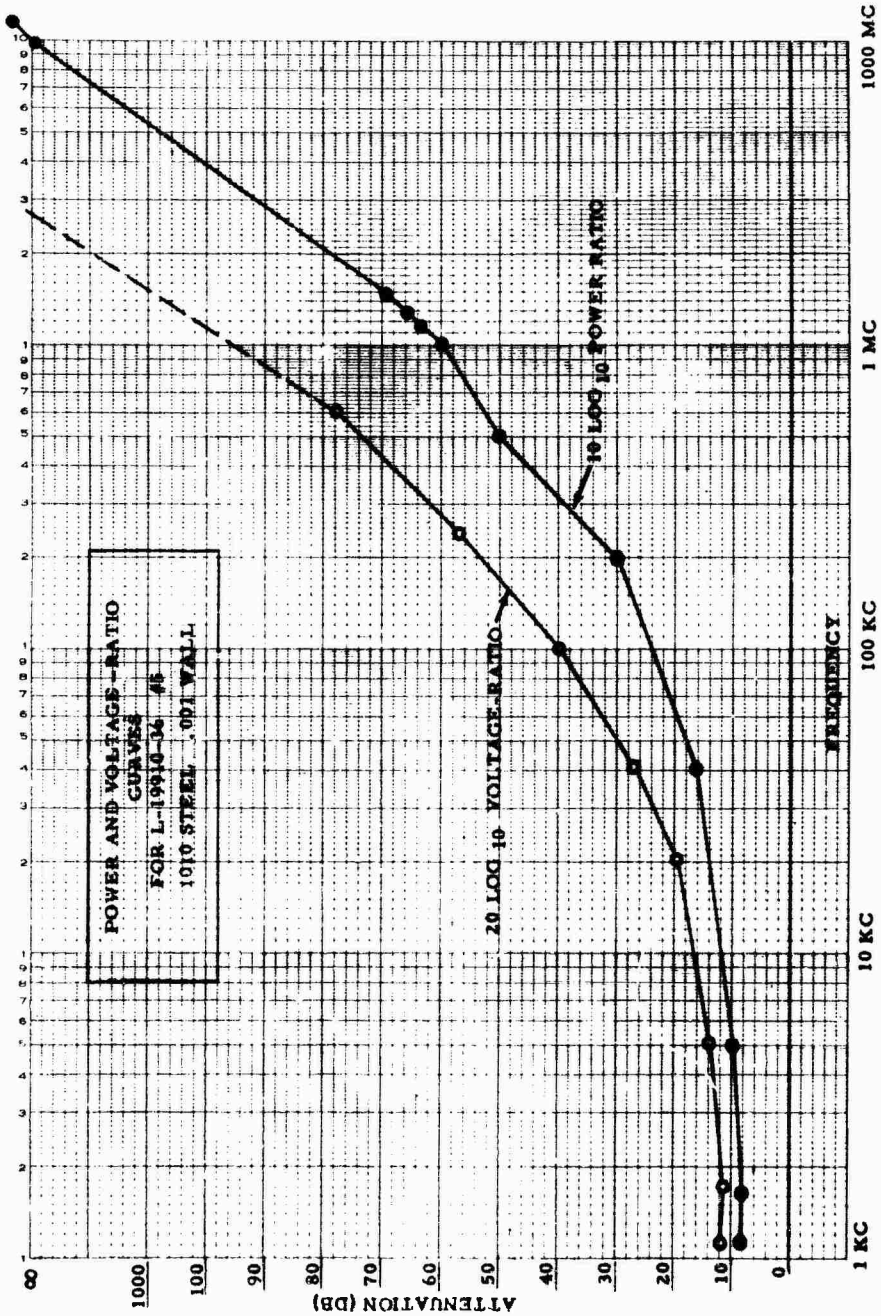
POWER AND VOLTAGE RATIO CURVES FOR L-19910-36 #5 1010 STEEL .001 WALL
10 LOG 10 POWER RATIO
20 LOG 10 VOLTAGE RATIO
ATTENUATION (DB)
FREQUENCY
1 KC
10 KC
100 KC
1 MC
1000 MC

Figure 13

Figure 10 contains a general diagrammatic representation of the impedance and voltage measurements which have been used for obtaining an attenuation or insertion loss in db.

$$\text{Attenuation} = 10 \log 10 \frac{P_1}{P_2}, \text{ db}$$

P_1 is the total power absorbed by the RIG and the load (or, power in) and P_2 is the total power absorbed by the load (or, power out).

The devices were tested for power attenuation from DC to 1 megacycle and from 1 MC to 2000 MC.

The curves in Figures 11 and 12 represent voltage and power measurements of the RIG taken from DC to I MC. It was not necessary to employ matching techniques to obtain measurements in this range. Information illustrated in Figures 11 and 12 indicates that the device is performing as expected and that attenuation increases with frequency. Furthermore, it shows that 99% iron has a higher $\mu\sigma$ factor than 42 alloy or 1010 steel.

An experiment was set up to prove: (1) that the RIG is a dissipative device and that it cannot be rendered ineffective by matching to an RF power source and (2) that attenuation on the device increases with frequency.

Power measurements, illustrated in Figure 13, were made at 10, 100, 156, 1000, and 2000 MC under matched conditions, by applying RF power of up to 15 watts. No measurable output was detected with micro-watt detectors when the RIG was terminated in 0.75 and 50 ohm loads. Rapid heating of the RIG was noted. This proves that the RIG is a dissipative device.

One more test, to determine whether RF power is reflected when the device is not matched, was performed. This test consisted of placing the device into a 50 ohm line and terminating the RIG in 0.75 and 50 ohm loads. A Microwave Devices (formerly M. C. Jones) Type 703 RF power meter for measuring incident and reflected power was placed in front of the RIG. RF power of up to 15 watts was applied at 5, 15, 30, 50, 100, and 150 MC. The

power reading of the incident versus the reflected power was the same in all cases when the RIG was terminated in 0.75 and 50 ohm loads. This proves that all RF power is reflected when the device is not matched.

In conclusion, it can be said that the RIG is an effective device in protecting EED's from RF radiation. When matched to an RF source, the RIG attenuates the RF power in a dissipative manner and can dissipate up to 10 watts of RF power. When it is not matched, it effectively employs reflective attenuation, which provides additional protection against overheating.

BIBLIOGRAPHY

T.M. No. W-7/62 Series and Parallel Arrangements of Electrically Initiated Explosives by Wing Commander R. I. Gray.

"A Note on The Use of Attenuators in Balanced and Unbalanced Networks" by Wing Commander R. I. Gray. (10 Nov 1962)

Memo on Attenuation of RIG of DC by Lyde S. Pruett of NWL, dated Nov. 13, 1962.

Requirements of The Radio - Frequency Interference Guard (RIG) by J. W. L. Lewis.

The author acknowledges contributions made by Tullio Tognola, Assistant Director of Engineering, Dr. W. E. Morris, Chief Engineer, Research, Donald Clark, Senior Project Engineer, and Frederick Hanni, Project Engineer, all of Scintilla Division, The Bendix Corporation.

20. DISCUSSION

Mr. Adelman of Picatinny Arsenal asked if any estimate was made of the cost in mass production. Mr. Kraus and Wing Cmdr. Gray declined to estimate the cost.

A voice, commenting on the film (presumably the "Achilles Hell of Modern Weapons"), mentioned it was undesirable to go to insensitive EED's because of the increased power supply requirements. A missile may have as many as 200 EED's. With all of these protective devices, 10 pounds of additional power supply may be required in addition to the weight of the protective devices.

Commander Gray said that no additional power is required. This design operates from a standard power supply as used with more sensitive EED's. The input requirements will be the same as a Mark 1 Squib for example.

A questioner asked how much one or two hundred of these devices would weigh. Commander Gray recognized this as a good question and commented that some compromise is necessary to solve the problem adequately.

Mr. Blank asked what temperatures were developed. Mr. Kraus said that the maximum surface temperature for a small device was 300°F.

Mr. Kilpatrick of General Dynamics asked what sources of power could pose a problem in light of the 10 watt dissipation and the 25 db attenuation. Mr. Kraus answered that much of the normal losses would be in reflection. It will afford 25 db of attenuation and at the same time dissipate 10 watts of power. These are limitations that can be used for calculation in individual problem areas.

Mr. Barkham of Lockheed asked if this device prevented electrical noises from the exploding EED from being fed back into the firing line. Commander Gray said that this device is not suitable for high impedance. It was designed for low impedances like 1 ohm bridgewires. He stated that we don't talk about EBWs since the last Congress. Mr. Kraus commented that it passes the high peak and therefore could not be used for an EBW device.

21. RADHAZ PROOF MAGNETIC COUPLING

Author: Edward A. White, Jr.
U. S. Naval Ordnance Laboratory

INTRODUCTION

The RADHAZ problem for free fall weapons has been attacked from various directions, where a multitude of partial solutions have been proposed. A complete solution to the problem is to completely encase the weapon in a conducting shield so that high frequency signals are not able to penetrate the skin. Now the problem arises as to how does one communicate with the weapon. The following report deals with a method of communication by propagating low frequency electromagnetic radiation through a conducting medium. The discussion is restricted to one dimensional magnetic field flow perpendicular to the conducting material. Essentially two cases are considered, a sinusoidal input and a step function input. It is shown theoretically and experimentally that energy from a low frequency magnetic field will penetrate the conductor and that energies from signals whose frequencies are above 10 KC will be attenuated to a negligible value, yielding a device which is a low frequency band pass filter.

THEORETICAL STUDY

The discussion in this section will be concerned with the transfer of magnetic energy through various media and

boundaries. The problem can be briefly pointed out in Figure 1(a). A current i_1 flows in windings N_1, producing a magnetic field H_1, which is propagated through a new medium (x) as H_x and into the secondary core as H_2 and produces the current i_2 in the windings N_2. The evaluation of these parameters and their dependence upon the physics of the machine is best described through an interpretation of Maxwell's equations, i.e.,

$$\nabla \cdot \vec{B} = 0 \tag{1}$$

$$\nabla \cdot \vec{E} = \rho/\epsilon \tag{2}$$

$$\nabla \times \vec{H} = \vec{I} + \epsilon (\partial \vec{E}/\partial t) \tag{3}$$

$$\nabla \times \vec{E} = -\partial \vec{B}/\partial t \tag{4}$$

where

$\vec{B}$ is the magnetic flux

$\vec{H}$ is the magnetic field

$\vec{I}$ is the true current density

$\vec{E}$ is the electric field intensity

ρ is the charge density

t is the time

The current density $\vec{I} = \bar{\sigma}\vec{E}$ where $\bar{\sigma}$ is the electrical conductivity tensor. If one takes the curl of equation (3) and (4) and assumes that the medium is a good conductor,

so that $\nabla \cdot B$ and $\nabla \cdot E = 0$, then a diffusion equation can be written for the quantities H, E and i, i.e.,

$$\nabla^2 \vec{H} = \sigma\mu \, (\partial \vec{H}/\partial t) \tag{5}$$

$$\nabla^2 \vec{E} = \sigma\mu \, (\partial \vec{E}/\partial t) \tag{6}$$

$$\nabla^2 \vec{i} = \sigma\mu \, (\partial \vec{i}/\partial t) \tag{7}$$

where

μ is the magnetic permeability

First let us consider the case where the current flowing in windings H_1 and the magnetic field produced by the current are sinusoidal as $e^{j\omega t}$. Equation (5) then becomes

$$\nabla^2 \vec{H} = j\omega\sigma\mu\vec{H} \tag{8}$$

The case in general may be approximated by Figure 1(b), where the magnetic field H is directed in the x direction only, producing a current i in the copper media in the z direction only. Equation (7) is written as

$$\frac{\partial^2 i_z}{\partial x^2} = j\omega \sigma\mu i_z = \gamma^2 i_z \tag{9}$$

where

$$\gamma^2 = j\omega \sigma\mu$$

Hence

$$\gamma = (1 + j) \sqrt{\frac{\omega\sigma\mu}{2}} = \frac{1 + j}{\delta} \tag{10}$$

where

$$\delta = \sqrt{\frac{2}{\omega \mu \sigma}} \tag{11}$$

Which is called the skin depth, i.e., that penetration where the induced current and associated magnetic field H_x is reduced to 1/e of its value at the surface x = 0.

Equation (8) in our case can be written in the same form as equation (9), i. e.

$$\frac{\partial^2 H_x}{\partial x^2} = j\mu\omega\sigma H_x \tag{12}$$

When the appropriate boundary conditions are applied the solution of equation (12) is written as

$$H_x = H_o e^{-(1 + j)\, x/\delta} \tag{13}$$

where H_o is H_x when x = 0.
Which describes the complex magnetic field in the conductor as is shown in Figure 2.

By coupling equation (13) with Faraday's induction law, i.e.

$$V = \mu \int_0^A \frac{\partial}{\partial t} H \cdot dA \tag{14}$$

The voltage developed in the secondary windings N_2 is then

$$V_2 = j\omega \mu A N_2 H_o e^{-(1 + j)\, x/\delta} \tag{15}$$

whose absolute value is

$$|V_2| = \omega A N_2 \mu H_o e^{-x/\delta} \tag{16}$$

Assuming at this point that H_o is constant with frequency than a plot of V_2 versus ω will show a peak at

$$\omega_c = \frac{8}{x^2 \mu \sigma} \tag{17}$$

as is shown in Figure 3 for various values of x. In practice however H_o is not a constant with μ since it is a direct function of i_1. At very low frequencies i_1 is not a severe function of ω, but at frequencies above 100 cycles per second i_1 is definitely affected by ω since

$$i_1 = \frac{V_o}{R_1 + j \omega L_{s1}} e^{j\omega t} \tag{18}$$

where the equivalent circuit is shown in Figure 4(a). The resistance R_1 is more than the dc resistance of the windings N_1. The conducting sheet (x) acts as a single turn load to the primary and is essentially resistive, although it is frequency depended. Hence at frequencies above about 100 cycles per second H_o is written as

$$H_o = \frac{N_1}{2\pi r} \frac{V_o}{R_1 + j\omega L_{s1}} e^{j\omega t} \tag{19}$$

where r is the radius of the solenoid.

The magnitude of V_2 in this case is then

$$|V_2| = K_1 \frac{\omega e^{-x/\delta}}{\sqrt{\omega^2 L_{s1}^2 + R_1^2}} \tag{20}$$

where

$$K_1 = \frac{N_1 N_2 \mu_{Fe} A V_o}{2\pi r}$$

μ_{Fe} representing the permeability of iron. The maximum frequency here is given by

$$\omega_c = \frac{\delta}{x^2 \mu \sigma} - f(L,R) \tag{21}$$

where f (L,R) varies with the core geometry turns ratio and the material and thickness of the conducting material.

To investigate energy transfer from a step input function we begin again with Figure 4. When switch S is closed the current flowing in windings N_1, is

$$i_1 = i_o (1 - e^{-(R_1/L_{s1})t}) \tag{22}$$

where $i_o = V_o/R_1$, and the associated magnetic field produced is

$$H_1 = H_o(1 - e^{-(R_1/L_{s1})t}) \tag{23}$$

where

$$H_o = \frac{N_1}{2\pi r} \quad i_o = \frac{N_1}{2\pi r} \quad \frac{V_o}{R_1}$$

A solution of equation (12) after applying the appropriate boundary condition, is in this case

$$H_x = H_o e^{-x/\delta_s} \left(1 - e^{-(R_1/L_{s1})t}\right) \tag{24}$$

where δ_s is

$$\delta_s = \left[\frac{1 - e^{-(R_1/L_{s1})\,t}}{\sigma\mu\,(R_1/L_{s1})\,e^{-(R_1/L_{s1})\,t}}\right]^{1/2} \tag{25}$$

The skin depth (δ_s) from a step input is therefore dependent on time as well as the electrical conductivity σ, the permeability μ and the circuit parameters R_1 and L_{s1}. The voltage V_2 developed across N_2 is then

$$V_2(t) = N_2\mu \frac{\partial}{\partial t} \int_0^A H_x \cdot dA$$

$$= \frac{N_1 N_2 A \mu_{re}}{2\pi r} \frac{V_o}{L_{s1}} e^{-x/\delta_s} \left(e^{-(R_1/L_{s1})t} + \frac{x}{2\delta_s}\right) \tag{26}$$

The energy (W) delivered to the load resistor R_L is given by (c.f. Figure 4(b))

$$W = i_2^2(t)\, R_L T \tag{27}$$

where T = the duration of $V_2(t)$ and

$$i_2(t) = \frac{N_1 N_2 A \mu_{Fe}}{2\pi r} \frac{V_o}{L_{s1}} \frac{e^{-x/\delta_s}}{R_2 + R_L} \left\{ \frac{x}{2\delta_s} \right.$$

$$(1 - e^{-((R_2 + R_L)/L_{s2})t})$$

$$+ \left(\frac{R_1 L_{s1} L_{s2}}{L_{s1}(R_2 + R_L) - R_1 L_{s2}} \right)$$

$$\left. (e^{-(R_1/L_{s1})t} - e^{-((R_2 + R_L)/L_{s2})t}) \right\} \quad (28)$$

The energy delivered to a load is then dependent on the size, geometry and turns ratio of the transformer and highly dependent on the thickness and physical properties of the conducting shield. The dependence on L_{s1} and L_{s2} is in turn essentially constant with x, as will be shown in the next section.

PARAMETER EFFECTS AND EXPERIMENTAL RESULTS

In the preceding section we developed both voltage and current equations, which describe the energy propagation process from one medium to another, when the input signal is sinusoidal and when it is a step function. In this section we hope to confirm these expressions, at least in part, by some experimental results that have been obtained.

Let us take the sinusoidal case first where only a limited amount of experimental work was performed. In this case voltage measurements were made across a secondary load of 0.75 ohms as a function of the driving frequency $\omega/2\pi$. A plot of the output to input voltage ratio versus the driving frequency ($\omega/2\pi$) is given in Figure 6. The physical properties of the device are shown in the figure. Over the frequency range of 1 KC to 200 KC the variation of V_{out}/V_{in} ranges from 10^{-1} to 2×10^{-5} indicating a very definite filtering action. The corresponding curves shown in Figure 3 show that the curve should have peaked at about 20 KC, but a closer look at the equation (22) indicates a term dependent upon the resistance and inductance of the circuit which is subtracted from the term $8/x^2\mu\sigma$, which compensates for the variation in the two curves.

The bulk of the experimental work was performed where the input was a step function. The information desired was the energy transmitted through the conducting shield to the resistive load connected across the secondary windings. Figure 6 shows plots of the energy delivered to the resistive load R_L as a function of the shielding thickness x and the core area cross section. The physical parameters of the materials are given in the figure. The input voltage in all cases was 28 volts. The energies transferred range from 1000 to 800,000 ergs, which are

adequate for firing electro-explosive or semiconductor devices. The theoretical curves and experimental data (points) on the curve fit very well. The values of the leakage inductance looking from the secondary L_{s2} was constant with the turns ratio N_2/N_1 and both the primary and secondary leakage inductances L_{s1} and L_{s2} were constant with the shielding thickness x.

All the discussions of this report have been restricted to electrical energy transfer. It is also possible to transmit electrical energy by doing mechanical work, such as separating two sections of a magnetic core. This type of investigation has been conducted at the Naval Ordnance Laboratory by Mr. Roland Schlie.

Figures (8) and (9) are possible communication systems, using the aforementioned principlesas the communication link. Figure (8) shows a system which uses a sinusoidal input to drive different tuned circuits. Each tuned circuit operating at a different frequency would be a selection for the pilot. Prior to separation or bomb release the core is energized with a dc current, and as the bomb is released a signal on the secondary windings arms the weapon. Figure (9) shows a system which incorporates a series of step input voltages to select the arming and fuzing sequences desired. The second transformer is energized prior to separation and the pulse generated at separation arms the weapon. Both systems would have to be armed deliberately

by the pilot so that an accidental release or a desired jettison would leave the weapon in a safe condition.

CONCLUSIONS

A transformer whose primary and secondary windings are wound on iron cores will exhibit the behavior of a low frequency band pass filter, if the iron cores are separated by a thin conducting sheet. This has been shown theoretically and experimentally. For a copper sheet .040 inches thick the attenuation of the magnetic field at 100 KC is greater than 2 orders of magnitude, and at one megacycle it is attenuated by seven orders of magnitude. The associated electric field is attenuated some 8 orders of magnitude below that of the magnetic field. If then a weapon is completely encased in a conducting material the internal components of the weapon will not be affected by radar. The split transformer, however, provides a method of communication which, while not very efficient, has been demonstrated to be quite feasible from an energy transfer, reliability and size viewpoint.

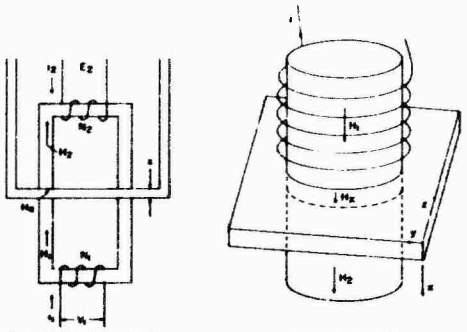

FIG 1

FIG. 2 MAGNETIC FIELD ATTENUATION IN COPPER

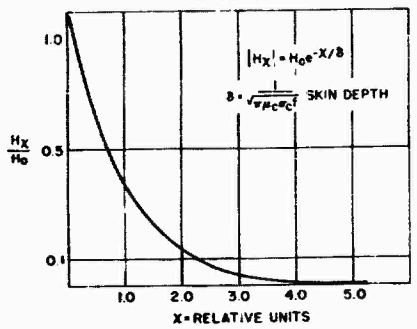

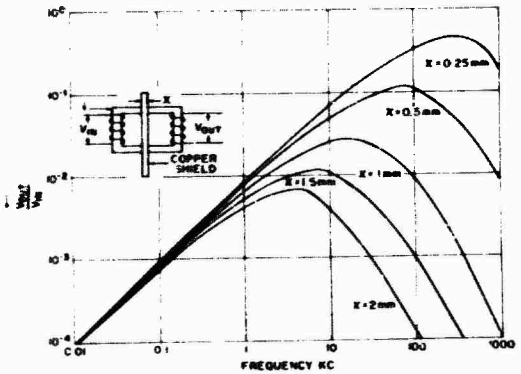

FIG 3 THEORETICAL V_{OUT}/V_{IN} vs FREQUENCY AS A FUNCTION OF SHIELD THICKNESS

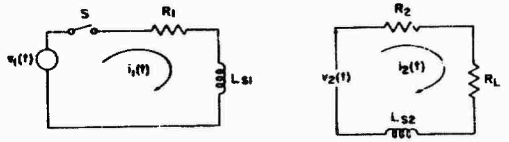

FIG. 4 INPUT AND OUTPUT EQUIVALENT CIRCUITS

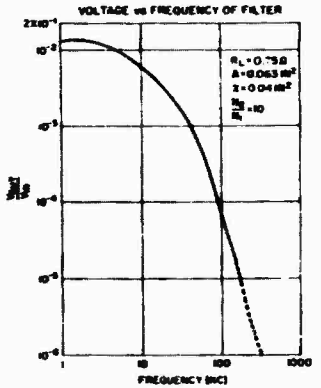

FIG. 5 V_{OUT}/V_{IN} vs FREQUENCY OF EXPERIMENTAL MODEL

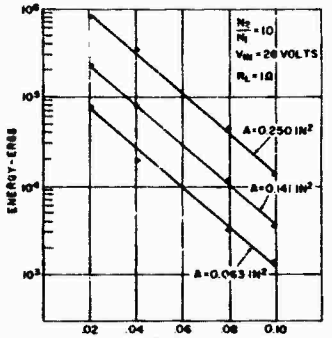

FIG. 6 TRANSMITTED ENERGY vs SHIELD THICKNESS

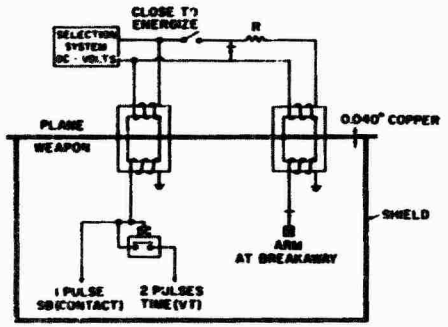

FIG. 8 PLANE TO WEAPON COMMUNICATION BY PULSED SIGNAL

FIG. 7 PLANE TO WEAPON COMMUNICATION TUNED CIRCUITS

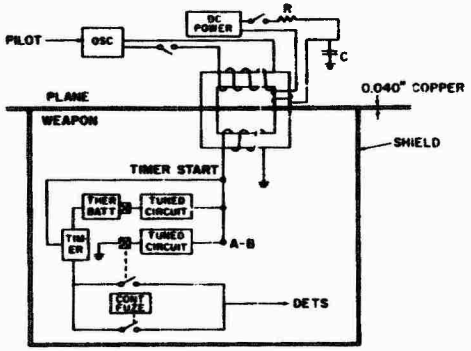

21. DISCUSSION

A questioner asked the power supply requirement for multiple, simultaneous release. Mr. White answered that the efficiency was poor. With as many as 54 bombs on the plane requiring arming at the same time, you might have a problem but with higher voltage it looks as though this problem could be circumvented.

Mr. Warren of The Franklin Institute commented that the .04 inch shield would reduce the permeability of the core. Even a 0.001 inch would be adequate thickness for the shield. The shield could be made of a high permeability material. Each of these would improve the efficiency of the device. Mr. White added that shields smaller than .04 inches were used.

Mr. Altman of Dahlgren asked if repeated use of the device could be made. He asked if studies had been made of mating surfaces in order to extend the magnetic core through the shield and simply shield the flux linkage. The answer was that a method similar to this was designed and used in a weapon. Signals were passed through it. The intent was to use it as a fix, but it could also be used for communication. Mr. Schlie will probably answer that question in more detail in the next presentation.

22. A MECHANICAL PULSE TRANSFORMER

Roland W. Schlie

U. S. Naval Ordnance Laboratory
White Oak, Silver Spring, Maryland

INTRODUCTION

The application of electroexplosive devices (EED) in fuze systems has many advantages. Their susceptibility to radio frequency (RF) signals continues to be a major justification for substitutions which, while not susceptible to RF, do not have the inherent advantages of the EED.

It is the purpose of the paper to present a device which could provide RF isolation to a bomb fuze incorporating an EED. This device may be called a mechanical pulse transformer which will enable the fuze circuitry to be completely shielded and yet permit the application of aircraft electrical signals to initiate fuze function.

A properly designed transformer can provide effective isolation from RF signals. Reference (a). However, the efficiency with which a d.c. firing pulse can be transformed to the secondary load has been a major limitation. In the case of the mechanical pulse transformer the bulk of the energy output is introduced mechanically. While d.c. excitation is required for function, output energy resulting from excitation or de-excitation is negligible.

DESCRIPTION

A reactive circuit containing stored magnetic energy will accept additional energy if the reactance is forcibly changed (references (b)(c)(d)). A transformer having separate primary and secondary coil assemblies is such a reactive circuit. If mechanical energy is used to forcibly separate the transformer, part of this energy will be dissipated in the connected load resistance.

Figure 1 shows a cross section of the test model. Both primary and secondary cores are made of mild unannealed steel, chosen to have a maximum core loss for a.c. excitation. The 0.009-inch gap tends to hold down residual flux. A large number of primary turns are chosen to obtain as much primary inductance as possible. High primary inductance provides better distribution of the energy pulse to the secondary load and a large time constant for excitation and de-excitation pulses. Secondary turns are chosen for best power transfer to the secondary load resistance.

A possible design configuration for application with a bomb is shown in Figure 2. The shield shown would most likely be made of soft copper, pressfit in the secondary or primary core to provide complete shielding of the two coils. The power dissipated in the shunt is dependent upon the ratio of N^2/R for the shunt as compared to N^2/R for the secondary coil. Calculations indicate that ample shield thickness can be obtained without decreasing power output by more than 20 percent. Other configurations are also feasible.

It should be noted at this point that the applications envisioned to date would employ the Navy Aircraft "Fuze Function Control Set AN/AWW-1" for a source of 195- or 300-volt d.c. excitation power. With this conception, an intent-to-drop input signal for the system is initiated by the pilot; the bomb fuze system is initiated after actual separation of the bomb from the aircraft has occurred. Thus, the application of the mechanical pulse transformer can provide:

1. Dual input signals for bomb system initiation.
   (a) Excitation by pilot.
   (b) Separation of bomb from aircraft.
2. Complete separation and shielding between the aircraft and bomb electrical systems.

TEST PROCEDURES

Preliminary tests indicated that the relationship of power output and excitation flux density was well known and easily verified within the limits of unsaturated cores. Output power as a function of the velocity of separation was far less understood. Test efforts were therefore directed toward obtaining data which would demonstrate this relationship. A theoretical analysis of the behavior of the mechanical transformer is shown in Appendix A.

Measurements of energy pulses are at best a cumbersome task. "Erg-meter" techniques were tried with reasonable success but did not provide a very visual indication of the parameters of interest, maximum power output and time durations. The simple test arrangement shown in Figure 3 proved to be the most useful.

Photographs of the oscilloscope traces were analyzed to obtain the relationship of output load voltage as a function of time.

Dropping a weight a measured distance proved to be the simplest method of imparting a known velocity of separation to the secondary core and coil assembly. The test fixture for accomplishing this is shown in sketch form by Figure 4. Drop distance S was increased to obtain higher velocities of separation. The weight used had to be relatively large compared to the core and coil in order to overcome magnetic attraction without a serious change in velocity. Nineteen pounds were used to obtain the test data given in this paper. The secondary core and coil plus stem and stop weighed three-quarter pounds.

PERFORMANCE

It appeared that the best method of evaluating and understanding the performance of a mechanical transformer would be to make a graphic comparison of the actual performance curves with those calculated from theoretical equations. Appendix A contains the theoretical equations which were derived on the basis of the following assumptions:

1. Reluctance of the magnetic circuit is proportional to the square root of the air gap distance.

2. Velocity of separation is constant.

Appendix B contains the theoretical equations for which transformer constants were calculated from test data. Logarithmic graphic presentations are included in Appendix B, Figures 9 and 10, but

these plots do not present the voltage-time and power-time curves in their most familiar form. Figure 5 is a plot of output load voltage versus time for (1) the mechanical pulse transformer, (2) the calculated theoretical equation, and (3) a conventional capacitor discharge. Figure 6 is a plot of output power versus time. Included in Figure 6 are the total energy quantities obtained by integrating the power curves.

The close correlation between the voltage and power curves, as well as the total energy calculations, justifies the assumptions used in deriving the theoretical equations.

Load resistance as a function of relative output energy is shown in Figure 7. Maximum energy output occurred for a load resistance of 1.4 times the secondary coil resistance. Optimum power output can be obtained by selecting the wire size and number of secondary turns to match the load resistance. Maximum utilization of the coil volume space will result in a higher efficiency.

Unwanted energy pulses will occur when the transformer is (1) excited, (2) de-excited, or (3) separated while residual flux remains in the core. Consider first the case of excitation. Energy equal to that stored in the magnetic circuit must be dissipated in the resistance of the primary coil, secondary coil and load. In the case of de-excitation, only the secondary coil resistance and load resistance dissipate the stored energy. Therefore the unwanted energy pulse resulting from de-excitation is greater. A simple method of reducing the unwanted energy pulse resulting from de-excitation is to connect a resistor in parallel

with the primary coil as shown in Figure 3. The reduction, while significant, was not as much as expected. Output pulses due to de-excitation were about 10 percent higher than those due to excitation. The test fixture did not lend itself to a measurement of the unwanted output pulse caused by separation while residual flux existed. The properties of the core material and the use of a gap should hold residual flux to a minimum, but further investigation is warranted.

Figure 8 is a plot of output voltage versus time for (1) a forced separation with an impact velocity of 4.63 feet per second and an excitation of 32 milliamperes, and (2) de-excitation from 32 milliamperes. A ratio of the energy pulses is shown to be 21:1. This ratio of output pulses is increased if the core gap is decreased. However, if the gap is decreased, a larger energy pulse will result from separation as a result of residual flux. A compromise between the lower de-excitation pulse obtained by decreasing the gap and the resulting larger pulse caused by residual flux must be made.

DESIGN PROBLEMS

The success in obtaining maximum energy at the secondary load terminal with minimum energy going to the primary coil is due, in part, to the fact that the primary is designed for maximum inductance. Number forty wire was used in the test model. Wire of this size is difficult to work with. Using still smaller sizes would improve performance. Wafer-coil techniques for transformers (reference (e)) may well be the answer.

Conventional winding techniques and lead attachment methods were very costly in coil space. Methods of attaching the leads and of securing the coil in the core need to be improved upon.

CHARACTERISTICS TO INVESTIGATE

There are several performance characteristics about which more must be known before design calculations can be made to adequately predict actual performance. Effects of shielding methods on the efficiency with which the transformer will convert mechanical energy is one such characteristic. It is a basic premise of this paper that complete shielding will prevent RF coupling between the primary and secondary coils and that the solid core materials together with the very high inductance of the primary will result in a very minor transformation of RF to the secondary. However, there are several methods of achieving these goals. Their effects on performance as a mechanical pulse transformer have not been determined.

Adjusting load resistance to achieve maximum output is easy enough. Selecting secondary wire size and the number of secondary turns to obtain maximum output with a specified load resistor is another matter. A theoretical approach is being developed.

Minimum travel distance of the core and coil assembly would facilitate a more compact unit. Effects of travel distance on power output have not been determined.

The magnitude of residual flux and the corresponding output pulse caused by forced separation must be kept to a minimum. Output per unit volume can be increased if the gap length can be reduced.

SUMMARY

A major drawback to the use of a transformer to couple energy to an EED is its efficiency in transforming a d.c. firing pulse. The device presented in this paper takes advantage of the mechanical energy available during a bomb release. For example, 1000 pounds are ejected from the bomb rack at better than 10 feet per second; ample energy is thus readily available.

Advantages of the mechanical pulse transformer concept, if employed in a fuze bomb system, are summarized as follows:

1. Complete separation of aircraft and bomb electrical systems.
2. Complete shielding from RF.
3. High energy availability for EED.
4. Dual input requirements for system function.

REFERENCES

(a) Development of a Universal Radio Frequency Protected Squib, by Paul F. Mohrbach and Melvin R. Smith. Report Number F-B1856, The Franklin Institute, 1962.

(b) Survey of Possible Explosive Electric Energy Transducers, by Stuart E. Whitcomb. Sandia Corporation SCTM 231-58-51, July 1958.

(c) Electromechanical Energy Conversion, by David C. White and Herbert H. Woodson. John Wiley and Sons, New York, 1959.

(d) Electromechanical Energy Conversion, by Samuel Seely. McGraw-Hill Book Co., Inc., New York, 1962.

(e) Wafer-Coil Techniques for Transformers, by Albert Zack and James Heffernan. Electrical Manufacturing, February 1955.

APPENDIX A

DERIVATION OF VOLTAGE AND ENERGY RELATIONS

Albert Preisman

U. S. Naval Ordnance Laboratory
White Oak, Silver Spring, Maryland

Assume the velocity of separation of the mechanical pulse transformer is a constant, v , and that the reluctance of the air gap $R_{(x)} = k\sqrt{x}$ where x is the length of the air gap caused by the separation and k is a constant. Since $x = vt$, where t = time, $R_{(t)} = k\sqrt{vt}$

In order to obtain a manageable mathematical equation, assume that the reluctance of the iron structure is negligible compared to that of the air gap, and that the primary ampere turns $N_p I_p$ are negligible compared to that produced by the induced secondary current I_s flowing through the N_s turns of the secondary coil. It can be shown that this is essentially true for the major portion of the travel distance of the secondary coil structure.

The flux ϕ set up at any time t corresponding to a reluctance $R_{(t)}$, is then given by

$$\phi = \frac{N_s I_s}{R_{(t)}} = \frac{N_s I_s}{k\sqrt{vt}} \qquad (1)$$

But

$$I_s = \frac{E_s}{R} \qquad (2)$$

where E_s is the voltage induced in the secondary by the decreasing flux:

$$Es = -Ns \, d\phi/dt \qquad (3)$$

and R . 3 the total resistance of the secondary circuit and is the sum of the secondary winding resistance R_w plus that of the connected load, R_L.

Substituting equations (2) and (3) in (1) we obtain

$$\phi = \frac{-Ns^2}{Rk\sqrt{v}t} \, d\phi/dt \qquad (4)$$

The variables, $t \notin \phi$, can be separated and integrated to yield

or $$\log \phi/\phi_m = -\frac{2Rkv^{1/2}t^{3/2}}{3Ns^2}$$

$$\phi = \phi_m \varepsilon^{-\left(\frac{2Rkv^{1/2}t^{3/2}}{3Ns^2}\right)} \qquad (5)$$

where ϕ_m is the maximum value of the flux just prior to the separation of the mechanical pulse transformer.

From equation (3) we have

$$Es = \frac{\phi_m Rkv^{1/2}t^{1/2}}{Ns} \, \varepsilon^{-\left(\frac{2Rkv^{1/2}t^{3/2}}{3Ns^2}\right)} \qquad (6)$$

and since $$EL = Es \, \frac{RL}{R}$$

$$EL = \frac{\phi_m RL kv^{1/2}t^{1/2}}{Ns} \, \varepsilon^{-\left(\frac{2Rkv^{1/2}t^{3/2}}{3Ns^2}\right)} \qquad (7)$$

where E_L is the voltage applied to the load R_L connected to the secondary coil.

The power developed in R_L is $P_L = \frac{E_L^2}{R_L}$

or $$P_L = \frac{\Phi_m^2 R_L k^2 v t}{N_s^2} \varepsilon^{-\left(\frac{4Rkv^{1/2}t^{3/2}}{3N_s^2}\right)} \qquad (8)$$

and the energy $$W_L = \int_0^\infty P_L dt = \int_0^\infty \frac{\Phi_m^2 R_L k^2 v t}{N_s^2} \varepsilon^{-\left(\frac{4Rkv^{1/2}t^{3/2}}{3N_s^2}\right)} dt \qquad (9)$$

From the integral table we have

$$\int_0^\infty y^n \varepsilon^{-ay} dy = \frac{\Gamma(n+1)}{a^{(n+1)}}$$

now let $y = t^{3/2}$, then $t = y^{2/3}$ and $dt = \frac{2}{3} y^{-1/3} dy$

Substituting the equations for y in equation (9) yields

$$W_L = \int_0^\infty \frac{2\Phi_m^2 R_L k^2 v y^{1/3}}{3N_s^2} \varepsilon^{-\left(\frac{4Rkv^{1/2}y}{3N_s^2}\right)} dy \qquad (10)$$

Evaluating equation (10) by the formula given in the integral tables we have

$$W_L = \frac{2}{3}\left(\frac{3}{4}\right)^{4/3} \Gamma(4/3) \frac{\Phi_m^2 R_L k^{2/3} v^{1/3} N_s^{2/3}}{R^{4/3}}$$

or $$W_L = .4035 \frac{\Phi_m^2 R_L k^{2/3} v^{1/3} N_s^{2/3}}{R^{4/3}} \qquad (11)$$

APPENDIX B

CALCULATION OF EQUATION CONSTANTS

U. S. Naval Ordnance Laboratory
White Oak, Silver Spring, Maryland

The equations of Appendix A may be used as the basis for calculating constants which represent the characteristics of the model mechanical pulse transformer. The derivations of Appendix A can then be evaluated in terms of the assumptions used. Also, the test results obtained with the model can be extrapolated to predict performance beyond the test parameters chosen.

Equation (7) is rewritten in the following form

$$E_L = \frac{\Phi_m k R_L}{N_s} v^{1/2} t^{1/2} \varepsilon^{-\left(\frac{Rk}{N_s^2} \frac{2}{3} v^{1/2} t^{3/2}\right)}$$

The values of k and N_s are constants for a specific transformer. The values of R_L and Φ_m can be held constant for a specific test series. Therefore, let

$$Q = \frac{\Phi_m k R_L}{N_s} \tag{12}$$

and

$$q_0 = \frac{Rk}{N_s^2} \tag{13}$$

Substituting equations (12) and (13) in equation (7) yields

$$E_L = Q v^{1/2} t^{1/2} \varepsilon^{-\left(\frac{2}{3} q_0 v^{1/2} t^{3/2}\right)} \tag{14}$$

The value of E_{Lmax} may be determined by taking the derivative of E_L with respect to t and equating the derivative to zero.

$$dE_L/dt = Q v^{1/2}\left\{t^{1/2}(-2/3\, g v^{1/2} t^{1/2})\, \varepsilon^{-\left(2/3\, g v^{1/2} t^{3/2}\right)} + 1/2\, t^{-1/2}\, \varepsilon^{-\left(2/3\, g v^{1/2} t^{3/2}\right)}\right\} = 0$$

Then for $E_{L\,max}$ $$t = 2^{-2/3}\, g^{-2/3}\, v^{1/3} \qquad (15)$$

or $$v = 4 g^{-2} t^{-3} \qquad (16)$$

Substituting equations (15) and (16) in equation (14) yields

$$E_{L\,max} = \frac{Q v^{1/3}}{2^{1/3} g^{1/3}}\, \varepsilon^{-1/3} \qquad (17)$$

or $$E_{L\,max} = \frac{Q}{2gt}\, \varepsilon^{-1/3} \qquad (18)$$

A test series was conducted holding R_L & ϕ_m constant. A simple test fixture was used for dropping a 19 pound weight a pre-selected distance S, see Figure (4). At the end of the travel distance, S, the weight engages the secondary core and coil assembly of the test model. The weight and core and coil assembly were allowed to travel a distance g, 3-1/4 inches. The kinetic energy of the weight separated the mechanical pulse transformer. While this simple test procedure did not produce a constant velocity of separation, it did yield satisfactory test data for evaluating the performance of the model and provided the data required to evaluate the equations of Appendix A. Table I is a summary of the test results.

The values of $E_{L\ max}$ and t were taken from a scope trace of E_L and t. Velocity of separation was assumed to be equal to the impact velocity of the weight. Table 1 values were first substituted in equation (18) to obtain an average value for (Q/q). An average for q was obtained by substituting in equation (16). Based upon these calculations, the following values were selected, Q = 70 & q=1792.

With these values for Q & q and expressing time in millisecond, equations (14), (15), (16), (17) and (18) may be written as

$$E_L = 2.214\, v^{1/2} t^{1/2} \varepsilon^{-.0378 v^{1/2} t^{3/2}} \text{ volts} \tag{19}$$

At $E_{L\ max}$ $$t = 4.27\, v^{-1/3} \text{ ms} \tag{20}$$

$$v = 77.85\, t^{-3} \text{ ft/sec.} \tag{21}$$

$$E_{L\ max} = 3.28\, v^{1/3} \text{ volts} \tag{22}$$

$$E_{L\ max} = \frac{14}{t} \text{ volts} \tag{23}$$

A similar treatment of equation (8) yields

$$P_L = \frac{Q^2 v t}{R_L} \varepsilon^{-4/3 q v^{1/2} t^{3/2}} \text{ watts} \tag{24}$$

$$W_L = \int_0^\infty \frac{Q^2 v t}{R_L} \varepsilon^{-4/3 q v^{1/2} t^{3/2}} dt \tag{25}$$

$$W_L = \frac{.404\, Q^2 v^{1/3}}{R_L q^{4/3}} \text{ watt - seconds} \tag{26}$$

$$W_L = \frac{908,000}{R_L} v^{1/3} \text{ ergs} \qquad (27)$$

$$W_L = 174,000\, v^{1/3} \text{ ergs} \qquad (28)$$

Figure 9 presents equations (19) through (23) in graphic form. The straight line is a plot of E_{Lmax} at specific velocities and the corresponding time at which peak load voltage occurs. The curved lines are a plot of load voltage as a function of time. The intersection of the straight line and the curves identifies the velocity of separation and maximum load voltage. It should be noted that these curves represent a specific transformer for which excitation current and load resistance are held constant.

Figure 10 is presented to compare the test values of the model taken from an oscilloscope trace with calculated values from equations (19) through (23). Maximum voltage is identified for tests (2), (3) and (5). The complete curve is shown for tests (1) and (4). The dash curve is a calculated curve added to aid in the comparison.

Table 1. TEST RESULTS

Test Number	Drop Distance S	Impact Velocity V	$E_{L\ max}$	t at $E_{L\ max}$	R_L
1	0.5 inches	1.64 ft/sec	3.70 volts	3.7 ms	5.22 ohms
2	1.0	2.32	4.24	3.5	5.22
3	2.0	3.28	4.80	3.0	5.22
4	4.0	4.63	5.40	2.5	5.22
5	8.0	6.55	5.85	1.85	5.22

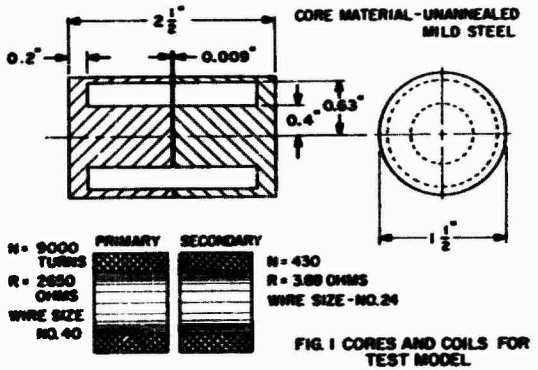

FIG. 1 CORES AND COILS FOR TEST MODEL

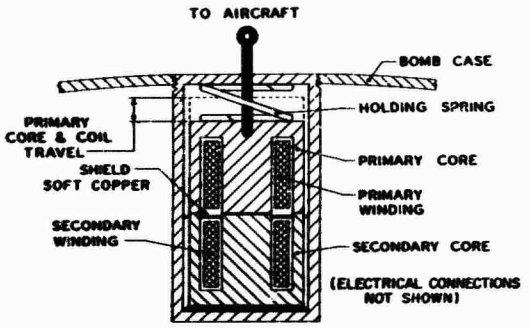

FIG. 2 DESIGN CONCEPT OF MECHANICAL PULSE TRANSFORMER FOR BOMB APPLICATION

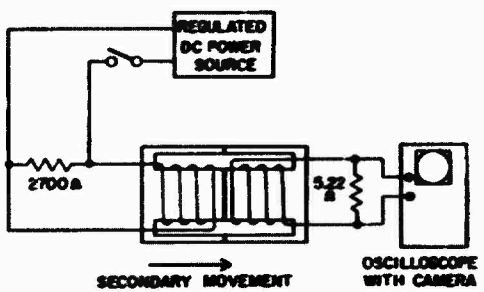

FIG. 3 TEST CIRCUIT FOR MEASUREMENT OF PERFORMANCE OF THE MECHANICAL PULSE TRANSFORMER

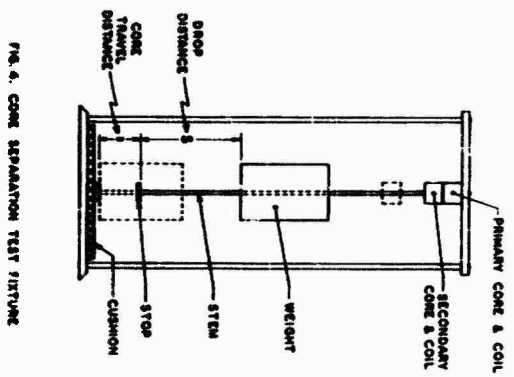

FIG. 4. CORE SEPARATION TEST FIXTURE

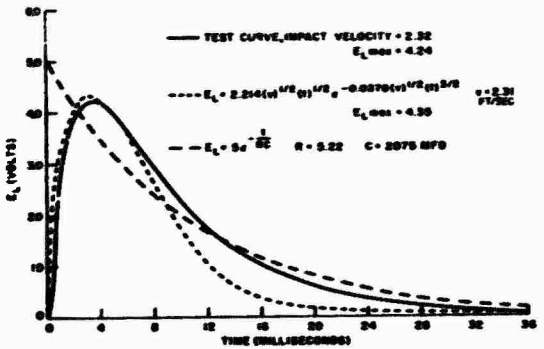

FIG. 5 COMPARISON OF
OUTPUT VOLTAGE OF MECHANICAL PULSE TRANSFORMER

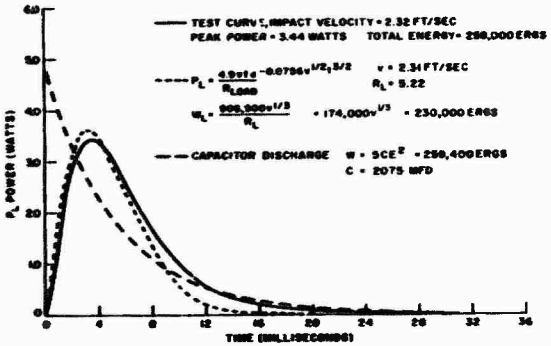

FIG. 6 COMPARISON OF
OUTPUT POWER OF MECHANICAL PULSE TRANSFORMER

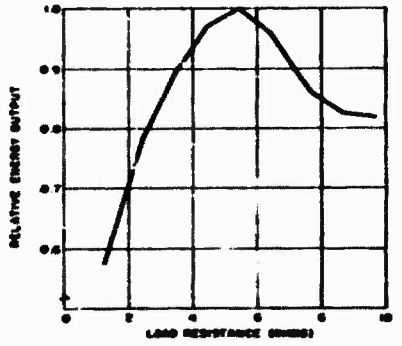

FIG. 7 RELATIVE ENERGY OUTPUT
AS A FUNCTION OF LOAD RESISTANCE

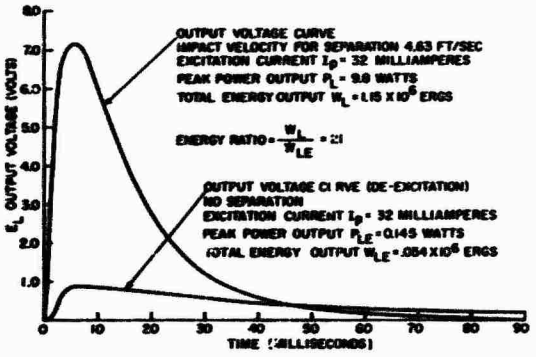

FIG. 8 OUTPUT VOLTAGE RESULTING FROM DE-ENERGIZING TRANSFORMER

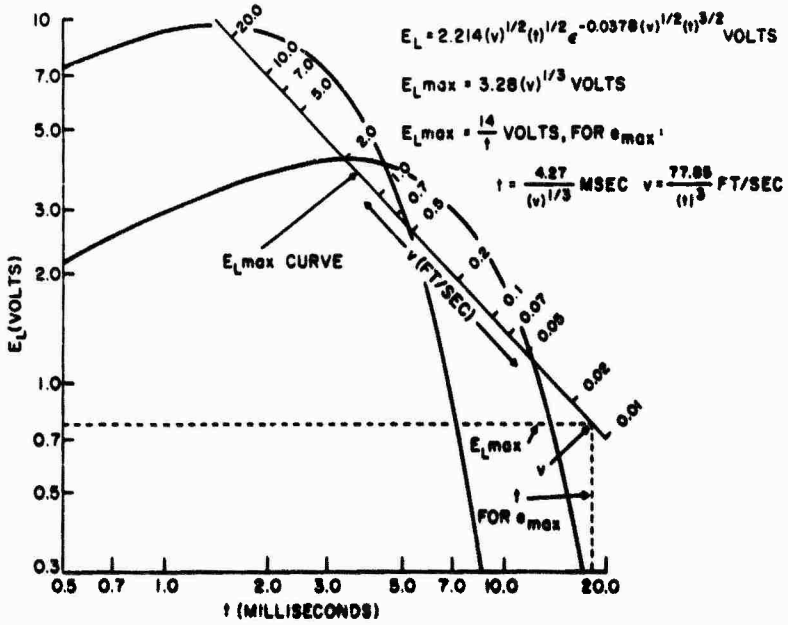

FIG. 9 MECHANICAL PULSE TRANSFORMER-OUTPUT VOLTAGE

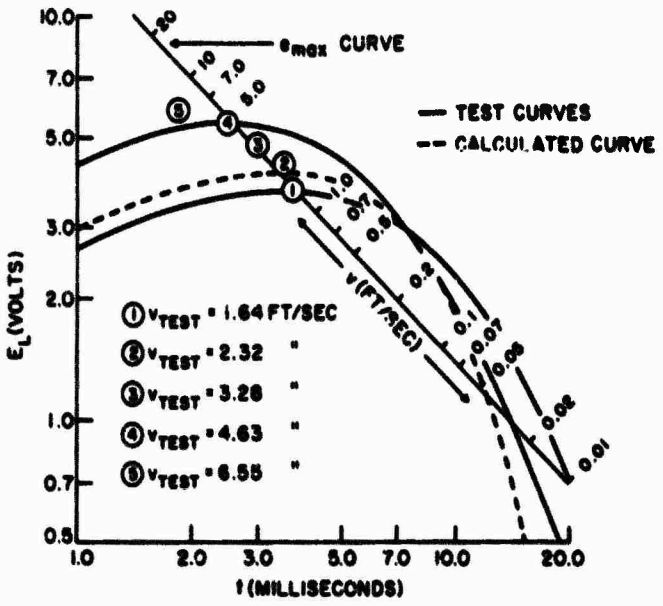

FIG. 10 TEST RESULTS OF
MECHANICAL PULSE TRANSFORMER-OUTPUT VOLTAGE

23. RF SENSITIVITY OF CONTROLLED RECTIFIERS

Author: Richard J. Sanford

U. S. Naval Ordnance Laboratory

INTRODUCTION

The controlled rectifier, also known as the controlled switch or pnpn switch, is a semiconductor device which closes an electrical connection between its anode and cathode when a suitable electrical signal is applied between gate and cathode. This connection remains closed as long as a current passes through it, whether the gate signal remains or not.

STRUCTURE AND OPERATION

The heart of a silicon controlled rectifier is a single crystal of very pure silicon consisting of four alternating layers of p- and n- type material, which form three interacting p-n junctions. From bottom to top of Figure 1, these are the emitter or cathode junction, the collector junction, and the conjugate emitter or anode junction. The lower two junctions form, in effect, a high gain n-p-n transistor, and the upper two junctions form a low gain p-n-p transistor, both transistors using the same collector. The α of each transistor increases with collector current at low currents. Since the transistors are connected for position feedback, the device switches "on" when the collector current rises

to such a value that the sum of the α's exceed unity. A forward voltage of about ½ volt must be placed across the emitter junction to raise the collector current to this value, and so any signal, DC or RF, which can raise the gate voltage to this level can fire the switch.

GATE RF SENSITIVITY

A controlled rectifier has some inherent protection against RF signals introduced at its gate lead. The capacitance of its emitter junction combines with the resistance around the gate contact to form a simple RC filter which attenuates the RF. The action of this filter decreases the sensitivity of the switch as the frequency of the gate signal is increased, as is shown in Figure 2, for two pnpn switches. Figure 3 shows a simplified diagram of the test circuit used. Moreover, the controlled rectifier can "remember" whether it is "on" or "off" only so long as DC is applied to the anode. Since these switches are not damaged by gate powers much higher than those required to fire them, the controlled rectifiers in an unarmed weapon may be subjected to large RF signals and still operate satisfactorily at some later time. This contrasts sharply with the explosive switch which, once fired, cannot be reset.

ANODE RF SENSITIVITY

Normal

Controlled rectifiers can also be fired by spurious RF applied between anode and cathode. In this case, the RF

voltage is divided between the reactance of the anode capacitance and the impedance across the emitter junction. Figure 4 shows that a controlled rectifier can be fired by progressively lower RF voltages as the frequency increases. Moreover, the anode capacitance of the switch (30 pf for the 2N1882) allows even an unfired unit to pass appreciable current at the higher frequencies. Figure 5 shows the circuit used in this test and the two to follow.

Two Methods of Protection

The voltage divider model of the pnpn switch suggests two methods of protection against RF which inadvertently reaches the anode. One method is to apply a reverse bias to the gate, so that a larger voltage swing must be produced at the emitter if the RF is to fire the switch. Figure 6 shows that this method is effective at all frequencies tested. A simpler method is to place a capacitor between gate and cathode. This capacitor acts as a low impedance shunt path to reduce the voltage across the emitter. Figure 7 shows the effect of the gate capacitor. It provides effective anode protection at the lower radio frequencies, but the gate resistance of the switch limits the usefulness of the capacitor at higher frequencies.

PROTECTION FOR EED'S

Circuit

One possible application of the silicon controlled rectifier is as a low pass filter to protect the bridge wire

of an electro-explosive device from low frequency radio signals. At low radio frequencies such as 150 KC, conventional LC filters tend either to be physically bulky or to have prohibitively high series resistances. The circuit of Figure 8 was designed to protect bridge wire devices against 32 volt RMS signals between 100 KC and 30 MC. The low frequency protection is provided entirely by the circuitry to the right of the dashed line. The gate capacitor enables the controlled switch anode to withstand 32 volt RMS signals up to about 3 MC. The gate is isolated from the RF input by an RC filter. The circuitry to the left of the line is a rudimentary LC filter to provide protection at higher frequencies. Its effectiveness is limited by the shunt capacitance of the particular choke used. A more appropriate conventional filter can extend the protection to much higher frequencies.

Response

Figure 9 shows the measured audio-frequency response of the model that was built. The model begins to protect against 32 volt RMS (45 volt amplitude) signals at about 20 KC.

Figure 10 shows the model switch protector with an explosive switch and a copper shield. The model, which uses only conventional components, is built into a lucite cube ½ inch on a side. At the bottom the protector, switch and shield are shown assembled.

SUMMARY

The RF gate voltage to fire a pnpn switch increases monotonically withfrequency.

A fired pnpn switch may be reset and reused.

The RF anode voltage to fire a pnpn switch decreases with frequency.

Some anode protection can be obtained by use of reverse gate bias or a gate capacitor.

The pnpn switch may prove useful in protecting electro-explosive devices against low-frequency radio signals.

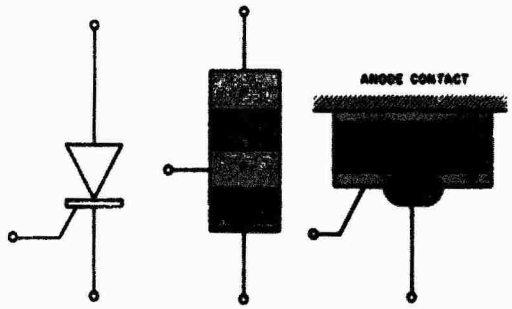

PNPN SWITCH
(SILICON CONTROLLED RECTIFIER)
FIG. 1

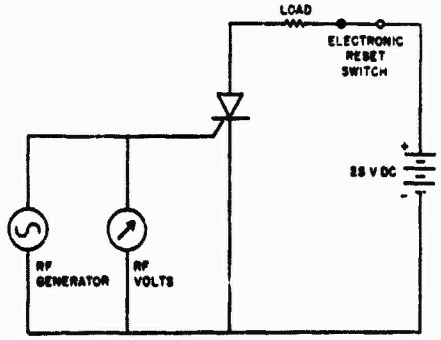

SIMPLIFIED RF SENSITIVITY TEST
FIG. 2

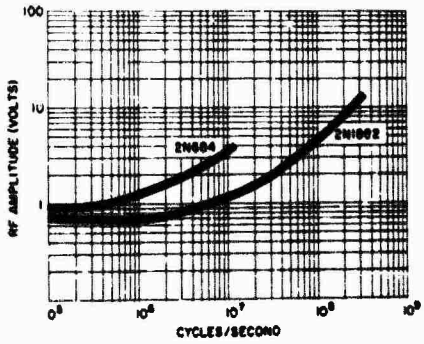

GATE RF FIRING
FIG. 3

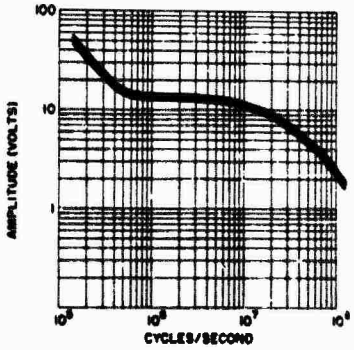

ANODE RF FIRING OF 2N1682 @ 7
FIG. 4

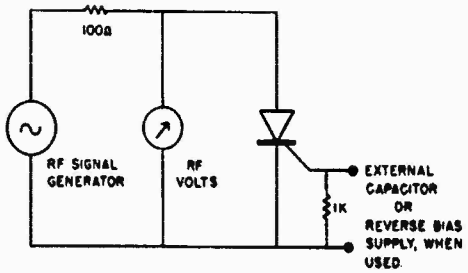

SIMPLIFIED CIRCUIT TO TEST RESPONSE OF SCR TO RF ON ANODE
FIG. 5

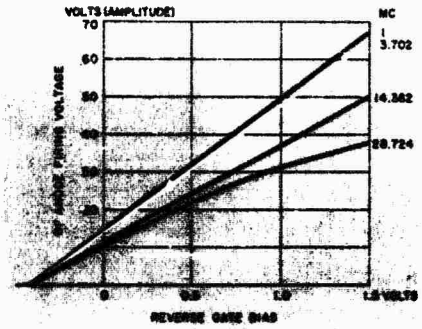

ANODE PROTECTION BY GATE BIAS
FIG. 6

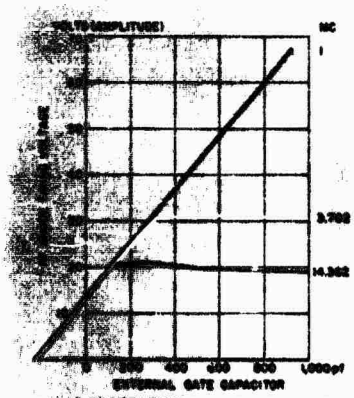

ANODE PROTECTION BY GATE CAPACITOR
FIG. 7

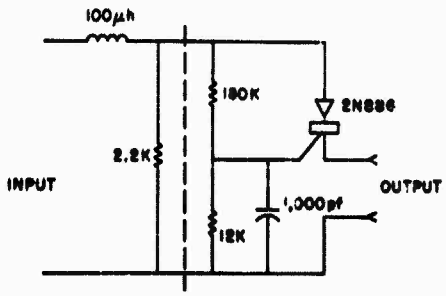

RF PROTECTOR
FIG. 8

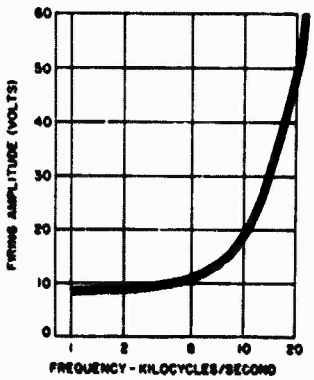

RESPONSE OF RF PROTECTOR
FIG. 9

FIG. 10
RF PROTECTOR

23. DISCUSSION

Mr. Sanders asked for the DC current rating on the device and the normal operating voltage. Mr. Sanford gave the rating at 300 milliamperes with much higher pulsed rating. Where one shot only is required, up to 5 amperes can be used. The lead wire length will affect the voltage rating.

It was pointed out that power input, from an RF standpoint, is more truly indicative of performance than voltage ratios. The quasi-dc analysis showing protection is not necessarily an effective one for RF. Mr. Sanford answered that the need for proper RF design is obvious and that assembly of the physical circuit must be such as to eliminate RF.

A comment was that the device does not naturally lend itself to RF protection because all of the leads come out of the same end. Mr. Sanford replied that he expected no problem at communication frequencies. At higher frequencies, a voice replied, there will be resonances and cross bands. This effect may cause the curve to come down again. Mr. Sanford commented that this device was not intended to cover the entire electromagnetic spectrum.

Comments were made that some of these lend themselves to coaxial configurations and can be sealed completely in a metal can. A bridgewire is located across the anode encased in a metal shield. This is very similar to the General Electric silicon controlled rectifier. These can be purchased in various voltage ratings and in current ratings up to 100 amperes.

There was a question concerning series inductance in the input circuit in regard to the possibility of resonances that could be created. No information was available on this.

A comment from a representative of Douglas Aircraft was that RF susceptibility tests were run on control rectifier firing circuits. With a low-power signal generator in a screen room it was possible to trigger the control rectifier consistently at frequencies up to 2.5 Mc. Filtering eliminated the problem but it is worth noting that the basic unit is susceptible to RF at low frequencies.

Mr. Sanford commented that he had made similar measurements, but by measuring current into a known input impedance. This technique permits the actual power to be deduced. A number of resonances occur however, even with these dips, the device still provides good RF protection over a frequency range from 10 KC to 400 Mc.

24. Skin Effect Filter-Attenuator for Electroexplosive Device RF Protection — H. B. Warner, R. H. Klamt

An integral RF filter-attenuator utilizing the high skin effect resistance of a miniaturized TWINAX shielded conductor has been provided for rocket motor initiators. Small size and extremely broad band attenuation regardless of source reactance characterize this unique approach to increased RF and electrostatic safety.

25. Development of RFI Shielded Connectors — W. J. Mashek

The feasibility of achieving the Navy's requirements for a multi-conductor RFI shielded cable connector suitable for use in missile firing circuits and electrically detonated ordnance has been verified by designing, constructing, and testing connector prototypes.

26. Two-Conductor Low-Pass Transmission Line Theory — H. G. Tobin, L. J. Greenstein, R. J. Arndt, E. W. Weber

The use of attenuating, low-pass transmission lines to limit the propagation of RF energy to an EED is considered. Such a line would provide little or no attenuation to the desired firing signal but would filter higher frequencies which are induced when the cable is placed in a high level electromagnetic field environment. The presentation is divided into three main areas. The first is a theoretical study of various transmission line configurations in order to determine the optimum filter effects which can be obtained. The second area considers the practical aspects of material availability and fabrication of the selected lines. The final portion of the paper outlines the measurement techniques and the response characteristics obtained from both laboratory and commercial models of attenuating lines.

28. High Voltage Hybrid Initiators — Leonard Katz

The effort to produce electroexplosive devices which will be safe versus the increasing RF fields, strong stray signals and other electrical hazards, has resulted in a new family -- the high voltage, hybrid initiator. The hybrid initiator combines high voltage no-fire characteristics with the conventional 1 amp, 1 watt no-fire bridgewire, resulting in an exceptionally safe, though simply fired, initiator. The characteristics and advantages are described.

29. Development of RF Protected Electroexplosive Devices — Frederick M. Correll

In order to alleviate the possibility of premature initiation or change in sensitivity of initiators due to RF energy, the Army has endeavored to make all of its initiators "RF Proof". To date, the T24E1, M36A1, T20E1, T77 detonators; M2 squib, and M6 blasting cap have been provided with RF attenuators.

30. The Lossy Filter and Its Application to Protection of Electromagnetic Radiation Sensitive Ordnance Devices — Merrill O. Murphy

The problems of filter applications and design criteria in ordnance are discussed briefly. The design features of a lossy filter, useful from 200 kilocycles upward, is described together with test results and test methods.

31. A Miniature Filter for Squib Protection — J. L. Hinds, Jr.

Size reduction and impedance matching were problems in the design of π-Section RF filter, to fit a limited space, 2 inches by 11/32 inch. The use of tantalum feed-thru capacitors and ferrite toroids led to a solution which, which not the ultimate, is entirely practical within certain limits, and is inexpensive.

32. Development of Broadband Electromagnetic Absorbers for Electroexplosive Devices — Robert W. Wood, Daniel J. Mullen, Jr.

Ferrite materials can attenuate RF energy, ranging from 3 db/cm at 1 Mc to 100-150 db/cm at 100 Mc. Problems of low resistivity and poor machinability are probably not insurmountable. Equations relating attenuation to material parameters have been developed; they will result in improved materials. Use can be made of certain other materials having very high dielectric constants to improve both insulation and attenuation.

33. An Inductively Coupled Filter Providing Complete RF Shielding of an EED — Dale G. Holinbeck

A filter is described based upon protecting an EED from RF hazards by completely enclosing it within a metallic shield that has no openings or leads passing through. Intentional firing is accomplished by inductive coupling through the shield. Experimental power attenuation vs. frequency curves and the delivered intentional firing energy of a filter of practical size and weight are presented.

24. SKIN EFFECT FILTER-ATTENUATOR FOR ELECTROEXPLOSIVE DEVICE RF PROTECTION

By

H. B. Warner

R. H. Klamt

Douglas Aircraft Co., Inc.
Santa Monica, California

1. INTRODUCTION

Discussion of the Problem

There is, at this time, a weapon system under development that makes use of radars more powerful than any used in previous systems. Early in this program it became evident that the extreme RF environments induced by the missile system radars as well as by range RF equipments at the various R and D launch sites would cause severe hazards to the missile electroexplosive systems. There has been considerable effort expended to define the nature and degree of these hazards.

After the real and potential environments were defined, analyses were performed to determine the limits of the coupling characteristics of the initiator circuits. Of course, the ultraconservative approach of assuming the terminals of the electroexplosive to be a resonant dipole showed in almost every condition of importance that the electroexplosives would be initiated. It was obvious that a more exact study was needed.

Approach to Solution

Analysis techniques utilizing computer methods were developed for calculating coupling characteristics of the several electroexplosive circuits. Other, more realistic limits were established as to the antenna characteristics that might exist. It was found that among the antenna models that best described the existing cases were the whip, loop, dipole, and two-wire models. Realistic estimates were made of the antenna-load impedance mismatches. Extensive investigation showed that use of these configurations was realistic, yet conservative from the standpoint of safety. Additionally, a study was made of the initiator response to pulses, and pulse trains, as well as average power. As a result of these studies a requirement was created for the inclusion of RF protective systems.

The following ground rules were established pertaining to the development of any RF protective system to be used:

1. One year lead time allotted.
2. No major changes allowed to the missile or ground power systems.
3. Minimum changes allowed to checkout equipment.
4. Protective system to provide protection regardless of voltage source reactance.
5. The system must be compact, light, simple, and must exhibit apparent reliability.
6. It should provide protection over a frequency range of 500 kc/s to 10 G/cs.

Method of Solution

Relationships between power transfer from antennae and various loss and matching mechanisms suggested fundamentals for a special purpose insertion loss device. After a short study to support the feasibility of such a device, a patent disclosure was made at Douglas.

A contract was awarded to General Laboratory Associates in Norwich, New York for the development of the insertion loss device (filter-attenuator) who in turn awarded a subcontract to Franklin Institute for testing of the device during development.

2. SKIN EFFECT DEVICE DESCRIPTION

Orientation

Block schematics of the original and modified systems are shown in figure 1. The original (unprotected) system consisted of a power supply, current limiting resistance, switching provision and initiator. The modified system differs by the insertion of the filter-attenuator in front of the initiator bridgewire. The modified system contains the same limiting resistance to direct current as the original, but this resistance is now located in the filter-attenuator.

Theory of Operation

When a firing circuit such as this acts as an antenna, it will have a characteristic source impedance determined by many factors among which are component and circuit geometry. Schematics with these parameters represented are shown in figure 2.

The insertion loss of a device placed between an antenna and load will differ at various frequencies because of frequency dependent antenna characteristics. The standard 50 ohm pad insertion loss tests that are so useful for most applications in which fixed impedances are involved will not give a true indication of performance under these varying frequency conditions.

The upper limit of the source resistance characteristic is very important and fortunately fairly easy to estimate. This characteristic, known as the radiation resistance, is fixed by the length of the circuit in wavelengths. At low frequency it will be very small, but it may be quite large at higher frequencies. These facts have significance germane to the adequacy of protection by voltage division, which will be discussed later.

In view of the wide range of significant variables, it is not possible to define the source reactance characteristics of a circuit acting as an antenna inside a missile. Consequently the insertion loss device for broad band coverage must be effective regardless of source reactance. The simple expedients of adding large inductors, bypass capacitors, or other devices subject to resonant effects are not acceptable.

The fundamentals of the method by which the device provides the necessary loss can now be explained. The basic mechanism exploited is the increase of resistance by virtue of skin effect. Along with this, other features that contribute to transmission line attenuation have been embodied in the design.

Referring again to figure 2 it can be seen that as long as source resistance is sufficiently small and the limiting resistance large compared to the bridgewire resistance, a voltage division of the applied potential will result which is proportional to the ratio of the resistance of the initiator to that of the limiting resistance. By using wire for the limiting resistances that has a high magnetic permeability, or wire adequately coated with such a material, the resistance and therefore the voltage division will be greater at radio frequencies than in the DC case.

Another benefit accrued by this method of protection is that total power dissipated in the system is reduced, and therefore less heat must be transferred away from the explosive. For a single loop circuit as discussed, the power dissipated is inversely proportional to resistance. If loop resistance is increased by a factor of 100, total dissipated heat is reduced by the same factor.

The high distributed resistance exhibited at high frequencies also contributes to transmission line attenuation independent of load resistance; and in fact is present even at open circuit. Other characteristics involved in transmission line attenuation are distributed capacitance, distributed inductance, and loss factor of the dielectric. The upper diagram in figure 3 grossly illustrates the circulating currents, and resultant voltage distribution that play a part in the attenuating process. At a high enough frequency, line attenuation alone could give the insertion loss needed regardless of source and load impedance.

Actually, by designing the line for maximum attenuation as well as skin effect, both mechanisms can be utilized as is depicted in the loaded circuit. By packaging a sufficient length of a lossy two wire transmission line within a shield, it can be used for high attenuation of conducted energy.

Design

An LCR filter is often designed to function in the same manner as discussed above and by adding lumped capacitors across the load, the effects already described are more pronounced. It would seem proper to call such an arrangement a skin effect LCR filter, and it turns out to be a very effective broad band filter-attenuator for radio frequencies. This scheme is depicted in figure 4. There are two sections of the balanced pair line previously described, a capacitor, and two trimming resistors added to the bridgewire circuit with a continuous shield applied along the length of the wire as shown in figure 6. The trimming resistance is a necessary evil peculiar to this one application to provide the exact proper DC resistance. The operation is analogous to a series of LCR filters.

The features that contribute most to the effectiveness of the device may be summarized as follows:

1. The conductors are a balanced pair coated with a layer of high permeability material to maximize skin effect and inductance.
2. The conductors are closely spaced for maximum capacitive coupling.
3. The input is adequately isolated from the output by the outer sheath of the cable.

4. A feed-through capacitor is added where it does the most good; that is, about two thirds of the way down the line.

As produced, the entire filter/squib assembly may be pictured as shown in figure 5. The assembly consists of two principal elements, the squib and the filter. The squibs are essentially the same as those used on the earlier firings of this missile system. However, the connector portion was redesigned to accept the mating connector of the filter. The joining of the filter and squib is accomplished by a slip fit and final fastening is done by a 360 degree soft solder joint. The connector is a standard Bendix six pin receptacle soft soldered to the case.

The lossy transmission line is the heart of the filter. A cross section of it is shown in figure 7. The line is a two conductor shielded cable. The outer sheath is made of 50 per cent nickel - 50 per cent iron alloy and is about 0.063 inch in diameter. Each of the conductors is also sheathed in the same material but has a core of copper. The conductors are 0.011 inch in diameter and have a center to center separation of some 0.019 inch. The dielectric is magnesia (magnesium oxide). The technique for drawing similar miniaturized cable was originally developed for high temperature thermocouple wire. However, these nickel iron alloys had not been used before. The total length of twinax cable used on this filter is approximately 13 feet.

Performance

Numerous tests have been conducted to establish the performance of the device

To start with, tests reveal that the transmission line has the following characteristics.

R_{DC} = 0.333 ohm/loop-foot

R at 500 kc/s = 11 ohms/loop-foot (refer to figure 8)

C = 70 pf/foot

Additional analytic studies have given the following characteristics:

L at 500 kc/s = 4 microhenries/loop-foot

Transmission line attenuation at 500 kc/s = 0.37 db/foot

Transmission line attenuation at 10 Mc/s = 3.5 db/foot

At about 20 Mc/s the thirteen feet of the wire as used in the device provide 60 db of attenuation.

To establish the insertion loss of the entire device a rigorous test procedure was specified. One purpose was to assure that adequate protection would be available under any and all source reactance conditions. Another purpose was to use a source that more realistically simulated the source resistance of the circuit-antenna. Since line attenuation alone exceeds 60 db at frequencies of 20 Mc/s and higher, for these higher frequencies the protection is available regardless of source resistance. It is known from previous studies that the radiation resistance of the circuit could never be greater than 2 ohms at frequencies lower than 100 Mc/s so the test generators were modified accordingly. The results obtained were conservative because with

any source resistance less than 2 ohms, the loss will be greater. In field use the device will always have more insertion loss than that measured in the tests. The tests were conducted by the Franklin Institute and a graphical resume is given in figure 9. The filter-attenuators provide an insertion loss greater than 60 db for all frequencies above 1 Mc/s. The original design objective of 60 db down to 500 kc/s is not realized on all filters, but the loss always exceeds 50 db, and since there was a liberal pad at this extreme of the frequency span, 50 db is acceptable. It is apparent that the actual insertion loss exceeds the limits of the measuring equipment at all frequencies greater than 3 Mc/s. The device provides this insertion loss even after being subjected to full environmental testing.

Other characteristics of the device have been established by further tests at General Laboratory Associates and Douglas. A number of squib-filter units were subjected to a no-fire test at various radio frequencies the lowest of which was 2 Mc/s. In this test, potentials of approximately 100 volts were applied directly to the units for a 30 second period. This is a time duration larger by a factor of 1000 than the device will ever experience a potential of this magnitude in the field. None of the squibs fired and in later firing tests it was found that the shape and amplitude of the pressure output curves was not affected by the tests.

Naturally heat is dissipated in the device. In tests to establish the failure limits, potentials of approximately 200 volts were applied at 2 Mc/s until failure. Failure by open circuit occurred in the two units so tested after approximately two minutes. A picture of one of these units is shown in figure 10. The soldered end near the connector was melted,

and the connector was pushed out by thermal expansion of the potting material. The squibs did not fire, but did fire in a later firing test when subjected to DC inputs.

It is not hard to imagine what happens when a static electric source is discharged into the filtered squib. Theoretically most of the energy should be dissipated in a ringing action in the first loop of the filter-attenuator. This is pictured in figure 11. The current in the first loop alternates at a high frequency after a static source is applied, and only a small current is present in the bridgewire loop. Tests with 500 pf capacitors charged to 5000 volts reveal that the energy delivered to the bridgewire during the heating portion of discharge is less by a factor of 10,000 than that which would be delivered without the filter-attenuator. Since the bridgewire temperature rise for inputs of such short duration is proportional to energy, the significance is obvious.

Another test was performed to show that with a step input of a DC potential, the voltage at the load end reaches 95 per cent of the steady state in less than 100 microseconds. Firing tests confirm that there is no measurable firing delay introduced by the filter-attenuator.

All firings of the RF protected squibs to date have been successful including igniter and motor tests.

3. POTENTIAL FURTHER DEVELOPMENT

Variations of Requirements

Possibilities of improvement of this device are greater if some of the original constraints are not imposed.

For many similar systems of good circuit design the insertion loss needed probably could have been realized with the transmission line alone of the type used in these devices.

Then too, if the choice of initiator is not limited to a specific unit, it would be beneficial to choose one having a lower bridgewire resistance. Since voltage division is involved, less current limiting resistance would be necessary, less line could be used, and the device would be smaller.

Optimization of Electrical Characteristics

Although time and reliability considerations did not permit it for the present program the filter attenuator design could be refined for greater efficiency; that is, greater insertion loss to size ratio, with attendant cost reductions.

Since the largest and most expensive element of the filter-attenuator is the transmission line, optimization with respect to materials, size, and geometry of the line is most important. The use of materials with high magnetic permeability for the wire, or for the wire coating is all important for maximizing skin effects.

The ratio of AC to DC resistance is critical and this could be much increased by use of materials of higher magnetic permeability. If the conductors were coated with supermalloy, it is estimated that the insertion loss of the present design could be 20 db greater.

The transmission line described earlier is overdesigned, and can be made smaller as confidence in the drawing technique develops. Since twin axial thermocouple wires can be bought off the shelf with outer sheath diameters of 0.011 inch having separate conductor diameters of 0.002 it is felt that wire of the present design could be drawn much smaller than the 0.063 used presently. This miniaturization would result in:

1. Increased distributed capacitance caused by closer spacing of the conductors.
2. Increased resistance of the conductors per unit length because of the reduced conductor cross section.
3. Savings in weight and volume by virtue of the above as well as the reduced cross section.

If the cross section were reduced to one half, the bulk of the transmission line could be reduced to about one sixth of its present volume.

Another approach lies in optimization of the geometrical cross section of the transmission line. There are several exotic things that could be done in a twin axial design. However, to take an easy approach with simple shapes, considerable improvement could be obtained in a design of two flat wires, inside a circular sheath. This design is shown in figure 12. It would utilize the space better with regard to area of dielectric needed for a given area of wire, and results in greatly increased capacitance between wires, with more pronounced skin effect both from the rectangular cross section and increased proximity effects. It should also be mentioned that

this drawn wire, twin axial design does not appear to be the optimum production method for obtaining the type of transmission line needed, although it does solve the isolation problem neatly, and meets the requirement for flexibility. Other fabrication techniques such as thin film, look more promising for greatest efficiency and smallest bulk.

The literature indicates that capacitors adequate for this application either are available, or soon will be, in very small packages occupying perhaps one fifth the present volume of the feed-through capacitor.

Possible Configurations

Two possibilities for improved versions of the device are shown in figure 13, in comparison to the device in present use. They are representative of the improvements that could be realized with improved drawn twin axial wire only and do not reflect thin film possibilities.

In looking to potential developments we look forward to the advantageous application of the possibilities of optimization, and envision applying this to another new concept developed at Douglas for initiator design.

On one of our current programs at Douglas we are making use of a detonator mounted at the missile skin, which can be installed or removed with only a standard screwdriver. The detonator output, by means of small shaped charges in the detonator, initiates a mild detonating fuse train which in turn is routed over to a solid propellant gas generator of a hydraulic pumping unit (HPU) see figure 15.

The detonator itself is shown in cross section in figure 14. Note the swiveling head and indexing key that make this detonator skin insertable. This scheme allows the HPU to be easily and convincingly armed and disarmed.

This detonator type equipped with integral loss line protection as illustrated in figure 16 and making use of the improvements suggested above can provide a new order of simple, convincingly safe, easy to install electroexplosives.

4. SUMMARY

Present Device

By way of summary, the filter squib in production, having been fully proof tested has the following important features.

1. Firing Voltage . . . . . 26 volts DC
2. No-Fire Voltage . . . . . .4 volts DC
3. Insertion loss of filter - attenuator

   50 db from 0.5 to 1 Mc/s

   60 db above 1 Mc/s

   80 db above 3 Mc/s
4. RF no-fire for all frequencies greater than 500 kc/s:

   Designed to withstand a 400 volt potential for several seconds with no damage or dudding. With present circuits this corresponds to electromagnetic fields up to 1.5 million w/m^2.

Demonstrated ability to withstand 100 volt potential for 30 seconds with no damage or dudding. Corresponding electromagnetic field is 100,000 w/m^2.

Designed to withstand a 30 volt potential indefinitely. This corresponds to an electromagnetic field of 10,000 w/m^2.

5. Physical Package

Weight . . . . . 4 1/2 ounces
Total length. . . . . .3 1/2 inches
Largest diameter. . . . . .1 1/4 inches

Future Devics

With those changes felt to be immediately possible with negligible development outlay, the same performance could be obtained in the following physical package:

Weight . . . . . 1 1/2 ounces
Length . . . . . 2 1/2 inches
Diameter . . . . . 3/4 inches

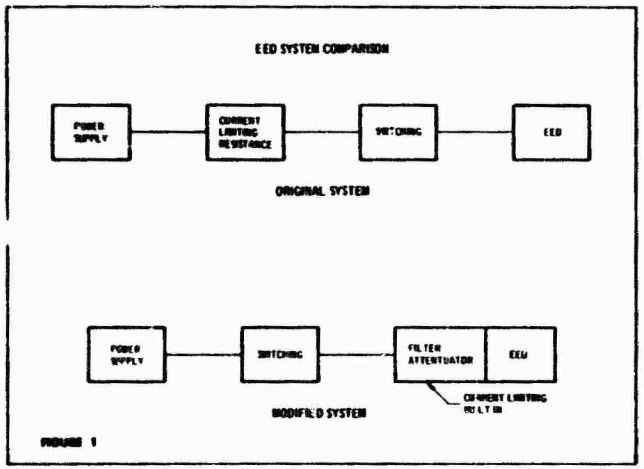

FIGURE 1

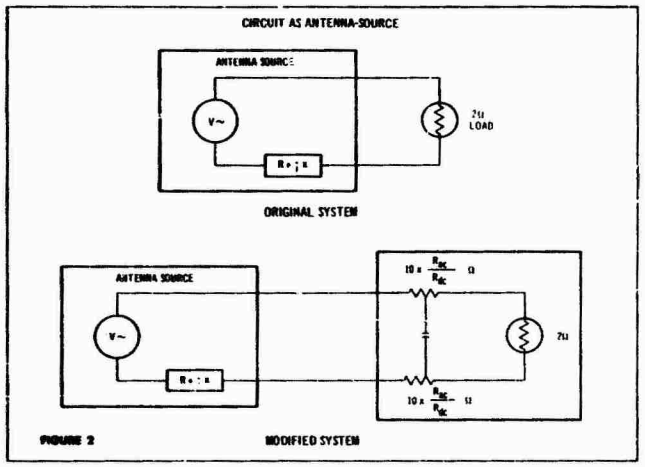

FIGURE 2

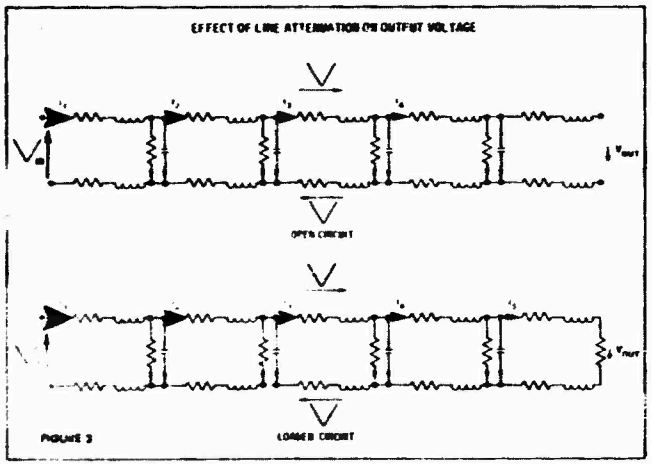

FIGURE 3

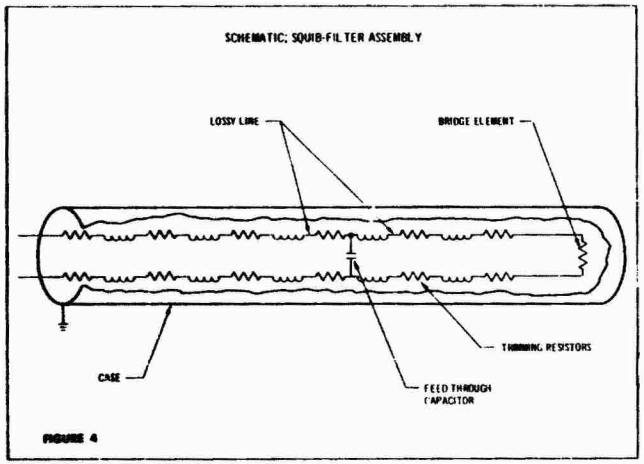

FIGURE 4

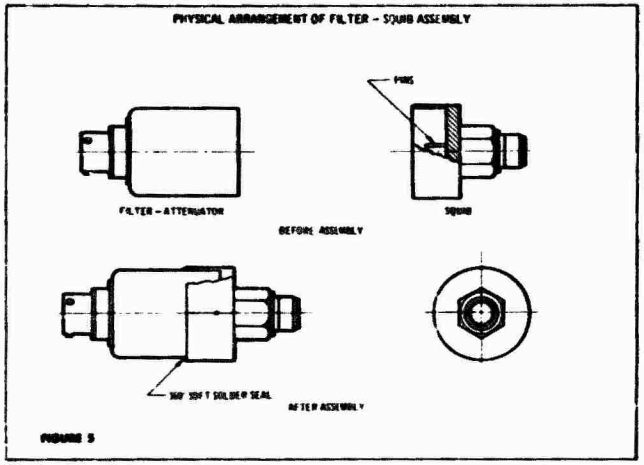
PHYSICAL ARRANGEMENT OF FILTER – STUB ASSEMBLY
PINS
FILTER – ATTENUATOR
STUB
BEFORE ASSEMBLY
360° SOFT SOLDER SEAL
AFTER ASSEMBLY
FIGURE 5

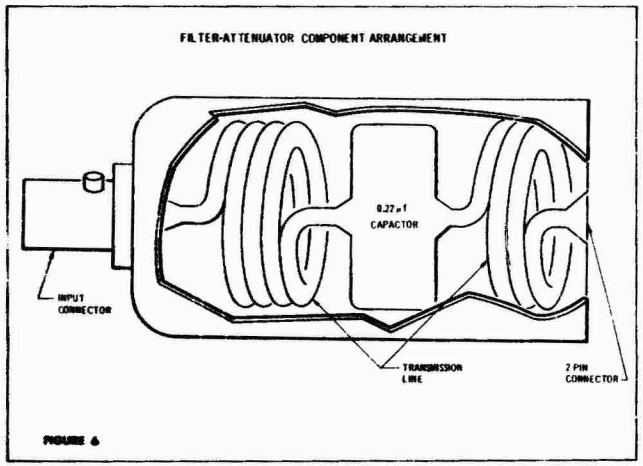
FILTER-ATTENUATOR COMPONENT ARRANGEMENT
0.27 pf
CAPACTOR
INPUT
CONNECTOR
TRANSMISSION
LINE
7 PIN
CONNECTOR
FIGURE 6

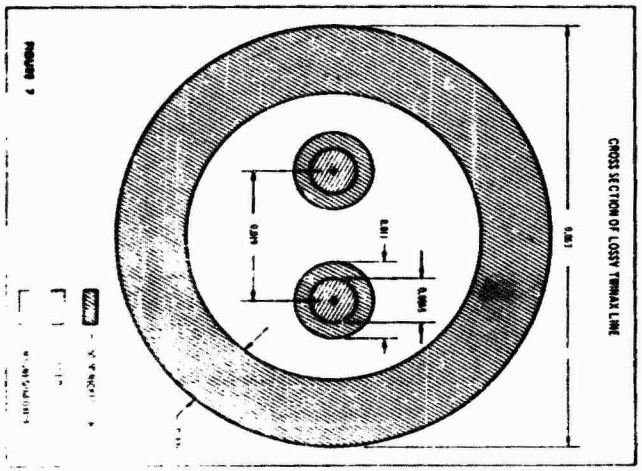
CROSS SECTION OF LOSSY TRIPLATE LINE

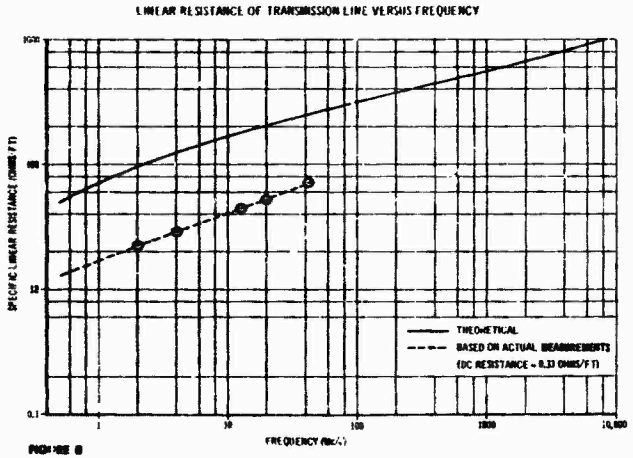
LINEAR RESISTANCE OF TRANSMISSION LINE VERSUS FREQUENCY
SPECIFIC LINEAR RESISTANCE (OHMS/FT)
FREQUENCY (MC/S)
THEORETICAL
BASED ON ACTUAL MEASUREMENTS
(DC RESISTANCE = 0.33 OHMS/FT)

INSERTION LOSS VS FREQUENCY

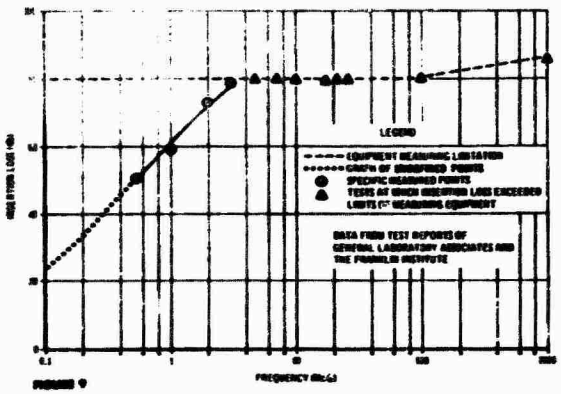

FIGURE 9

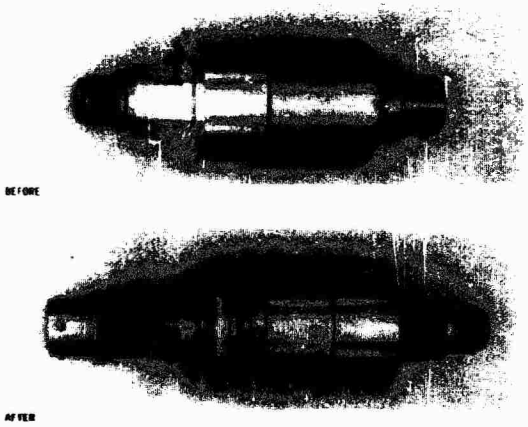

FIGURE 10 DAMAGE DUE TO EXTENDED APPLICATION EXTREME RF POTENTIALS

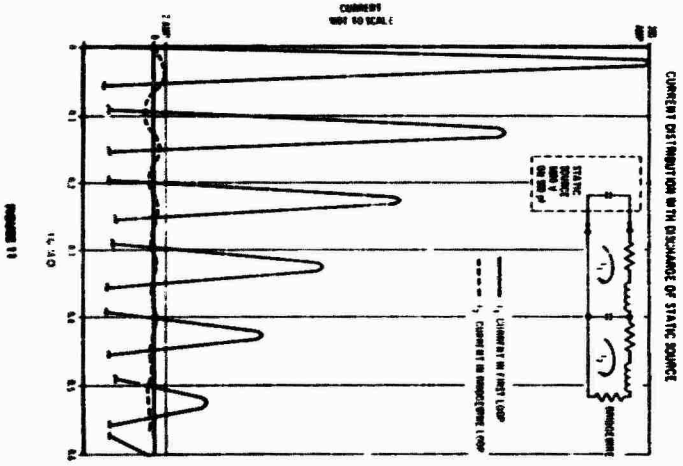

FIGURE 11

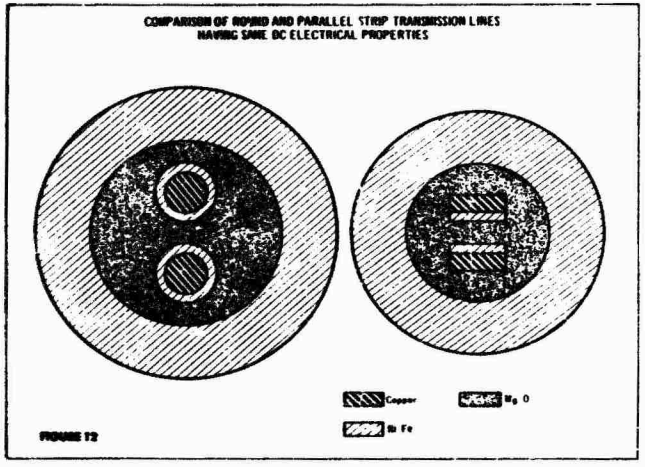

FIGURE 12

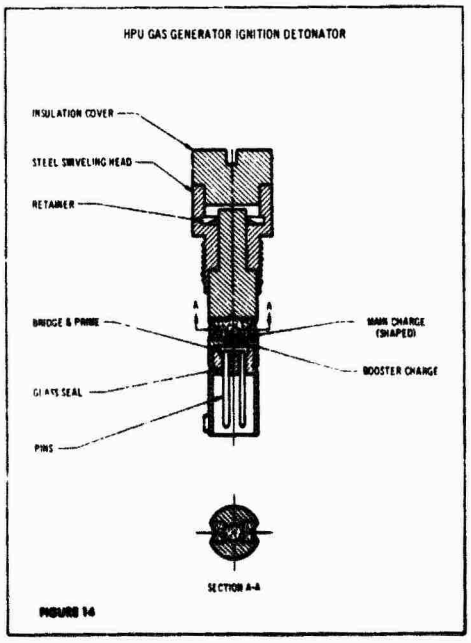
HPU GAS GENERATOR IGNITION DETONATOR
INSULATION COVER
STEEL SWIVELING HEAD
RETAINER
BRIDGE & PANNE
GLASS SEAL
PINS
MAIN CHARGE (SHAPED)
BOOSTER CHARGE
A
A
SECTION A-A

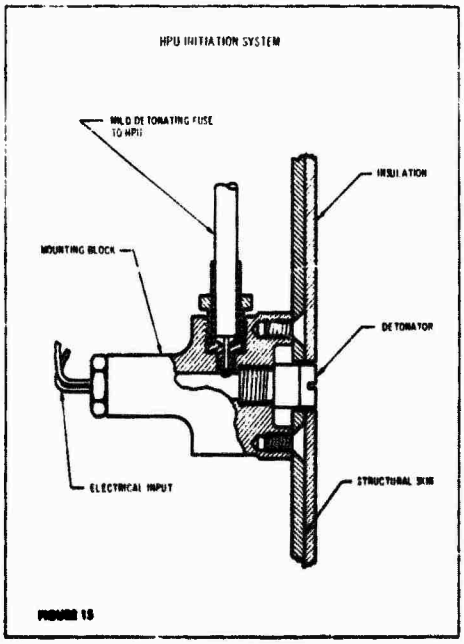
HPU INITIATION SYSTEM
MILD DETONATING FUSE TO HPU
INSULATION
MOUNTING BLOCK
DETONATOR
ELECTRICAL INPUT
STRUCTURAL SKIN

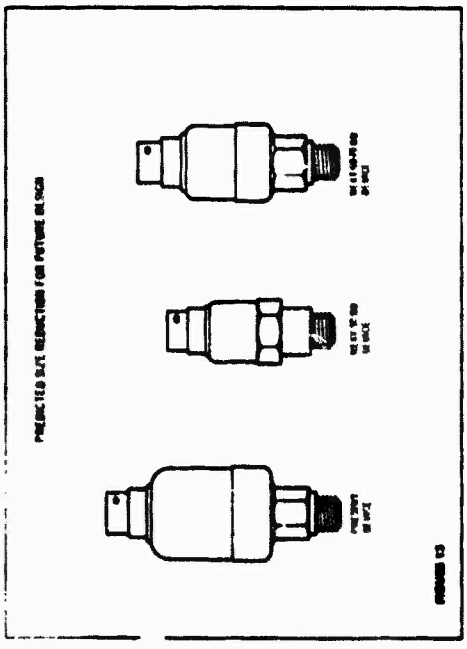
PREDICTED SIZE REDUCTION FOR FUTURE DESIGN

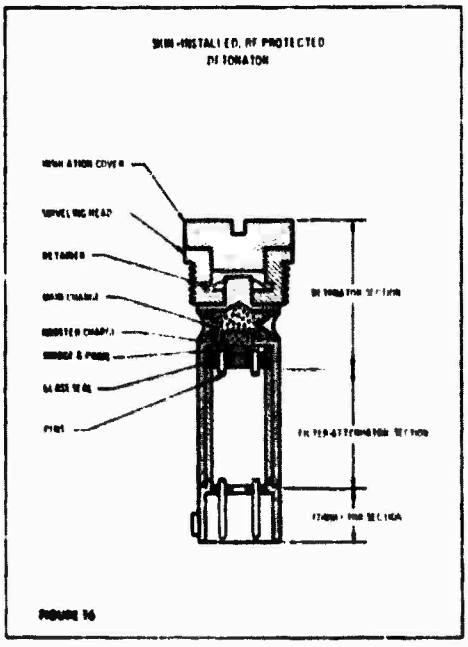
SKIN-INSTALLED, RF PROTECTED DETONATOR

24. DISCUSSION

A man from Picatinny Arsenal requested clarification of the term " insertion loss" under conditions where input and output were matched. He asked if, under these conditions, the loss should not be termed attenuation. Mr. Warner confirmed that The Franklin Institute had matched the device during measurements. The questioner reported that this is usually known as attenuation. Insertion loss is the term applied when no attempt is made to match. Mr. Warner answered that these measurements did not follow MIL 220.

Mr. Brown asked the unit cost. Mr. Warner answered between 300 and 400 dollars. If the device is fired repeatedly a corresponding unit cost correction can be added.

Mr. Simpson asked if the filter materially lengthened the ignition time and what ignition time is available. Mr. Warner answered that the ignition time is a few milliseconds and that 95% of max voltage is achieved within 100 microseconds.

An unidentified questioner asked what the attenuation was for DC input. Mr. Warner approximated the attenuation to DC at 20 db.

25. Development of RFI Shielded Connectors

W.J. Hashek
Amphenol Connector Division
Amphenol-Borg Electronics Corporation
Chicago 50, Illinois

This paper comprises a summary of work accomplished on Navy Contract 178-7933.

The feasibility of achieving the Navy's requirements for a multi-conductor RFI shielded cable connector suitable for use in missile firing circuits and electrically detonated ordnance has been verified by designing, constructing, and testing connector prototypes.

DISCUSSION

The connector developed as a result of this contract will be used to make a shielded electrical connection from a remote power supply to a missile firing circuit. The ambient conditions will include high intensity electromagnetic radiation. Hence, shielding is mandatory. In addition, the connectors should be capable of withstanding environments typical of present-day aircraft and missile applications.

The missile firing circuit is composed of a sensitive resistance wire which when heated by the passage of electrical current will ignite an explosive charge or squib.

A potentially hazardous condition is created by the presence of environmental electromagnetic radiation. Under certain conditions, it is possible that the various components of the firing system, cable, connectors, etc. will act as antenna and energize the firing circuit as the connectors are unmated, mated, or in the process of being mated or unmated.

As a result, the Naval Weapons Laboratory, Dahlgren, Virginia, granted a

contract to the Amphenol Connector Division for the primary purpose of developing a connector design concept which would alleviate this hazardous misfiring characteristic.

In order to shield and otherwise prevent electromagnetic radiation from entering the missile firing circuit at the connector, the following design features are significant.

1. The shielding effectiveness of the mated connector should equal or exceed that of an equal length of the cable utilized in the firing circuit.

2. The connector shield at the interface of the two connector halves must make positive contact before the two power contacts mate and maintain contact until after the power contacts break.

3. The contacts in the receptacle connector half should be isolated sufficiently to preclude the possibility of field personnel accidentally touching the socket contacts with their fingers or with the mating connector shell during the mating and unmating cycle or while the connectors are unmated.

4. There should be no break in the shield through the connector and cable which would allow RFI to "leak" into the power circuit.

5. The "skin" mounted receptacle connector should reduce the antenna effect of the contacts as much as possible while in the unmated state.

6. The connector should be able to withstand environmental conditions (vibration, high and low temperatures, corrosion, etc.) without degradation of the shielding characteristics of the connector.

7. The design concepts to be developed should be applicable to connectors employing a large number of contacts.

Cable Selection

The Navy specified that a two-conductor shielded cable should be used with the connector to be developed. The exact designation or construction of the cable was not indicated for the reason that any number of existing or other future cables may be used. Variations in cable would involve minor connector design changes in order to adapt the cable to the connector and hence should not affect any basic connector design concepts which relate to shielding effectiveness.

The two-conductor cable arbitarily selected by Amphenol to be used in conjunction with the developed connector was the Military No. RG-22B/U cable.

This cable was selected mainly because it utilizes a double layer braided shield which provides improved shielding over other cable types which have only a single layer of shield braid. In addition, this cable was readily available and its selection expedited the work of the contract.

Prototype Connector Design

Achievement of the connector design requirements previously outlined is revealed in the prototype receptacle and plug connector designs.

Those design features pertaining to environmental resistance are presently utilized by Amphenol in its 48 Series line of miniature, multi-contact, environmentally resistant electrical connectors in accordance with the requirements of the governing Air Force Specification MIL-C-26500.

Fig. 1 shows a drawing of the prototype plug connector.

This design is very similar to the mating receptacle connector shown in Fig. 2. The prototype designs have many features which favor highly effective and reliable shielding and environmental resistance characteristics.

For example, a hard dielectric disc with integral retention clips, Item 1 of the drawing provided for secure attachment of the contacts in the connector. This device will prevent axial movement of the contacts due to rugged use, cable flexing, or temperature changes. The retention clips require the use of tools for removing contacts from the connector and for inserting contacts into the connector.

Various O-rings and resilient seals are utilized to prevent the entry of moisture or corrosive elements into the mated connectors.

Because the contacts are crimped to the conductors prior to assembly into the connector, an elongated grommet ferrule, Item 2 of the drawing allows sufficient free conductor length to facilitate contact insertion.

Copper alloys were used in the majority of the connector components as well as aluminum. An all aluminum connector of suitably plated alloys should be considered for future applications to provide the necessary electrical properties as well as desireable light weight characteristics.

All mechanical junctions between the piece parts which make up the connector were made metal to metal compression loaded at the full circumference of the contracting areas. This approach eliminated all gaps in the connector shield. Small gaps in the shield can significantly degrade shielding effectiveness.

A major improvement in the prototype samples is the introduction of a shield contact. The shield contact, Item 3 of the drawing is provided for two main reasons.

1. The shield contact will provide a positive method for connecting the cable shield before the power contacts are mated and to break the cable shield after the power contacts are unmated.

2. The shield contact will provide effective shielding for the contacts when the connectors are either mated or unmated or in the process of being mated or unmated.

The first shield contact design is shown in Fig. 3.

This is a four tine male cylindrical contact. The feature of this design which enhances its shielding effectiveness is its close peripheral fit to the mating socket member. The features of this design which would possibly degrade its shielding effectiveness are: (1) only four point contact with the mating socket member and (2) axial slots which are required to provide its resilient characteristics. These axial slots may permit the entry of strey RFI into the connector.

This geometry can be considered as a wave guide operating below the cut off frequency because the inside diameter of the shield contact is .350 inch. Calculation yields a cut off wavelength of .598 inch or a cut off frequency of 19.7 kMc/sec.

In this particular shield contact design, the contact length provided will cause the tips of the central power contacts to be recessed 1/2 inch from the front end of the shield contact. This will yield a calculated 39.2 db wave guide attenuation at 10 kMc/sec. and a maximum calculated attenuation of 45.3 db at lower frequencies (below approximately 2 kMc/sec.)

The second shield contact design is shown in Fig. 4.

This shield contact basically consists of a length of brass tubing terminated

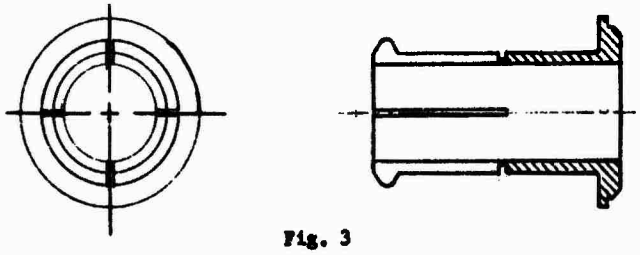

Fig. 3

FOUR TINE SHIELD CONTACT

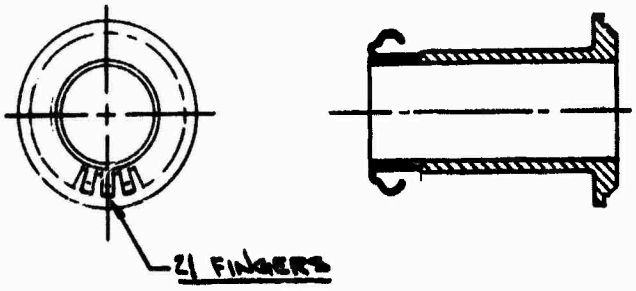

Fig. 4

FINGER TYPE SHIELD CONTACT

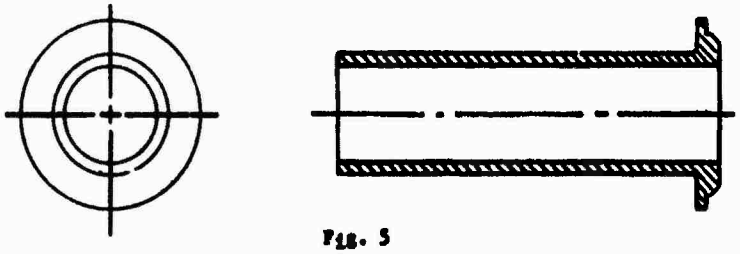

Fig. 5

EXTRA LONG SHIELD CONTACT

at one end with a circular ring of radially projecting spring fingers or contacts which will make the required electrical contact with the mating socket member.

The features of this design which will probably enhance its shielding effectiveness are: (1) a multiplicity of points of electrical contact depending upon the number of fingers utilized in the contact design (in this case, twenty-one), and (2) the absence of any axial slots which could allow leakage of stray electromagnetic radiation into the connector. The one disadvantage of this design are the spaces between the contact fingers which could be a source of inward leakage. The calculated shielding characteristics of this design when analyzed again as a waveguide below cutoff will be of the same magnitude as described previously because the controlling parameters of length and inside diameter are equal in both contact designs. In actual testing, this shield contact configuration offered more attenuation than the previously discussed design.

The third shield contact design is shown in Fig. 5.

This design consists of a length of brass tubing. This contact is identical to the previous contact design except that it does not have a means for making electrical contact with the mating socket member and is 1/2 inch greater in length. Hence, the power contacts would be recessed 1 inch from the front of the shield contact. Since this is not a complete contact, it was only used when evaluating the shielding effectiveness of the connector in the unmated state. Analysis of this geometry as a waveguide gives an indicated attenuation at 10 kMc/sec. of 78.4 db and a maximum attenuation below approximately 2 kMc/sec. of 91.0 db. The construction and testing of a connector utilizing this contact provided a comparison with the other alternate shield contact designs when determining shielding effectiveness of the unmated open-faced connector.

Testing

The next phase of contractual work was the laboratory evaluation of the connector prototypes.

The connectors tested consisted of the MIL-C-26500 connectors which are Amphenol standard production items and were tested as a basis for comparison with the contractually developed connectors where such a comparison was applicable. The next two fig. (6 & 7) show the standard plug and receptacle connectors so tested. The 12 size shell with No. 20 contacts was used because the prototype also utilized this approximate shell and contact size.

Three receptacle prototypes were tested. Fig. 8 showing one type of receptacle utilizes a tined shield contact having four axial slots. Fig. 9 showing another receptacle utilizes a tubular shield contact having radially projecting spring fingers. Fig. 10 showing still another receptacle utilizes a tubular shield contact of extended length. This connector was only used in those tests involving unmated connectors. All 3 receptacle prototypes were identical except for the variations in the shield contact design.

Fig. 11 shows the prototype plug connector. This same plug was used in all tests involving mated connectors.

Three types of laboratory tests were used to evaluate the RFI shielding capabilities of the two conductor power connectors. They were:

1. Fully mated Connector Shielding Effectiveness Test
2. Unmated or Open Connector Coupling Test
3. Connector Proximity Coupling Test

The first test conducted evaluated fully mated connector shielding effectiveness. A parallel plate or slab transmission line was fabricated to permit

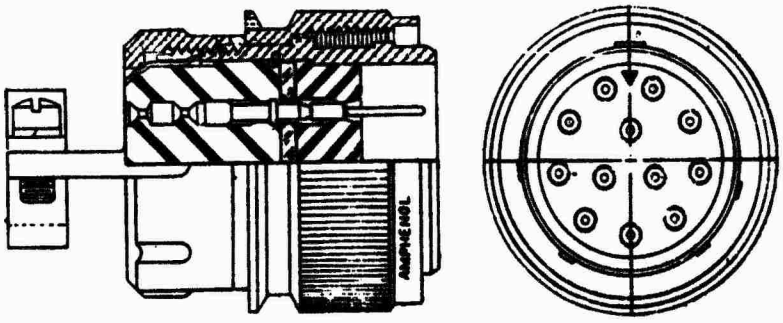

Fig. 6

STANDARD PLUG

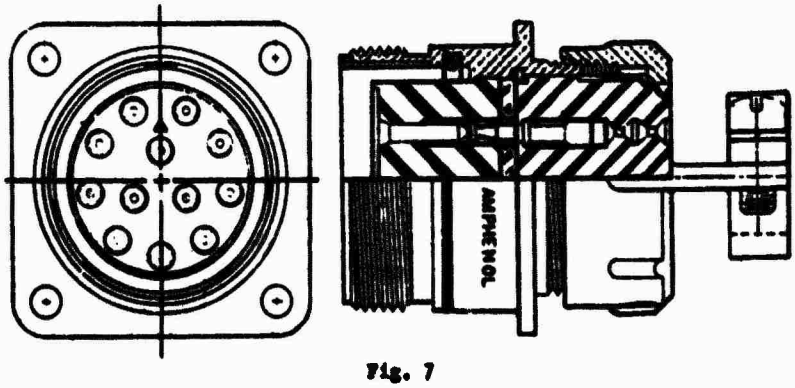

Fig. 7

STANDARD RECEPTACLE

the insertion of coupling loops of fully mated connectors assembled to cable. A coupling loop of RG-22B/U cable without connectors was used as the reference for the comparative measurements.

At each test frequency, the RG-22B/U cable coupling loop was precisely set into the slab line and the RF detector output level was recorded. This loop was replaced, in turn, by the RG-22B/U cable loop with fully mated connectors attached as in service.

Fig. 12 shows the test schematic and describes the details of the test setup. Important details affecting the test results included:

1. The length of the cable loop without connectors was equal to the length of cable loop with connectors.

2. The 5/8 inch distance from the centerline of the cable loop to the surface of the center conductor of the slab transmission line was maintained throughout all tests.

The test equipment was varied to suit the test frequency. Tests were conducted in the frequency range of 2 to 625 Mc/sec.

Fig. 13 is a photograph of the test setup. On the left are two types of RF detectors covering the frequency range of 40 to 625 Mc/sec. In the center is shown an RF oscillator and power supply. On the right is the slab line with test sample cable leads projecting from its top. The side and end plates of the slab line are of aluminum stock. The center conductor is brass and is terminated with connectors for coupling to standard laboratory test equipment.

The test results show that the RG-22B/U cable loop with connectors is, within experimental accuracy, superior to the RG-22B/U cable loop without connectors. The test results have been plotted on Graph No. 1.

CHART 1

SHIELDING EFFECTIVENESS OF CONNECTOR RELATIVE TO CABLE (db.)

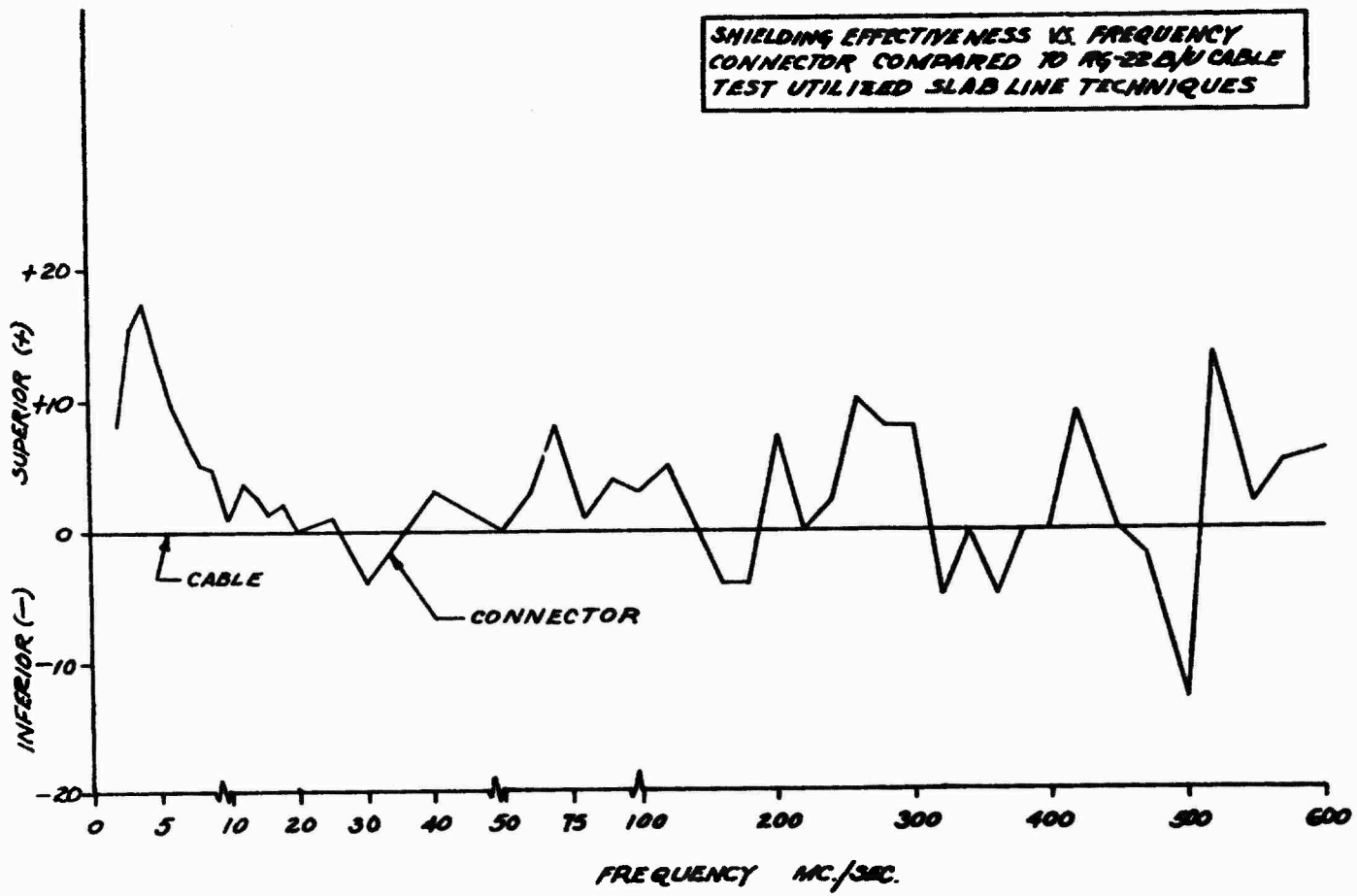

This graph plots test frequency against shielding effectiveness. The zero datum line is the shielding effectiveness of the cable loop without connectors. The jagged curve representing the shielding effectiveness of the connector was determined by actual test measurements. At any particular frequency, a positive value indicates the connectors are superior to the cable and a negative value indicates the connectors are inferior to the cable. Even though some of the values for connector shielding effectiveness are less than the cable, the majority of the values are better than or equal to the cable. Hence, on the average, the connectors exhibit superior shielding capabilities to the RG-22B/U cable. The variations in shielding effectiveness between the cable and cable with connectors is probably due to two effects. They are:

1. Distortion of the field in the slab line test fixture due to differences in the size and shape of cable and connector test samples.

2. Phasing effects which alter the net voltage introduced into the coupling loop. Phasing effects are especially noticeable at higher frequencies when the length of the coupling loop is a large fraction of the slab line wave length.

The second test was conducted at X-band to determine which unmated receptacle configuration presented the best rejection to RFI. Three different prototype receptacle connectors utilizing three different shield contact designs, as previously described, were tested in addition to a standard MIL-C-26500 receptacle.

Fig. 14 describes the test schematic and test setup. The Varian X-13 Klystron has a rated minimum output of 100 milliwatts in an optimum load. This coupled with a pyramidal horn gain of 22 db and an isolation pad loss of 3 db did not yield sufficient radiation power levels to permit far field testing of

receptacles mounted on metallic ground planes. Detectable signals were observed only when the receptacle-ground plane was brought up to within 20 inches from the horn aperture. This resulted in considerable signal reflection back into the horn with corresponding erretic test results.

The near field tests conducted utilizing a microwave absorbing material as a ground plane as shown in the test schematic was found to yield reproducible results.

The brass tube which is attached mechanically and electrically to the back of the test connector maintains a tight fit to the microwave absorber. By this means, the conductors and detector are shielded to spurious RFI. After passing through the brass tube and dielectric block, the conductors are terminated to a type N coaxial receptacle.

When tested in this manner, all three contractially designed connectors show superior shielding effectiveness in comparison with standard connectors. At the single test frequency of 9,680 mc/s, the following order of excellence was noted.

The connector using the extended shield contact was the most effective being 17 db superior to the standard connector.

The connector using the tubular shield contact with radially projecting spring fingers was 16 db superior to the standard connector.

The connector using the four tined shield contact was 8 db superior to the standard connector.

The standard MIL-C-26500 connector was least effective. This inferiority is common to all unshielded connectors and not only the MIL-C-26500 connector.

The third and last test conducted was the connector proximity coupling test. The purpose of this test was to evaluate the shielding effectiveness of the mating plug and receptacle as they are in the process of being coupled. Fig. 15 shows the test setup.

In this test, the standard MIL-C-26500 and the prototype plug connectors were used as transmitting antennas. This was accomplished by terminating the contacts of the connectors in 100 ohms while maintaining insulation to the shell and energizing the connectors coaxially. The outer shells of the plugs were connected to the inner conductor of the transmitter's coaxial output and the coaxial line's outer conductor terminated on the 6 foot square stationary ground plane. This effectively made the plug shells stub antennas with a voltage maximum at the outer or mating end of the connectors. The standard MIL-C-26500 connectors and the prototype test connectors were successively mounted on a portable three foot square ground plane and brought into the proximity of the energized plugs. Double stub tuners were used to match the connector plugs used as antennas to the transmitter.

Detectable output was observed during the test only when the plug and receptacle were mated metallically. The results show that at 2.8 kMc/sec. all combinations yielded the same output level. No output was observed to be due to proximity only. A Hewlett-Packard oscillator used as the transmitter has an output of 10 milliwatts. A higher power transmitter might reveal proximity coupling before the inner contacts touch.

This concluded the test program.

CONCLUSIONS

1. The connector is superior to an equivalent length of RG-22B/U cable in shielding effectiveness.

2. The receptacle connector in the unmated or open face state will have superior shielding effectiveness to standard connectors.

3. An outer shielding contact of cylindrical shape will make contact before the power contacts mate and maintain contact until after the power contacts break. This contact will also provide RFI shielding while the connectors are unmated.

4. The contacts in the receptacle half have been isolated to preclude the possibility of field personnel accidentally touching the contacts.

5. The connector will be able to withstand severe environments without degradation of shielding effectiveness and can employ a range of contact sizes and quantities.

---

25. DISCUSSION

A voice asked for numerical or comparative leakage values for a regular connector. Mr. Mashek answered that this was not checked because of the similarity of RF cable and open wiring. It was feared that results would be inconclusive.

Another voice commented that equipment is available to check the leakage of any connector or joint. Mr. Mashek replied that he had no way of doing this.

Mr. R. Walsh of NWL asked, with new applications in mind, if the connector was matched to the line. Mr. Mashek answered that the characteristics of the connector were not considered at all.

A questioner asked for the overall length. He asked if the length was the same as the 26500 J. Mr. Mashek answered that it was not because of the additional length required to insert the contacts. These contacts are removable and require additional length for mechanical insertion. The contact will release either front or rear. The present unit is about 3 inches long and 3/4 inch in diameter. This is the practical limit in size unless a single contact is desired in which case it could be compressed considerably.

In reply to a question concerning the performance of this device under high arc conditions, Mr. Mashek said that no evaluations have been made.

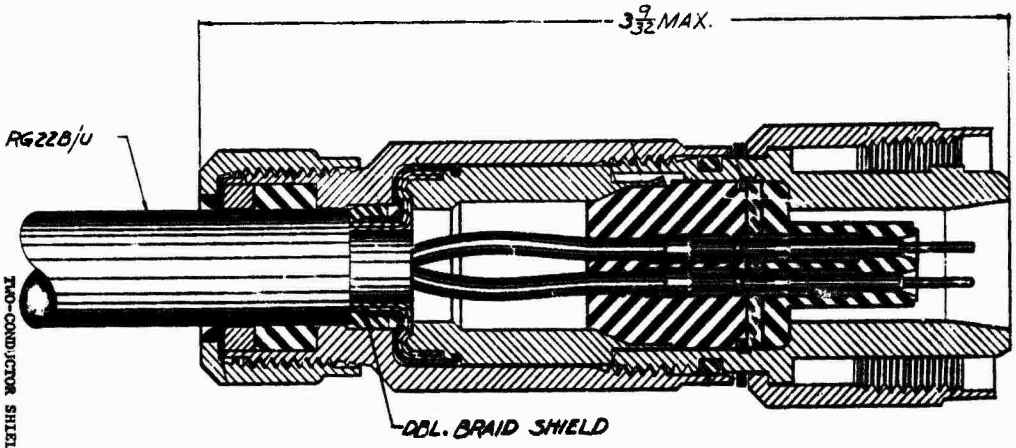

Fig. 1. TWO-CONDUCTOR SHIELDED CABLE PLUG CONNECTOR ASSEMBLY

TWO-CONDUCTOR SHIELDED CABLE PI
Fig. 1

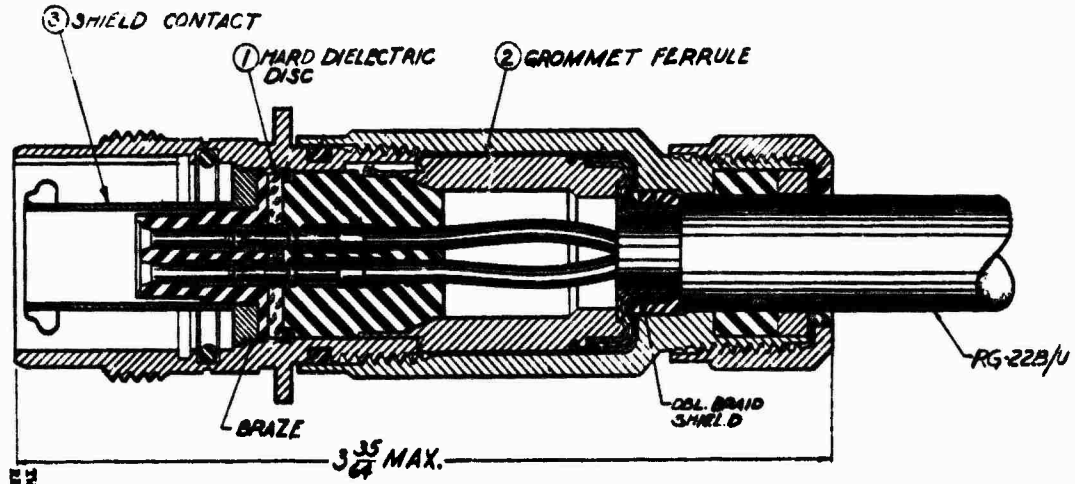

Fig. 2. TWO-CONDUCTOR SHIELDED CABLE RECEPTACLE CONNECTOR ASSEMBLY

TWO-CONDUCTOR SHIELDED CABLE RECEPTACLE CONNECTOR ASSEMBLY
Fig. 2

Fig. 8

TWO-CONDUCTOR SHIELDED CABLE
RECEPTACLE CONNECTOR ASSEMBLY

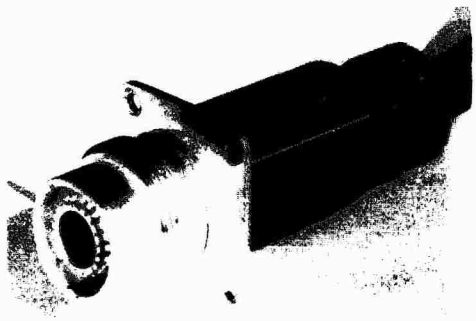

Fig. 9

TWO-CONDUCTOR SHIELDED CABLE
RECEPTACLE CONNECTOR ASSEMBLY

Fig. 10

TWO-CONDUCTOR SHIELDED CABLE
RECEPTACLE CONNECTOR ASSEMBLY

Fig. 11

TWO-CONDUCTOR SHIELDED CABLE
PLUG CONNECTOR ASSEMBLY

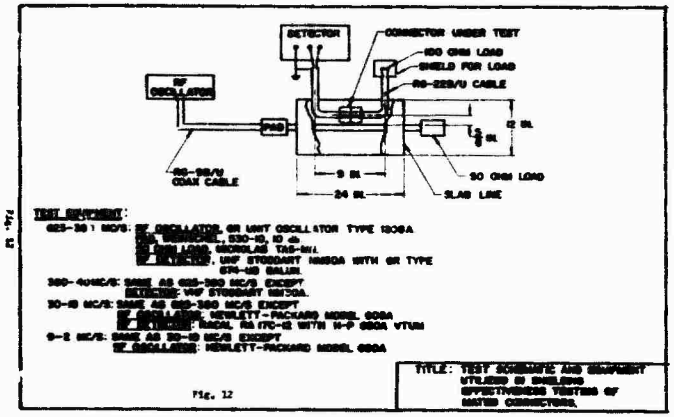

Fig. 12

TITLE: TEST SCHEMATIC AND EQUIPMENT UTILIZED IN SHIELDING EFFECTIVENESS TESTING OF MATED CONNECTORS.

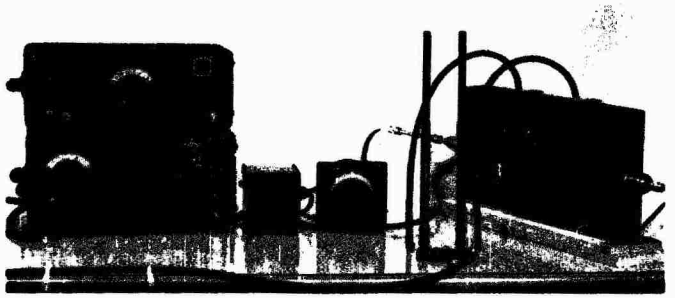

Fig. 13

TEST SET-UP UTILIZED IN SHIELDING EFFECTIVENESS TEST OF MATED CONNECTORS AND CABLE BY THE COUPLING LOOP METHOD IN AMPHENOL-BORG CONSTRUCTED SLAB LINE.

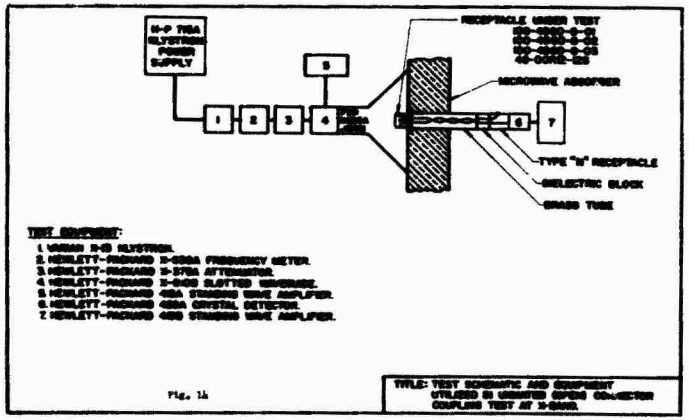

Fig. 14

TITLE: TEST SCHEMATIC AND EQUIPMENT UTILIZED IN VARIOUS SPEED CONNECTOR COUPLING TEST AT X-BAND.

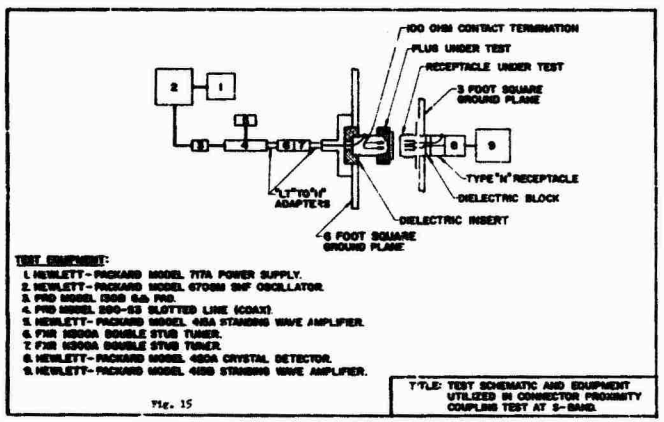

Fig. 15

TITLE: TEST SCHEMATIC AND EQUIPMENT UTILIZED IN CONNECTOR PROXIMITY COUPLING TEST AT S-BAND.

26. TWO-CONDUCTOR LOW-PASS TRANSMISSION LINE THEORY

H. G. Tobin, L. J. Greenstein, R. J. Arndt, and E. W. Weber
Armour Research Foundation
of
Illinois Institute of Technology

INTRODUCTION

The operational effectiveness of Naval vessels on which ordnance functions coexist with communication and radar functions requires safeguards to preclude inadvertant firings of electro-explosive devices by means of transmitter outputs. To reduce the danger of such undesirable occurrences, without remoting the ordnance and communications operations in either distance or time, several techniques could be employed. The most noteworthy of these are:

(1) Shielding each firing cable to minimize the leakage of spurious electromagnetic energy into the fire control circuits.

(2) Providing a lumped-circuit low-pass filter at the electrical input to each actuating device, so that only energy contained in the frequency band of the control signal is passed.

(3) Developing firing cables which pass control signals satisfactorily, while providing high attenuation at frequencies above the bandwidth of the control signals, i.e., performing the above-mentioned low-pass filtering in the transmission line itself.

It may well be that the most effective and economical techniques for minimizing the danger of unintentional firings consists of some combination of

the above approaches. To limit the necessity for external shielding and filtering, however, it appears desirable to first obtain the maximum benefit from the inherent filtering capabilities of transmission lines. Such a line should provide no more than 3 db attenuation per meter at frequencies up to 20 kc, while providing considerable attenuation, perhaps 50-60 db per meter, at radio frequencies.

It was with the above objectives in mind that Armour Research Foundation undertook a research program for the U. S. Navy Mine Defense Laboratory to study the feasibility of the development of attenuating cables. The work was carried out in three phases. The first phase of the work involved theoretical analysis of various transmission line configurations to determine how the objectives of the program might best be met. A second phase of the program was concerned with a study of material properties and, in particular, those properties of materials which appeared to be of interest on the program. In connection with the material survey, investigation was also made of the fabrication difficulties encountered with various dielectric materials. The final phase of the work is concerned with an experimental verification of the attenuating properties of transmission lines which have been fabricated both commercially and in the laboratory. Work is still continuing in these areas. This paper will attempt to give an up-to-date report on the progress obtained.

THEORETICAL ANALYSIS

Introduction

The first phase of the program involved the analysis of various line configurations in order to determine the theoretical limitations of different lines. Depending on the criterion applied, any number of procedures could be used to optimize a given line configuration. The particular technique used in the analysis performed is as follows: An attenuation of 3 db/meter was

specified at 20 kc (f_1). The RF attenuation desired above 0-20 kc pass-band was then selected. The optimization technique then consisted of minimizing the frequency (f_2) at which this attenuation occurs.

Expressions of the attenuation as a function of frequency were derived for various line configurations. The optimum line design using the above techniques was then found. Only the results of these analyses will be presented here. Detailed derivations are given in Quarterly Reports on "Two-Conductor Low-Pass Transmission Line Theory," Contract No. N178-7927, submitted to the U. S. Naval Weapons Laboratory, Dahlgren, Virginia. Copies of these reports have been submitted to ASTIA and are available from that agency.

The optimum line design, as found from the procedure outlined above, will not always be a realistic one. The limitations of material properties and the fabrication techniques possible with these materials may require that compromise be made between the optimum design and one which may be achieved with relative ease. The analysis, together with considerations of the above practical limitations, will allow a judicious compromise to be made between the various requirements of protection, cost, weight, etc.

Conventional Distributed Transmission Line

A differential length of conventional transmission line may be represented as shown in Figure 1. The circuit behavior of this line may be characterized in terms of its characteristic impedance, Z_0, and its propagation constant, γ . For a line with a series impedance of Z ohms per meter and a shunt admittance of Y mhos per meter, the values of the transmission parameters are given by

$$Z_o = \sqrt{Z/Y} \quad \text{ohms} \qquad (1)$$

$$\gamma = \sqrt{ZY} \qquad (2)$$

In order to determine the attenuating properties of any particular line, it is necessary to find the real part of the propagation constant. The real part is called α and is the attenuation of the line in nepers/meter. For the line in Figure 1, α may be shown to be

$$\alpha = \left\{\frac{1}{2}\left[\sqrt{(R^2+\omega^2L^2)(G^2+\omega^2C^2)}+RG-\omega^2LC\right]\right\}^{1/2} \text{ nepers/meter} \qquad (3)$$

At low frequencies, α is given by

$$\alpha_0 = \sqrt{RG} \qquad \text{nepers/meter} \qquad (4)$$

while at high frequencies, the value of the parameter asymptotically approaches

$$\alpha_H = \frac{R}{2}\sqrt{\frac{C}{L}} + \frac{G}{2}\sqrt{\frac{L}{C}} \qquad \text{nepers/meter} \qquad (5)$$

A series of curves giving the attenuation as a function of frequency for different values of the high frequency attenuation are shown in Figure 2. In plotting these curves it was assumed that the low frequency attenuation was very close to zero. A value of other than zero attenuation at low frequencies causes a toe in the attenuation curve at the low frequency end. The same curves are replotted in Figure 3 so that all curves have the same attenuation at some specified frequency. One technique for determining the optimum line configuration is to fix the attenuation at some low frequency and then minimize the frequency at which the attenuation rises to a specified value.

From Figure 3, it can be seen that all curves initially rise at the same rate as the curve indicated by $\alpha_H = \omega^{1/2}$. Along this line, the attenuation increases in proportion to the square root of frequency. This then is the optimum condition we are interested in. In order that the attenuation will increase as the square root of frequency, it is necessary that α_0 be very small and α_H be very large. These limiting conditions can be obtained by requiring that

either

$$R = C = 0 \tag{6}$$

or

$$L = G = 0 \tag{7}$$

If (6) holds, then

$$\alpha = \sqrt{\frac{\omega L G}{2}} \quad \text{nepers/meter} \tag{8}$$

while if (7) holds,

$$\alpha = \sqrt{\frac{\omega R C}{2}} \quad \text{nepers/meter} \tag{9}$$

A line which satisfies (6) will be called an LG line while one which satisfies (7) will be called an RC line.

Double-Layer Line -- Circuit Analysis

The preceding analysis has shown that the optimum conventional transmission line will give an attenuation which increases in proportion to the square root of frequency. In an attempt to determine whether this rate of change of attenuation could be increased, several other types of transmission lines were studied. The analysis of the response of any transmission line may be determined by analyzing a circuit model similar to that analysed for the conventional distributed line. This circuit representation is valid if the propagating wave on the line is comprised of the TEM mode only. If this is not the case, the circuit approach may be used only in those ranges of the frequency spectrum where the longitudinal component of the electric field is small compared to the radial component.

One type of line which was investigated was the double-layer line. Consider a line (Figure 4) in which the inter-conductor region is composed of two media, such that the boundary between them is equipotential with respect to the conductors. Assume that one medium consists of a low-loss dielectric,

while the other consists of a conducting, or partially conducting, material.

If the material whose parameters are designated by the subscript 1 in Figure 4 is a semiconductor or conductor, and the second material is a dielectric, then the circuit element representation of the distributed line can be given by the configuration of Figure 5a. The lossiness of the dielectric material and the dielectric constant of the lossy material can be neglected to a first approximation, thus leading to the configuration of Figure 6b where G_2 and C_1 have been removed.

The normalized attenuation of such a line is

$$g = \left[\gamma\sqrt{\frac{1+\lambda^2\gamma^2}{1+\gamma^2}} + \gamma\,\frac{1+\lambda\gamma^2}{1+\gamma^2}\right]^{1/2} - \left[\gamma\sqrt{\frac{1+\lambda^2\gamma^2}{1+\gamma^2}} - \gamma\,\frac{1+\lambda\gamma^2}{1+\gamma^2}\right]^{1/2} \qquad (10)$$

where

$$\left.\begin{aligned} g &\equiv \frac{2\alpha}{\sqrt{RG}} \\ \gamma &\equiv \frac{\omega C}{G} \\ \lambda &\equiv \frac{L G}{R C} \end{aligned}\right\} \qquad (10')$$

Figure 6 shows curves of normalised attenuation g vs. normalised frequency y, with k as a parameter. For very large k and very low y it can be shown that g(y) has a square-low variation, i.e., $g \propto y^2$. This represents the steepest variation of attenuation with frequency ($\alpha \propto \omega^2$) that can be thsoretically attained with this line.

Assume that the attenuation below some frequency f_1 is not to exceed some specified value α_1, and that we wish to minimise the frequency $f_2 > f_1$ above which the attenuation equals or exceeds some cutoff attenuation $\alpha_2 > \alpha_1$. To minimise f_2 within the constraint that $\alpha \leq \alpha_1$ for all $f \leq f_1$, we can employ the curves of Fig. 6 and solve for f_2 and the corresponding line parameters for various values of k. The simplicity of this approach attests to the utility of the normalised representation, and can be described as follows:

For a curve corresponding to a specific value of k, two points (y_1, g_1) and (y_2, g_2) are selected which have the following properties:

(1) $g_2/g_1 = \alpha_2/\alpha_1$

(2) $g < g_1$ for $y < y_1$

(3) $g > g_2$ for $y > y_2$

(4) The average slope of g with respect to y between g_1 and g_2 is the maximum average slope attainable between any two points which satisfy the above three conditions.

The values of y_1, y_2, g_1 and g_2 obtained in this manner are the normalized values of ω_1, ω_2, α_1, and α_2, respectively, where the normalizations are given by (10'). If $\omega_1 (\equiv 2\pi f_1)$, α_1, and α_2 are specified then $\omega_2 (\equiv 2\pi f_2)$ can be determined for each k, and represents the minimum cutoff frequency for that k.

The above technique was applied to a coaxial line having an outer conductor of 1" diameter, an inner conductor of 0.25" diameter, and a dielectric film of thickness 1 mil as region 1. In addition, it is assumed that a non-magnetic conducting material is used. For such a line, the inductance is $L = 0.3\ \mu h/m$. The specified values of f_1, α_1, and α_2 were 20 kc, 0.33 nepers/m., and 16.7 nepers/m., respectively. The values of f_2 calculated using the above technique are tabulated for various k in Table 1. The corresponding optimum line parameters R, G, and C are also given, as well as the relative dielectric constant of the film and the conductivity of the conducting medium required to achieve the calculated values of C and G for the assumed line dimensions.

Double-Layer Line -- Field Analysis

As previously indicated, the use of an equivalent circuit to determine the behavior of a transmission line is valid as long as the propagating wave can be approximated by a wave having only a radial component of electric field and

an angular component of magnetic field, i.e. a TEM wave. In order to determine whether such a wave is present on a two-layer line, a field analysis of this type of coaxial configuration was performed. The analysis assumes no losses in the conducting walls (inner and outer conductors) of the line. This corresponds to the assumption R = 0 in the circuit model analysis.

The electric and magnetic fields in both layers of the line must obey Maxwell's equations. If a TEM mode exists, then

$$E_z = E_\varphi = H_r = H_z = 0 \tag{11}$$

A two-layer line with a cross section as shown in Figure 4 is considered. It can be shown that a TEM mode will exist only when

$$\mu_1 \epsilon_1 = \mu_2 \epsilon_2 \tag{12}$$

and

$$\frac{\mu_1 \sigma_1}{\epsilon_1} = \frac{\mu_2 \sigma_2}{\epsilon_2} \tag{13}$$

Even in a lossless line, both these conditions will not in general be satisfied. Therefore, a TEM mode will not in general exist.

Since the TEM mode cannot propagate, there must exist another mode with a cutoff frequency of zero which degenerates into the TEM mode when both layers are the same. It has been shown that a TM mode has these properties. We define

$$\beta_{c_n} = \gamma^2 + \omega^2 \mu_n \hat{\epsilon}_n \tag{14}$$

where

r = propagation factor

n = 1 in region 1

= 2 in region 2

Then the fields which exist in the two-layer line can be shown to be

$$E_{z_m} = [A_m J_0(\beta_{c_m} r) + B_m Y_0(\beta_{c_m} r)] e^{-\gamma z} \tag{15}$$

$$E_{r_m} = -\frac{\gamma}{\beta_{c_m}} [A_m J_0'(\beta_{c_m} r) + B_m Y_0'(\beta_{c_m} r)] e^{-\gamma z} \tag{16}$$

$$H_{\phi_m} = -j \frac{\omega \hat{\epsilon}_m}{\beta_{c_m}} [A_m J_0'(\beta_{c_m} r) + B_m Y_0'(\beta_{c_m} r)] e^{-\gamma z} \tag{17}$$

J_0 and Y_0 are Bessel functions of zero order and of the first and second kind respectively and the primes indicate their derivatives and

$$\hat{\epsilon} = \epsilon - j\frac{\sigma}{\omega} \tag{18}$$

When the boundary conditions are applied, it is possible to find the propagation constant of the line. However, the solution is rather formidable in appearance. In order to derive useful information about the behavior of the line, two different approximating approaches were tried. In the first case, the Bessel function evaluated at r = a and r = c are approximated by the first two terms of a Taylor series about r = b. If this is done, γ is found to be given by

$$\gamma^2 = -\omega^2 \hat{\epsilon}_1 \hat{\epsilon}_2 \frac{(b-a)\mu_1 + (c-b)\mu_2}{(b-a)\hat{\epsilon}_2 + (c-b)\hat{\epsilon}_1} \tag{19}$$

Note that if $\hat{\epsilon}_1$ and $\hat{\epsilon}_2$ are real, γ is purely imaginary and propagation results. In addition, if $\hat{\epsilon}_1 = \hat{\epsilon}_2$ and $\mu_1 = \mu_2$, the equation for the propagation factor for the TEM mode results. For small values of $\beta_{c_1} r$ and $\beta_{c_1} a$, we may write

$$\left| E_{\phi_1} / E_{r_1} \right| = \left| \frac{\beta_{c_1}}{\gamma} \right| \ln \frac{a}{r} \beta_{c_1} r \tag{20}$$

The maximum magnitude of this expression will be found when r = b = 2a. For

$$\mu_1 = \mu_2 = \mu_0 = 4\pi \times 10^{-7} \quad \text{henries/meter} \qquad (21)$$

$$\epsilon_1 = \epsilon_0 = \frac{1}{36\pi} \times 10^{-9} \quad \text{farads/meter} \qquad (22)$$

$$\epsilon_2 = 9\epsilon_1 \qquad (23)$$

$$\frac{b-a}{c-a} = 0.5 \qquad (24)$$

$$a = 1 \text{ cm.} \qquad (25)$$

we find

$$\left|\epsilon_{21}/\epsilon_{11}\right| = 9.13 \times 10^{-11}\ \omega \qquad (26)$$

which indicates the validity of the circuit model at frequencies below 100 Mc.

Another expression for the propagation factor may be obtained by using an alternate set of approximations for the Bessel functions. For small values of the argument, the Bessel functions may be replaced by the first few terms of their power series expansions. For the case where

$$\beta_{c_1} b \ll 1 \qquad (27)$$

and

$$\beta_{c_1} c \ll 1 \qquad (28)$$

we find

$$\gamma^2 = -\omega^2 \frac{\mu_2 \ln c/b + \mu_1 \ln b/a}{\frac{\ln b/a}{\epsilon_1} + \frac{\ln c/b}{\epsilon_2}} \qquad (29)$$

By finding the real part of the square root of (29) we may determine α. It can be shown that, by proper substitution, this is the same propagation factor as would be found from a circuit representation of this line. It is also of interest to note that an increase in μ will not increase the rate of change of attenuation but merely increase the magnitude of the attenuation throughout

the range. Although not readily apparent, it can be shown that, over certain frequency ranges, the attenuation as found from (29) will vary in proportion to the frequency squared. This is a similar result to that found for the circuit model originally proposed. We may conclude that the circuit model is certainly valid, with small error at frequencies in the communications band.

Discontinuous Transmission Lines

Discussion thus far has been concerned with lines which provide dissipative attenuation only. It is well known that filters which incorporate only reactive elements will exhibit the steepest cutoff characteristics. As loss is introduced into the filter, the cutoff of the device becomes more gradual. Unfortunately, those filters with extremely sharp cutoffs generally also exhibit pass-bands at frequencies above those for which the filter is designed to operate. Thus, if it is of importance to allow no energy to be propagated above a certain limiting frequency, (low-pass filter), some loss must be introduced to minimize the effect of higher frequency pass-bands.

A similar situation exists in transmission lines. Lines can be designed which will not propagate energy in a given frequency range. Rejection of the unwanted signals is accomplished through the introduction of discontinuities in the line so that signals are reflected back to the source rather than being transmitted to the load. As a result of the reflections, the loss of the line will be greater than that to be expected from dissipative attenuation alone. An analysis of such a line was performed for establishing criteria for the design of the line in order to obtain the sharpest possible cutoff consistent with the maintenance of a minimum value of attenuation in the stop band.

The model assumed for the study is shown in Figure 8. It is a composite line consisting of alternate sections of two types of transmission lines. The line was considered to be of semi-infinite extent in order that the effects of load end reflections could be neglected and that the impedances

appearing at corresponding points in successive sections would be identical. Significant parameters of the line are given in Table 2. Using these parameters and the conventional transmission line voltage and impedance relationships we may find the ratio of the input voltage to one section of the line to the voltage at the output of the second section of the line. This relationship is found to be given by

$$e_1/e_3 = \frac{(K+1)^2}{8K\eta_1\eta_2}\left[1+\eta_1^2\eta_2^2-\left(\frac{K-1}{K+1}\right)^2(\eta_1^2+\eta_2^2)\mp\sqrt{\left[1+\eta_1^2\eta_2^2-\left(\frac{K-1}{K+1}\right)^2(\eta_1^2+\eta_2^2)\right]^2-\frac{64K^2\eta_1^2\eta_2^2}{(K+1)^4}}\right] \quad (30)$$

Equation (30) is certainly formidable in appearance. Its difficulty is compounded by the fact that the terms involved are in general complex numbers. However, considerable in information can be derived from this expression. The equation is symmetrical with respect to η_1 and η_2. Furthermore, the result is unchanged if K is replaced by 1/K.

An understanding of (30) is facilitated by a breakdown of the individual factors involved. The attenuation loss and the phase shift of the individual section is represented by η_1 and η_2. The factor $(K + 1)/2\sqrt{K}$ will be recognized as proportional to the mismatch loss between two lines having characteristic impedances Z_{0_1} and Z_{0_2}. The remaining portion of (30) is due to second and higher order reflections which occur as the wave is reflected first toward the source, then toward the load, and so on. The importance of these higher order reflections will depend upon the dissipative attenuation of the individual sections of the line. If the individual attenuations are small, the wave after its second reflection is of the same order of magnitude as the primary wave. If attenuation is present, the influence of higher order waves will be negligible.

When the ratio of characteristic impedances is high, and a moderate amount of attenuation occurs in each of the elements of the line, (30) may be simplified to

$$e_1/e_3 \approx \eta_1 \eta_2 \frac{(K+1)^2}{4K}\left(1-\frac{1}{\eta_1^2}\right)\left(1-\frac{1}{\eta_2^2}\right) \qquad (31)$$

For mismatch ratios of greater than 50 to 1 and attenuations of at least 1 db per section, (31) will be in error by less than ten percent. In addition, no great error will be involved in using (31) even for the low-loss case unless the electrical length of one or the other of the elements of the line is nearly an integral number of half-wavelengths.

On the basis of the foregoing discussion, several generalizations can be formulated regarding the behavior of a quasi-lumped transmission line over the entire frequency range.

(1) In the low-frequency range the attenuation of such a line will be relatively low and will be approximately equal to the sum of the dissipative losses in the elements which comprise it.

(2) At higher frequencies the attenuation will rise more rapidly than the losses of the individual elements because of the mismatch loss resulting from phase shift in the line sections.

(3) As the frequency approaches that at which the individual elements represent a quarter-wavelength, the attenuation of the composite section passes through a peak.

(4) The attenuation then decreases with rising frequency until the point at which each element represents a half-wavelength at the signal frequency. The value of the attenuation at this minimum point is a function of the losses of the two elements and will usually be greater than their sum.

(5) At still higher frequencies the attenuation displays a cyclical variation wit' peaks occurring at frequencies corresponding to odd numbers of

quarter-wavelengths and valleys at frequencies corresponding to even numbers of quarter wavelengths.

(6) In a physical line, the amplitudes of successive fluctuations tend to decrease progressively as the attenuations of the elements increase with frequency.

(7) The attenuation characteristic of the composite line oscillates about a curve whose value is equal to the sum of the attenuation of the two elements plus twice the mismatch loss between their characteristic impedances.

In order to get a more quantitative idea of the behavior of such a line, a specific value of K was assumed. Figure 9 gives a family of curves of the maximum and minimum values of attenuation in terms of the attenuation of the individual elements calculated for a value of K equal to 1000. The minimum value of attenuation will occur only if both lines represent an integral number of half-wavelengths at the same frequency. The same may be said for the maximum value. One interesting feature is the fact that for a given attenuation of the individual elements, the attenuation of the composite line will be greatest if each section has the same loss as the other. Between the curves giving the upper and lower limits of the composite attenuation, a curve is drawn which is equal to the sum of the individual attenuations plus twice the mismatch loss. This curve represents an asymptote which both sets of curves approach. It should be noted that for each value of K a new set of curves could be generated.

Although a complete design specification cannot be found by use of the above analysis the curves can be used to obtain the minimum values of individual attenuation necessary to insure that the total attenuation will remain above a specified limit as the frequency is varied. Specification of the design parameters for a line of this type will, in general, be an empirical process involving a number of compromises. However, some suggestions might be

made which should facilitate the process and minimize the number of burdensome calculations which must be performed.

In most applications, the required length of the overall line will be known. Determination of the number of sections into which this length should be divided will involve a compromise among several factors. Close agreement between the theoretical performance capabilities described above and the behavior of an actual line requires that the line contain a large number of identical composite sections in cascade. However, fabrication of a line becomes more difficult, and perhaps even impractical, if an unduly large number of sections is specified. Furthermore, the range of values particularly of the reactive parameters, which can be realized in a reasonable line configuration is limited by available materials and techniques and this, in turn, restricts the extent to which each section can be shortened while still obtaining adequate phase shift over the frequency range of interest. Nevertheless, it is suggested that the line be divided into as large a number of sections as is feasible and that a minimum of perhaps five composite sections is necessary if reasonable agreement between theoretical results and actual performance is to be obtained.

ATTENUATION MEASUREMENTS

Measurement Techniques

The attenuation of a transmission line may be determined by a measurement of the input impedance of a line under open-circuit and short-circuit load conditions. If the open-circuit input impedance is denoted by Z_{oc} and the short-circuit input impedance by Z_{sc}, then the propagation constant of the line will satisfy the following relationship:

$$\tanh \gamma l = \sqrt{\frac{Z_{sc}}{Z_{oc}}} \qquad (32)$$

This equation can be solved to determine γ and thus α .

As α increases, however, the input impedance under any load conditions approaches Z_0, the characteristic impedance of the line. It then becomes difficult to determine the line parameters by a measurement of the input impedance.

An alternate scheme has been devised to make these determinations. For an open-circuit load, the magnitude of the ratio of receiving end to sending end voltages can be shown to be

$$A = \left| V_R / V_S \right| = \left| \frac{2 e^{-\gamma \ell}}{1 + e^{-2\gamma \ell}} \right| \tag{33}$$

For $\cos 2\beta \ell \approx 1$, the attenuation may be approximated by

$$e^{-\alpha \ell} \simeq \frac{1}{A} \left[1 - \sqrt{1 - A^2} \right] \tag{34}$$

For values of $A < 0.4$, this can be further simplified to

$$e^{-\alpha \ell} \simeq \frac{A}{2} \tag{35}$$

with better than one percent accuracy.

Experimental Results

The experimental setup for both voltage and impedance measurements is shown in Figure 9. A ground plane of 1/32" copper sheeting was placed on a bench-top, with all of the instruments and the line under measurement being grounded to this plane. The following will give the results of measurements performed upon certain of the lines. The attenuation values given for these lines were in most cases derived through a measurement of the ratio of input and output voltages under open circuit load conditions. Impedance measurements were generally made to obtain a check of the attenuation at one or two frequencies at the low end of the frequency band.

The first line which was fabricated and measured was a strip RC line. The response of this line as a function of frequency is shown in Figure 10. Included is the theoretical response of a line with the measured values of R and C determined by input impedance measurements. The constancy of the attenuation at frequencies above one megacycle is due to the presence of inductance which is neglected in the theoretical derivation.

The results obtained with several additional line types are shown in Figure 11. Included in this Figure is the response of the RC line for comparison. The lumped element line indicated consisted of series coils and shunt capacitors with a theoretical attenuation of 3 db/section at 320 kilocycles.

Attenuation measurements performed upon the two-layer lines which were fabricated indicated that little correlation existed between the theoretical and obtained values of attenuation. One of the main difficulties encountered with all models of the two-layer line was the prohibitively high value of series resistance which was present. In one strip line, the series resistance at dc was measured as 190 ohms. In addition, the conducting epoxy which was employed as the conducting medium was found not to meet the specifications of the manufacturer. One type was found to have a resistivity four orders of magnitude greater than the manufacturer's literature claimed. It is felt, therefore, that a good physical model of the two-layer line has not yet been constructed. In addition, it should be noted that the requirements on the material as indicated in Table 1, may preclude the construction of the type of two-layer line described here.

Some of the most interesting lines tested were gelatinous filler lines. Five different types of filler were tested. The compositions of the filler are given in Table 3. The attenuation of these lines as a function of frequency are shown in Figure 12. It will be noted that the variation in

attenuation as a function of frequency is much more rapid than the one-half power, at least until the high frequencies are reached. This appears to be due to the variation in the resistivity of the material as a function of frequency. For the purposes of attenuating lines, this variation is in the proper direction, i.e. the resistivity decreases with increasing frequency. Once again, it can be seen that the attenuation tends to become constant at frequencies above one megacycle.

Recent efforts have been concerned with two commercially manufactured types of cable. The first is fabricated with a conducting polyethelyne dielectric. The second's dielectric is a conducting silicone rubber compound. Receipt of these lines was only recently made and the initial results are reported. Portions of both of these cables were braided with a one hundred percent coverage. Preliminary indications are that neither of these cables will meet the contract requirements as far as the exact attenuation requirements are concerned. However, it can be seen that the variation of attenuation as a function of frequency is approximately as predicted. The responses of several of these commercially fabricated lines are shown in Figure 13. Included in this figure are the results of measurements on a polyethelene dielectric, copper braided line, and two rubber dielectric lines. Of these latter two, one was braided while the other used a mixture of conducting paste and a silicon adhesive as the outer conductor.

CONCLUSIONS

The feasibility of using the signal leads to an electroexplosive device to provide attenuation to unwanted rf energy has been analytically demonstrated. For a conventional line, however, attenuation above the pass-band will increase at a rate no greater than the square root of frequency. The use of a double-layer line will in theory allow this to be increased to the second power of

frequency. However, the practical difficulties of fabricating such a line may not allow full benefit to be derived from its use. If reflective losses are permitted, a theoretically infinitely sharp cutoff can be achieved. Such a cutoff will, however, give higher frequency pass-bands.

Commercially fabricated lines have demonstrated that attenuating lines can be constructed. The lines tested thus far have not fully met the design specifications. If, however, the cost of such lines is not prohibitive, the amount of attenuation which has been achieved should allow the use of ordnance devices in higher intensity field strength areas than is presently possible. Further investigation of fabrication techniques should allow the original design goals of this program to be met. It is felt that the incorporation of such lines into new systems would be of definite benefit to the HERO program.

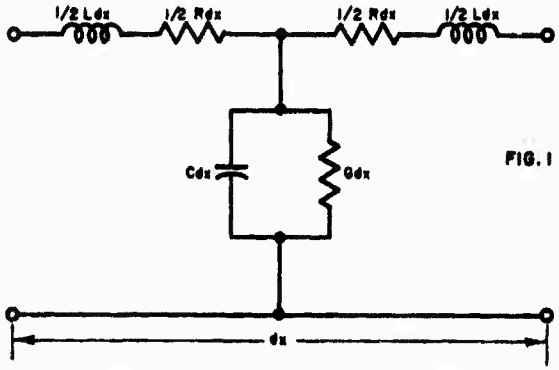

FIG. 1 CIRCUIT REPRESENTATION OF A CONVENTIONAL DISTRIBUTED TRANSMISSION LINE

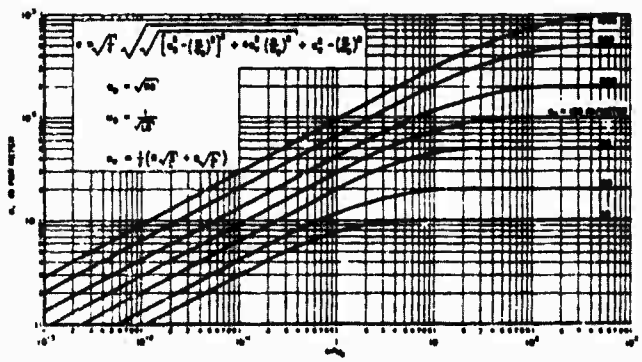

FIG. 2 NORMALIZED ATTENUATION CHARACTERISTICS OF CONVENTIONAL TRANSMISSION LINE, $a_0 = 0$

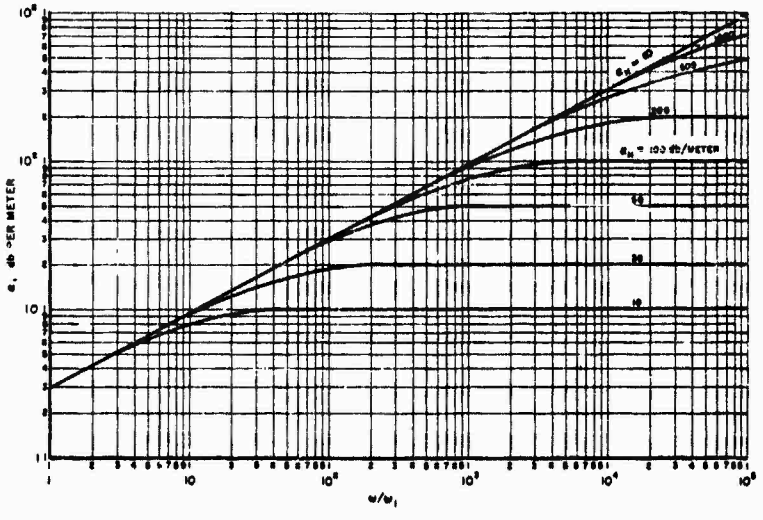

FIG. 3 NORMALIZED ATTENUATION CHARACTERISTICS OF CONVENTIONAL TRANSMISSION LINE, $\alpha_0 = 0$

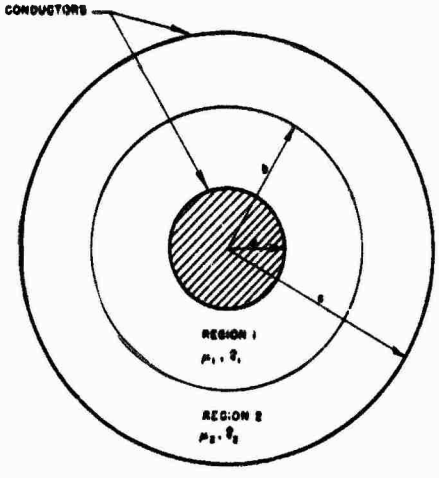

FIG. 4 TWO-LAYER COAXIAL TRANSMISSION LINE, CROSS-SECTIONAL VIEW

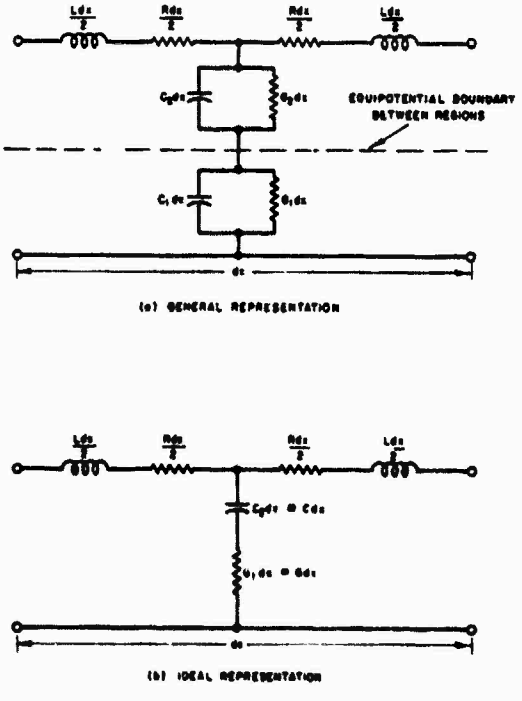

FIG. 5 CIRCUIT REPRESENTATION OF LINE

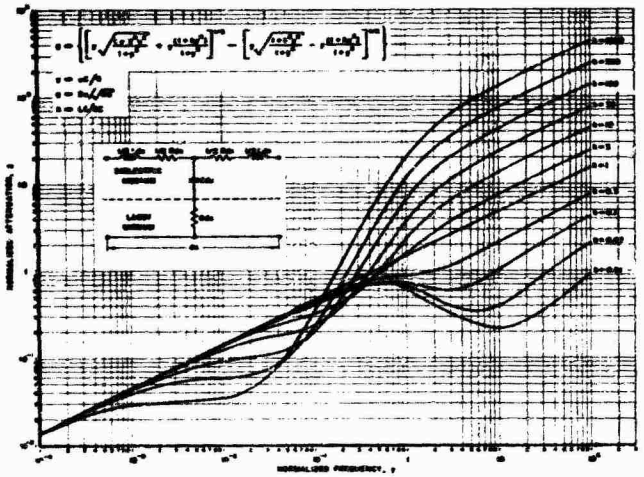

FIG 6 NORMALIZED ATTENUATION — FREQUENCY CURVES TWO LAYER TRANSMISSION LINES

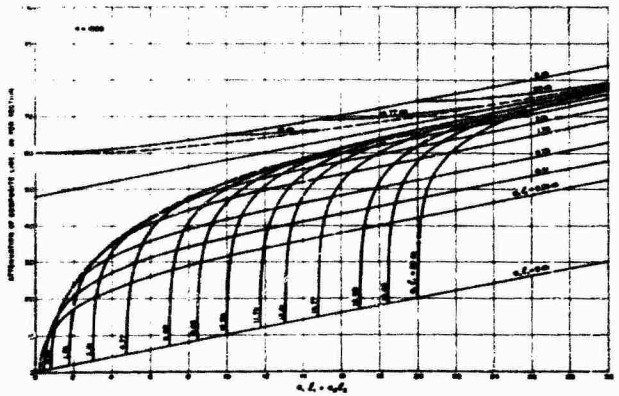

FIG 8

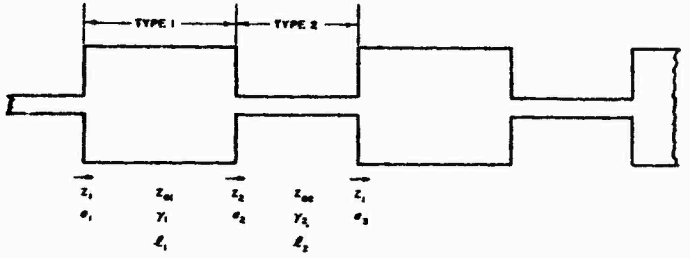

FIG. 7 MODEL OF DISCONTINUOUS TRANSMISSION LINE

FIGURE 9 EXPERIMENTAL TEST SETUP

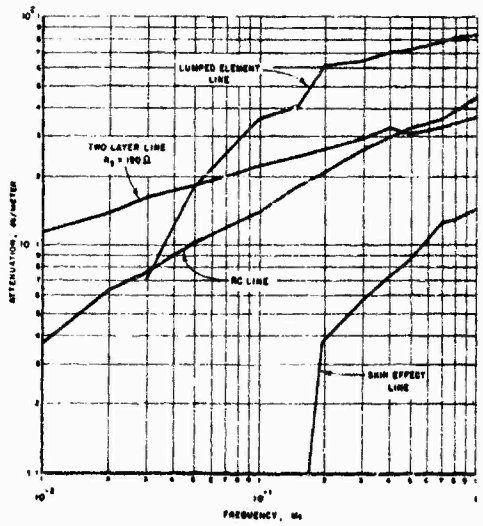

FIG. 11 ATTENUATION OF REPRESENTATIVE LINES

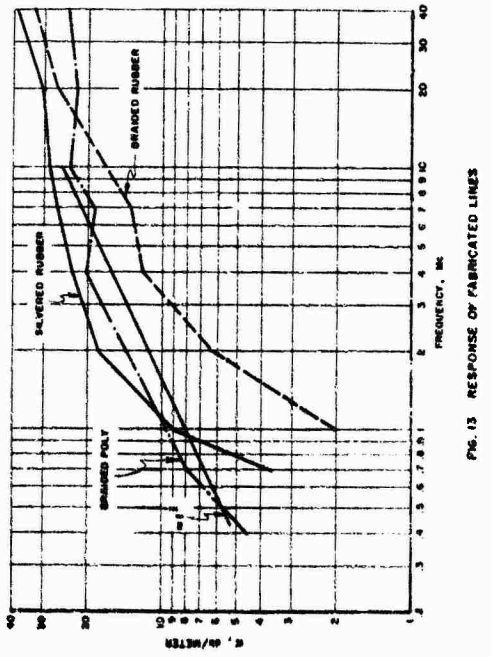

FIG. 13 RESPONSE OF FABRICATED LINES

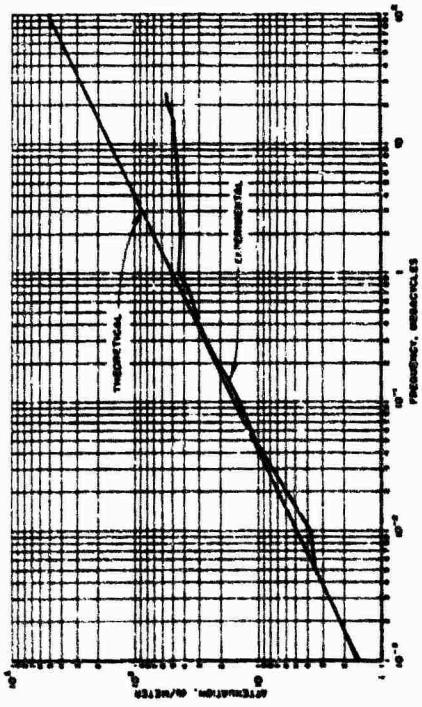

FIG. 12 ATTENUATION OF RC LINE

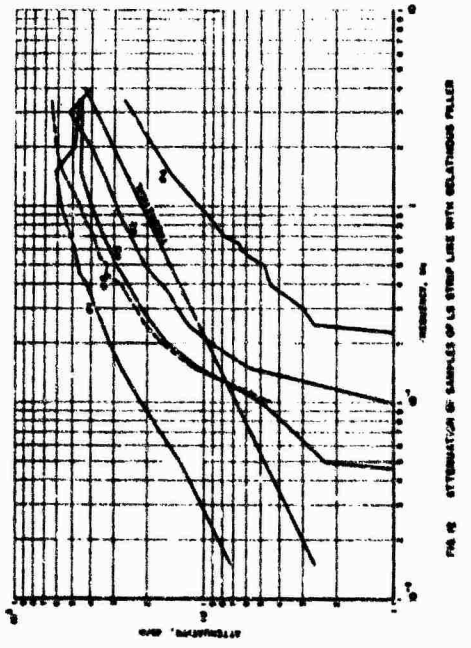

FIG. 14 ATTENUATION OF SAMPLES OF LS STRIP LINE WITH DIELECTRIC FILLER

28. HIGH VOLTAGE HYBRID INITIATORS

Leonard Katz, Rocketdyne, Div. of
North American Aviation Corp.
Canoga Park, California

The past few years have seen the rapid development of new families of electro-explosive devices. This development is necessitated by increasing subjection of these electro-explosive devices to inadvertent firing by other than the proper command signals. The improper signals might be contributed by powerful RF fields, by strong system currents or voltages, or by erroneous electrical connections. A lesser emphasized but quite real hazard is the possibility of firing a unit by static discharge pin-to-pin and pin-to-ground.

One of the safe families has been attained by moderate, evolutionary "upgrading" of the conventional bridge wire devices, i.e., the 1 amp, 1 watt no-fire, 4 amp all-fire unit. Proponents of this improved class point to the following advantages:

1. The no-fire capabilities are more than adequate versus RF fields.
2. There is negligible susceptibility to pin-to-ground static discharge firing.
3. There are no electrical connector or electrical transmission line difficulties; no electrical system alterations are required (twisted, shielded pairs are assumed).
4. A simple 28 volt supply is all that is required; no black boxes needed.
5. An extensive background of storage, surveillance and behavior data exists.

The disadvantages include:

1. Danger of being fired inadvertently by application of available excessive power; i.e., plugging in of high voltage systems which may be a portion of the missile system or ground supply.

A second safe family of electro-explosive devices is the Exploding Bridge Wire group, known variously as EBW, XB, High Voltage, and others. There have been many contributions to this development and many facets to the resultant characteristic features. Basically, though, the unit features a fine bridge wire through which a great amount of electrical energy is passed in a very short time. This energy is usually provided by the discharge of a capacitor through the wire. When the energy pulse hits the wire, the wire is said to "explode" with a resultant shock wave which can initiate relatively insensitive explosives.

Most of the units in this family include voltage blocking devices to protect the wire. The advantages include:

1. The use of relatively insensitive explosive material.
2. Excellent no-fire characteristics under a wide range of relatively high voltages, temperatures, RF and shock.
3. High simultaneity capability.

The disadvantages include:

1. Possibility of dudding when subjected to certain no-fire values if blocking devices are absent or rendered inoperative.

2. Permissible transmission line lengths from the power source (condenser) to unit are quite short (approx. 4 ft. max. length).
3. A multiplicity of black box techniques is required to provide condenser charge as needed, bleed as needed, and discharge as needed, including protection of the triggering device.
4. New connector developments are required.

Because of the various interpretations of the AFMTC "Standards with Regard to RF Ratiation Hazards", a new, third group of electro-explosive devices is developing.

One of the interpretations of the AFMTC policy letter regarding range safety is a stipulation that a unit must not fire upon the application of one watt for five minutes and one ampere five minutes as applied directly to the bridge wire, without the use of voltage blocks or shunting devices. Dudding is acceptable. For those who accept dudding of the unit as a consequence of the one watt-one ampere treatment, one of the EBW units with voltage blocking devices would be adequate. For those who do not or cannot accept dudding of the unit, and who also require a high voltage capability, a new class has been developed.

In the absence of any present nomenclature, I have been referring to this category as High Voltage Hybrid Initiators.

The hybrid unit combines most of the major advantages of the two classes just described. Typically, it has a no-fire voltage higher than that of

the highest available as ground support or system power. This no-fire (usually above 230 volt AC RMS systems) is accomplished by diodes, gaps, or similar voltage blocking devices. An especial note here: The devices fire as a consequence of applied power. If the power (which usually, in this context, means heat) can be dissipated, rather than "blocked", the unit would be simpler. The required firing voltage is some higher amount, consistent with safety, reliability and type of power supply. The bridge wire portion is the conventional one amp no-fire, 4 amp fire unit.

The advantages include:

1. Meeting all requirements of Range Safety AFMTC, without dudding.
2. Use of established (well-documented) pyrotechnics.
3. If firing voltages are kept relatively low (1000 volts or less, preferably 500) transformers can be used, eliminating transmission line length worries, triggering devices, and associated techniques.
4. No connector problems.

The disadvantages include:

1. The detonating types of devices would not have an insensitive material in lieu of the primary explosive.

In the presenting of the classes, their advantages and disadvantages, the listings have been purposely kept to the major points. In the same sense, there have been avoided, for the sake of brevity, the recitals to each of the disadvantages listed.

For instance, in discussing the disadvantages of the short transmission line length in EBW devices, a rebuttal would be that mild detonating fuse can be used. (Mild detonating fuse is a cord with an explosive material disseminated along its length. It transmits explosive shock waves.) The rebuttal to the rebuttal would be that MDF must be replaced after each test, that MDF transmits shock and that if deflagration is required rather than detonation, an additional pyrotechnic technique is necessary - etc. and so on for each of the possible solutions.

For those who are interested in the specific details of the hybrid unit, there are herein listed some of the major operating characteristics of the igniter unit of the solid propellant gas generator used for starting the turbine on Rocketdyne's H-1, Saturn engine. (Note: Though the unit described fits the hybrid definition, the conventional bridge wire portion of this particular unit is not a one amp no-fire, 4 amp fire unit; it is of slightly lower no-fire, all-fire amperage. The unit has been in use for over three years. Upgrading it to the full 1 amp, 1 watt no-fire would require only a formal request to the vendors to provide the available 1 amp, 1 watt portion.)

No-fire characteristics:

Pin to Pin and Both Pins Individually to the Initiator Case Ground

1. 36 V. DC from 0.1 ohms impedance or less. The impedance between the power supply and initiator shall be held to 0.1 ohms or less.
2. 115 V. AC 60 cycle from a power supply capable of delivering 3 amperes continuously with 5 percent voltage regulation. The impedance between the power supply and initiator shall be held to 0.2 ohms or less.

3. 250 V. AC 60 cycle power supply capable of delivering 3 amperes continuously with 5 percent voltage regulation. The impedance between the power supply and the initiator shall be held to 0.2 ohms or less.

4. 115 V. AC 400 cycle power supply capable of delivering 3 amperes continuously with 5 percent voltage regulation. The impedance between the power supply and the initiator shall be held to 1.0 ohms or less.

5. 250 V. AC 400 cycle power supply capable of delivering 3 amperes continuously with 5 percent voltage regulation. The impedance between the power supply and initiator shall be held to 1.0 ohms or less.

6. Discharge from a one-microfarad capacitor charged to 500 volts.

7. Discharge of 1,000,000 ergs minimum from approximately a 500 micro-microfarad capacitor charged to approximately 20,000 volts. The capacitor and voltage values may vary, but the adjustment to obtain the 1,000,000 shall be according to the following equation: 1,000,000 ergs = 1/2 x capicator rating in farads x $(\text{voltage})^2$ x 10^7.

8. 250 Volts AC with no current limitations other than the initiator shall be applied to the bridge wire circuit for a period of 5.0 minutes. The initiator shall not operate.

All-fire characteristics:

1. 500 Volts AC with no current limitations other than the initiator shall be applied to the bridge wire circuit. The initiator shall operate satisfactorily.

HIGH VOLTAGE HYBRID INITIATORS

250 VAC NO FIRE - 500 VAC FIRE

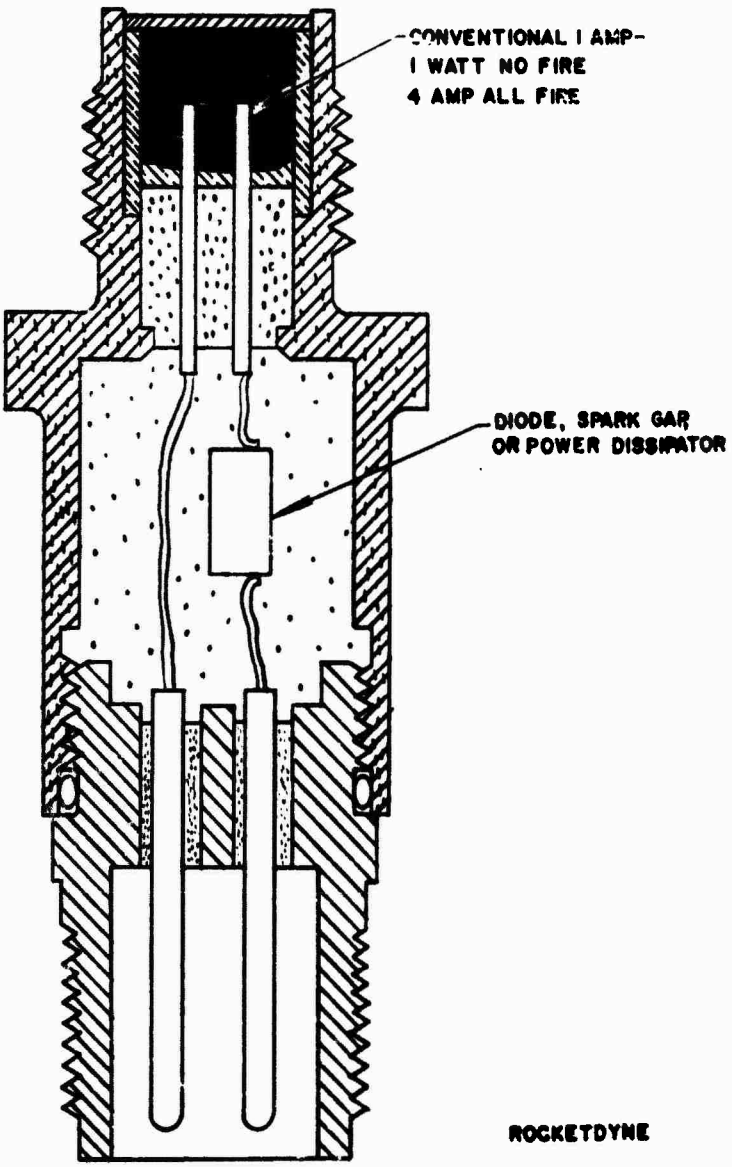

ROCKETDYNE

29. DEVELOPMENT OF RF PROTECTED ELECTRO-EXPLOSIVE DEVICES

Frederick M. Correll
Picatinny Arsenal, Dover, New Jersey

Many electro-explosive devices (EED) utilized in weapon systems have been shown to be vulnerable to electromagnetic radiation emanated from radio and radar transmitters. The results of a premature initiation of an EED can be the unprogrammed launching of a missile, detonation of a warhead, premature stage separation, or any one of a series of events commenced by an EED. Also, an EED can be rendered unreliable after being subjected to current below the firing level for an extended period of time. This is no less serious than premature initiations in some systems.

In order to alleviate the possibility of premature initiation or change in sensitivity of an EED due to electromagnetic energy, we have endeavored to make all EED's "RF Proof". The most obvious solution is to discard all EED's and utilize non-electric initiators only. However, the many advantages inherent to EED's such as small size, light weight, cheapness, reliability and relative simplicity made them highly desirable when compared with non-electric initiators.

In a study of solid state materials, it was observed that some of these materials act as broadband RF absorbers or attenuators. The advantages of utilizing attenuator materials for RF protection are many. First, these materials can be incorporated within the existing exterior configurations of initiators with no great difficulty and at reasonable cost. This is accomplished by substituting a plug composed of the attenuating material in place of the plastic sealing plug through which the lead wires pass.

No external device or fitting is necessary thus eliminating the possibility of a faulty assembly which would provide no RF attenuation at all or possibly even attenuate or short out a normal firing pulse. Since the material compressed into the attenuating plug is a single component device, it is far more reliable than multi-component filtering devices. Another advantage is that there are no resonant points. Other important advantages in the utilization of RF attenuators are that this approach can be universally applied to all initiators; no additional space or weight requirement is necessary; and this is a low cost solution.

Requirements for the RF attenuating material to be utilized in EED's were set up as follows.

a. It must provide adequate attenuation of RF energy.

b. It must not significantly alter the normal firing response of the EED.

c. It must be easily molded or formed into configurations and sizes identical to those of the plug it replaces.

d. When assembled into an EED, the EED must still be capable of passing all functioning, reliability, environmental stability, rough handling and other required MIL Standard Tests.

e. In all, the attenuator plug must meet all of the requirements met by the orginal plastic plug and in addition must provide significant RF absorption.

The material selected was phosphated powdered iron which orginally was mixed with expoxy resin binder and molded at high pressures. However, product refinement by The Franklin Institute has led us to a standardized product prepared as follows. The iron powder utilized is pure 10 micron iron powder made by the carbonyl process. The iron powder is then insulated

by wetting it with acetone; adding a stock solution of dilute phosphoric acid to the wetted powder; and stirred until dry under a heat lamp. The molding powder is pressed into plugs at pressures well over 50,000 psi. These high pressures are necessary in order that the concentration of iron powder in the plug be high so that high attenuation values are obtained. This is exemplified in Figure 1 which shows the dependency of attenuation upon density by the very steep slope of the curve.

The first item to be provided with RF protection was the T24E1 detonator shown in Figure 2. This detonator was provided with protection because it was the most sensitive (500 ergs) Army wirebridge EED. The lead wires which pass through the phenolic plug are kinked. Figure 3 shows the attenuated T24E1 detonator. The phenolic plug was eliminated and an attenuator plug substituted. There is absolutely no difference in the shape or dimensions of the plug or of the initiator. The only difference is that the lead wires are now tapered instead of being kinked. This change was necessary because the high pressure necessary for molding the attenuator plug caused breaks in the kinked wires. Insofar as pull-out strength is concerned there was no loss. Results of extensive engineering tests on the RF protected T24E1 detonator showed that there is absolutely no difference between these two detonators except that the attenuated detonator provides around 15 db of attenuation at 500 mc whereas the original detonator provided none. Figure 4 shows attenuation vs frequency for the .13 inch RF attenuator plugs for the T24E1. Note how the steep slope of the curve gives us very high attenuation values at high frequencies but very low atienuation at low frequencies. We are attempting to correct this low frequency deficiency. The RF protected T24E1 detonator has entered the production engineering phase of its development.

Figure 5 shows the T20E1 detonator. It is very similiar to the T24E1 detonator except that the spot charge is colloidal lead azide instead of milled lead styphnate which makes the normal functioning energy 5,000 ergs rather than 500 ergs as required for the T24E1 detonator. Figure 6 shows the RF protected version of the T20E1 detonator. Attenuation values for the RF attenuator plug for the T20E1 are identical to the T24E1 plug.

The T77 wirebridge, button-type electric detonator is shown in Figure 7. This detonator was the first of its kind to be provided with RF protection. The changes in design for the RF protected T77 detonator included the deletion of the formvar coating and araldite bonding between the pin and plug; and the addition of a steel cup for holding the attenuator which was required for assembling the bridgewire. This is shown in Figure 8. Figure 9 is an attenuation vs frequency curve for the .125 inch long plugs. A pilot lot testing program carried out with the RF protected T77 detonator proved it to be practically identical with the unattenuated version in functioning, sensitivity, environmental stability and ability to withstand rough handling. RF attenuators have been provided for the MK2 Mod 0 and MK7 Mod 0 ignition elements under Navy sponsorship. The MK7 Mod 0 ignition element is shown in Figure 10. Figure 11 shows the RF protected version. Modification of the MK7 Mod 0 electrode to a tapered shape was to permit molding the attenuator plug and also to permit the element to withstand the 50,000 psi blowback test. The grove added below the tapered portion holds the attenuating material in place during assembly. Complete functioning, sensitivity, reliability and rough handling tests have established that there is no degradation in performance with this RF protected ignition element in comparison with the unprotected version except that it provides the attenuation shown in Figure 12.

RF attenuators have been provided for the M6 blasting cap, M2 squib, M36A1 detonator, XM66E2 detonator, M51 detonator, and T77 conductive mix detonator. However, extensive pilot lot studies have not been conducted on these items.

The new Army electric blasting cap, the M6, is shown in Figure 13. Figure 14 shows the RF Protected M6 Blasting Cap utilizing a new non-proprietory ignition mix. The attenuation provided by the attenuator plug is necessarily much greater than any of those before mentioned because of its almost three fold length increase over the longest attenuator plug incorporated into EED's up to this time.

Production engineering studies are presently being planned for the RF protected version of the M2 squib utilized in many rocket igniters and the M36A1 detonator utilized in VT fuzes. The RF protected versions of the M2 squib and M36A1 are shown in Figures 15 and 16 respectively. Also the XM66E2 detonator, utilized in the Type 19 Spotting Device has recently been provided with RF protection.

All of the previously described EED's which have been provided with RF protection were wirebridge, wire lead items except for the T77 detonator and the MK2 Mod 0 and MK7 Mod 0 ignition elements. Studies have been conducted on a piggy back design of the phosphatized iron on top of bakelite for the RF protected M51 carbon bridge, wire lead detonator. This design is shown in Figure 17. Also an attenuated face gap plug design with a spot charge of gold and colloidal lead azide to make up an RF protected T77 conductive mix detonator has been studied and is shown in Figure 18.

Presently studies are being made to incorporate ferrites such as Ceramag 27 and T1 into the T24E1 detonator, M2 squib and M6 blasting cap. These materials exhibit superior low frequency attenuation to that provided

by the present phosphatized powdered iron. We are also studying organic polymeric semiconductors which show promise of good broadband attenuation under contract with Midwest Research Institute.

The work previously described was carried out with support from The Franklin Institute, Atlas Chemical Industries, and Atlantic Research Corporation.

Our goal is to provide the munitions designer with safe, reliable EED's which are safe from electromagnetic radiation. We can at the present time come close to realizing this goal with the promise of coming even closer in the near future. In the meantime, we are doing our utmost to make available the products of the present state-of-the-art.

(Discussion appears in Supplement, Section 55.)

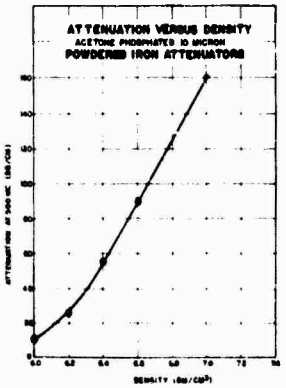

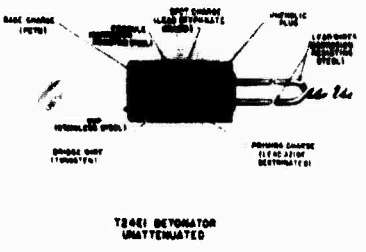

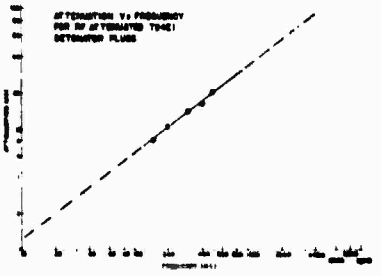

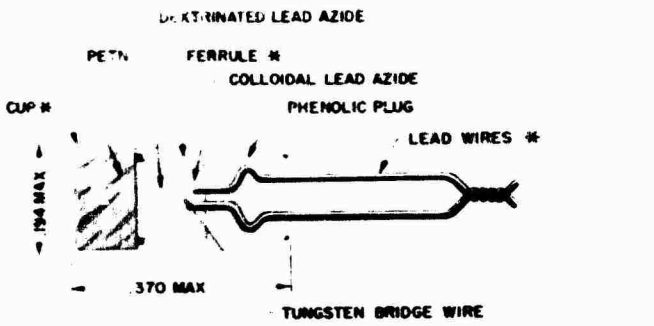

T20E1 ELECTRIC DETONATOR

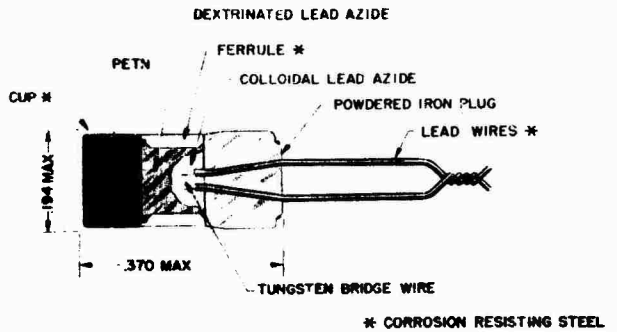

RF PROTECTED T20E1 ELECTRIC DETONATOR

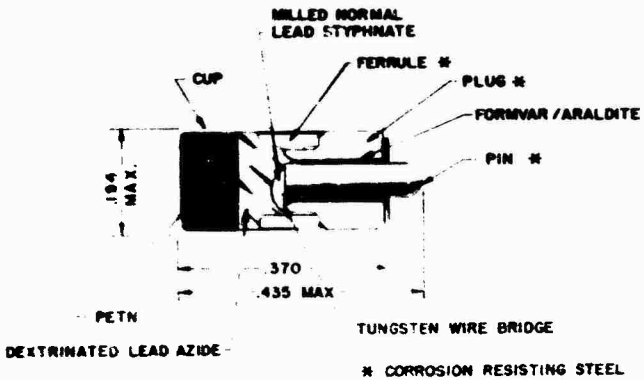

T77 ELECTRIC DETONATOR

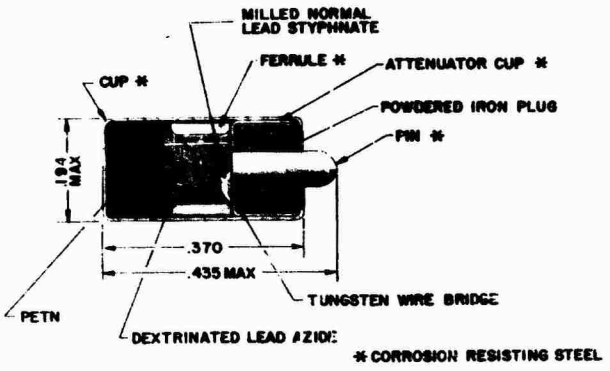

RF PROTECTED T77 ELECTRIC DETONATOR

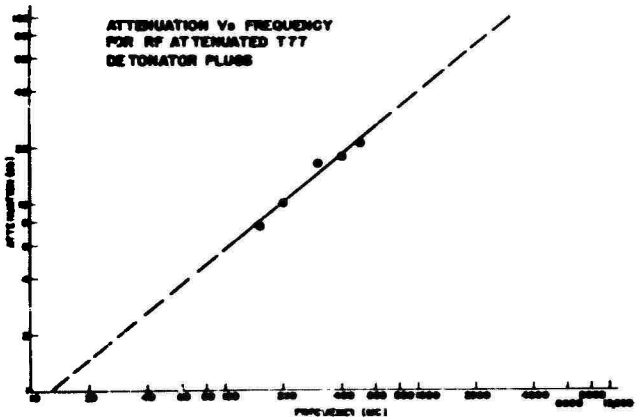

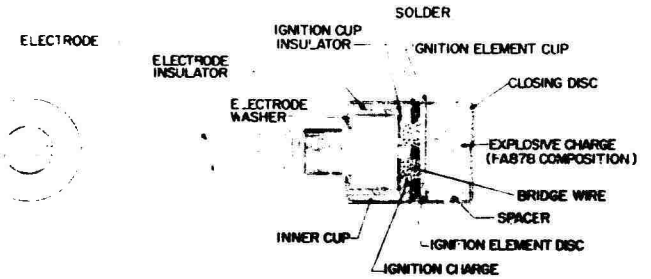

MK-7-MOD O ASSEMBLY

FIGURE 10

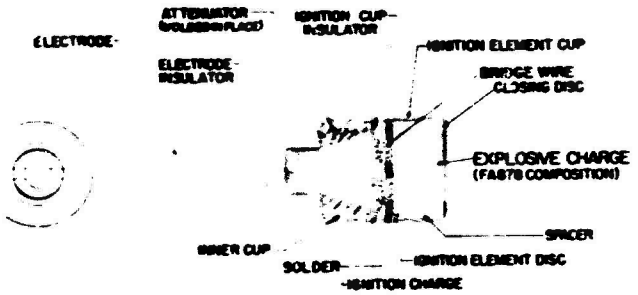

ATTENUATED MK-7-MOD-O ASSEMBLY

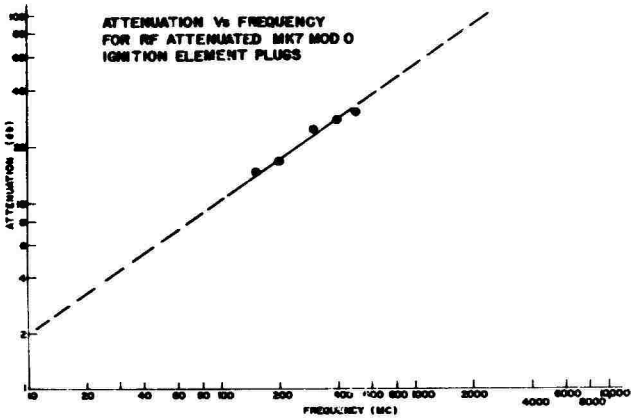

FIGURE 12

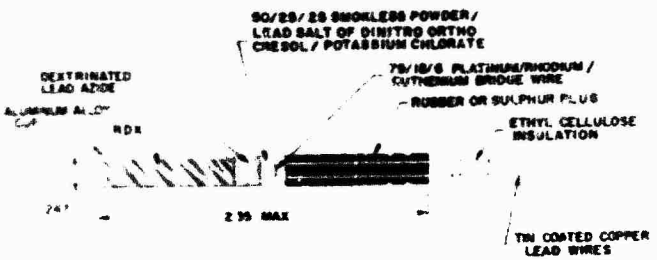

M6 ELECTRIC BLASTING CAP

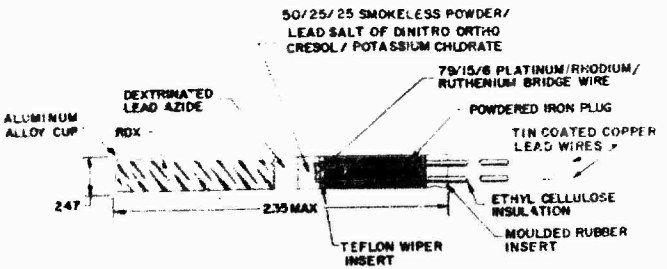

RF PROTECTED M6 ELECTRIC BLASTING CAP

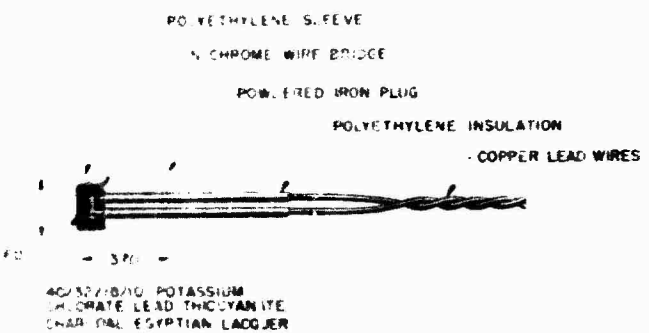

RF PROTECTED M2 ELECTRIC SQUIB

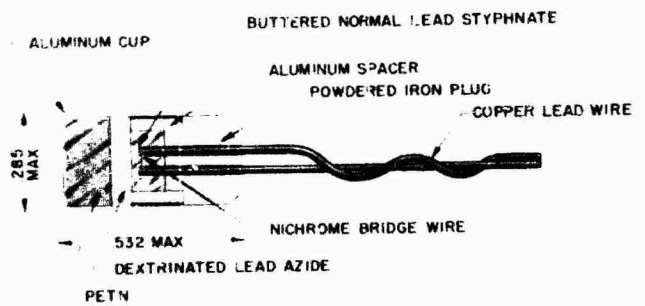

RF PROTECTED M36A1 ELECTRIC DETONATOR

30. THE LOSSY FILTER AND ITS APPLICATION TO PROTECTION OF ELECTROMAGNETIC RADIATION SENSITIVE ORDNANCE DEVICES

By

Merrill O. Murphy
Sandia Corporation, Division 1423

Summary

The requirements placed on a filter for protection of radiation sensitive weapon devices are discussed in some detail. The problems brought about by those requirements are described and solutions are discussed. The lossy ferrite core material is advocated as a means of meeting the unknown impedance driving source and load conditions. Use of this material and its heat sinking is described. An actual multichannel filter using ferrites is described and a test program is briefly outlined to indicate the test procedures necessary to obtain a reliable product.

Multichannel lossy filter packages are being developed at Sandia for several weapon applications. Each of these filters must meet certain requirements peculiar to the weapons field. These special requirements are:

1. Attenuation Over a Wide Frequency Range.

   Each filter channel must provide at least 50 decibels of attenuation to radio frequency currents in the frequency range of one megacycle to 50 megacycles. Below one megacycle and above 50 megacycles the required attenuation level slopes off at six decibels per octave to end frequencies of 200 kilocycles and 1000 megacycles. (See Figure 1)

2. High Input Voltage Operation.

Each filter channel must provide the above stated attenuation for a 30 minute period with an input of 125 volts rms at all frequencies between one and 50 megacycles. Below one megacycle and above 50 megacycles the filter channels are required to provide the attenuation indicated in Figure 1 at input voltage levels which also decrease at six decibels per octave from the 125 volt maximum.

3. Operation With Unknown Driving Impedances.

The impedance of the energy source which drives the filter is unknown. It is a function of frequency and of the aircraft to weapon wiring variations. No two cases will result in the same input impedances.

4. Operation With Unknown Load Impedances.

The true value of the load impedance is also unknown and subject to individual weapon wiring variations.

5. Direct Current Resistance.

(a) Each channel must exhibit less than 0.20 ohms DC series resistance.

(b) Each channel must exhibit a shunt resistance exceeding one megohm.

6. Reliability (90% Confidence Level).

(a) Each filter channel must be capable of providing the specified attenuation with a 0.999 probability.

(b) Each filter channel must provide a 0.999 assurance that the DC series resistance will not exceed 0.20 ohms.

(c) Each filter channel must provide a 0.999 assurance that the DC shunt resistance exceeds one megohm.

7. Environmental

(a) Each filter channel must meet the preceding requirements at any temperature between -65°F and 165°F.

(b) Depending on the weapon application, the filter package must be operable after subjection to shocks as great as 1000g.

(c) The filter package must not be degraded by vibration levels as high as 5g at 2000 cps applied in four, fifteen minute cycles.

Each of the preceding requirements presents its own special problems. Attenuation over a wide frequency range requires capacitors exhibiting no resonances below the highest frequency of interest. Such a capacitor was found. It is an oil impregnated paper, feed-through capacitor made by Sprague Electric Company. It has very excellent bypass characteristics to frequencies at least as high as 1000 megacycles.

The unknown impedance characteristics of the driving source and of the load present a very real problem. These impedances, if largely reactive and of proper value, could resonate with elements of the filter at frequencies within the rejection band. Such resonance would result in marked degradation of the attenuation of a lossless filter. The use of lossy ferrite core inductors so lowers the circuit Q at frequencies of interest that series resonance effects do not seriously degrade filter performance. The high permeability W-01 ferrite, made by Allen-Bradley, has been used in Sandia filter designs. The high permeability allows use of a minimum number of coil turns, resulting in low DC resistance and low winding capacitance. The loss characteristics of the W-01 ferrite are shown in Figure 6.

The lossy ferrite cores solved the problem of operation with unknown driving and load impedances but added the problem of how to cope with heat developed in the loss resistance. Ferrite is not a good heat conductor. Application of 125 volts

rms signal at one megacycle to the input of a T-section filter will drive the ferrite of the first inductor beyond its Curie temperature in a matter of seconds if special heat-sink designs are not used. The best method found to date consists of using the cup core design which encloses the winding. The core and cover are clamped together to provide the required inductance. A 0.005 to 0.010 inch thick jacket of copper is sprayed onto the entire core surface using the Metco or the Plasmadyne flame spraying processes. The copper jacket channels the heat to a heavy metal plate. The copper jacket also serves to clamp the cores permanently with the proper tension to produce the desired inductance.

The reliability level required necessitates circuit simplicity and sturdy components. It also demands careful design and construction. The simple T-section filter design has best met weapon use requirements. The circuit is illustrated by Figure 7. Note the self-shielding effect of the components used.

At frequencies above 100 kilocycles the loss resistance of the ferrite core begins to appear as is shown in Figure 8. At frequencies of a few megacycles and above the equivalent filter circuit becomes quite complex. Figure 9 illustrates the major components of the complex circuit. At some frequency in the range of five to ten megacycles, the path through the shunt winding capacitances, C_s, becomes a lower impedance than the path through the inductors and C_s begins to limit the attenuation contribution of the inductors. At frequencies above ten megacycles, C and C_s form a capacitive voltage divider with the greatest portion of the input voltage dropped across C_s.

The photograph, Figure 10, depicts the various components used in a filter channel. The threaded brass slug is soldered to the copper jacketed ferrite as a means of mounting and to conduct heat from the copper shell to a heavier heat-sink as

is shown in Figure 11. Figure 11 illustrates how a single filter channel is used. Note the use of shielded input cable and the modified conductive connector, all designed to prevent radio frequency energy from escaping into the weapon case where it could bypass the filter and enter sensitive elements.

The photograph, Figure 12, shows the application of these principles to a nine channel filter package. Each channel is capable of meeting the requirements specified previously in this report. It weighs 2.9 lbs. and occupies a volume of 33.68 cubic inches.

Testing procedure, on a filter package of the type described, is broken into three phases, developmental laboratory tests, field tests, and product acceptance tests. In the developmental tests, each component is evaluated separately and in conjunction with the others. A great many tests are run to evaluate the design and to determine which tests shall be required for product acceptance. Most of these tests are routine; three of them are of prime importance and are worthy of description.

1. Low Power Attenuation Testing

   The test setup is shown in the block diagram Figure 13. If a number of frequencies are chosen through the rejection band of interest an accurate attenuation curve can be drawn for each filter channel as it would react to a zero impedance driving generator and a specified load. The results of such a test are shown in Figure 14.

2. High Power Attenuation Tests

   The test setup for high power testing is shown in the block diagram Figure 15. A 200 watt generator is used. It is capable of output at a large number of frequencies between 1.75 megacycles and 30 megacycles.

Testing consists of selecting a voltage equal to or greater than that specified in Figure 1 and applying it to the input of a filter channel. The filter attenuation is noted and the time measured until the input inductor core has reached Curie temperature. At the Curie point a sudden change in generator loading is noted.

3. Pulse Current Tests

Pulse current tests are performed to provide proof of the filter capability to pass direct currents, low frequency sine wave currents and low frequency pulse currents of relatively long duration. The testing equipment consists of a charged bank of capacitors which is discharged through the filter when a silicon controlled-rectifier is triggered. The current pulse is terminated by a second silicon controlled-rectifier. Pulse currents to 100 amperes amplitude and ten milliseconds duration are obtainable by this means to determine actual failure levels.

Field tests are run with the filter mounted in the weapon as in end use. The weapon with the umbilical cable attached is then irradiated with radio frequency energy at the highest level expected in end use of the weapon. The filter protected devices are monitored during the test to determine that radio frequency currents reaching them are at a safe level.

The input ferrites of each channel may also be monitored during the field test to determine how much energy is being dissipated at the various frequencies. Field testing provides the final proof of the design.

Acceptance tests are those selected as proof of a reliable manufactured product. They include such tests as series resistance, shunt resistance, inductance, and capacitance tests run on all units. Shock, vibration, attenuation, humidity

cycling, and temperature cycling tests are run on randomly selected production units.

Conclusion

The use of lossy ferrite inductors and high quality feed-through capacitors in a simple filter network can provide a means of protecting sensitive weapon devices from radio frequency energy. An adequate development and acceptance testing program is manditory.

FIG. 5

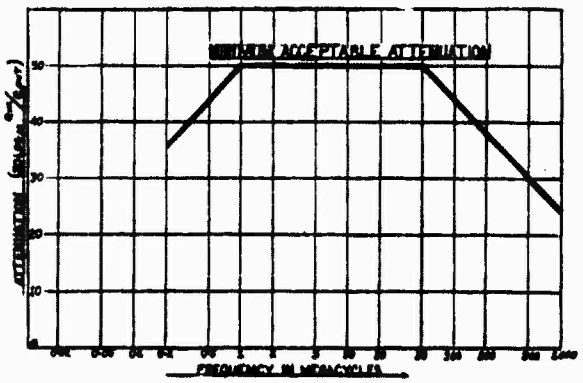

ATTENUATION REQUIREMENTS

FIG. 6

CORE LOSS VS FREQUENCY
LOSSY FERRITE 25°C.

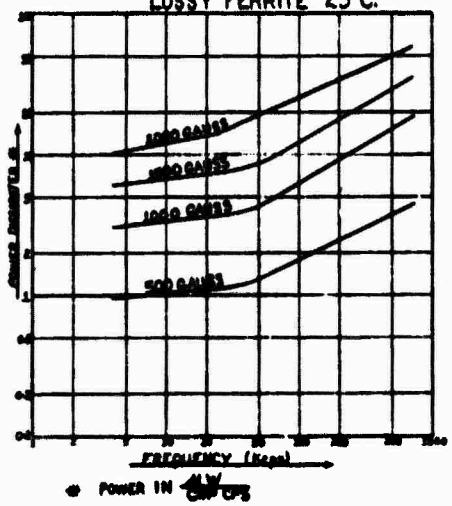

POWER IN

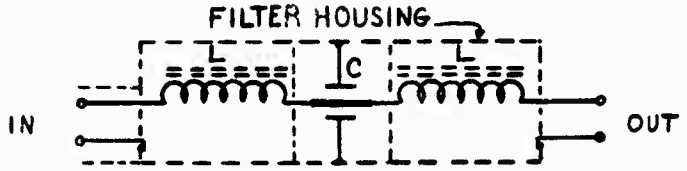

FIG. 7

LOSSY FERRITE FILTER- LOW FREQUENCY

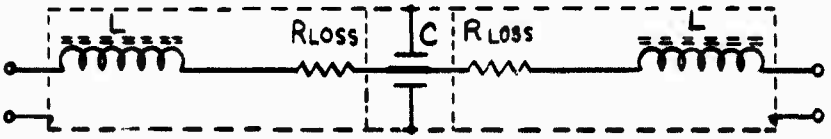

FIG. 8

LOSSY FERRITE FILTER— MID-FREQUENCY

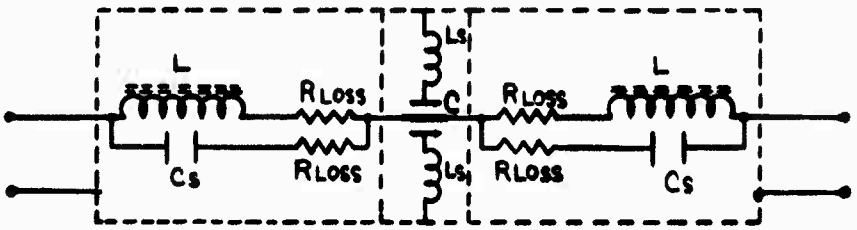

FIG. 9

LOSSY FERRITE FILTER—HIGH FREQUENCY

FIG. 10

CAPACITOR

FERRITE CORES

BOBBIN

WOUND BOBBIN (ENCAPSULATED)

COPPER COATED INDUCTOR

THREADED SLUG

COMPLETE INDUCTOR

LOSSY FILTER COMPONENTS

FIG. 11

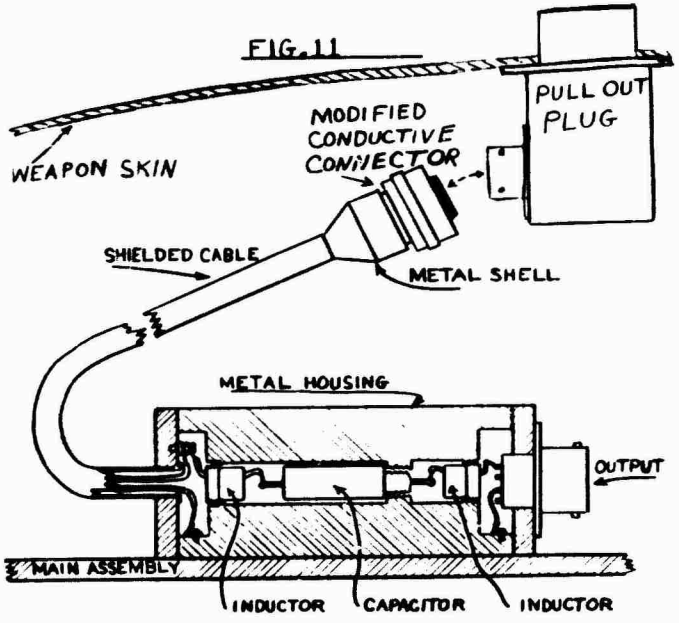

IDEAL FILTER LAYOUT

FIG. 12

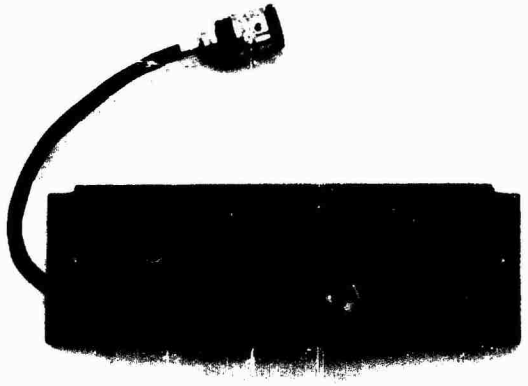

TYPICAL MULTICHANNEL LOSSY FILTER

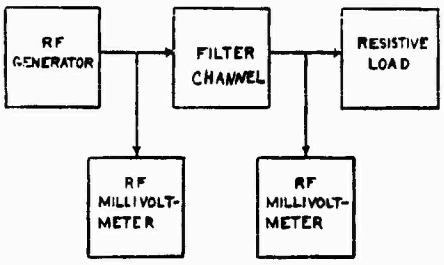

FIG. 13

LOW POWER ATTENUATION TESTING SETUP

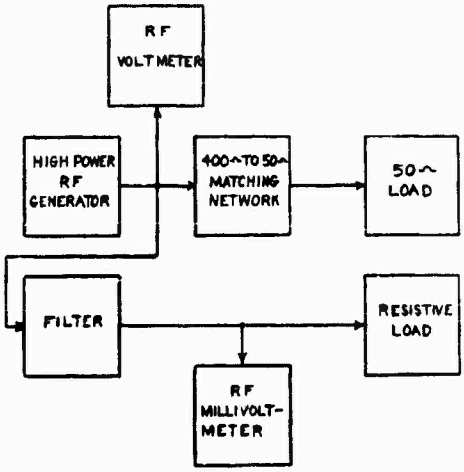

FIG. 15

HIGH POWER TEST SETUP

FIG. 14

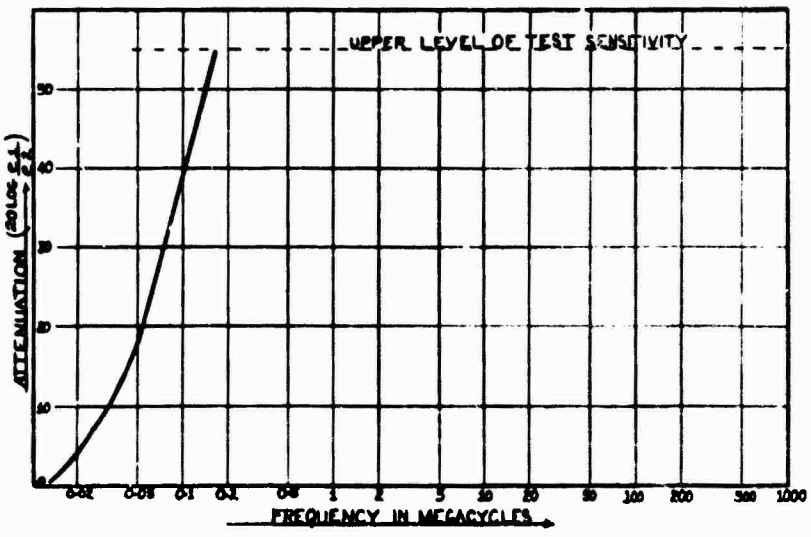

TYPICAL LOW POWER ATTENUATION CURVE

30. DISCUSSION

Mr. Algeo of the Naval Air Development Center asked for the origin of the 125 volts. Mr. Murphy answered that he was afraid someone would ask this be but answered that the results are based on tests on shipboard and at Dahlgren. Conditions are the worst encountered with a safety factor of two.

Mr. Grinoch of Picatinny Arsenal asked if, in evaluating the filter, the filter was terminated with a load equivalent to that of the EED, (about one ohm) and if the input was provided with a realistic match. Mr. Murphy answered that the load used most often was 4.5 ohms. If a one-ohm load was used, a higher attenuation would have been measured. No matching device was used with the low frequency measurements. This is not necessarily the effect one would have in the field nor is it the worst-case. It is a reasonable requirement for manufacturers.

Commander Gray commented that the indicated measurements were simply input and output voltages. He asked if any attempts were made to resolve power. In answer Mr. Murphy said that some power calculation and measurements were made. Each channel is capable of dissipating a maximum of about 14 watts. There are, in addition to the dissipative losses, reflective losses. Each inductor is 220 microhenries, that is made of a low Q coil of 16 turns. This prevents series resonance conditions. If the input to the filter is matched you will probably get less attenuation. It may be difficult to obtain this match.

Mr. Senn commented that at very high values of attenuation or insertion loss the question of whether the device is matched or not is purely academic. The reflective loss compared to the attenuation becomes relatively small.

Mr. Murphy said that his experimental efforts had verified this. Commander Gray added that one can avoid matching the input with the provision that impedance, frequency and voltage are known. The real power in can be computed.

A person injected a comment that prototypes of the filter have been tested at Dahlgren with no responses indicated in the EED circuit with maximum power applied during handling procedures.

31. A MINIATURE FILTER FOR SQUIB PROTECTION

J. L. Hinds, Jr.
U. S. Naval Air Development Center
Johnsville, Penna.

In designing a filter for squib protection it would be quite desirable to have feed-thru capacitors available which have large capacitance, low dissipation factor, miniature size and which are low in cost. Capacitors of this type are beginning to appear in the development laboratories as experimental models and utilize high dielectric constant ceramics. However, these are not yet available in production quantities.

In present applications where a miniature feed-thru capacitor of high capacitance is needed, there is one choice; the solid tantalum feed-thru capacitor. While review of the technical specifications indicates a potential trouble area in the form of a high dissipation factor, extensive testing has indicated that it is not. In actual practice the large capacitance units have such a low transfer impedance that even when the rf source (the aircraft weapon interface) is at its lowest impedance which is around 3 ohms, the capacitor is still a relatively effective short circuit and very little dissipation occurs within the tantalum feed-thru capacitor.

SELECTION OF A FILTER:

A high insertion loss requirement indicates that a π section or T section filter might be effective. The π section was chosen over the T section primarily because of the impedance stabilization properties of the input and output capacitors. Even if an appreciable length of line must be used between the filter and the squib and a quarter wave length of line is approached, the line is still short circuited. If the T section were used, when a quarter wave length of line separated the squib from the filter, the filter would see a high impedance[1], the effectiveness of the series element would be lost and a current maximum would occur at the squib.

(1) $Z_{in} = R_o\left(\dfrac{Z_1 \cos Bl + j R_o \sin Bl}{R_o \cos Bl + j Z_1 \sin Bl}\right)$ for a quarter wave line $Bl = 90°$

$Z_{in} = \dfrac{R_o^2}{Z_1}$ for a 50Ω line, 1Ω squib $Z_{in} = \dfrac{50^2}{1} = 2500.$

Since the source impedance of the aircraft weapon interface as a generator is in the 3 to 500 ohm range, a capacitor with a transfer impedance which is 0.3 ohm or less will reflect a minimum of 82% of the energy back to the source and will prevent an impedance match between the source and the series element of the π section over the frequency band.

A 6.8 mfd at 35 volt unit meets this requirement, figure 1.

The insertion loss (measured in a 50Ω system) of the solid tantalum feed-thru capacitor is compared with the insertion loss of a typical 0.22 mfd metallized mylar feed-thru capacitor, figure 2. It is seen that the tantalum feed-thru capacitor has a rather unique characteristic; rather than rising at the usual rate of 6 db/octave, up to the first resonant point, it remains almost flat from 100 kc to 100 mc. This is caused by the high leakage characteristics. Effectively, the 6.8 mfd tantalum feed-thru has the transfer impedance of a 6.8 mfd capacitor up to 50 kc, a 3.0 mfd capacitor at 100 kc and a 0.1 mfd capacitor at 20 mc, figure 3. In order to plot the 1 ohm characteristics, the transfer impedance of a 50 ohm and 1 ohm circuit were plotted in figure 4. From this data and figure 3, figure 5 was plotted. It will be noted that the .22 mfd has practically zero insertion loss at 100 kc. A metallized mylar capacitor having the same insertion loss as the tantalum at 1 mc requires 10 times the volume.

Since the power in the 100 kc to 4 mc range is being increased and there is a strong possibility of going even lower in frequency, low frequency protection is an important consideration for the near future.

The ferrite[2] used for the A-60 toroidal assembly was chosen because of its high permeability at 100 kc and the high magnetic loss characteristic in the high frequency range. The permeability is 2000 at 100 kc, the volume resistivity is a few ohms-cm and the curie temperature is 180°C. The resistive and reactive components of the impedance of the toroidal assembly is shown in figure 6. At the present time the frequency range which tends to be the most troublesome in aircraft weapon systems exposed to high level rf fields is the range from 4 to 26 mc. It will

---

[2] This ferrite is manufactured as T-1 material by Indiana General, WO-3 material by Allen Bradley and Ceramag 20 by Stackpole Carbon.

be noted that the resistive and reactive components are greater than 250 ohms over this range. The sharp reactive drop out at 26 mc is more than compensated for by the high resistive component at this frequency.

Figure 7 is a plot of the impedance of the toroidal assembly as a function of the rf voltage drop at 10 mc. The filter normally operates on the level portion of the curve due to the large mismatch caused by the input capacitor which in turn severely limits the voltage input to the toroidal unit.

Figure 8 is a schematic of the final A-62 filter.

Figure 9 is a plot of the insertion loss of the A-62 as a function of frequency for 50 ohm and 1 ohm circuits. The curve for the high level input represents the maximum insertion loss capable of being measured due to dynamic range limitations of the instrumentation and the unavailability of high power pads. It will be noted that a high insertion lose is maintained down to 100 kc.

To permit meaningful insertion loss measurements a 400 watt rf source, figure 10, has been set up which consists of a low level signal generator, 50 millivolts output, driving a chain of distributed amplifiers to 400 watts into a 90 ohm load. The system requires no tuning, thus permitting a continuously varying frequency from 150 kc to 300 mc to be applied to the input of the filter to detect resonant points in minutes, rather than days, by older methods.

The detecting system used is a 1.5 ohm UHF vacuum thermocouple which was made to NADC specifications so that a current of 2 milliamps can be detected at the heater with a sensitive electronic dc microvoltmeter having a full scale deflection of 1 microvolt.

One method which has been used to obtain relative performance data on various filter configurations is shown in figure 11. A frequency scan is made from 150 kc to 250 mc at a power input into a dummy load of 100 watts at a VSWR of 1.8, the power being coaxially switched between the dummy load and the filter terminated in 1.5 ohms. This method, while it has several drawbacks, the main one of which is the lack of isolation between the source and the filter, has proven to be useful for design purposes. Empirically it has been found that the probability of a filter successfully withstanding the ground plane or operational environment is high when a filter withstands this laboratory test.

A method, figure 12, which is presently being set up and which circumvents the problems associated with the previous system will be ready upon completion of the high power pads. It consists of the 90 ohm source stepped down to 5 ohms by means of a broad band transformer. Originally it has been planned to transform the impedance down to 1 ohm but the transformer designer found that it was not possible to make an impedance transformation greater than 18:1 and meet the other requirements. However, one must admit that it is much more feasible to match a 5 ohm source to 1 ohm than to match a 90 ohm source to 1 ohm. The π section pads terminate the generator in its characteristic impedance whether the line is open or short circuited.

The insertion loss is then calculated from the difference in level on the microvoltmeter when the 70 db pad is in the circuit as compared with the 10 db pad and the filter in the circuit. 10 db is then subtracted from the reading to get the net insertion loss.

The basic A-62 in line design, figure 13, has been used without change in several applications utilizing a bulkhead isolation arrangement.

A proposed filter design for another application is one step further in miniaturization. Due to the limited space available - 2" x 11/32" - it became necessary to investigate the possibility of reducing the size of the tantalum feed-thru capacitors. The actual tantalum slug is small, the major portion of the volume being taken up by the case and the end-seals. The capacitor manufacturer's design group was able to reduce the case size and the size of the internal end-seal, thus enabling the full π section to be incorporated in a common hermetically sealed case measuring 2" by 11/32".

One area in filter technology which has not been explored in depth is the effect which source and load impedances have on the insertion loss of a filter. In order to explore this area a general computer program is being set up on the IBM 650 to analyse several types of filters under all possible combinations of source and load impedances in sufficiently small increments to insure complete data.

The schematic in figure 14 gives the mathematical notation used in the loop equations in figure 15, which pertain to the A-62 filter. The functions for the feed-thru capacitors and the toroidal assembly will not be those of ideal or theoretical components but will be those

computed using curve matching techniques on impedance measurements made on the actual components. Thus the non-linear characteristics of the ferrite assembly and the feed-thru capacitors will all be taken into account in the solutions. Having these solutions it will be a relatively easy task to establish the insertion lose under known conditions of source and load impedances for various aircraft and weapon system combinations.

The A-62 filter is by no means considered to be the ultimate in solutions for the protection of EED's. First of all there is no substitute for a well designed aircraft weapon system which permits the establishment of an effective and reliable rf ground between the weapon and aircraft prior to making connections between the aircraft's electrical system and the weapon. Secondly, the design of the receptacle and connector at the aircraft rack and weapon interface should be such that a good effective and reliable rf ground is made between the cable shielding and the aircraft rack structure before any other connections are made. Unfortunately, this second requirement is not easily attained within size, weight, and cost limitations.

Such components as miniature high capacitance ceramic feed-thru capacitors, high lose coaxial dissipative devices, rf proof relays, and lossy transmission lines show considerable promise and when brought into the area of practicality may offer better solutions. The A-62 does, in the meantime, offer an interim solution which is effective and inexpensive for many applications.

REFERENCES

1. J. L. Hinds - "A Filter Approach for Hero & Radhaz Situations", First Hero Congress May 1961.

2. J. C. Senn, "Ferrites in Radio Interference Filters: Proceedings of the Fourth Conference on Radio Interference Reduction and Electronic Compatibility" held at Armour Research Foundation Oct. 1 - 2, 1958, pp 458-474.

3. H. M. Schliche, "Essentials of Dielectromagnetic Engineering" published by John Wiley, New York 1961.

4. "Lines, Waves and Antennas" - Brown, Sharpe and Hughes published by Ronald Press, New York 1961.

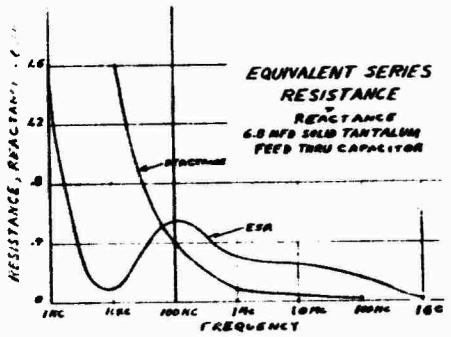

FIGURE 1

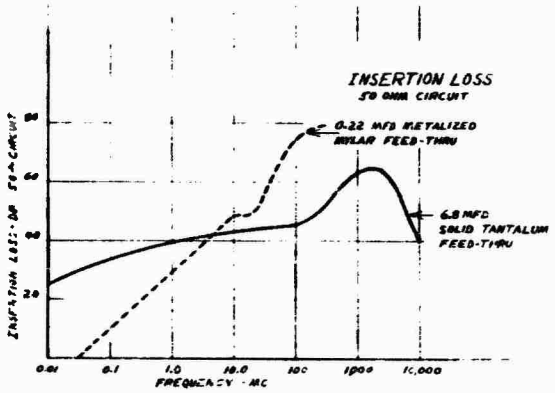

FIGURE 2

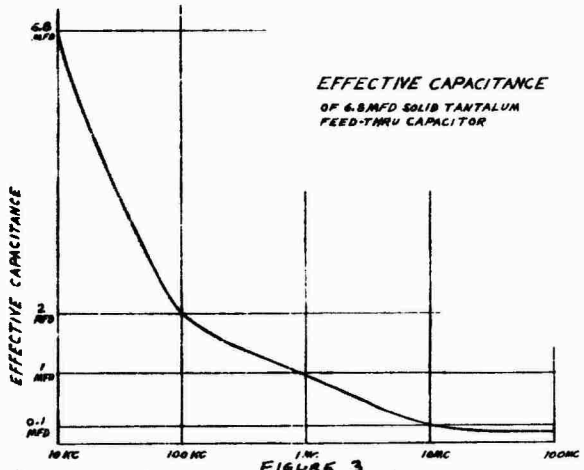

FIGURE 3

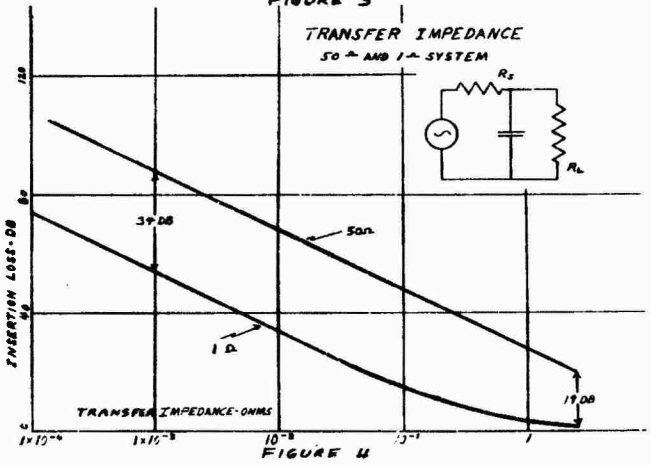

FIGURE 4

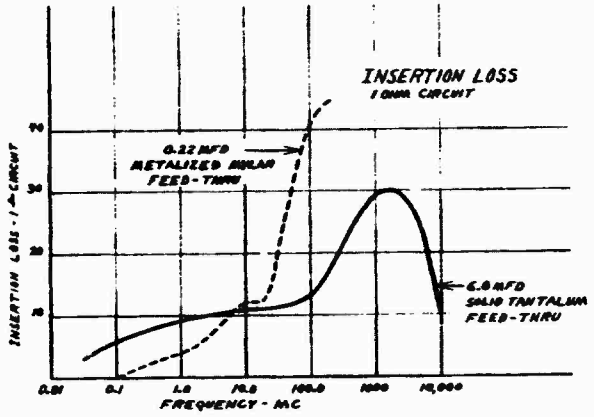

FIGURE 5

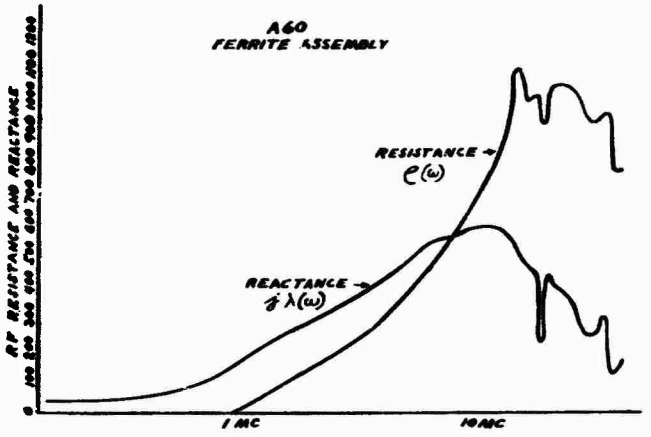

FIGURE 6

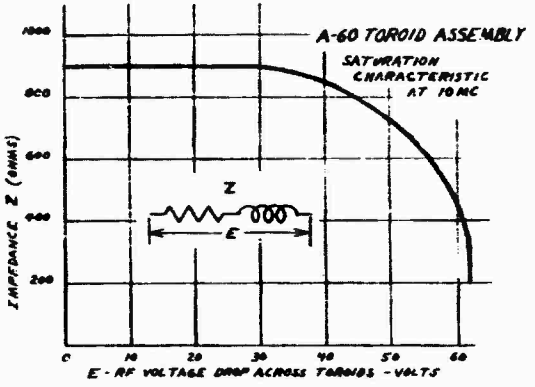

FIGURE 7

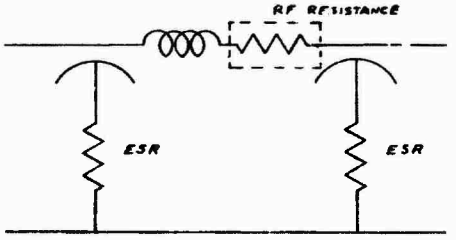

A-62 FILTER

FIGURE 8

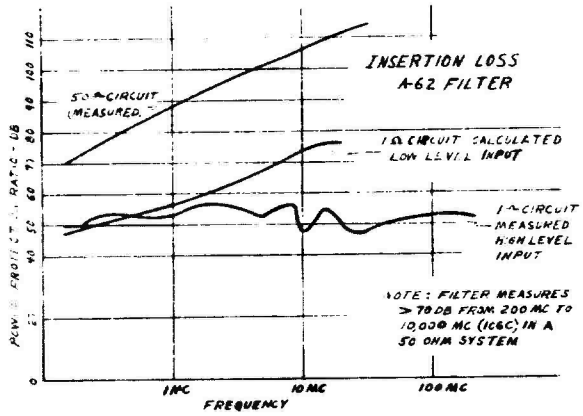

FIGURE 9

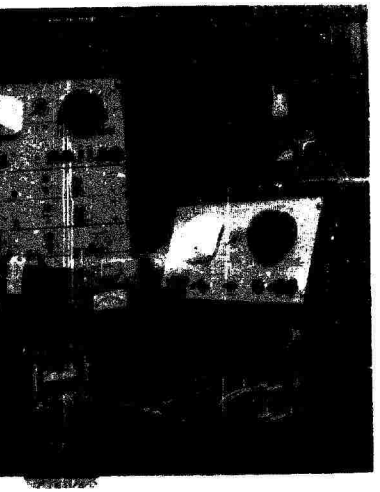

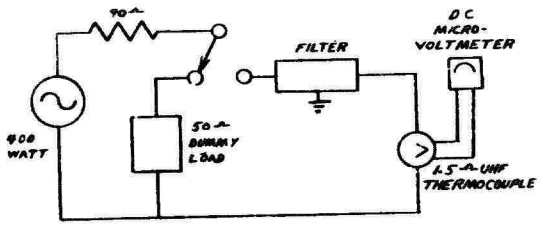

FILTER TEST SET UP

FIGURE 11

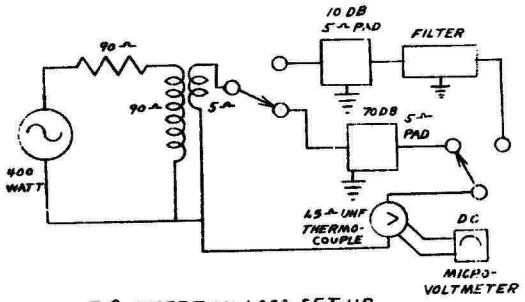

5Ω INSERTION LOSS SET UP

FIGURE 12

FIGURE 13

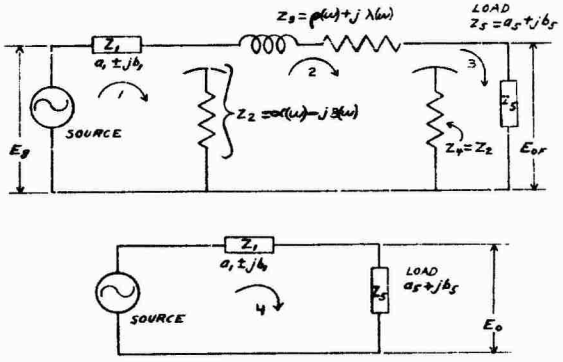

FIGURE 14

FILTER IN LOOP EQUATIONS

$$E_g = I_1\left[a_1 \pm jb_1 + \alpha(\omega) - j\,\beta(\omega)\right] - I_2\left[\alpha(\omega) - j\,\beta(\omega)\right] - I_3(\omega)$$

$$0 = I_1\left[\alpha(\omega) - j\,\beta(\omega)\right] + I_2\left[2\alpha(\omega) - j2\beta(\omega) + \phi(\omega) + j\,\lambda(\omega)\right] - I_3\left[\alpha(\omega) - j\,\beta(\omega)\right]$$

$$0 = -I_1(\omega) - I_2\left[\alpha(\omega) - j\,\beta(\omega)\right] + I_3\left[\alpha(\omega) - j\,\beta(\omega) + a_S \pm jb_S\right]$$

SOLVE FOR I_3

FILTER OUT EQUATIONS

$$I_4 = \frac{E_g}{2R \cdot I_3} \qquad 12\,R = \frac{I_4}{I_3}$$

FIGURE 15

32. DEVELOPMENT OF BROADBAND ELECTROMAGNETIC ABSORBERS FOR ELECTRO-EXPLOSIVE DEVICES

By
Robert F. Wood, Daniel J. Mullen, Jr., Paul F. Mohrbach
of The Franklin Institute

I. INTRODUCTION

The Franklin Institute, under contract to the Naval Weapons Laboratory and Picatinny Arsenal, has during the past several years been active in the search for materials which absorb radio frequency energy and for means of making optimum use of these materials. The first significant result of this study was the development of a material consisting of iron particles insulated with iron phosphate. This material not only proved the feasibility of the approach, but also proved to be quite adaptable to many immediate uses in the field of electroexplosive ordnance.

Figure 1 shows a typical curve of attenuation versus frequency for samples made of carbonyl iron coated by the acetone-phosphate process. It is evident that when this information is plotted on log-log coordinates a straight line results with a slope of 53° to the x axis. This is characteristic of all of the phosphate coated irons which we have studied. While this material has ample attenuation at high frequencies (50 db/cm at 500 Mc for example) it has fallen to 6 db/cm at 100 Mc and less then 1 db/cm at 10 Mc. All attempts to increase this have produced only marginal gains. It became obvious that better materials would be needed for low frequency applications.

2. FERRITES AS ATTENUATING MATERIAL

At the present point in the investigation the class of materials that have shown the most immediate promise is the ferrites. A ferrite, according to one of the more commonly accepted definitions, is a ceramic ferromagnetic material with the general chemical composition of $XO \cdot Fe_2O_3$, where X is a divalent metal such as manganese, nickel or zinc.

Figure 2 shows plots of attenuation versus frequency for three types of ferrites and a typical carbonyl iron sample. Two of these ferrites are commercially available; the third curve shows a ferrite made at The Franklin Institute. It can be seen from these curves that ferrites can offer a considerable gain in attenuation over insulated iron at the low frequencies. However, there is much work yet to be done.

Figure 3 shows a derived equation which indicates the relationship of the attenuation (α) to a number of the parameters characterizing RF attenuating material. Figure 4 is a table based on this equation, which gives one set of minimum acceptable values, necessary to produce 60 db/cm down to 1 Mc and 30 db/cm at 0.1 Mc. This particular set was projected on the basis of materials available today so that no completely unreasonable demands would be called for. In the lower half of Figure 4 is a table which gives the corresponding parameters for a typical ferrite commercially available today which has good RF loss characteristics. It can be seen from a comparison of the two sets of data that the primary changes required are a sizeable increase in the permeability at all frequencies with increases in the loss tangents and the conductivity also required at the lower frequencies. While such a material is not now available, it does not seem beyond the realm of feasibility.

One other point should be noted. Ferrite materials that show promise as good attenuators also have very large conductivities. When used in actual applications such materials can produce very small shunt resistance across the firing lines with a corresponding result that the

dc sensitivity of an explosive item may be greatly reduced. While such a condition can be accepted in many existing firing circuits and can be allowed for in any new circuit, it is desirable to avoid the condition by having large shunt resistances. Furthermore, any method which is used to increase the shunt resistance should, ideally, not decrease the normal firing sensitivity even if normal firing is by means of a condenser discharge pulse.

The elimination of low shunt resistance by insulating the firing leads passing through the attenuating material with either an insulating material that has a large dielectric constant or is itself lossy is being investigated.

These requirements applying to the insulation have grown out of the fact that any material interposed between the conductors and the attenuating materials produces a sizeable decrease in the effectiveness of the attenuating materials. Dielectrics with large dielectric constants (greater than 100) tend to minimize this condition. An alternative is to introduce an insulator which in itself contributes to the attenuation to compensate for the decrease in attenuation. In this connection, a combination of tantalum pentoxide and manganese dioxide (as used in tantalum capacitors) is of considerably interest and is being investigated. Figure 5 shows a comparison, (attenuation versus frequency) of a ferrite mounted directly on the center conductor with the same ferrite mounted on insulators with a dielectric constant of 1200 and a wall thickness of 19 mils.

A summary of performance characteristics of carbonyl iron versus ferrite is presented in Figure 6. Values for both insulated and uninsulated samples are tabulated.

This, then, sums up the general abilities of ferrites today; what must be done to improve them and some special problems if the materials are to be incorporated directly into electroexplosive devices. In the interim, however, there are a number of approaches to the general problem which can be considered if the materials can be placed in an attenuating device which can be plugged in ahead of the electroexplosive devices.

3. FERRITE ATTENUATORS

In Figure 4 we showed design parameters which were aimed at producing ferrites with an attenuation of 60 db/cm at 1 Mc and considerable attenuation even at lower frequencies. This value of attenuation was chosen to provide at least 20 db of power attenuation in a typical initiator design where the plug is approximately 1/3 of a centimeter in length. If one were to remove the length restriction imposed by initiator design one could make considerable use of presently available materials.

Figure 7 shows one model of an experimental attenuator. The overall length of the device is 4-3/8 inches and the diameter is 3/4 inch. However, the size was dictated primarily by the size of standard available components and could be reduced considerably. Basically, it consists of a metal sleeve, which is the outer conductor; a brass rod, which is the center conductor; approximately 6 centimeters of ferrite material, and two metal caps with BNC connectors. The dc shunt resistance of this model was 4 ohms. The curve of attenuation versus frequency for this design is shown in Figure 8. At one megacycle we have 18 db and at ten megacycles this has risen to over 200 db. Insulation of this model with a large dielectric constant insulator would drop the attenuation at one megacycle to about 10 db and at ten megacycles to 70 db.

The principle demonstrated here, however, opens up several possible avenues which are at present under study. It is apparent that one need only increase the effective path length of the conductor in the material to increase the attenuation and therefore the problem becomes one of utilizing the available volume for maximum effectiveness rather than just the length. There are several pitfalls on such an approach but these are being evaded. One of the simplest approaches to this long path solution is shown in Figure 9. This barrel attenuator places several small cylinders of ferrite in the same length formerly occupied by a single length. In this case, the nine such cylinders produce approximately nine times the attenuation normally obtainable with a single full-diameter attenuator. There is evidence that one need only mold several wires into a single slug of material and then connect them on the faces of the slug to form one continuous conductor through the material. Along these lines, many other more sophisticated approaches come to mind, and a number of these are under investigation at the present time.

Let us return for a moment to the straightforward model, shown in Figure 7, which has also been insulated. As stated before, the attenuation is down to 10 db at 1 Mc but is already 70 db by 10 Mc. This model has exhibited the ability to withstand 1500 volts. The dc input resistance is in the neighborhood of 10^8 ohms. Constant current and constant voltage input pulses are essentially unaffected. Finally, if a 1 μ f capacitor is discharged through this device into a one-ohm load the waveform is only slightly altered.

In summary, one can expect to use presently available ferrites with considerable effectiveness in attenuators which would be external to the electroexplosive devices. There is every reason to believe that these devices could be produced quite simply, with reasonable compactness and attenuation, and could avoid some of the problems which occur with filters and other kinds of protection. For example, good attenuation could probably be obtained with very little deterioration of any type of presently used firing pulse - - - a very valuable feature, particularly in retrofit problems.

4. THE FUTURE

What can the future hold along the lines of attenuating materials? First of all we have already indicated that there is a strong likelihood of producing much lossier ferrites than are now available; this would seem to be an approach to be pursued immediately.

In addition to ferrites, however, there are other materials now being developed which would bear study for low frequency attenuation problems. Among these one might consider the tantalum pentoxide - manganese dioxide combinations mentioned earlier as a possible insulator. These are the two essential ingredients of tantalum capacitors at the present time and such capacitors are known to have considerable RF attenuation. While the literature contains some theories regarding the loss mechanisms of these capacitors, the general problem is not fully understood and there is room for study in this field. In addition, there are high polymer materials now being developed which show promise of having very large dielectric loss tangents - one of the essential parameters for RF attenuation.

Finally there is an entire region of possibility growing out of composite materials. Unusual results have been obtained, for example, by placing a cylinder of the basic carbonyl iron attenuating material around a cylinder of a lossy ferrite. Attenuation appears to be greatly improved at the lower frequencies. One theoretical approach indicates a very large possible attenuation if a very thin layer of very large dielectric constant material is placed on a ferrite with carefully chosen parameters. Many other possibilities suggest themselves and are being studied.

In conclusion, it can be stated that iron, phosphate insulated, has demonstrated ability to provide adequate attenuation in the available size of present electroexplosive devices down to frequencies in the range of 200 Mc. Its use is now quite practical for wire-bridge initiators,

and with proper high-dielectric-constant insulation, the material will work for other types. Presently available ferrites make it possible to extend the lower frequency limit down to 10 Mc for wire-bridge initiators, while staying within the dimensions of typical electroexplosive devices. By placing the attenuators outside of the electroexplosive devices, thus permitting more freedom in size and configuration, presently available ferrites can probably be used effectively down to 100 Kc and lower with increasing mechanical complexity. These devices could be so designed to work with all types of electroexplosive devices; that is, they would not be restricted to hot wire types. Finally there is considerably reason to hope that substances and combinations of substances can be developed in the near future which will greatly reduce the amount of material necessary to provide attenuation at low frequencies, thereby bringing us back toward the ideal of incorporating the protection as an integral part of the electroexplosive devices themselves.

32. DISCUSSION

A questioner asked if the position of the carbonyl iron and ferrite had been reversed. Mr. Wood said that this makes no difference.

A person expressed interest in the meane of insulating the ferrite. Mr. Wood explained that the carbonyl iron is used as an insulator. In order to keep attenuation high, the iron portion is made thin. This process reduces the insulation resistance from the normal 2 megohms down to 250 ohms.

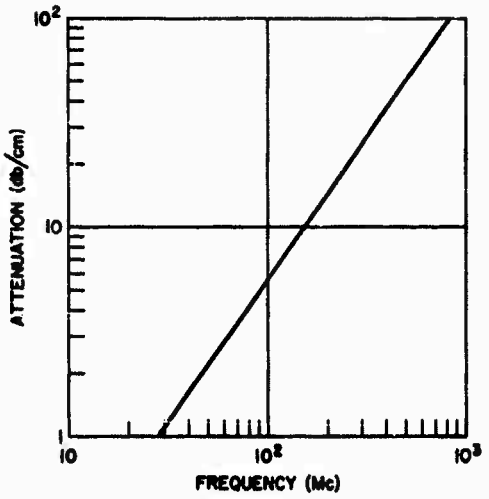

FIG. 1. ATTENUATION VERSUS FREQUENCY FOR CARBONYL IRON

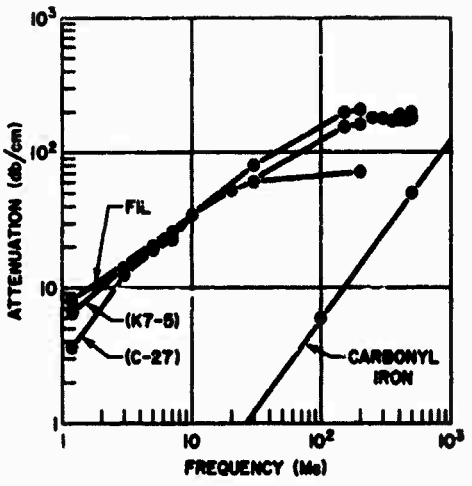

FIG. 2. ATTENUATION MEASUREMENTS OF THREE TYPES OF FERRITES AND CARBONYL IRON

$$\alpha = 128 \times 10^{-11} f \left[\frac{\epsilon'}{\epsilon_0} \frac{\mu'}{\mu_0} \left((\tan\delta_\epsilon \tan\delta_\mu - 1) + \sqrt{1 + \tan^2\delta_\epsilon \tan^2\delta_\mu + \tan^2\delta_\epsilon \tan^2\delta_\mu'} \right) \right]^{\frac{1}{2}}$$

WHERE α, THE ATTENUATION IN db PER CENTIMETER, IS GIVEN AS A FUNCTION OF f, THE FREQUENCY IN CYCLES PER SECOND

$\frac{\epsilon'}{\epsilon_0}$ = REAL PART OF RELATIVE PERMITTIVITY

$\frac{\mu'}{\mu_0}$ = REAL PART OF RELATIVE PERMEABILITY

$\tan\delta_\epsilon$ = DIELECTRIC LOSS TANGENT

$\tan\delta_\mu$ = MAGNETIC LOSS TANGENT

FIG. 3. RELATIONSHIP OF ATTENUATION (α) TO MATERIAL PARAMETERS

Figure 4

Ferrite Parameters

(a) Minimum Acceptable Parameters of Ideal Ferrite

Frequency (cps)	Calculated Attenuation (db/cm)	$\frac{\epsilon'}{\epsilon_o}$	$\frac{\mu'}{\mu_o}$	Tan δ_ϵ	Tan δ_μ	Calculated Conductivity (Mho/M)
10^5	30	2.5×10^4	9×10^3	20	6	2.8
10^6	60	2.0×10^4	3.2×10^3	5	3.4	5.5
10^7	60	15.5×10^3	$.580 \times 10^3$	0.7	1.72	6.0
10^8	60	$.0625 \times 10^4$	100	2	0.86	7.0
10^9	60	48	13	3	0.58	8.0

(b) Typical Parameters of Commercial Ferrite

Frequency (cps)	Calculated Attenuation (db/cm)	$\frac{\epsilon'}{\epsilon_o}$	$\frac{\mu'}{\mu_o}$	Tan δ_ϵ	Tan δ_μ	Calculated Conductivity (Mho/M)
10^5	0.7	3×10^4	0.4×10^3	2	0.02	0.332
10^6	3.0	1.6×10^4	0.5×10^3	0.8	0.04	0.71
10^7	20.0	6×10^3	$.050 \times 10^3$	0.9	4.0	3.00
10^8	42.0	$.05 \times 10^4$	2.6	3.0	13.0	8.35
10^9	70.0	50	0.6	3.5	25.0	9.70

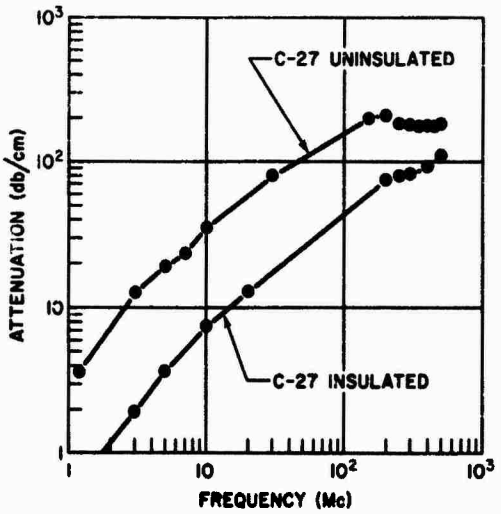

FIG. 5. COMPARISON OF UNINSULATED AND INSULATED FERRITE

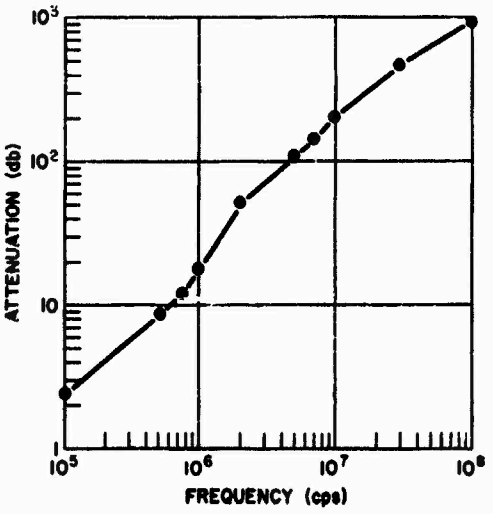

FIG.6. ATTENUATION VERSUS FREQUENCY OF FERRITE ATTENUATOR

	IRON	IRON AND INSULATOR	FERRITE	FERRITE AND INSULATOR
RESISTANCE	10^9 OHM	10^9 OHM	10^2 OHM	10^9 OHM
BREAKDOWN VOLTAGE	30V	1500V	—	1500 V
α (db/cm) 1Mc	0.01	0.01	4	0.8
α (db/cm) 10Mc	0.25	0.25	34	7.5
α (db/cm) 100Mc	6	6	160	52
α (db/cm) 500Mc	50	50	170	100
TEMPERATURE	-65°F TO 300°F	—	-65°F TO 300°F	—
EFFECT ON CAPACITOR DISCHARGE	NONE	NONE	SHUNTS LOAD	NONE
EFFECT ON SQUARE WAVE PULSE	NONE	NONE	SHUNTS LOAD	NONE

FIG.8. SUMMARY OF PERFORMANCE CHARACTERISTICS OF CARBONYL IRON VERSUS FERRITE

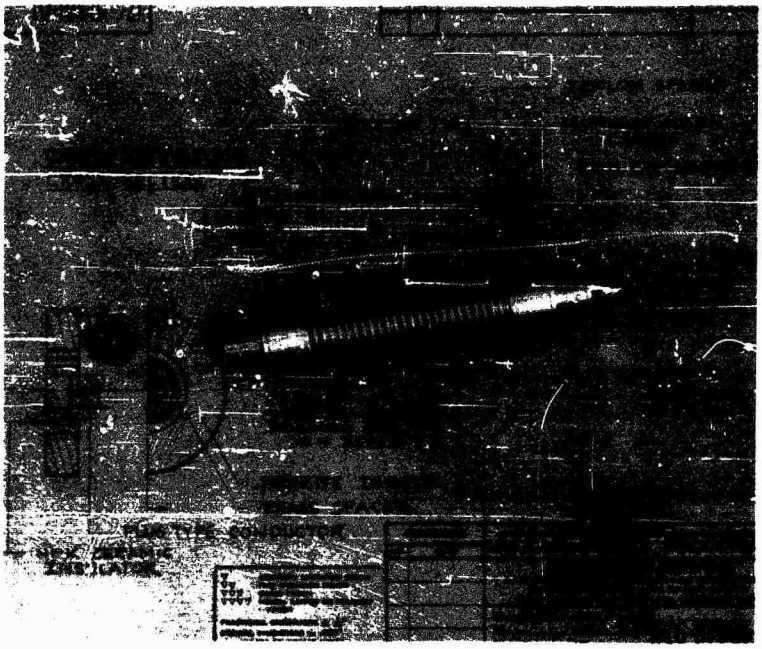

FIG. 7. AXIAL ATTENUATOR

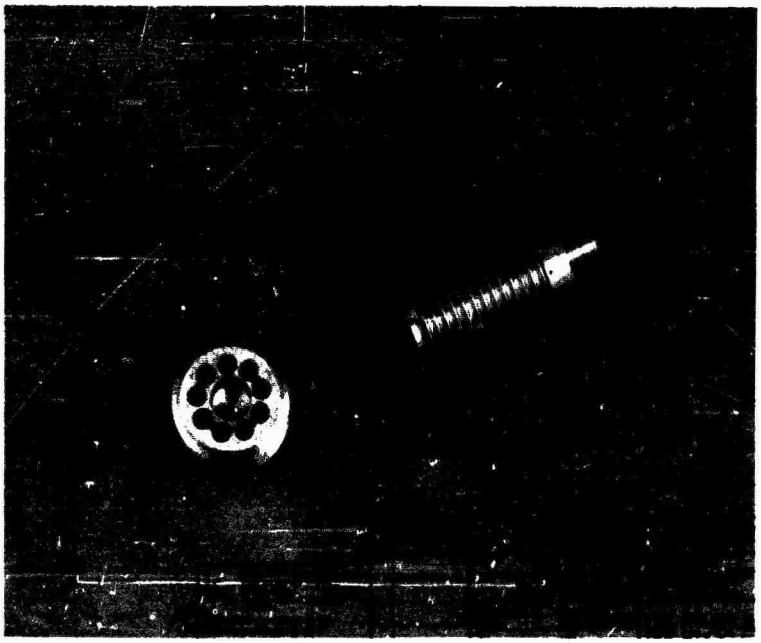

FIG. 9. BARREL ATTENUATOR

33. AN INDUCTIVELY COUPLED FILTER PROVIDING COMPLETE RF SHIELDING OF AN EED

Dale G. Holinbeck

Bjorksten Research Laboratories, Inc.
Madison, Wisconsin

ABSTRACT

A filter is described based upon protecting an EED from RF hazards by completely enclosing it within a metallic shield that has no openings or leads passing through. Intentional firing is accomplished by inductive coupling through the shield. Experimental power attenuation vs frequency curves and the delivered intentional firing energy of a filter of practical size and weight are presented.

INTRODUCTION

The use of an electroexplosive device (EED) in an RF environment presents two simultaneous requirements -- RF protection must be provided and intentional firing capability must be preserved.

As far as the RF problem is concerned, a simple and foolproof solution is to enclose the EED within a continuous shield of adequate thickness that has no openings whatsoever for the entry of RF energy. Because of the inverse relationship between skin depth and frequency, such a shield provides unquestioned protection against all frequencies above some lower limit.

As far as the intentional firing problem is concerned, a simple solution that is compatible with the presence of a continuous shield around the EED is the use of low frequency inductive coupling. Because of the relative penetrability of the shield at low frequencies, enough energy can be transferred to insure reliable firing of the EED within the shield. Figure 1 illustrates this general approach.

The cross-hatched member represents the continuous metallic shield which completely encloses the EED. It is clear that RF energy can not reach the EED without first penetrating this shield.

For intentional firing, closure of the switch in Figure 1 allows current from either a battery, a low-frequency generator, or a discharging condenser to flow in the outer coil. If this current in the outer coil is produced by a battery, it will establish a final steady-state flux that links the inner coil. Since a time rate of change of flux will occur in the inner coil as the flux changes from its initial to its final value, an activating pulse of current will flow through the EED. Similarly, if the current in the outer coil is produced by a generator of a low frequency such as 60 cps, 400 cps, or even 1000 cps, an alternating flux will penetrate the shield, link the inner coil, and cause an activating current to flow through the EED. Finally, if the current in the outer coil is produced by a discharging condenser, the flux associated with this transient will also penetrate the shield, link the inner coil, and cause an activating current to flow through the EED.

Of course, energy transfer to the EED is improved by the use of magnetic materials. Figure 2 illustrates one geometry where the flux through the inner coil closes through a continuous path of magnetic material. It is seen that this geometry does not destroy the integrity of the shield; the only difference between the shields of Figures 1 and 2 is that a magnetic material explicitly forms at least a part of the shield in Figure 2.

These completely shielded, inductively coupled filters have been under development by the Bjorksten Research Laboratories since early 1961 when this approach was conceived by us. Work on these filters has been supported by the Air Force Special Weapons Center for the past year under Contract No. AF 29(601)-5358. Data obtained on this Air Force program constitutes the major part of this paper.

A FILTER FOR THE MK-1 SQUIB

Intentional Firing

Figure 3 is a photograph of a filter designed for the MK-1 squib and a 28-volt dc firing system. This filter has a weight of 1.6 ounces, a length of 1.4 inches, a diameter of 0.67 inch, and a dc input resistance of 8.9 ohms. The 8.9 ohm input resistance insures that the current drawn from a 28-volt supply does not exceed 3.15 amperes. While a squib is shown as being directly joined to the filter, it could be located a distance from the filter if the integrity of the shielding were preserved by some suitable means such as copper, or perhaps soft iron, tubing.

Figure 4 shows a 28-volt step wave input to the filter of Figure 3 together with the corresponding output voltage pulses that are obtained when the load is either a 1-ohm resistor or a MK-1 squib. The voltage pulses for these two loads are easily identified because of the discontinuity associated with the firing of the squib. In this instance the squib has fired 0.2 millisecond after application of the input voltage. Taking 1.7 millijoules as the maximum energy required to fire a MK-1 squib under these conditions and noting that the total energy delivered to the 1-ohm resistor is 13.9 millijoules, the safety factor for firing the squib is found to be at least 8.

There is also more than an adequate amount of energy delivered to a squib by the filter of Figure 3 if the input voltage is as low as 20 volts. This is illustrated by the curves of Figure 5 that show a 20-volt step wave input and the output voltage pulses that are obtained when the load is either a 1-ohm resistor or a MK-1 squib. In this case the squib has fired 0.33 millisecond after application of the input voltage and the total energy delivered to the 1-ohm resistor is 9.5 millijoules. The safety factor for firing the squib is therefore about 5.6.

While it is very unlikely that an input voltage would accidentally have a time constant as long as 1 millisecond if it were intended to be a step wave, the filter of Figure 3 would fire a MK-1 squib with such an input even if it rose to only 20 volts. This "worst case" is shown in Figure 6. The input voltage to the filter rises exponentially to 20 volts with a time constant of 1 millisecond (i.e., it reaches 90% of its final value in about 2.3 milliseconds) and the MK-1 squib fires 1.37 milliseconds after the start of the input pulse. The total energy delivered to a 1-ohm load in this case is 7.0 millijoules, and the safety factor for firing the squib is therefore about 4.1.

Figure 7 shows the energy delivered to the load as a function of load resistance when the input to the filter is a 28-volt step wave. It is seen that this energy varies by only 10% over the range from 0.7 ohms to 1.3 ohms which is the range of bridge wire resistance for MK-1 squibs. Of course, if the filter had been designed for a squib of a different resistance, then this curve would be centered at that value of resistance.

Figure 8 illustrates the effect of contact bounce in the switch that applies the input voltage to the filter of Figure 3. In this case the switch was specially selected to have a large amount of contact bounce. For reference, the "clean" curve shows the output voltage across a 1-ohm load when the input to the filter is a "clean" 28-volt step wave. The other curve shows the corresponding output voltage that results when the switch in the input circuit has a large amount of contact bounce. It is seen that this bounce only delays the output pulse; the energy content of the output pulse is essentially unaffected.

Figure 9 illustrates the effect of lead resistance in the input circuit to the filter of Figure 3. A 28-volt step wave was first applied directly to the input of the filter and then to the input through resistive leads having a total resistance equal to 10% of the dc input resistance of the filter. The output voltages across a 1-ohm load show that the effect of the resistive input leads on the energy content of the pulse is slight; they simply decrease the peak value of the pulse a small amount and increase its total duration. The net result is about a 5% decrease in total energy delivered to the 1-ohm load. In this case the resistive leads comprised a 30-foot length of a twisted pair of No. 22 (7 x 30) hookup wire and their resistance of 0.89 ohms is judged to be the greatest that one might expect in any practical application. Tests have also been conducted with 30-foot lengths of coax and twinax cables that have a high capacitance per unit length. The capacity of these cables was found to have no effect upon the output voltages; their resistance was the only significant cable parameter.

It should be noted that the curves of the previous figures were obtained by first applying step wave input voltages to the filter several times so that the magnetic core material was biased in the same direction as it was driven in obtaining these curves. Thus, as far as the residual induction of the core material is concerned, the results presented in each case represent the minimum energy that will be delivered by the filter. If, instead, the filter is first biased in the backward direction and then has a 28-volt step wave applied to its input, somewhat more energy is delivered to the load. This is illustrated in Figure 10 for the case of a 28-volt step wave input and a 1-ohm resistive load. The

output voltage across the 1-ohm load that lasts the longer time corresponds to the condition of backward bias and it delivers about 5% more energy than the shorter pulse. The shorter pulse corresponds to the condition of forward bias and is identical to the pulse shown in Figure 4.

RF Protection

Since power attenuation specifies the fraction of total input power that reaches a load, it is the most meaningful description of a filter's protective ability. Unlike insertion loss measurements which give different results for different generators, input line lengths and configurations, power attenuation is a unique characteristic of the filter itself and is independent of mismatches or resonances on the input leads to the filter. Thus, if the power attenuation of a filter is 30 db, for example, one can be certain under all conditions that exactly 1/1000 of the total power delivered to the filter will reach the load.

Power attenuation measurements were conducted on the filter of Figure 3 with a 0.65-ohm load up to a frequency of 10 kmc. No resonances were observed and the number of measurements was sufficient to insure that none went unobserved. For these measurements, the output power above 2 mc was less than the minimum detectable level of about 0.02 microwatts. With the input powers available, this indicated that the power attenuation is greater than 68 db from 2 mc to 100 mc and greater than 80 db from 100 mc to 10 kmc. However, it is most likely that the power attenuation is much greater than this because it is 59 db at 1 mc and increasing at the rate of about 30 db per decade. Thus, at 10 mc one would expect the power attenuation to be at least 59 + 30 = 89 db.

The power attenuation of the filter in Figure 3 with various loads is shown by the curves of Figure 11. By interpolation, the power attenuation at 200 kc for loads of 0.7, 1.0, and 1.3 ohms is, respectively, 33, 32, and 31 db. (The bridge wire resistance of a MK-1 squib varies from 0.7 to 1.3 ohms.) Since a MK-1 squib requires a minimum power of about 0.1 watt for ignition, this means that an input power in excess of 100 watts would have to be delivered to the filter at 200 kc in order to ignite the squib.

The input power for these power attenuation measurements was determined by calorimetric methods. For each measurement, power was delivered to the filter for 30 seconds and the temperature rise it produced was measured by a system consisting of a thermocouple attached to the filter case, a dc amplifier, and a recorder. Input powers as low as 0.1 watt were measurable to within about 5% accuracy with this system. Calibration was achieved by delivering known amounts of dc power to the filter.

The output power was determined by using an insulated heater type of vacuum thermocouple as the load and measuring its output with an amplifier-recorder system. Vacuum thermocouples having different heater resistances were used for the various loads and each was calibrated with dc power. Depending upon the particular vacuum thermocouple that was used, the minimum detectable output power ranged from about 0.005 to 0.03 microwatts.

Effects of Nearby 60-cps and 400-cps Currents

The effects of large 60 cps and 400 cps currents flowing near the filter of Figure 3 were also investigated. With one turn of a single lead

carrying 20 amperes of either 60 cps or 400 cps current wound directly on the filter itself, the voltage across the 1-onm load resistor of the filter was less than 2.5 millivolts. With the input leads to the filter comprising 30 feet of unshielded twisted pair and with a single lead carrying 10 amperes of either 60 cps or 400 cps current taped to the twisted pair that were either "open" or shorted together, the voltage across the 1-ohm load resistor of the filter was less than the 40-microvolt sensitivity of the measurement. While these tests are quite severe compared to what might actually occur in practice, they do serve to indicate that there should be little concern about the existence of nearby large currents.

GENERAL DISCUSSION

Filters employing the complete shielding concept can be designed to a wide variety of specifications. Some units have been designed to deliver as much as 125 millijoules (1,250,000 ergs) to a load when a 28-volt step wave is applied and to have a power attenuation greater than 30 db at all frequencies above 20 kc; some units have been designed for use with EED's having dual bridge wires that provide reliability through redundancy; other units have been designed for ac firing systems; still other units have been designed for 300-volt dc low current drain firing systems. In this latter instance, the current drawn from the 300-volt supply is no more than 170 milliamperes since the dc input resistance of the filter is 1750 ohms and yet the filter delivers a peak current in excess of 2.3 amperes to a 1-ohm load. More particularly, 1 millisecond after the 300-volt step wave is applied, the current drawn from the supply

is only 105 milliamperes and the current in the 1-ohm load is 2.35 amperes. This 22-fold step up in current illustrates that these filters can also be used to advantage in matching high impedance power supplies, both ac and dc, to low impedance EED's.

The photograph in Figure 12 shows a filter that is being developed for use with Eagle-Picher automatically activated batteries. This filter has two separate outputs that are connected to the two independent bridge wires of the gas generator which is joined to the left-hand end of the filter. The dc input resistance of this filter is 7 ohms to insure that the current drawn from a 28-volt supply does not exceed 4 amperes.

The weight and volume of these filters are essentially determined by considerations relating to the intentional firing of an EED; the continuous shield that provides the RF protection need, by itself, contribute very little to weight or volume. Thus, when the input voltage to a filter and its load resistance are specified, the two most important factors in determining the weight and volume of the filter are the energy that it must deliver to the load and the minimum input resistance that it may have. Naturally enough, the smaller each of these is, the smaller the filter can be. Other factors that may affect the size of a filter are the time in which the specified energy must be delivered to the load and the amount of attenuation that the filter must provide at the lowest frequency of concern.

To illustrate the lightness and weight-saving potentialities of these filters, it is instructive to express their weight in terms of well known components used in EED firing systems. Feet of 1/8-inch ID shielding braid is an appropriate choice because braid is often used over twisted pair input leads and it is unnecessary with these filters which additionally provide

far greater RF protection. In terms of this new "unit of weight," the filter of Figure 3 "weighs" only 8 feet of standard 1/8-inch ID shielding braid. This shows how little it takes to actually save weight with these filters. Comparison of the degree of RF protection obtained in terms of the weight of components required by other systems should be equally favorable.

It should be noted that these filters do not automatically open-circuit themselves as squibs usually do when they fire. Since some systems place critical reliance on the squibs opening the circuit to the firing supply, the use of these filters in those systems would require installation of a circuit opening device.

Many systems, however, would not require the installation of a circuit opening device. In some systems, circuit opening is already provided, either by switches or as a consequence of firing the EED (e.g., cable disconnect in rocket firing). In other systems, such as most pulse-firing or capacitor-discharge firing systems, circuit opening is immaterial. It is also immaterial with single function firing supplies where the fate of the supply after firing the EED is of no concern (e.g., warhead detonation).

In addition to their relatively light weight, these filters have many other advantages. They are simple, passive, and rugged. They contain no semiconducting materials and they are operable over a temperature range at least as great as that of the EED's they are to be used with. They can be designed for ac, dc, pulse, or capacitor-discharge firing systems. They can be used advantageously to match a high impedance firing supply to a low impedance EED. They protect an EED from dc ground currents which, even though they may not fire the EED, can degrade an EED so that it may never be operable. The outstanding advantage of these filters, however, is that they provide an EED with unquestioned immunity to all RF frequencies.

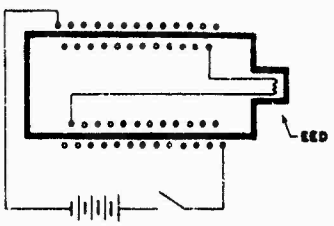

Figure 1. A Schematic Illustration of a Completely Shielded, Inductively Coupled Filter

Positive protection from RF is achieved by totally enclosing the squib circuit within a shield of adequate thickness. Intentional firing is accomplished by low frequency inductive coupling.

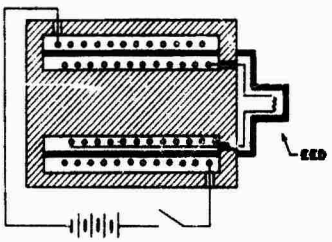

Figure 2. A Schematic Illustration of a Filter Having Flux Closure Through a Magnetic Material

This illustrates one way of obtaining flux closure through a counter-axe path of magnetic material without destroying the integrity of the continuous RF shield.

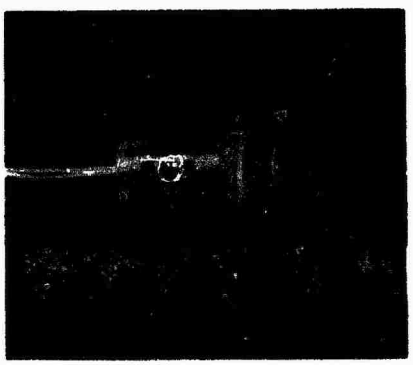

Figure 3. A Photograph of a Filter Designed for the MK-1 Squib

This filter delivers 13.9 millijoules to a 1-ohm load upon application of a 28-volt step wave input. This is more than 9 times the energy needed to fire a MK-1 squib which is shown at the right-hand end of the filter. The power consumption of this filter when terminated by a 1-ohm load is 32 db at 200 kc.

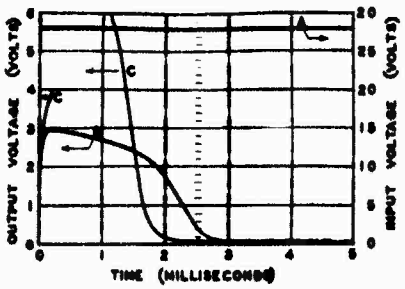

Figure 4. A Graph of Output Voltages for a 28-Volt Step Wave Input

Curve B shows the output voltage across a 1-ohm load for the filter of Figure 3 when a 28-volt step wave (curve A) is applied to its input. Curve C shows the corresponding output voltage across a MK-1 squib load. In this instance the squib has fired 0.2 millisecond after application of voltage to the input of the filter.

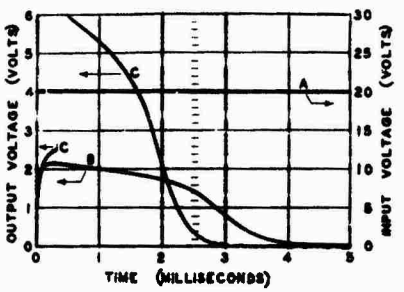

Figure 5. A Graph of Output Voltages for a 20-Volt Step Wave Input

Curve B shows the output voltage across a 1-ohm load for the filter of Figure 3 when a 30-volt step wave (curve A) is applied to its input. Curve C shows the corresponding output voltage across a MK-1 squib load. In this instance the squib has fired 0.33 millisecond after application of voltage to the input of the filter.

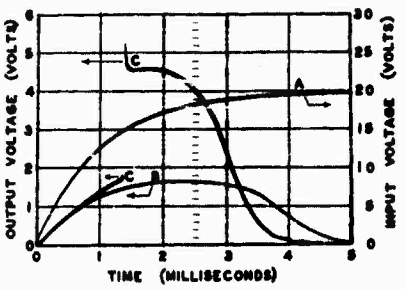

Figure 6. A Graph of Output Voltages for an Input Voltage Rising Exponentially to 20 Volts with a Time Constant of 1 Millisecond

Curve B shows the output voltage across a 1-ohm load for the filter of Figure 3 when the voltage shown by curve A is applied to its input. Curve C shows the corresponding output voltage across a MK-1 squib load. In this instance the squib has fired 1.37 milliseconds after the start of the input voltage to the filter.

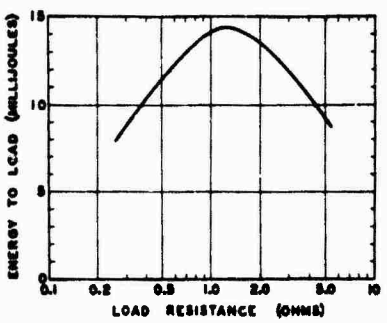

Figure 7. A Graph of Total Energy Delivered to the Load vs Load Resistance

For a 28-volt step wave applied to the input of the filter of Figure 3, this graph shows the total energy delivered to a load as a function of load resistance. This energy varies by only 10% over the range from 0.7 ohm to 1.3 ohms which is the range of bridge wire resistance for MK-1 squibs.

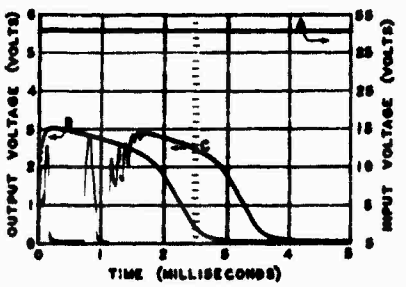

Figure 8. A Graph Showing the Effect of Contact Bounce in the Input Circuit of the Filter of Figure 3

For reference, curve B shows the output voltage across a 1-ohm load for the filter of Figure 3 when a "clean" 28-volt step wave (curve A) is applied to its input. Curve C shows the output voltage across a 1-ohm load when a switch specially selected to have a large amount of contact bounce is used to connect a 28-volt dc supply to the input of the filter. It is seen that this contact bounce only delays the output pulse a corresponding time; the energy content of the output pulse is essentially unaffected.

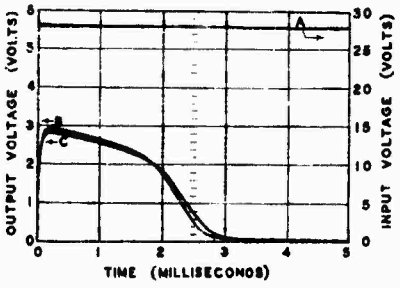

Figure 9. A Graph Showing the Effect of Lead Resistance in the Input Circuit of the Filter of Figure 3

Curve B shows the output voltage across a 1-ohm load for the filter of Figure 3 when a 28-volt step wave (curve A) is applied directly to its input. Curve C shows the corresponding output voltage when the input leads to the filter have a resistance equal to 10% of the dc input resistance of the filter. This lead resistance decreases the total energy delivered to the 1-ohm load by about 5%.

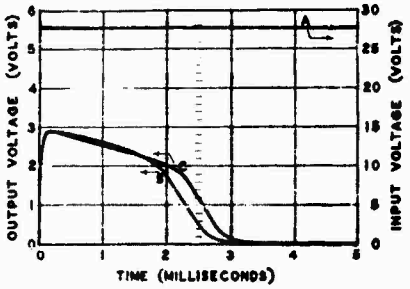

Figure 10. A Graph Showing the Effect of Backward Bias

For reference, curve B shows one of a succession of output voltage pulses across a 1-ohm load when a succession of 28-volt step wave inputs (curve A) is applied to the filter of Figure 3. Curve C shows the corresponding output obtained when the core material initially has its maximum residual induction in the backward direction. The voltage pulse of curve C delivers to the 1-ohm load about 5% more energy than does that of curve B.

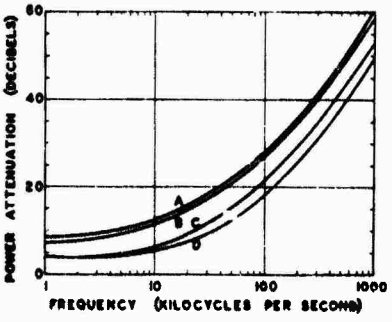

Figure 11. A Graph of Power Attenuation vs Frequency for Various Resistive Loads

The curves A, B, C, D show power attenuation vs frequency for the filter of Figure 3 when terminated by loads of 8.60, 8.68, 1.98, and 4.67 ohms, respectively. By interpolation, the power attenuation for a 1.0 ohm load is 32 db at 200 kc.

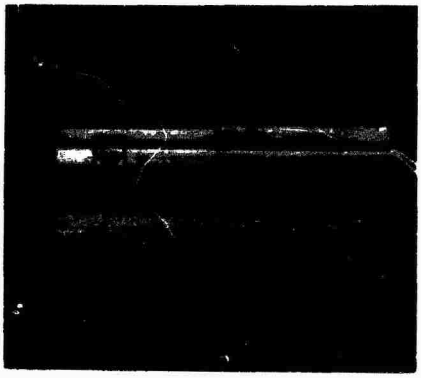

Figure 12. A Photograph Showing a Filter Designed for Use with Eagle-Picher Automatically Activated Batteries

This filter has two separate outputs that are connected to the two independent bridge wires of the gas generator which is joined to the left-hand end of the filter. The dc input resistance of this filter is 7 ohms to insure that the current drawn from a 28-volt supply does not exceed 4 amperes.

ABSTRACTS - SESSION V

34. The Prediction of Very Low EED Firing Probabilities

L. D. Hampton
J. N. Ayres
I. Kabik

EED sensitivity information must be used in the prediction of unintentional RF firing probabilities. Too often poor data, improper statistical methods, unwarranted assumptions, and ambiguous concepts (e.g. "All-Fail" and "All-Fire" point(s)) cause highly imprecise predictions. Methods are presented for improving unavoidable extrapolations and increasing the precision of firing probability estimates.

35. A Survey of 1-AMP, 1-Watt EED's

Gunther Cohn

This survey was made to compile a list of manufactured EED's meeting the 1-Amp, 1-Watt specification. We are not concerned here with the merits of this specification. It can be seen from the compilation that a large variety of initiators in this category are now available.

36. Systems Approach to Minimize EMR Hazards to Ordnance

Lt. Col. C. W. Smith
Morris Rosenthal

Hazards of EMR to ordnance are considered to be an overall system problem. Ordnance desensitization is not a panacea for overcoming hazards ascribable to wandering electrons. The Titan II and AFBSD/STL approach is determining the sensitivity of the EED's to EMR and insuring, by proper system design and procedures, that the EED's are protected from dudding or actuating inadvertently as a result of EMR. The need for an impartial test and information agency is emphasized.

37. Effects of Lightning on Air Force Systems

Capt. James H. Scharff

When the tremendous energy of natural lightning is directed against USAF systems on and in the ground, as well as in the air, serious damage and/or consequences can result. This paper discusses some aspects of the problem, approaches to better understand the phenomena, some of the detailed effects, and some means to provide protection.

38. Some Calculations Involving the Amount of Energy Electromagnetically Coupled to an Electroexplosive Device by a Lightning Stroke (U) — D. E. Merewether

Measured sinusoidal steady state data are used to determine transfer functions which relate the response of electroexplosive devices (EED's) in selected circuits to a transient environment which will electromagnetically couple energy into EED's. These transfer functions are then used to estimate the amount of energy which is electromagnetically coupled into the bridgewire of the EED's from the environment produced by a lightning strike.

39. Distribution of RF Fields Over a Carrier Deck — E. H. Smith

A theory is developed which yields the electromagnetic fields of whip and monopole antennas located at the edge of the carrier deck. Calculations are presented and compared with shipboard measurements. Some discussion is given on the behavior of the antenna field at the deck edge, and the relation of the results to classical diffraction theory.

40. The Utilization of Gamma Radiation for Weapon Control Systems (U) — Martin J. Cohen, Rudolph N. Griesheimer

This paper will treat the properties of gamma radiation arising from radioisotopes in the design of weapon control systems. Sources, sensors and equipment for communication, evaluation and decision determination for control of weapons will be considered. The performance capability of this equipment as related to environment, physical characteristics and reliability will be discussed.

41. Organic Polymers as RF Attenuating Materials — Howard W. Christie, Bernard F. Jones, James J. Downs

The development of carbonyl iron solid state attenuators has provided adequate attenuation at frequencies above 100 Mc. As there appears to be little possibility of increasing the low frequency attenuating abilities of these materials the investigation of other classes of lossy materials becomes of importance. There are a number of materials that can be considered for use in attenuators; among these are organic compounds and organic polymers that show high dielectric constants and appreciable electrical conductivity.

42. Thermal Analyses of Primary Explosives — George Svadeba

Decomposition of primary explosives which had been heated to elevated temperatures, has been studied by a variety of techniques. Application of differential thermal analyses to the study of diazodinitrophenol is discussed together with gas chromatographic studies of lead azide.

34. THE PREDICTION OF VERY-LOW EED FIRING PROBABILITIES

By J. N. Ayres, L. D. Hampton, I. Kabik
U. S. Naval Ordnanca Laboratory
White Oak, Silver Spring, Maryland

INTRODUCTION

1. The assessment of the hazards of electromagnatic radiation to axplosive ordnance centers largely about the determination of the probability or inadvertantly firing electro-explosiva devicas by RF energy. A major part of this paper will be devoted to expounding the thesis that, in general, the firing probability of EED's has not been determined with sufficient accuracy to allow the hazard assessment to be mada with raalistic precision. A second objective will be to set forth techniques by which the firing probabilities of EED's can be determined with greater accuracy at input stimuli associated with low firing response. Finally, it is hoped that this paper will give enough insight into the problam of predicting EED rasponsa, that the presently used ambiguous concepts of "All-Fira" and "No-Fire" points will be eradicatad.

2. The safaty-dasign goal for Naval weapon fuzas has long bean that there be no more than one weapon in a million wharein the warhead charge shall be initiated unintentionally at any time from manufactura to targat dalivery. This fact is citad to indicata tha high laval of safaty desirad in the Navy's detonating munitions and as point of rafarenca for establishing safety goals for today's modern weapons of larger range and potency. The demonstration of such probability lavels is virtually impossible by diract testing methods. Inferential methods must be used to amass relevant data and to make accaptable estimates.

RESPONSE OF EED'S

3. The major portion of tha HERO problem arises from the RF vulnerable EED's usad throughout weapon systems. It is necessary that EED sensitivity to electrical anergy (power) be related to the ambient electrical anvironment if an estimate of safety is to be mada. Furthermora tha sansitivity (probability of response to a particular intensity of anvironment) is needad at a very low probability of firing level.

c. That the sample is representative of the batch or lot from which it was taken.
d. That the sampled batch (or lot) is representative of all possible batches (or lots) of that particular EED.
e. That the distribution function employed in making the extrapolation does in fact describe the sensitivity of the EED.

8. If extrapolation is so dangerous why is it used? Why are not the extreme functioning responses measured directly rather than by this tenuous method? The obvious reason is that the number of EED's (often very costly) needed to make a direct measurement is prohibitive. Suppose one is interested in knowing the current which will cause not more than one in ten thousand EED's to fire. It would be necessary to observe thirty thousand trials without a single fire before one could say with reasonable assurance (a risk of one chance in twenty) that the current will not cause more than one in ten thousand EED's to fire.

CHOICE OF DISTRIBUTION FUNCTION

9. There is no other way out than extrapolation in the present state of the art. There is considerable hope that knowledge of the electro-thermal parameters coupled with the hot-spot theory[1] will eventually make it possible to establish safe currents through EED bridgewires. Until such time we must therefore select a distribution function which will be used as a basis for making the desired estimates.

10. To our knowledge only in two instances have there been sufficiently detailed tests made to give a quantitative picture of the sensitivity distribution function of EED's. One of these was carried out here at Franklin Institute on 4362 carbon bridge EED's. The other, carried out on 7890 wire bridge EED's, was reported at the last HERO Congress[2] by two of the present authors[3]. This work leads to the following conclusions concerning the proper choice of distribution function:

a. The horizontal axis should be in logarithmic units, i.e., log current, log energy, or log voltage.
b. The Gaussian probability curve is not a good fit since it predicts too high a reliability above the 50% point and too low a probability (greater safety than actually exists) below the 50% point.
c. The logistic distribution function[4] does not give an accurate fit but at least it seems to err on the side of over conservatism.

It has been the authors' recommendation that in the absence of more definitive information, the log-logistic distribution function be used for making extreme-functioning probability estimates of wire bridge EED's. Much, if not most, of the estimates currently

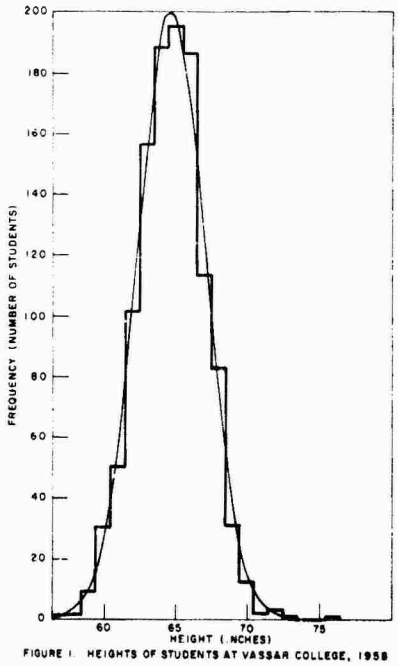

FIGURE 1 HEIGHTS OF STUDENTS AT VASSAR COLLEGE, 1958

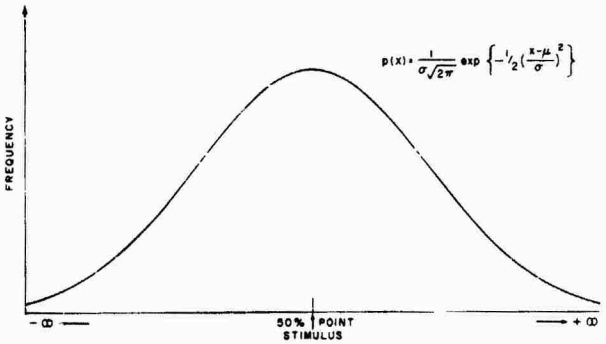

FIGURE 2 DISTRIBUTION FUNCTION DISPLAYED AS A FREQUENCY CURVE (BELL CURVE)

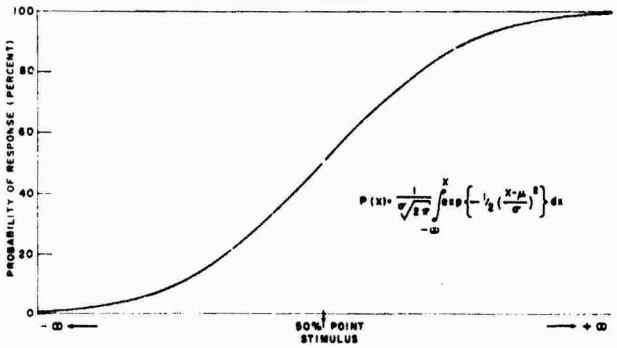

FIGURE 3 CUMULATIVE DISTRIBUTION FUNCTION, DISPLAYED AS A SIGMOIDAL FUNCTION

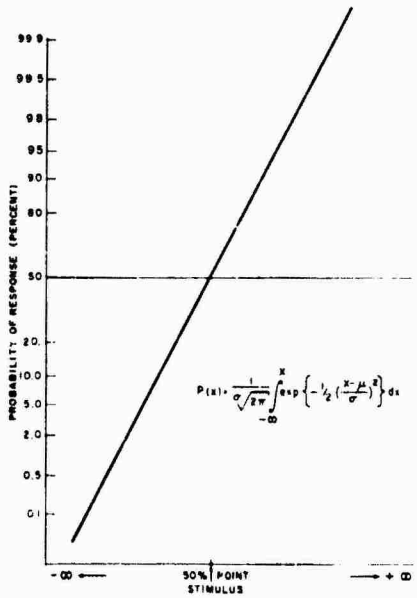

FIGURE 4 CUMULATIVE DISTRIBUTION FUNCTION DISPLAYED AS A STRAIGHT LINE IN A PROBABILITY SPACE

available in the litarature, manufacturing data, and specifications are based on the Gaussian distribution rather than the logistic.

11. In passing, wa would like to point out an extra advantage in using the logistic distribution function. Being of tha form:

$$L=\ln\frac{p}{q} = \frac{x-\bar{X}}{r}$$

where p is probability, $q=1-p$, x is tha stimulus, $\bar{x}$ is tha mean stimulus, and r is tha reciprocal of the slope in tha logistic probability space. This function can be evaluatad with a set of leg tables for desk computations and can be programmed very simply for high-spaad computars. The cumulativa Gaussian function cannot be evaluated in terms ef elementary functions and is tharefore difficult to incorporata into high-spead computer programs.

LIMITATIONS OF THE BRUCETON DATA-COLLECTION PLAN

12. Tha Brucaton plan is tha most widely used method today for obtaining and analyzing firing data, undoubtsdly becausa of tha censarvative sample size and the aase of making statistical calculations. But the Bruceton plan is extremely poor for making tha large extrapolations needed in the estimatien of extreme firing levals. Tha testing is conducted close to the 50% firing lavel raquiring that the distribution function be very well known to allow leng extrapolations. Furthar the Bruceton plan tends to give poor astimates of the standard deviation, which is one of the parameters by which the extrapolatien is made. Work carried out in England by J. W. Martin of the Royal Armament Research and Develepment Establishment, Waltham Abbey[6], shows that poor estimatas of the standard deviation occur even with reasonable sample sizes (100 firings, fer example). The situation is dapicted graphically in Figures 5 and 6, which were obtained by making high-speed computer Bruceten runs with a known normal distribution. Here it can be seen that the standard deviatien tends to be underastimated, in some cases by as much as fifty per cent. Underestimating the standard deviation, of course, will give ovarly optimistic predictions ef both safety and reliability. To underastimate the true standard daviation by thirty-three or fifty per cent will give unreasonable estimates of the various firing points as shown below where extrapolation is made from the fifty per cent firing level.

True Firing Probability Per Cent	Predicted Firing Probability Per Cent	
	$s=0.5\sigma$	$s=0.67\sigma$
0.873	0.0001	0.0182
1.644	0.001	0.069
3.148	0.01	0.264
6.118	0.10	1.024
12.24	1.0	4.054
26.08	10.0	16.81
33.68	20.0	26.38

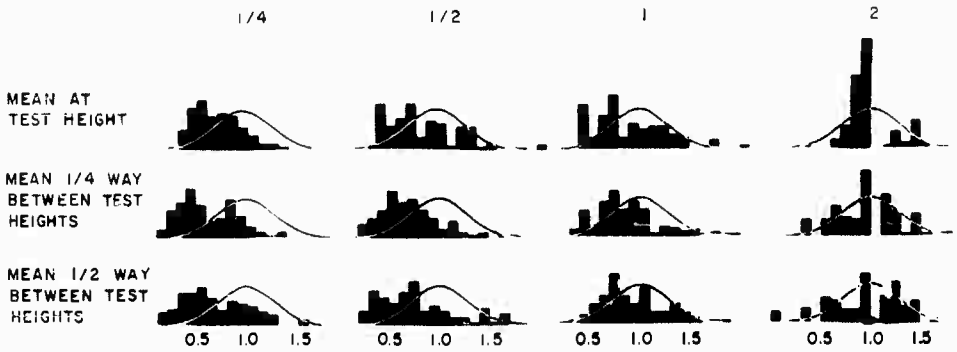

FIGURE 5. SPECTRUM OF STANDARD DEVIATIONS. EACH HISTOGRAM GIVES THE RESULT OF 100 TRIALS OF 25 ITEMS. THE X AXIS SHOWS THE RATIO OF "FOUND" TO "TRUE" STANDARD DEVIATION.

TAKEN FROM PRIVATE COMMUNICATION OF
J.W. MARTIN, RARDE
FORT HALSTEAD, ENGLAND

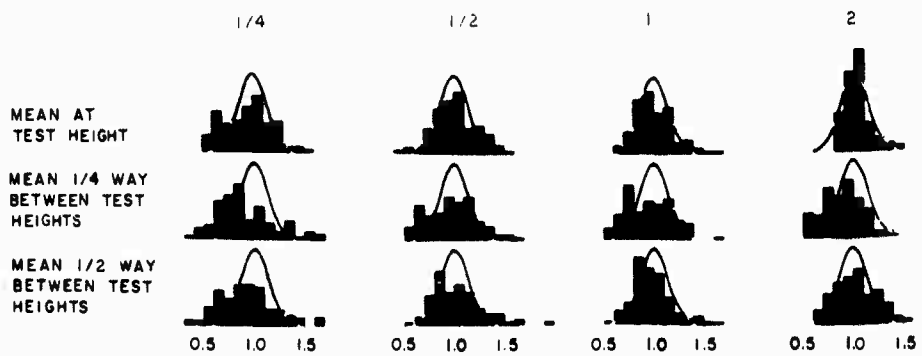

FIGURE 6. SPECTRUM OF STANDARD DEVIATIONS. EACH HISTOGRAM GIVES THE RESULT OF 100 TRIALS OF 100 ITEMS. THE X AXIS SHOWS THE RATIO OF "FOUND" TO "TRUE" STANDARD DEVIATION.

TAKEN FROM PRIVATE COMMUNICATION OF
J.W. MARTIN, RARDE
FORT HALSTEAD, ENGLAND

4. In order to understand the various methods of predicting extreme firing probability levels a passing understanding of probability distribution functions is of benefit. It has been found that the values of many naturally occurring phenomena can be sufficiently well described for many purposes by the normal (Gaussian) distribution function, for example, the heights of 1162 Vassar students in 1958 (Figure 1). Here we can see that the Gaussian curve describes the distribution of heights quite well except at the upper tail where only one or two students would be expected to be over 6 feet tall. Actually there were five.

5. The normal distribution can be represented graphically in a number of different ways: the bell-shaped frequency curve (Figure 2), the cumulative curve or ogive curve (Figure 3), and the cumulative curve transformed to a straight line by plotting in an appropriate probability space (Figure 4). While these three forms appear to be different they are equivalent. They all demonstrate the fact that the function is asymptotic at both extremes. That is, the probability of initiation does not become zero until the stimulus is decreasing without limit. Similarly 100% probability is approached but never actually attained. Whether or not this asymptotic property is an accurate description of the nature of EED's will be brought out in later discussions, particularly when considering "All-Fire" and "No-Fire" concepts.

6. The cumulative function is the more useful one for making estimates of extreme firing probability levels, particularly when in the straight-line form*. From the straight line relation it is obvious that a particular distribution can be fully identified by two data points: either a particular functioning stimulus-and-probability point and the slope of the line, or else two functioning-stimulus-and-probability points.

THE METHODS FOR ESTIMATING EXTREME FUNCTIONING PROBABILITY POINTS

7. Extreme functioning probability points for EED's have usually been estimated by extrapolating on the basis of an experimentally determined mean and standard deviation. As is the way with extrapolations, this process can lead to seriously faulty answers. There are certain assumptions inherent in the extrapolation:

a. That the sample size is adequate
b. That the sample is used efficiently. (This is controlled by the design of the experiment and the accuracy of the apparatus.)

---

* It should be noted that the point of intersection of the line with the 50% firing level is designated as μ, the fifty per cent firing stimulus, while σ, the standard deviation is the reciprocal of the slope at μ. It is a statistical convention to reserve the Greek symbols μ and σ for expressing the properties of the parent population and $\bar{x}$ and s respectively as the estimates based on measurements on samples from the population.

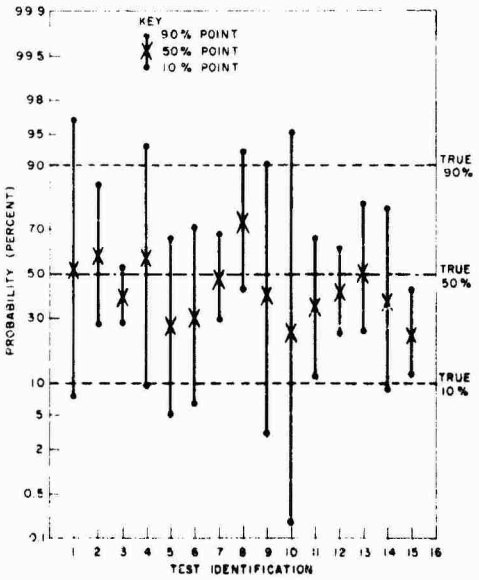

FIGURE 7 VARIABILITY OF ESTIMATES OF 90, 50, AND 10% POINTS BASED ON 20-SHOT BRUCETON SAMPLES FROM A KNOWN POPULATION

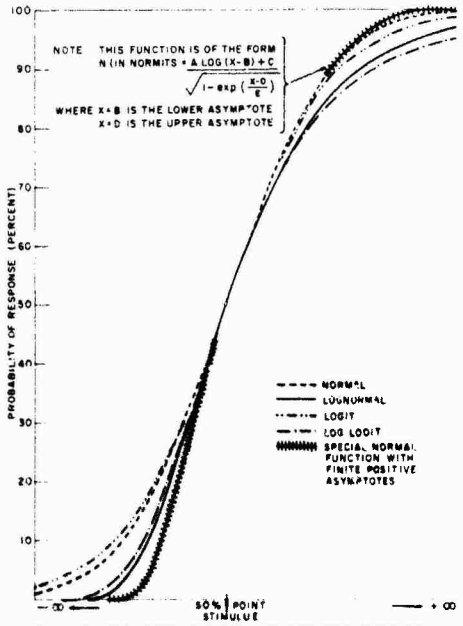

FIGURE 8 COMPARISON OF DISTRIBUTION FUNCTIONS HAVING THE SAME MEAN AND THE SAME SLOPE AT THE MEAN

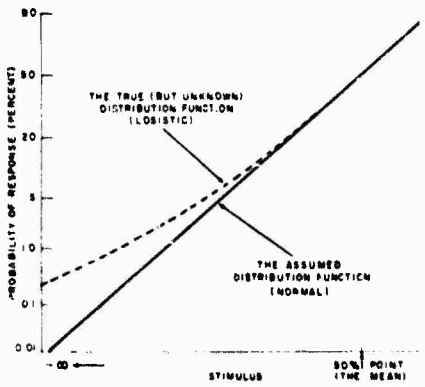

FIGURE 9 THE EFFECT OF FITTING THE ASSUMED DISTRIBUTION FUNCTION TO A MEAN AND SLOPE MEASURED AT THE MEAN

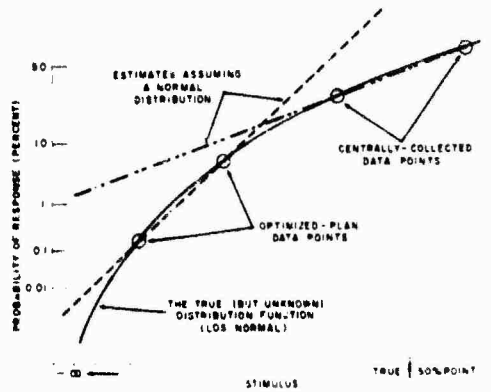

FIGURE 10 OPTIMIZATION OF DATA COLLECTION PLAN TO REDUCE CENTRAL ERROR BY CONCENTRATING DATA BELOW THE 50% POINT FOR SAFETY ESTIMATES

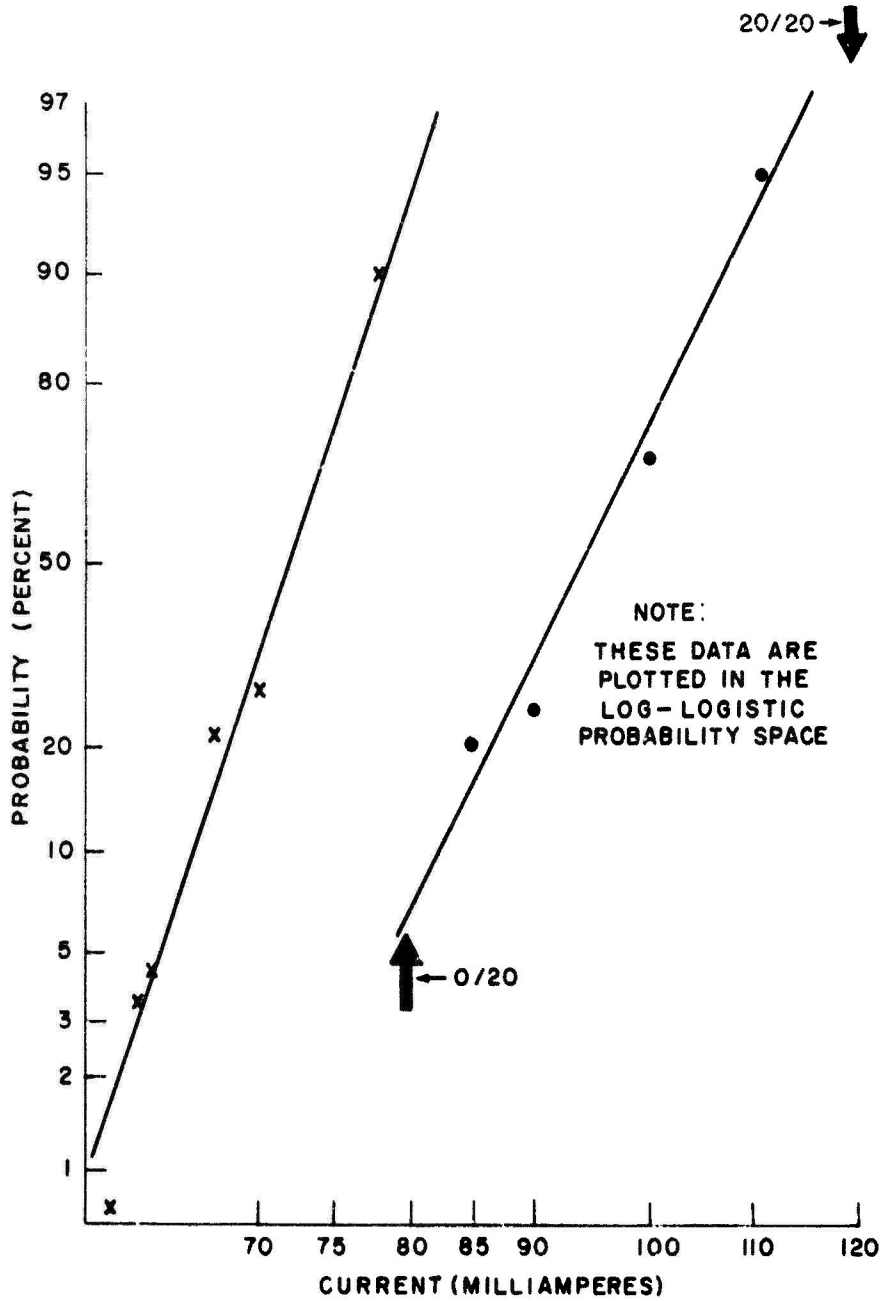

FIGURE II. LOT-TO-LOT VARIABILITY OF THE CONSTANT-CURRENT SENSITIVITY OF MK. 114-TYPE PRIMERS

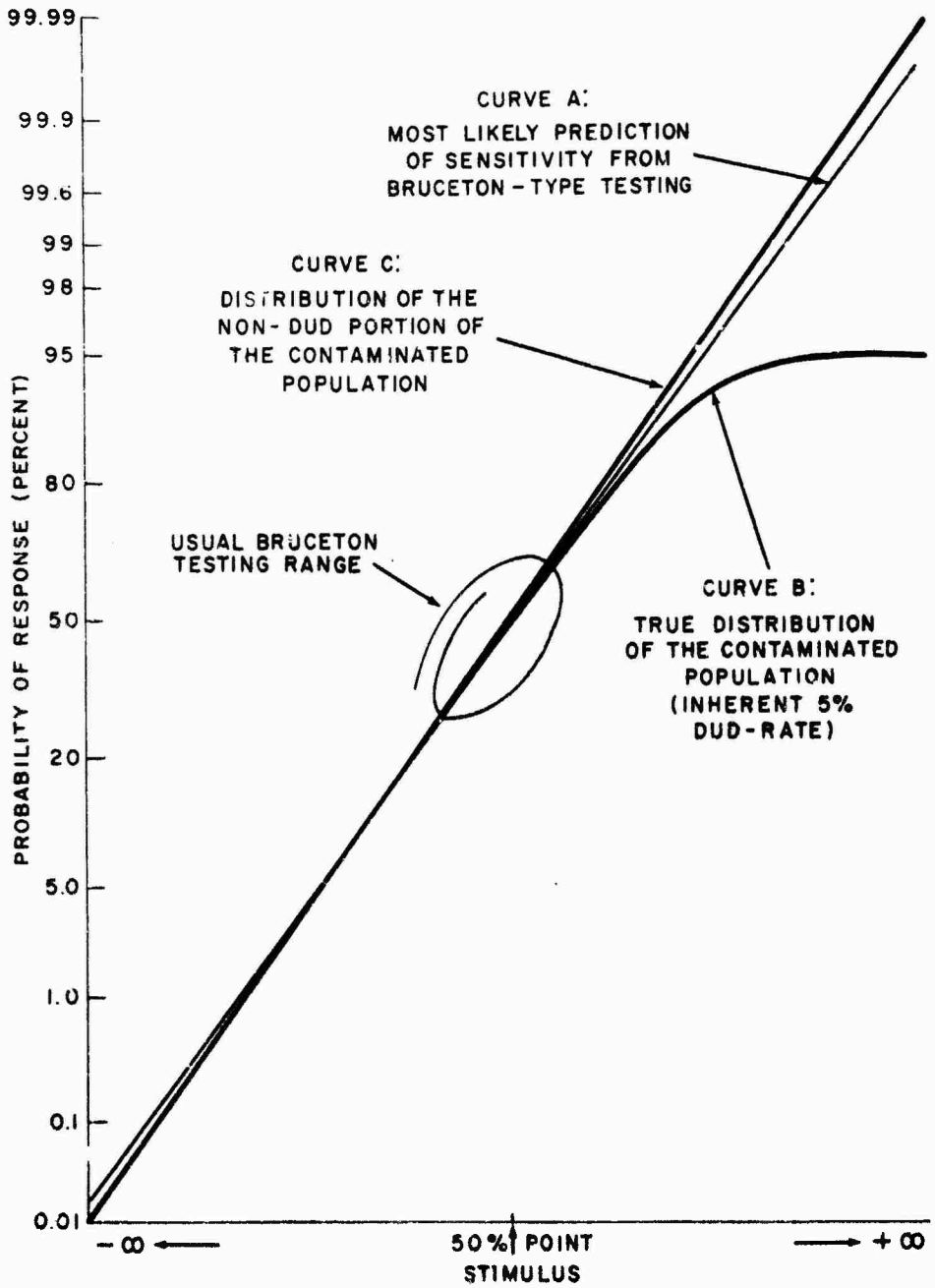

FIGURE 12. FAILURE OF BRUCETON TEST AND ANALYSIS TO DETECT AN INHERENT DUD RATE

would be in the form of a statement that the error is probably less than a certain amount. In a certain proportion of the tests, five per cent for example, the error will be greater than this amount.

21. Remember that these error estimates will be valid only if the sample was taken randomly. A random sample is one in which the selection of the individual items does not depend upon any property of the item. Every item must have an equal chance of being selected as a member of the sample. In many cases the selection of a truly random sample becomes difficult if not actually impossible. For example, we cannot obtain a random sample of all Mk 114 Primers. The sample must, for practical reasons, be drawn from the items on hand at a particular time and place. The result is that one does not estimate the characteristics of the Mk 114 Primer but of some particular lot or group of these Primers. As was pointed out in the preceding paragraph any attempt to consider these results as a characterization of the Mk 114 Primer is fallacious. This is the same error as that made by the European who thinks that he knows what Americans are like because he has seen a few American movies or has spent a day or two in New York City.

THE "ALL-FIRE" "NO-FIRE" TRAP

22. Over the past few years there has been an increasing tendency to use as concepts for characterizing EED's:

a. The "No-Fire" level, i.e., the largest input stimulus which can be applied to an EED without initiating it.
b. The "All-Fire" level, i.e., the smallest input stimulus which must be applied to an EED to initiate it with certainty.

These concepts are very handy from the engineering standpoint. They may even be true. But to date we have not been able to devise a method for locating these points or levels or of verifying their existence.

23. The usual process for estimating the "All-Fire" and "No-Fire" levels involves a measurement of response at a number of levels and then an extrapolation in the appropriate direction with an assumed distribution function. But the asymptotic limits of the distribution function are automatically assumed since they are part of the distribution function. And these limits are the desired "No-Fire" and "All-Fire" levels. Since they have been assumed a priori, they cannot be estimated or measured by the assumed distribution function. These limits are $-\infty$ and $+\infty$ for a linear normal or linear logistic function. Since a negative firing energy or power is meaningless the logarithmic transform is usually used. With the logarithmic transformation, the "No-Fire"

level becomes zero energy or power and the "All-Fire" level remains + ∞. Other distribution functions could easily be conjured up which would be asymptotic at finite non-zero levels, but they would have to be based on absolute knowledge before their limits could be identified with certainty as the desired "All-Fire" and "No-Fire" levels.

24. There is a way of getting an idea whether or not a particular test level is above or below the "All-Fire" level. For instance, let us assume that 3 million units of a particular type of EED are to be tested at 3.0 amperes. If there is a mixed response (both fires and fails) we know with certainty that the "All-Fire" level, if it exists, is greater than 3.0 amperes. If all of the units respond we may have exceeded the "All-Fire" level. But there is still one chance in twenty that we are at as low a probability as a 0.999,999*. There is an even greater chance that we have not exceeded the "All-Fire" level. But to get this assurance of only one in a million failure level at 95% confidence we had to use a fantastic sample size and we still are not sure that we have reached an "All-Fire" level or even that it exists.

25. The term "No-Fire" is an idea which seems to us to be similar to the idea of an upper boundary to the earth's atmosphere. All of the initiators of a given kind, the entire population in statistical language, correspond in this analogy to the atmosphere. The population of initiators is made up of individuals each of which will have a minimum stimulus requirement just as the atmosphere is made of individual molecules each having a certain height** above the earth. If there is atmosphere at any given height above the earth's surface then there will be some gas molecules at a slightly greater height. A similar situation exists with initiator sensitivity. If a few initiators will fire at a given stimulus, it is impossible to say that a decrease of an erg in the energy or a milliampere in the current would never result in a fire.

26. It is our contention that the terms "All-Fire" and "No-Fire" do not mean literally what they say. Is there, then, a meaning for these terms which, though different from the literal translation, is generally accepted. It is certainly possible that an

---

*The sample size needed to make this same sort of a prediction at other probabilities can be computed very simply by:

$$N=\frac{3P}{1-P}$$

where N is the number of items in the sample, P is the lower 95% confidence limit for the estimate of the probability of having observed N fires out of N trials.

**For the purposes of this analogy it is immaterial that the minimum stimulus requirement of the initiator is fixed while gas molecule heights vary with time. The atmosphere analogy is restricted to a single instant in time.

13. Other Monte Carlo studies carried out independently at the Naval Ordnance Laboratory show dramatically the imprecision to be expected with small-sample size Bruceton determinations. Fifteen Bruceton type tests, twenty shots per test , were carried out using a population with a known mean of 5.60 and a known standard deviation of 2.00. Figure 7 compares the individual estimates of the 90, 50 and 10 per cent points with the known population. Note,for instance, that the predicted 10 per cent point of the eighth run is higher than the predicted 90 per cent point of the fifteenth run.

14. Still another instance can be quoted. Recently one thousand Primers Mk 114 were fired under constant current conditions at the Naval Ordnance Laboratory. A preliminary 30 shot Bruceton run yielded a 50 per cent point of 71.8 milliamperes which is virtually the same as was observed for the 1000 shot rundown tests. The Bruceton predicted 1 per cent firing level was 62.7 milliamperes. Experimentally in the rundown at a level of 62.5 milliamperes 3.85% functioning was actually observed.

15. The original paper on the analysis of the Bruceton method gives a test for normality. This is based on what is known as the Chi-square test. Unfortunately use of this test will never prove that the distribution is normal. Failure to psss the test is usually taken as proving that the distribution is not normal whereas passing the test merely shows that it could be, but is not necessarily, normal. What is even more disquieting, unless the distribution differs greatly from the normal s lsrge number (i.e., many hundreds) of trials will be required to estsblish the non-normality of the distribution. The usual Bruceton test does not have a sufficient number of trials to do this.

16. Another very serious limitation lies in the fact that the Bruceton test collects the data near the fifty per cent point. There are many possible distribution functions which would match the data collected over this range in a very satisfsctory manner but which would differ to a very considersble extent for low or high per cent response points. Figure 8 shows several such curves fitted to data of a typical Bruceton test. To state this problem in another way, if the true distribution function should be even slightly peaked, or slightly flattened, near the mesn (as compared with the assumed function) then we find that the true and assumed functions would have diverged greatly by the time the extreme functioning probability levels were reached. For instsnce, in Figure 9 we see a case where the true function had longer tsils than the assumed function. Even if we had a perfect Bruceton, one in which the mean and the standard deviation messured at the mean were without error, we would be making overly optimistic estimates at both ends. In Figure 10 we show a way we can collect the dsta to reduce the effect of lack of agreement of the true snd assumed functions.

17. For emphasis, we repeat that the Bruceton collection plan should not be used for this work. We realize that the Bruceton plan is an old friend,apopular and tried-and-trusty tool, It has its uses. But it is not the tool for this job. Here we must find some way of allocating our samples so that we approach more closely to the functioning level we wish to estimate but yet not get so far away from the mean that we get almost meaningless (saturated*) data.

BATCH-TO-BATCH AND LOT-TO-LOT VARIABILITY

18. It is usual to treat electro-explosive devices as if each had individual fixed characteristics. We think in terms of a fixed firing energy for a particular design of EED under given conditions, and publish data to show what its characteristics are. For example, the Mk 1 Squib requires 10,000 ergs for 50% firing under adiabatic input. But it is known that when each of two different manufacturers make the squib the firing characteristics will probably be different. These differences can occur from slightly different bridge wire lengths, bridge wire diameters, fineness of explosive about the bridge wire, etc. It has even been found that when the same manufacturer makes the same EED over a period of time the firing characteristics may vary widely. An example of this is shown for the bridge-explosive combination of the Mk 114 Primer, manufactured by the same company with an interval of approximately 10 years between the two manufactured batches, (Figure 11).

19. That an EED cannot be considered to be of fixed firing characteristics is thus apparent. This fact should not be surprising when it is realized that manufacturers using the same plant, equipment, and processes can turn out both acceptable and unacceptable lots of EED's during a given production. What should not be expected or assumed is that a given variety of EED is invariant in its characteristics; consequently safety estimates cannot be realistically made assuming invariant firing properties.

SAMPLING ERROR

20. In estimating the firing characteristics of a group of EED's test firing must be made with a sample taken from the group. The results of this test firing can be taken as estimates for the group as a whole. These estimates will, of course, differ from the true, but unknown, values. These differences constitute the sampling errors. Their possible magnitudes for random samples can be estimated by standard statistical methods. These estimates

---

* By saturated data we mean a level at which all fails or else all fires were observed. Since we compute $p = \frac{\text{No. of fires}}{\text{No. of trials}}$ we would find p=0 or ∞ respectively. We would be unable to plot it in our straight line cumulative probability space

some measure of the variability of the sample such as s, the standard deviation, we must be assured that the variability introduced by instrumentation errors is small compared to the variability inherent in the EED. Reference 6 is suggested as a detailed analysis of the quantitative problems of firing EED's by capacitor discharge. And finally, the importance of choosing the right distribution function has been discussed in detail elsewhere in this report.

DESIGN OF A DATA COLLECTION PLAN OPTIMIZED FOR MAKING EXTREME FUNCTIONING PROBABILITY ESTIMATES

32. In order to minimize the importance of assumptions regarding the frequency distribution it is desirable to base these estimates on data taken as close as possible to the per cent point to be determined. The simplest such test would be one which calls for testing at two stimulus levels near to the region in question. One of the two levels will be further from the mean and closer to the desired point than the other. This will be designated the remote stimulus level. The data obtained can then be extrapolated to determine the stimulus associated with the desired per cent point. In planning such an experiment the following conditions should be met:

a. The difference between the stimuli used should not be small compared to the extrapolation distance (the difference between the desired point and the observed remote stimulus)
b. The number of trials at the remote stimulus level and the expected response at this level must be such that the probability of observing either all-fires or all-fails is small
c. The number of trials made at the remote functioning level should be greater than the number of trials at the level closer to the mean. A good choice is to take the number so that the product np (1-p) is the same for both levels where n is the number of trials and p is the expected probability of fire.

33. The general approach in implementing this method is to run a preliminary short Bruceton which is used to estimate two stimulus levels at which the remainder of the sample will be fired. At the first level (the one closer to the mean) the smaller portion of the remaining sample is fired. If the observed response is not too different from what was expected from the Bruceton test, the remainder of the sample is fired at the previously selected remote level. If the response at the first level is greatly at variance with the expected response, the test plan is altered to reallocate the sample remainder.

34. The following is a step-by-step procedure for firing two hundred samples:

a. Fire twenty items in a Bruceton test to obtain preliminary estimates of the mean, m, and the standard deviation, s. A log-transform of the dosage (current, potential, energy) is taken as the stimulus
b. Compute the magnitude of the two test levels near stimulus (first level) = m-0.4s, remote stimulus (second level) = m-1.3s
c. Test fifty items at the near stimulus level

(1) if five or fewer fires are observed, redefine the near stimulus level as the remote level by continuing firing at this level until one hundred-thirty items are expended. Fire the remaining fifty at m-0.2s
(2) if more than five fires are observed (the usual circumstance) fire the remaining one hundred-thirty units at the original remote stimulus level.

35. The foregoing procedure is set up for use when a low per cent point is desired. This method can be used for determining a high per cent point by making the appropriate changes. The test levels should be computed by adding, rather than subtracting, the appropriate multiple of s. The criterion for altering test levels, i.e., "five or fewer fires", would be changed to "five or fewer fails".

36. There is one problem in reliability determination which does not have its counterpart at low per cent points. This is the possibility of the presence of duds which would not respond to any stimulus, no matter how great. Obviously if more than one per cent of the population were duds, a 99% functioning point would be a fiction. It could not exist. Figure 12 shows the expected response of a normally distributed population contaminated by 5% duds. As can be seen from the figure, if an experiment were made covering the range from 15 to 80% response, the data obtained could be represented quite well by a straight line. Hence any test made entirely in this interval would give completely erroneous predictions for responses above 90%. This would completely eliminate the Bruceton test for estimating high functioning probabilities unless the absence of duds is assumed. Ordinarily the proportion of duds is smaller and therefore harder to detect.

38. The data collection plan described above ordinarily yields some centrally-collected Bruceton data plus data at two levels which mixed responses are observed. Because the Bruceton data are collected at the mean and at levels most remote from the

arbitrary definition could be made and generally accepted in the same way as other empirical parameters such as Flash point of oil, yield point of steel, etc. At present there are many interpretations of the concepts ranging from carefully computed points to engineering hunches and guesses.

27. For instance, we find in the specifications for the Squib Mk 1 that either forty-five or seventy-five items (depending upon the lot size) are to be tested with a current of 200 milliamperes. If none fire the lot is accepted. This 200 milliampere level is quoted as the "No-Fire" current for this initiator. But the ghastly truth is that the chances are five out of eight that forty-five failures would be observed at a level which in reality was the 1% functioning level. Or, to look at it another way, a manufacturer could be producing Mk 1 Squibs which will function 0.1% of the time at this 200 milliampere "All-Fail" and have 19 out of 20 lots accepted.

28. Recently certain groups at the Bureau of Naval Weapons have decided to define the "m-4s" and the m+4s" levels as the "All-Fail" and All-Fire" levels respectively. These correspond to probabilities of 34 in a million that an adverse result is expected in either case, i.e., 0.000034 or 0.999966. The choice of 4 standard deviations away from the mean is purely arbitrary. It is a seat-of-the-pants compromise between what one might like to be able to say (one in a million) and what one might be really justified in saying (one in a hundred).

THE WAY OUT

29. By now the picture we have painted must indeed be bleak. We have said that even if a good random sample is taken from the lot being tested there is no assurance that the other lots will not differ from it. We have said that the normal distribution and the Bruceton data-collection plan should not be used to make extrapolations. We have said that the "All-Fire" and "No-Fire" levels probably do not exist or else if they do exist they cannot be determined by direct experiment. We will say further that it will almost always be the case that safety estimates must be made by extrapolating hopefully with a surmised distribution function on data derived from an inadequate sample size taken from a lot which probably will be different from the lot that is used in the weapon.

30. The first purpose of this paper is to post a warning as to the nature and degree of the problem. The second is to show ways to reduce the likelihood of making faulty estimates:

a. Get the largest possible sample size
b. Make sure that the sampling was random
c. Make sure that the firing instrumentation is in good order. (The inherent experimental error should be known.)
d. Carry out the firing according to a plan which has been optimized for the purpose of making the desired estimate

e. Choose the distribution function which will yield conservative estimates
f. Estimates should be made realistically in view of the limitations inherent in the process. Assumptions should be recognized and stated with the deduced sensitivity figures.

31. What is meant by "largest possible sample size"? How big is a large sample size? As was mentioned previously 1000 Primers Mk 114 were fired under constant-current conditions. The following firing data were obtained:

Current	Observed Response		
Milliamperes	Fires	Fails	Per Cent
94.0	2	0	100.00
77.0	9	1	90.00
70.0	4	9	30.77
67.5	10	35	22.22
64.0	8	171	4.47
62.5	15	375	3.85
61.0	1	349	0.29

Using the log-logistic distribution function, and fitting the data using the least-squares method, the sensitivities are estimated:

Probability of Functioning (per cent)	Predicted Level milliamperes
50.0	71.19
5.0	63.70
1.0	59.85
0.1	54.85
0.01	50.28
0.001	46.09

The 95% tolerance interval (upper and lower confidence band) about the 0.1% point is from 50 to 57 milliamperes. The estimate of the 0.1% point is not particularly precise. Had the sample size been in the order of 100 units, this interval would have been over three times larger. Thus it can be seen that a sample of a few hundred units really cannot be expected to give a reliable and precise estimate much beyond the 1% point. It begins to be evident that the definition of a large sample size is: a quantity much larger than one can hope for.

32. The next three items listed in paragraph 30 are quite clear. The necessity for random selection of the sample from the population is a basic tenet of proper experimental and statistical procedures. Next, since we must extrapolate on the basis of

desired estimation level it seems best to discard them and to perform the analysis on the two mixed response levels. This analysis can be carried out very simply by plotting the two points in the proper probability space and running a straight line through them.

39. More sophisticated statistical treatments, experimental designs, etc. can be used and in many cases will lead to better answers. Other papers are being prepared at the Naval Ordnance Laboratory which will describe in much greater detail some of the experimental techniques, statistical theory, and high-speed computer programs for data processing and for carrying out Monte Carlo experiments.

CONCLUSIONS

40. It is not possible to estimate precisely the functioning probability levels of EED's at the extremes needed for good safety and reliability estimates. There are practical procedures for reducing estimation errors: These are proper sampling, proper instrumentation, optimization of data collection procedures, and selection of proper statistical tools. There are certain areas, such as lot-to-lot and batch-to-batch variation, for which we cannot at present make adequate correction to our estimates. The gathering and study of relevant data would probably be quite difficult, yet would give information of great value in this type of work. We feel that even though it is not possible to solve all of the problems accurately it is much better to know the inherent limitations and possible sources of serious error in making safety and reliability estimates than it is to go blithely along in blissful ignorance of life as it really is.

REFERENCES

1. NOLTR 61-20, "The Response of Electro-Explosive Devices to Transient Electrical Pulses", A. Selem, I. Kabik, L. Rosenthal, 17 Apr 1961.

2. "Statistical Methods in Initiator Evaluation", The Franklin Institute Laboratories for Research and Development, Interim Report No. I-1804-1, Carl Hammer, May 1, 1955.

3. NAVWEPS Report 7347, "Characterization of Squib Mk 1 Mod 0 Determination of the Statistical Model", L. D. Hampton and J. M. Ayres, 30 Jan 1961.

4. "A Statistically Precise and Relatively Simple Method of Estimating the Bio-Assay with Quantal Response on the Logistic Function", Joseph Berkson, Jour. of Amer. Stat. Assoc., 48, 565-599 (1953).

5. Private Communication, J. W. Martin to I. Kabik, Apr 4, 1962.

6. NAVWEPS Report 7308, "Characterization of Squib Mk 1 Mod 0 Capacitor Discharge Sensitivity with Instrumentation", J. M. Ayres, 10 Jan 1961.

34. DISCUSSION

A questioner desired reference to published tables of tolerance factors if such tables exist. Mr. Hampton answered that this depended upon the mean and standard deviation. The same questioner said that he appreciated this but that the tolerance factor table takes into account the errors in the mean and standard deviation, and asked if there was an equivalent table for this function. Mr. Hampton answered no, but added that information on this will be published in the next Association Journal.

Mr. Benedict commented that the table for the normal distribution was published about three years ago. It was questioned whether the other one was as up to date as this. He continued that various people, notably Kerr and Davis had pointed out shortcomings of the Bruceton test. The interval for Bruceton testing should hold a definite relation to the standard deviation. It is necessary to adjust testing to meet this condition. There is no law for this and he for one has adjusted the interval to give the customer the desired results.

Mr. Benedict inquired if the interval was controlled before the test to have a certain relationship to the standard deviation or were they taken as they came. Mr. Hampton answered that in his own test he did not, but that Mr. Martin in his test in England did. He said that the slides he had shown indicated columns for different size steps.

Mr. Hedges of the Martin Company commented of his interest in this table and agreed with everything that was said. With respect to the previous speaker he expressed a desire to add to his comments. It is beleived that most of the criticism of the Bruceton method is unjustified to a large extent. In reviewing Bruceton data that is supposed to prove that a particular explosive device meets the AFMTC safety requirement, he failed to follow the computor's method. If he was using the NAVORD report, he didn't even follow the right section of the curve in certain areas. In most cases the log function is not used. When the log function is not used, the result is a conservative estimate of the safety point and

perhaps not too conservative estimate of the all fire point. To this end, Mr. Hedges proposed to the JANAF subcommittee on Explosive Components that a Standard be sponsored that would describe a Bruceton technique easy to follow, with simple tables that would make computation easy, eliminating all curves.

Mr. Hedges continued that the speaker had mentioned a true sigma and that he would like to know what a true sigma is. He also commented on the testing of samples at several year intervals. He suspects that these were actually two different items with the same label. He commented further that the baseball player example is poor because of different stimulus. He made his main point that he is not concerned who wants to use the Bruceton method or what they want to do with it; predict the 99.9 or 99 with nine 9's behind it. But he advocates a standard Bruceton method in which independent workers can validly compare results.

Mr. Hampton answered that with a random number approach standard deviation can be computed for the entire population. By sampling from this population standard deviation of the sample can be obtained by different methods and compared with the true standard deviation. He commented that Bruceton data accumulates near the 50% point and that the distribution is assumed. A figure included in the paper but omitted from the presentation shows a normal distribution and a logistic distribution together. It shows that the 0.1 percent point predicted by a Bruceton is actually the 3 or 4 percent point if the true distribution is logistic.

Mr. Kabik added that in attempting to predict extremes that are many standard deviations from the mean, from data collected around the mean, we are fairly sure to come up with the wrong answer. The Bruceton should not be used in this case. A standard for the Bruceton may still produce the wrong answer.

Weaknesses in assuming that items are "the same" were pointed out. They may be tagged with the same label, for example, MARK 114. But examining the facts may show that they were different lots, different manufacturers or different batches. It was pointed out that from a limited sample on one batch or one lot it cannot forever be said that these are the responses of the device.

Mr. Hampton commented that at least all of these go by the same name.

Mr. Amicone of The Franklin Institute commented that he had reviewed Martin's work and that we owe it to him to mention the small sample sizes that were used. Mr. Hampton said that the slides showed, he beleived, samples of 25. Mr. Amicone replied that most of the people present know that this sample size is entirely too small to make any kind of estimate.

Mr. Kabik added that Martin used sample sizes as high as 100 with a resultant improvement in the estimate. The results still did not fit the normal distribution. Further even with batches of 25, 50 and 100 good estimates are not made.

Mr. Hedges commented that his standard showed what would happen with sample sizes of 20 to 500. The sample size can be given a degree of calculated accuracy. The point of best return, which appears to be at a slope of 45 degrees, occurs at just slightly over 100 samples. The proposed method involves 120 samples of which 20 will be used to obtain an estimate of the mean and standard deviation.

The discussion was suspended by the chairmen in order not to fall too far behind schedule.

35. A Survey of 1-Amp, 1-Watt EED's

by Gunther Cohn
The Franklin Institute

Background

Over the years, a number of methods have been proposed to cope with the hazards of radio frequency electromagnetic radiation to ordnance. Certainly, this hazard is of serious concern to the agencies of the Department of Defense and its Contractors. Even a sketchy description of the various approaches used to wrestle with the RF problem would be of such length as to warrant a separate paper. Suffice it to say that the approach has been one of long range planning through design changes to fixes for specific applications.

We are concerned today with one of the proposed design changes, known as the 1-Amp, 1-Watt solution. It is defined in the "Interim Standards to Minimize the Hazards of Electromagnetic Radiation to Electroexplosive Devices" which were issued 1 October 1962 by the Safety Division, Office of Inspector General, Headquarters, Air Force Systems Command, Andrews Air Force Base, Washington, D.C. The interim standards state in part that:

> "EED's are required to meet one of the following standards:
>
> "(1) EED's will not fire as a result of the application of one watt of direct current power for five minutes and as a result of the application of one ampere of direct current for five minutes. This requirement must be met without the use of external shunts. Suitable testing, such as the Bruceton type statistical test, will be performed to validate a no-fire reliability of 0.999 with a 95 per cent confidence level.
>
> "(2) EED's with electroexplosive elements that do not meet the above one watt/one ampere/five minute standard will be designed so that the integral unit will survive in an electromagnetic field intensity of 100 watts per square meter. Approved testing will be performed...."

Before proceeding, let us set the boundary conditions of this paper. I should make clear that I do not intend to discuss the merits of the 1-Amp, 1-Watt specification. Whatever you may think of the 1-Amp, 1-Watt approach as a solution to the HERO problem, the fact is that such EED's are now being specified, manufactured, and tested. This paper is being presented as a part of our technical documentation work which is designed to record and disseminate information on current ordnance topics. Hence, it is the purpose of this paper to discuss the various EED's now available which can withstand inputs of at least one ampere and one watt of direct current for five minutes or longer without initiation or degradation.

I might comment on these two requirements. Failure to initiate or fire pertains to safety and is spelled out in the specification. Failure to degrade pertains to reliability and as such is implied in the specification. Both attributes are important. The conventional hot wire bridge electric initiator is too sensitive to meet these requirements.

Survey

In March 1963, we wrote to two Government agencies and 32 manufacturers asking them for information about their 1-Amp, 1-Watt EED's. We received 6 replies stating that such devices were not yet in their line and heard nothing from 11 others. Fleming Industries indicated that they had an RF-insensitive EED but no 1-Amp, 1-Watt. Positive replies came from 14 manufacturers. We must admit that the time for reply was short so that it is entirely possible that some companies did not have a chance to write.

A summary of the 1-Amp, 1-Watt EED's now available is shown in the accompanying table. The 1-Amp, 1-Watt devices now appear in catalogs as regular shelf items. They come in a variety of sizes, types and functioning characteristics and most manufacturers indicate that their lines are to be extended. We did not attempt to list every available initiator but merely gave the ranges covered. Little would be gained by attempting

to achieve completeness of listings because most companies indicate their ability to make changes to suit a customer's specific needs. In addition to the summary table we also attach a list of manufacturers with contact names and phone numbers.

Methods of achieving the 1-Amp, 1-Watt insensitivity differ. There seems to be no best solution. Dual bridges, insensitive mixes, internal shunts, and heat sinks, all are being used, often in combination. The use of an insensitive mix appears to be convenient to solve retrofit problems.

This summary then is meant to help designers and users of EED's get started in their search for 1-Amp, 1-Watt devices. We would be amiss if we did not include in this presentation a serious note of warning: 1-Amp, 1-Watt devices are brand new, they have not been tested extensively, they do not have history of use behind them. We know from past experience that it is dangerous to assume that a change in the primary operation of an EED, however small, can be ignored. There is as much reason to assume that there is a tremendous change in performance as there is that the change is insignificant.

Probably the most efficient sensitivity testing procedure is the so-called Bruceton test. Its validity is based on the assumptions that

(1) the response is normally distributed (Gaussian) with respect to the stimulus.

(2) no duds (manufacturing freaks) are in the lot.

The validity of the Bruceton test for the conventional sensitive hot-wire initiator has been demonstrated by tests of entire lots according to the Bartlett plan. We therefore test with the Bruceton method near the 50% point and infer what happens at the extremes. Let us suppose now that it might turn out that the changes introduced to make 1-Amp, 1-Watt devices are such that the assumption of normalcy no longer holds. For example,

say that the bridge wire burns out at a certain high current so that the curve is discontinuous. Such a condition would not only invalidate the Bruceton test, it may well result in consistent performance failures at so called all-fire currents.

Non-conventional designs may also exhibit different failure mechanisms which should be taken into consideration. For example, a multi-bridge initiation may become more sensitive if one or more bridge filaments are broken. This condition poses the question, does the item have fail-safe characteristics from a safety standpoint? Further, storage stability, compatibility of mixes, new construction materials, and degradation due to prepulses should all be considered.

Both designers and users then have no choice but to insist on complete test results for the contemplated item. Many of the manufacturers furnish test data results. This is good. We can then examine the data to make certain that it characterizes the item fully. We can conclude that one should shop for 1-Amp, 1-Watt devices the same way as we used to shop for EED's some years ago before they became standardized.

Summary of EED's

Manufact.	Item	Size	Funct.	Achieves 1A/1W by	Status
Nav. Ord. Plant	Ignition Element EX 5 MOD 0	.5D x .65L	2 Amp 10 ms	Heat Sink	Design proof
Atlas	Blasting Caps Nos. 6, 8, 9	1-7/16 x 2L	6 Amp	Heat dissip. resistor	Product.
	Min. Switches 2 to 8 poles	3/8 square $1\frac{1}{2}$ to $5\frac{1}{2}$L		"	"
	OM Switches 4 to 12 poles	$\frac{1}{2}$ sq x to 3.7L .5 x 1.6 x 1.6		"	"
	Piston Activator	.38D x 2.8L	6 Amp	"	"
	Bellows	9/16D x 1-3/4L	6 Amp	"	"

Summary of EED's (Cont.)

Manufact.	Item	Size	Funct.	Achieves 1A/1W by	Status
Conax	Primers	.19 to .29D	3-5 Amp	Insensitive	Product.
	CC 61, 62, 63	.46 to .64L	3.5 ms	mix	"
	Primer	.285D x .75L	4-5 Amp 3.8 Amp	2 Bridges Resistors	"
	Primer Cartridge		3.5 Amp 6 ms	2 Bridges Heat Sink	Proposed
Flare	Phenolic plug squibs F-N 126, 127	.27D x .4L	5 Amp 1 ms	Insens. mix	Product.
	Detonator, G.T.M.S. F-N 1017, 1042	5/8 hex x .84L	5 Amp 1 ms	"	Devel.
Gould	Igniter, G156227-D7P-02B-1NF	3/4 hex x .6L	4-5 Amp 8-10 ms	2 Bridges Double fil. Heat Sink	Pilot lot
Hercules	Delay Squibs	3/4 hex 2 to 3.4L	4.5 Amp to 5.6 sec.	Various methods	Product.
	Squibs	.28 to .3D .42 to 1.4L	4.5 Amp 4 ms	"	"
	Primers	.29D .52 to .63L	4.5 Amp 3.5 ms	"	"
	Bellows	.33D x 2L	5 Amp 2.2 ms	"	"
Hi-Shear	Squibs, PC Series	9/16 to 1-1/8 hex 1 to 1.5L	4-5 Amp 3 ms	Insensitive mix	Product.
	Detonators, PD	5/8 hex x 1.125L	"	"	"
Holex	Pressure Cartr. Series 3000, 3100	3/4 to 1 hex 1 to 1¼L	4.5 Amp 9ms	Heat sink 2 Bridges	Product.
	Ignition Cartr. Series 3200, 3300	3/4 hex x 1L	4.5 Amp 9 ms	Heat sink 2 Bridges	"
Lorasc.	Propellant Inits. RI-75, RI-76	5/8 hex x 1.06L	4 Amp	Insensitive mix	Pilot lot
McC. Selph	Squibs M-88, M-102	5/8 hex .84 to .96L	2 to 5A 4 ms	2 Bridges Insens. mix	Pilot lot
	Pressure Cartr. M-103, M-104	5/8 hex x .86L	2-3 Amp	2 Bridges Insens. Mix	"
Olin	Squib Flame Model	9/16 hex x .6L	5 Amp 20 ms		Pilot lot
Spec. Devices	Cartridges	5/8 hex x 1L	5 Amp 8 ms	Heat sink	Product.
Uridyanm.	Detonator UMD 1025	.3D x 1L	4.5 Amp 8 ms	Heat sink	Test

Manufacturers of 1-Amp/1-Watt EED's

Commander
U.S. Naval Ordnance Plant
Macon, Georgia
Mr. J.L. Pertsch, Code PD270,
Devel. Engr. Div.
788-6700 ext 418

Aerojet General Corp.
Solid Rocket Plant
Sacramento, California
Mr. Herbert Askwith
YU 5-5111

Atlas Chemical Industries, Inc.
Aerospace Components Div.
P.O. Box 271
Tamaqua, Pa.
Mr. R. McGirr, Superv.
Des. & Devel. Group
Mantzville 4

Conax Corporation
Explosive Products Division
2300 Walden Avenue
Buffalo 25, N.Y.
Mr. Ted Pierson, Engr.
NT 4-4500

Flare Division
Atlantic Research Corporation
19701 W. Goodvale Rd.
Saugus, California
Mr. P.M. Kirkegaard,
Res. Engr.
STate 8-7260

Gould Laboratories
North Delsea Drive
Pitman, New Jersey
Mr. W.F. Gould, Vice Pres.
LUther 9-5753

Hercules Powder Co.
Port Ewen, N.Y.
Mr. W.R. Thomas
FEderal 8-2144

Hi-Shear Corporation
2600 West 247th Street
Torrance, California
Mr. Monte W. Korb, Mgr.
Ordnance
SPruce 5-3181

Holex, Inc.
2751 San Juan Rd.
Hollister, California
Mr. S.A. Moses, Dir.
Res. & Engr.
MErcury 7-5306

Librascope Division
General Precision, Inc.
Information Systems Group
Mr. D.F. Finochio, Jr.
Proposal Mgr., Ord. Systems
REgent 6-9290

McCormick-Selph Assoc.
Hollister Airport
Hollister, California
Mr. William Frey, Mgr.,
Applicat. Engr.
MEcury 7-3731

Olin
Organics Div., Defense Products
East Alton, Ill.
Mr. J.L. Caspari
CLinton 4-7311

Special Devices, Inc.
16830 W. Placerita Canyon Rd.
Newhall, California
Mr. E.M. Shurtleff, Dir. R&D
EMpire 5-3171

Unidynamics
Division of Universal Match Corp.
Crab Orchard Operations
P.O. Box 231
Marion, Ill.
Mr. Robert D. Smith, Staff Engr.
WYandotte 2-2941 ext 281

INTERIM STANDARDS TO MINIMIZE THE HAZARDS OF ELECTROMAGNETIC RADIATION TO ELECTROEXPLOSIVE DEVICES (1 October 1962)

SAFETY DIVISION -- OFFICE OF THE INSPECTOR GENERAL
HEADQUARTERS, AIR FORCE SYSTEMS COMMAND

1. PURPOSE. To minimize the hazards of electromagnetic radiation to electroexplosive devices and to minimize the requirements for radio frequency silence at the National Ranges, the following standards will be used. The standards will apply to the design, selection, and application of electroexplosive devices for future development programs, and will be incorporated in current development programs in an orderly but expedient manner. These standards are applicable to all elements of the Air Force Systems Command engaged in the design and development of systems that use electroexplosive devices.

2. REQUIREMENTS. Systems using electroexplosive devices (EED) will be designed to preclude spurious functioning of any system EED or degradation of any EED with respect to reliability or performance characteristics by environmental electromagnetic radiation. Established techniques for reducing the susceptibility of electroexplosive devices to electromagnetic radiation are to reduce the sensitivity of the electroexplosive element to RF energy and to deny access of RF energy to the EED.

3. STANDARDS. Guidance for the design or selection of electroexplosive devices will include, but not be limited to the following:

a. EED's will not be used when the system requirement can be met by other reasonable means.

b. Sensitivity of electroexplosive devices will be the minimum compatible with design requirements and limitations such as space, weight, power, reliability, and performance characteristics.

c. EED's are required to meet one of the following standards:

(1) EED's will not fire as a result of the application of one watt of direct current power for five minutes and as a result of the application of one ampere of direct current for five minutes. This requirement must be met without the use of external shunts. Suitable testing, such as the Bruceton type statistical test, will be performed to validate a no-fire reliability of 0.999 with a 95 percent confidence level.

(2) EED's with electroexplosive elements that do not meet the above one watt/one ampere/five minute standard will be designed so that the integral unit will survive in an electromagnetic field intensity of 100 watts per square meter. Approved testing will be performed to establish a no-fire reliability of 0.999 with a confidence level at 95 percent. Tests will include exposure to electromagnetic fields, pulsed and continuous wave, with frequencies ranging from 100 kilocycles to 40 gigacycles. Testing will include: Evaluation of the RF sensitivity of the basic electroexplosive element; evaluation of the uninstalled EED in all normal modes of storage, transporting, handling, and installing; and evaluation of the complete EED system in the installed configuration.

d. For the purposes of this standard, the firing circuit of an installed EED will include all electrical circuits and components between the initiation power source and the electroexplosive element of the EED. Prior to installation, an EED includes all leads and connectors electrically connected to the electroexplosive element. To deny access of RF energy to electroexplosive devices, the following specifications are applicable:

(1) EED firing circuits will be isolated from other circuits and each other by means of individual shields. Shielded EED circuits may be routed together in a common secondary shield.

(2) Circuits to EED's will be balanced to and isolated from the EED case and other conducting parts of the weapon. If a circuit must be grounded, there will be only one interconnection with other circuits. Static discharge resistors of 100,000 ohms or more may be connected to firing circuits.

(3) Firing circuit conductors will be twisted to maintain electrical balance and reduce induction.

(4) Firing circuit wiring will be kept to a minimum.

(5) All conductors that connect the EED with other weapon components will be provided with metallic shields to provide an integral shield without electrical discontinuities or gaps.

(6) Connectors will be kept to a minimum. Connector construction will be such that, when being mated, the shield contacting surfaces will mate before any of the inner conductors and will not break contact until after all inner conductors have broken contact. Also, the inner conductors of the connector on the EED side will be recessed in the shield opening.

(7) Wiring within an EED will be isolated from any metallic case or enclosure. The impedance to case from each conductor will be equal and high as practicable.

(8) Carefully designed and tested RF attenuating filter elements can be effective in suppressing RF currents. These may be used to protect against nearby sources of RF energy, such as missile borne radar beacons, telemetry transmitters, or very high power ground transmitters.

e. EED's that use devices other than conventional bridgewire initiators must also demonstrate survivability in electromagnetic field intensities at 100 watts per square meter with a no-fire reliability of 0.999, 95 percent confidence level.

4. RESPONSIBILITIES.

a. The agency responsible for the management of a system program will:

(1) Assure that electroexplosive devices used in the system conform to the specifications of this standard.

(2) Monitor validation testing procedures to assure proper scope and quality.

(3) Provide documented certification of EED's selected for use in the system.

(4) Assure that adequate quality control techniques are adopted to provide continued qualification of production items.

b. The Commander, AFMTC will be responsible for:

(1) Identifying areas within the range boundaries where the electromagnetic radiation intensity exceeds 100 watts per square meter.

(2) Granting waivers to the requirements of this standard when adequate justification is presented, and assuring adequate protection for EED systems that are granted waivers.

c. Headquarters AFSC (SCIZM) will monitor this interim standard until a more comprehensive and complete exhibit or military specification is developed. Remarks and recommendations pertaining to this interim standard will be forwarded to this Headquarters.

NOTE: A formal presentation by a representative of the AFMTC, Patrick AFB, Florida, describing the latest Standard is planned for the Fourth Electric Initiator Symposium to be held October 1 and 2, 1963 at The Franklin Institute, Philadelphia, Pennsylvania.

35. DISCUSSION

Mr. Guinn said that the most of the fixes discussed are rated at 10 or 20 watts. Other people have mentioned 14 amperes being induced. This represents a power of 196 watts into a 1-ohm load. If there is the possibility of this much power, he asked why we are considering 10 to 20 watt fixes and 1 amp-1 watt no fire devices. Mr. Cohn referred this question to Cmdr. Gray who replied that he could make any size dissipater desired. He asked how big the questioner wanted it. Mr. Adelman of Picatinny Arsenal pointed out that most of the devices that provide insertion loss are quite large. Most of them are from 3 to 4 inches. Most applications allow for a half an inch or so for the entire initiator and fix.

Mr. Benedict of JPL said that in the room there are people on both sides of a very hot political argument. He commented that people came to the Congress in order to leave the meeting with a better understanding of the one-amp, one-watt requirement. He asked if this could be started.

Mr. Rawls of the RCA Service Company was asked to comment on the speakers reference to the Atlantic Missile Range (AMR) policy requiring one-amp, one-watt initiators. Mr. Rawls stated that there is no one-amp, one-watt policy as such, but only in conjunction with many other provisions including shielding. He added that the current policy requires validation of the capability of survival in a field of 100 watts/square meter from 50 Mc up and 2 watts/square meter (28 volts per meter) below 50 Mc or compliance with proper shielding and other circuit design features plus one amp, one watt initiators. The user should bring his procedures to AMR, Safety Division and they will check it and offer an opinion. The one-amp one-watt requirement is not claimed to be a cure-all but in conjunction with proper shielding and good circuit design should improve safety with reference to the 100 watt per square meter maximum RF field intensity.

In a meeting at Bedford, Massachusetts last year a Navy representative stated that they were considering a one-amp, one-watt no-fire requirement and also specifying that the bridgewire circuit should open after firing. This becomes a matter for the ordnance manufacturers to adjust properly.

Mr. Warner of Douglas Aircraft asked if anyone had looked into the possibility of having a highly sensitive condition from pin-to-case in the one-amp, one-watt devices. Mr. McAdams of Redstone Arsenal commented that this was similar to problems encountered in encased relays. Mr. Adelman of Picatinny Arsenal commented that at least one initiator or possibly two were more sensitive in the pin-to-case mode of excitation than pin-to-pin.

A person from Douglas Aircraft found that many manufacturers are applying the "no fire" current to all of the items they produce. Although this may assure that the device will not fire under these conditions, there is a reluctance on the part of ordnance people to accept devices that have been pulsed in this fashion. He asked for comments on this practice.

Mr. Rosenthal of STL commented that he believed the 100% prepulsing to be a stupid practice. In some devices sensitivity will increase; in others it will decrease. The result is that predictions of firing levels are difficult to make. He expressed his belief that a sampling technique should be used and destructive testing performed including sequential environmental tests. A Bruceton may also be used as a quality control test to compare later production with design development lots.

Mr. McGirr of Atlas Chemical industries commented that his firm tests all items that are shipped. The method has been approved only as a result of statistical test on the procedure, however; Mr. Kelly of The Franklin Institute commented that in discussing pin-to-case and pin-to-pin modes of initiation we should be aware of the possibility that the pin-to-case mode is voltage phenomena and that the pin-to-pin mode is a power or energy phenomena.

Mr. Sheng of Aerospace commented that he has seen a growing tendency by missile manufacturers to accept a one-amp, one-watt criterion without concern for what they are really buying. We should keep in mind that we are seeking RF protection and accept no substitute.

Mr. McGirr asked that if a device fires at 4 amperes DC does this not guarantee that it would be more RF resistant than a correspondingly more DC sensitive device. There was not a direct answer to this question.

Someone suggested that the system needs a more general approach, The pin-to-pin mode represents a low impedance and is subject to inductive coupling. In the pin-tc-case mode the device has a high impedance and is more subject to coupling of a capactive nature.

The inductive coupling is hard to control, but may best be defeated by twisting the leads. Capacitive coupling can best be defeated by shielding. Di- ectric heating of the explosive around the bridgewire presents a problem that needs further examination.

A person from the Air Force Special Weapons Center commented that RF-proof is just a term. We can never make a device completely RF proof, only RF resistant. He commented further that there is no arbitrary environment that can be stated as safe. Enough energy can be found to do the job of inadvertent firing somewhere. The problem will be in establishing acceptable energies for a given job and sufficiently insensitive EED's to withstand the environment. These are the reasons that AFSWC has been against specification of any general level, one-amp or one-thousand amps. Our feeling is that the environment should be included.

A person from AVCO expressed his thinking that it is not hazardous to test an initiator before it is used. If one-amp, one-watt is chosen, it had better pass that specification. Another person voiced his agreement with the speaker except for the statement that capacitive coupling can be corrected by shielding. This may not be true with "worse-case loads" that occur in servicing with shields removed.

Mr. Rosenthal of STL once more objected to 100% exposure of device to one-amp, saying that testing is O.K. for receiving tubes or tuning forks but explosive devices degrade. Mr. Katz suggested that a middle path could be taken by subjecting a sample to the one-amp, 5-minute test and then, the remaining items for only a quarter second; this is a compromise. The effects of the one-ampere exposure could also be examined by a Bruceton technique.

Someone remarked that he failed to see the problem as long as the unit is designed to carry the heat away. He remarked further that the device his company manufactured does not degrade under the one-ampere tests in the slightest degree. This was proved by repeated Bruceton tests.

Mr. Kelly added that The Franklin Institute and NOL White Oak, are both attempting to develop a non-destructive test for individual EED's that will predict the firing sensitivity of individual devices. The input energy or power required for this measurement is no higher than that needed to measure bridge resistance.

Mr. Kelly continued that tests are necessary to determine if the non-destructive test was truly so. Measures of the mean fire sensitivity and standard deviation before and after exposure prove that these was no effect whatsoever in his experience.

Mr. Goldie of The Franklin Institute warned that these tests cannot be applied across the board to EED's. The test will tell whether a particular type of device is sensitive to prepulsing or not; present status of the investigation does not permit a general statement covering all explosive devices.

A person from Douglas Aircraft commented that previous statements have been in regard to initiators having lead azids and lead styphnats and similar primary explosives. He claimed that these materials are obsolete as primary charges now that the one-ampere, one-watt requirement is with us. He also claimed that manufacturers have scrapped all past knowledge and are starting over again. He asked if anyone is attempting to measure the dielectric properties of the one-amp, one-watt explosive material or of those used in EBW initiators.

Mr. Rosenthal of STL mentioned a case in which the same item was purchased by two installations; one required prepulsing, the other did not. These were both tested for RF sensitivity and the results were very different. These are indications of what prepulsing can do. He commented further that his remarks were directed against the 5-minute part of the test.

Mr. Roberts of Ordnance Associates suggested that Bruceton tests be run to determine if the stimulus does degrade the unit in question.

Mr. Benedict of JPL expressed a desire to describe political aspects of the one-amp, one-watt. He said that two or three years ago someone came up with a political solution to the HERO problem by saying let's make initiators one-watt, one-amp and all our problems will be solved.

Numbers of people grasped this like drowning men after the proverbial straw. This concept was politically inspired and not technically sound. It did bring some stability into the industry for a while until technical repercussions came home.

Several alternatives have been proposed and hinted at here this morning. One alternative is going to a particular vehicle by calculation and bench testing, evaluating the environmental effect and squib sensitivity. Another is that every weapon type should be tested at every use site. One more is that every component and assembly should be engineered from the RF standpoint. The one-ampere, one-watt requirement, much like the building code to the construction trade, has done good in reducing the careless use of unduly sensitive initiators.

There are various possibilities with which we are now faced. We can use one-amp, one-watt across the board. This will not afford protection in every case and will cause the use of excess firing energy in some instances. The analysis advocates want to determine theoretically whether or not a device will fire but the commentor's personal belief is that this is impossible.

Elaborate testing is not feasible for missile and space programs that number only a few flights each as opposed to some weapons that may be built by the thousands. He stated that he had asked one of the earlier speakers for an estimate of the time required to check one weapon at one installation. The estimate was 100 weapon hours, 500 engineer hours and 1000 technician hours. The test equipment cost was not discussed. Good engineering entails establishment of the integrity of the design and the professional competance of every man working on a particular scheme.

The commenter said that none of these things alone is a cure-all. He warned against completely abandoning of the one-amp, one-watt criteria. In addition, he stated that he did not want to be driven into tests nor did he believe that engineering analysis is the beginning and end of all RF programs.

Mr. Sheng of Aerospace stated that the person who is buying one-amp, one-watt is missing something. NOL has shown coincidence of DC and RF power up to 5 Mc. Extension of the work to 10KMC might show that one-amp, one-watt does offer RF protection. Until this is done, one-amp, one-watt cannot be specified as RF protection.

Mr. Katz of Rocketdyne mentioned the deadline of 14 months, saying that anything not meeting one of these specs by the time will not fly in national ranges. This applies on a retrofit basis as well. That we like or dislike a particular method does not change the fact that the deadline must be met with one of the methods.

Mr. Waddington commented concerning Mr. Sheng's remarks regarding comparison of DC to RF power. This may have been true for one device but it will be necessary to look further to assure that this is universally true.

Mr. Taiani, of NASA, Cocoa Beach, commented that AMR has advocated the one-amp, one-watt criterion for two and one half years. They waive this requirement under certain circumstances. The environment is important, as Mr. Rawls said this morning. If the environmental tests can be passed use of the device will probably be permitted. Systems and program managers know what they want in the vehicle. Some companies use the one-amp, one-watt criteria, others want to use EEDs tailored to the system and will face the environmental aspects of AMR. He commented further that his problem is not the same as with aircraft carriers and Air Force, high intensity radars. His organization has only two C band radars that are far from the site. Their biggest problem are static and lightning.

A man from Douglas Aircraft mentioned the large amount of work on decreasing the DC sensitivity of EED's. It appears that the DC sensitivity has been reduced a small amount while the RF sensitivity has been reduced by the same small amount. Filters and equivalent circuitry produce large values of isolation but are large in size and difficult to incorporate. System design can produce large isolation with little additional cost, weight or bulk. This program is called electromagnetic compatibility. This program is not only applied to EED's but also to trigger circuits.

Mr. DeMaris of General Electric Co. commented on the long term storage aspects of the composition used in one-amp, one-watt devices. He said that a knowledge of the chemical kinetics of some of the newer compounds has not been thoroughly established and that this does not create great confidence in them.

36. BALLISTIC SYSTEMS APPROACH TO MINIMIZE ELECTROMAGNETIC RADIATION HAZARDS TO ORDNANCE

Space Technology Laboratories, Inc.

H. L. Busuttil
M. Rosenthal

Air Force Ballistic Systems Division

Lt. Col. C. W. Schmidt

1. RELIABILITY AND SAFETY

The prime consideration in the design of a weapon system is the ability of the weapon to deliver its warhead, be it a steel slug or a thermonuclear device, to its target with the maximum reliability consonant with its tactical mission. A single low cost warhead (such as a rifle bullet slug) delivered in a spray pattern need not be as reliable in hitting its target as an ICBM warhead because of its tactical mission, which includes cost, logistics, etc.

There is a second consideration - safety - which most people agree goes hand in hand with reliability. The authors agree with this thesis, provided it has this single clarification: A reliable weapon is a safe weapon but a safe weapon is not necessarily reliable.

For the Air Force Ballistics System Division weapons, maximum reliability attainable under the time schedule and funding appropriated is the prime consideration. Any item serving to degrade reliability must be eliminated (ultimate reliability, of course, is achieved by using no components) unless it is necessary in achieving the weapon system objective.

Much progress has been made with AFBSD weapon systems since the THOR program in achieving this high reliability. Increase in reliability has been achieved by the simplification of design and function rather than by the addition of complex and expensive safeguards. Knowledge accumulated from earlier programs (AFBSD and those of other organizations) has been found to be of inestimable value. Information interchange, although it could be improved tremendously, has resulted in more rapid attainment of reliability at lower cost to the government. These sessions, for example, will return to the government many times the costs incurred in gathering the top caliber of personnel together here. The time saved by weapon systems because of these sessions will be significant.

Into this wonderful single track world of achieving weapon systems reliability came those charging knights in shining armor - our safety personnel - also operating in a single track world of their own. Unlike the result expected from the head-on collision of locomotives on a single track, this clash of the worlds, we are happy to state, has resulted finally in mutual understanding and betterment for all AF weapon system programs.

2. AFMTC RANGE SAFETY

Because of the increasing neglect, by weapon systems designers responsible for ordnance, of the effect of electromagnetic hazards on electrically actuated ordnance initiators and electro-explosive devices (EEDs), EEDs were becoming more and more sensitive. After several incidents at the Atlantic Missile Range and subsequent discussions with range users, AFMTC range safety personnel issued their oft damned, sometimes praised 7 September 1961 "AFMTC Ordnance Standards with Regard to RF Radiation Hazards" in which the 1 ampere, 1 watt no-fire for 5 minutes criteria were established.

The uproar raised by various Air Force divisions and System Program Offices, spearheaded by the authors, was that all the accumulated data on EEDs was being discarded, that the designers were being handcuffed arbitrarily, and that costs would be increased and schedules slipped, among other things. Lt. Col. R. B. Moody of DIG/Safety at Norton Air Force Base even proved mathematically that by assuming:

a. That the EED is immersed in the very strong electromagnetic field density of 100 watts per square meter over the full rf frequency range,

b. That the leads to the EED are exposed and configured as an antenna,

c. That the leads are of a precise length to provide a resonant circuit for the wave length of the electromagnetic field,

d. That the leads are oriented in a three-dimensional space in order to accommodate the polarization and directivity of the EM field,

e. That the EED itself is configured as an antenna load,

antenna configurations most likely assumed by an EED and its leads (half-wave dipols, quarter-wave grounded stub, and short stub, $\lambda/20$, grounded antennas) could deliver 9 1/2, 1 1/4, and 1 1/4 watts, respectively to a one ohm load EED at 250 mc. These conditions, of course, are highly idealized.

The big argument of the anti-range regulation camp was that 1 watt no-fire gave a false sense of security and that the logical way to overcome the hazards of rf radiation was to use techniques designed to destroy EED antenna and antenna transmission line characteristics and use EED's having the largest possible no-fire current compatible with the EED application. The decision as to the approach taken to overcome the specified EMR environment should be left to the weapon system designer.

The giant step forward resulting from the September 1961 AFMTC regulation was bringing to a halt the uncontrolled use of sensitive EED's. Subsequent frequent and often highly heated meetings between range safety personnel and the SPOs brought about an understanding of each others problems. A new set of AFMTC range regulations, acceptable to all AFSC parties - without compromising any of the technical points or design freedom policies - was agreed to by representatives of the AFSC divisions, including AFMTC, at a 12, 13 March 1963 meeting at AFSC Headquarters, Andrews AFB.

The new regulation requires as minimums the use of a 1 watt/1 ampere for five minutes no fire EED or the use of an EED which at all stages of handling and installation must be capable of withstanding a RF power density field of 100 watts per square meter at 50 mc and above and a power density of 2 watts per square meter from 150 KC to 50 mc. The big item which reconciled all camps concerning validity of the regulation for safety was the stipulation that certain firing circuit design requirements must be met regardless of which approach was taken for EED selection.

Whereas it was believed that the worst conditions of RF power density for AFBSD weapons occurred at the test ranges, it has been found subsequently that operational bases occasionally have more severe environments. Thanks are in order for the role of the AFMTC regulation in alerting the SPOs to hazards of EMR to ordnance. It is hoped that missile designers and safety officers come to the realization that we all live in one world. It is hoped we here do not lose sight of the fact that not just rf but <u>all</u> stray electrical energy poses a hazard to ordnance systems.

3. STRAY ELECTRICAL ENERGY

Prior to the 1961 range regulation, the Titan II and Minuteman programs both were aware of the hazards of stray electrical energy to the electro-explosive ordnance systems of both missiles and proceeded to attack them. The STL Program Offices prepared AF Ballistic Missile Exhibits and other design criteria documents to give systems engineering and technical direction to the various contractors on the weapon systems. The preparation of documentation concerning the ordnance items had to be such that each portion of the weapon system having an effect on the reliability and safety of the ordnance firing circuitry would be controlled adequately without needlessly restricting the designer or having an adverse affect on that non-ordnance weapon system portion. Because ordnance items are used widely on these missiles, interfaces between ordnance and other sub-systems were numerous.

Ordnance is considered a black art by other missile sub-systems and, therefore, little thought is given the EED actuation cause and effect by non-ordnance personnel until the missile test flights begin unless the ordnance designers educate themselves and others about the interaction between other weapon system components and the EEDs. For the Titan II and Minuteman programs full-time assignments of ordnance personnel to the Program Offices were made so that ordnance interfaces could be handled before they became problems and so that ordnance detail design and test would run smoothly.

EMR and stray electrical energy effects on EED's were handled by analyzing the reasons for encountering stray energy in EED firing leads and determining experimentation and test work required to determine susceptibility. BSD Exhibit 63-8 is a set of guide lines containing a distillation of knowledge gleaned to date. Some of the primary causes of stray electrical energy determined, but not necessarily encountered on the programs, are (not in order of importance):

a. Static electricity.

This could cause stray electricity in missile wiring from the handling of improperly electrically bonded parts, from missile ionization in flight, or from dust storms, among other things. Kilovolts of peak potential from such causes have been built up and dumped into ordnance and other circuitry with disastrous results. EEDs can and have been set off by the electrostatic discharge from personnel handling EEDs who did not wear conductive shoes or grounding bracelets, who did not ground themselves before handling ordnance, who reached for ordnance leads with probes already charged with static electricity, and in the many other ways in which static charges are built up.

These modes of malfunction by static electricity are handled by requiring compliance with MIL-B-5087A for electrically bonding all metal parts and the missile to its launcher, by providing for static electricity bleeders during flight as necessary, by requiring EEDs not to fire or dud when subjected to electrostatic discharges of up to 200,000 ergs from a 500 micromicrofarad capacitor (charged to about 9000V) under all firing modes, and by procedural and equipment regulations, including use of anti-static straps and conductive coatings.

b. Human Factors.

The possibility of introduction of stray electricity into EEDs or into Electro-Explosive Ordnance Subsystems (EEOS) by personnel actions on and in the vicinity of the EEOS is the major accident factor. After ordnance initiators are mechanically installed or electrically connected, introduction of current generating equipment or hot

instrumentation leads on the weapon system, around umbilicals and ordnance firing circuitry and around the firing console should be forbidden or permitted only under extremely tight, knowledgeable supervision. Good design dictates that a minimum of two human errors, independent in nature, should be able to occur at each EEOS/human interface without ignition. All other weapon subsystems and external environmental stray energy sources should be operating when the evaluation is made. Further, careful evaluation should be made of human factors in conjunction with missile system power mode changes because electric pumps, solenoids, etc. are a major source of stray electrical energy when in the switching mode. The replacement of ordnance initiators with stray energy detectors during tests of missile system power mode change effects on electro-explosive ordnance systems is invaluable in detecting human factor errors.

c. Water Leak Paths and Corrosion.

An unfortunately common occurrance has been sloppy workmanship around misciles which has resulted in moisture entering the wiring to form a conductive path from a hot circuit at one location to an ordnance firing lead at another location. Mysterious accidental firings and duddings have been traced to such causes. Wiring and connectors should be moisture-proof.

"Unless suitably protected, dissimilar metals capable of electrolytic corrosion shall not be used in intimate contact with each other. If dissimilar metals are used, tests must be made for SEEBECK e.m.f. and corrosion to insure system safety." Compliance with this requirement, however, has frequently caused conflict with the

good electrical bonding requirement (conductance of 100 mhos). Both requirements can and must be met simultaneoulsy. There are excellent elsctrically conductive coatings that serve as corrosion barriers and there are numerous mechanical ways to comply with both requirements. Care must be taken that, in meeting the dissimilar metals requirement by insulating metal parts, static electricity vulnerability is not increased.

d. Induced Transients and Circulating Currents.

These two causes of stray electrical energy can be further broken down into many detailed headings. They have been and still are an important source for reports of actuating and dudding EEDs inadvertently. They can be overcome by good design practices but should be checked for their absence by the use of stray voltage or stray energy detectors installed electrically in place of the EEDs when all electrical systems except the ordnance subsystems are operated. These detectors should have the same impedances as the EEDs but should be sensitive enough to detect stray electrical energy A.C. and D.C. which may cause dudding. Stray electrical energy checks should be made on each installed missile, and not just initially for a design check, because human factors probably make each installation different, with respect to stray electrical energy environments.

Design requirements included in BSD Exhibit 63-8 to overcome such causes of stray electrical energy are:

1. EEOS inductance and capacitance both series and parallel shall be kept to a minimum.

2. Isolate ordnance firing circuits physically from other power, control, electronic or other current carrying circuits.

3. Use balanced (ungrounded) two-wire feeder circuits for ordnance systems. Designs should be analyzed to insure that this balance is maintained in all operational system configurations.

4. Control the circuit configuration of these two-wire systems by using methods that maintain the geometrical symmetry between the two wires in the feeder systems. Tightly twisted pairs should be used where possible.

5. The formation of multiple ground paths shall be avoided to preclude inductive stray electrical energy coupling.

It should be noted that any sudden surge of power required from the power supply will cause a transient which either must be lived with without causing malfunction or which must be protected against. Conversely, EEDs are prone to short for either a transient period or for a long period of time after being fired. Accordingly, other weapon system components may be adversely affected and the ordnance designer should issue appropriate warnings so that remedial measures may be taken.

e. Leakage Resistance.

This properly may belong with the discussions in previous paragraphs, but is included separately to mention that, although electrical wiring insulation is provided universally, it is not uncommon

to find missiles with insulation eroded or abraded from the wiring because of physical interference with another subsystem, incompatibility with environmental factors, or because of poor workmanship. BSD requires the leakage resistance between all mutually insulated parts to be at least 100 megohms at a D.C. potential of 500 volts. A study is made of the wiring installations for physical interaction during and after missile build-up and the effects of environment (such as vibration) on the wiring and physical relations with adjacent components or structure are analyzed and tested, if necessary.

f. Circuit Continuity Checks.

There is no reason for permitting the use of EED circuit continuity checkers having an output of more than 25 milliamperes. With the selection of a sufficiently high D.C. no-fire current (1 ampere), it is not expected that any number of EED circuit continuity tests at 25 ma. will degrade the EED. Unfortunately, some unauthorized ohmmeters, ballistic galvanometers and AC operated VTVM's capable of delivering 0.5 amps are available at military installations. Accidents have happened. However, these are caused by procedural errors which should be controlled by the cognisant safety officer who should be guided by very clear and emphatic publications warning about use of unauthorized test gear.

g. Incorrect Wiring.

Incorrect wiring of ordnance firing leads has been done on many programs at various installations. The obvious cures are to minimize the number of connections in wiring circuit, label the wiring clearly, use connectors with polarized pins, lands and grooves

to minimize the possibilities of mismatch, and elimination of spliced cables. Circuit continuity checks should be made to identify leads prior to electrically mating EEDs to them.

h. Electromagnetic Radiation.

There is no need to describe EMR hazards to this group except to state that transmitters are springing up like weeds around the country with one group not bothering to coordinate with another. What BSD/STL originally considered to be chiefly a range problem is now an operation problem as well.

Steps taken to handle the rf radiation problem are discussed herein.

In order to afford maximum design flexibility to the missile designers, certain performance reliability and safety criteria were issued. In the case of the Minuteman missile solid rocket engine igniters and all BSD missile destruct systems, out-of-line powder train rotors are used to insure that, with the rotors in the safe position, accidental initiation of the EEDs would not result in actuating the rest of the powder train.

The basic approach used to minimize the rf radiation hazard (dudding or premature ignition) to both EEDs and EEOS was: (a) to require the use of techniques which destroy EEOS antenna and antenna transmission line characteristics, (b) to require that the EEDs have 1 ampere D.C. for five minutes minimum no-fire characteristics with a 0.9995 reliability at a 95% confidence level, (c) to require that EEDs use wire bridges instead of carbon bridges to reduce susceptibility to peak power, (d) to require that the susceptibility of EEDs to rf radiation power coupled into the bridgewire be determined from 1 to 10,000 mc, and (e) that analyses and

tests be performed to demonstrate ability of the EEOS to survive successfully expected RF environmental conditions.

In close cooperation with the Franklin Institute, which has been found to be one of the most knowledgeable sources on rf radiation - EED interactions information, a test program as follows has been established as the general basic from which to determine rf sensitivity of EEDs.

4. EVALUATION OF RF SENSITIVITY OF EEOS

The minimum procedures discussed below are used by the Titan II and Minuteman programs to determine the extent of the rf hazard to a particular missile circuit. These procedures are offered as candidates for standardized use in validating ability of EEOS in meeting test range and operational environments. Steps in the procedures are as follows:

a. Statistical RF Sensitivity Tests.

The first step is conducting laboratory tests to determine the rf sensitivity of each type of initiator used on the weapon system to application of rf power directly to the input pins, using a closed system in which impedances of source, line, connectors and load are matched to assure maximum transfer of power. The frequency range from below 5 mc to 10,000 mc is explored in at least four bands, using continuous wave forms at all bands to the upper limit of the equipment and using 500 to 1000 pps pulsed wave forms beginning at 2500 mc. Where the upper power limit of the equipment is reached without EEDs firing when using the continuous wave form at any frequency band, then the pulsed wave form should be used. Power application should be controlled and should last 10 to 15 seconds.

Either the Bruceton or Probit Plans should be followed. From the data generated in these tests, curves should be calculated and plotted for average power vs frequency at the 0.999, 0.500, and 0.001 firing probabilities at the 95% confidence level. The CW data probably will form a smooth, continuous curve whereas the pulsed data probably will fall on a separate curve.

b. Pin-To-Case Mode RF Sensitivity Tests.

It has been noted that certain initiators (such as the U. S. Flare Model 207A squib) are more sensitive to rf power in the pin-to-case mode than through the bridgewire circuit at certain frequencies. Accordingly, it has been found necessary to test initiators with rf power applied in the pin-to-case mode at the 0.999 firing probability level determined from the pin-to-pin rf susceptibility tests. Greater susceptibility in the pin-to-case mode is the exception, rather than the rule. Consequently, a two initiator test (using initiators not fired in the pin-to-pin mode) at each frequency band generally is sufficient.

c. RF Dudding Sensitivity Tests.

An important, but much neglected, aspect of hazards to ordnance from EMR isdudding EEDs by the application of EMR at levels below that required for actuation to EEDs for extended periods of time. Dudding occurs when bridgewire temperatures or pyrotechnic temperatures are raised to a critical point where chemical decomposition or physical degradation is initiated and then held at or above these temperatures for extended time periods. Two methods employed to determine initiator

dudding characteristics are: (1) Determine the critical pyrotechnic temperature versus time relationship and then determine the dc or rf electrical power input required to raise the bridgewire or pyrotechnic composition to the critical temperature corresponding to the time period of interest; (2) Experimentally determine the dc and rf electrical power inputs versus time which will cause the EED to change performance significantly. Pulsed power as well as continuous wave power should be employed.

d. Measurement System Calibration.

In these tests, rf power is applied through the bridgewire of the EED in a closed system using coaxial cables or wave guides to connect the rf generator and initiator. No rf should be permitted to radiate from the system or to be received by the EED from external sources. The impedances of the transmitter, the transmission line and connectors, and the EED should be matched closely to permit maximum power transfer. To compensate for expected mismatches, some tuning device is required. However, at the higher frequencies the losses in the tuning device and the transmission line to the EED are substantial because of the high voltage standing waves and the correspondingly high currents. The system, therefore, should be calibrated to determine the extent of the losses and the test results should be corrected accordingly.

e. DI Bruceton Analyses.

In order to have a statistical standard of comparison for the rf power susceptibility tests discussed herein, it is essential that

Probit or Bruceton tests to determine sensitivity to dc be conducted. Data should be obtained over a range of current levels and pulse times to afford maximum information for rf test control purposes and for the firing circuit designers.

f. Pulsing Information Tests.

It is not feasible to conduct rf tests over the entire frequency spectrum using pulse modulated transmitters and various pulse times and repetition rates. Because pulsed transmitters usually have peak power about 1000 times their average power, it is possible that an EED might be more sensitive to pulsed rf than to continuous wave rf. The much greater power in a short pulse may cause rapid heating of the bridgewire and, if the time until the next pulse is short compared to the cooling time of the bridgewire, repeated pulses will result in "thermal stacking". This may cause the EED to fire at average power levels that are lower than those for the continuous wave method of applying power. In order to obtain qualitative data with regard to these effects, the dynamic resistance (the rate of change of resistance and rate of change of bridgewire temperature increase with respect to current) and the thermal time constant (the rate at which the bridgewire system cools) should be measured.

g. Lead Wires, Connectors and Assembly Tests.

Because almost all initiators are used in conjunction with other components to form an assembly, it is essential in validating rf sensitivity of EEDS to determine the rf susceptibility of each individual EED and its associated assembly and circuitry. Normally,

adding components to the initiator provides shielding and attenuation which increase greatly the level of rf power which can be withstood safely, as compared to the initiator alone. Tests are conducted with assembled units in which the initiator is replaced with an instrumented simulator having the same impedance as the initiator. RF energy is pumped into the system at various points where rf might conceivably enter under normal service. The rf energy is injected in a closed, matched system and the incident power is measured accurately. Comparison of the incident power and power reaching the initiator gives an indication of the degree of attenuation or safety margin provided by the additional components. Measurements are made at several frequencies over the rf spectrum.

h. Assessment of Susceptibility.

Having determined experimentally the rf sensitivity of the EED and the degree of protection afforded by the other components and circuitry with which the EED is used, the next step is to derive ideal antennas based on information gathered from range safety personnel, system designers, and - it is hoped - a central rf information library to be established in the near future. With this information, it is possible to calculate the minimum rf field intensity which conceivably could present a hazard to the particular EED involved. This value then would be compared with the expected environments at the test ranges and operationally.

Examination of possible receiving antennas associated with the EED should be examined first so that any wiring changes that obviously

need to be made can be done at an early date. The concurrency concept makes early action an economic necessity. Long unshielded leads might act as rhombic, loop, dipole, or long wire antennas and be effective in absorbing rf energy from the environment and transferring it to the EED. Criteria now applicable to AFBSD programs, of course, are designed to preclude unshielded lead wires, and wiring configured as effective antennas.

However, it is necessary to analyze the lead wire configurations and determine the possible ideal antennas that can be made and then calculate their maximum effective apertures. The maximum effective aperture multiplied by the rf field power density gives the maximum rf power that could be received by the EED. The rf power actually reaching the EED bridgewire will be reduced by the amount lost in the transmission line, associated circuitry components, and the initiator plug If the calculated amount of rf power (backed up by obtainable experimental data where necessary) actually reaching the bridgewire is lower than the rf power for the 0.001 probability of initiation with 95% confidence level of the basic initiator, then it can be concluded that the EEOS is safe in the specified rf field power density environment.

The EED must be evaluated under conditions expected during handling, processing, transport, storage, and during and after installation.

The AFMTC has already prepared forms to be employed by range users to validate the safety of EEDs and EEOS under AMR guaranteed rf field intensity environments. As was mentioned earlier the environments are:

a. From 150 kc to and including 50 mc, the field intensity is 2 watts per square meter or 28 volts per meter.

b. From 50 mc to 40,000 mc, the field intensity is 100 watts per square meter or 194 volts per meter.

AFMTC will require users to plot relative DB above or below a zero DB reference level as the linear ordinate scale on semi-logarithmic paper versus frequency as the logarithmic scale. The DB values will be calculated as:

a. From 50 mc and Below: $DB = 10 \log \frac{P}{2}$ or $DB = 20 \log \frac{E}{28}$

b. Above 50 mc: $DB = 10 \log \frac{P}{100}$ or $DB = 20 \log \frac{E}{194}$

Positive DB values will indicate EED susceptibility to rf fields greater than specified at AFMTC and negative DB values indicate EED susceptibility to rf field less than those specified at AFMTC.

It is believed similar criteria are required for all operational and test environments to which EEDs will be exposed.

5. FIELD APPLICATIONS

After employing the best available design means for protecting EEOS and EEDs from stray electrical energy, including rf, it is essential to determine (a) whether sloppy fabrication techniques or improperly fabricated parts themselves for each individual weapon have not introduced some new stray energy problem (items such as wiring errors, improper bonding, grounds, shorts, unexpected transients, etc.), and (b) whether the environmental conditions on which the design has been based have not been underestimated or been changed adversely (unexpected interactions when communications links are activated, ground reflections, etc.).

The means employed to answer these questions must include tighter quality assurance provisions and actual tests at the test and operational sites. The ability to employ tight quality assurance controls must be a consideration in the design of components and assemblies. Actual tests in the field include the obvious such as: EED circuit continuity checks, firing lead circuit continuity checks, and checks to determine that firing circuitry leads are dead prior to electrical connection of EEDs. BSD weapons are checked for stray electrical energy by means of stray energy or stray voltage detectors electrically installed in place of the EED initiators to determine if a predetermined stray voltage is detected in the EED firing leads when the electrical energy generating equipment is turned on during missile and launch verification exercises. Such procedures are followed on other than BSD programs, of course.

Because Murphyisms can occur on a random basis, however, it is good practice to perform this stray energy check on every missile after installing the missile at its site or launch platform.

It should be noted that, in order to obtain stray energy or stray voltage detectors which are more sensitive to EMR fields than the EED initiator for which they are substituted, pyrotechnic actuated detectors usually have bridgewire resistances greater than the EED initiator. It is desirable to duplicate the EED initiator bridgewire resistance and still have the stray energy or stray voltage detector more sensitive - to a predetermined and logical degree - than the EED. Non-pyrotechnic operated stray energy detectors, such as those produced by Hughes Aircraft and Assembly Engineers, can perform in this manner. The advantages of non-pyrotechnic actuated stray energy detector are that they pose no explosive hazard and can be tested and reset without renewing them and can be reused.

In order to keep designers abreast of EMR environments expected to be encountered, it would be useful for "electrodetic" maps to be made and kept up to date - where feasible - of the test ranges and military bases where EEDs are employed. GEEIA performs such services when requested for Air Force installations and, no doubt, other agencies do this for the other services. However, it is important that the weapon system program offices have this information throughout the design phase so that they know if the EMR environment in which the weapon must sit or through which the weapon must fly is different from what was expected. The national test ranges do provide such information when requested.

6. TRIGGER CIRCUITS

The study of Ordnance hazards should not be limited to the inadvertent initiation of an electro-explosive device by means of electromagnetic radiation. It is one of the purposes of this paper to emphasize the most critical hazard, the susceptibility of the electronic triggering circuit.

Electronics has seen some remarkable advances in the last ten years, with the advent of the fast switching transistor, silicone controlled rectifier and sensitive switching relays. The trend has been toward faster response time, lower power consumption and extreme compactness. Then to further complicate the susceptibility problem, digital computers and programmers have been developed that can respond to switching signals in milli-microseconds at extremely low power amplitude. It has been through these advances that our long range missiles have been made possible. But these very characteristics have complicated the problem of protecting ordnance systems from premature initiation.

There have been a number of instances where the electronics system was caused to malfunction by electro-interference, consequently initiating ordnance devices prematurely. The average power required to fire an ordnance initiator, squib,

in a conventional ordnance system is about a 1/4 watt for one millisecond. On the other hand, most triggering circuits can be initiated by a pulse-gate transient with much less power with a duration measured in microseconds. The susceptibility of the electronics in an ordnance firing circuit has now passed that of the initiator and now requires the close scrutiny of the systems engineer to establish that the proper isolation, shielding and good design is used in the firing circuits. The ever increasing power densities that are being produced by high-power radar are indeed demanding that the environmental requirements for these systems be raised.

Another contributor to the ordnance system hazard is the electrostatic charge developed by our new solid propellant boosters. The phenomenon of an electrostatic charge that is developed by the hot droplets of metallic oxides impinging on the exit nozzles, has caused some very high arc discharges to occur between isolated pieces of metallic structure in a booster. The electro-interference caused by this phenomenon has affected the guidance systems of some vehicles. The same vehicle contained some 1 amp no-fire initiators which were not directly affected by the interference. This again proves that our electronics systems are the weak links. Other surveys have also proven that the electronics were more susceptible to R-F pulse radiation than the initiator.

Therefore, as a result of this increased awareness of the weakness, STL has established the viewpoint that the ordnance system must be an integrated design with the major objectives being reliability and safety in the expected environment. This requires the complete analysis of an ordnance design to determine its susceptibility to the electromagnetic hazards. The enforcement of these design objectives is accomplished by the issuance of an ordnance design criteria which includes the ground rules for safe electrical, electronic and ordnance design. Grounding and shielding

criteria with verification tests are also included. Furthermore, the implementation of the design objectives demands a constant surveillance of the design especially in the new space and ICBM systems which are utilizing ordnance functions in ever-increasing numbers.

7. INFORMATION AGENCY

This paper has indicated that there is no single cause or cure for all electromagnetic radiation hazards to ordnance any more than there is a single cause or cure for war, worry or women. Although the problem of EMR hazards is complex, it has been worked on by many government and private agencies for many years. It is wasteful of time and money if the experiences of all those participating in the HERO field are not available readily to neophyte and veteran alike. The solid and liquid propellant rocket fields each have a central information agency which gathers data, abstracts data and publishes the abstracts, distributes reports, serves as a central library and serves in the capacity of arranging periodic meetings of groups and committees.

The SPIA and LPIA are agencies sponsored by the Army, Navy, Air Force and now, probably, NASA as joint funding ventures under the cognizance of one of the Department of Defense agencies. Such an information agency is needed in the HERO field.

Under such an agency, a catalogue of all electrically actuated ordnance initiators could be prepared which would enable designers to take advantage readily of the current state-of-the-art. A form requiring all pertinent performance and safety information for ordnance initiators and the like could be prepared which military and NASA contracts could state must be filled out by the vendor. It is true that some agencies now require and publish such information, but <u>all</u> agencies do not do so. The information agency concept, if followed, should make such action mandatory.

Cross-fertilization of ideas and experiences, such as is occurring at this meeting, is essential to rapid progress. By being the funnelling and distributing central point for all information regarding HERO and other stray electrical energy hazards to ordnance and their trigger circuitry, the required cross-fertilization could be achieved through a central information agency.

8. CONCLUSION

The authors would like to reiterate several points:

a. The EMR hazards to ordnance problem should not be confined to the effects of rf radiation on EEDs but should be expanded to consider hazards from all stray electrical energy on electro-explosives ordnance systems - including trigger circuits.

b. The rf hazards to ordnance problem is primarily an antenna and antenna transmission line problem and the optimum solutions lie in the direction of destroying EEOS antenna characteristics, employing filters and attenuators in the circuitry, and using the least current sensitive EED initiators. There is no universal panacea. Each missile is a problem unto itself and the solution requires use of open, informed minds.

c. It is essential that the rf and d.c. sensitivity of all EED initiators be determined by themselves and in their assemblies so that it is possible to determine the EMR environment to which they may be exposed and the auxiliary means required, if necessary, to protect them.

d. It is necessary that any criteria established provide weapon system designers with maximum design latitude but also with well defined environmental requirements and means of validation. Early definition of stray energy environment, although not completely accurate, is preferable to too late a more accurate definition of environment.

e. It is important that field tests be conducted for each installation to ensure against the presence of unacceptable levels of stray electrical energy in the EEOS under the most adverse expected test or operational conditions.

f. Full use of statistics and random sampling techniques is required in order to conduct evaluations economically. Those not believing in random sampling should give up all their blood for analysis the next time they visit their doctor.

g. Establishment of an impartial central information agency to serve all military, space and air traffic agencies is recommended to enable maximum use of information developed in the field of stray electrical energy hazards to ordnance systems.

36. DISCUSSION

Mr. Cormack pointed out that the Navy has put a great deal of effort forth in developing WR27. This document, a design plan to preclude electromagnetic hazards, has been circulated to Army, Navy and Air Force Activities for consideration as a MIL standard. The Air Force replied first, suggesting that we hold off publishing this as a MIL standard until they could come up with enough information to comment on it. The second reply was from Frankford Arsenal who spoke for the entire Army. Not all of the papers sent out have been returned. This document attempts to serve as a guide for weapons designers and contain all of Commander Gray's statements plus the results of studies in this country.

Mr. Cormack commented further that the results represent a three-year effort inside the Navy and that the document is now crossing the Services boundary. Some new requirements have been brought up as a result of requirements peculiar to Army and Air Force problems. These certainly should be considered but it is along, slow process.

Mr. Rosenthal thanked the Navy for this contribution and commented

that the Air Force has had internal disputes with the Atlantic Missile Range which resulted in mutual agreement. The AMR requirement has been accepted and has actually been extended because of more severe requirements elsewhere. It is hoped that once the Air Force has its own house straight that coordination will be possible with the Army, Navy and NASA. The present document must not include too many hard and fast mandatory criteria because each weapons system has its own individual problems. Its nature should be: here's advice, here are some mandatory things, here's a standard set of tests and so forth. Within a year we hope to have this document.

Mr. King commented that he has been connected with the work since 1946 and that his organization (NASA, Cocoa Beach) feels that the Franklin Institute is doing what probably is the best work in this field.

He commented further that he and probably others are bothered by the fact that every two or three years a fresh wave of experts come in and shout their answers on the same old bulwarks. Then we regroup and assemble our forces and go back to what we have contemplated: good clean circuitry, shielding, grounding, bonding and so forth. We did this in Army circuit designs back in 1946. We seem at beating ourselves to death without showing any gain. Mr. King asked if there are any break-throughs or new scientific approaches that will eliminate problems other than good circuit design techniques, shielding and wave traps. He asked if there were any new hopes on the horizon.

Mr. Rosenthal admitted that this kind of work can be frustrating. He explained that the job of moving from research and development to production is painfully slow. Sometimes frustration creates anger and angry people sometime accomplish results. As in warfare, some good comes from the results of heated discussion. Red tape and empire building that are characteristic of a democracy also tend to slow progress.

A man from Patrick Air Force Base commented on the AFMTC policy saying that he had contacted a well-known ordnance manufacturer who commented that there is no need to worry about amperage or wattage only keep the temperature of the mix below 140°F and there will be no problem. He commented further that astronaut Cooper's Mercury capsule reached 160°F inside. If the engineer supplying this information built all the items for this capsule, Cooper would not be with us today.

A man commented that AMR expects complete compliance to several directives including one-amp, one-watt or alternatives. He questioned whether any agencies existed that have procedures which can be used and which AMR will accept by the complete RF environmental testing route.

Mr. Rosenthal answered that a procedure exists now for the Minuteman Missile that has been submitted to the Cape. We are trying to get the accepted method published for industry. AMR wants the validation program submitted and approved before any money is spent. The program we have on Titan II and the Minuteman are basically similar. It is a Franklin Institute program which AMR has reviewed and accepted as a valid test program. The first results need to be looked at however, not only analysing the EED, but the complete circuit. The Titan II test program should be completed by October. We are trying to get the Franklin Institute to analyse circuits and present data. These analyses will include a connector type EED and one with pigtails.

Mr. Weintraub of AVCO commented that everything we now send into space must be sterilised at 135°C. This must be survived before the device get off the ground. This requirement will probably outstrip existing science and may require something new in the place of existing, old-fashioned EED's.

Mr. Teres of General Electric commented that the one-watt, one-amp requirement by inference specifies a one ohm bridge. He has been using a device on Titan with a resistance of 0.2 ohms. He asked if the five-fold increase in bridge resistance would not increase the hazard.

Mr. Rosenthal answered that there is a study by Lt. Col. R. B. Moody (paper no. 54) that indicates only a device with an impedance of zero or infinity would offer complete protection in an antenna circuit. As a general rule increasing the resistance may make the EED impedance closer in value to that of the source (antenna) impedance and therefore make the system more RF susceptible.

Mr. Warren of Douglas Aircraft asked if any problems had arisen from RF radiation from nuclear bursts. Mr. Rosenthal commented that this question was not of the scope and security classification of this meeting.

39. DISTRIBUTION OF RF FIELDS ON CARRIER DECKS

by E. H. Smith

E. H. Smith and Company, Inc.

It is the intention of this paper to give only the briefest summary of the theoretical work from which rf fields on the deck of an aircraft carrier are computed, reserving for the appendix the detailed mathematical derivation of the solution. Here, we shall be more concerned with how accurately the theory predicts the actual carrier deck fields.

The whip and monopole antennas on an aircraft carrier are located at the edge of the catwalk which runs along the flight deck of the carrier. Thus, we remark that the chief disturbing influence on the antenna fields is the deck edge itself and that this edge behaves more nearly like the edge of a half-plane than any other simple geometrical shape. Consequently, we shall be interested initially in the field of an electric dipole as modified by the presence of a perfectly-conducting, semi-infinite plane.

The problem can best be formulated using a cylindrical coordinate system, with the z-axis taken to lie along the edge of the half-plane. The dipole antenna shall be located at a point P with coordinates ρ_o, ϕ_o in a polar coordinate system in the z = o plane, as shown in Figure 1 below. The perfectly conducting half-plane is taken to coincide with the semi-infinite surface defined by the equation $x' \geq 0$.

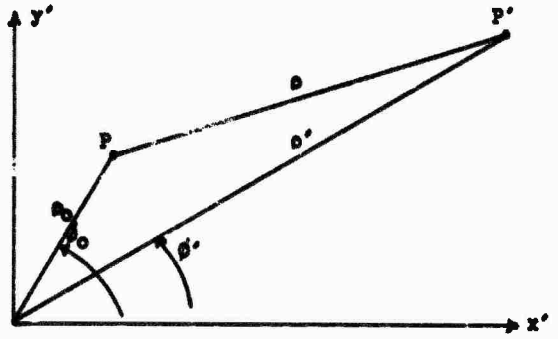

Figure 1: The z = o plane

We shall wish to determine the electric and magnetic fields at a point in space having coordinates ρ', ϕ', z. Note that point P' is the projection of this point onto the z = o plane.

Two series expressions, from which one can obtain the vector potential of the total field, are given below. The notation used in these expressions is standardized in the literature, and since the terms are all well defined in the appendix the definitions will not be repeated here.

$$\psi_1' = 1/2 \int_o^\infty \sum_{m=o}^{\infty} \epsilon_m J_{m/2}(t\rho_o) J_{m/2}(t\rho') \cos\left[\frac{m}{2}(\phi' - \phi_o)\right] \frac{e^{-z\sqrt{t^2 - k^2}}}{\sqrt{t^2 - k^2}} t\,dt$$

$$\psi_2' = 1/2 \int_o^\infty \sum_{m=o}^{\infty} \epsilon_m J_{m/2}(t\rho_o) J_{m/2}(t\rho') \cos\left[\frac{m}{2}(\phi' + \phi_o)\right] \frac{e^{-z\sqrt{t^2 - k^2}}}{\sqrt{t^2 - k^2}} t\,dt$$

These series solutions contain the complete set of eigen functions for the diffraction problem. It should be noted that one forms a solution to the problem of a dipole oriented horizontally above the semi-infinite plane (Dirichlet problem) by taking the linear combination $\psi_1' - \psi_2'$ as the expression for the Herts vector potential; while a solution to the problem of a dipole oriented vertically above the horizontal semi-infinite plane (Neumann Problem) is obtained by taking the linear combination $\psi_1' + \psi_2'$ as the expression for the Herts vector potential.

It can be shown that these series expressions are identical with the diffraction integrals first given by Carslaw and later simplified by Mac Donald, which in turn have been shown to satisfy the wave equation. The series expression ψ_2' can be shown to possess no singularities anywhere, while the series expression ψ_1' approaches $\frac{e^{ikR}}{R}$ as the distance from the

point of observation to the dipole (R) decreases to zero. In addition, by using the diffraction integrals, it can be shown that various limiting cases such as the plane wave excitation of a half-plane fall out of these solutions. These facts should be ample to demonstrate the validity of the solutions obtained.

For the special case of the dipole oriented along the x'-axis where $\phi_0 = 0$ - i.e., the dipole assumes the position taken by the horizontal whip antenna - the electric and magnetic fields along the deck have the very simple form:

$$H_{z'} = \frac{i\omega}{\rho} U$$

$$E_{\phi'} = \frac{\partial}{\partial \rho'} \left(\frac{U}{\rho'}\right)$$

$$\text{where } U = \frac{ik\sqrt{\rho_0 \rho'}}{R} H_1^{(1)}(k R)$$

This result is very pleasing from both a theoretical and a computational standpoint.

For other orientations and locations of the dipole, the series expressions, ψ_1' and ψ_2', are useful for near field computations since one may approximate to $J_\nu(t\rho')$, which is contained in the integrand of expressions ψ_1' and ψ_2', by the first term in its Bessel function series, i.e.,

$$J_\nu(t\rho') \approx \frac{\left(\frac{t\rho'}{2}\right)^\nu}{\Gamma(\nu+1)}$$

and this approximation is used for $\rho' < \rho_0$. When $\rho' > \rho_0$, the opposite approximation is used, i.e.,

$$J_\nu(t\rho_0) \approx \frac{\left(\frac{t\rho_0}{2}\right)^\nu}{\Gamma(\nu+1)}$$

In either case, the indicated integration can be carried out using an integral given in Watson's "Bessel Functions". One of these

approximations or the other will always be available so long as either ρ' or ρ_0 is small compared to the wavelength.

Once our expression for the elementry dipole field is obtained the fields produced by a whip or monopole antenna can be found by integrating over the effective length of the antenna, using the appropriate antenna current distribution as a multiplier of the dipole fields in the integrand.

Calculations were carried out for an antenna in a vertical position at the deck edge. The antenna was operating in a quarter wave length mode of excitation at about 3 Mc. Calculations were made for one watt output from the transmitter with an assumed radiation efficiency of 50%. Results are shown in Figure 2.

One should note that the calculated field is of the order of 0.10 volts/meter near the far edge of the deck. The effect of reflection from the far edge has not been put in, but this effect is not large in this case except for distances a few feet from the edge. The field fall-off in the theoretical calculation along the near edge is rather rapid and, as we shall see later, the measured fields at the near edge fall off more slowly. There is some evidence that the aircraft carrier catapult slots affect the fields although, theoretically, one would not expect this effect to be large. The catapult slots are located between the centerline and port side of the ship and, starting near the base of the monopole antenna, run forward parallel to the landing area. It appears that, perhaps, the catwalk may be the major geometrical feature

which has been left out of the calculation. It is planned to add a first order correction for the effect of the catwalk in a crude way by estimating the normal component of H at deck level over the catwalk from potential theory, deriving tangential E over the catwalk, and then obtaining the first order perturbation to the normal electric field on the deck due to presence of the catwalk. This correction will not be entirely satisfactory but it will, at least, show whether our surmise as to the effect of the catwalk is correct.

It might be added that the effect of the far edges of the deck can be estimated rather accurately by the same method used to calculate the effect of the near edge. This correction for the far edge will be most important for the whip antennas located on the narrow deck section near the bow.

In Figure 3, we have the measured fields. The comparison between experimental and calculated values is good as we go across the deck from the antenna, the field falling to 0.10 volts/meter at about the same place as in the theoretical calculations. As mentioned before, the comparison is not so good in the field behavior close to the near edge of the deck. The inclusion of an approximation for the effect of the catwalk will, perhaps, improve the result. Reflection of the field from corners in the deck outline can also be considered and taken into account to a first approximation.

In addition, we note that the large aircraft carrier at sea cannot be expected to provide an environment in which measurements of accuracy can be made. One cannot interfere with necessary shipboard operations

to any extent and further, even if one could, the large distances involved preclude the use of all the experimental checks which one would wish to make, at least in any reasonable length of time. These considerations are the consequence of the essential difference between operational conditions and small scale controlled laboratory conditions.

Our greatest concern in making these calculations was to get a good comparison of the size of the vertical electric field for a vertical antenna as against the size of the same field for the same antenna in a horizontal outboard position. As you know, we can use antennas in the vertical position only for ground plane measurements whereas the horizontal antenna position is the position normally used when the fleet is underway.

In Figure 4 we show the computed normal electric field for the same antenna in the horizontal outboard position under the same condition of radiated power. In general, the calculated field strengths are lower by about a factor of twenty. Further, without going into details, it seems reasonable that the effect of the catwalk will be small in this new field configuration. We hope at a later time to have a scaled laboratory deck plane on which the fields of horizontal and vertical antenna configurations can be measured. This will provide a useful experimental check. For the present, however, it appears that one can say with considerable confidence that the horizontal configuration does indeed give lower fields by about a factor of twenty over most of the deck.

Before closing, I wish to again call attention to Figure 2 which shows the calculations for the vertical antenna. Across the deck, where the field for the horizontal antenna was about 0.005 volts/meter, we note that the field of the vertical antenna is about 0.10 volts/meter. Very close to the antenna, the differences are not so pronounced. For most of the deck area, however, we would expect the field of the horizontal antenna to be much lower, and this would include the region of the catapult.

We are aware that the calculations do not, and cannot, include all of the small irregularities which are actually present on board ship. Any comparison between measured and calculated results is, of course, quite sensitive to how close the measurement was taken to the deck edge or to any other small irregularity such as the catapult slots, stanchions, or to other inert antennas. We were looking for an average comparison of field strengths under the two conditions, with the feeling that corrections for some of the local obstacles and irregularities could be made if such improvements in the calculations seemed useful.

Finally, for those who are interested in the mathematics of the situation, a few remarks about the mathematical differences between the calculations for the vertical antenna and the horizontal antenna are of interest. In the case of the vertical antenna, the total field on the deck is first made up of 1/2 the field of the antenna and its image as these would appear for an infinite plane. The rest of the field arises due to the fact that the plane is not infinite and the antenna is at the edge of a semi-infinite plane. In the case of the horizontal antenna, however, the antenna field and its image field, as viewed for an infinite plane, exactly cancel, and we are left with the odd terms in the series expression only. This difference is, perhaps, the major theoretical difference between the two cases.

Figure 2
Contour Map
Monopole Antenna
3.395 Mc

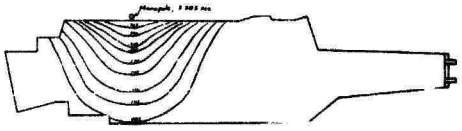

Electric Field Normal to the Deck in volts/meter for a Reading of One Watt at the Transmitter Output Meter (50% Radiation Efficiency)

Figure 3
Contour Map
Monopole Antenna
3.395 Mc

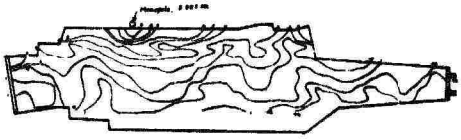

Vertical Component of the E Field (V/M) for One Watt Radiated Power

Figure 4
Contour Map
Monopole Antenna
3.395 Mc

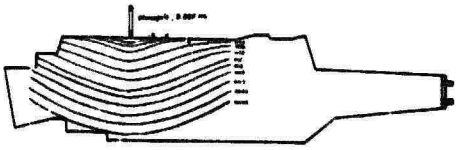

Electric Field Normal to the Deck in volts/meter for a Reading of One Watt at the Transmitter Output Meter
(50% Radiation Efficiency)

DISTRIBUTION OF RF FIELDS OVER A CARRIER DECK

by E.H. Smith
E.H. Smith and Company, Inc.

The whip and monopole antennas on an aircraft carrier are located at the edge of the catwalk. The general geometry of the deck edge resembles the edge of a semi-infinite plane more than it does any other simple geometry. Thus, we shall be interested in the fields of antennas as modified by the deck edge which we shall treat, for the first approximation, as the edge of a thin plane.

In the discussion to follow, we shall connect a series expression for the field with some diffraction integrals first obtained by MacDonald (Ref. 1) by reduction of some infinite integrals due to Carslaw (Ref. 2). We shall then present calculations for the monopole antenna in the horizontal outboard position.

The paper would be much too long if we included calculations for vertical antennas. Hence, we limit the presentation here to the horizontal case together with a few remarks on use of the series solutions to calculate vertical antenna fields.

PART I

THE FIELD OF A DIPOLE ABOVE A SEMI-INFINITE PLANE

We wish to look at the problem of an electric dipole above a semi-infinite plane of infinite conductivity.

The coordinate system chosen for the problem is shown below.

Figure 1.

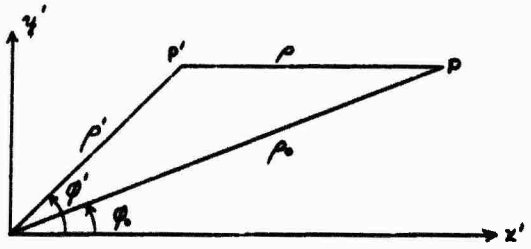

The edge of the semi-infinite plane is put at $x' = y' = 0$ and it lies along the z-axis, which is positive normal to the paper. The dipole is located at point P with coordinates ρ_0, φ_0 in a polar system in the $z = 0$ plane. ρ', φ' form another polar system in the same plane. We wish to express the dipole Hertz vector in terms of the (ρ', φ', z) coordinate system. The dipole may be obtained either normal to the plane or parallel to the plane.

Now, if $\hat{\imath}_\ell$ is a unit vector along the dipole direction, the Hertz vector of the dipole field is

$$\underline{\Pi} = \frac{-Id\ell\,\hat{\imath}_\ell}{4\pi i\omega\epsilon_0}\,\frac{e^{ikR-i\omega t}}{R} \tag{1}$$

where

I = the current amplitude

$d\ell$ = the dipole length

R = the distance from the dipole

ω = angular frequency

ϵ_0 = dielectric constant for free space in the MKS system.

The electric field is given by

$$\underset{\sim}{E} = \nabla(\nabla\cdot\underset{\sim}{\Pi}) + k^2\underset{\sim}{\Pi} \tag{2}$$

and the magnetic field by

$$\underset{\sim}{H} = -i\omega\epsilon_0\nabla\times\underset{\sim}{\Pi} \tag{3}$$

with

$$k = \frac{\omega}{c}$$

First, we take the scalar quantity $\frac{e^{ikR}}{R}$ and express it in the (ρ', φ', z) system. Watson* (Ref. 3) gives the integral

$$\int_0^\infty J_0(bt)\frac{e^{-a\sqrt{t^2-y^2}}}{\sqrt{t^2-y^2}}\,t\,dt = \frac{e^{\mp iy\sqrt{a^2+b^2}}}{\sqrt{a^2+b^2}} \tag{4}$$

The value of $\sqrt{t^2 - y^2}$ is defined so that $\sqrt{t^2 - y^2} > 0$ for $t > y$ and the sign of the exponential on the right is determined by whether the contour passes above or below the branch point at $t = y$. Thus, the positive sign is chosen in the expression on the right if the contour looks as follows:

Figure 2.

Thus, in our case we set

$$\frac{e^{ik\sqrt{\rho^2+z^2}}}{\sqrt{\rho^2+z^2}} = \int_0^\infty J_0(\rho t)\frac{e^{-z\sqrt{t^2-k^2}}}{\sqrt{t^2-k^2}}\,t\,dt \tag{5}$$

* This integral was used by Sommerfeld in a discussion of propagation of waves over the earth. This work is summarized in Ref. 4.

with the contour chosen as shown above. Now, setting

$$\rho^2 = \rho_0^2 + \rho'^2 - 2\rho_0\rho' \cos(\varphi' - \varphi_0)$$

and using the addition formula for Bessel functions, we have

$$J_0(\rho t) = \sum_0^\infty \epsilon_m J_m(\rho_0 t) J_m(\rho' t) \cos m(\varphi' - \varphi_0) \tag{6}$$

where

$$\epsilon_m = 1, \; m = 0; \quad \epsilon_m = 2 \text{ otherwise.}$$

Thus, in the (ρ', φ', z) system,

$$\frac{e^{ikR}}{R} = \int_0^\infty \sum_0^\infty \epsilon_m J_m(\rho_0 t) J_m(\rho' t) \cos\left[m(\varphi' - \varphi_0)\right] \frac{e^{-z\sqrt{t^2 - k^2}}}{\sqrt{t^2 - k^2}} \, dt \tag{7}$$

Now, if we set

$$\psi(\rho', z, \varphi' - \varphi_0) = \int_0^\infty \sum_0^\infty \epsilon_m J_{m/2}(\rho_0 t) J_{m/2}(\rho' t) \cos\left[\frac{m}{2}(\varphi' - \varphi_0)\right] \frac{e^{-z\sqrt{t^2 - k^2}}}{\sqrt{t^2 - k^2}} \, dt \tag{8}$$

we would guess that the expressions

$$\psi(\rho', z, \varphi' - \varphi_0) \pm \psi(\rho', z, \varphi' + \varphi_0) \tag{9}$$

would be solutions to the problem. The combination in (9) with the positive sign would satisfy boundary conditions for a dipole oriented normal to the plane and the combination with the negative sign would be correct for a dipole in one of the two horizontal orientations. Further, we note that when m is even in (8), we get back our original field and when m is even in (9), we get the original field plus the reflected field. One would think, then, that (9) would be the solution to the problem. This conclusion turns out to be correct, except for a multiplying factor of one-half. The result is not, however, nearly as obvious as it seems at this point. The crux of the matter is whether the terms for odd m in (9) result

in a field which is free of singularities, particularly at the dipole position. Thus, we proceed by looking at the terms, m-odd, in (9). We set

$$\psi_i = 2\int_0^\infty \sum_0^\infty J_{n+\frac{1}{2}}(t\rho_0) J_{n+\frac{1}{2}}(t\rho') \cos\left[(n+\tfrac{1}{2})(\phi'-\phi_0)\right] \frac{e^{-z\sqrt{t^2-k^2}}}{\sqrt{t^2-k^2}}\, t\,dt \qquad (10)$$

We shall need several expressions, mostly taken from Watson (1915). Thus, we shall use

$$\int_0^\infty J_{n+\frac{1}{2}}(bt) \frac{e^{-a\sqrt{t^2-y^2}}}{\sqrt{t^2-y^2}}\, t^{n+\frac{1}{2}}\, dt = i\sqrt{\frac{\pi}{2}}\, b^{n+\frac{1}{2}} \left(\frac{y}{\sqrt{a^2+b^2}}\right)^{n+\frac{1}{2}} H_{n+\frac{1}{2}}^{(1)}\left[y\sqrt{a^2+b^2}\right] \qquad (11a)$$

(Watson, page 416*)

$$J_{n+\frac{1}{2}}(t\rho_0) J_{n+\frac{1}{2}}(t\rho') = \frac{t^{\frac{1}{2}}\sqrt{\rho_0\rho'}}{\sqrt{2\pi}} \int_0^\pi \frac{J_{\frac{1}{2}}\left[t\sqrt{\rho_0^2+\rho'^2-2\rho_0\rho'\cos\beta}\right]}{\sqrt{\rho_0^2+\rho'^2-2\rho_0\rho'\cos\beta}} C_n^{\frac{1}{2}}(\cos\beta)\sin\beta\, d\beta \qquad (11b)$$

(Watson, page 367)

$C_n^{\frac{1}{2}}$ is the Gegenbauer polynomial or, in this case, the Legendre polynomial P_n. From the definition of the Gegenbauer functions

$$\sum_0^\infty C_n^{\frac{1}{2}}(\cos\beta)\cos\left[(n+\tfrac{1}{2})\Theta\right] = \frac{1}{\sqrt{2(\cos\Theta-\cos\beta)}} = \sum_0^\infty P_n(\cos\beta)\cos(n+\tfrac{1}{2})\Theta \qquad (11c)$$

$$\cos\Theta > \cos\beta$$

This sum is positive for $|\Theta| < \pi$, $\cos\Theta > \cos\beta$; it is always zero for $\cos\Theta < \cos\beta$; and negative for $\pi < \Theta < 2\pi$, $\cos\Theta > \cos\beta$.

If we set (11b) in (10) and use (11c), and carry out the integration over the infinite range using (11a), then we find

$$\psi_i = i\pi\sqrt{\frac{k\rho_0}{2}} \int_{\phi'-\phi_0}^{\pi} \frac{\sin\beta\, H_0^{(1)}\left[k\sqrt{z^2+\rho_0^2+\rho'^2-2\rho_0\rho'\cos\beta}\right]}{\sqrt{\cos(\phi'-\phi_0)-\cos\beta}\sqrt{z^2+\rho_0^2+\rho'^2-2\rho_0\rho'\cos\beta}}\, d\beta \qquad (12)$$

* There is a misprint in Watson's book in this formula.

for $-\pi < \varphi' - \varphi_0 < \pi$. The result has a negative sign when $\pi < \varphi' - \varphi_0 < 3\pi$. Further, $\psi_1(\varphi' - \varphi_0 + 2\pi) = -\psi_1(\varphi' - \varphi_0)$, i.e., ψ_1 has period 4π.

Now, put

$$z^2 + \rho_0^2 + \rho'^2 - 2\rho_0\rho'\cos\beta = z^2 + \rho_0^2 + \rho'^2 - 2\rho_0\rho'\cos(\varphi' - \varphi_0) + 2\rho_0\rho'\left[\cos(\varphi' - \varphi_0) - \cos\beta\right]$$

$$= R_1^2 + 2\rho_0\rho'\left[\cos(\varphi' - \varphi_0) - \cos\beta\right]$$

where R_1 is the distance from the source dipole. We can now substitute

$\mu = \cos(\varphi' - \varphi_0) - \cos\beta$ throughout (12) and obtain

$$\psi_1 = \pm ikR\sqrt{\frac{\rho_0\rho'}{2}} \int_0^{1+\cos(\varphi' - \varphi_0)} \frac{H_1^{(1)}\left[kR\sqrt{R_1^2 + 2\rho_0\rho'\mu}\right]}{\sqrt{R_1^2 + 2\rho_0\rho'\mu}} \frac{d\mu}{\sqrt{\mu}} \qquad (13)$$

where the + sign holds for $-\pi \le \varphi' - \varphi_0 \le \pi$ and the - sign for $\pi \le \varphi' - \varphi_0 \le 3\pi$.

If now we put $2\rho_0\rho'\mu = R_1^2 v^2$, we obtain

$$\psi_1 = \pm ikR \int_0^{v_1'} \frac{H_1^{(1)}\left[kR_1\sqrt{1+v^2}\right]}{\sqrt{1+v^2}}\, dv \qquad (14)$$

with $v_1' = \frac{2\sqrt{\rho_0\rho'}}{R_1}\left|\cos\left(\frac{\varphi' - \varphi_0}{2}\right)\right|$, and we find that the sign change indicated in (14) is taken care of if we remove the absolute value notation from the $\cos\left(\frac{\varphi' - \varphi_0}{2}\right)$. Thus, finally,

$$\psi_1 = ikR \int_0^{v_1'} \frac{H_1^{(1)}\left[kR_1\sqrt{1+v^2}\right]}{\sqrt{1+v^2}}\, dv \qquad (15)$$

with $v_1' = \frac{2\sqrt{\rho_0\rho'}}{R_1}\cos\left(\frac{\varphi' - \varphi_0}{2}\right)$. We note again that

$$\psi_1(\varphi' - \varphi_0) + \psi_1(\varphi' - \varphi_0 + 2\pi) = 0$$

i.e., ψ_1 has period 4π.

Next, one should examine the behavior of ψ_1 near $R_1 = 0$. To do this, we set

$$\psi_1 = -ik\int_0^{\infty} \frac{H_1^{(1)}\left[kR_1\sqrt{1+v^2}\right]}{\sqrt{1+v^2}}\,dv - ik\int_{v_1'}^{\infty} \frac{H_1^{(1)}\left[kR_1\sqrt{1+v^2}\right]}{\sqrt{1+v^2}}\,dv$$

Near R = 0, $\rho' \longrightarrow \rho_0$, $\varphi' \longrightarrow \varphi_0$, so that

$$v_1' \longrightarrow \frac{2\rho_0}{R_1}$$

Further,

$$\int_0^{\infty} \frac{H_1^{(1)}\left[kR_1\sqrt{1+v^2}\right]}{\sqrt{1+v^2}}\,dv = \frac{1}{ik}\,\frac{e^{ikR_1}}{R_1}$$

So,

$$\psi_1 \longrightarrow \frac{e^{ikR_1}}{R_1} - ik\lim_{R_1\to 0}\int_{v_1'}^{\infty} \frac{H_1^{(1)}\left[kR_1\sqrt{1+v^2}\right]}{\sqrt{1+v^2}}\,dv$$

In the integral, we put

$$u = kR_1\sqrt{1+v^2}$$

then

$$\lim_{R_1\to 0}\int_{v_1'}^{\infty} \frac{H_1^{(1)}\left[kR_1\sqrt{1+v^2}\right]}{\sqrt{1+v^2}}\,dv = \lim_{R_1\to 0}\int_{k\sqrt{\rho_0^2+R_1^2}}^{\infty} \frac{H_1^{(1)}(u)}{\sqrt{u^2-k^2R_1^2}}\,du = \int_{2k\rho_0}^{\infty} \frac{H_1^{(1)}(u)}{u}\,du$$

Thus, ψ_1 approaches $\frac{e^{ikR_1}}{R_1}$ plus a function which is bounded at $R_1 = 0$. Thus, ψ_1 does have a singularity as $R_1 \longrightarrow 0$ and hence (9) as it stands cannot be correct.

The corresponding function for $\varphi' + \varphi_0$ is

$$\psi_2 = -ik\int_0^{v_2'} \frac{H_1^{(1)}\left[kR_2\sqrt{1+v^2}\right]}{\sqrt{1+v^2}}\,dv \qquad (16)$$

with

$$v_2' = \frac{2\sqrt{\rho_0\rho'}}{R_2}\cos\left(\frac{\varphi'+\varphi_0}{2}\right)$$

$$R_2^2 = z^2+\rho_0^2+\rho'^2-2\rho_0\rho'\cos(\varphi'+\varphi_0)$$

To form a solution which fits all boundary conditions and has the proper singu-

larities and the proper boundary conditions at infinity, we take combinations of the two functions

$$\psi_1' = \frac{1}{2}\left(\frac{e^{ikR_1}}{R_1} + \psi_1\right)$$

$$\psi_2' = \frac{1}{2}\left(\frac{e^{ikR_2}}{R_2} + \psi_2\right)$$

By reasoning identical to that just applied to ψ_1, $\psi_2 \longrightarrow -\frac{e^{ikR_2}}{R_2}$ plus bounded function as $R_2 \longrightarrow 0$. The negative sign appears since $v_2' < 0$ at $\varphi' = 2\pi - \varphi_0$. Thus, ψ_2' does not have a singularity at $R_2 = 0$, or, in fact, anywhere; and ψ_1' has the proper singularity as $R_1 \longrightarrow 0$, i.e., $\psi_1' \longrightarrow \frac{e^{ikR_1}}{R_1}$ plus a bounded function as $R_1 \longrightarrow 0$. ψ_1' has no other singularities. Further, $\psi' + \psi_2'$ satisfied Neumann conditions $\left(\frac{\partial}{\partial n}(\psi_1' + \psi_2') = 0\right)$ on the conducting half plane and $\psi_1' - \psi_2'$ satisfies Dirichlet conditions $(\psi_1' - \psi_2' = 0)$ on the conducting plane. In other words, the solution to the diffraction problem is given by (9) except for a factor of one-half.

One should note further that

$$\psi_1'(\varphi' - \varphi_0) + \psi_1'(\varphi' - \varphi_0 + 2\pi) = \frac{e^{ikR_1}}{R_1} \tag{17a}$$

$$\psi_1'\Big|_{\varphi' - \varphi_0 = \pi} = \frac{1}{2}\frac{e^{ikR_1}}{R_1} \tag{17b}$$

$$\psi_2'(\varphi' + \varphi_0) + \psi_2'(\varphi' + \varphi_0 + 2\pi) = \frac{e^{ikR_2}}{R_2} \tag{17c}$$

$$\psi_2'\Big|_{\varphi' + \varphi_0 = \pi} = \frac{1}{2}\frac{e^{ikR_2}}{R_2} \tag{17d}$$

The asymptotic expressions for ψ_1 and ψ_2 follow immediately from (15) and (16). Thus, starting with (15), $v_1' \longrightarrow 0$ as $R_1 \longrightarrow \infty$. The first term in the

asymptotic expansion is then

$$\lim_{R_1 \to 0} i\beta H_1^{(1)}(\beta R_1)\frac{2\sqrt{\rho_1\rho'}}{R_1}\cos\left(\frac{\varphi'-\varphi_1}{2}\right) = 2\sqrt{\frac{2}{\pi}}\sqrt{-i\beta\rho_1\sin\theta}\,\frac{e^{-i\beta R_1}}{R_1}\cos\left(\frac{\varphi'-\varphi_1}{2}\right) \qquad (18)$$

where we have used the first term in the asymptotic expression for $H_1^{(1)}$ and have set $\rho' = R\sin\theta$ (θ = angle with z-axis in spherical coordinates). Thus,

$$\psi_1' \sim \frac{e^{-i\beta\left[R-\rho_1\sin\theta\cos(\varphi'-\varphi_1)\right]}}{R}\left[\frac{1}{2}+\sqrt{\frac{-2i\beta\rho_1\sin\theta}{\pi}}\cos\left(\frac{\varphi'-\varphi_1}{2}\right)\right] \qquad (19)$$

$$\psi_2' \sim \frac{e^{-i\beta\left[R-\rho_2\sin\theta\cos(\varphi'+\varphi_2)\right]}}{R}\left[\frac{1}{2}+\sqrt{\frac{-2i\beta\rho_2\sin\theta}{\pi}}\cos\left(\frac{\varphi'+\varphi_2}{2}\right)\right] \qquad (20)$$

$$R = \sqrt{\rho'^2+z^2}$$

As $\rho_2 \longrightarrow 0$

$$\begin{cases} \psi_1' - \psi_2' \sim 0 & \text{(dipole fields cancel)} \\ \psi_1' + \psi_2' \sim \dfrac{e^{-i\beta R}}{R} & R = R_1 = R_2 \end{cases}$$

Further, if we set $U = \psi_1' - \psi_2'$, we note that

$$\left.\frac{\partial U}{\partial \rho'}\right|_{\substack{\varphi_1=\pi \\ \varphi'=0}}$$

reduces to the simple expression

$$\left.\frac{\partial U}{\partial \rho'}\right|_{\substack{\varphi_1=\pi \\ \varphi'=0}} = \frac{-i\beta\sqrt{\rho_1\rho'}}{R}H_1^{(1)}\left[\beta\sqrt{z^2+(\rho_1+\rho')^2}\right] = \frac{i\beta\sqrt{\rho_1\rho'}}{R}H_1^{(1)}(\beta R) \qquad (21)$$

$$R = \sqrt{z^2+(\rho_1+\rho')^2}$$

This means that, on the conducting plate, the electric and magnetic fields of a dipole oriented as shown below reduce to a simple form.

Figure 3.

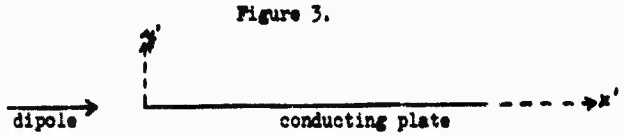

The result (21) can also be verified directly from the series solution (9).

As one further check on the theory, we can examine the behavior of $\rho_0\psi_1'$ as $\rho_0 \longrightarrow \infty$. This should give us the diffraction integral for a plane wave.

Using (13), we can write

$$\psi_1' = \frac{1}{2}\frac{e^{ikR_1}}{R_1} + \frac{ik}{2}\sqrt{\frac{\rho_0\rho'}{2}}\int_0^{1+\cos(\varphi'-\varphi_0)} \frac{H_1^{(1)}\left[k\sqrt{R_1^2+2\rho_0\rho' u}\right]}{\sqrt{R_1^2+2\rho_0\rho' u}}\,\frac{du}{\sqrt{u}} \qquad (22)$$

where $\varphi'-\varphi_0$ is restricted, for the present, to values $0 < \varphi'-\varphi_0 < \pi$. Now,

$$\rho_0\psi_1' \to \frac{1}{2}e^{ik\rho_0 - ik\rho'\cos(\varphi'-\varphi_0)} + \frac{ik}{2}\sqrt{\frac{\rho'}{2}}\rho_0^{3/2}\int_0^{1+\cos(\varphi'-\varphi_0)} \frac{H_1^{(1)}\left[k\sqrt{R_1^2+2\rho_0\rho' u}\right]}{\sqrt{R_1^2+2\rho_0\rho' u}}\,\frac{du}{\sqrt{u}}$$

as $\rho_0 \longrightarrow \infty$. But,

$$H_1^{(1)} \to \sqrt{\frac{2}{\pi k\rho_0}}\, e^{ik(\rho_0+\rho' u)-\frac{3\pi i}{4}-ik\rho'\cos(\varphi'-\varphi_0)}$$

asymptotically as $\rho_0 \longrightarrow \infty$. Thus,

$$\rho_0\psi_1' \to \frac{1}{2}e^{ik\rho_0 - ik\rho'\cos(\varphi'-\varphi_0)} + \frac{e^{-i\pi/4}}{2\sqrt{\pi}}e^{ik\rho_0 - ik\rho'\cos(\varphi'-\varphi_0)}\sqrt{\frac{2}{\pi k}}\int_0^{1+\cos(\varphi'-\varphi_0)} e^{ik\rho' u}\,\frac{du}{\sqrt{u}}$$

If we set $\lambda^2 = k\rho' u$, this reduces to

$$\rho_0\psi_1' \to \frac{1}{2}e^{ik\rho_0 - ik\rho'\cos(\varphi'-\varphi_0)} + \frac{1}{\sqrt{\pi}}e^{-i\pi/4}e^{ik\rho_0 - ik\rho'\cos(\varphi'-\varphi_0)}\int_0^{\sqrt{2k\rho'}\cos\left(\frac{\varphi'-\varphi_0}{2}\right)} e^{i\lambda^2}\,d\lambda \qquad (23)$$

Since

$$\int_{-\infty}^{\infty} e^{i\lambda^2}\,d\lambda = \sqrt{\pi}\, e^{i\pi/4}$$

This last equation can be written as

---

* In taking the limit, we retain all terms which affect the phase of the incident wave. These terms may be neglected in any multiplying factors which appear.

$$\rho_0 \psi_1' \to \frac{1}{\sqrt{\pi}} e^{-i\pi/4} e^{ik\rho_0 - ik\rho'\cos(\varphi'-\varphi_0)} \int_{-\infty}^{\sqrt{2k\rho'}\cos\left(\frac{\varphi'-\varphi_0}{2}\right)} e^{i\lambda^2} d\lambda \tag{24}$$

Again the restriction of $\varphi' - \varphi_0$ to the interval $0<\varphi'-\varphi_0<\pi$ may be relaxed. Equation (23) is the usual form of the plane wave diffraction integral. The corresponding equation for $\varphi'+\varphi_0$ is to be added to or subtracted from (24) depending on whether $\underset{\sim}{H}$ or $\underset{\sim}{E}$ is tangent to the conducting plane. The phase term $e^{ik\rho_0}$ is, of course, meaningless in the limit $\rho_0 \to \infty$. One can drop this term which would be a constant for any fixed, large ρ_0. The resulting expression is identical to the result of Sommerfeld.

Finally, if one takes equation (12) and integrates over z, the result for a cylindrical source of infinite extent will be obtained. In this way, one finds for the cylindrical source

$$\psi_1 = \frac{2}{i\pi} \int_0^{\frac{2\sqrt{k\rho'}}{R_1}\cos\left(\frac{\varphi'-\varphi_0}{2}\right)} \frac{e^{ikR_1\sqrt{1+v^2}}}{\sqrt{1+v^2}}\, dv \tag{25}$$

where now $R_1 = \sqrt{\rho^2+\rho'^2-2\rho\rho'\cos(\varphi'-\varphi)}$. A similar result is obtained for ψ_2. We also note that

$$\frac{2}{i\pi} \int_0^{\infty} \frac{e^{ikR_1\sqrt{1+v^2}}}{\sqrt{1+v^2}}\, dv = H_0^{(1)}(kR_1) \tag{26}$$

Thus, the complete solution for the cylindrical source is

$$\psi_1' = \frac{1}{2}\left\{ H_0^{(1)}(kR_1) + \frac{2}{i\pi} \int_0^{\frac{2\sqrt{k\rho'}}{R_1}\cos\left(\frac{\varphi'-\varphi_0}{2}\right)} \frac{e^{ikR_1\sqrt{1+v^2}}}{\sqrt{1+v^2}}\, dv \right\} \tag{27}$$

$$\psi_2' = \frac{1}{2}\left\{ H_0^{(1)}(kR_2) + \frac{2}{i\pi} \int_0^{\frac{2\sqrt{k\rho'}}{R_2}\cos\left(\frac{\varphi'+\varphi_0}{2}\right)} \frac{e^{ikR_2\sqrt{1+v^2}}}{\sqrt{1+v^2}}\, dv \right\} \tag{28}$$

Here, of course,

$$R_2 = \sqrt{\rho_0^2 + \rho'^2 - 2\rho_0\rho' \cos(\varphi' + \varphi_0)}$$

$$R_1 = \sqrt{\rho_0^2 + \rho'^2 - 2\rho_0\rho' \cos(\varphi' - \varphi_0)}$$

APPENDIX A TO PART I

Particular forms of the following integrals have been used.

$$\int_0^\infty J_\mu(bt) \frac{e^{-a\sqrt{t^2+y^2}}}{\sqrt{t^2+y^2}} t^{\mu+1} dt = i\sqrt{\frac{\pi}{2}}\, b^\mu \left(\frac{y}{\sqrt{a^2+b^2}}\right)^{\mu+\frac{1}{2}} H_{\mu+\frac{1}{2}}\left[y\sqrt{a^2+b^2}\right] \tag{A1}$$

$$\int_0^\infty \frac{H_\nu^{(1)}\left[a\sqrt{t^2+x^2}\right]}{(t^2+x^2)^{\nu/2}} t^{2\mu+1} dt = \frac{2^\mu \Gamma(\mu+1)}{a^{\mu+1} x^{\nu-\mu-1}} H_{\nu-\mu-1}(ax) \tag{A2}$$

for

$$R_e\left(\frac{\nu}{2} - \frac{1}{4}\right) > R_e\,\mu > -1$$

When $\nu = 1$ and $\mu = -1/2$, this latter formula gives

$$H_{\frac{1}{2}}^{(1)}(ax) = \sqrt{\frac{2}{\pi a x}}\, \frac{e^{iax}}{i}$$

on the right hand side, i.e.,

$$\int_0^\infty \frac{H_1^{(1)}\left[a\sqrt{t^2+x^2}\right]}{\sqrt{t^2+x^2}} dt = \frac{e^{iax}}{iax} \tag{A3}$$

If one sets $\nu = 1/2$, $\mu = -1/2$ in (A2), then

$$\frac{2}{i\pi} \int_0^\infty \frac{e^{-kR_1\sqrt{1+v^2}}}{\sqrt{1+v^2}} dv = H_0^{(1)}(kR_1) \tag{A4}$$

PART II

THE CALCULATION OF ANTENNA FIELDS

We wish now to write down the series expressions for the dipole fields corresponding to the closed form results given by $\psi_1' \pm \psi_2'$. Thus, we can write

$$\psi_1' = \frac{1}{2}\int_0^\infty \sum_0^\infty \epsilon_m J_{m/2}(t\rho_0) J_{m/2}(t\rho') \cos\left[\frac{m}{2}(\phi' - \phi_0)\right] \frac{e^{-z\sqrt{t^2-k^2}}}{\sqrt{t^2-k^2}}\, t\,dt \qquad (29)$$

$$\psi_2' = \frac{1}{2}\int_0^\infty \sum_0^\infty \epsilon_m J_{m/2}(t\rho_0) J_{m/2}(t\rho') \cos\left[\frac{m}{2}(\phi' + \phi_0)\right] \frac{e^{-z\sqrt{t^2-k^2}}}{\sqrt{t^2-k^2}}\, t\,dt \qquad (30)$$

For a dipole normal to the deck, the geometry is as shown below.

Figure 4.

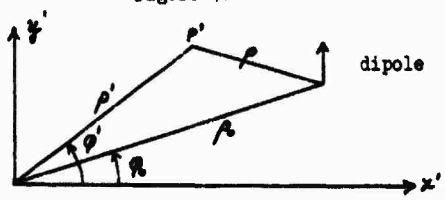

The edge of the deck is at x' = y' = 0 and it lies along the z-axis, which is positive normal to the paper. The dipole is located at $(\rho_0, \phi_0, z=0)$ and the field is expressed at P' in terms of (ρ', ϕ', z). In this case, the solution to the diffraction problem is $\pi_R^{(1)} = \psi_1' + \psi_2'$, or in series form,

$$\pi_R^{(1)} = \int_0^\infty \sum_0^\infty \epsilon_m J_{m/2}(t\rho_0) J_{m/2}(t\rho') \cos\frac{m}{2}\phi' \cos\frac{m}{2}\phi_0 \frac{e^{-z\sqrt{t^2-k^2}}}{\sqrt{t^2-k^2}}\, t\,dt \qquad (31)$$

If the dipole is oriented horizontal to the deck, then $\pi_R^{(2)} = \psi_1' - \psi_2'$, or in series form

$$\pi_R^{(2)} = 2\int_0^\infty \sum_0^\infty J_{m/2}(t\rho_0) J_{m/2}(t\rho') \sin\frac{m}{2}\phi' \sin\frac{m}{2}\phi_0 \frac{e^{-z\sqrt{t^2-k^2}}}{\sqrt{t^2-k^2}}\, t\,dt \qquad (32)$$

In the case of the whip antenna in the vertical position, equation (31) is, of course, used with $\phi_0 = \pi/2$. This puts the orientation of the dipole along the

y' axis as shown in the figure below.

Figure 5.

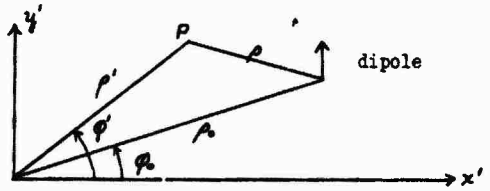

Equation (31) gives the Hertz vector for the dipole field at point P when the dipole itself is located in the general position $\rho' = \rho_0$, $\varphi' = \varphi_0$, z = 0. The deck edge is along the z-axis, which is normal to the paper at x' = y' = 0. If $\varphi_0 = \frac{\pi}{2}$, the dipole is then located at distance ρ_0 above the deck edge with orientation in the positive y' direction.

The electric and magnetic fields due to the dipole are given by

$$\underset{\sim}{H} = -i\omega\epsilon\, \nabla \times \underset{\sim}{\Pi}_R^{(i)} \tag{33}$$

$$\underset{\sim}{E} = \nabla \times \nabla \times \underset{\sim}{\Pi}_R^{(i)} = \nabla(\nabla \cdot \underset{\sim}{\Pi}_R^{(i)}) + k^2 \underset{\sim}{\Pi}_R^{(i)} \tag{34}$$

If we now write the components of $\pi_R^{(i)}$ in the (ρ', φ', z) system, these are, of course, $(\pi_R^{(i)} \sin\varphi', \pi_R^{(i)} \cos\varphi', 0)$ respectively, so that

$$H_{\rho'} = i\omega\epsilon \cos\varphi' \frac{\partial \pi_R^{(i)}}{\partial z} \tag{35}$$

$$H_{\varphi'} = -i\omega\epsilon \sin\varphi' \frac{\partial \pi_R^{(i)}}{\partial z} \tag{36}$$

$$H_z = -i\omega\epsilon \left[\cos\varphi' \frac{\partial \pi_R^{(i)}}{\partial \rho'} - \frac{\sin\varphi'}{\rho'} \frac{\partial \pi_R^{(i)}}{\partial \varphi'}\right] \tag{37}$$

Similarly,

$$E_{\rho'} = -\frac{1}{\rho'}\left\{\frac{\partial}{\partial \varphi'}\left[\frac{\sin\varphi'}{\rho'} \frac{\partial \pi_R^{(i)}}{\partial \varphi'} - \cos\varphi' \frac{\partial \pi_R^{(i)}}{\partial \rho'}\right] + \rho' \sin\varphi' \frac{\partial^2 \pi_R^{(i)}}{\partial z^2}\right\} \tag{38}$$

$$E_{\varphi'} = \frac{\partial}{\partial \rho'}\left[\frac{\sin\varphi'}{\rho'}\frac{\partial \pi_R^{(i)}}{\partial \varphi'} - \cos\varphi'\frac{\partial \pi_R^{(i)}}{\partial \rho'}\right] - \cos\varphi'\frac{\partial^2 \pi_R^{(i)}}{\partial z^2} \tag{39}$$

$$E_{z'} = \frac{1}{\rho'}\left\{\sin\varphi'\frac{\partial}{\partial \rho'}\left(\rho'\frac{\partial \pi_R^{(i)}}{\partial z}\right) + \frac{\partial}{\partial \varphi'}\left(\cos\varphi'\frac{\partial \pi_R^{(i)}}{\partial z}\right)\right\} \tag{40}$$

The fields at the surface of the deck itself are, of course, mainly of interest. Thus, for the case $\varphi' = 0$, the fields reduce to

$$H_{\rho'} = i\omega\epsilon\left.\frac{\partial \pi_R^{(i)}}{\partial z}\right|_{\varphi'=0} \tag{41}$$

$$H_{\varphi'} = 0 \tag{42}$$

$$H_{z'} = -i\omega\epsilon\left.\frac{\partial \pi_R^{(i)}}{\partial \rho'}\right|_{\varphi'=0} \tag{43}$$

$$E_{\rho'} = E_{z'} = 0 \tag{44}$$

$$E_{\varphi'} = \left(-\frac{\partial^2 \pi_R^{(i)}}{\partial \rho'^2} - \frac{\partial^2 \pi_R^{(i)}}{\partial z^2}\right)_{\varphi'=0} \tag{45}$$

Since $\pi_R^{(i)}$ satisfies the wave equation, (45) may also be written

$$E_{\varphi'} = \left[\frac{1}{\rho'}\frac{\partial \pi_R^{(i)}}{\partial \rho'} + \frac{1}{\rho'^2}\frac{\partial^2 \pi_R^{(i)}}{\partial \varphi'^2} + k^2 \pi_R^{(i)}\right]_{\varphi'=0} \tag{46}$$

For the case of equation (32) where the dipole orientation is parallel to the deck, the dipole could be directed either along the x'-direction or along the z-direction. The former orientation is, of course, the one of interest for the

whip antenna or the monopole antenna in the horizontal outboard position. Thus, with the dipole oriented along x'-direction, the fields are

$$H_{\rho'} = -i\omega\epsilon \sin\varphi' \frac{\partial \Pi_R^{(2)}}{\partial z} \tag{47}$$

$$H_{\varphi'} = i\omega\epsilon \cos\varphi' \frac{\partial \Pi_R^{(2)}}{\partial z} \tag{48}$$

$$H_z = \frac{i\omega\epsilon}{\rho'}\left[\rho' \sin\varphi' \frac{\partial \Pi_R^{(2)}}{\partial \rho'} + \cos\varphi' \frac{\partial \Pi_R^{(2)}}{\partial \varphi'}\right] \tag{49}$$

$$E_{\rho'} = \cos\varphi' \frac{\partial^2 \Pi_R^{(2)}}{\partial \rho'^2} - \frac{\sin\varphi'}{\rho'} \frac{\partial^2 \Pi_R^{(2)}}{\partial \rho' \partial \varphi'} + k^2 \Pi_R^{(2)} \cos\varphi' \tag{50}$$

$$E_{\varphi'} = \frac{1}{\rho'} \frac{\partial}{\partial \varphi'}\left[\cos\varphi' \frac{\partial \Pi_R^{(2)}}{\partial \rho'} - \frac{\sin\varphi'}{\rho'} \frac{\partial \Pi_R^{(2)}}{\partial \varphi'}\right] - k^2 \Pi_R^{(2)} \sin\varphi' \tag{51}$$

$$E_z = \cos\varphi' \frac{\partial^2 \Pi_R^{(2)}}{\partial z \partial \rho'} - \frac{\sin\varphi'}{\rho'} \frac{\partial^2 \Pi_R^{(2)}}{\partial z \partial \varphi'} \tag{52}$$

On the deck, i.e., when $\varphi' = 0$, these fields reduce to

$$H_z = \frac{i\omega\epsilon}{\rho'} \left.\frac{\partial \Pi_R^{(2)}}{\partial \varphi'}\right|_{\varphi'=0} \tag{53}$$

$$E_{\varphi'} = \left\{\frac{1}{\rho'} \frac{\partial^2 \Pi_R^{(2)}}{\partial \varphi' \partial \rho'} - \frac{1}{\rho'^2} \frac{\partial \Pi_R^{(2)}}{\partial \varphi'}\right\}_{\varphi'=0} \tag{54}$$

and all other components are zero.

We have seen earlier, (21), that

$$\left.\frac{\partial \Pi_R^{(2)}}{\partial \varphi'}\right|_{\substack{\varphi'=0 \\ R=W}}$$

reduces to the very simple form

$$\frac{ik\sqrt{\rho_0\rho'}}{R} H_1^{(1)}(kR)$$

Thus, for a dipole oriented along x' with $\varphi_0 = \pi$, i.e., for the dipole along the position of the horizontal whip antenna, both the electric and magnetic fields on the deck have the very simple form

$$H_z = \frac{i\omega\epsilon}{\rho'} \psi \tag{55}$$

$$E_{\varphi'} = \frac{\partial}{\partial \rho'}\left(\frac{\psi}{\rho'}\right) \tag{56}$$

where

$$\psi = \frac{ik\sqrt{\rho_0\rho'}}{R} H_1^{(1)}(kR)$$

and

$$R = \sqrt{(\rho_0+\rho')^2 + z^2}$$

The dipole is located at distance ρ_0 from the deck edge as shown below.

Figure 6.

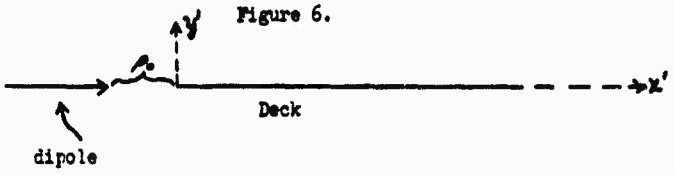

H_z and $E_{\varphi'}$ are the only non-zero field components on the deck in thie case.

At the risk of being repetitious we shall derive the reeults (55) and (56) again in the next eection by summing the φ' derivative of the seriee expreesion (32) for the case $\varphi' = 0$, $\varphi_0 = \pi$.

Finally, if the dipole is parallel to the deck but oriented along the positive z-direction, the fields are again obtained from (32) with $\pi_{z\pi}^{(2)} = i_z \pi_R^{(2)}$, i.e., vector $\pi_R^{(2)}$ ie along z.

One has

$$H_{\rho'} = \frac{-i\omega\epsilon}{\rho'} \frac{\partial \Pi_R^{(2)}}{\partial \varphi'} \tag{57}$$

$$H_{\varphi'} = i\omega\epsilon \frac{\partial \Pi_R^{(2)}}{\partial \rho'} \tag{58}$$

$$H_z = 0 \tag{59}$$

$$E_{\rho'} = \frac{\partial^2 \Pi_R^{(2)}}{\partial \rho' \partial z} \tag{60}$$

$$E_{\varphi'} = \frac{1}{\rho'} \frac{\partial^2 \Pi_R^{(2)}}{\partial \varphi' \partial z} \tag{61}$$

$$E_z = \frac{\partial^2 \Pi_R^{(2)}}{\partial z^2} + k^2 \Pi_R^{(2)} \tag{62}$$

It is clear at this point that our theoretical calculations can be presented rather simply for the horizontal outboard antenna. One has the result exactly for the dipole field and one can, in principle at least, integrate over the antenna current distribution to obtain the field of the entire antenna. For the vertical antenna, neither the closed form results of Part I nor the series expression (51) present an immediate approach to numerical calculation. Later, we wish to present some approximate methods and to discuss a possible further simplification based on the integral expressions derived in Part I.

In the next part, however, we will consider the calculation of a horizontal monopole antenna field excited in approximately a 1/4 wave length mode. The calculation will involve use of the exact result for the dipole field plus an approximate integration over the antenna current. Since the antenna current has a loop at the near end, there will be an end loading term equivalent to the field of a point charge oscillating sinusoidally with time.

PART III

EVALUATION OF FIELDS OF HORIZONTAL ANTENNAS

As mentioned earlier, at the expense of repetition, we shall derive the field normal to the deck for a horizontal dipole, located outboard of the deck, directly from the series expression (32). The geometry of the situation is shown in Fig. 6 of Part II, i.e., we have $\frac{\partial \Pi_R^{(2)}}{\partial \rho'}$ to evaluate at $\rho' = 0$, $\phi_0 = \pi$. Differentiating (32) and setting $\rho' = 0$, $\phi_0 = \pi$, one obtains

$$\psi = \left.\frac{\partial \Pi_R^{(2)}}{\partial \rho'}\right|_{\substack{\rho'=0 \\ \phi_0=\pi}} = 2\int_0^\infty \sum_0^\infty J_{n+\frac{1}{2}}(t\rho_0) J_{n+\frac{1}{2}}(t\rho')(n+\tfrac{1}{2})(-1)^n \frac{\epsilon^{-z\sqrt{t^2-k^2}}}{\sqrt{t^2-k^2}}\, t\,dt \qquad (63)$$

It happens, in this case, that the infinite sum involved in ψ can be evaluated. Thus, on page 522, Watson gives the result due to Gegenbauer, i.e.,

$$\frac{J_\nu(\omega)}{\omega^\nu} = 2^\nu \Gamma(\nu) \sum_0^\infty (\nu+m) \frac{J_{m+\nu}(R)}{R^\nu} \frac{J_{m+\nu}(r)}{r^\nu} C_m^\nu(\cos\varphi) \qquad (64)$$

where

$$\omega^2 = R^2 + r^2 - 2rR\cos\varphi$$

and where $C_m^\nu(t)$ is the coefficient of α^m in the expansion of $(1-2\alpha t+\alpha^2)^{-\nu}$ in the ascending powers of α (the C_m^ν's are Gegenbauer functions). One sees that for $\nu = 1/2$ and $t = -1$ ($\varphi = \pi$), $C_m^{\frac{1}{2}} = (-1)^m$. Thus, from (64) one has

$$\sum_0^\infty (-1)^n (n+\tfrac{1}{2}) J_{n+\frac{1}{2}}(t\rho') J_{n+\frac{1}{2}}(t\rho_0) = \frac{J_{\frac{1}{2}}\left[t(\rho_0+\rho')\right]}{\sqrt{t(\rho_0+\rho')}} \frac{t\sqrt{\rho_0\rho'}}{\sqrt{2\pi}} \qquad (65)$$

In obtaining this last formula we have set $R = t\rho_0$, $r = t\rho'$ and $\cos\varphi = -1$, so that $\omega = t(\rho_0 + \rho')$.

The reader will note that the procedure followed here is basically a special case of the procedure involved in obtaining the results of Part I.

Now, substituting (65) in (63)

$$\psi = \frac{2\sqrt{\rho_0\rho'}}{\sqrt{2\pi(\rho+\rho')}} \int_0^\infty J_{1/2}\left[t(\rho+\rho')\right] \frac{\epsilon^{-z\sqrt{t^2-k^2}}}{\sqrt{t^2-k^2}} t^{1/2}\, dt \qquad (66)$$

This last integral is, however, just a special case of the integral given in (A1) of Appendix A to Part I. Thus, referring to Appendix A, one finds immediately

$$\psi = ik\sqrt{\rho_0\rho'}\ \frac{H_0^{(1)}(kR)}{R} \qquad (67)$$

with

$$R = \sqrt{(\rho+\rho')^2 + z^2}$$

ψ is an outgoing wave on the deck plane, as it should be. This result is the same as the result obtained earlier in Equation (21) of Part I.

Now, although ψ is the quantity of interest for a dipole field, we shall need a reasonable approximation to the field of the entire antenna. Taking the monopole antenna in the horizontal position, the current distribution is approximately that of a 1/4 wave antenna at a frequency of 3.385 mc. We wish to take into account the entire antenna to a reasonable approximation together with the end effect due to the current maximum at the near end.

The expression (67) is correct for a dipole at distance ρ_0 outboard of the deck. For the entire antenna, we replace ρ_0 by ρ and let ρ range from ρ_1 to ρ_2, where $\rho_2 - \rho_1 = \ell$ = length of the antenna in meters and ρ_1 is the distance of the antenna base from the deck.

To obtain the effect of the near end loading, let the current at the near end be $I_0\epsilon^{-i\omega t}$. Then the charge accumulated at the near end is

$$\frac{dQ}{dt} = +I_0\epsilon^{-i\omega t} \qquad \text{or} \qquad Q = \frac{I_0}{-i\omega}\,\epsilon^{-i\omega t}$$

The scalar potential of this charge is then

$$\psi_2 = \frac{-I_o}{4\pi i\omega\epsilon_o}\,\frac{e^{-ikR_1}}{R_1} \tag{68}$$

$$R_1 = \sqrt{(\rho+\rho')^2+z^2}$$

To obtain the solution which fits boundary conditions on the plane, it is clear that we replace

$$\frac{e^{-ikR_1}}{R_1} \qquad \text{by} \qquad \pi_R^{(2)}(\rho,\rho',z)$$

as given by (32) and compute the normal field by taking

$$\frac{-1}{\rho'}\left.\frac{\partial\pi_R}{\partial\rho'}\right|_{\rho'=0}$$

Thus, the normal field due to end loading is (67)

$$E_{rs} = \frac{+I_o k}{4\pi\omega\epsilon_o}\sqrt{\frac{\rho}{\rho'}}\,\frac{H_1^{(2)}(kR_1)}{R_1} \tag{69}$$

This term would appear naturally in the integration of the current over the length of the antenna. We present it separately here since it may be desirable at some later time to change this end loading term if details of the input circuit require such a change.

Now, the actual current on the antenna is usually approximated by a quarter sine wave. We know, however, that the current decay is more rapid than a sine function. If we take the current distribution to be $I_o\sqrt{\frac{\rho}{\beta}}$, we have a function which decays more rapidly than the sine function over most of the antenna but which does not lead to zero current at the far end. This make little difference, however, for we shall leave out the far end loading induced by our assumption and we shall also leave out the near end loading since it has already been taken into account.

Thus, returning to (67) we multiply ψ by $\frac{-I_0\sqrt{\rho'}\,d\rho}{4\pi\omega\epsilon_0}$ and integrate from ρ_1 to ρ_2 being careful to leave both end loading terms out. ρ_0 in (67) is, of course, replaced by ρ. We shall call the result ψ_a. Thus,

$$\psi_a = \frac{-jI_0}{4\pi\omega\epsilon_0}\sqrt{\rho\rho'}\int_{\rho_1}^{\rho_2}\frac{H_0^{(2)}(kR)}{R}\,d\rho \tag{70}$$

with

$$R^2 = (\rho+\rho')^2 + z^2$$

We now note that

$$\frac{\partial}{\partial\rho}\left[H_0^{(2)}(kR)\right] = \frac{-H_1^{(2)}(kR)}{R}\,k(\rho+\rho')$$

and thus,

$$\psi_a = \frac{I_0}{4\pi\omega\epsilon_0}\sqrt{\rho\rho'}\int_{\rho_1}^{\rho_2}\frac{1}{\rho+\rho'}\,\frac{\partial}{\partial\rho}\,H_0^{(2)}(kR)\,d\rho \tag{71}$$

Since the phase of the field is contained in the Hankel function term, it is a sufficient approximation to replace $\frac{1}{\rho+\rho'}$ by $\frac{1}{\bar{\rho}+\rho'}$ where $\bar{\rho}$ is some average value of ρ to be selected later. The final result will not be critical to a reasonable selection of $\bar{\rho}$. Thus, we have finally

$$\psi_a = \frac{I_0}{4\pi\omega\epsilon_0}\,\frac{\sqrt{\rho\rho'}}{\bar{\rho}+\rho'}\left[H_0^{(2)}(kR_2) - H_0^{(2)}(kR_1)\right] \tag{72}$$

$$R_2^2 = (\rho_2+\rho')^2 + z^2$$

$$R_1^2 = (\rho_1+\rho')^2 + z^2$$

In computing the normal field on the deck, we must leave out the end effects. Referring to Eq. (56) of Part II, the normal field in terms of ψ_a is

$$E_{na} = \frac{1}{\rho'} \frac{\partial \psi_a}{\partial \rho'} - \frac{1}{\rho'^2} \psi_a = \frac{\partial}{\partial \rho'}\left(\frac{\psi_a}{\rho'}\right) \tag{73}$$

Thus, we put the expreesion (72) for ψ_a in (73). In computing the derivative with respect to ρ', however, we leave out the derivativee of the Hankel functions since these give the end loading terme. Thus, we find finally for E_{na}

$$E_{na} = \frac{I_o}{4\pi\omega\epsilon_o}\left[H_o^{(1)}(kR_1) - H_o^{(1)}(kR_2)\right] \frac{\partial}{\partial \rho'}\left[\frac{\sqrt{\rho_1}}{\sqrt{\rho'}(\bar{\rho}+\rho')}\right] \tag{74}$$

or

$$E_{na} = \frac{I_o}{4\pi\omega\epsilon_o}\left[H_o^{(1)}(kR_1) - H_o^{(1)}(kR_2)\right]\left[\frac{\sqrt{\rho_1}(\bar{\rho}+3\rho')}{2\rho'^{3/2}(\bar{\rho}+\rho')^2}\right] \tag{75}$$

The total normal field for the antenna is then $E_{na} + E_{ns}$.

These results are very pleasing from a theoretical etandpoint. The final formulas are in closed form and are very nearly exact under the original assumptions; and the case treated is, fortunately, the moet important case for the shipboard monopole and whip antennas. These results should, therefore, be quitc useful.

Calculations for the monopole antenna are shown in Figure 7 for thc case

ν = 3.385 mc

ℓ = antenna length = 60' = 18.3 meters

ρ_1 = distance from catwalk to antenna near end

= 1.5 meters.

The calculations are normalized to a radiated power of 1 watt. Thus, if one writes the radiated power as

$$\omega = \frac{1}{2} R_a I_o^2$$

we assume a 1/4 wave excitation with R_a = 36.6 ohms. This gives I_o = .233 amperes for the maximum antenna current (the maximum occurs at the base of the antenna) when the efficiency is 100%. If the transmitter output reads 1 watt, and if the efficiency is 50%, the current at the base would then be $.233/\sqrt{2} = .165$. Thus, the calculations have been made setting $I_o = .165$.

It is now of interest to see with what accuracy the field of the horizontal antenna can be represented by a simple dipole field alone. To do this, we return to the expression (67) for ψ and note that the electric field normal to the deck is $\frac{\partial}{\partial \rho'}\left(\frac{\psi}{\rho'}\right)$, with

$$\psi = ikR\sqrt{\rho_o \rho'}\ \frac{H_1^{(1)}(kR)}{R} \tag{76}$$

and

$$R = \sqrt{(\rho_o+\rho')^2 + z^2}$$

ψ is, of course, to be multiplied by the normalizing factor

$$\frac{iI_o\,dl}{4\pi\omega\epsilon}$$

For a quarter wave current excitation, we replace

$$I_o\,dl \quad \text{by} \quad I_o\int_0^{l} \cos\frac{\pi}{2}\frac{z}{l}\,dz = \frac{2}{\pi}\,l\,I_o$$

As before, we set I_o = .165 and, since for the monopole the antenna length is a little less than 1/4 wave length, we have $kl = 1.3$ instead of 1.57. This is a minor correction. Thus, differentiating (76) and substituting the value of the normalizing factor, we have for the field normal to the deck

$$E_n = \frac{2W}{kR}\sqrt{\frac{\rho_o}{\rho'}}\left[\frac{H_1^{(1)}(kR)}{2k\rho'} + \frac{(R+\rho')}{R}\,H_2^{(1)}(kR)\right] \tag{77}$$

The result will not be very sensitive to the selection of ρ_o, the distance of the dipole from the catwalk edge, hence we shall set this value at $\rho_o = 8$ meters.

We can now compare the results calculated from (77) with our previous results for the whole antenna as given by $E_{na} + E_{ns}$, with E_{na} given by (75) and E_{ns} by (69). This comparison will be made at selected points as given in the Table below.

Table III(1)

Comparison of Results for the Simple Dipole Field with Previous Calculations for the Entire Antenna

Case 1. $\rho' = 3$ meters; z varied

z (meters)	E_n (from (77))	$E_{na} + E_{ns}$ (From (75)and(69))
0	3.0	2.7
5	2.3	1.7
15	.93	.69
25	.39	.39

Case 2. $z = 0$; ρ' varied

ρ'	E_n (from (77))	$E_{na} + E_{ns}$ (from (75)and(69))
6	.91	.75
15	.15	.11
30	.035	.026
50	.012	.008

Although the agreement is not spectacular, it is probably adequate enough for use in field predictions. In other words, the use of the simple dipole field (76) which fits boundary conditions for the edge is probably sufficient for most purposes.

The Choice of $\bar{\rho}$

A reasonable choice of $\bar{\rho}$ would appear to be to set

$$\bar{\rho} = \frac{\int_{\rho_1}^{\rho_2} \rho I(\rho) d\rho}{\int_{\rho_1}^{\rho_2} I(\rho) d\rho}$$

This yields

$$\bar{\rho} = \frac{1}{3}\left[\ell + 2\rho_1 + \sqrt{\rho_1(\ell+\rho_1)}\right]$$

where $\rho_2 = \ell + \rho_1$ and ℓ = length of the antenna. For

$$\ell = 18.3 \text{ meters}$$

$$\rho_1 = 1.5 \text{ meters}$$

$$\bar{\rho} = 8.9 \text{ meters}$$

In addition to $\bar{\rho}$, one needs some sort of an efficiency factor for the antenna, i.e., the ratio of power radiated to power input. Or, since the calculations involve the near field mostly, an effective efficiency factor can be obtained by normalizing the calculated field to the measured field at a suitable point.

Figure 7

Contour Map of the Computed Electric Field Normal to the Deck for a Horizontal Outboard Antenna

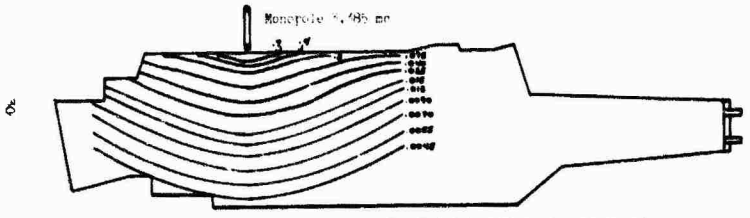

Electric Field Normal to the Deck in volts/meter for a Reading of One Watt at the Transmitter Output Meter (5.5% Radiation Efficiency)

PART IV

THE VERTICAL ANTENNA

In the interest of keeping this report to reasonable length, we shall not present the results for the vertical antenna in detail, although calculations have been made. We shall merely remark here that the series for the Hertz vector for the vertical dipole is

$$\pi_R = \int_0^\infty \sum_0^\infty \epsilon_m J_{m/2}(t\rho_<) J_{m/2}(t\rho') \cos\frac{m}{2}\varphi' \cos\frac{m}{2}\varphi \, \frac{e^{-z\sqrt{t^2-k^2}}}{\sqrt{t^2-k^2}} \, t\,dt$$

The m-even terms of this series give one-half the field due to a dipole and its image for the case of an infinite plane. For the m-odd terms, we can calculate the series to good approximation by using the first term in the Bessel function series for

$$J_{m/2}(t\rho_<) \quad \text{i.e.,} \quad J_{m/2}(t\rho_<) \simeq \frac{\left(\frac{t\rho_<}{2}\right)^{m/2}}{\Gamma(m/2+1)}$$

for the case $\rho_< < \rho'$. For $\rho_> > \rho'$ we approximate the $J_{m/2}(t\rho')$ in the same wave. In either case, the series then becomes integrable term by term using the integral (A1) of Appendix A to Part I.

References

1. H.M. MacDonald, Proc. London Math. Soc. 14 (1915), page 410.
2. Carslaw, Proc. London Math. Soc., (1), 30 (1899), page 121.
3. Watson, Bessel Functions, Second Edition, Cambridge, 1944.
4. A. Sommerfeld, Partial Differential Equations, Academic Press, Inc. 1949.

41. ORGANIC POLYMERS AS RF ATTENUATING MATERIALS

by

Howard W. Christie
Bernard F. Jones
James J. Downs
Midwest Research Institute
Kansas City, Missouri

INTRODUCTION

The development of carbonyl iron solid state attenuators has provided adequate attenuation at frequencies above 100 mc. As there appears to be little possibility of increasing the low frequency attenuating abilities of these materials the investigation of other classes of lossy materials becomes of importance.[1/] There are a number of materials that can be considered for use in attenuators, among these are organic compounds and organic polymers that show high dielectric constants and appreciable electrical conductivity.

The program currently being carried out at Midwest Research Institute under sponsorship of Picatinny Arsenal* is aimed at the development of organic polymers that will have the characteristics required of attenuating materials. The types of polymers being studied are not of the kind normally associated with the electrically insulating materials. Organic polymers are normally excellent insulators and have relatively low, 2 to 6, dielectric constants and low dielectric loss factors at frequencies in the low megacycle

*Contract No. DA-23-072-DRD-1781.

range. The polymers under study at MRI exhibit electrical and dielectric properties that are rather unique for organic materials. These polymers have been called, perhaps erroneously, semiconductors. The term has arisen from the fact that many of these compounds and polymers show conductivities in the range normally associated with the inorganic semiconductors, that is, from 100 to 10^9 ohm-cms volume resistivity, and possess a negative temperature coefficient of resistivity, that is, their resistance decreases with increasing temperatures.

The program at MRI is concerned with preparation of a series of polymers exhibiting semiconductor behavior, the determination of the complex dielectric and magnetic properties (ϵ^* and μ^*) so that the intrinsic attenuation factor, α, can be determined, and examination of the paramagnetic properties of these materials by electron paramagnetic resonance techniques.

BACKGROUND

In the past five years, the study of organic semiconductors has become a focal point of considerable interest and speculation in research. The early work on pyrolyzed polymers and crystalline condensed benzenoid compounds such as anthracene has led to the development of some highly conductive crystalline organic compounds such as tetracyanoquinodimethane.[2/] This work has stimulated work on the electrical behavior of high polymers.

The electrical conductivity of semiconducting polymers is created by the presence of a highly conjugated (alternate single and double bonds between

carbon and/or nitrogen bonds of the polymer backbone) system of chemical bonds. The presence of a highly conjugated bond system reduces the energy required to remove an electron from its bond. For example, in polyethylene each carbon-carbon bond is formed by a pair of electrons. The energy required to remove these electrons is very high, in the order of 3 to 5 e.v. If one removes every other hydrogen to form a series of conjugate double bonds the binding energy holding the electrons in the bond is reduced as the length of the conjugate bond system increases. Linear polyenes prepared by the dehydrochlorination of polyvinyl chloride have been shown to be semiconductors with rather high resistivities and activation energies in the 0.7 e.v. range.[3/]

The d.c. resistivity of the organic semiconductors decreases with increasing temperatures according to the Arrhenius equation

$$\rho = \rho_0 e^{\frac{\Delta E}{kT}}$$

ρ = Resistivity at temperature, °K

ρ_0 = Extrapolated resistance at infinite temperature

k = Boltzman Constant, 8.616 ev/°K

ΔE = Activation energy, e.v.

The activation energy can be determined by measuring the change of resistivity with temperature and the preparation of a log resistivity-reciprocal temperature plot of the data obtained. The slope of the line is the activation energy and the intercept of the line with the y-axis at infinite temperature ($1/T = 0$) is the ρ_0.

In addition to showing some degree of electrical conductivity conjugated polymers exhibit paramagnetic properties. That is, they have susceptibilities (x, relative) that are positive but small. There is a direct correlation between the number of conjugate double bonds and the degree of paramagnetic properties exhibited. This property is due to the existence of unpaired electrons in the polymers. These electrons are probably of both the localized type found in free radicals and those created by conjugate systems that are unlocalized. The unlocalized electrons can perhaps be best visualized as existing in a cloud surrounding the conjugate system (a high degree of π bonding). These unpaired electrons have been found in many types of conjugated polymer systems in concentrations ranging from 10^{15} to 10^{21} per gram of polymer. The presence of these electrons is determined by electron paramagnetic resonance techniques. In addition to providing information about the concentration of these electrons, electron paramagnetic resonance (EPR) techniques can be used to determine the character and interactions of these electrons with the polymer under certain conditions.

Although a considerable amount of effort toward description of the behavior of organic semiconductors has been made many questions remain to be answered. The theory of semiconductivity has been developed to a very useful state for inorganic semiconductors, but the basic theoretical relations in organic semiconductors is still obscure. The nature of the band gap, and the mechanism of charge transport in these materials is largely unexplained. Experimental areas such as doping, dielectric behavior, and carrier injection remain largely unexplored.

APPROACH TO THE PROBLEM

Radio frequency attenuators should possess very high attenuation at high frequencies and relatively low attenuation for low frequencies on d.c. transmission. In principle this is possible because the power absorbed (P) by an attenuator varies directly with frequency, according to the relation

$$P = h\omega\varepsilon''$$

where h and ω are Planck's constant and the angular frequency, respectively and ε'' is the dielectric loss.[4] If ε'' can be held constant, an increase of 90 db attenuation will be observed in going from d.c. to 1 kMc.

Organic semiconductors have been chosen for this application because they show low charge carrier mobilities.[5] If carrier mobilities are sufficiently low, then conductivity and attenuation may be controlled by such processes as space-charge polarization[1] and orientation polarization[1] occurring in the bulk of the material. These processes would lead to an increase of dielectric loss at higher frequencies, with a consequent increase of radio frequency attenuation.

Conductivity in organic semiconductors depends on four factors:

1. Carrier concentration;
2. Carrier charge;
3. Carrier mass; and
4. Carrier mobility.

It is difficult to assess the relative value of these factors until more is known about the charge transport process in organic semiconductors. Carrier concentration is expected to be roughly dependent on the number of unpaired electrons in the semiconductor. This is so, in fact. Carrier charge should be relatively constant for organic semiconductors. The effective mass of positive holes may vary, but that for electron carriers should be relatively constant. We feel that the essential problem in development of rf attenuators using organic semiconductors lies in alteration of carrier mobilities to give a maximal dielectric loss at the frequencies to be attenuated.

The approach to this problem has been very empirical, but insofar as possible, our physical measurements have been used to clarify the charge transport process as well as describe bulk attenuation properties in the organic polymers which have been studied.

EXPERIMENTAL

The following discussion is broken into four parts following the steps used in the experimental work carried out during this program.

1. Polymer Syntheses

During the course of this program several types of polymers have been prepared. Only four of these will be discussed:

1. Xanthene polymers[5]
2. Pyrolyzed polyacrylonitrile[7]

3. Polyaminoquinones[8]

4. Metal chelating polymers derived from diisothiocyanates[9]

The xanthene polymers are prepared by the reaction of dianhydrides such as pyromellitic dianhydride and diphenols. The condensation reaction is carried out in the presence of zinc chloride at temperatures of 200° to 250°C. An extremely black, infusible, insoluble polymer is obtained. The basic structure is shown below. The high degree of conjugation is evident.

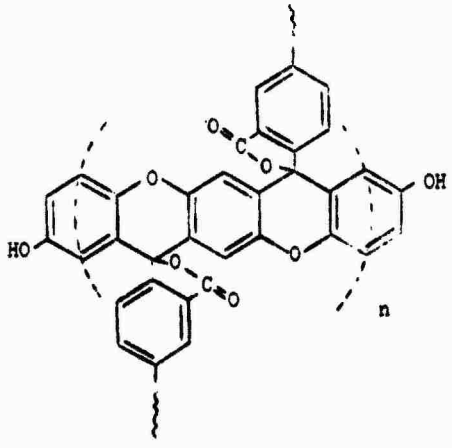

Pyrolized polyacrylonitrile has been the subject of several investigations and has produced semiconducting materials with interesting properties. Those studied during this program were prepared by two methods. Pyrolysis of fibrous samples of the polymer and preparation of thin films of the polymer from solution in dimethyl formamide and subsequent pyrolysis. The polymer changes fromas colorless material to an extremely black material on exposure to temperatures in the 200° to 250°C range. The incorporation of small quantities of copper ion into the polymer prior to pyrolysis was found to increase

the conductivity of the black polymer and also produced lowered activetion energy of conduction. The chemical structure proposed for the pyrolized polymer is shown below.

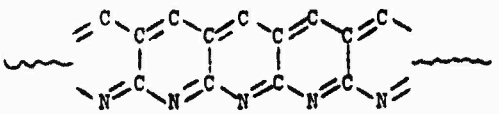

Pyrolized Polyacrylonitrile

A large number of polymers were prepared by the reaction of tetrachloroquinone (chloranil) and various aromatic and aliphatic diamines. These polymers were prepared in two different solvent systems at reflux (boiling) temperatures. Ethanol and dimethyl formamide were used as reaction solvents. The reaction scheme is shown below.

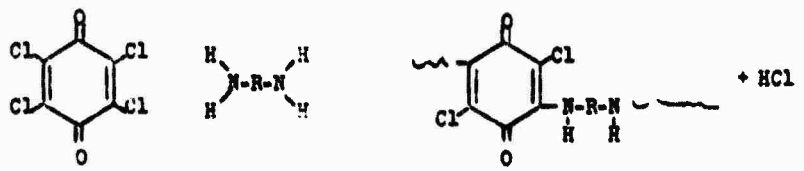

Chloranil Diamine Polyaminoquinone

Twenty-five of these polymers were prepared from various amines as shown in Table I. The polymers precipitated from the reaction media during the course of reaction. The various amines used were chosen to produce polymers of varying degrees of conjugation in their structure. The color of the polymers varied from extremely black to light brown as shown in Table I. Yields varied

from values as low as 5% to 82%. The polymers were insoluble in the normal laboratory solvents and were infusible at temperatures below their decomposition temperatures. A brief examination of the thermal stability of the polymers derived from the phenylenediamines indicated that they were stable at temperatures up to 240°C. Similar stability would be expected of the other polymers. It should be pointed out that the thermal stability of the highly conjugated polymers in inert atmospheres should be relatively good. The increase in resonance observed in these materials should add to their stability.

The fourth class of polymers under consideration are somewhat different than those discussed above. The previous polymers were prepared by condensation of suitable chemical reactants to yield a polymeric material containing a high degree of conjugate bonding. The last class of materials under study are metal chelate polymers, that is, the structure of the polymer is such that metallic ions can be incorporated into the polymer by chemical bonding after the polymer has been prepared. These polymers are of two chemical classes polythioureas and polythiosemicarbazides. The reaction of an organic diisothiocyanate and a diamine yields a polythiourea polymer as shown below.

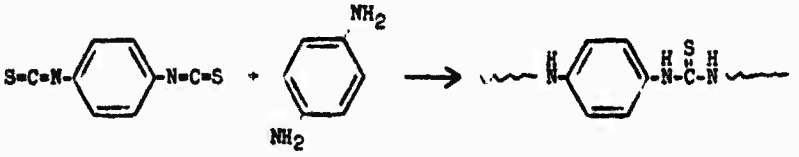

diisothiocyanate diamine A polythiourea

The reaction of a diisothiocyanate and an N-substituted diamine such as N,N-diaminopiperazine yields a polythiosemicarbazide:

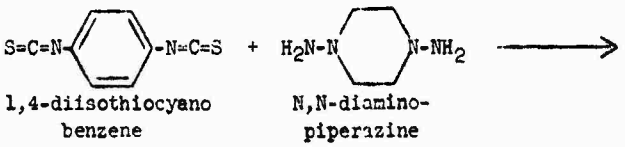

1,4-diisothiocyano benzene

N,N-diamino-piperazine

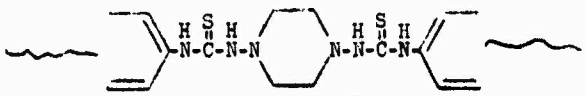

A polythiosemicarbazide

The polythiosemicarbazides have been shown to be excellent chelating agents for copper.[9] Work at MRI on the polythiourea polymers has indicated that certain derivatives of this polymer are also good chelating agents for heavy metals such as copper, silver and lead. The preparation and evaluation of the series of metal chelate polymers is not yet complete, however some data have been collected on the d.c. electrical conductivity of one metal chelate polymer derived from paraphenylenediamine and metadiisothiocyanobenzene.

II. D.C. Electrical Properties

The goal of this program is the correlation of electrical, dielectric and magnetic properties with the polymer's structure. The determination of the change in resistivity with increasing temperatures for the polymers under study was carried out using powdered samples under pressure of approximately [illegible] psi, and a field of 20 to 400 v/cm. There are a number of difficulties

encountered in determining the resistivity of powdered samples. There is some doubt as to what relations between bulk and surface conductivities are observed. Thus it was felt that measurement under high pressures would be desirable. It should be noted that these polymers are piezoresistive, that is, their resistance decreases with increasing pressure and in addition there is a reduction in the observed activation energy of conduction with increasing temperatures. The resistivity parameters determined for a number of the polymers under study are shown in Table II.

Some of the more pertinent data obtained are shown in Figure 1. It should be noted that the volume resistivity and activation energy (slope of line) decreases with increasing conjugation and with the presence of condensed benzenoid structures in the cases of the naphthalene and anthraquinone based polyaminoquinone polymers. The xanthene and copper-doped acrylonitrile polymers are comparable. The polythiourea-copper chelate polymer is a good conductor and has an extremely low activation energy (0.03 e.v.).

III. Determination of Dielectric Properties

As this program is concerned with an investigation of the electrical properties of polymeric semiconductors, the determination of the intrinsic impedance, z, and the intrinsic propagation constant, γ, was desired. The relations

$$z = \sqrt{\mu^*/\epsilon^*}$$

$$\gamma = j\omega\sqrt{\mu^*\epsilon^*} = \alpha + j\beta$$

α = attenuation factor

β = phase constant

exist between these values and complex permitivity $\epsilon^* = \epsilon' - j\epsilon''$ and complex permeability, $\mu^* = \mu' - j\mu''$. Several methods were considered for determining these values. The measurement of the open and short circuit impedance of a coaxial line filled with the polymer under investigation was selected. The impedance measurements were made using a Boonton RX Meter, Type 250-A. Doughnut samples of the polymers were molded at pressures in the range of 30,000 to 40,000 psi. These samples were then fitted into a coaxial sample holder for measurements on the RX meter. Figure 2 shows the mold used for forming the sample and the coaxial sample holder. Reduction of the impedance and geometry measurements to the desired dielectric properties was mathematically quite complicated and is beyond the scope of this discussion. A program for reduction of the experimental data on an IBM 1620 computer was prepared and has been used in all calculations.

Impedance measurements were made at frequencies between 0.5 mc. and 200 mc. Measurements have been made on 32 different polymer samples over these frequencies. Some of the highly pertinent data obtained are summarized in Figure 3.

It is interesting to note that the dielectric constant for several of these polymers is considerably higher than that normally found with organic polymers, whose constants usually range from 2 to 5. In the case of the xanthene polymer the dielectric constant at lower frequencies is approximately 50. The rapid drop in dielectric constant with increasing frequencies is accompanied by an increase in the loss factor (ϵ''/ϵ'). The attenuation values

are quite low and do not increase as rapidly with frequency as might be expected. This phenomenon is probably due to a decrease in (ϵ'') with increasing frequency. The one exception to this trend is found in the AG-NCS sample which is the silver complex formed on reaction with a derivative of paraphenylenediisothiocyanate. For this reason it is hoped that the metal chelate polymers currently under investigation will provide increased attenuation.

EPR PROPERTIES OF POLYAMINOQUINONES

Electron paramagnetic resonance (EPR) spectra show the presence of unpaired electrons in a sample by measuring energy absorbed from a radiation field when the electrons undergo a transition from the +1/2 to a -1/2 spin state. The resonance frequency of the transition is adjusted by orienting the unpaired electrons in a magnetic field. EPR has proved to be very useful for studying the properties of unpaired electrons, and is particularly applicable to the present study.[10]

Electron paramagnetic properties of the polyaminoquinones have been studied rather extensively during this program to aid in the understanding of the charge transport process. Spin concentrations for most of the polymers prepared have been measured by comparing the area of the absorption curve with that of a standard pitch sample. Spin concentrations show a rough relation to conductivity.

In addition to spin concentration, the shape and structure of the absorption curve and its saturation and phase behavior may also give useful information about the nature of the electrons making up the EPR signal.

The important EPR properties of the polyaminoquinones are these:

(1) Spin concentrations are approximately 10^{19} electron spins/gram;

(2) Spin lattice relaxation times (T_1) are about 10^{-7} sec., and transverse relaxation times (T_2) about 10^{-8} sec.;

(3) Phase behavior measured using 100 kc. phase sensitive detection[12] shows that some of the signals are inhomogeneous, and possible composed of two or three kinds of electrons.

(4) The shape of the signal is either Gaussian or Lorentzian. The Lorentzian shape indicates intermolecular electron exchange,[11] and polymers showing a Lorentzian signal have increased conductivity in comparison to similar polymers having Gaussian shapes.

(5) The structure of the signal is that of a single broad absorption band, except in the case of the meta polymers. These show small extra absorptions at the extremities of the main absorption which also indicate that two kinds of electrons make up the signal.

We think that these wings may be caused by an unpaired electron localized at the nitrogen atom, and split into three equal components by interaction with the nitrogen quadrupole moment.

The single EPR characteristic which seems to bear directly on the charge transport mechanism for these polymers is the change of shape of the

absorption curve from Gaussian to Lorentzian. Intermolecular electron exchange is strongly indicated by this effect, and further substantiated by the fact that general comparisons with conductivity data show increased conductivity for those polymers exhibiting a Lorentzian EPR signal. In view of the phase behavior of the signal, and the small "wings" shown on the meta-PAQ polymers, we are inclined to believe that the unpaired electrons in these polymers are associated with positively and negatively charged centers in the molecule, and that p-type conduction indicated by the Seebeck effect proceeds by the electron exchange at the positive centers and resultant motion of positive holes through the bulk polymers.

CONCLUSIONS

The polymer systems described here are probably intrinsic semiconductors, showing moderate conductivity and fairly low activation energies for conduction.

Considered as rf attenuators for the 10 mc. region, those including metals in their formulation seem to be best. The dielectric and magnetic loss tangents are high and fairly constant in the frequency range 10 - 200 mc.; dielectric constant and magnetic permeability are also high and fairly constant. The PAQ polymers seem to be less promising because dielectric constant and magnetic permeability vary inversely through the frequency region of interest.

Neither type of polymer has shown remarkably high attenuation properties, but these can probably be improved with experimentation and as we understand the charge transport process better.

Currently, we are preparing a series of polymers containing chelated metal in their structure, and we expect these to have much improved conductivity and attenuation properties in the 10 mc. region.

41. DISCUSSION

Mr. Steinmark of Picatinny Arsenal asked if it was true that a metal filler was required in order to obtain attenuation. Mr. Christie answered that low values of attenuation were measured without metal fillers. About 90 tests were run on 54 different polymers. Materials were polymers that are not thermoplastic; they have good stability up to about 250°C at which temperature they melt. They were molded at high pressures but it was found that they were fused powders and not solid materials after this process.

Dr. Harvalik mentioned that lead azide may, itself make a fairly good attenuator, especially after it is heated to 145°C over a not-too-projected period of time. Of course, it could blow up the ship (laughter). Mr. Christie commented that metal salts can be easily polarized and decomposed to form free electrons. This is a possible explanation of the larger values of attenuation achieved with metal polymers.

Someone from Dahlgren inquired of the endurance and flexibility of the polymers. Mr. Christie answered that they are of low molecular weight, stable in the presence of oxygen and reasonably stable with temperature. The most stable forms are organic.

REFERENCES

1. Mohrbach, P. F., Wood, R. F., Monthly Progress Report No. P-B1981-8, "Dev. of Broad Band Electromagnetic Absorbers for Electroexplosive Devices," Franklin Institute, Feb. 1963.
2. Kerpler, R. G., Bierstedt, P. E., and Merrifield, R. E., Phys. Rev. Letters, 5, 503 (1960).
3. Bohrer, J., Trans. N. Y. Acad. Sci., Sec. II, 20, 5, 367 (1958).
4. Von Hippel, A. R., "Dielectrics and Waves," John Wiley and Sons, 1954, p. 26.
5. Ann. Rev. Phys. Chem., 13, 319 (1962).
6. McNeil, R., Weiss, D. E., Aust. J. Chem., 12, 643-56 (1959).
7. Topchev, A., et al., Doklady Akad. Nauk. USSR, 128, 312 (1959).
8. Berlin, A. A., Matveeva, N. G., Visokomol. Soedin., 1, 1647-1651 (1959).
9. Campbell, T. W., and Tomic, E. A., J. Pol. Sci., 62, 379-399 (1962).
10. Ingram, D. J. E., "Free Radicals," Butterworths, London, 1958, Chap. 7.
11. Hyde, J. S., Phys. Rev., 119, 1483 (1960).
12. Ingram, D. J. E., ibid., p. 127.

TABLE I

POLYAMINOQUINONES

No.	Diamine	Color	Yield % Theory*
1	p-Phenylenediamine	Black	64
2	m-Phenylenediamine	Black	34
3	o-Phenylenediamine	Black	64
4	4,4'-Diaminobiphenyl	Dk. brown	70
5	4,4'-Diaminodiphenylmethane	Brown	75
6	4,4'-Diaminodiphenylsulfone	Lt. brown	69
7	1,5-Diaminonaphthalene	Black	46
8	1,8-Diaminonaphthalene	Black	39
9	1,4-Diaminoanthraquinone	Black	5
10	1,5-Diaminoanthraquinone	Black	10
11	2,4-Diaminotoluene	Black	65
12	2,5-Dichloro-3,6-diaminobenzoquinone	Black	64
13	o-Tolidene	Dk. brown	64
14	2,4-Diaminophenol	Black	75
15	2,4-Diaminoanisole	Black	79
16	2,4-Diaminobenzoic acid	Black	69
17	1-Nitro-2,4-diaminobenzene	Black	74
18	Triamino-s-triazene	Dk. brown	82
19	Urea	Black	38
20	Diethylenetriamine	Brown	50

*Prepared in N,N-dimethylformamide.

TABLE II

RESISTIVITY PARAMETERS

(from $\rho = \rho_o e^{\frac{\Delta E}{kT}}$)

Polymer Description	$\rho_{30°C}$ (ohm-cms)	ρ_o (ohm-cms)	ΔE (e.v.)
Xanthene	7.5×10^{4}	0.57	0.30
PA-HQ	3.8×10^{5}	0.83	0.34
Copper-Doped Polyacrylonitrile	6.2×10^{5}	0.29	0.40
Polyaminoquinones (See Table I)			
1	8.3×10^{12}	1.59×10^{-3}	0.93
2	3.7×10^{12}	3.55×10^{-3}	0.77
3	5.8×10^{12}	2.51×10^{-2}	0.85
4	9.6×10^{14}	7.94×10^{-4}	1.07
5	2.8×10^{18}	1.26×10^{-7}	1.50
6	2.61×10^{17}	2.89×10^{-4}	1.24
7	1.83×10^{10}	1.42×10^{2}	0.48
8	2.4×10^{10}	0.11	0.69
9	6.8×10^{9}	7.94×10^{-3}	0.76
10	6.1×10^{9}	1.50×10^{-4}	0.80
11	3.0×10^{11}	7.94×10^{-3}	0.76
12	3.3×10^{10}	2.51×10^{-4}	0.59
13	1.8×10^{8}	1.12	0.50
14	1.2×10^{10}	0.64	0.40
15	5.8×10^{11}	21.5	0.64
16	1.3×10^{12}	1.32	0.73
17	1.4×10^{12}	50.1	0.64
18	1.7×10^{13}	0.82	0.62
19	1.2×10^{10}	2.50×10^{-5}	0.89
Copper (Cu^{++}), Polythiourea Complex*	9.80×10^{3}	3.17×10^{3}	0.03
Silver-p-phenylenediisothiocyanate Complex	1.25×10^{6}	2.40×10^{-4}	0.70

*Prepared from p-phenylenediamine and m-diisothiocyanobenzene.

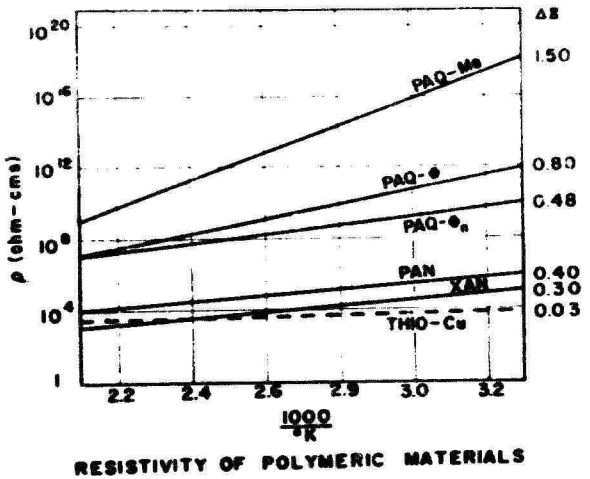

RESISTIVITY OF POLYMERIC MATERIALS

Figure 1 - Resistivity of Polymeric Materials

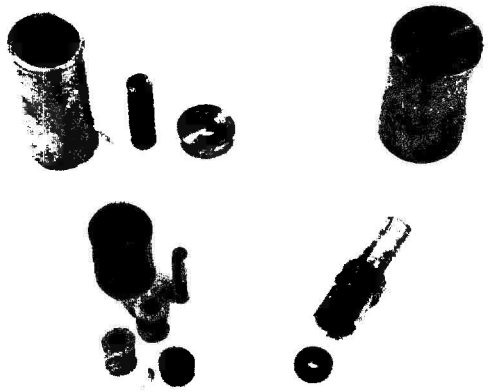

Figure 2 - Sample Mold and Holder

$$\alpha \cong \omega\left[\frac{\mu'}{\mu_0}\cdot\frac{\epsilon'}{\epsilon_0}\left(\frac{\mu''}{\mu'}+\frac{\epsilon''}{\epsilon'}\right)\right]$$

	ϵ'/ϵ_0	μ'/μ_0	ϵ''/ϵ'	μ''/μ'	α (db/cm)
POLYAMINO-QUINONES	4-5 CONST.	2-4 CONST.	0-0.08 DECREASING	10-0.1 DECREASING	0.01-0.16
CHELATES, METAL MIXTURES	10-30 CONST.	1-2 CONST.	0.5 CONST.	0.5 CONST.	0.05-1.2
XANTHENE	3-15 DECREASING	1.5 CONST.	1.3-0.2 DECREASING	0.5 CONST.	0.04-0.10

Figure 3 - Changes in Dielectric Properties from 1 to 100 mc.

42. THERMAL ANALYSIS OF PRIMARY EXPLOSIVES

by:

George Svadeba
Research & Development Division
U.S. Naval Weapons Station, Yorktown, Va.

I. INTRODUCTION

Let me begin the Weapons Station's presentation by taking you to a day in the future. The HERO program assignment has been completed and turned over to appropriate personnel for use. A ship has just returned from its tour at sea. On shore, HERO program personnel from the Naval Weapons Laboratory, Dahlgren, are waiting to determine the levels of electromagnetic radiation encountered by the EEDs since the ship left port. A single EED is selected from shipboard stocks for analysis and forwarded to their laboratory. Upon examination, it is found that the explosive around the bridgewire of the EED has been decomposed by 7%. Since the item selected was a newly manufactured item just released to the fleet, it is known that the total decomposition occurred during a single tour. Checking with available conversion tables, a cumulative frequency-time factor of electromagnetic radiation exposure is obtained. A second table indicates that 40% additional energy will be required to initiate thie EED to provide the same probability of fire, and that this

is still within the energy available from the S&A device. It is further determined, that based on the data just obtained, the probable reliable life under similar conditions of exposure will be one additional trip, after which time, probability of function of the EED will be below acceptable levels, with a high percentage of duds to exist in this stock of EEDs.

This hypothetical situation describes the basic program objectives at the Naval Weapons Station, Yorktown - namely; (1) DETECT changes which have occurred in the EED; (2) DETERMINE what conditions are necessary to effect these changes; and, (3) based on the existing condition of the EED, DETERMINE what the reliability or hazard of the EED will be, or what conditions of exposure will make the EED a hazard or dud.

II. EXPERIMENTAL APPROACH

With these basic program objectives in mind, let me briefly review what we have done, where we are, and where we are going. The first objective is to detect changes in the EED as a result of exposure to electromagnetic radiation. It was assumed and verified during the early phase of the program, that the effect of electromagnetic radiation and consequently, heat, would result in a complex pattern of decomposition of the

primary explosives surrounding the bridgewire of an EED. It was further observed that no single method of analysis was capable of detecting or resolving all the effects associated with decomposition. Accordingly, a variety of techniques were used to approach the problem of analysis, each with a slightly different viewpoint. The total approach has been combined under the program heading of Thermal Analysis. The first technique under study is Differential Thermal Analysis.

A. Differential Thermal Analysis is a technique used to study the effect of heat on any material. The method involves heating the sample under study and a thermally inert reference material to elevated temperatures at a constant rate (variable between 1/2 to 20°C/min.), while continuously recording the temperature difference between them as a function of sample or reference temperature. All of the reactions which can occur in the sample as it is heated are accompanied by energy changes which generally manifest themselves as heat energy. Some produce heat and are called exothermic; some require heat for the reaction to proceed and are called endothermic. On a rising temperature basis, endothermic heat effects can be caused by vaporization, decomposition, inversion, reduction and fusion. The exothermic ones are due to oxidation, crystallization and autocatalytic decomposition. The curves obtained by DTA, called thermograms, may

then be used to characterize the system under study in terms of its thermal reactions, both physical and chemical.

(1) Differential Thermal Analyzer

A Differential Thermal Analyzer is composed of three major components: a sample holder, a controlled source of heat, and a device for the measurement of the heats of reaction. Fundamentally, only a few basic ideas exist, although practically no two units are exactly alike in detail because they are generally assembled individually. The actual design employed, in addition to personal preference, is controlled by the ultimate purpose of the collected data.

The analyzer used in this work was developed by the Robert L. Stone Company of Austin, Texas, and modified for the Naval Weapons Station in order to obtain maximum information about the explosives under study with the minimum size samples. The instrument is capable of producing data under controlled pressure and under a gaseous atmosphere of known, controlled composition. The desired pressure is created by using Nitrogen or compressed air. This allows studies in accordance with the LeChatelier-Braun principle which states that whenever stress is placed on any system in a state of equilibrium, the system will always react in a direction which will tend to counteract the

applied stress. The literature cites a number of reactions which are unexpectedly and quite profoundly affected by pressure.

Gases of known composition may also be swept through the sample during the DTA run to carry off any other gases being evolved through decomposition. This allows studies of reactions with and without the reaction-participating gases present.

A second technique used to study the effect of heat on solid explosives is Infrared Spectroscopy.

B. Infrared Spectroscopy

Infrared spectroscopy is based on three laws of physics: (1) that molecules and the atomic nuclei of molecules are in constant motion, (2) that all molecular motions occur with fixed and characteristics frequencies, and (3) that when the frequency of radiation is equal to a natural frequency of the molecule, then the molecule will absorb radiation. (If the frequency of radiation differs from the frequency of the molecule, the molecule will transmit or reflect the radiation).

The absorption of the molecule depends upon the natural modes of the motion, particularly the vibration of the molecule. Since the vibration pattern of the molecule is determined by the vibrational frequencies of the masses of atoms present in the molecule, the various structural groups and configurations of

molecules will yield characteristic absorptions. Just as each component has its own characteristic infrared absorption spectrum, a mixture of components will yield an absorption spectrum containing the characteristics of all the components. The absorption at each wavelength is the sum of the absorbances for the individual components at a given wavelength, the contribution of each component depending upon its concentration and absorptivity at that wavelength.

The infrared spectrophotometer measures the absorption of the sample by illuminating it with infrared radiation - one wavelength at a time - and plotting (recording) the transmittance of the sample vs the wavelength of radiation. The recorded infrared spectrum is thus a true "fingerprint" of the sample - the most characteristic physical property of the sample.

(1) Equipment

The instrument used in this program is a Beckman IR-5 Infrared Spectrophotometer and is an automatic recording double beam instrument. Equipped with NaCl optics, the IR-5 has a wavelength range of 2 to 16 microns and scans the entire wavelength range in 16 minutes, recording linearly in transmittance and wavelength.

The explosives under study are prepared for sampling

using the Potassium Bromide technique. This method consists of diluting the materials in solid Potassium Bromide and then pressing the mix to give a fused disk which can be introduced into a light beam of a spectrophotometer. Since the Potassium Bromide is transparent over the range of interest, the resulting spectrum is that of the sample.

The third major technique used in the program is Gas Chromatography.

C. Gas Chromatography

The fact that gaseous mixtures are separated into their component parts as they are passed through a packed column of certain solid materials has given rise to a method of analysis known as gas-solid chromatography. This separation is accomplished through the phenomena of ad-and absorption of the gas by the solid. One of the most prominent materials used in gas-solid chromatography is the molecular sieve. The molecular sieve is a dry, crystalline material containing small diameter pores that act not only as a sorbent for certain gases, but is so manufactured that it is capable of separating molecules on the basis of size. In an operating gas chromatograph, the sample to be analyzed is injected into an injection port where it is picked up by a carrier gas and transported through a separating

column. As the sample gases are of a different size, the smaller ones may pass through the pores of the sieve practically unhindered, while the larger ones may require a considerable period of time to find its way through the column. If a detector is placed at the end of the column, the time for the gas to appear and the quantity of gas present may be determined. A simplified block diagram as well as a flow schematic of a typical gas chromatograph is shown below.

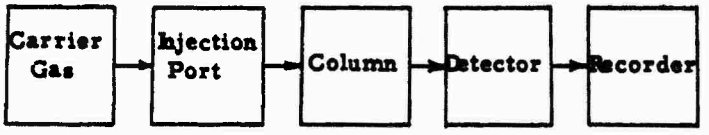

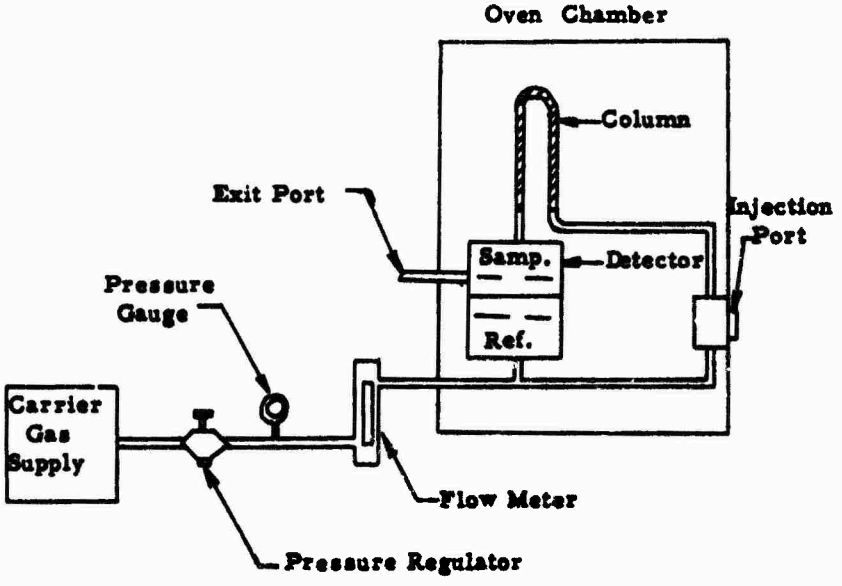

FLOW SCHEMATIC

Figure 1

(1) Equipment

The equipment used for this study was a F&M Model 500 linear programmed high temperature gas chromatograph. It is capable of either programmed or isothermal temperatures to 500°C and has separate and independent temperature controls for column, detector and injection port. The detector is a thermal conductivity cell and its response is based on the difference in thermal conductivity between the carrier gas and the sample components, and furnishes the signal for a Minneapolis-Honeywell Model No. Y143X Recorder. The column used was a six foot stainless steel, coiled column packed with Molecular Sieve No. 5A, (5 Angstrom pores).

III. EXPERIMENTAL PROGRAM

With a number of techniques available for use in the study of thermal effects on primary explosives (including several not described which include TGA and microscopy), we are now able to proceed to the second program objective - namely, determine what conditions were necessary to effect the changes noted. This work is currently in process, but I would like to give you a preview of what information is available to date, and the direction of our present work. The following curve, Figure 2, is a plot of decomposition of Lead Azide as a function of time at fixed temperature.

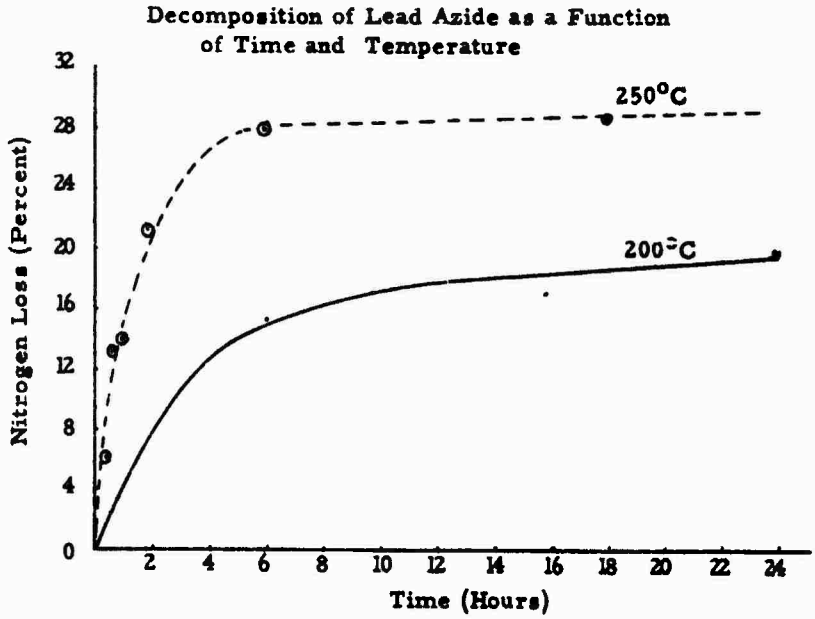

Figure 2

The completed curve is based on studies at 250°C and shows that at relatively high temperatures, Lead Azide decomposes quite rapidly. During this decomposition under atmospheric conditions, the lead oxidizes forming a number of oxides. The oxides formed depends on the decomposition temperature. Let me call your attention to the points on the 200°C and 250°C curves for six hours. At 250°C, the sample is virtually completely decomposed insofar as the Lead Azide is concerned. The oxides formed at this temperature, however, are chemically active. The decomposition at 200°C for six hours is roughly 60% complete with lower oxides

formed. Let us now look at a comparison of weight losses of the explosive and degree of decomposition. It is immediately seen in Table 1

Table 1

Nitrogen Loss vs Weight Loss of Lead Azide

200° C.			250° C.		
Time	Weight Loss	Nitrogen Loss(GC)	Time	Weight Loss	Nitrogen Loss(GC)
6 hrs.	15.1	15.1	20 min.	6.2	6.7
6 hrs.	15.1	15.2			
			30 min.	11.5	13.1
16 hrs.	14.8	16.4			
16 hrs.	14.8	16.1	1 hr.	11.6	13.9
24 hrs.	18.7	20.5	2 hrs.	13.7	20.7
24 hrs.	18.7	18.2			
			6 hrs.	16.3	27.8
65 hrs.	20.3	21.8			
			18 hrs.	19.7	28.1

that at 200°C, weight losses are nearly comparable to the degree of decomposition as determined by the loss of nitrogen, while weight losses at 250°C show much smaller losses in weight. This indicates a higher degree of oxidation taking place at the higher

temperature. Why is this important, or is it? The indications right now are that it is important, particularly when we attempt to apply this information to the third phase of the program. In this phase, we are attempting to correlate the reliability of the EED with the degree of decomposition. The curve illustrated below (Figure 3), shows the energy requirement for 50% fire of Lead Azide versus the degree of decomposition.

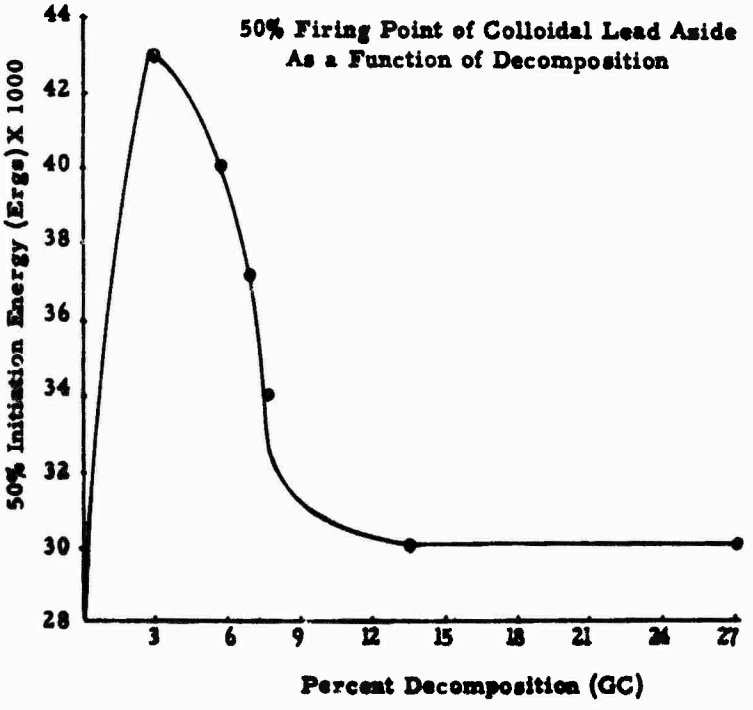

Figure 3

A Mk 1 Mod 0 Squib was used as a standard test vehicle. The curve shows that as the explosive begins to decompose, the energy

required for the 50% point increases until a maximum is reached at 7% nitrogen loss or 25% decomposition. Up to this point, this is as expected. As the explosive initially decomposes, it may act as an insulator, requiring greater initiation energy to reach the remaining undecomposed explosive. Beyond this point, however, the energy requirement drops until it stabilizes at and beyond 14% nitrogen loss or 50% Azide decomposition. How can this be explained? First, let me note that as the energy drops from the peak required for initiation, the acoustic intensity of the detonated squib also drops. To distinguish between "go's" and no-go's) in this region, we are presently attempting to coat the bead with a second coat of undecomposed Lead Azide. We hope that detonation of the second stage Azide can be used to distinguish burning or sparking from lower energy detonation which can still build up to full detonation of the EED. Let me return to the weight loss versus decomposition curves which showed the formation of different oxides, depending on the decomposition temperature. The indications to date are that the higher oxides are not inert, but are capable at least of ignition. The drop in acoustic intensity noted, therefore, would be explained by the reduction of active Lead Azide into lower energy oxides plus the remaining undecomposed Lead Azide. The conclusion of the second stage Azide firings will thus

provide us with the first part of the third program objective, namely - predict the degree of hazard or dud in an EED. Since we have now touched on the three phases of the program at Yorktown, let me cover briefly the work that has been done to date on Diazodinitrophenol or DDNP as it is generally known.

DDNP was one of the explosives studied early in our program which responded to analysis by infrared spectroscopy. I mention it here only to illustrate the point that it is quite probable that different explosives will respond to different analytical techniques. While the data available is sketchy, it shows that infrared analysis of DDNP offers a potential for resolving decomposition. The curve in Figure 4 illustrates the absorption spectra of DDNP.

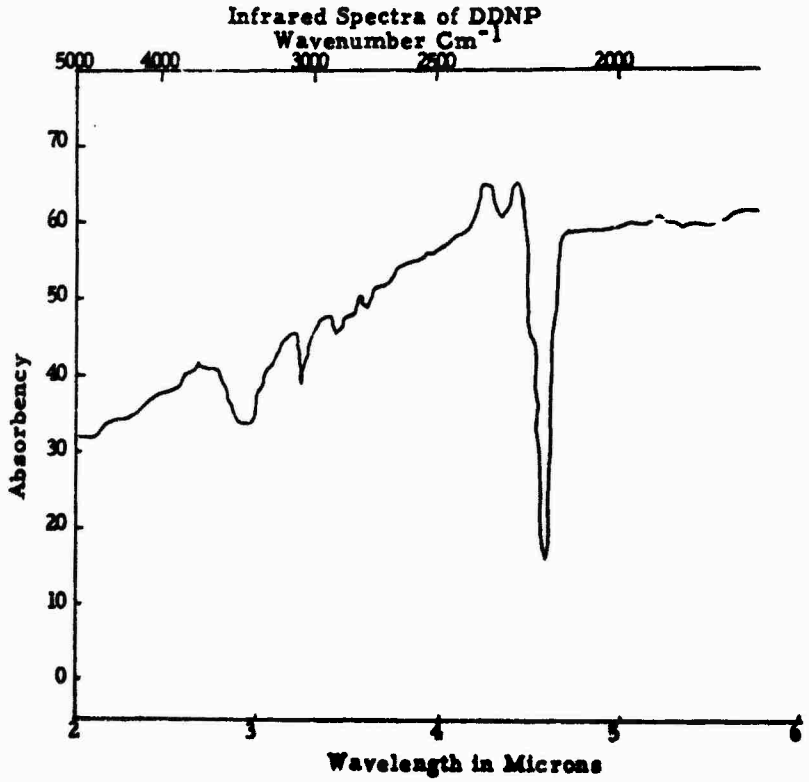

Figure 4

Samples of DDNP were heated under various conditions and carefully weighed after heating to determine the loss in weight. The decomposed samples were retested and showed a decrease in the absorption band at 2200 cm^{-1} until the band completely disappeared. The decrease and final disappearance of this band appears to be directly related to the decomposition of the DDNP as illustrated in Figure 5.

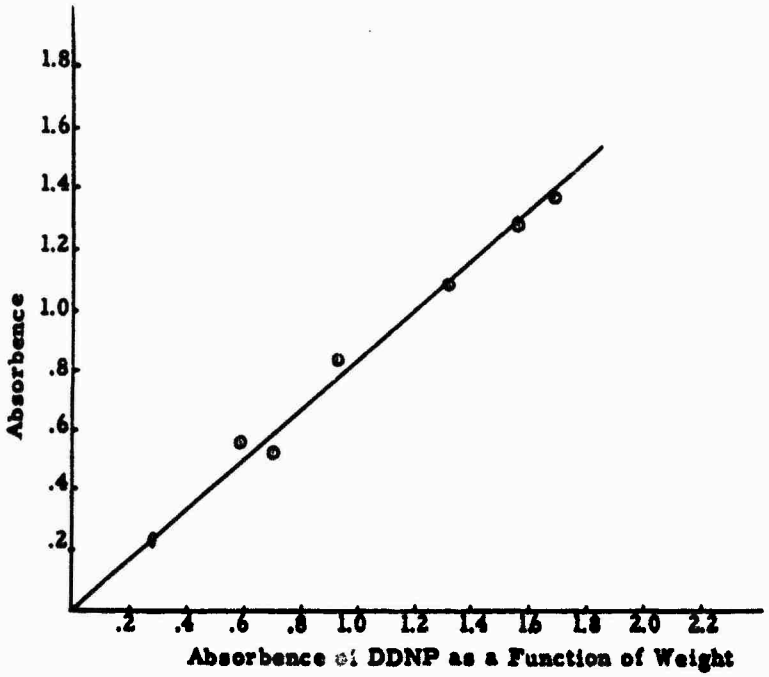

Figure 5

Should this method for determining the degree of decomposition of DDNP be accurate within limits required for this program, it can be used to relate firing-decomposition-time data as illustrated earlier for Lead Azide.

IV. SUMMARY

The information obtained to date indicates that the objectives of the program at the Naval Weapons Station can be achieved. We have developed or applied a number of techniques to the analysis of primary explosives to determine the degree of decomposition

of primary explosives. We are in the process of completing work which we feel will enable us to determine what conditions of temperature and time the explosives have been exposed to. And, finally, we have illustrated that decomposition of the explosive can affect the firing of an EED. There is still much to be done. Some of the things we plan to do in the future are:

(1) Continue second stage firings simulating a complete EED in an attempt to redefine a failure or "no go" in our tests.

(2) Complete studies of Colloidal Lead Azide. This will include completion of time-temperature-decomposition curves with related firings of Mk 1 Mod 0 squibs.

(3) Extend present studies to ignition systems presently used in EEDs in the fleet today, or proposed for use. Lead Styphnate is next on our list for study.

(4) Study the problem of sampling the explosive from the EED for testing. Areas such as effect of solvents on decomposition products, interference of binder on test results, etc.

(5) Evaluation of new techniques where required (Thermovolumetric Analysis, which plots gas evolution from DTA tests as a function of temperature).

PAPERS NOT PRESENTED ORALLY

43. Picatinny Arsenal RF Facilities, Test Results and Future Plans (U) — A. Grinoch

A transmitter has been developed for this program to cover the frequencies from 300 Mc to 10,000 Mc. A miniature tape recorder is being developed to handle the output of 20 sensors. Some limited RF tests on ordnance items have been performed. Future plans include an indoor RF transmitting facility with RF simulation chambers for the lower frequency range.

44. Transient Electromagnetic Field Propagation Through Infinite Plates and Into Hollow Cylinders and Spherical Shells of Finite Conductivity — Charles W. Harrison, Jr.

Gaussian electromagnetic field pulses of several standard deviations are propagated through infinite plates, into the interior of hollow cylinder and spherical shells. It is shown that gaussian pulse fields of relatively long-time duration (standard deviation of 24μ-sec or more) defined on the surface of plates and cylinders are propagated through the metal walls with some diminution in amplitude. When the incident pulse undergoes reflection at the boundary surface as well as transmission through the metal wall, the total attenuation sustained by the field is enormous.

45. The Sandia RF Testing Facility Using Low Level Electromagnetic Radiation: A Status Report — C. W. Cook

The Sandia Corporation low level RF testing system is now a fully operational test facility. The changes necessary to develop the experimental system into a fully operational system are described in detail. Its capabilities, its advantages and disadvantages and the techniques of testing as well as the methods of automatic data acquisition are described. Anticipated future uses for this type of test facility are discussed.

46. Slot Receiving Antennas as Related to Radio Frequency Hazards to Ordnance — Charles W. Harrison, Jr.

These types of slot receiving antennae are discussed quantitatively in this paper. The general theory is applied to solve specific problems. The results are presented in the form of curves relating the power to the frequency. These curves may be regarded as transfer characteristics for the slot receiving systems because from them the power in the load for any given value of field strength may be determined immediately. In the low-to-medium frequency region, most of the curves have a positive slope of 6 db/octave with increasing frequency, and beyond 10 Mc/sec they are oscillatory in nature.

47. A Study of the Simulation of Instrumented to Loaded EED's — D. Boyd Barker, Richard K. Fry

With the assumption that both instrumented and loaded EED's behave as linear systems, the analysis predicts the degree of simulation in terms of basic thermal parameters. Measured values of parameters and evidence supporting the model are given. Graphs are presented characterizing the degree of simulation for devices under various conditions.

48. Measurement of the Least Possible (Worst Case) Attenuation of Protective Devices for Electroexplosive Devices — Ramie H. Thompson

The attenuation of a protective arrangement may result from reflection, or energy absorption and dissipation, or some combination of the two. That part which is due to reflection can be cancelled or reduced under some conditions of impedance relationship; the least possible (worst case) attenuation is that due to absorption alone. This value is shown to be that which is measured in a system employing matching networks on both sides of the sample under test. Formulas are derived by analysis of equivalent circuits, and experimentally verified. This method is particularly useful for the 20Kc - 100Mc range, where impedances are easily measured, but matching systems may have objectionable inherent loss.

49. Anti-RADHAZ Device for Bombs (U) — L. L. Woolston

This device protects electroexplosive components in the bomb's fusing system by providing total impermeability to electromagnetic radiation from radar and communication transmitters at all frequencies. This is accomplished by using a conductive barrier, penetrated only after bomb release, between the bomb connector and the electrical charging cable to the aircraft. RADHAZ tests and recent functional tests have been so successfully indicated that the design principle used may be useful in future weapons as well as for the current application.

50. Picatinny Arsenal Artillery Ammunition Laboratory Program — Stanley M. Adelman

The Artillery Ammunition Laboratory at Picatinny Arsenal has for several years been engaged in a program to determine the vulnerability of electroexplosive devices and to safeguard electroexplosive devices from RF radiation. This has included theoretical analysis, laboratory testing and field testing where possible, and also the incorporation of RF attenuators in electroexplosive devices.

51. Infrared Detector Techniques for Estimating the RF Power in a Heated Bridgewire — John P. Warren

A detector is mounted close to, but not touching, the bridgewire, to measure infrared radiation. This measurement is an indication of the amount of RF energy input which causes the radiation. The system is calibrated with DC input, because measurement of DC power presents no problems. Two such detestors are described in detail, with their instrumentation; capabilities and limitations are discussed.

52. Non-Electric Stimulus Transfer Systems and Through-Bulkhead Ignition — Robert C. Allen

Non-electric stimulus transfer systems (NESTS), incorporating completely contained mild or miniature detonating fuse and through-bulkhead detonation or ignition transfer units, can be designed to accomplish any number of one-shot functions from ignition and destruct to the actuation of valves and switches. Properly designed NESTS are completely insensitive to RF, stray currents, and other induced or even deliberately applied electric currents and also eliminate the need for primary explosive compositions, ground check-out equipment, and critical interface tolerances.

53. A Feasibility Study for a Sonic Arming/Safing System for Aircraft Weapons System (U) — James A. Rummel

Sonic energy is mechanical energy--not electromagnetic energy. Thus sonic energy cannot induce electrical current in firing circuits of squibs or fuzes. This premise prompted a study which demonstrated the feasibility of a sonic arming/safing system for air-dropped weapons.

54. EMR Hazards to EEDs — Lt. Col. Reuben B. Moody

Concern over electromagnetic radiation hazards to electroexplosive devices (ord EEDs) arises from the fact that electrical leads to an EED can, under certain conditions, act as an antenna. There have incidents, albeit very few, when leads to an EED have extracted sufficient energy from an electromagnetic field environment to cause inadvertent detonation.

44 TRANSIENT ELECTROMAGNETIC FIELD PROPAGATION THROUGH INFINITE SHEETS, INTO SPHERICAL SHELLS, AND INTO HOLLOW CYLINDERS

by

Charles W. Harrison, Jr.
Member of the Technical Staff,
Sandia Corporation, Albuquerque, N. M.

Introduction

This study was undertaken to determine the shielding characteristics of thin-walled infinite sheets, spherical shells, and cylindrical tubes, illustrated by Figure 1, under transient conditions. The shields are made of aluminum and contain no slots. Gaussian electromagnetic field pulses are propagated through the infinite sheets, and from outside to the inside of closed containers in the geometrical shape of spheres and cylinders. Time histories of the attenuated pulses are computed. For the case of the infinite conductive sheets the propagated pulses are compared to the associated impinging pulses on the basis of available energy per unit area.

Finally, the field is calculated in the interior of cylindrical tubes of finite lengths, when the ends are connected by wire to a generator delivering a current pulse of gaussian shape. From the theoretical point of view, this problem is closely related to that of calculating the field within a missile stripped of interior components, when subjected to a direct lightning strike.

The Impinging Gaussian Pulse

The description of the impinging pulse in the time domain employed in this paper is

$$e(t) = Ae^{-\frac{1}{2}\left(\frac{t}{t_1}\right)^2} \tag{1}$$

where A is the value of e(o), t is the time, and t_1 is a measure of the pulse width. The spectrum of the pulse is obtained by taking the Fourier transform of (1). Thus,

$$E(f) = A\int_{-\infty}^{\infty} e^{-\frac{1}{2}\left(\frac{t}{t_1}\right)^2} e^{-j2\pi ft}\,dt = At_1\sqrt{2\pi}\,e^{-\frac{1}{2}\left(\frac{f}{f_1}\right)^2} \tag{2}$$

where

$$f_1 = \frac{1}{2\pi t_1}. \tag{3}$$

In evaluating Fourier transforms by numerical methods it is often convenient to truncate the frequency spectrum in passing from the frequency to time domain, and truncate the limits of integration when computing the frequency spectrum of a given time function.

Let $e_1(t)$ be the new time function obtained by taking the transform of the truncated frequency function. Assume that the cutoff frequency is $f_c = 2.6f_1$. The error is then

$$\eta(t) = |e(t) - e_1(t)| = \left| \int_{-\infty}^{-2.6f_1} E(f)e^{j2\pi ft}\,df + \int_{2.6f_1}^{\infty} E(f)e^{j2\pi ft}\,df \right|. \tag{4}$$

Thus,

$$\eta(t) \leq 2\int_{2.6f}^{\infty} |E(f)|\,df. \tag{5}$$

Substituting (2) into (5) and integrating, $\eta(t) \leq 0.0093A$. Thus, $e_1(t)$ does not depart from $e(t)$ by more than 1 percent at any time.

If $e(t)$ is a plane wave, the energy in the pulse is given by

$$U_t = \frac{1}{\zeta_0}\int_{-\infty}^{\infty} [e(t)]^2 dt = \frac{1}{\zeta_0}\int_{-\infty}^{\infty} |E(f)|^2\,df, \tag{6}$$

where the last relation follows from Parseval's identity.

The energy lost by truncation of the spectrum is

$$U_f = \frac{2}{\zeta_0}\int_{2.6f_1}^{\infty} |E(f)|^2\,df. \tag{7}$$

In these expressions $\zeta_0 = 120\pi$ ohms is the characteristic resistance of space. Substituting (2) into (6) and (7), and performing the integration, it is found that $U_f = 0.000236U_t$. Thus, 0.0236 of 1 percent of the energy is lost by truncation of the frequency spectrum at $f = 2.6f_1$.

In this paper the highest significant frequency contained in a gaussian pulse is taken to be $f_c = 2.6f_1 = 2.6/2\pi t_1$. The "significant" base width of the time function is $2 \times 2.6t_1 = 5.2t_1$. Thus, when $t_1 = 12\ \mu s$ the pulse duration is considered to be $62.4\ \mu s$. The highest significant frequency in this pulse is 34.48 kcs. The half-amplitude width of a gaussian pulse is $2.355t_1$.

The Transfer Functions for Sheets, Spheres, and Cylinders

It is readily shown from elementary principles of electrodynamics that the transfer functions for an infinite sheet of thickness d for parallel incidence of the electric field are [1,2]

$$\frac{E_t(f)}{E_0(f)} = \frac{2\zeta_0\zeta}{2\zeta_0\zeta\cos kd + j\left(\zeta_0^2 + \zeta^2\right)\sin kd}, \tag{2}$$

and

$$\frac{E_i(f)}{E_t(f)} = \frac{\zeta_o}{\zeta_o \cos kd + j\zeta \sin kd}, \tag{9}$$

where $E_i(f)$ is the electric field emerging from the far side of the sheet, $E_s(f)$ is the incident electric field, and $E_t(f)$ is the tangential electric field on the near side of the sheet.* This field is the vector sum of the incident and reflected fields. $E_o(f) >> E_i(f)$, and when $f > o$, $E_t(f) > E_i(f)$ because of skin effect (refer to Figure 1).

$$\zeta = \sqrt{\frac{\pi f \mu}{\sigma}}\,(1 + j), \tag{10}$$

$$k = \sqrt{\pi f \mu \sigma}\,(1 - j), \tag{11}$$

where $\mu = 4\pi \times 10^{-7}$ henry/m is the permeability of space and $\sigma = 3.72 \times 10^7$ mhos/m is the conductivity of aluminum.

In deriving (8) and (9), a time dependance of the form exp(j2πft) is assumed.

The transfer function for a spherical shell is[3]

$$\frac{H_i(f)}{H_s(f)} = \frac{1}{\cosh \gamma d + \frac{1}{3}\gamma a \sinh \gamma d}. \tag{12}$$

Here, H_i is the magnetic field inside the spherical shell, H_s is the incident magnetic field, a is the outer radius of the shell, b is the inner radius of the shell, and $d = a - b$ is the shell thickness.

$$\gamma = \sqrt{\pi f \mu \sigma}\,(1 + j). \tag{13}$$

The cylinder transfer functions are[4]

$$\frac{E_i(f)}{E_t(f)} = \frac{J_o(kb)N_1(kb) - N_o(kb)J_1(kb)}{J_o(ka)N_1(kb) - N_o(ka)J_1(kb)}, \tag{14}$$

and

$$\frac{E_t(f)}{I_o(f)} = \frac{1}{\pi a}\left(\frac{ka}{2}\right)\cot kd. \tag{15}$$

In deriving (14) and (15), a time dependence of the form exp (j2πft) is assumed. Here a and b are the outer and inner radii of the tube, respectively, and $d = a - b$ is the wall thickness.

---

* The subscripts i, o, and t on the fields mean inside, outside and tangential, respectively.

Now,[8]

$$J_e(kb)N_1(kb) - N_e(kb)J_1(kb) = -\frac{2}{\pi kb}. \tag{16}$$

(This is the Wronskian relation.) On combining (14) and (15), and making use of (16),

$$\frac{E_i(f)}{I_e(f)} = -\frac{\cot kd}{\pi^2 \sigma ab}\left[\frac{1}{J_e(ka)N_1(kb) - N_e(ka)J_1(kb)}\right]. \tag{17}$$

This expression permits calculation of the steady-state field within the cylinder in terms of the total current delivered by the current generator directly connected by wire to the ends of the cylinder. It is assumed that the current is uniform in this circuit. This will be the case if the circuit dimensions are small in terms of the wavelength of the highest significant frequency contained in the shortest current pulse employed in this study.

If a plane-wave electric field is directed parallel to the axis of an isolated cylinder, the current $I_e(f)$ at its mid-point is obtained from antenna theory. It is given by the relation

$$I_e(f) = \frac{2h_e(f)E_e}{Z_e(f)}. \tag{18}$$

The effective length of the cylinder is $2h_e$, and Z_e is its impedance. If $\Omega \geq 7$ and $\beta h = \frac{2\pi}{\lambda} h \leq \frac{2\pi f_c}{c} h \leq 0.5$,[9]

$$2h_e(f) = \frac{h(\Omega - 1)}{\Omega - 2 + \ln 4}, \tag{19}$$

and

$$Z_e(f) = \frac{\zeta_e}{6\pi}(\beta h)^2\left[\frac{1 + \frac{4\ln 2}{\Omega - 2}}{\left(1 + \frac{2\ln 2}{\Omega - 2}\right)^2}\right] - j\frac{\zeta_e}{2\pi\beta h}\left[\frac{\Omega - 2}{1 + \frac{2\ln 2}{\Omega - 2}}\right], \tag{20}$$

where Ω is the cylinder shape parameter. It is

$$\Omega = 2\ln\frac{2h}{a}. \tag{21}$$

The length of the cylinder is $2h$.

It is of interest to note that as $f \to 0$, the transfer functions (8), (9), (12), (14), and (15) become

$$\left.\frac{E_i(0)}{E_e(0)}\right|_{\text{plate}} = \frac{1}{1 + \frac{\zeta_e \sigma d}{2}}, \tag{22a}$$

$$\left.\frac{E_i(0)}{E_t(0)}\right|_{\text{plate}} = 1, \tag{22b}$$

$$\left.\frac{H_i(o)}{H_o(o)}\right|_{sphere} = 1, \tag{22c}$$

$$\left.\frac{E_i(o)}{E_t(o)}\right|_{cylinder} = 1, \tag{22d}$$

$$\left.\frac{E_t(o)}{I_o(o)}\right|_{cylinder} = \frac{1}{2\pi\sigma a}. \tag{22e}$$

Also, from (18) as $f \longrightarrow o$,

$$I_o(o)\Big|_{antenna} = 0. \tag{22f}$$

Let

$$G(f) = G_R(f) + jG_I(f) \tag{23}$$

represent any one of the foregoing transfer functions. It can be readily verified by expanding the trigonometric, hyperbolic, and Bessel functions in series, and examining the resulting expressions, that they satisfy the relation

$$G^*(f) = G(-f). \tag{24}$$

That this holds for (18) follows from the fact that $Z_o^*(f) = Z_o(-f)$, as an inspection of (20) shows. Expression (24) sets forth an important property of any transfer function applying to a physically realizable system.

From (23)

$$G(-f) = G_R(-f) + jG_I(-f), \tag{25}$$

and by definition

$$G^*(f) = G_R(f) - jG_I(f). \tag{26}$$

It follows that

$$G_R(f) = G_R(-f) \tag{27}$$

is an even function, and

$$G_I(f) = -G_I(-f) \tag{28}$$

is an odd function.

The Form of the Integrals to be Evaluated by a Computer

For illustrative purposes, let it be supposed that the time function of the electric field within a hollow cylinder is to be computed in terms of the gaussian pulse current the generator delivers by wire to the ends of the cylinder. In this instance, G(f) is the shorthand notation for the right-hand side of (17). Then,

$$E_i(f) = G(f)\, I_o(f). \tag{29}$$

$I_o(f)$ corresponds to (2), that is,

$$I_o(f) = At_1\sqrt{2\pi}\, e^{-\frac{1}{2}\left(\frac{f}{f_1}\right)^2} \tag{30}$$

for a current pulse in the time domain corresponding to (1). A is in amperes, and $I_o(f)$ in amperes/Hz for this particular situation.

The time history of the field on the interior of the cylinder is available from the integral

$$e_i(t) = At_1\sqrt{2\pi}\int_{-\infty}^{\infty} G(f) e^{-\frac{1}{2}\left(\frac{f}{f_1}\right)^2} e^{j2\pi ft}\, df$$

$$= At_1\sqrt{2\pi}\int_{-f_c}^{f_c}\left\{G_R(f)\cos 2\pi ft - G_I(f)\sin 2\pi ft\right.$$

$$\left. + j\left[G_R(f)\sin 2\pi ft + G_I(f)\cos 2\pi ft\right]\right\} e^{-\frac{1}{2}\left(\frac{f}{f_1}\right)^2} df, \tag{31}$$

provided the time dependence assumed in deriving G(f) is exp (j2πft). Since $G_R(f)$ and cos 2πft are even functions, and $G_I(f)$ and sin 2πft are odd functions, it follows that (32) reduces to

$$e_i(t) = 2At_1\sqrt{2\pi}\int_0^{f_c}\left[G_R(f)\cos 2\pi ft - G_I(f)\sin 2\pi ft\right] e^{-\frac{1}{2}\left(\frac{f}{f_1}\right)^2} df. \tag{32}$$

This is the final form of the integral to be evaluated on the computer. Note that the integral is necessarily real because $e_i(t)$ is a real function of time. All of the integrals encountered in this paper concerning the various shields are similar in form to (32). The constant A was taken as unity throughout the work. Of course, the units of A will depend on the shielding problem being considered.

Discussion of Graphs

Graph 1 shows the amplitude-time relation of some of the input gaussian pulses used in the numerical study. Specifically, pulses are drawn for values t_1 of 6, 12, 24, and 48 μs. Note that the peak amplitude of unity occurs at zero time. The pulses are symmetrical on the time scale.

Graph 2, based on (9), gives the steady-state transfer characteristic relating $E_i(f)$ to $E_t(f)$ for an infinite aluminum plate of thickness 1/32 inch, 1/16 inch, and 1/8 inch. For example, for a 1/16-inch plate at 15 kcs, the field emerging from the plate $E_i(f)$ is 30 db below the tangential field $E_t(f)$ on the other side of the plate.

Graphs 3, 4, 5, and 6 give the time history of the field $e_i(t)$ emerging from the plates of designated thicknesses in terms of $e_t(t)$ for values of t_1 of 6, 12, 24, and 48 μs, respectively. The value of $e_t(o)$ is 1 volt/m. Note that in all cases, the attenuation of the field is not great, but progressively increases with plate thickness and decreasing values of t_1. The waves are retarded in time in propagating through the plates, as should be anticipated. The delay increases with plate thickness.

Graph 7, based on (8), is like Graph 2, except that $e_o(t)$ replaces $e_t(t)$.

Graphs 8, 9, 10, and 11 correspond to Graphs 3, 4, 5, and 6, respectively, except that $e_o(t)$ replaces $e_t(t)$. Note that the wave shapes are very much alike, but the amplitude scale is vastly different. Graph 8 shows, for example, that when the peak value of $e_o(t)$ is 1 volt/m, $t_1 = 6$ μs, and $d = 1/32$ inch the peak value of $e_i(t)$ is about 1.61×10^{-7} volts/m, and occurs at 0.01 ms. If $e_o(t) = 10^5$ volts/m, $e_i(t) = 0.0181$ volts/m. Note that $e_o(t)$ undergoes reflection at the boundary surface, and this accounts for the large attenuation afforded by the sheet.

Graph 12, based on (12), gives the steady-state transfer characteristic relating $H_i(f)$ to $H_o(f)$ for a 36-inch spherical shell made of aluminum having wall thicknesses of 1/32 inch, 1/18 inch, and 1/8 inch. As an illustration, for a 1/18-inch wall 38-inch sphere at 7 kcs, the magnetic field $H_i(f)$ on the interior of the sphere is 56 db below the incident magnetic field $H_o(f)$.

Graphs 13, 14, 15, and 16 give the time history of the magnetic field $h_i(t)$ inside the 36-inch spheres of designated wall thicknesses when the magnetic field $h_o(o) = 1$ ampere/m for t_1 values of 24, 48, 96, and 1000 μs, respectively. As expected, as the pulse length increases, the field $h_i(t)$ increases. The thicker the shield, the more effective it becomes. Note the severe distortion of the incident pulse in propagating into the interior of the sphere.

Graph 17 is like Graph 12, except that it applies to a 72-inch spherical shell.

Graphs 18, 19, 20, and 21 correspond to Graphs 13, 14, 15, and 16, respectively, except that the computations were carried out for a 72-inch spherical shell.

Graph 22, based on (14), gives the steady-state transfer characteristic relating $E_i(f)$ to $E_t(f)$ for a cylinder 22.08 feet in length and 16 inches in diameter when the wall thicknesses are 1/32 inch, 1/16 inch, and 1/8 inch.

Graphs 23, 24, and 25 give the time history of the field $e_i(t)$ in the interior of the above cylinder when $e_e(o) = 1$ volt/m for t_1 values of 6, 12, and 24 μs. These graphs applying to finite cylinders have much in common with Graphs 3, 4, and 5 applying to infinite plates.

Graph 26, computed from (14), (15), and (18), permits one to obtain the db ratio of $E_i(f)$ to $E_e(f)$ under steady-state conditions for a cylinder 22.08 feet in length and 16 inches in diameter, when the plate thickness and frequency are specified.

Graphs 27, 28, and 29 furnish the time history of $e_i(t)$ for $e_e(o)$ of 1 volt/m for the designated cylinder for t_1 values of 6, 12, and 24 μs and for wall thicknesses of 1/32 inch, 1/16 inch, and 1/8 inch. Note that the interior field is extremely minute in terms of the incident field. Most of this attenuation is due to the fact that the incident field is reflected by the cylinder; the field $e_i(t)$ is extremely small compared to $e_e(t)$. Observe that the field on the interior of the cylinder is oscillatory in nature. This is accounted for by the fact that the transfer characteristic $E_i(f)/E_e(f)$, obtained by eliminating $I_e(f)$ between (17) and (18) rises with increasing frequency, and then falls off as the frequency is still further increased, as Graph 26 shows. No other transfer functions employed in this paper exhibit this property. The phenomenon is not to be attributed to antenna resonance. The cylinder remains short in terms of the wavelength of the highest significant frequency contained in the shortest pulse considered in the analysis.

Graph 30, computed from (17), furnishes the ratio of $E_i(f)/I_e(f)$ as a function of frequency for a cylinder 22.08 feet in length and 16 inches in diameter having wall thicknesses of 1/32 inch, 1/16 inch, and 1/8 inch. Thus, for a total current in any cross section of the cylinder of 1 ampere, the field in the interior of the cylinder will be 10^{-10} volts/m, if the frequency is 150 kcs and the cylinder wall thickness is 1/8 inch.

Graphs 31, 32, and 33 give the time history of $e_i(t)$, when $i_e(o)$ is 1 ampere, for the cylinders mentioned above for t_1 values of 12, 24, and 48 μs.

Graph 34 is the same as Graph 30, but is computed for a cylinder 105 inches in diameter, 60 feet 4 inches in height, and having a wall thickness of 1/4 inch. These dimensions are reported to apply to a Jupiter missile.

Graph 35 presents the time history of the electric field $e_i(t)$ inside a Jupiter missile stripped of interior components when $i_e(o)$ is 1 ampere for t_1 values of 24, 48, and 96 μs. Observe that the height dimension of the missile is sufficiently small that the current is uniform in the circuit connecting the ends of the missile to the current pulse generator.

Table I presents the decibel ratio of the energy available in the emerging plane-wave pulse from the far side of the plate to the energy in the impinging plane-wave pulse on the near side of the plate for the cases of tangential and incident electric fields. The decibel ratio of the propagated and impinging pulse peaks in the various situations described in the paper is easily obtained by inspection, hence tables are not provided.

TABLE I

Decibel Ratio of Energy Available in the Emerging Plane-Wave Pulse from the Far Side of a Plate to the Energy in the Impinging Plane-Wave Pulse on the Near Side of the Plate

(a) Case of the tangential electric field			(b) Case of the incident electric field		
d	t_1	db	d	t_1	db
1/32 inch	6 μs	- 4	1/32 inch	6 μs	-138
1/16 inch	6 μs	- 6	1/16 inch	6 μs	-147
1/8 inch	8 μs	-11	1/8 inch	6 μs	-158
1/32 inch	12 μs	- 3	1/32 inch	12 μs	-138
1/16 inch	12 μs	- 5	1/16 inch	12 μs	-145
1/8 inch	12 μs	- 9	1/8 inch	12 μs	-155
1/32 inch	24 μs	- 3	1/32 inch	24 μs	-138
1/16 inch	24 μs	- 4	1/16 inch	24 μs	-144
1/8 inch	24 μs	- 8	1/8 inch	24 μs	-153
1/32 inch	48 μs	- 3	1/32 inch	48 μs	-138
1/16 inch	48 μs	- 4	1/16 inch	48 μs	-144
1/8 inch	48 μs	- 5	1/8 inch	48 μs	-151

Table I was computed from the relation

$$db = 10 \log_{10} \left\{ \frac{\int_{-\infty}^{\infty} \left[e_1(t) \right]^2 dt}{\int_{-\infty}^{\infty} \left[e_{t_1}(t) \right]^2 dt} \right\} = 10 \log_{10} \left\{ \frac{\int_{-\infty}^{\infty} \left[e_1(t) \right]^2 dt}{t_1 \sqrt{\pi}} \right\}. \qquad (33)$$

Concluding Remarks

The shielding action of aluminum plates, spherical shells, and hollow cylinders to transient impinging fields and currents has been investigated rigorously. It has been assumed that the forcing pulses contain no frequencies sufficiently high to excite resonances in the spherical shells or hollow cylinders. The lowest mode of a perfectly conducting spherical shell is $\lambda_0 = 2.28b$, where b is the inner radius. The lowest radial mode for a perfectly conducting cylinder, when the exciting electric field is parallel to the axis of the cylinder, is $\lambda_0 = 2.61b$, where, again, b is the inner radius. The lowest longitudinal mode for the cylinder occurs when $2h \cong \lambda/2$. A moment's investigation will reveal that all of the cavity shields studied in this report have dimensions sufficiently small that no resonances can be excited by a frequency $f_0 = 68.96$ kcs, which corresponds to $t_1 = 6$ μs. This is the smallest value of t_1 of any gaussian pulse considered in the present analysis.

It should be evident to the reader that the use of gaussian pulses is not dictated by any theoretical considerations. Suppose $e_0(t)$ corresponding to a lightning flash is measured. Then, $E_0(f)$, the forcing function, can be found by numerical integration, by using a truncated form of the Fourier integral

$$E_e(f) = \int_{-\infty}^{\infty} e_e(t)\, e^{-j2\pi ft}\, dt,$$

for passing from the time to the frequency domain.

Having found the frequency spectrum $E_e(f)$ corresponding to the time function $e_e(t)$, one can find $e_i(t)$ numerically by using a truncated form of the Fourier integral

$$e_i(t) = \int_{-\infty}^{\infty} G(f) E_e(f) e^{j2\pi ft}\, df.$$

Thus, $e_i(t)$ can be found for any arbitrary wave shape $e_e(t)$--just as easily as was done for gaussian impinging pulses used in this report.

Center-loaded electric dipoles may be placed axially in the cylinders, and impedance-loaded loops in the spherical shells, and the energy in the loads evaluated under transient conditions. Consideration of these interesting problems is reserved for another paper.

ACKNOWLEDGMENT

Mr. C. S. Williams made many contributions to this work. The problems discussed in the paper were programmed for the Sandia Laboratory CDC-1604 computer by Mr. E. A. Aronson. Mrs. Margaret Houston plotted the graphs; they were inked under the direction of Mr. C. A. Tucker. The author extends thanks to all who participated in the preparation of this article.

APPENDIX I

THE NECESSITY FOR KNOWING THE TIME DEPENDENCE EMPLOYED IN DERIVING THE TRANSFER FUNCTIONS

It has been stressed that the time dependence employed in deriving the transfer functions given in this paper for sheets, spheres, and cylinders is exp (j2πft). If the time dependence exp (-j2πft)--favored by many electrodynamists--had been assumed in the development of (12), for example, the effect would have been to substitute k for γ. The transfer function then becomes $G^*(f)$ instead of $G(f) = H_t(f)/H_e(f)$. To obtain meaningful results in the solution of transient problems this change must be reflected by appropriate sign changes in the exponents of the Fourier transforms for passing from the frequency to the time domain, and vice versa.

Consider a series RL circuit (assumed to be linear). The driving voltage is e(t) and the current in the circuit is i(t). The differential equation is

$$e(t) = L\frac{di(t)}{dt} + Ri(t).$$

Let $e(t) = e^{j2\pi ft}$. Then, $i(t) = G(f)e^{j2\pi ft}$ where $G(f) = 1/(R + j\omega L)$. Construct the following table.

Input	Output	
e(t)	i(t)	
$e^{j2\pi ft}$	$G(f)e^{j2\pi ft}$	
$E(f)e^{j2\pi ft}df$	$E(f)G(f)e^{j2\pi ft}df$	(Property of linear systems - multiply by E(f)df)
$\int_{-\infty}^{\infty} E(f)e^{j2\pi ft}df$	$\int_{-\infty}^{\infty} E(f)G(f)e^{j2\pi ft}df$	(Property of linear systems - integrate)

Since $e(t) = \int_{-\infty}^{\infty} E(f)e^{j2\pi ft}df$, for consistency, $E(f) = \int_{-\infty}^{\infty} e(t)e^{-j2\pi ft}dt$.

Alternatively, if $e(t) = e^{-j2\pi ft}$ it follows that $G(f) = 1/(R - j\omega L)$,

$i(t) = \int_{-\infty}^{\infty} E(f)G(f)e^{-j2\pi ft}df$; $e(t) = \int_{-\infty}^{\infty} E(f)e^{-j2\pi ft}df$, and $E(f) = \int_{-\infty}^{\infty} e(t)e^{j2\pi ft}dt$.

APPENDIX II

NOTES ON THE MACHINE EVALUATION OF THE CYLINDER TRANSFER FUNCTION

Let

$$G(z_1, z_2) = \frac{J_0(z_1)N_1(z_1) - N_0(z_1)J_1(z_1)}{J_0(z_2)N_1(z_1) - N_0(z_2)J_1(z_1)} = \frac{M}{D},$$

where $z_i = z_{iR} - jz_{iI}$, $Z_{iR} = Z_{iI}$, $i = 1, 2$. Also define $z_2 = z_1 + \delta$ (δ small)

a. As mentioned in the body of the paper, as $f \to o$, $G(o, o) = 1 + jo$,

b. When $o \ll R_e(z_1) \leq 5$, $G(z_1, z_2)$ may be evaluated directly using single-precision arithmetic (36 bits); however, when $5 \ll R_e(z_1)$, $G(z_1, z_2)$ cannot be accurately evaluated directly using single-precision arithmetic because of loss of significant digits in the subtractions. In lieu of the extreme difficulties encountered in evaluating $G(z_1, z_2)$ with multiple-precision arithmetic, the following approximation was used.

Let

$$G(z_1, z_2) = \frac{M}{D} = \frac{M}{M + D - M},$$

where

$$D - M = N_1(z_1)\left\{J_0(z_2) - J_0(z_1)\right\} - J_1(z_1)\left\{N_0(z_2) - N_0(z_1)\right\}.$$

It is now possible to expand $J_0(z)$ and $N_0(z)$ in a Taylor series about z_1. Recalling that $z_2 = z_1 + \delta$,

$$J_0(z_1 + \delta) - J_0(z_1) = \delta J_0'(z_1) + \frac{\delta^2}{2!} J_0''(z_1) + \frac{\delta^3}{3!} J_0'''(z_1) + \ldots$$

A similar expansion holds for $N_0(z_1 + \delta) - N_0(z_1)$. Combining powers of δ and realizing that all Bessel functions now have z_1 for their argument, yields

$$D - M = \delta\left\{N_1 J_0' - J_1 N_0'\right\} + \frac{\delta^2}{2!}\left\{N_1 J_0'' - J_1 N_0''\right\} + \ldots = \sum_{n=1}^{\infty} \frac{C_n \delta^n}{n!};$$

when $C_n = N_1 J_0^{(n)} - J_1 N_0^{(n)}$. It remains to evaluate C_n.

By virtue of the relationships $J_0' = -J_1$ and $N_0' = -N_1$, it follows that $C_1 = 0$.

Since J_0 and N_0 satisfy Bessel's equation,

$$J_0''(z) = -\frac{J_0'(z)}{z} - J_0(z),$$

and

$$N_0'' = -\frac{N_0'(z)}{z} - N_0(z),$$

$$C_2 = N_1\left\{-\frac{J_0'}{z} - J_0\right\} - J_1\left\{-\frac{N_0'}{z} - N_0\right\} = -N_1 J_0 + J_1 N_0 = -M.$$

Differentiating $J_0^{(z)}$ and $N_0^{(z)}$ yields

$$J_0''(z) = -\frac{J_0'(z)}{z} + \frac{J_0(z)}{z^2} - J_0'(z),$$

$$N_0''(z) = -\frac{N_0'(z)}{z} + \frac{N_0(z)}{z^2} - N_0'(z).$$

As before, the terms involving J_0 and N_0 cancel and

$$C_3 = \frac{M}{z}\bigg|_{z=z_1} = \frac{M}{z_1}.$$

Differentiating again yields

$$J_0''' = -\frac{J_0''}{z} + 2\frac{J_0'}{z^2} - 2\frac{J_0}{z^3} - J_0''$$

a similar expression holds for N_0'''. Now,

$$C_4 = C_2\left[\frac{2}{z_1^2} - 1\right] - \frac{C_3}{z_1} = -M\left[\frac{2}{z_1^2} - 1\right] - \frac{M}{z_1^3} = M\left[1 - \frac{3}{z_1^2}\right].$$

It was decided that four terms of the expansion would be satisfactory for better than 1-percent accuracy in the range

$$5 < R_0(z_1) \leq 20.$$

One may now write

$$G(z_1, z_2) = \frac{M}{M + D - M} \approx \frac{M}{M - \frac{b^2}{2!}M + \frac{b^3}{3!z_1}M + \frac{b^4}{4!}\left[1 - \frac{3}{z_1}\right]M}$$

$$= \frac{1}{1 - \frac{b^2}{2!} + \frac{b^3}{3!z_1} + \frac{b^4}{4!}\left[1 - \frac{3}{z_1}\right]}.$$

This approximation was used for $5 < R_0(z_1) \leq 20$.

c. For $R_0(z_1) > 20$, two terms of the asymptotic expansion may be used.

We have,

$$M = -\frac{2}{\pi z_1},$$

$$D = -\frac{2}{\pi\sqrt{z_1 z_2}}\left\{\cos b\left[1 - \frac{3}{64 z_1 z_2}\right] + \frac{\sin b}{8}\left[\frac{1}{z_2} + \frac{3}{z_1}\right]\right\},$$

yielding

$$G(z_1, z_2) \simeq \sqrt{\frac{z_2}{z_1}} \left\{ \frac{1}{\left[1 - \frac{3}{64 z_1 z_2}\right] \cos \phi + \frac{1}{8}\left[\frac{1}{z_2} + \frac{3}{z_1}\right] \sin \phi} \right\}.$$

REFERENCES

1. Stratton, J. A., Electromagnetic Theory, McGraw-Hill Book Co., Inc., (1941), Chapter 9, Section 9.10, pp 511-513.

2. Kinsler, L. E. and Frey, A. R., Fundamentals of Acoustics, John Wiley and Sons, Inc., (1950), Chapter 6, Section 6.4, pp 149-154.

3. King, L. V., "Electromagnetic Shielding at Radio Frequencies," Philosophical Magazine and Journal of Science, Vol. 15, No. 97, pp 201-223, February 1933. There appear to be a number of inconsistencies in this paper. If the time dependence is taken to be exp(j2πft) King's formula (25) reproduced in this paper as (12) appears to be correct, provided $\alpha = \gamma = \sqrt{\pi\mu\sigma}\,(1 + j)$.

4. Harrison, C. W. Jr., and King, R. W. P., "Response of a Loaded Electric Dipole in an Imperfectly Conducting Cylinder of Finite Length," Journal of Research of the National Bureau of Standards - D. Radio Propagation, Vol. 64D, No. 3, Equations (15) and (28).

5. McLachan, N. W., Bessel Functions for Engineers, Oxford University Press, 1955 2nd Edition p 32.

6. King, R. W. P., Theory of Linear Antennas, Harvard University Press (1956), Chapter 2, Section 31, p 184, Equations (4a) and (4b), and Chapter 4, Section 9, p 487, Equation (21).

SUPPLEMENTAL REFERENCES

Anderson, W. L., and Moore, R. K., "Frequency Spectra of Transient Electromagnetic Pulses in a Conducting Medium," IRE Transactions on Antennas and Propagation, *AP-8*, pp 603-607, November 1960.

Richards, P. I., "Transients in Conducting Media," IRE Transactions on Antennas and Propagation, *AP-6*, pp 178-182, April 1958.

Wait, J. R., "Shielding of a Transient Electromagnetic Dipole Field by a Conductive Sheet," Canadian Journal of Physics, *34*, pp 890-893, 1956.

Wait, J. R., "Induction in a Conducting Sheet by a Small Current Carrying Loop," Applied Science Research B3, p 230, 1953.

Zisk, S. H., "Electromagnetic Transients in Conducting Media," IRE Transactions on Antennas and Propagation, *AP-8*, pp 229-230, March 1960.

Zitron, N. R., "Shielding of Transient Electromagnetic Signals by a Thin Conducting Sheet," Journal of Research of the NBS - D. Radio Propagation, *64D*, No. 5, pp 563-567, September-October 1960.

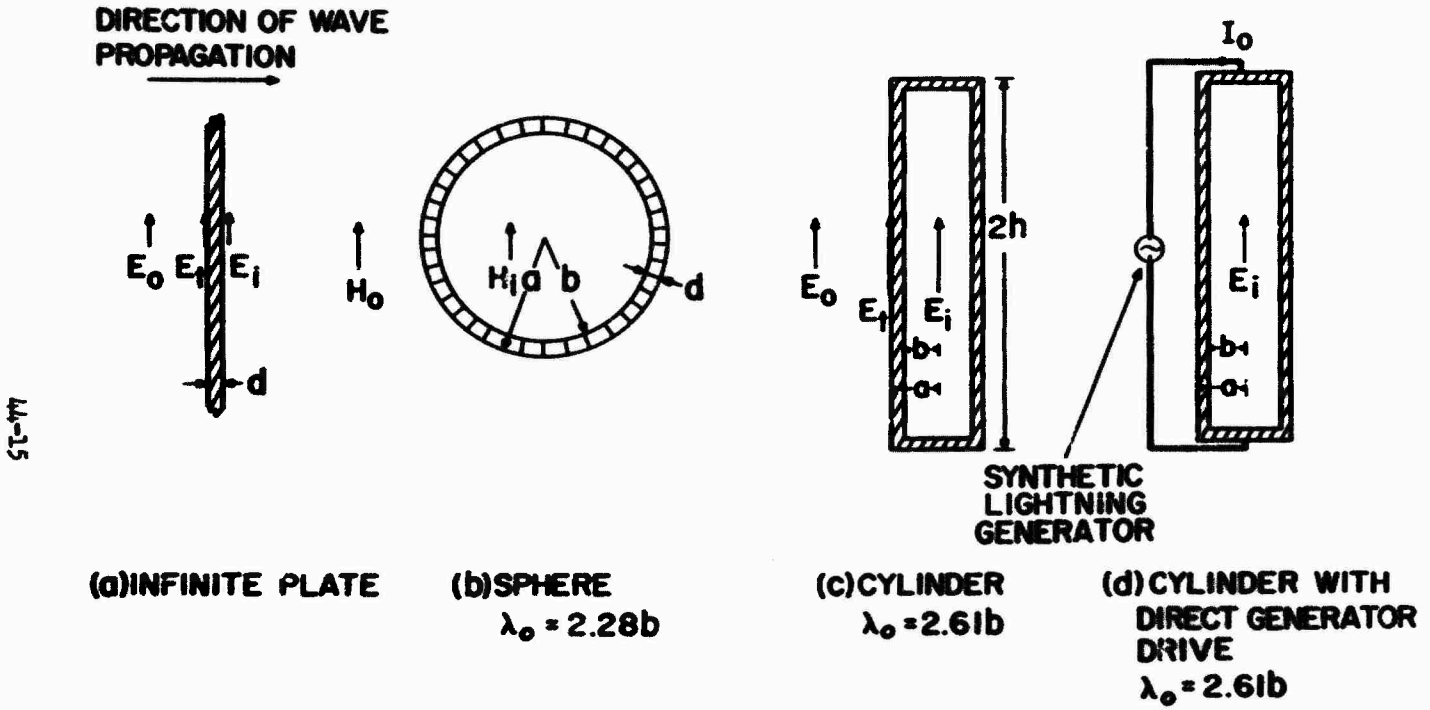

44-15

Figure 1 -- Configurations considered in the propagation of gaussian pulses through aluminum walls

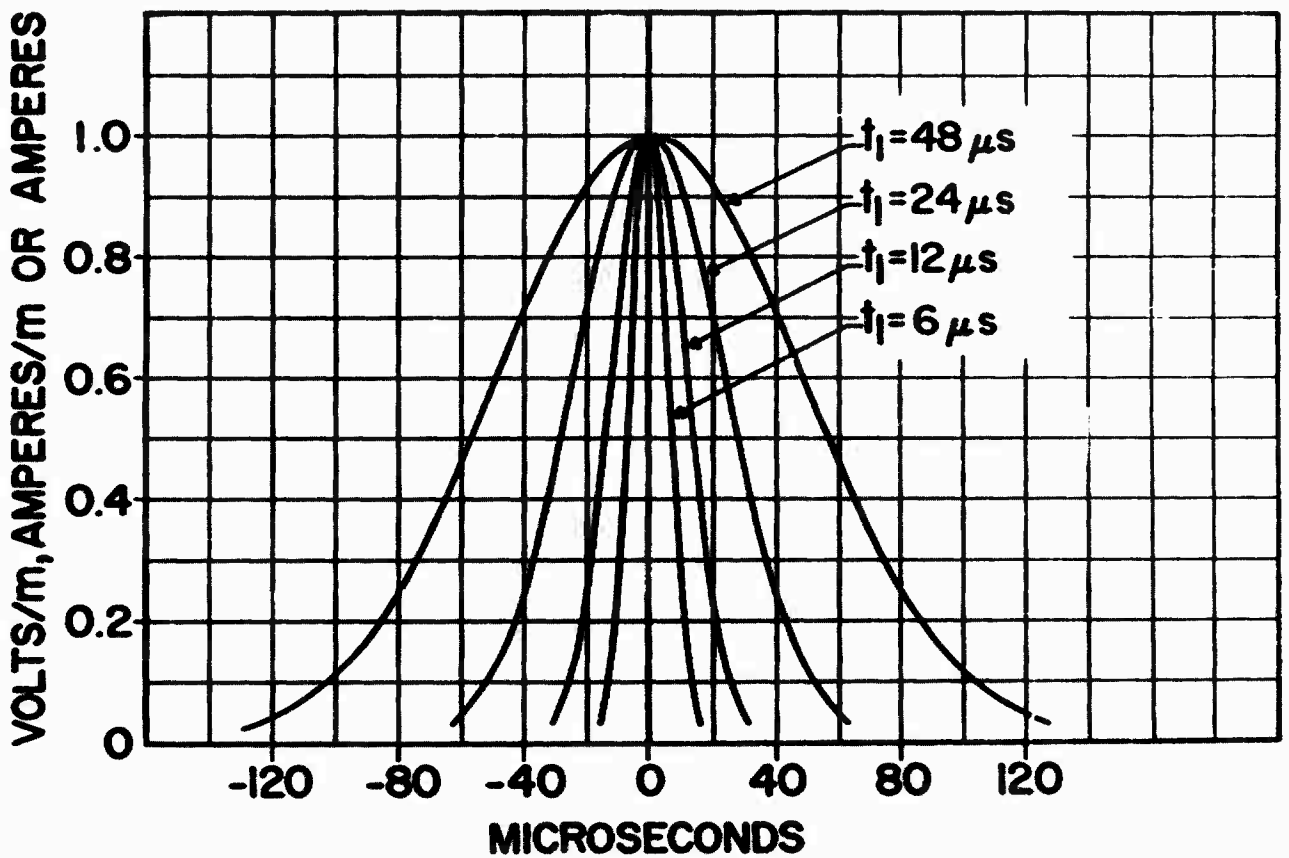

Graph 1 -- Input gaussian pulses

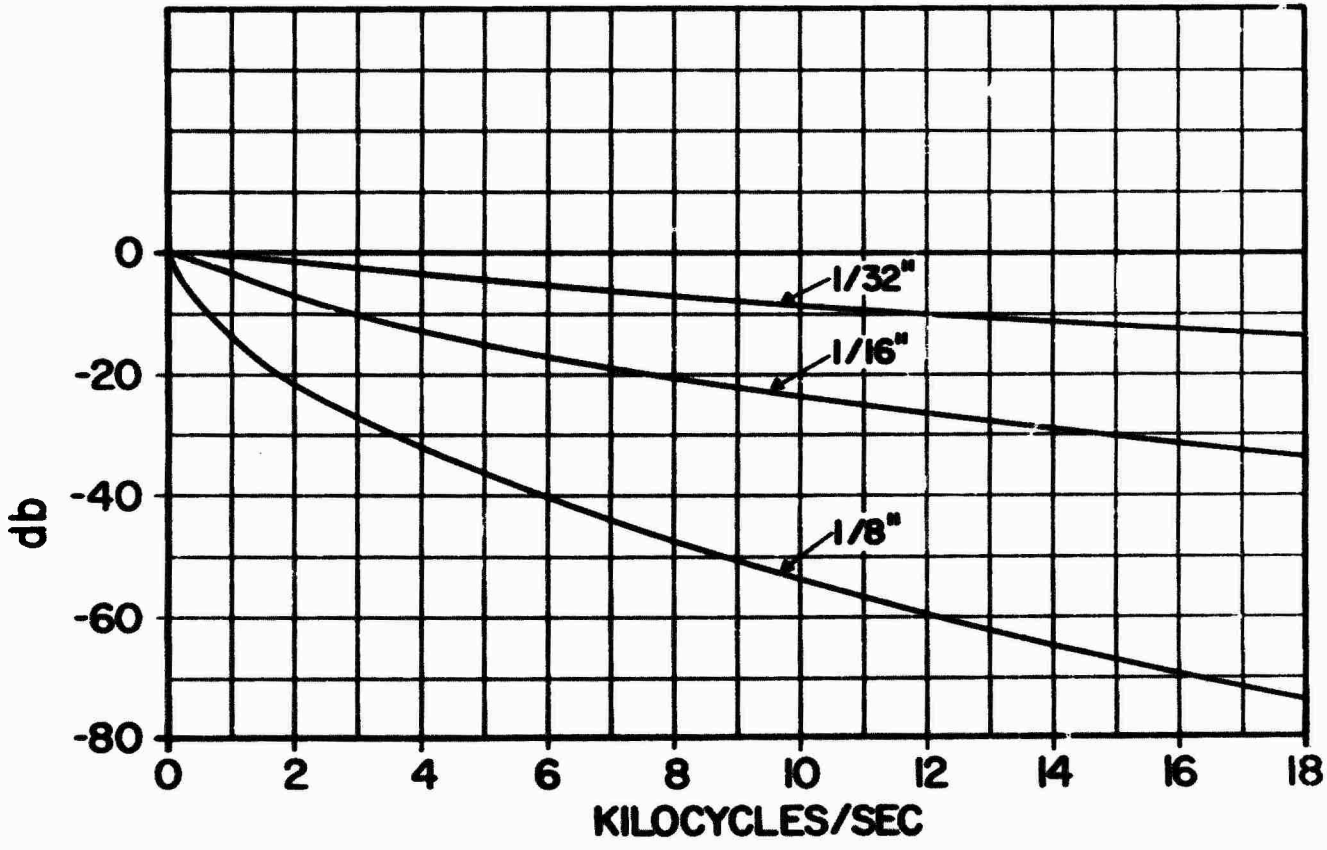

Graph 2 -- Infinite plate. Steady-state transfer characteristic relating E_i to E_t

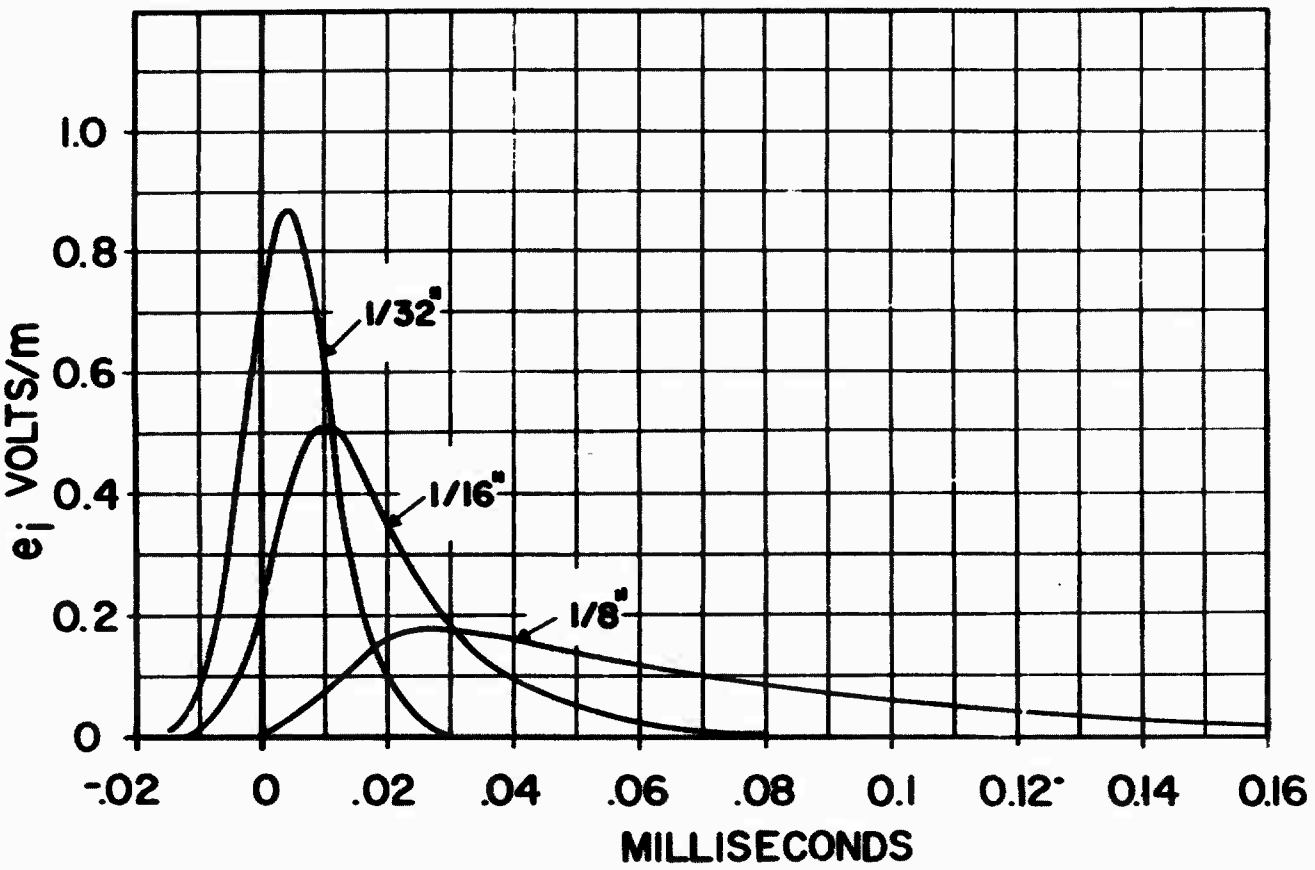

Graph 3 -- Infinite plate. $e_t(o) = 1$ volt/m; $t_1 = 6$ μs

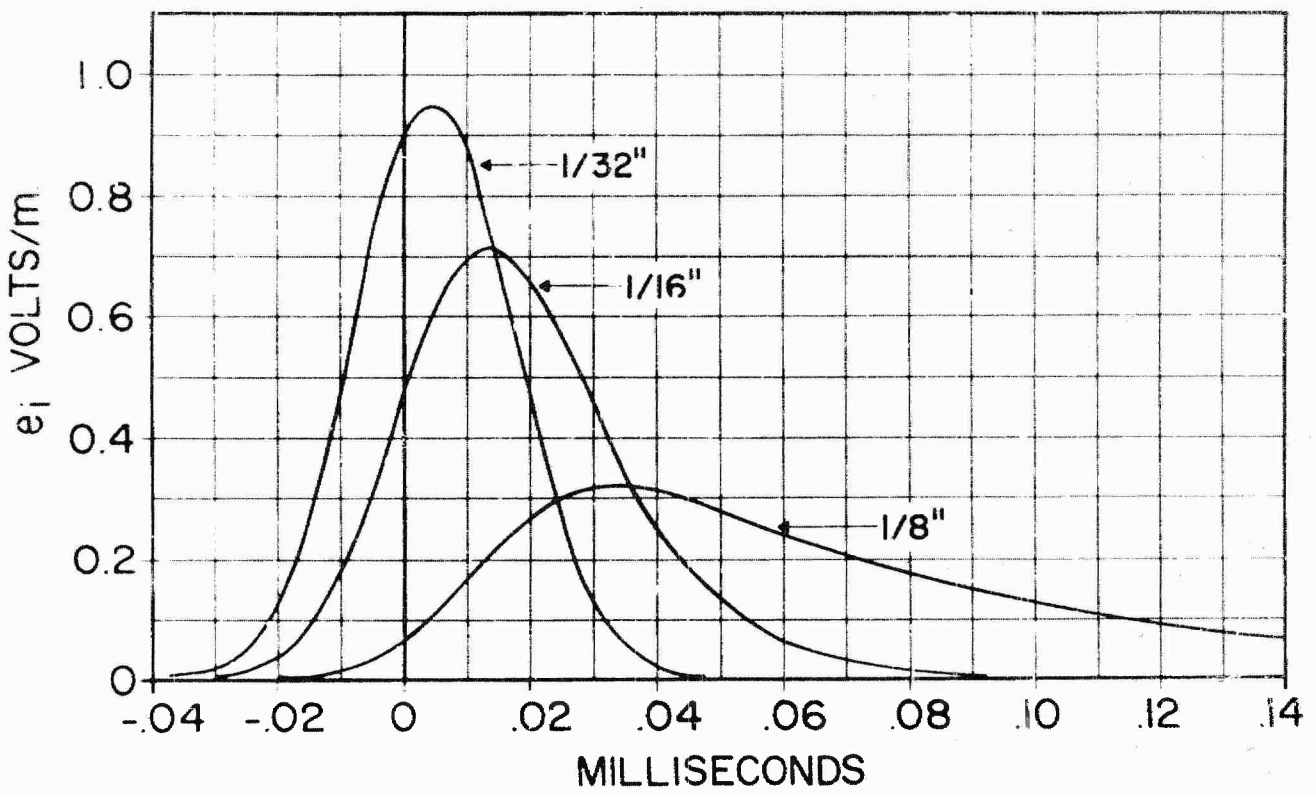

Graph 4 -- Infinite plate. $e_t(o) = 1$ volt/m; $t_1 = 12\ \mu s$

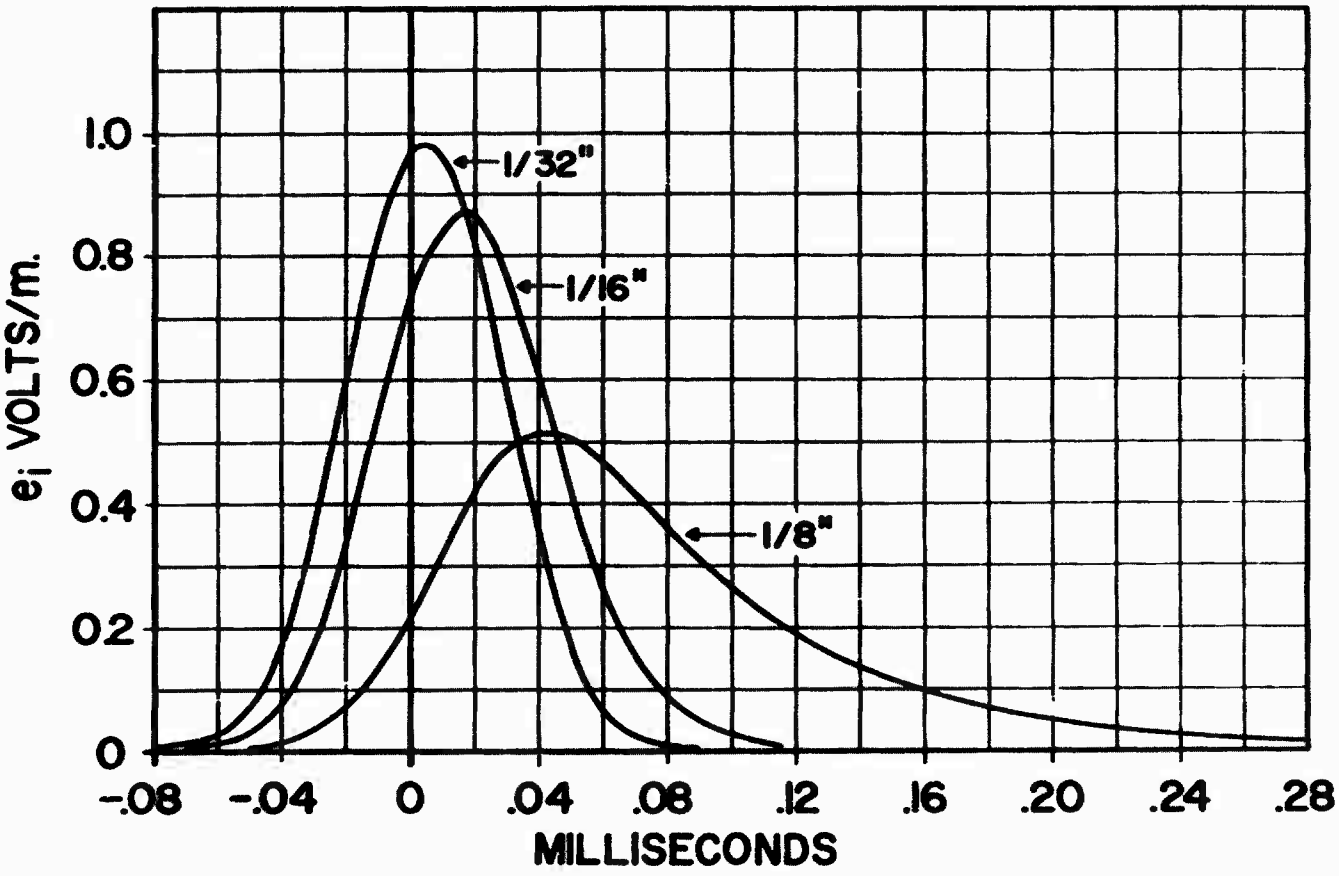

Graph 5 -- Infinite plate. $e_t(o) = 1$ volt/m; $t_1 = 24$ μs

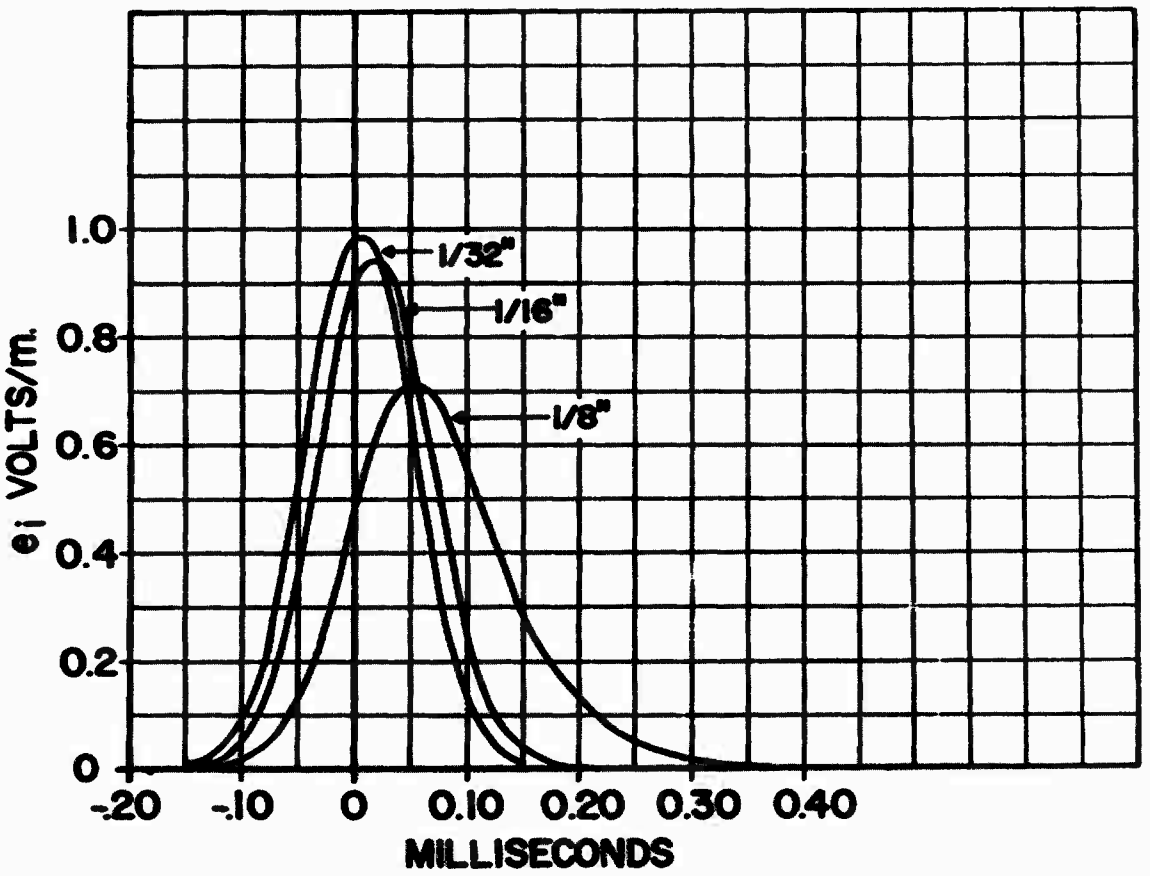

Graph 6 -- Infinite plate. $e_g(o)$ = 1 volt/m; t_1 = 48 μs

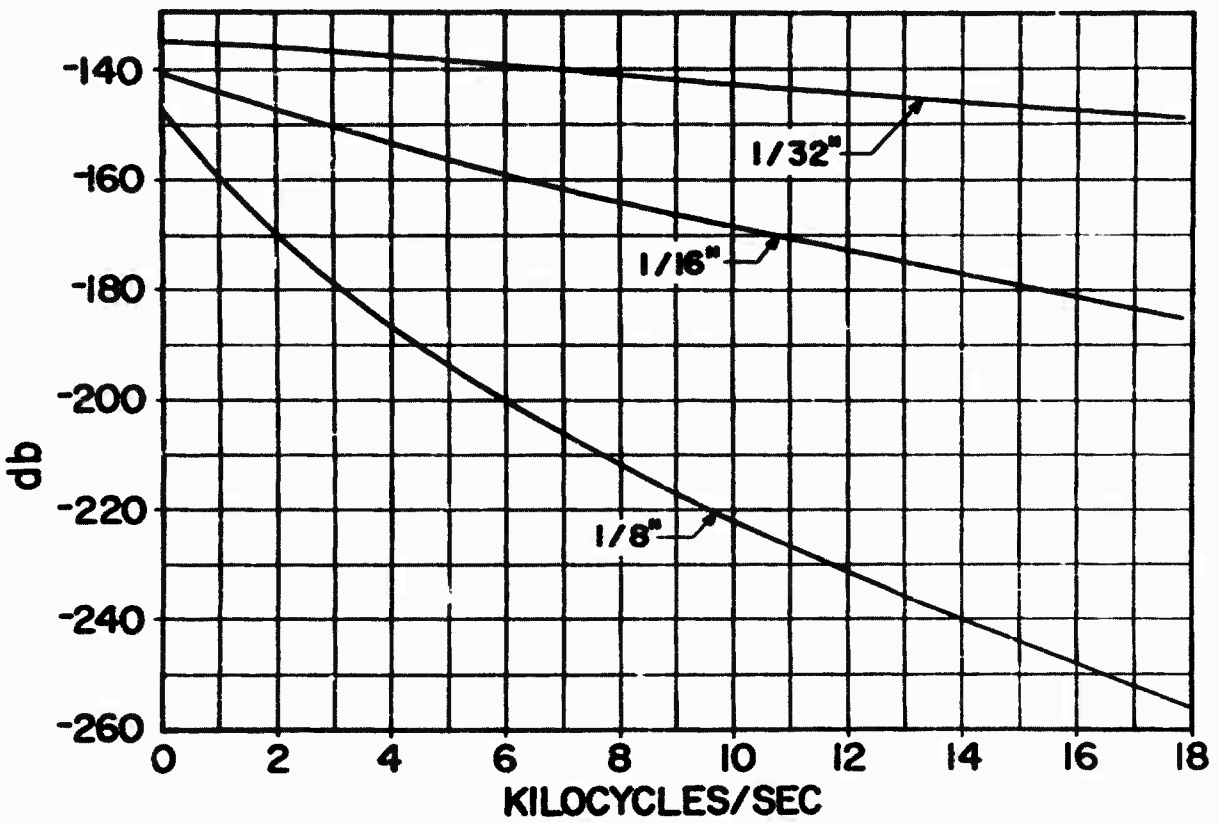

Graph 7 -- Infinite plate. Steady-state transfer characteristic relating E_i to F_e

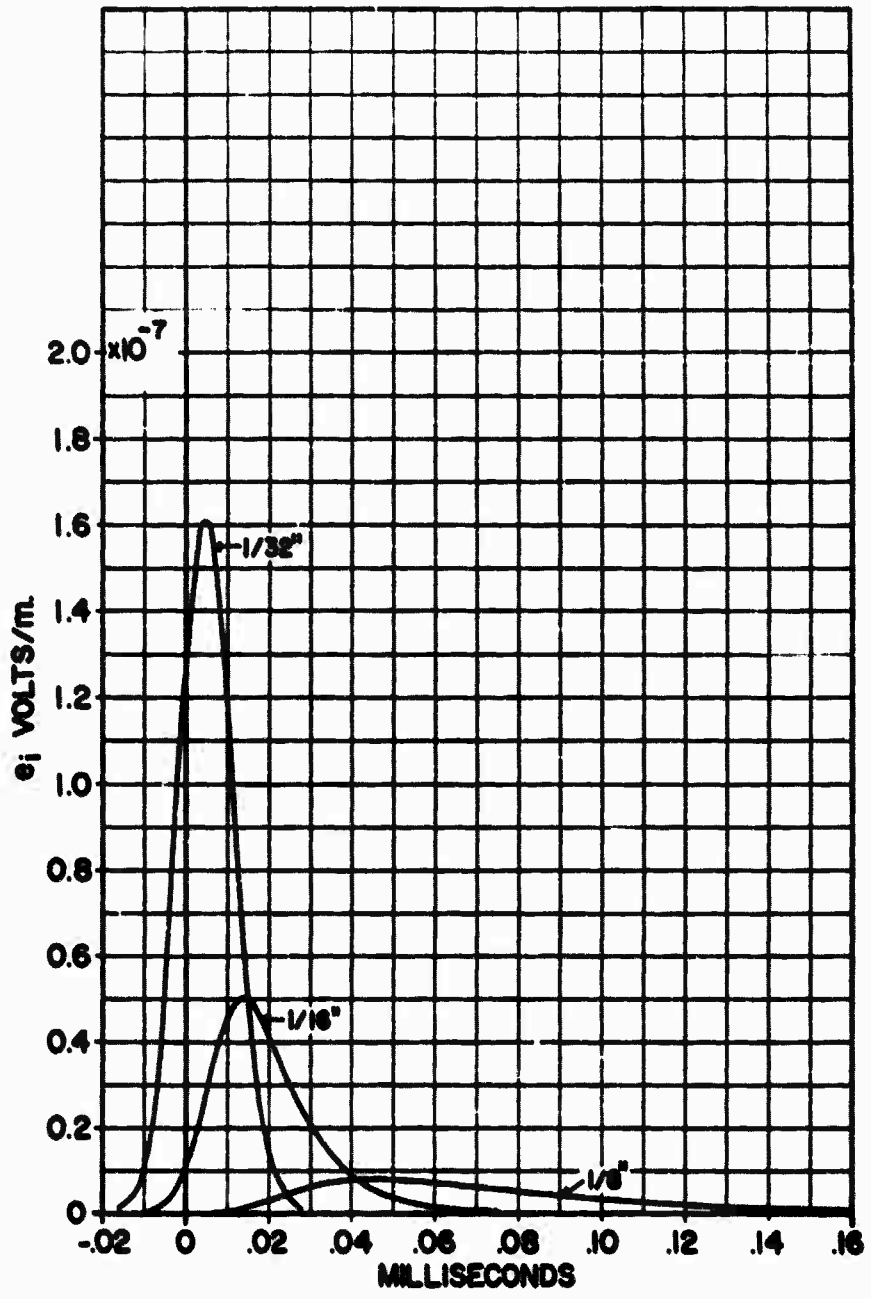

Graph 8 -- Infinite plate. $e_o(o)$ = 1 volt/m; t_1 = 6 μs

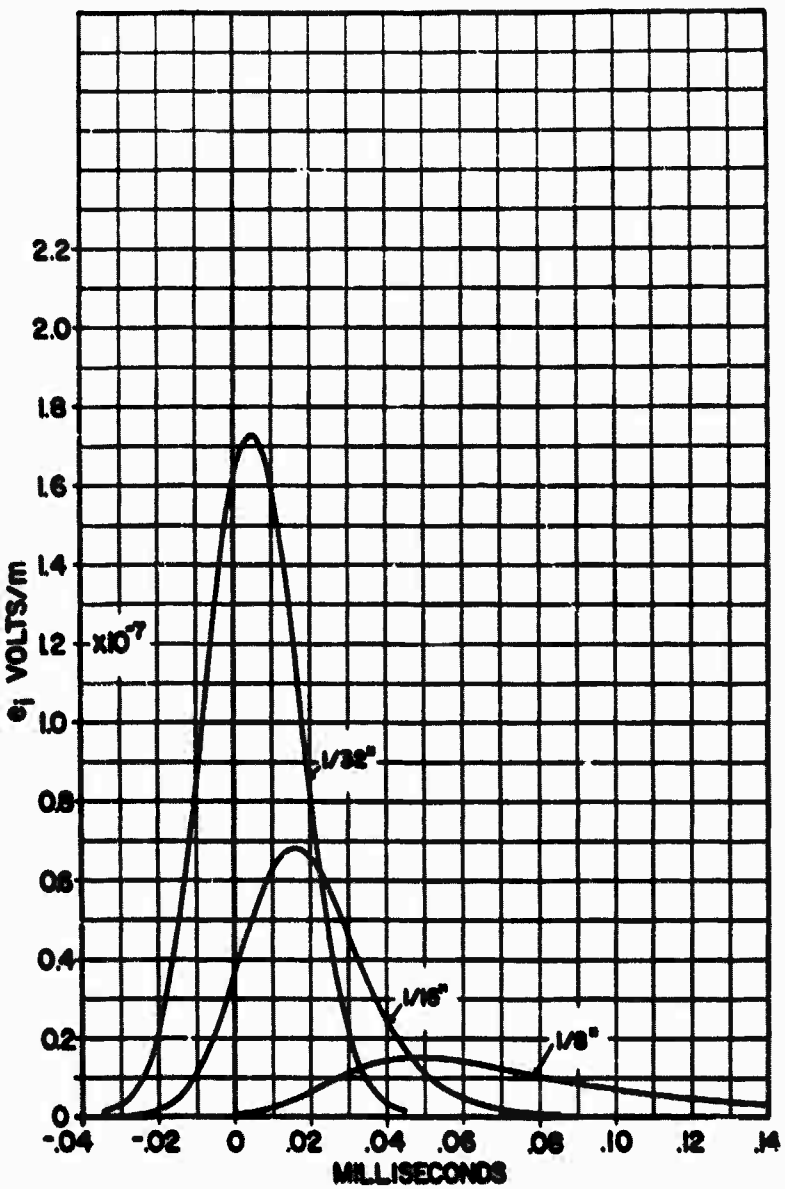

Graph 9 -- Infinite plate. $e_o(o) = 1$ volt/m; $t_1 = 12$ μs

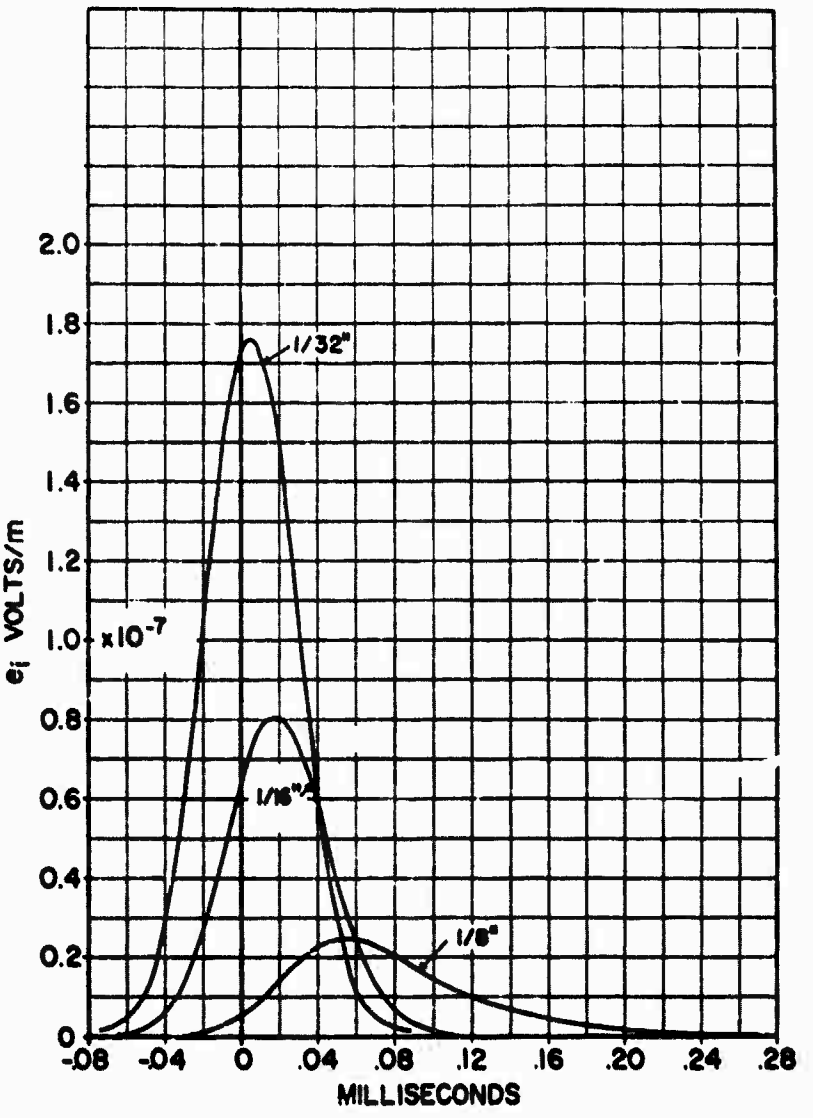

Graph 10 -- Infinite plate. $e_o(o)$ = 1 volt/m; t_1 = 24 μs

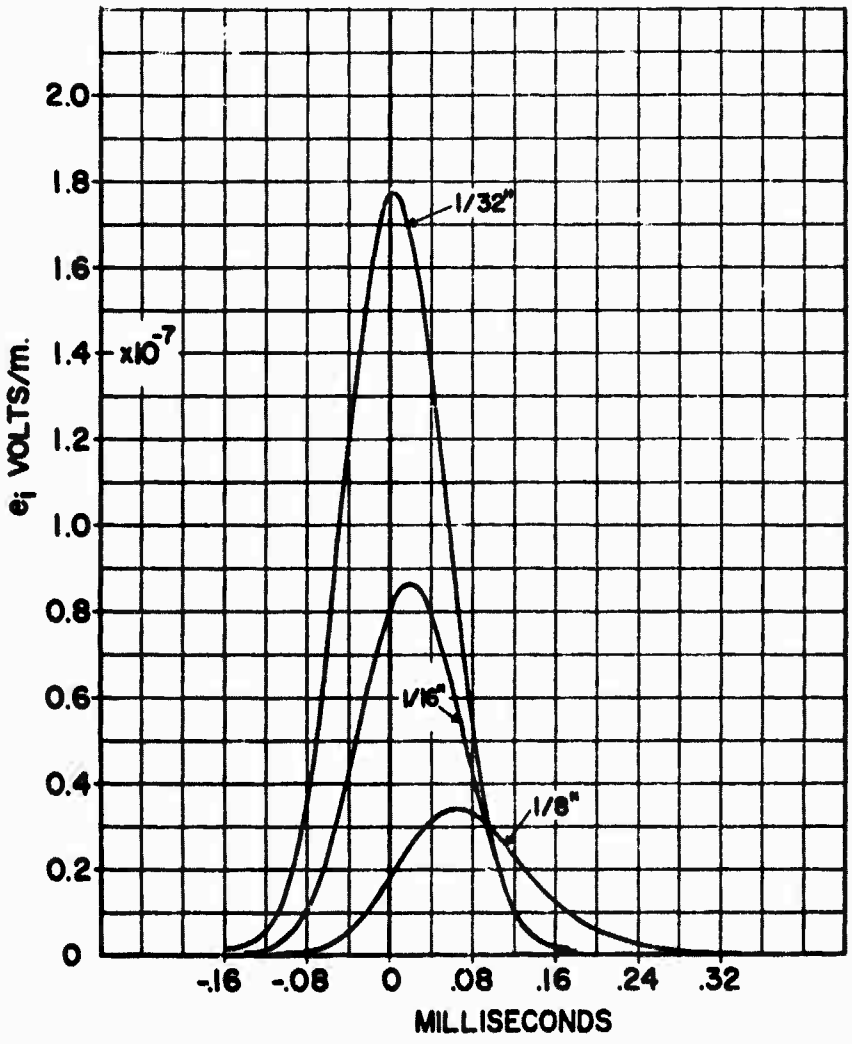

Graph 11 -- Infinite plate. $e_o(o) = 1$ volt/m: $t_1 = 48$ μs

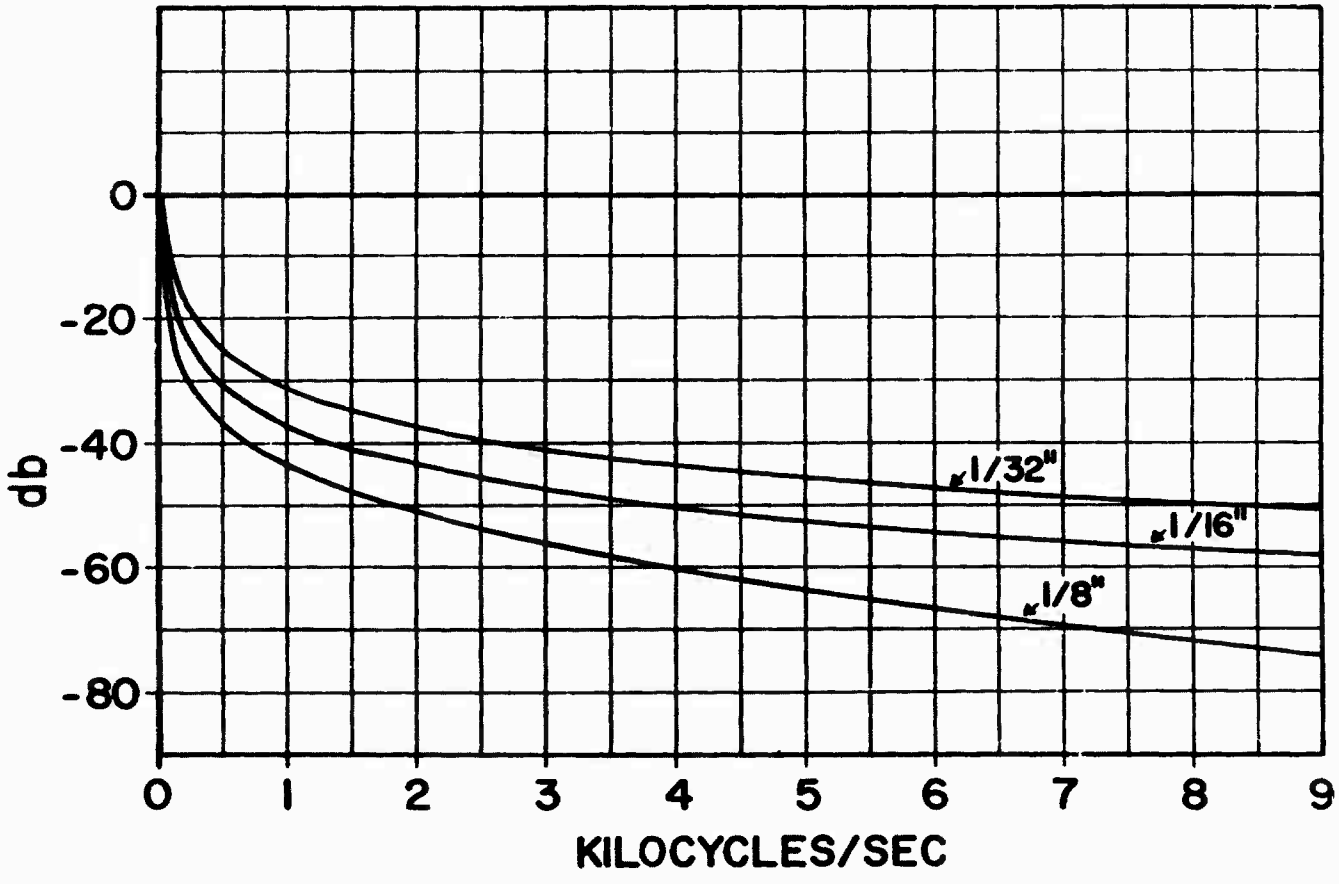

Graph 12 -- Sphere 36 inches in diameter. Steady-state transfer characteristic relating H_i to H_o

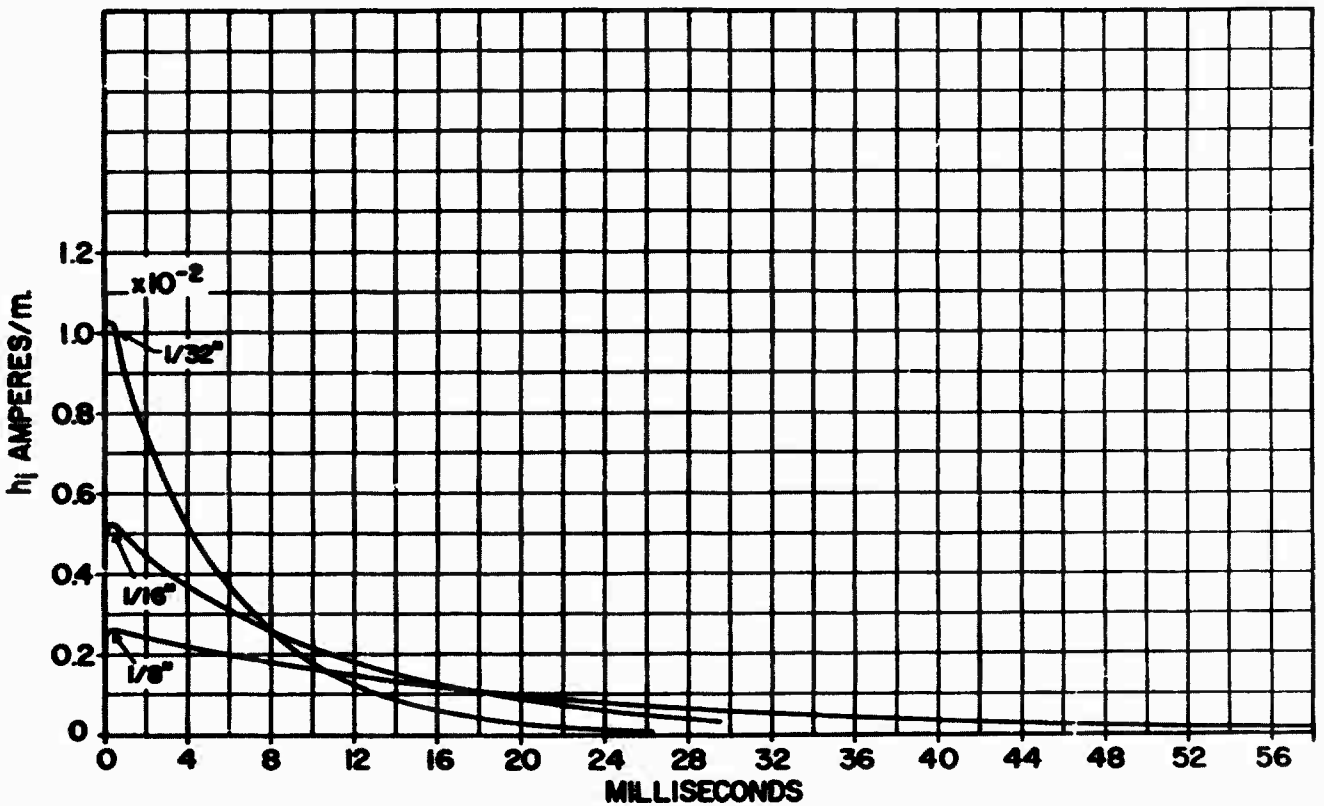

Graph 13 -- Sphere 36 inches in diameter. $h_o(o) = 1$ ampere/m; $t_1 = 24$ μs

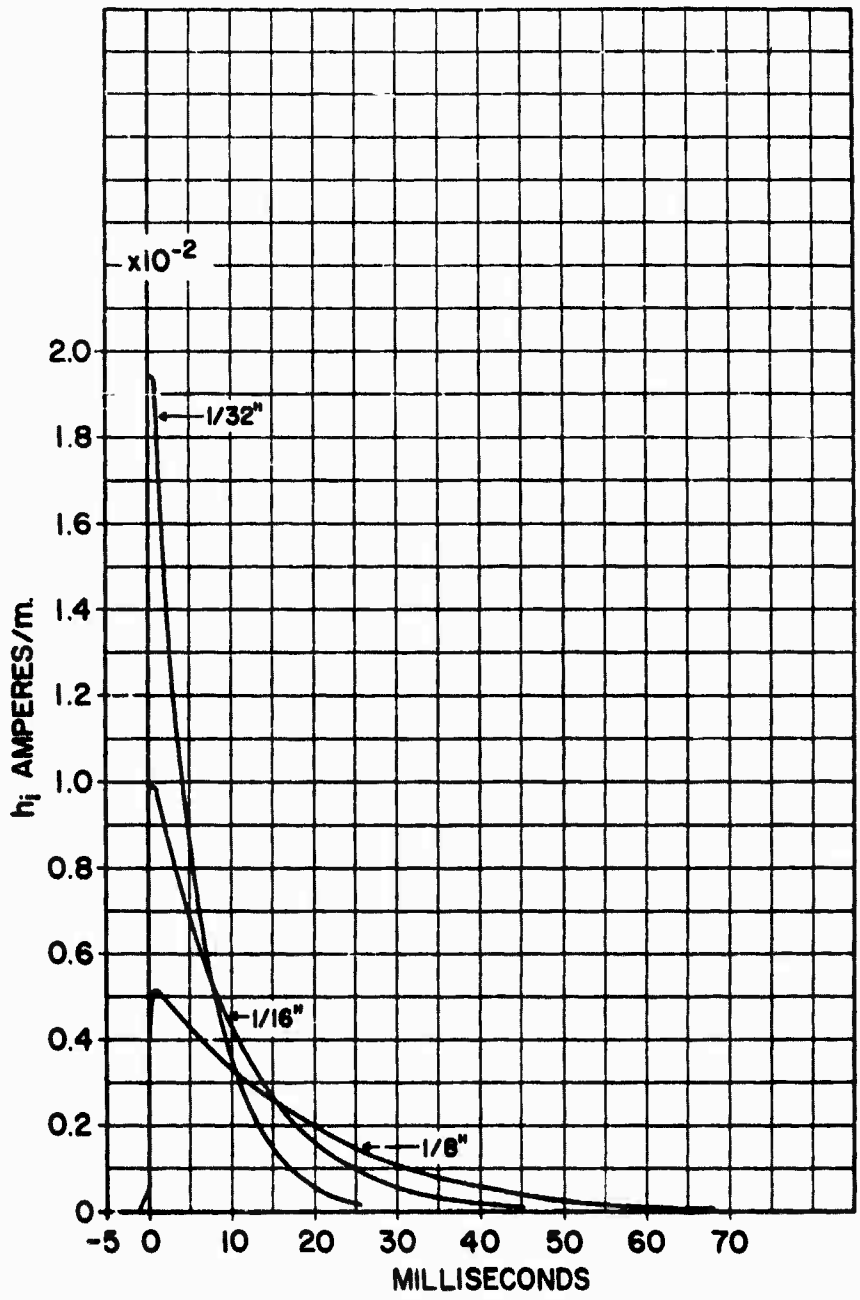

Graph 14 -- Sphere 36 inches in diameter. $h_o(o)$ - 1 ampere/m; t_1 = 48 μs

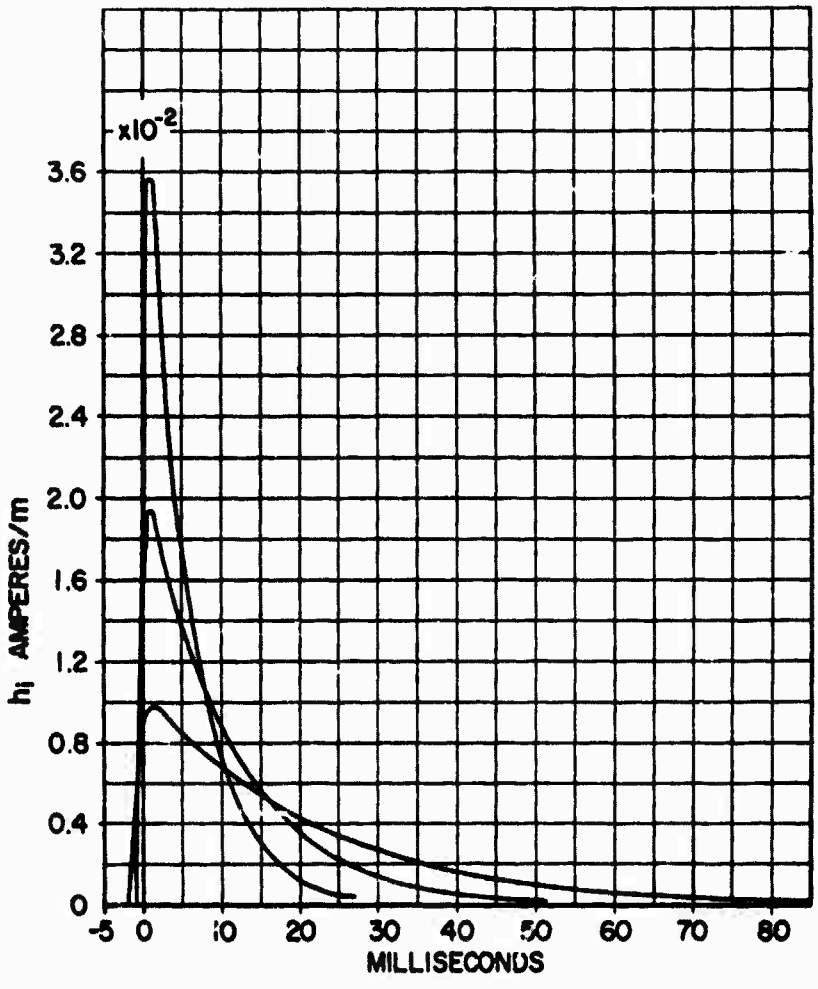

Graph 15 -- Sphere 36 inches in diameter. $h_o(o) = 1$ ampere/m; $t_1 = 96$ μs

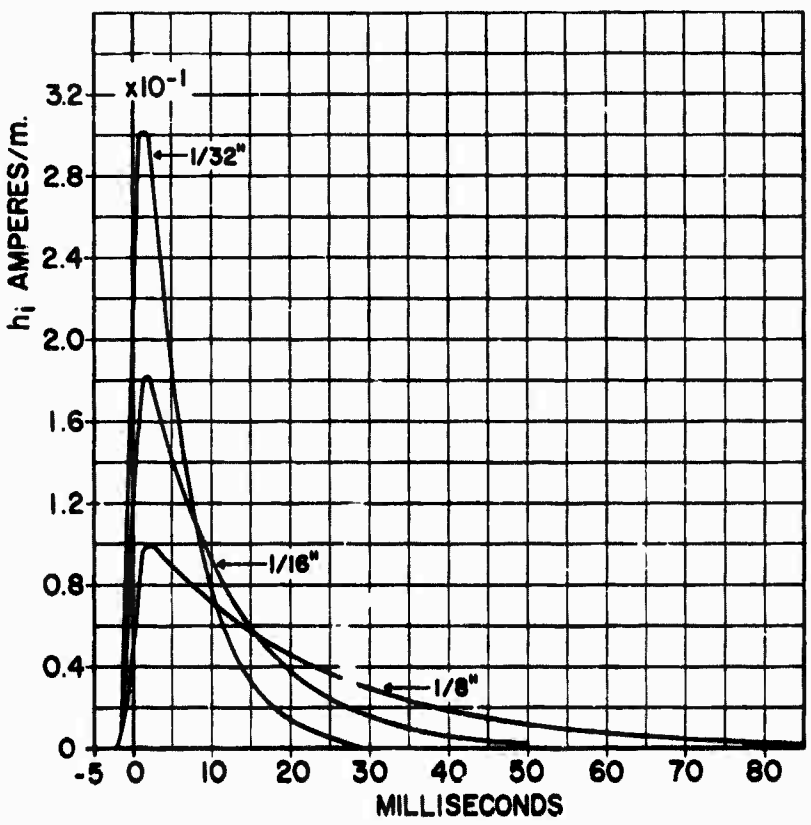

Graph 16 -- Sphere 36 inches in diameter. $h_o(o) = 1$ ampere/m; $t_1 = 1000$ μs

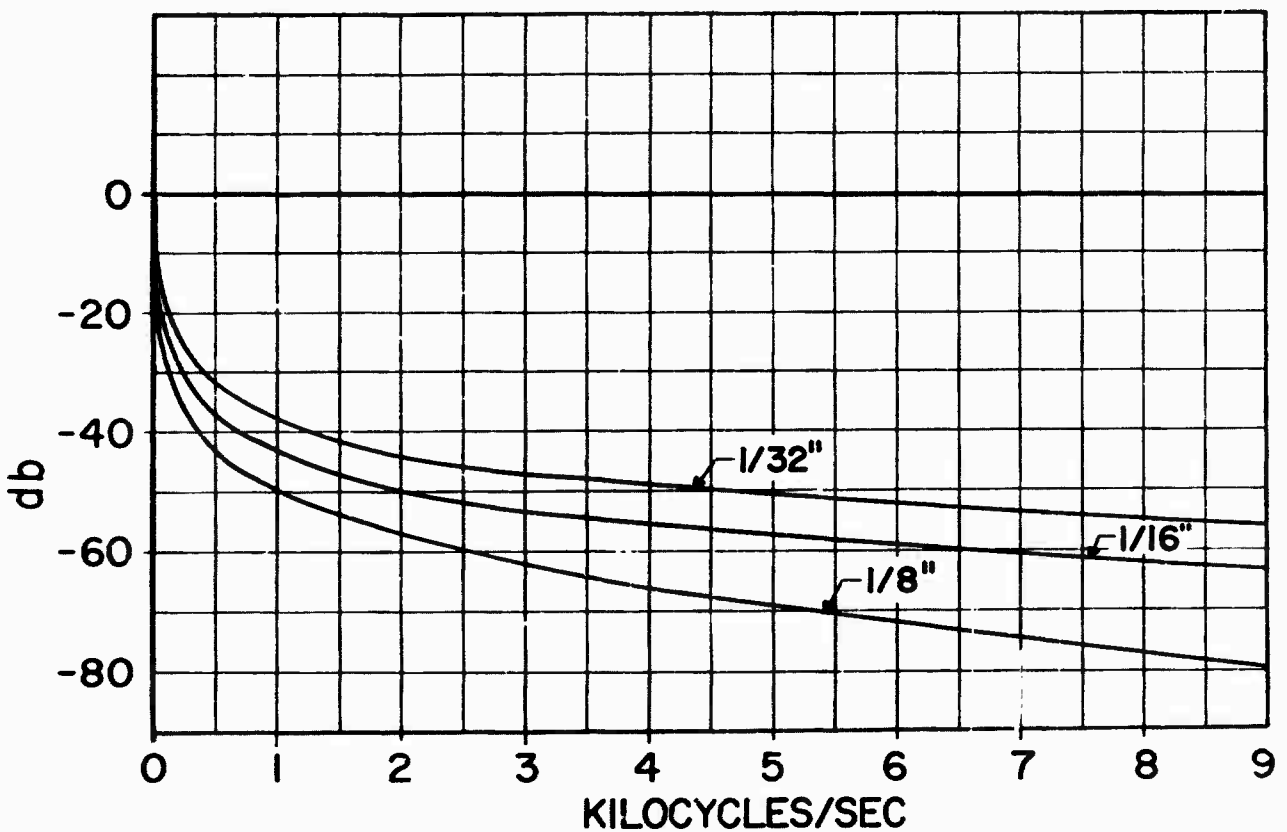

Graph 17 -- Sphere 72 inches in diameter. Steady-state transfer characteristic relating H_i to H_o

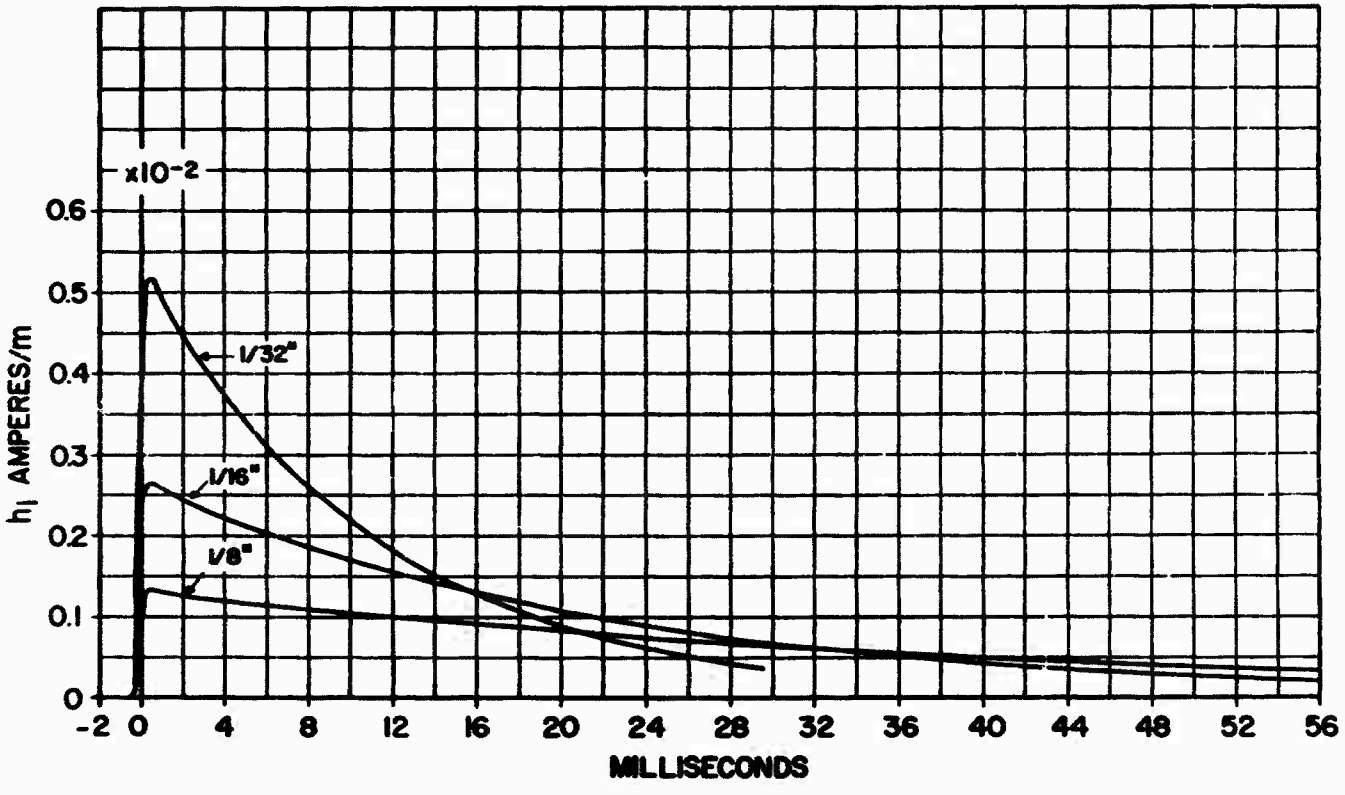

Graph 18 -- Sphere 72 inches in diameter. $h_o(o) = 1$ ampere/m; $t_1 = 24$ μs

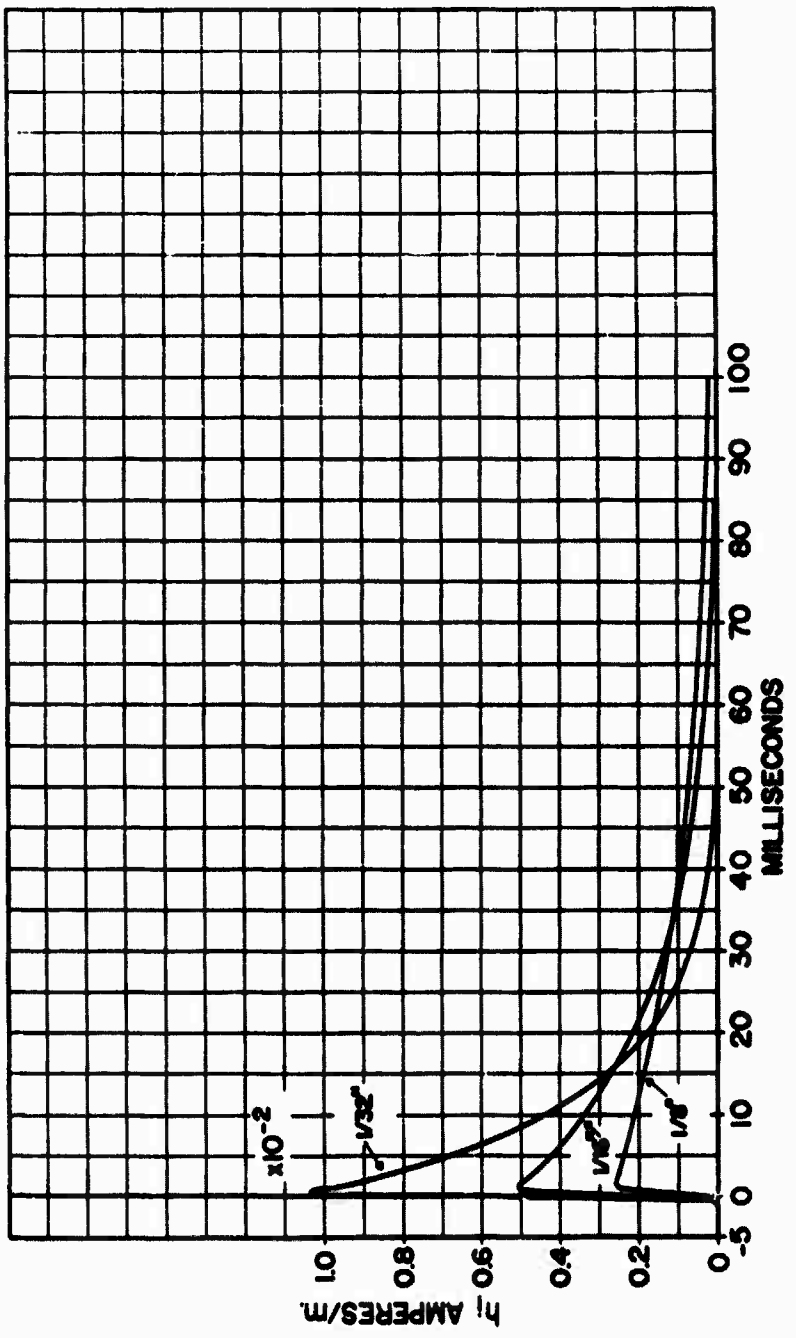

Graph 19 -- Sphere 72 inches in diameter. $h_o(o) = 1$ ampere/m; $t_1 = 48$ μs

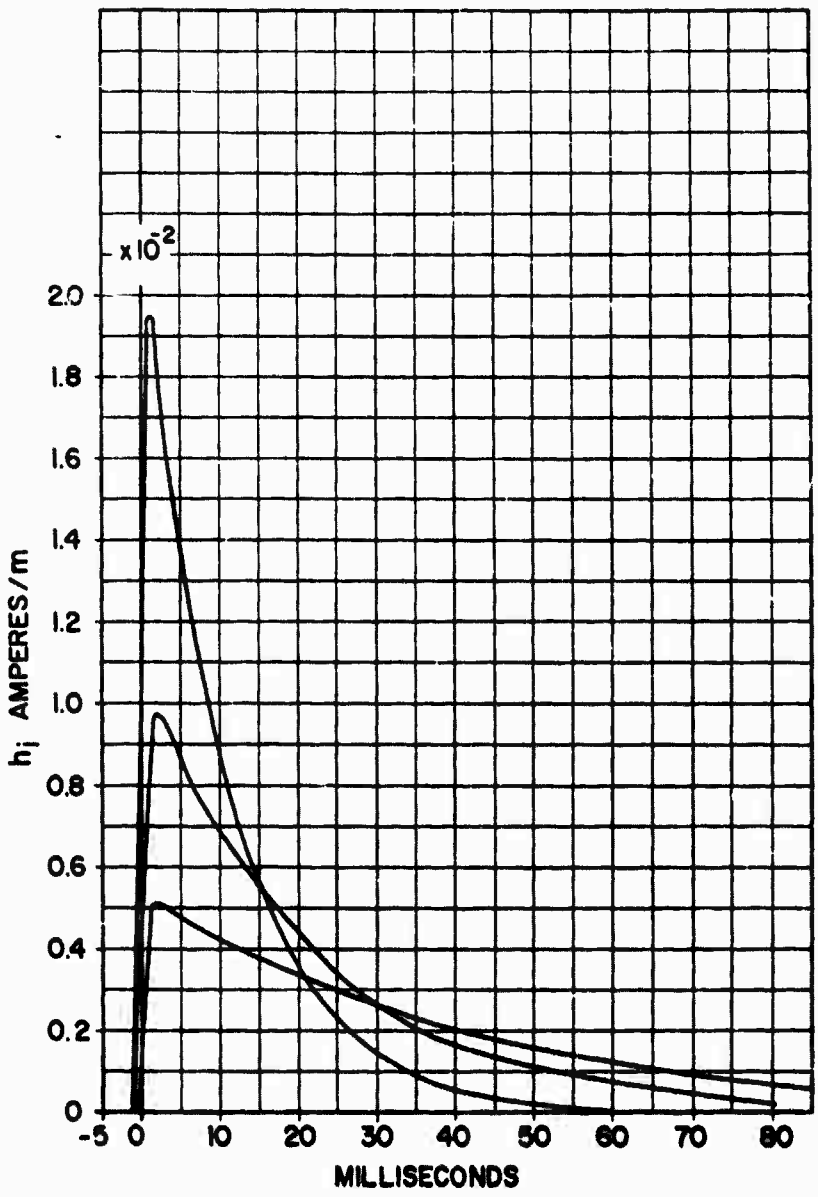

Graph 20 -- Sphere 72 inches in diameter. $h_o(o) = 1$ ampere/m; $t_1 = 96$ μs

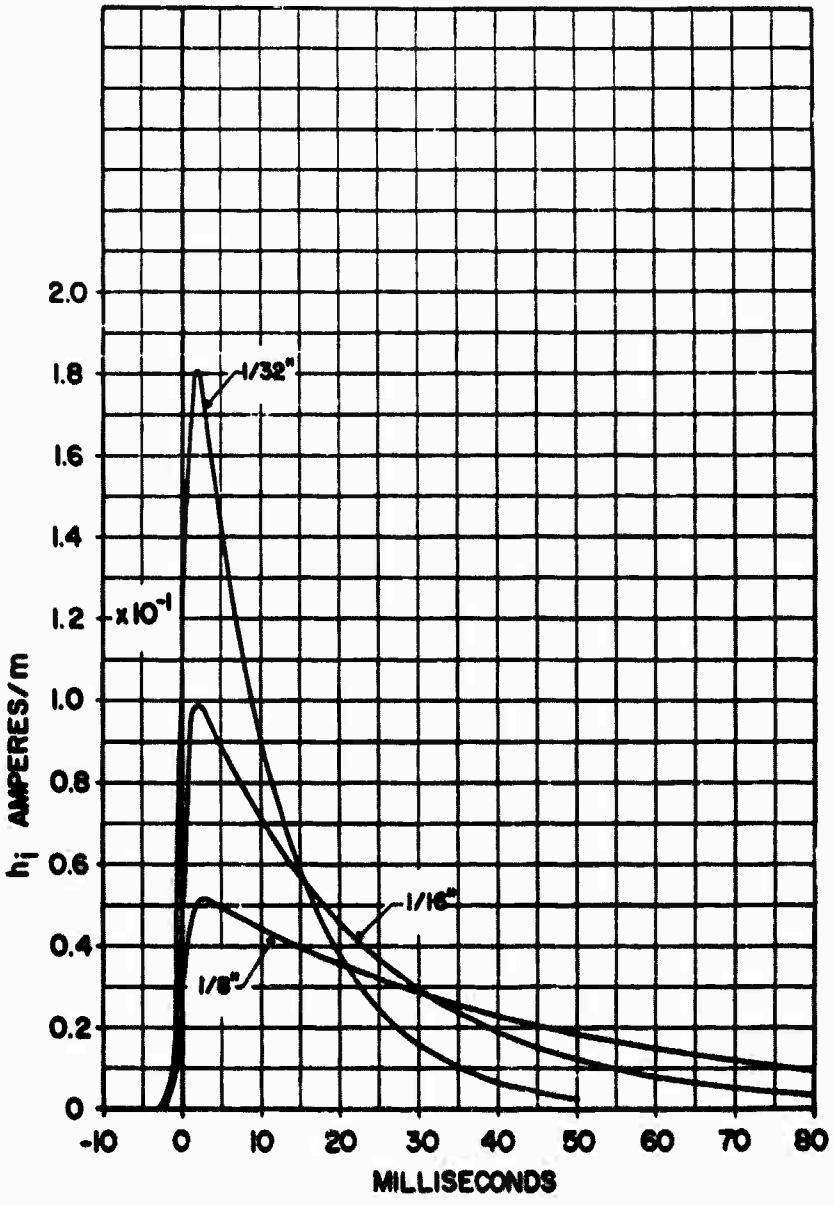

Graph 21 -- Sphere 72 inches in diameter. $h_o(o)$ = 1 ampere/m; t_1 = 1000 μs

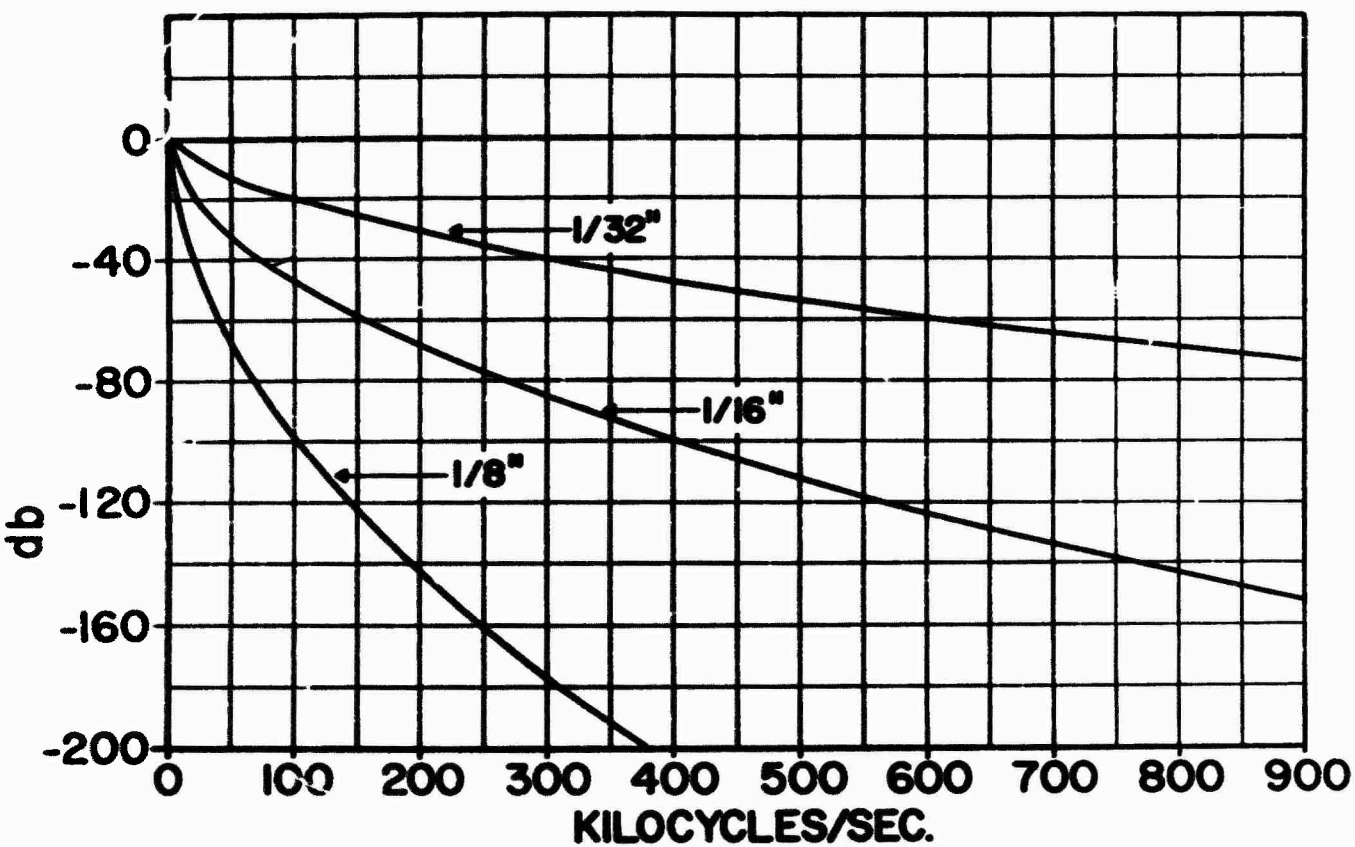

Graph 22 -- Cylinder. Steady-state transfer characteristic relating E_i to E_t

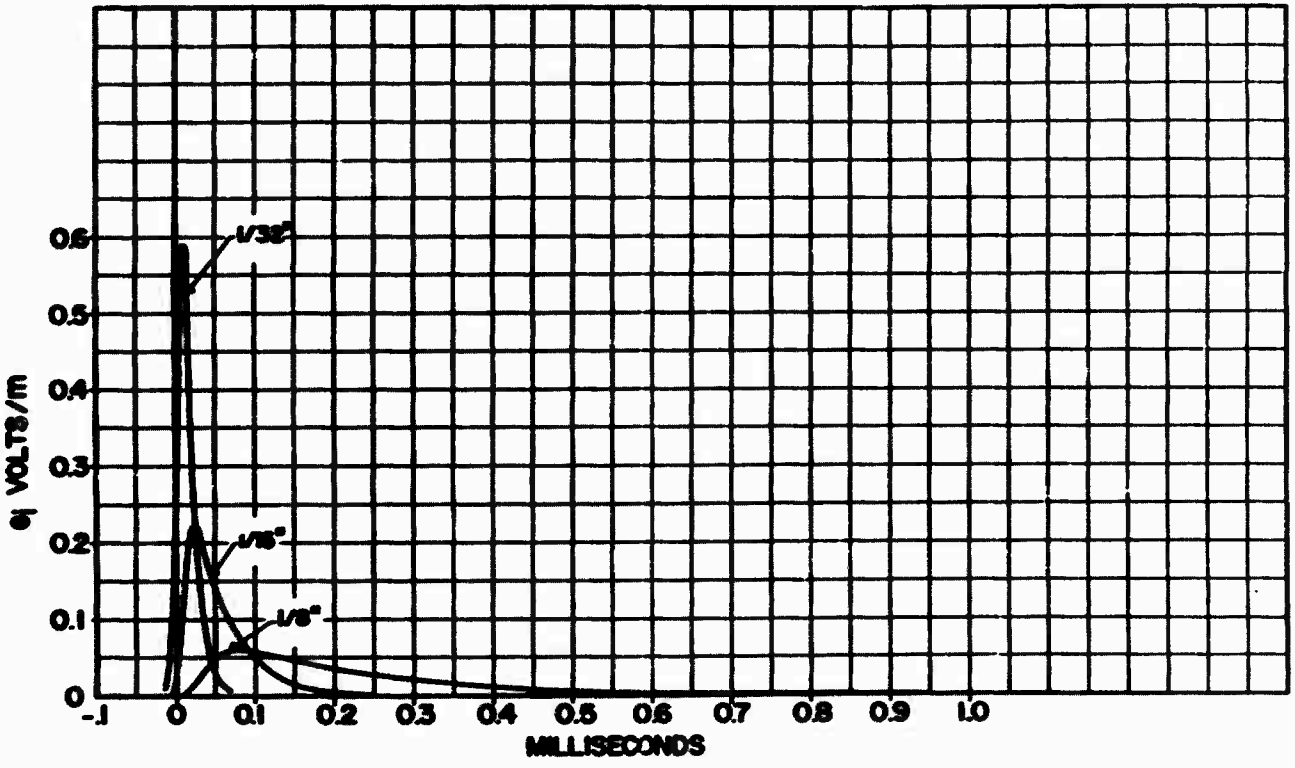

Graph 23 -- Cylinder. $e_t(o) = 1$ volt/m; $t_1 = 6$ μs

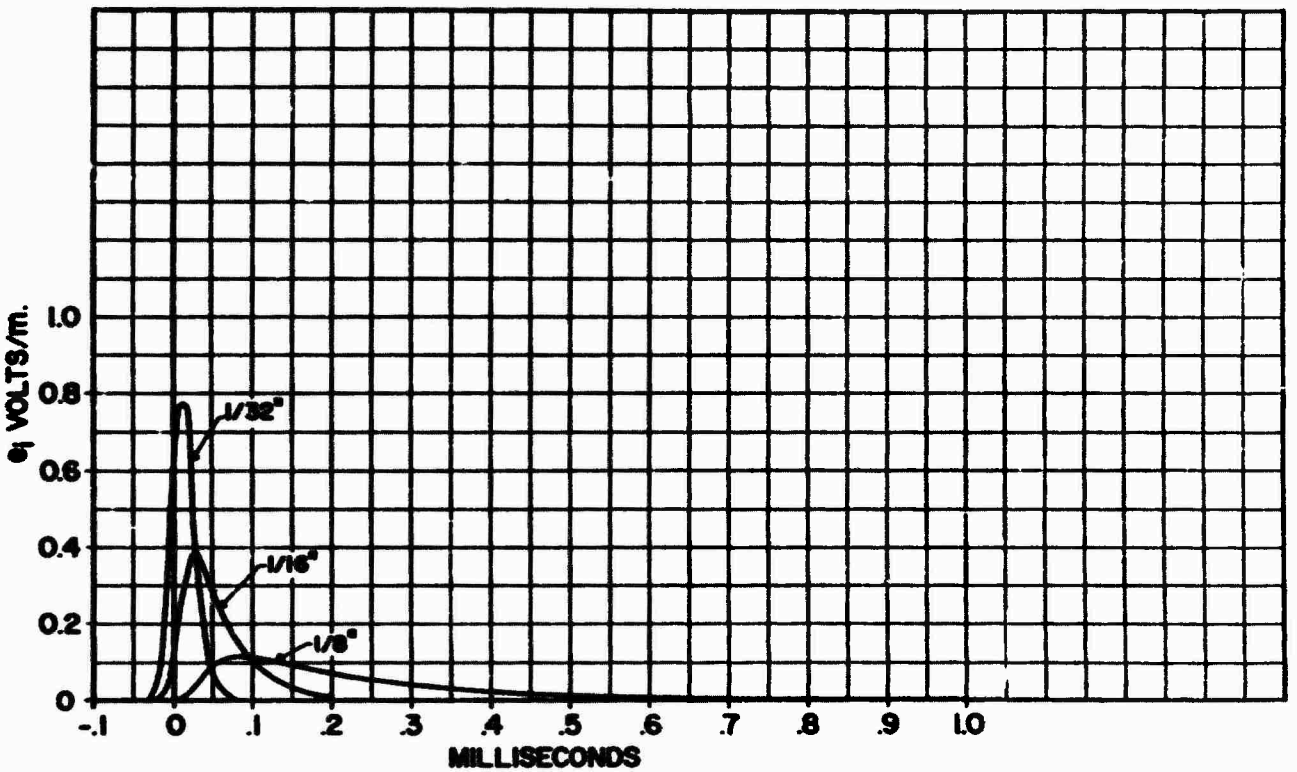

Graph 24 -- Cylinder. $e_t(o) = 1$ volt/m; $t_1 = 12$ μs

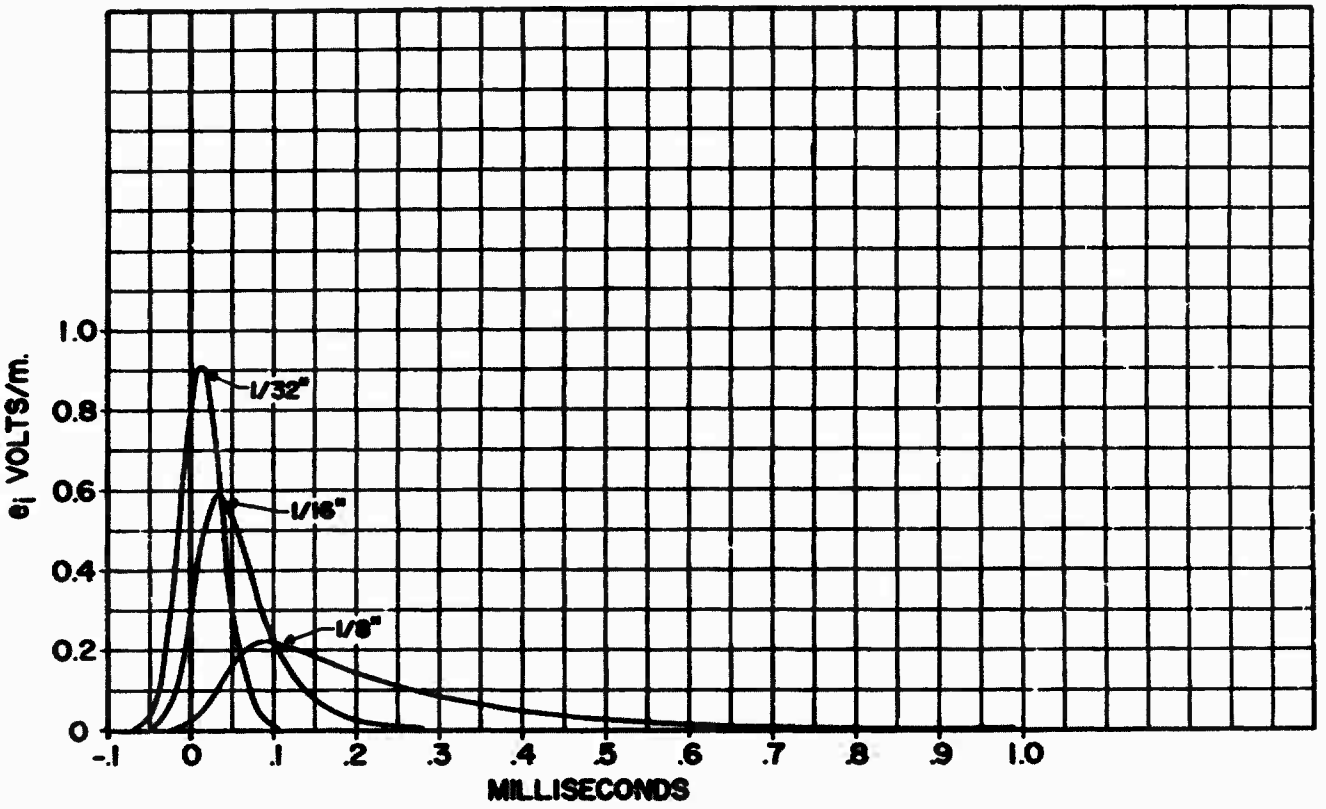

Graph 25 -- Cylinder. $e_t(o) = 1$ volt/m; $t_1 = 24$ μs

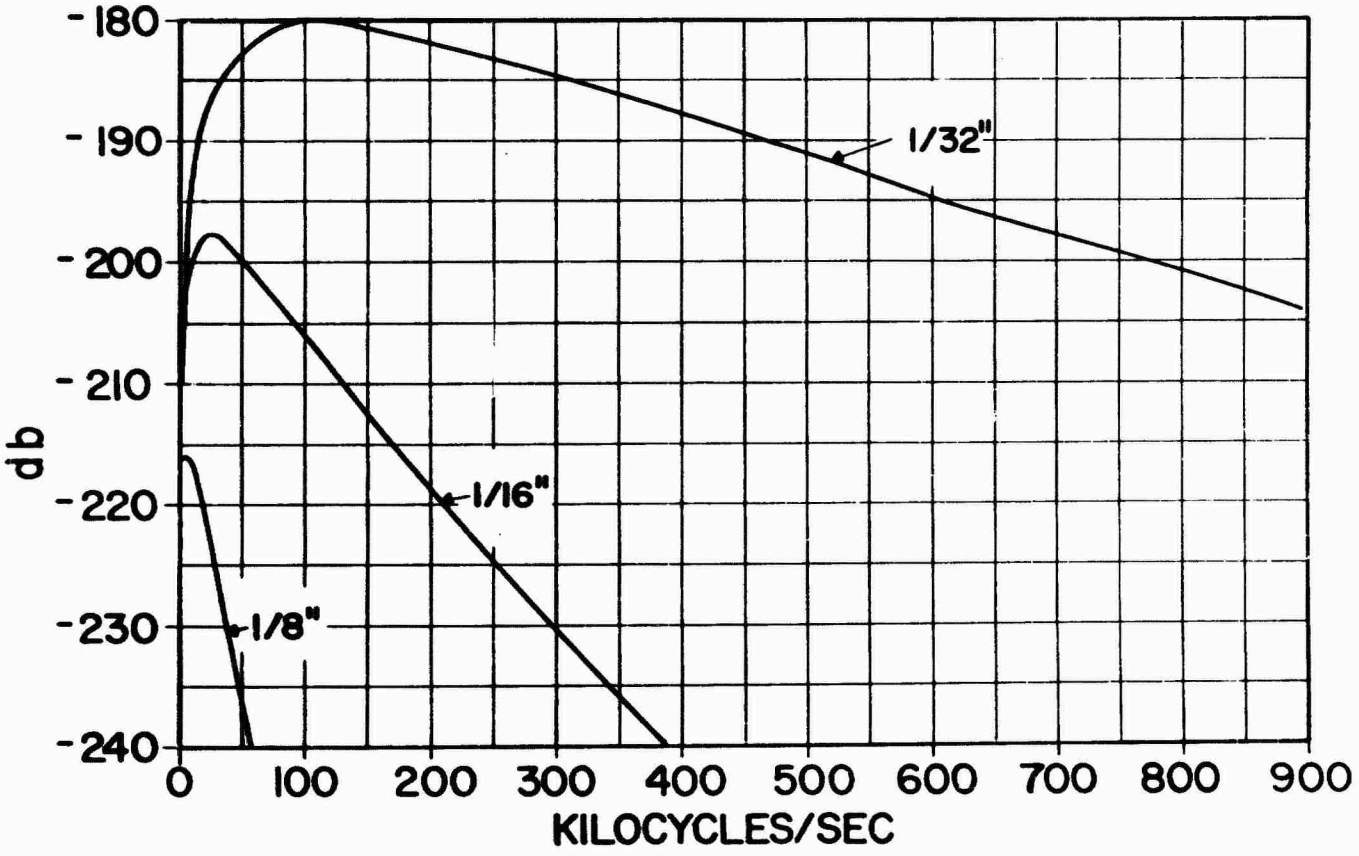

Graph 26 -- Cylinder. Steady-state transfer characteristic relating E_i to E_o

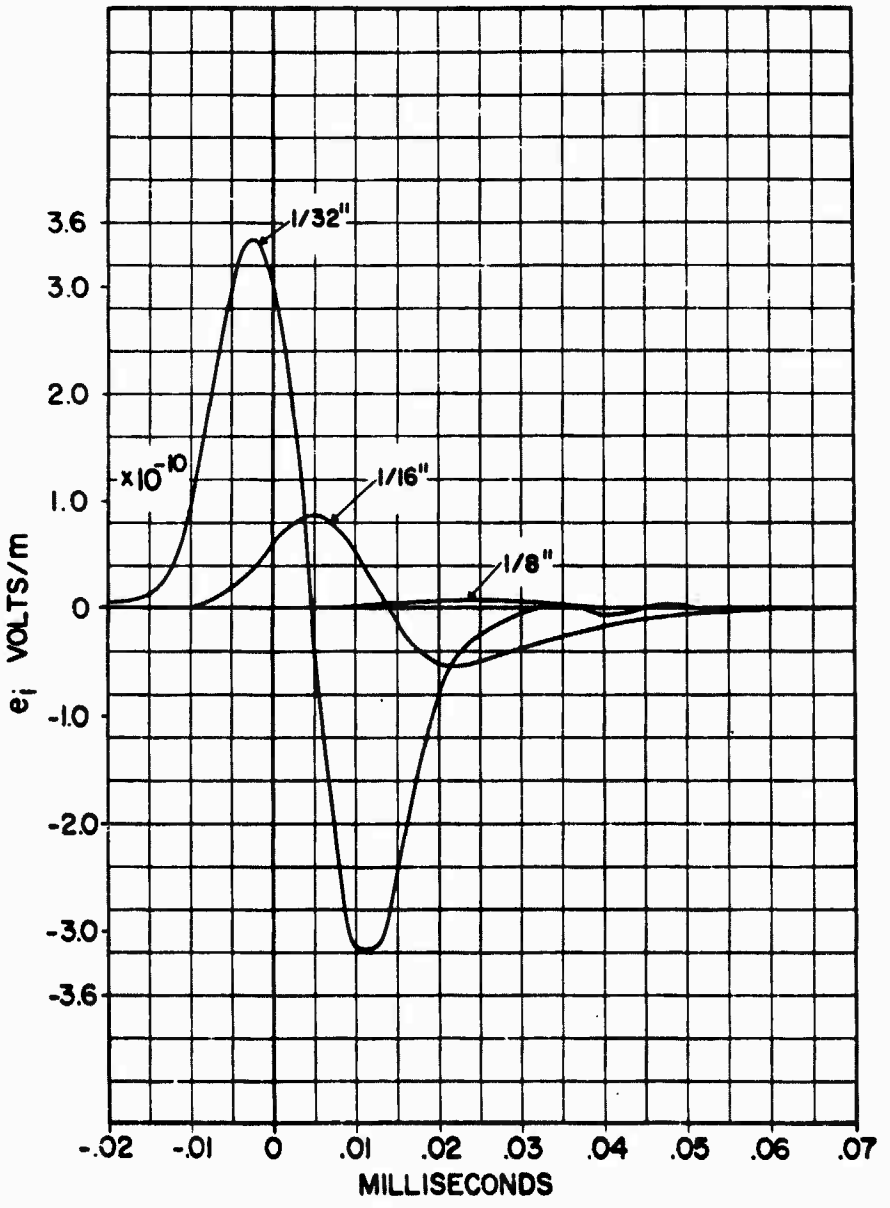

Graph 27 -- Cylinder. $e_o(o)$ = 1 volt/m; t_1 = 6 μs

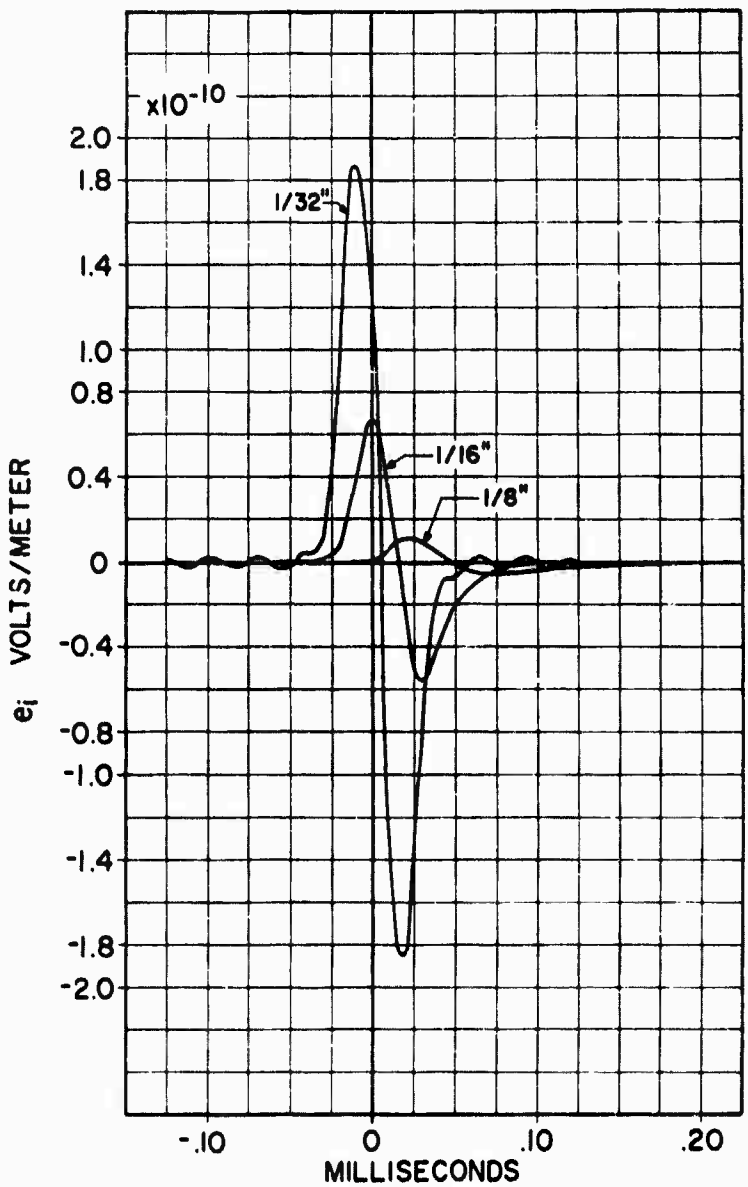

Graph 28 -- Cylinder. $\epsilon_o(o) = 1$ volt/m; $t_1 = 12$ μs

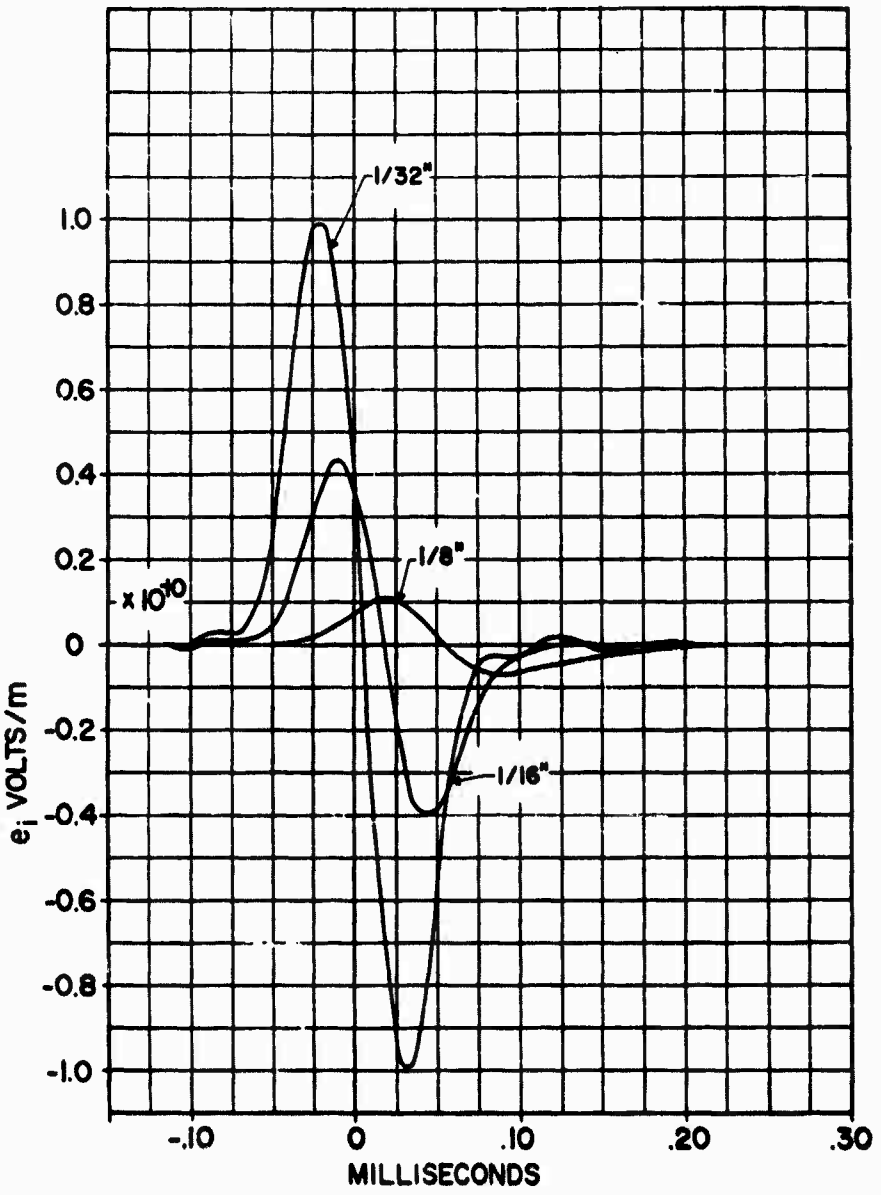

Graph 29 -- Cylinder. $e_o(o) = 1$ volt/m; $t_1 = 24$ μs

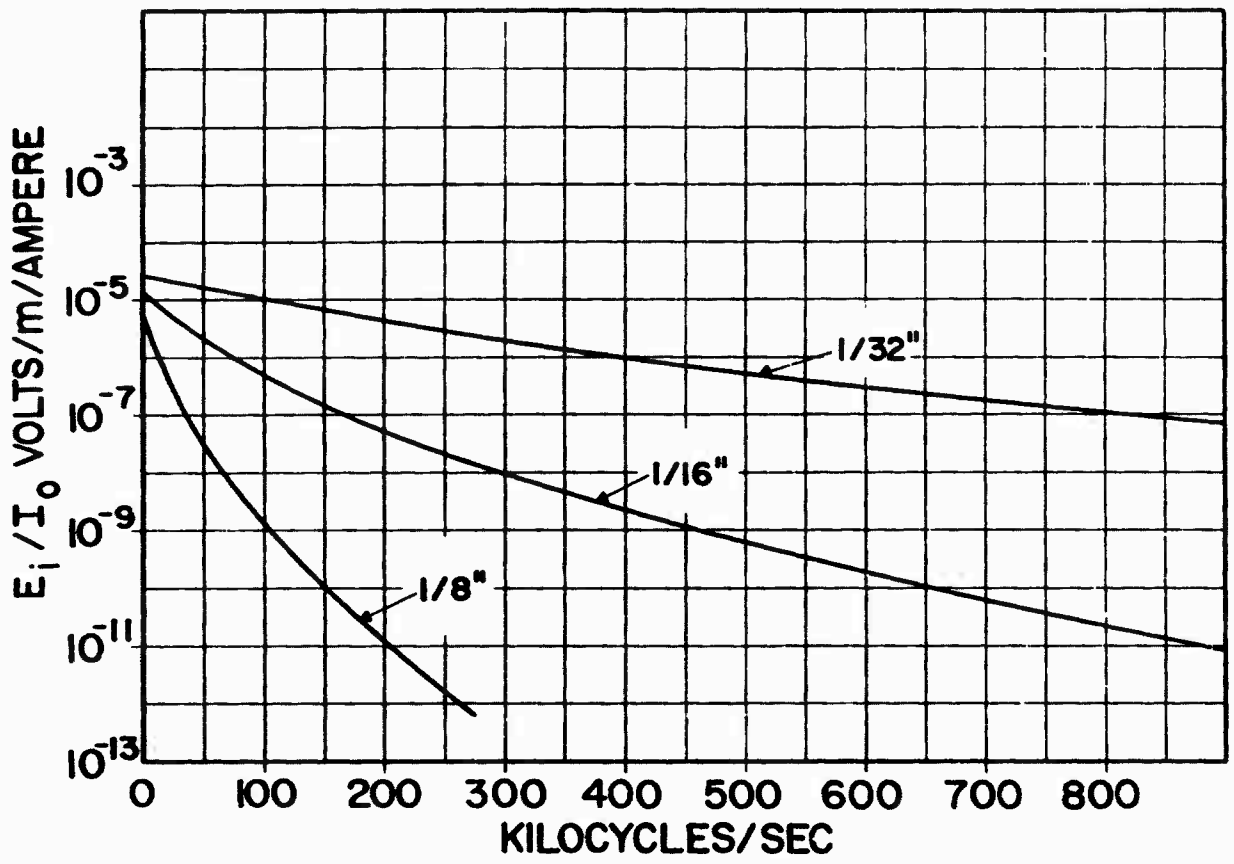

Graph 30 -- Cylinder. Steady-state transfer characteristic relating E_i to I_o

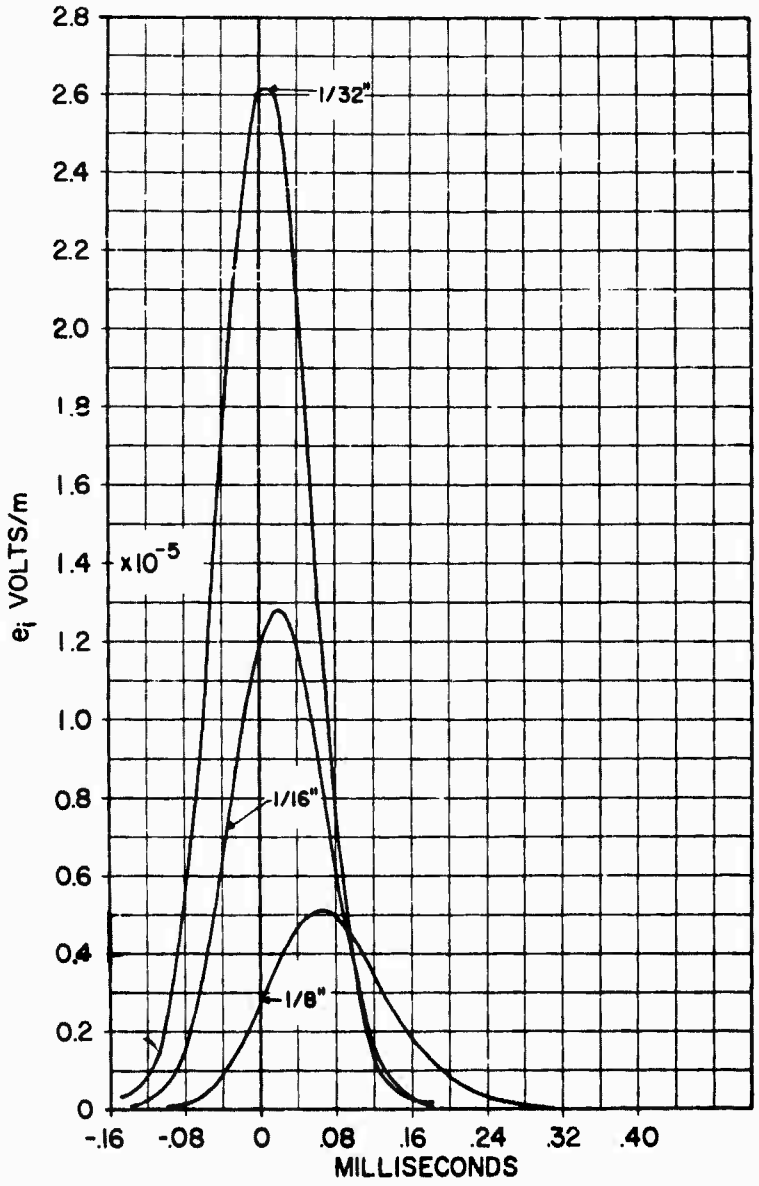

Graph 33 -- Cylinder. $i_o(\bullet) = 1$ ampere; $t_1 = 48\ \mu s$

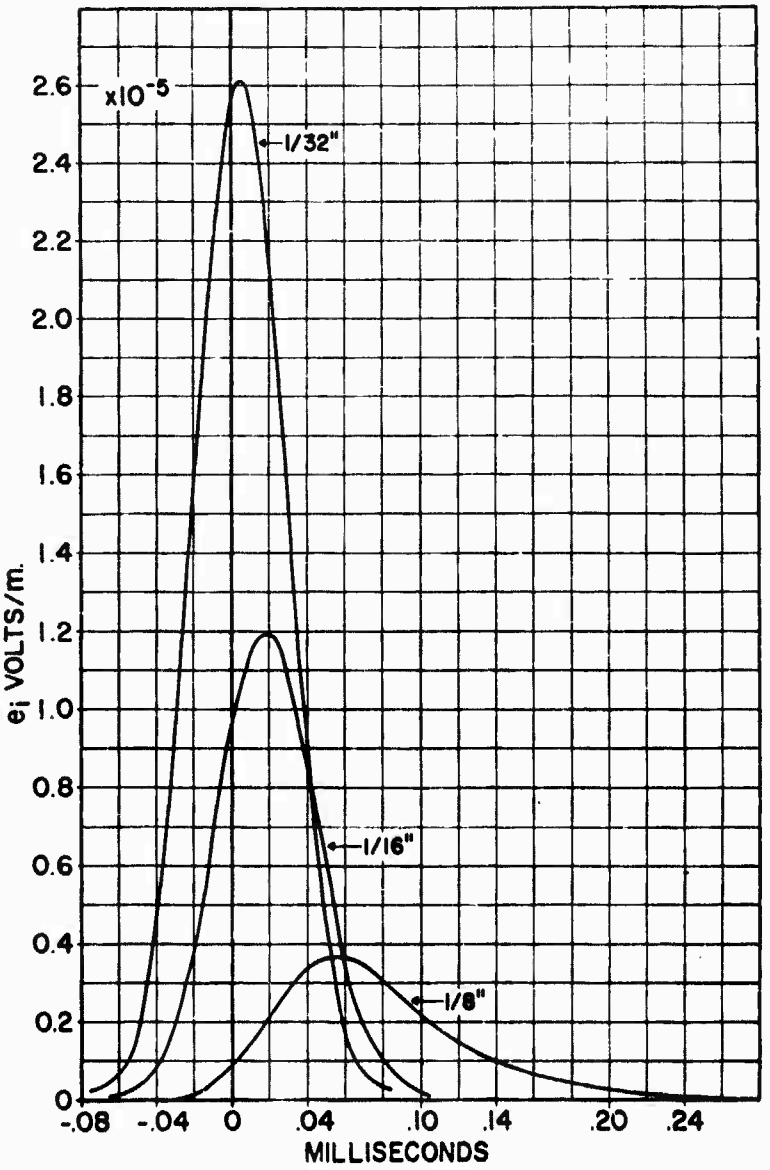

Graph 32 -- Cylinder. $i_o(o) = 1$ ampere; $t_1 = 24\ \mu s$

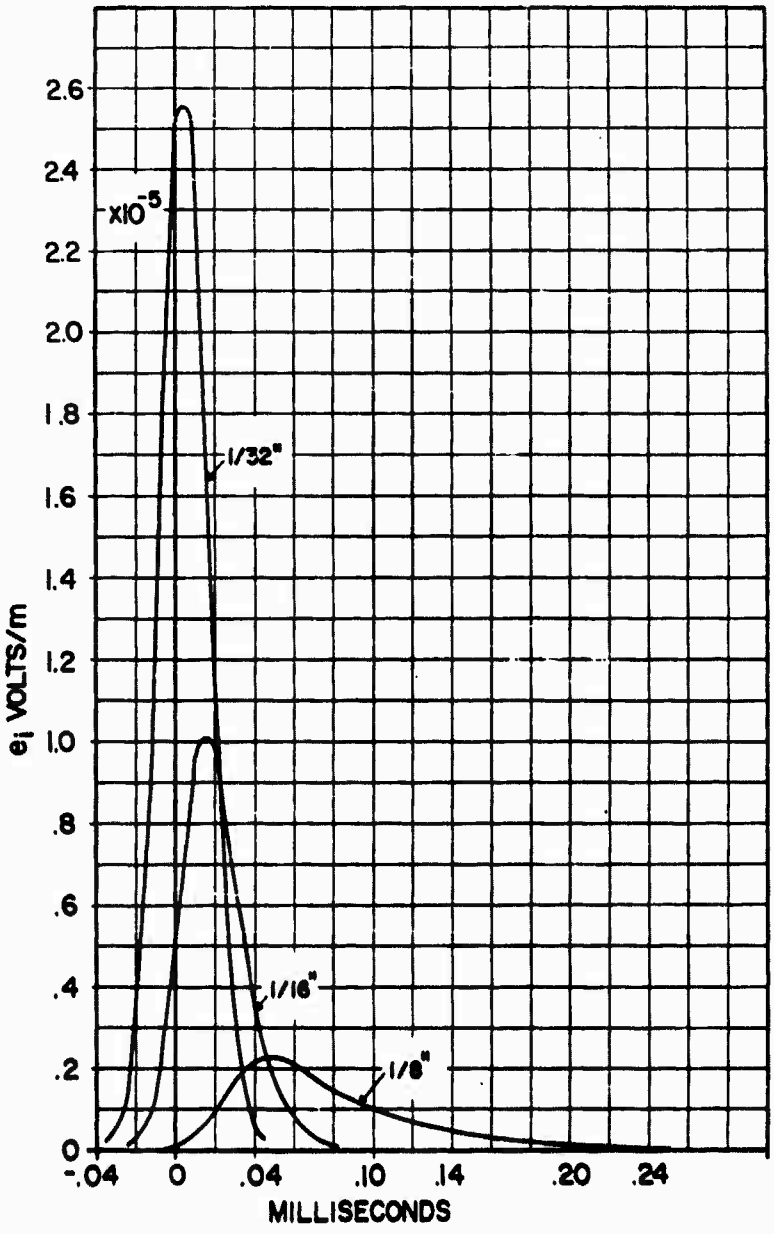

Graph 31 -- Cylinder. $i_3(o) = 1$ ampere; $t_1 = 12$ μs

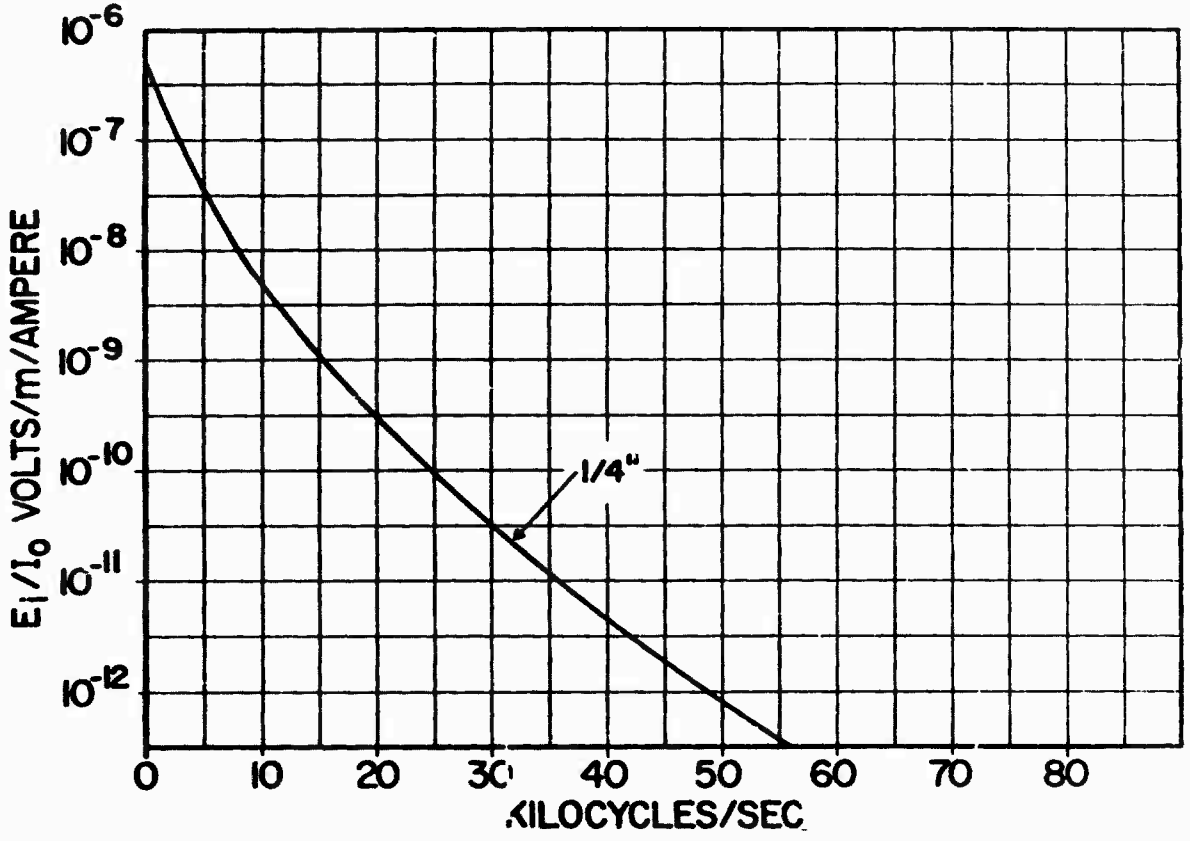

Graph 34 -- Jupiter missile. Steady-state transfer characteristic relating E_i to I_o

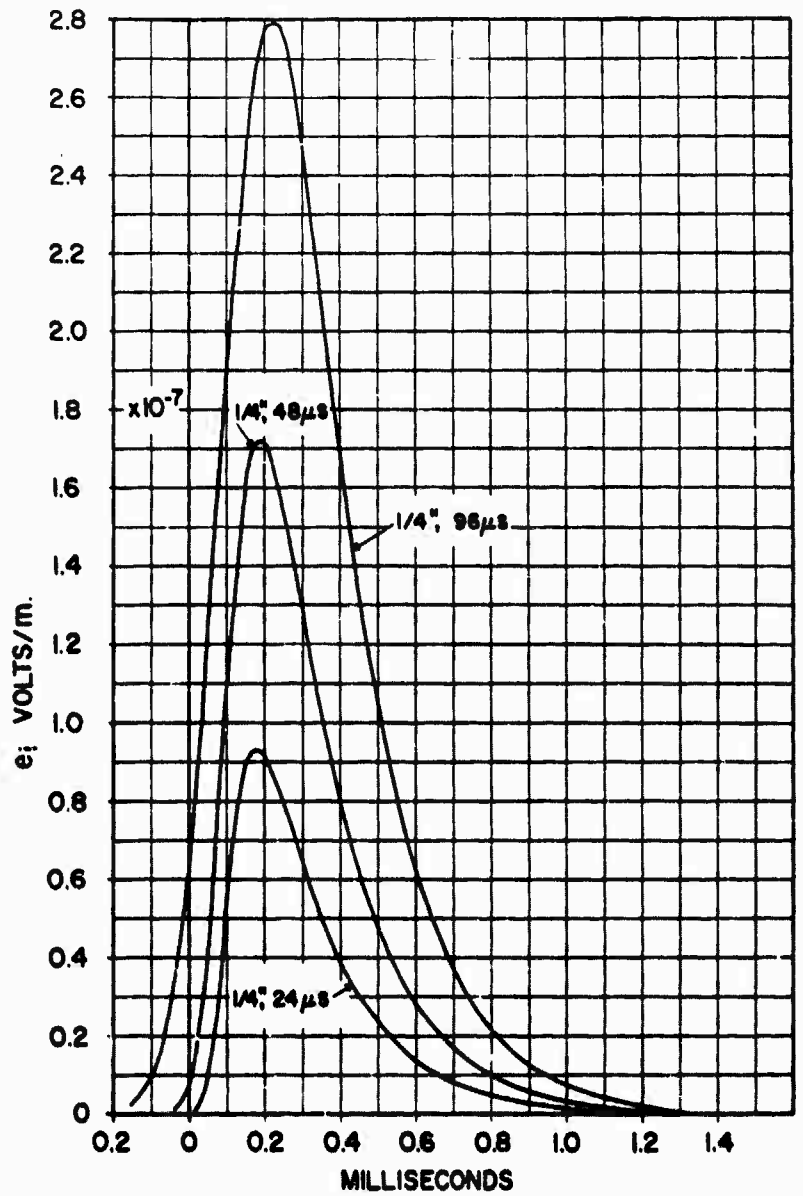

Graph 35 -- Jupiter missile. $i_o(o) = 1$ ampere; $t_1 = 24$, 48, and 96 μs

45. THE SANDIA RF TESTING FACILITY USING LOW-LEVEL ELECTROMAGNETIC RADIATION A STATUS REPORT *

C. W. Cook

Sandia Corporation
Albuquerque, New Mexico

INTRODUCTION

In 1958, Sandia Corporation (Organization 1424) started planning a radio frequency (RF) facility which would determine the susceptibility of a system to electromagnetic radiation (EMR). A low-power facility (less than 1 watt) was decided on.

The first consideration resulting from the selection of the low-power facility was that of developing a detector with which to instrument the electro-explosive device (EED) bridgewires so that the amount of energy being dissipated could be measured. Prior to this time, thermocouples had been used to instrument EED's; but the thermocouples weren't sensitive enough for the type of facility being built.

There are two basic means of detecting RF signals: the superheterodyne system and the crystal video system. Either one of these methods could probably have been developed into a satisfactory RF detector; but, after considerable study, the crystal video system was decided upon. The choice of this system eliminated one difficult problem: no RF switching was required in the receiver. However, the crystal video detector is not faultless; it is a very broad band detector and thus picks up many unwanted signals. To eliminate unwanted signals, a phase-locked receiver had to be employed. The detector and receiver currently used in the low-power facility are described in detail in this paper.

The capabilities and advantages, as well as the limitations, of the Sandia Corporation low-power RF test facility are discussed in this paper, and the techniques of testing and methods of automatic data acquisition are described.

---

*Developmental facility described in Proceedings of Hero Congress, 1961, reference paper No. 27.

CRYSTAL VIDEO DETECTOR

The criteria that controlled the design of this detector were:

1. The detector would have to be able to measure the power being absorbed in the bridgewire regardless of the balance of the input circuits to the bridgewire circuit. It would have to measure the actual power absorbed, no matter what else was happening.
2. Neither the detector nor its lead wires would pick up any stray RF which would result in a false indication.
3. The detector would have to present a very high impedance across the bridge circuit so that the system would be essentially the same as before the detector was put in place.
4. The cable which runs from the detector to the receiver would have to go through the configuration of whatever was being instrumented with as little disturbance as possible.

The present system has essentially met all of the above basic requirements.

The evolution of the video detector to its present configuration is illustrated by Figure 1. Detectors A and B were never used in a susceptibility test because they were too large for easy installation. Detector C has been used in five systems with good results. Detector D is the current miniaturized model.

The miniaturized detector is basically a Sylvania IN830 diode, as shown by the schematic (Figure 2). The small capacitors serve as RF filters. The 33 K resistors are used to insure good isolation. Resistors larger than 33 K increase the noise level of the whole system, thereby increasing the threshold. One-tenth volt was selected as the threshold output for the receiver (0.1 volt gives a fairly stable signal, well above the noise level). The amount of energy being absorbed by a bridgewire to produce this signal varies with each EED and with different frequencies. Consequently, each EED has to be calibrated

at each test frequency. Tests are now run in a band from 700 kc to 10 kmc. Fifty-seven discrete frequencies are used for each test.

The video detectors are calibrated by establishing a reference point with thermistor-instrumented EED's. A milliwatt of DC power is fed to the bridgewire of the thermistor-instrumented EED; the output obtained from the thermistor bridge is taken as a reference point. In order to find the equivalent heating due to RF, the same bridgewire is fed RF directly. When the bridge circuit responds the same to RF as it did to the DC, equivalent heating has been established. Once this reference point has been established, the signal generator setting is not changed. The thermistor-instrumented unit is then replaced with a video-detector- instrumented unit. With this setup, attenuation is added until the receiver has 0.1 volt output. The algebraic difference between these two readings is the sensitivity of the detector at the particular frequency being tested.

To limit component modification, the detector was miniaturized. The big advantage of the miniaturized video detector is that it requires no modification of the system external to the EED.

In 1962, Denver Research Institute developed a configuration for the commercial components which was much smaller than the detectors which had been used in several tests. The miniaturized detector which is installed within the EED case has characteristics very similar to the older models. Figure 3 is a calibration curve for a miniaturized video detector.

A note should be added about the instrumentation cable connecting the receiver and the video detector. Tests have shown that, to insure against stray RF pickups, a double shielded cable must be used. Commercial cables or fabricated cables have been used satisfactorily. The main requirements are that the shields be electrically isolated except at the termination and that the terminations make a good RF ground to the system's skin.*

*A more complete discussion of shielding can be found in the following reference: Cook, C. W., "Electromagnetic Radiation Susceptibility," Sandia Corporation Technical Memorandum 299-62(73); RS 3423/1137.

The output of the video detector is fed into a Tektronix Type E differential amplifier. The differential amplifier supplies 70 db of rejection for in-phase signals fed to its input. However, from Figure 2 it can be seen that a voltage appearing at one end of the bridgewire will be read to some degree by the receiver. Configurations can be envisioned where a voltage would be present at the ends of the bridgewire but not actually dropped across the bridgewire. Reading a signal of this nature would amount to false detection. An experimental measurement of the isolation from unwanted signals is shown in Figure 4.

The measured isolation indicates that meaningful data can be obtained from any EED; however, the type of circuit which would produce a condition for false detection is rare in present weapon systems.

HOMODYNE RECEIVING SYSTEM

Originally, one receiver (Figure 5) was used at the facility. Testing with one receiver was very time-consuming, and the old system had no efficient means of presenting the data for rapid processing. Early tests showed that there was a definite need to rotate the system being tested with respect to the transmitting antenna.

In planning the new receiving system, provisions were made for automatically rotating the hoist table. The new system has four identical receivers (Figure 6) which cut the time required to take the data by a factor of 4. Figure 7 is a block diagram of one of the receivers which comprise the present system.

A 1000-cps square wave with a variable time delay is used to obtain 100 percent modulation of the transmitter output. Another square wave from the same origin is used to switch a diode bridge in the homodyne.

By getting the detector output (1000-cps square wave) phased with the homodyne switching square wave, a peak is obtained from the output of the homodyne. The output of the homodyne is a DC voltage which is proportional

to power in the bridgewire of the instrumented EED. From the threshold of the video detectors to 40 db above this level the video detectors are square law.

As shown by the diagram, the necessary conversions are made so that the data is finally simultaneously typed and punched on paper tape. The typed copy gives an immediate survey of the data being taken.

Because of the broad band covered (700 kc - 10 kmc), the degree of susceptibility varies greatly. At frequencies above 50 mc, the angle of the system with respect to the transmitting antenna is an important factor. These two factors necessitated the incorporation of a memory circuit and an automatic attenuator. Since the maximum susceptibility for a given configuration is of most concern, a memory circuit has been employed which measures only the peak obtained during a complete rotation of the hoist table. The position of the hoist table which caused the maximum reading is also memorized. At the completion of a rotation, the channel number, peak response, and angle at which peak response occurred are recorded on the data tape. The homodyne has a dynamic range of approximately 10 db; therefore, to read signals larger than 10 db above threshold, an automatic attenuator on the input to the receiver had to be added.

To insure that all receivers are working properly and that the gains have not changed, a low-level signal is fed into each receiver before a scan is started. If the proper reading is obtained, the scan is made and recorded.

The present system which employs four receivers has completed a test of four configurations across a spectrum of 57 frequencies in 8 days. Two days after the completion of the test, the data had been corrected for field strength, detector sensitivity, and the 100 percent no-fire level (NF) of the EED. Figure 8 illustrates the final presentation of the data.

TEST ENVIRONMENT

For a system response to have meaning, it must be related to a specific environment. A defined and repeatable environment is also essential in evaluating system modifications or fixes.

The EMR environment at Sandia's facility is set up as accurately as possible and is then monitored continuously. The field strengths in the 700 kc - 1 kmc band are measured with an Empire Devices NF-205 field intensity meter. Since the measurements below 30 mc are made in the induction zone of the radiating antenna, a theoretical correction factor has to be applied to the readings below 30 mc.* Above 1 kmc, the field strengths are calculated from data provided by Polarad. For monitoring purposes a video-detector-instrumented EED is attached to an appropriate antenna and placed at a fixed location on the ground plane. This detector is read on each scan.

To facilitate rapid testing, direct tuning signal generators are now used. For comparison purposes Figures 9 and 10 show the old and new transmitter setups.

Figure 11 shows the relationship between the antenna locations and the hoist. The covered material between the antenna and the hoist is an RF absorbing material used to reduce ground plane reflections at the VHF and UHF frequencies.

*Correction factors from "Memo to File, March 1960" by P. Gelt, 1424, Sandia Corporation.

ADVANTAGES AND LIMITATIONS OF SANDIA'S LOW-POWER FACILITY

Advantages

The present system offers rapid testing over a very wide spectrum with continuous receiver checks. The data is immediately available for evaluation. Any susceptible areas are pinpointed as they are reached.

The facility is especially useful for evaluating internal fixes. Fix evaluation is made possible by results which are repeatable. Tests that have been repeated after several months indicate that the original responses can be repeated to within 1.5 db.

Above 150 mc, aircraft and umbilical cables have a diminishing effect; consequently, a system's response can be determined without any external simulation. The mode of entry for microwave energy is easily pinpointed by observing the position of the system at which the maximum response occurred. The increase in susceptibility due to open access doors, discontinuities, etc., is easily determined.

Limitations

The size of the system which can be tested is limited. Aircraft cannot be used. Results have shown that, below 50 mc, external cables are the only mode of entry for RF. To evaluate a system below 50 mc, the aircraft and the umbilical cable have to be simulated. For this simulation, an external cable is attached to the pullout plug. It should be emphasized that the external cable is merely simulating the mode of entry. However, comparisons with field data indicate that a resonant unshielded cable is a worse condition than an unracked weapon.

A second limitation is that all readings have to be extrapolated if the response to actual field conditions is desired. The system being tested can be considered to be a maze of R, L, and C. These are linear elements. Therefore, it is felt that a linear extrapolation is justified. The validity of low-power testing is discussed in further detail in another section.

AREAS THAT CAN AFFECT DATA VALIDITY

During the checkout of the present receiving system, several factors were discovered which can radically affect (variations greater than 6 db) the results of an EMR test. The automatic cycling and visual data readout of the receiving system permit easy checks of data reruns.

From many reruns it was discovered that moisture condensation inside a system can vary responses radically. The data indicates that moisture tends to increase responses although many cases were observed where the opposite was true. Repeatable data could be obtained only when the system was dry (no observable moisture). The dry condition is felt to represent the most realistic condition, since all WR systems are sealed and have desiccant inside.

A second variable was discovered when it was found that on some days all channels responded higher at frequencies below 30 mc than they had previously. This difference was finally traced to the grounded vertical antenna. The amount of energy radiated from the yertical antenna varied with ground and atmospheric conditions. When this was discovered, an Empire Devices NF-205 field intensity meter was employed to monitor the radiated field strength. After the environment was made repeatable, the data became repeatable.

VALIDITY OF LOW-POWER TESTING

How does low-power testing relate to the actual environment which produces much more than 50 microamps in the bridgewire (50 microamps is approximately the threshold level of the video detector)? One test has been run which verifies the validity of extrapolating from low levels to actual environment levels. This test was run at 10 kmc, using a parabola and a horn to transmit and a parabola to receive. A video-detector-instrumented EED was placed at the focal point of the receiving parabola. With the transmitter turned

down, the energy being absorbed by the instrumented bridgewire was measured. From this reading, a linear extrapolation was used to determine the power level which would set off a live EED located at the same point. The instrumented unit was replaced with a live EED. On three separate occasions, live EED's were fired within 3 db of the predicted level.

EMR tests have been run in Dahlgren, Virginia, at high-power levels. The main difficulty in correlating the results of the low-power tests with these tests is that of defining the environment. The EMR fields have not been defined precisely; however, using the data available, the results have been favorable.

DESIDERATA

The facility has already demonstrated that it can be used successfully for development and fix evaluation tests. It is anticipated that the facility will continue to be used for these tests. After more extensive correlation studies are made, it is hoped that most development tests can be run at the Sandia facility.

In an attempt to make continued improvement in the accuracy of the data acquired at the facility, the following areas will receive further investigation:

1. Improved calibration accuracy. A new calibration setup is being designed in an attempt to increase accuracy, especially at frequencies above 6 kmc.
2. Increased detector sensitivity. An increase in the detector sensitivity would provide more data than can now be obtained.
3. Improved environment definition. More research will be done in this area so that the number of tests required can be cut down.

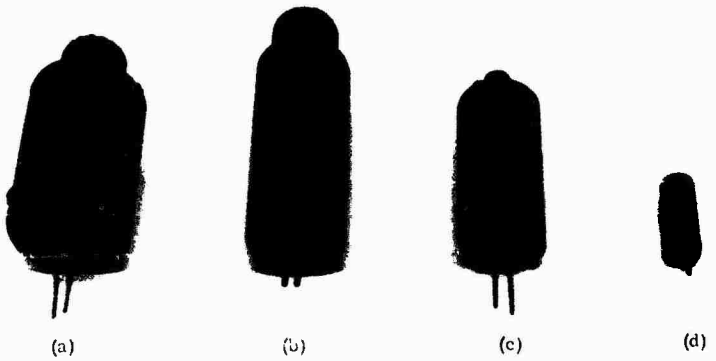

Figure 1. Video Detector Evaluation

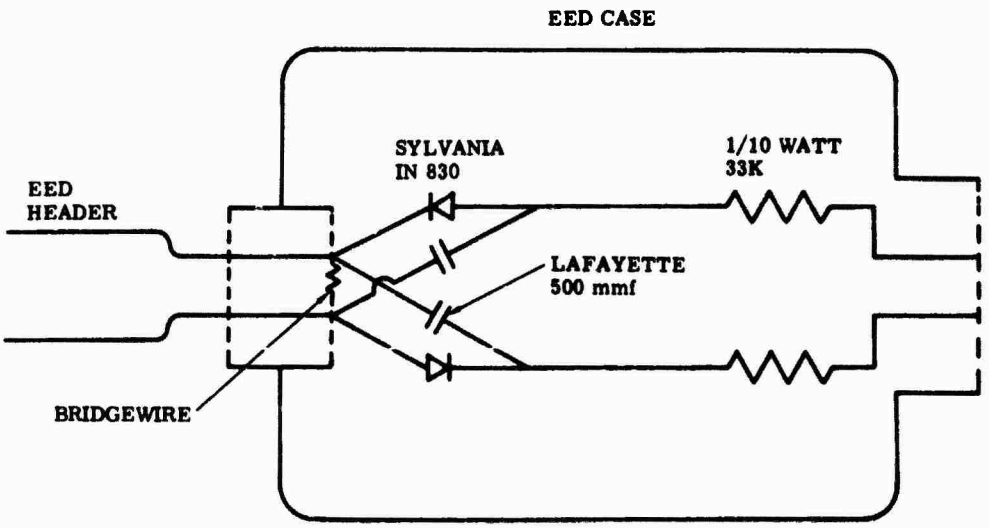

Figure 2 Crystal Video Detector

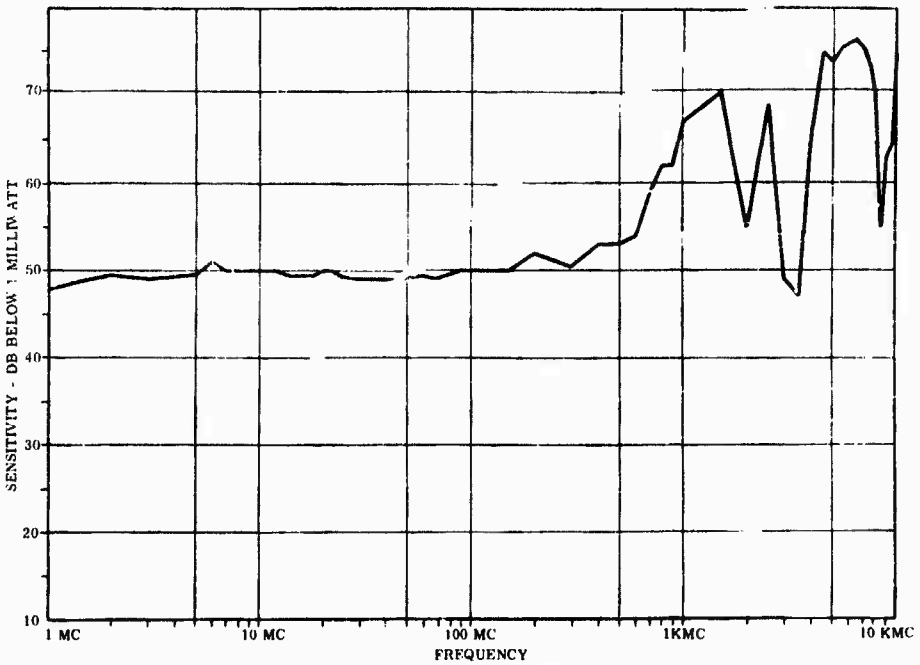

Figure 3. Calibration Curve for Miniaturized Video Detection

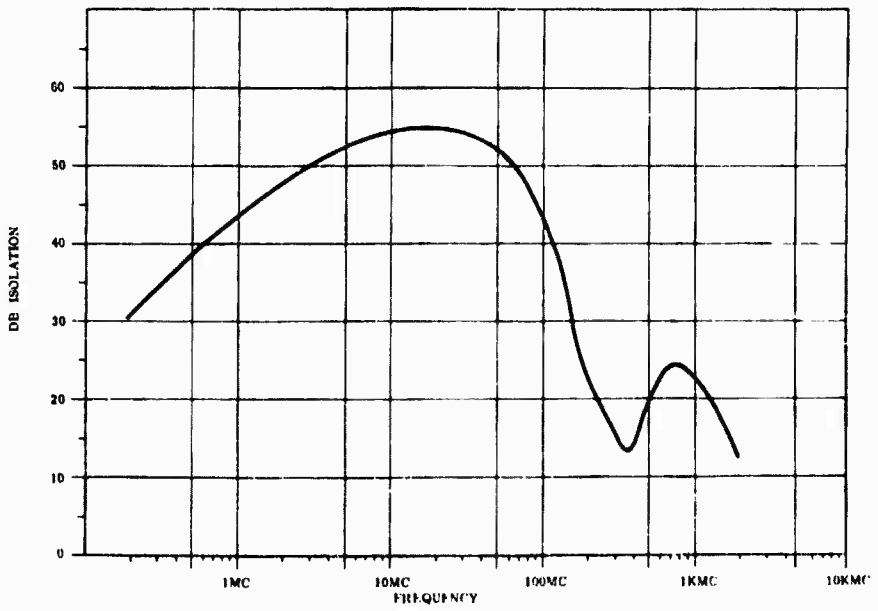

Figure 4. Isolation of Miniature Video Detection

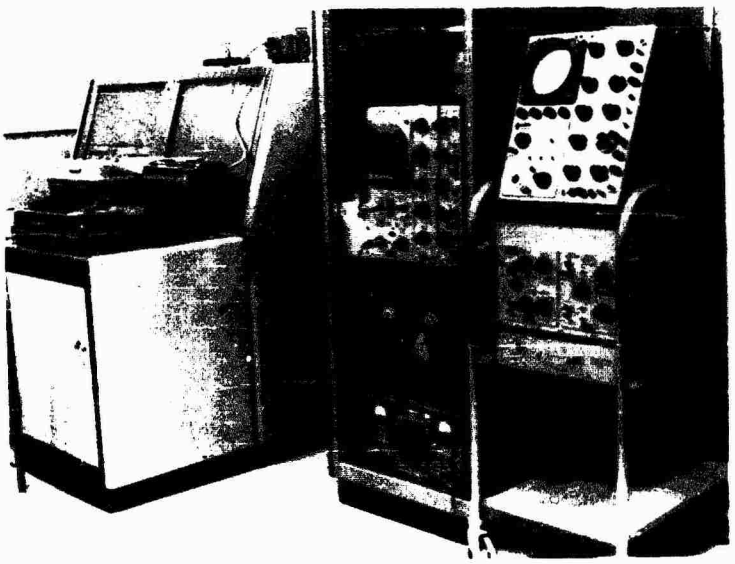

Figure 5. Original Receiver

Figure 6. New Automated Receiving Systems

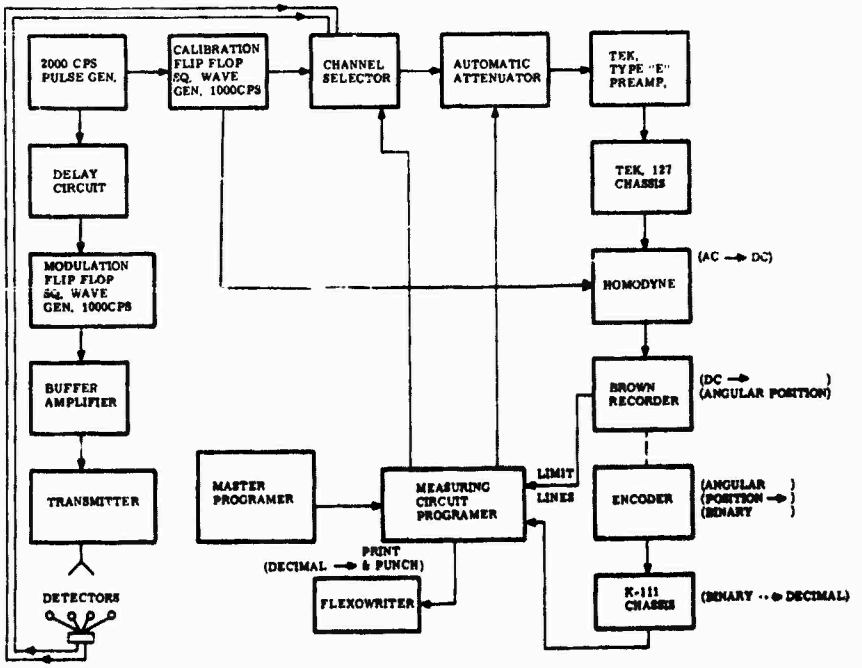

Figure 7. RF Facility Receiver

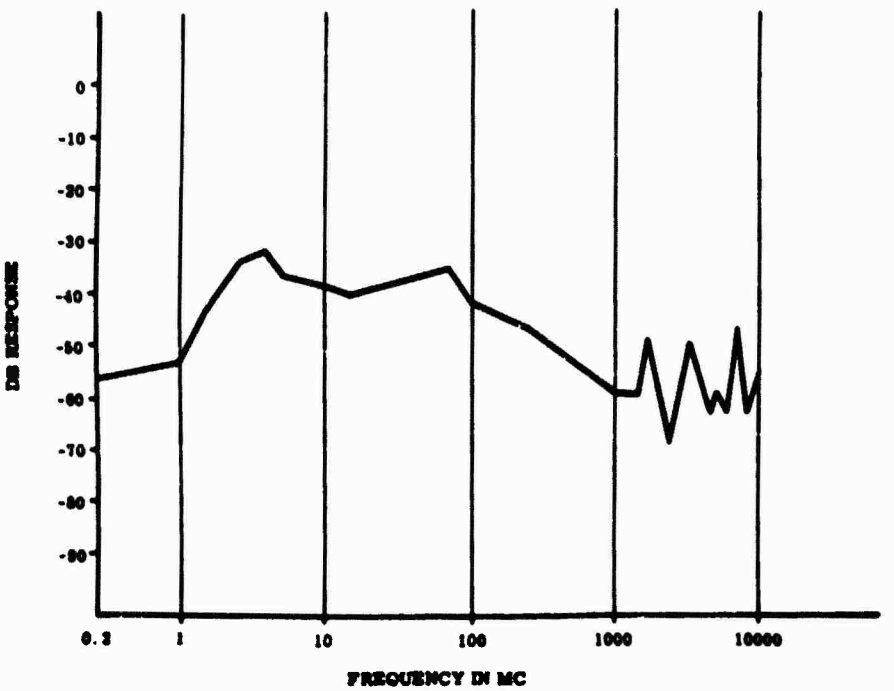

Figure 8. Arbitrary Response Curve

Figure 10. Present Direct Tuning Transmitters

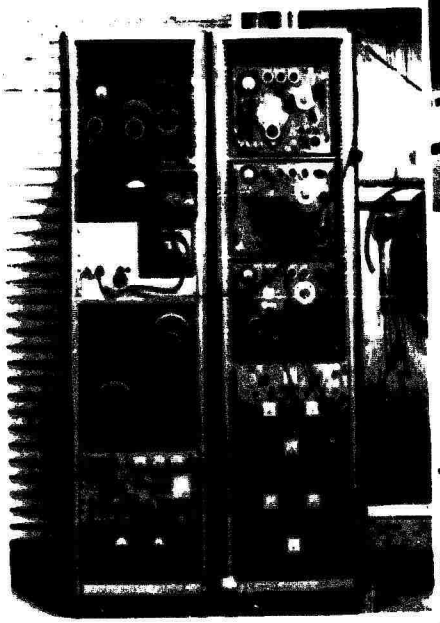

Existing Original Transmitters

Figure 11. Facility Ground Plane

46 SLOT RECEIVING ANTENNAS AS RELATED TO RADIO FREQUENCY HAZARDS TO ORDNANCE

by

Charles W. Harrison, Jr.
Member of the Technical Staff,
Sandia Corporation, Albuquerque, N. M.

Introduction

In the past several years, a number of problems in the field of radio-frequency hazards to ordance have been discussed in Sandia Laboratory reports.[1-6] This paper is another in the series—the objective being the evaluation of radio-frequency power transmission through an access door or circumferential anodized butt into the circuitry contained within a cylinder of finite length and radius. For convenience the cylinder is assumed to be perfectly conducting. This insures that no power may enter except by transfer through the slot. Transmission directly through the skin of a cylinder of even modest thickness, having no holes or cracks, has been proved to be negligible at all frequencies for which the cylinder is electrically short.[4-5]

The slot receiving antennas examined theoretically are:

1. A center-loaded slot cut in an infinite, perfectly conducting plane of infinitesimal thickness.

2. A thin-walled, perfectly conducting cylindrical tube of arbitrary length containing a center-loaded slot extending a portion of the way around the circumference of the tube.

3. A thin-walled, perfectly conducting cylindrical tube of arbitrary length containing a complete peripheral slot loaded (1) by an impedance across the slot, and (2) by internal impedances. The problem of stray capacitance shunting the load when connected across the slot is considered.

The general theory is applied to solve specific problems. The results are presented in the form of curves relating the power in a load resistance of 4.5 ohms (in decibels referred to a zero-power level of 50 milliwatts) to the frequency, for an incident electric field of 10 volts/m. The slot dimensions are 1.45 by 12 inches. In some instances, data is presented for a 4.5-ohm load with sufficient series reactance to produce resonance at each particular frequency considered. These curves may be regarded as transfer characteristics for the slot receiving systems because from them the power in the load for any given value of field strength may be determined immediately. In the low-to-medium frequency region, most of the curves have a positive slope of 6 db/octave with increasing frequency, and beyond 10 mc/sec they are oscillatory in nature.

Center-Loaded Slot Receiving Antenna Cut in an Infinite, Perfectly Conducting Plane

Figures 1a and 1b illustrate an impedance-loaded slot receiving antenna that is cut in an infinite, perfectly conducting sheet of infinitesimal thickness. The sheet coincides with the plane $z = 0$; the slot extends in length from $x = -h^s$ to $x = h^s$, and in width from $y = -\frac{w}{2}$ to $y = \frac{w}{2}$. The load terminals of the slot are located at $x = 0$, $y = \pm \frac{w}{2}$, and $z = 0$. The electromagnetic field incident upon the slot is assumed to originate with the dipole source of length ℓ and the image source shown in Figure 1a. For simplicity, the axes of the sources are oriented parallel to the y-axis. Their centers lie on the z-axis, a distance R measured normal to the sheet. The dimension R satisfies the inequalities $\beta R >> 1$ and $R >> \ell$, where β is the wave number. These conditions insure that the field incident upon the slot is a plane wave. The source and the image source carry currents that are in phase opposition, as shown.

Note that the incident field has no component of the electric field across the slot. The only components of the electromagnetic field that are tangential to the infinite conducting plane $z = 0$ and the slot cut in it are those of the magnetic field. Thus, the incident field may be regarded as generating surface currents on the conducting plane and these, in turn, produce separations of charge that maintain a transverse electric field across the slot.

In the analysis, two symmetrically placed sources are required in order to maintain complete symmetry between the half-spaces. Actually, the coupling between these half-spaces is not great and essentially the same results apply to either half-space, even if there is no source in the other. The contribution of the second source is provided almost completely by the image in the conducting plane—which is unbroken except for the slot. Thus the image source is almost perfect and differs little from the second source assumed in the analysis.

If the ground plane is not infinite in extent, the problem is fundamentally different. However, if the plane extends many wavelengths beyond the slot, and the distance R from the source to the ground screen is much less than the distance of the slot from the edge of the screen, the results obtained for the infinite ground plane may be expected to be reasonable approximations. If the ground screen is not large compared to the wavelength, the effective length of the receiving slot must include consideration of the finite size of the ground screen. Complementarity is not applicable since this actually assumes an infinite ground screen. Present results evidently throw no clear light on the problem of reception by a slot in a finite cylinder or other three-dimensional object, although a qualitative similarity may be expected if the metal surface is very large in extent compared with the wavelength.

The short-circuit current I_x^d at the terminals of the strip receiving antenna (the complement of the slot) is

$$I_x^d = \frac{2h_e E_x^{inc}}{Z^d} \tag{1}$$

where $2h_e$ is the effective length for parallel incidence of the electric field E_x^{inc}, and $Z^d = R^d + jX^d$ is the driving point impedance of the strip (viewed at the terminals $x = \pm\frac{\delta}{2}$, $y = 0$, $z = 0$) when used for transmission.

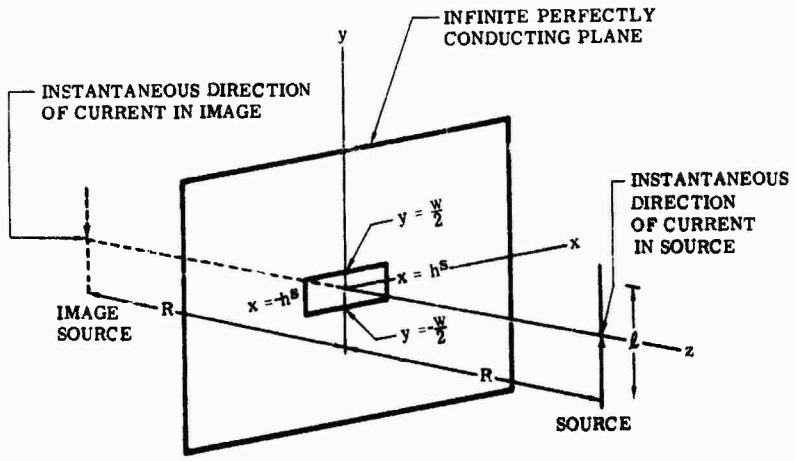

Figure 1a. Slot Cut in an Infinite Perfectly Conducting Plane of Infinitesimal Thickness

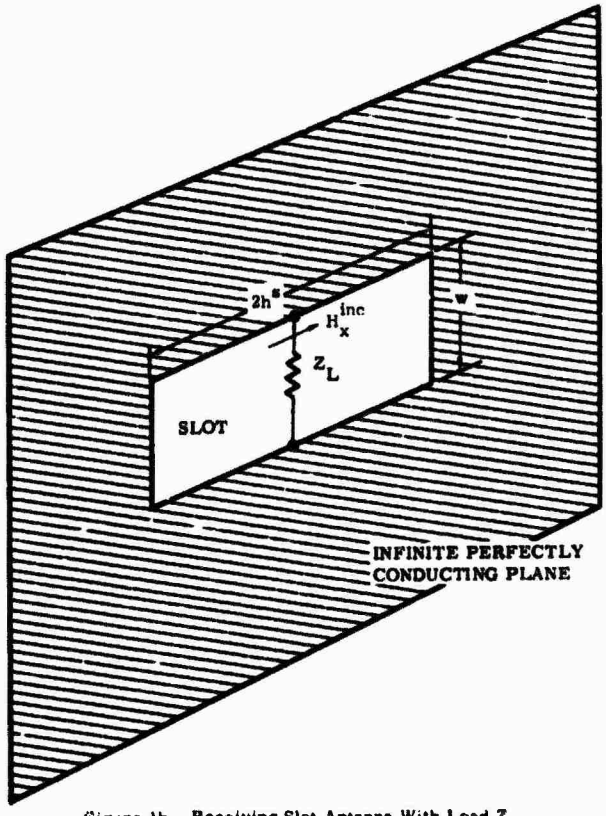

Figure 1b. Receiving Slot Antenna With Load Z_L

Evidently the current I_x^d is also given by the relation

$$I_x^d = 2\int_{-\frac{w}{2}}^{\frac{w}{2}} H_y^d dy . \tag{2}$$

Here H_y^d is the magnetic field transverse to the strip at $x = 0$.

The voltage appearing across the terminals of the strip antenna when they are open-circuited is

$$V_{oc}^d = \int_{-\frac{\delta}{2}}^{\frac{\delta}{2}} E_x^d dx . \tag{3}$$

In this relation E_x^d is the electric field across the gap in the strip. The principle of complementarity may now be applied, and conductor and air interchanged in the plane $z = 0$; also, the electric and magnetic fields are interchanged according to

$$\left.\begin{aligned} E^d &= -\zeta H^s \\ H^d &= E^s/\zeta \end{aligned}\right\} \tag{4a, 4b}$$

where $\zeta = 120\pi$ ohms.

Note that by this interchange the electric strip antenna having an air gap in the interval $-\frac{\delta}{2} \leq x \leq \frac{\delta}{2}$ now becomes a slot cut in an infinite perfectly conducting plane having a short-circuit of width δ connected to the slot terminals $y = \pm\frac{w}{2}$.

Substituting (4) into (2) and (3),

$$I_x^d = \frac{2}{\zeta}\int_{-\frac{w}{2}}^{\frac{w}{2}} E_y^s dy \tag{5}$$

and

$$V_{oc}^d = -\zeta\int_{-\frac{\delta}{2}}^{\frac{\delta}{2}} H_x^s dx . \tag{6}$$

But

$$\int_{-\frac{w}{2}}^{\frac{w}{2}} E_y^s \, dy = V_{oc}^s \tag{7}$$

and

$$-\int_{-\frac{\delta}{2}}^{\frac{\delta}{2}} H_x^s \, dx = -\frac{I_y^s}{2} . \tag{8}$$

Hence

$$V_{oc}^d = \frac{\zeta}{2} I_y^s \tag{9}$$

and

$$I_x^d = \frac{2V_{oc}^s}{\zeta} . \tag{10}$$

In these expressions V_{oc}^s and I_y^s are the open-circuit voltage and short-circuit current of the slot, respectively; E_y^s is the electric field across the slot at $x = 0$, and H_x^s is the longitudinal magnetic field in the slot at $x = 0$.

The short-circuit current at the terminals of the electric strip antenna multiplied by its driving point impedance gives the open-circuit voltage. The same relation holds for the slot. Thus,

$$Z^d = \frac{V_{oc}^d}{I_x^d} = \frac{\frac{\zeta}{2} I_y^s}{\frac{2}{\zeta} V_{oc}^s} = \frac{\zeta^2 I_y^s}{4V_{oc}^s} . \tag{11}$$

But $I_y^s / V_{oc}^s = Y^s = \frac{1}{Z^s}$ where $Z^s = R^s + jX^s$. Hence

$$Z^d Z^s = \zeta^2 / 4 , \tag{12}$$

a well-known result.

Substituting (10) into (1) and using (4), it becomes clear that the complementary formula for (1) is

$$V_{oc}^{s} = \frac{h_e H_x^{inc} \zeta^2}{Z^d} . \tag{13}$$

The equivalent circuit of the slot receiving system consists of V_{oc}^{s} driving a circuit comprising Z^s in series with the load impedance $Z_L^s = R_L^s + jX_L^s$. The current in the load is, therefore,

$$I_L^s = \frac{h_e H_x^{inc} \zeta^2}{Z^d \left(Z^s + Z_L^s \right)} \tag{14}$$

Using (12), (15) becomes

$$I_L = \frac{h_e H_x^{inc} \zeta^2}{\frac{\zeta^2}{4} + Z^d Z_L^s} . \tag{15}$$

The power in the load impedance is

$$P_L = |I_L^s|^2 R_L^s . \tag{16}$$

Equation (13) may be regarded as the fundamental formula of reception for a slot antenna. It gives the open-circuit voltage V_{oc}^{s} in terms of the effective half-length of an electric strip antenna h_e; the incident magnetic field H_x^{inc}, and the impedance of the strip antenna Z^d. Z^d is also the impedance of a center-driven cylindrical antenna of half-length h^s and radius a, where $a = \frac{w}{4}$.

Equations (15) and (16) were used to compute the power in a load impedance $Z_L^s = 4.5 + j0.0$ ohms connected to the terminals of a slot $2h^s = 0.3048$ m in length and w = 0.03681 m in width (12 by 1.45 inches). For these slot dimensions the shape parameter of the complementary dipole is $\Omega^d = 2 \ln 2h^s/a = 2 \ln 8h^s/w = 7$. It is necessary to determine Ω^d in order to evaluate h_e and Z^d appearing in (15). The values of Z^d and h_e for known Ω^d and βh^s may be computed from formulas or read from tables and curves appearing in the work of King.[7] Figure 2 shows the power in the load in decibels referred to $P_L = 50 \times 10^{-3}$ watts as zero-level as a function of frequency, for an incident magnetic field $H_x^{inc} = E_y^{inc}/\zeta = 2.655 \times 10^{-2}$ amperes/m, $\left(E_y^{inc} = 10 \text{ volts/m} \right)$. The slope of the curve in the low-frequency region is 6 db/octave, and rises with increasing frequency.

This slot receiving system may be tuned by adding a reactance $-X^s$ in series with R_L^s in the equivalent circuit. Alternatively, a resistance of value $\zeta^2 R^d / 4[(R^d)^2 + (X^d)^2]$ may replace Z^s in this circuit and give the same result. A curve for this case is shown in Figure 3. Again the slope is positive at 6 db/octave with increasing frequency to the point of break in the curve.

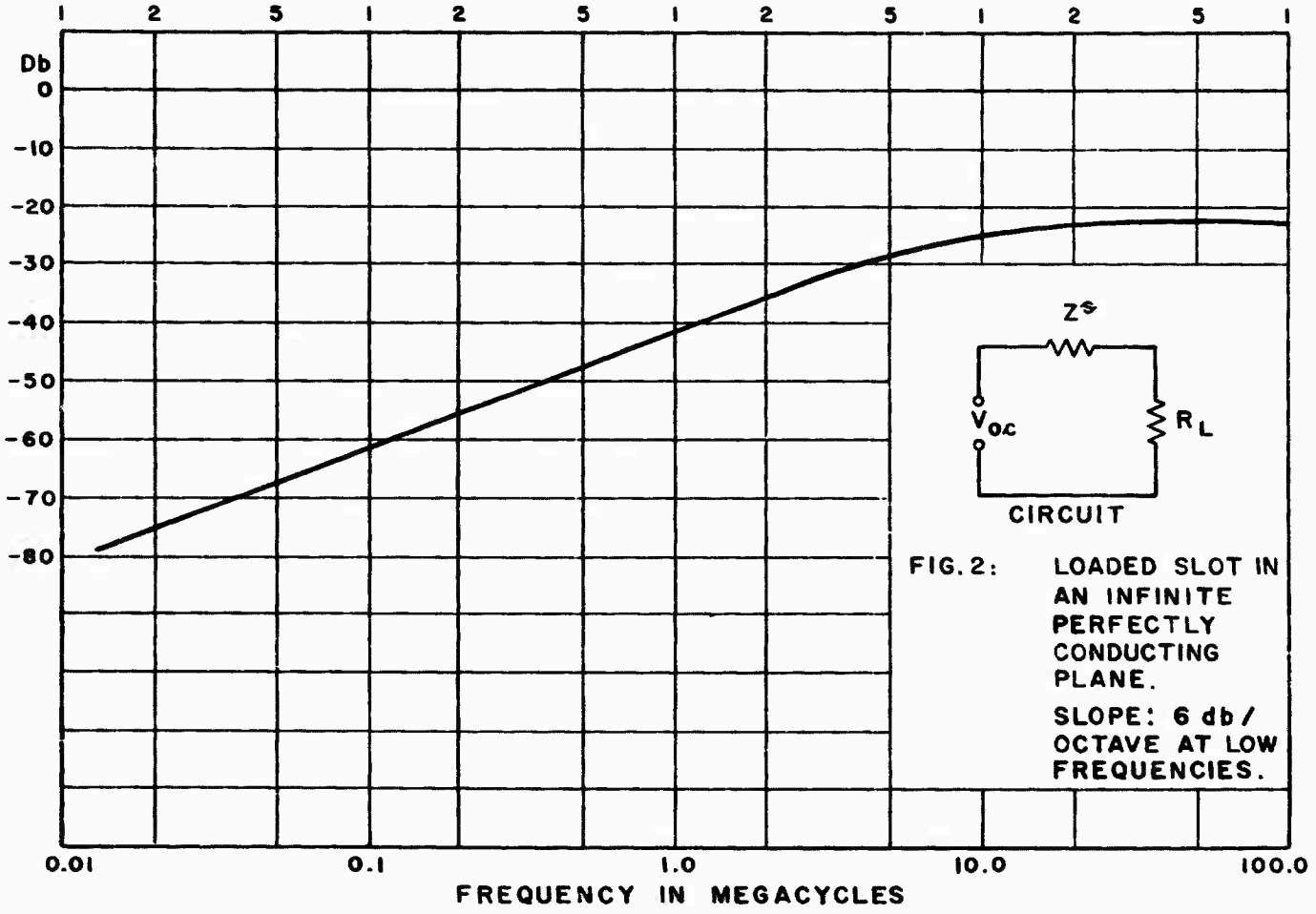

FIG. 2: LOADED SLOT IN AN INFINITE PERFECTLY CONDUCTING PLANE.

SLOPE: 6 db / OCTAVE AT LOW FREQUENCIES.

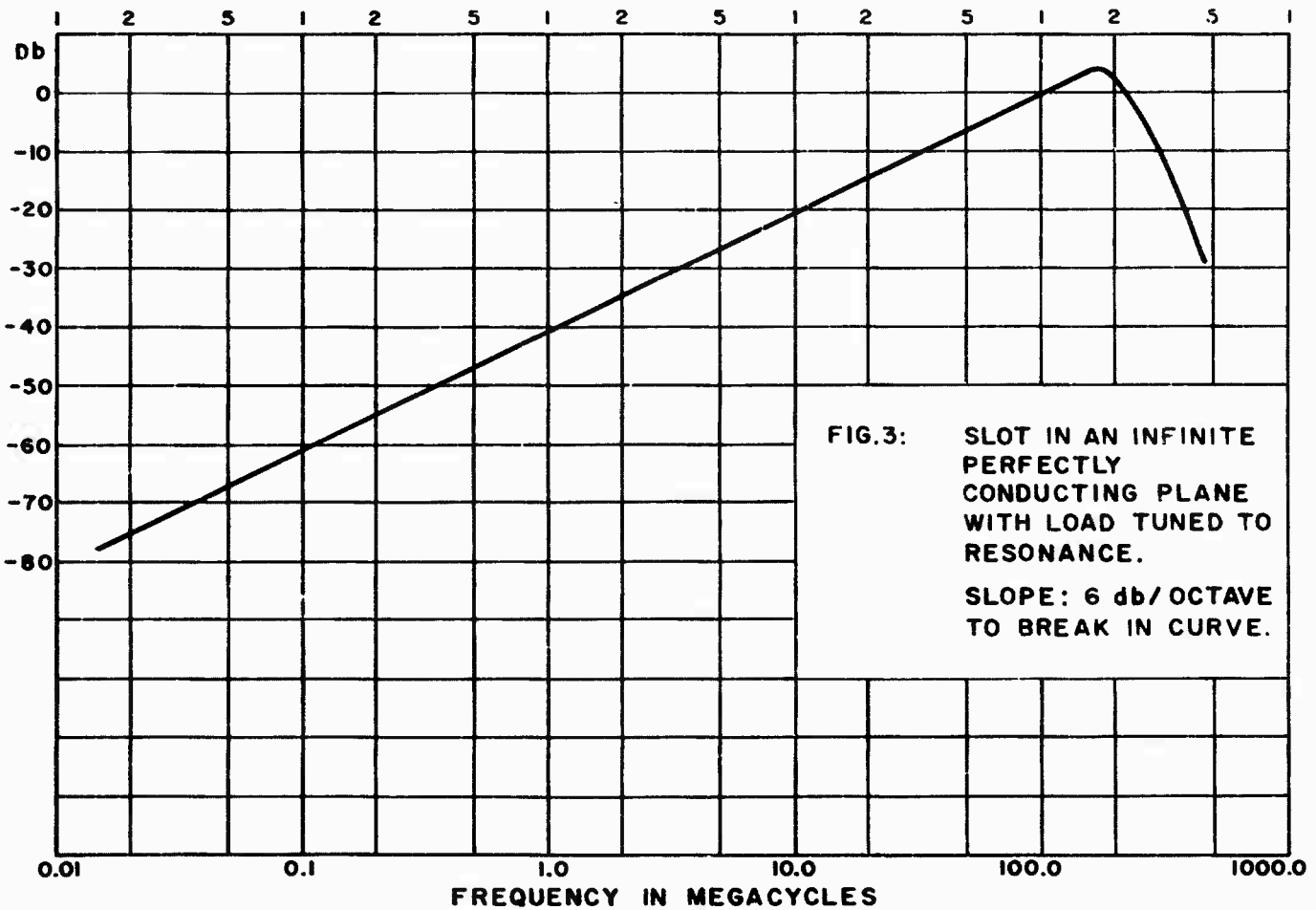

FIG.3: SLOT IN AN INFINITE PERFECTLY CONDUCTING PLANE WITH LOAD TUNED TO RESONANCE.

SLOPE: 6 db/ OCTAVE TO BREAK IN CURVE.

8-97

Evidently, for a slot of fixed dimensions, fixed load resistance, and fixed incident field strength, it is impossible for the power in the load to exceed the values given in this graph.

Hollow Cylindrical Antenna with Impedance-Loaded Slot

Consider a hollow cylindrical receiving antenna of arbitrary length $2h^c$ and radius a^c, illustrated in Figure 4a. Let the following inequalities be satisfied: $\beta a^c << 1$, $h^c >> a^c$, so that $\Omega^c = 2 \ln 2h^c/a^c \geq 7$. The terminals are located at the center of the antenna and are labeled a, b. The gap between the terminals may be thought of as a completely circumferential slot. (The impedance of this slot is normally considered to be infinite in antenna calculations.) If the impedance Z_L is connected to terminals a, b, it is clear that the slot and load impedances are in parallel.

Suppose now that one would like to fill in a portion of the peripheral slot with metal. The situation is pictured in Figure 4b. Evidently, the impedance of the slot is again in shunt with the load impedance. The question arises as to what value of slot impedance Z^s to employ in parallel with Z_L. Unfortunately, there is no available analytical expression for the impedance of a slot of finite dimensions cut in a hollow cylinder of finite length and radius. To circumvent this difficulty, impedance measurements were made at the Physical Sciences Laboratory, New Mexico State University, on (1) a slot 12 inches long by 1.45 inches in width cut in the middle of a 3-foot by 9-foot ground plane, and (2) the same configuration with the ground plane rolled up into a cylinder 11.46 inches in diameter and 108 inches in length.

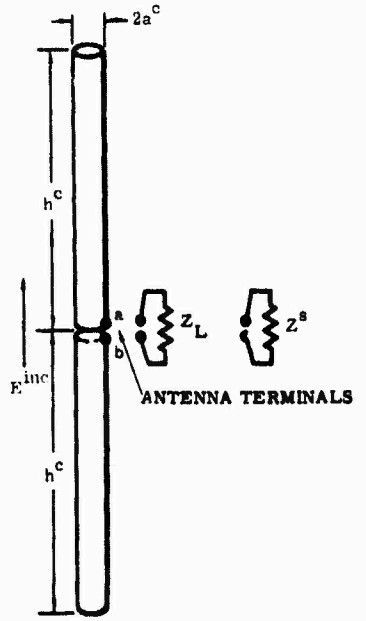

Figure 4a. Hollow Cylindrical Antenna

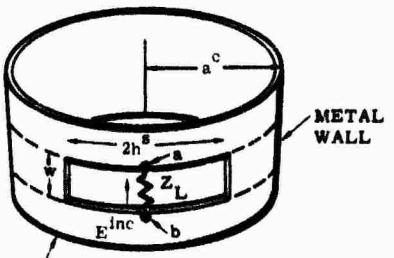

Figure 4b. Section of a Hollow Cylindrical Antenna With Impedance Loaded Slot

Figure 4. Hollow Cylindrical Antenna With Impedance Loaded Slot

Following this procedure minimizes discrepancies in the measured impedance caused by different feed arrangements. The results are shown in Tables I and II. Accurate measurements of Z^S for small βh^S could not be made because the slot behaves essentially as a pure reactance. It is noted that Z^S values in Tables I and II are not vastly different, and it is assumed that these differences are not accentuated at lower frequencies where measurements could not be made. Table III presents values of Z^S computed from (12) for a slot 1.45 by 12 inches cut in an infinite perfectly conducting plane of infinitesimal thickness. Evidently, one can work to an accuracy of better than an order of magnitude (10 db) by simply assuming that the impedance of a slot cut in a hollow cylinder is approximated adequately by (12).

TABLE I

Measured Impedance of a Center-Driven Slot Free to Radiate in Each Half-Space Cut in a 3- by 9-Foot Flat Plate. (The Long Dimension of the Slot is at Right Angles to the Long Dimension of the Flat Sheet.)
Slot Dimensions: 12 Inches Long by 1.45 Inches Wide.

βh^S	Z^S (ohms)	$\lvert Z^S \rvert$
0.3192	5.0 + j67.5	67.69
0.3830	8.5 + j80.5	80.95
0.4469	12 + j91.0	91.79
0.5107	18 + j116	116.9
0.5745	21 + j103	105.1
0.6384	28 + j133	135.9
0.7022	39 + j148	153.0
0.7660	53 + j150	158.4
0.8300	65 + j174	185.7
0.8937	125 + j228	260.0
0.9576	228 + j240	331.0
1.021	320 + j215	385.5
1.085	388 + j125	407.6
1.117	398 + j28	399.0
1.149	388 + j15	388.2
1.213	350 + j38	352.0
1.277	302 + j65	308.9
1.341	282 + j48	286.0
1.404	245 - j13	245.3
1.468	210 - j31	218.3
1.532	202 - j31	204.4
1.596	181 - j49	187.5
1.756	105 - j61	121.3
1.915	112 - j22	117.6
2.075	111 + j25	113.8
2.234	108 + j39	114.8
2.394	136 + j0.0	136.0
2.553	160 + j36	164.0
2.713	136 + j64	150.3
2.905	178 + j78	194.3

TABLE II

Measured Impedance of a Center-Driven Slot Cut Circumferentially in the Middle of a Cylinder 11.46 Feet in Diameter and 108 Inches in Length
Slot Dimensions: 12 Inches Long by 1.45 Inches in Width

βh^s	Z^s (ohms)	$\lvert Z^s \rvert$
0.3192	5.5 + j64	64.24
0.3830	8.0 + j72	72.44
0.4469	11 + j81	81.74
0.5107	14 + j96	96.95
0.5745	16 + j101	101.7
0.6384	20 + j112	113.8
0.7022	25 + j97	100.2
0.7660	29 + j110	113.8
0.7980	32 + j123	127.1
0.8300	40 + j137	142.7
0.8937	62 + j161	172.5
0.9576	101 + j191	216.1
1.021	145 + j203	249.5
1.085	194 + j219	292.5
1.149	183 + j190	263.8
1.213	184 + j175	253.9
1.277	160 + j156	223.5
1.341	150 + j156	216.4
1.404	147 + j140	203.0
1.468	176 + j130	218.8
1.532	185 + j94	207.4
1.596	202 + j58	210.0
1.660	191 + j56	199.1
1.756	160 - j20	161.2
1.915	116 - j4	116.1
2.075	80 + j30	85.44
2.234	59 + j41	71.55
2.394	65 + j62	89.63
2.553	118 + j64	134.1
2.713	67 + j79	103.2
2.873	52 + j77	92.28

TABLE III

Computed Impedance of a Center-Driven Slot Free to Radiate in Each Half Space.
Slot Dimensions: 12 Inches Long by 1.45 Inches Wide

βh^s	Z^s (ohms)	$\lvert Z^s \rvert$
0.100	0.0012 + j15.13	15.13
0.125	0.0030 + j18.91	18.91
0.150	0.0062 + j22.69	22.69
0.175	0.0115 + j26.47	26.47
0.200	0.0196 + j30.25	30.25
0.225	0.0315 + j34.04	34.04
0.250	0.0479 + j37.82	37.82
0.275	0.0702 + j41.60	41.60
0.300	0.0994 + j45.38	45.38
0.325	0.1369 + j49.16	49.16
0.350	0.1842 + j52.94	52.94
0.375	0.2427 + j56.73	56.73
0.400	0.3142 + j60.51	60.51
0.425	0.4004 + j64.29	64.29
0.450	0.5033 + j68.07	68.07
0.475	0.6248 + j71.85	71.85
0.500	1.255 + j94.58	94.60
0.700	6.531 + j149.4	149.5
0.900	28.79 + j232.4	234.1
1.100	134.5 + j366.8	390.6
1.200	293.6 + j419.1	511.7
1.300	518.9 + j307.9	803.4
1.400	551.8 + j39.47	553.2
1.500	414.9 + j101.1	427.1
1.600	297.2 - j124.1	322.1
1.700	222.3 - j108.5	247.3
1.800	175.8 - j83.65	194.7
1.900	145.9 - j58.05	157.1
2.000	125.7 - j33.34	130.1
2.100	111.6 - j9.808	112.0
2.200	101.4 + j13.19	102.2
2.300	93.87 + j36.00	100.4
2.400	87.70 + j58.97	105.7
2.500	82.86 + j82.55	117.0
2.800	78.79 + j107.2	133.0
2.700	75.28 + j132.8	152.6
2.800	72.19 + j159.9	175.4
2.900	69.89 + j188.4	200.9
3.000	68.06 + j218.7	229.1
3.100	67.95 + j250.8	259.8
3.200	69.90 + j284.4	292.9
3.300	75.48 + j320.6	329.4
3.400	86.01 + j359.0	369.1
3.500	103.3 + j399.6	327.8
3.600	130.9 + j442.8	461.7
3.700	173.5 + j488.3	518.2
3.800	238.9 + j533.1	584.2
3.900	338.5 + j566.6	660.1
4.000	482.3 + j562.7	741.1

The equivalent circuit of the receiving system is shown in the cut of Figure 5. It consists of V_{oc} driving a circuit comprising Z^c in series with the parallel combination of Z^s and R_L. The open-circuit voltage is given by the formula $V_{oc} = 2h_e E^{inc}$, where $2h_e$ is the effective length of a cylinder of half-length h^c and radius a^c, and E^{inc} is the incident electric field directed parallel to the axis of the cylinder. Z^c is the driving point impedance of the cylinder at terminals a, b, without slot or load. The graphs in Figures 5 and 6 were obtained under the following conditions:

$\Omega^c = 2 \ln 2h^c/a^c = 7$

$h^c = 8$ feet

Slot dimensions 1.45 by 12 inches

Load impedance $Z_L = 4.5 + j0.0$ ohms

Incident field strength $E^{inc} = 10$ volts/m

Zero level $P_L = 50 \times 10^{-3}$ watts

Note that the cylinder is below cutoff at the highest frequency at which the performance of the receiving system was computed.

Although Figure 5 holds for a tuned as well as for an untuned load, Figure 6 applies only to the untuned case. In obtaining the data for Figure 7, which depicts the tuned case, the Thévinen equivalent generator was utilized. The open-circuit voltage is the voltage appearing across Z^s with R_L disconnected. The internal impedance of the generator is obviously $Z^s Z^c/(Z^s + Z^c)$. The imaginary part of the generator impedance, with reversed sign, connected in series with R_L, effectively tunes the slot. It is absolutely impossible under the stated conditions for a greater transfer of power to take place to a 4.5-ohm load resistor than that predicted by Figures 5 and 7, no matter how arbitrary the circuit configuration within the cylinder, provided $Z^s = \zeta^2/4Z^d$ represents the slot impedance to a satisfactory degree of approximation.

An objection might be raised that when $h^c << \lambda$, Z^c is the controlling impedance element in the equivalent circuit (Figure 5). In reply, the writer mentions that the short-circuit current at the middle of the cylinder is always controlled by this impedance. The short-circuit current is given by the relation $I^c_{sc} = V_{oc}/Z^c$.

Dipole with Load Resistance Across a Circumferential Slot of Infinite Resistance and Zero Capacitance

Figure 8 gives the transfer characteristic of a dipole with a load resistance $R_L = 4$ ohms across a perfect circumferential slot, or gap, at its center. The voltage $V_{oc} = 2h_e E^{inc}$ drives a circuit consisting of Z^c in series with R_L, as shown in the drawing. For this computation, $h^c = 8$ feet; $\Omega = 7$, $E^{inc} = 10$ volts/m, and $P_L = 50 \times 10^{-3}$ watts is zero-level. As before, the electric field is directed parallel to the axis of the cylinder. The slope of the curve is 6 db/octave, and rises with increasing frequency.

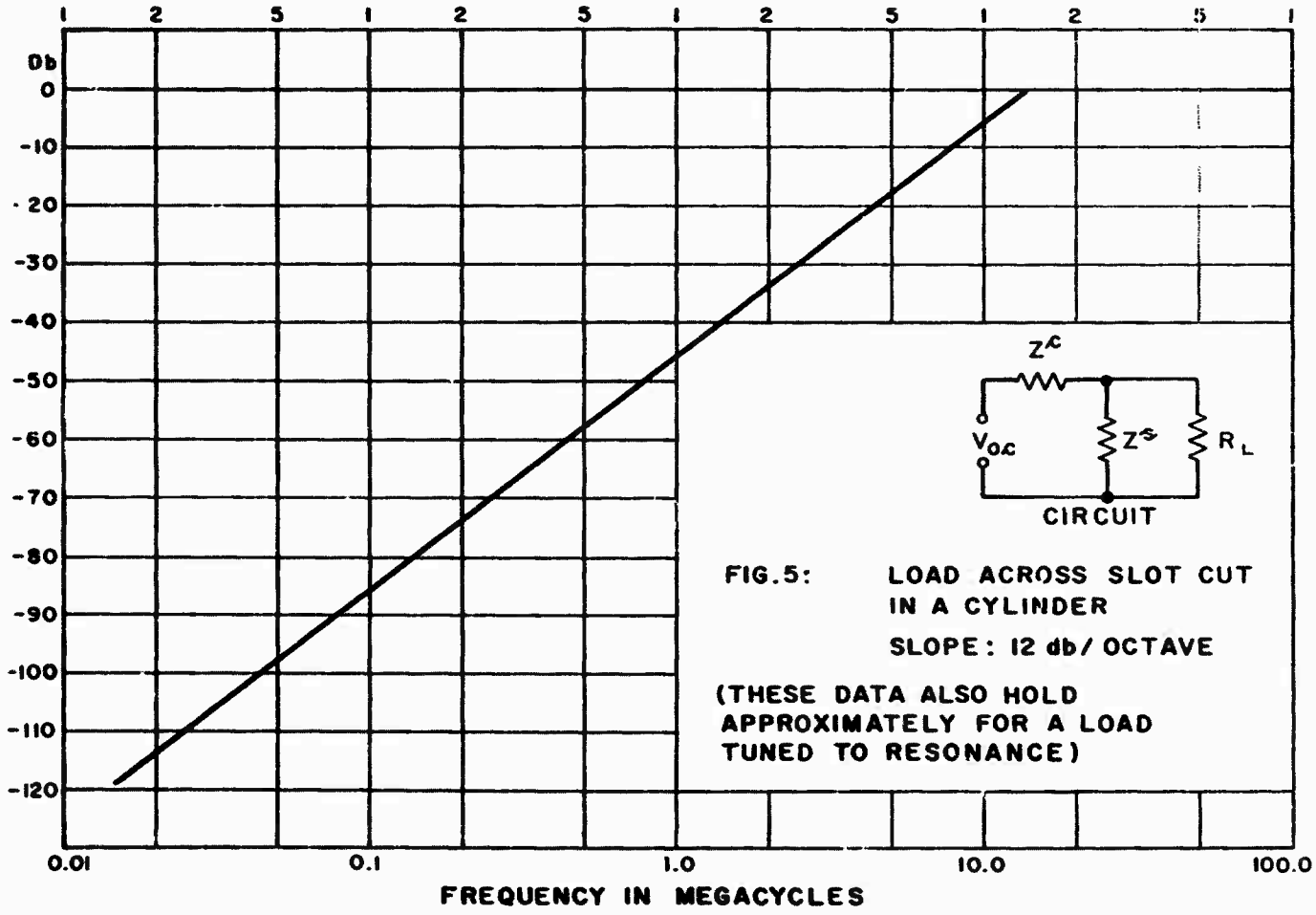

FIG.5: LOAD ACROSS SLOT CUT IN A CYLINDER

SLOPE: 12 db/ OCTAVE

(THESE DATA ALSO HOLD APPROXIMATELY FOR A LOAD TUNED TO RESONANCE)

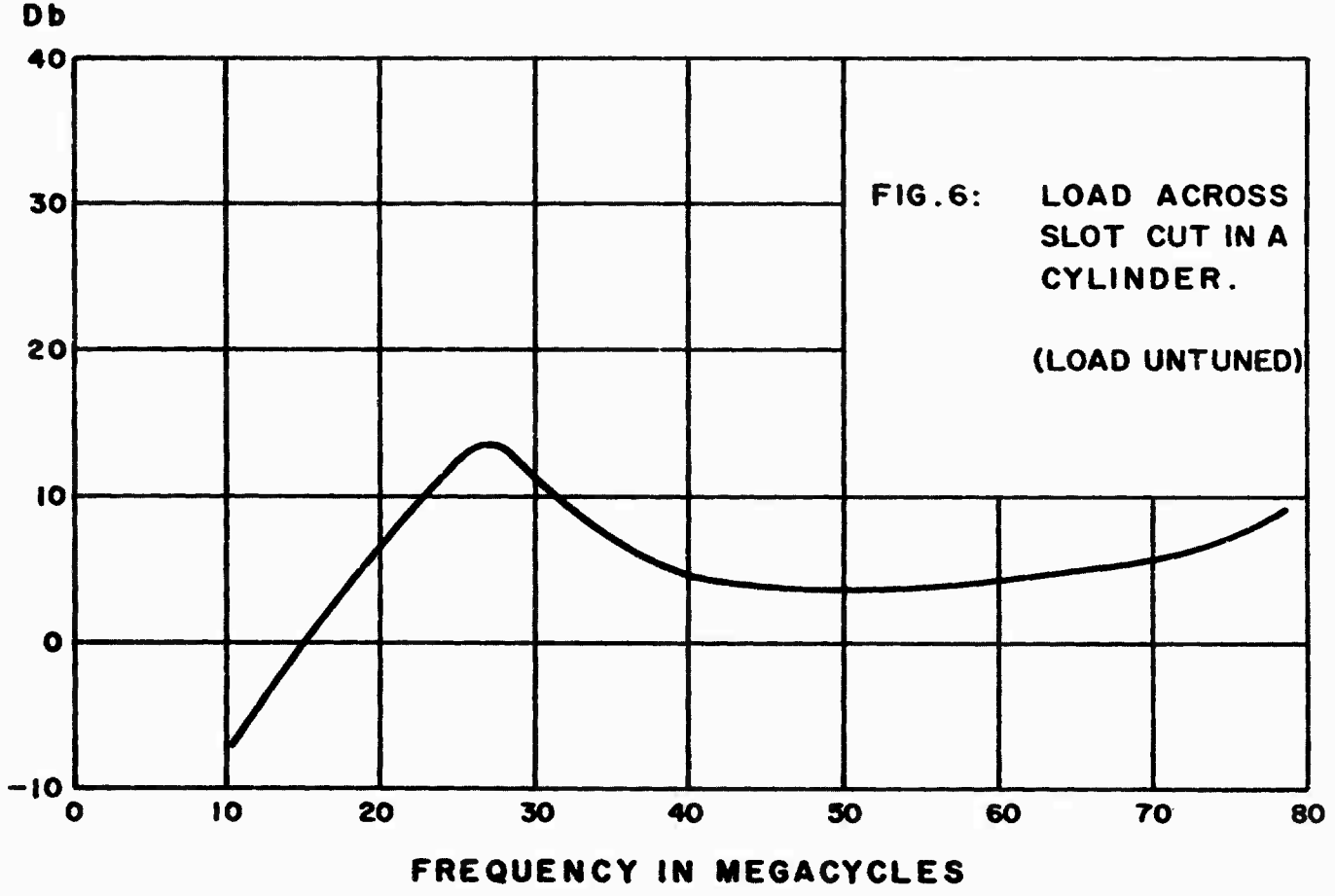

FIG.6: LOAD ACROSS SLOT CUT IN A CYLINDER.

(LOAD UNTUNED)

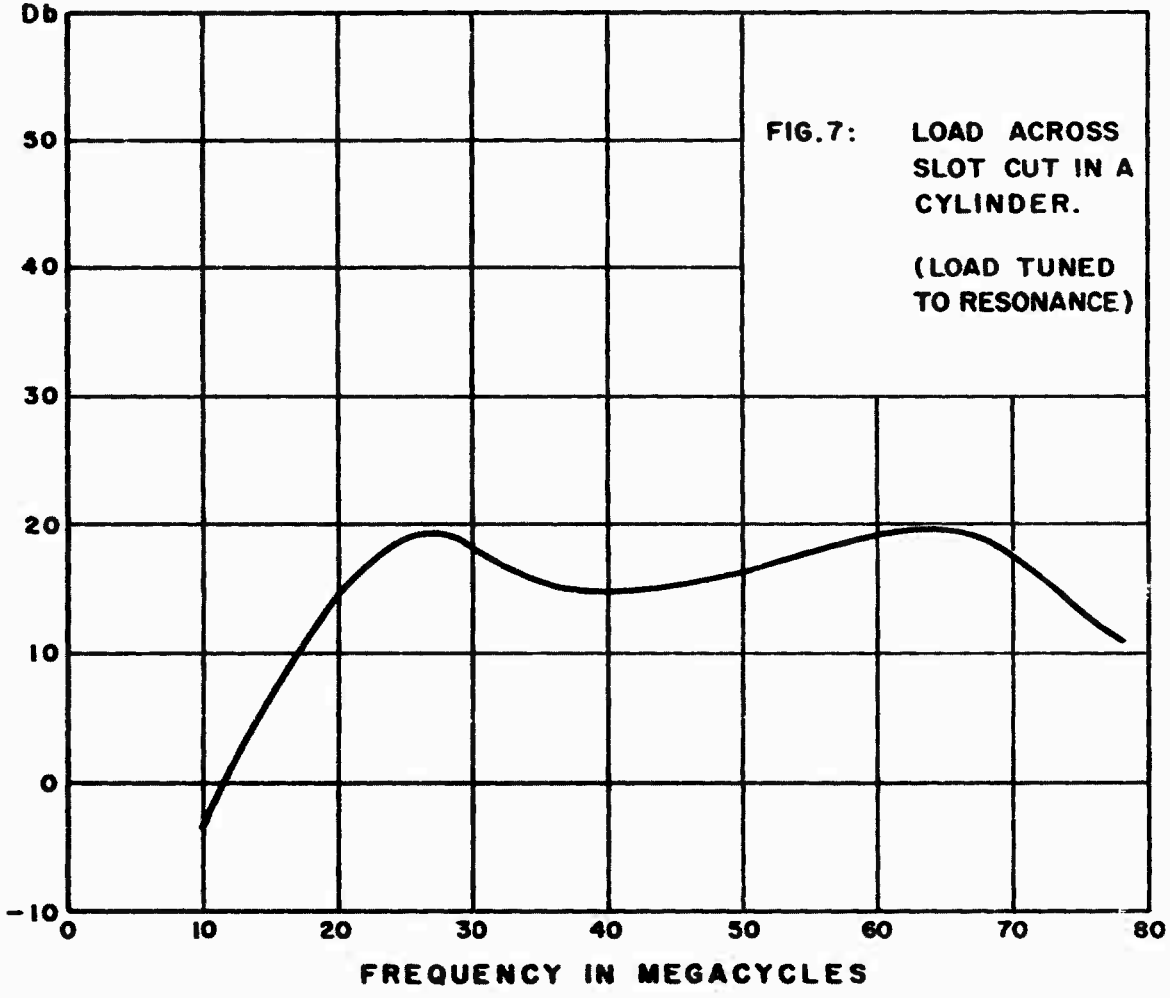

FIG.7: LOAD ACROSS SLOT CUT IN A CYLINDER.

(LOAD TUNED TO RESONANCE)

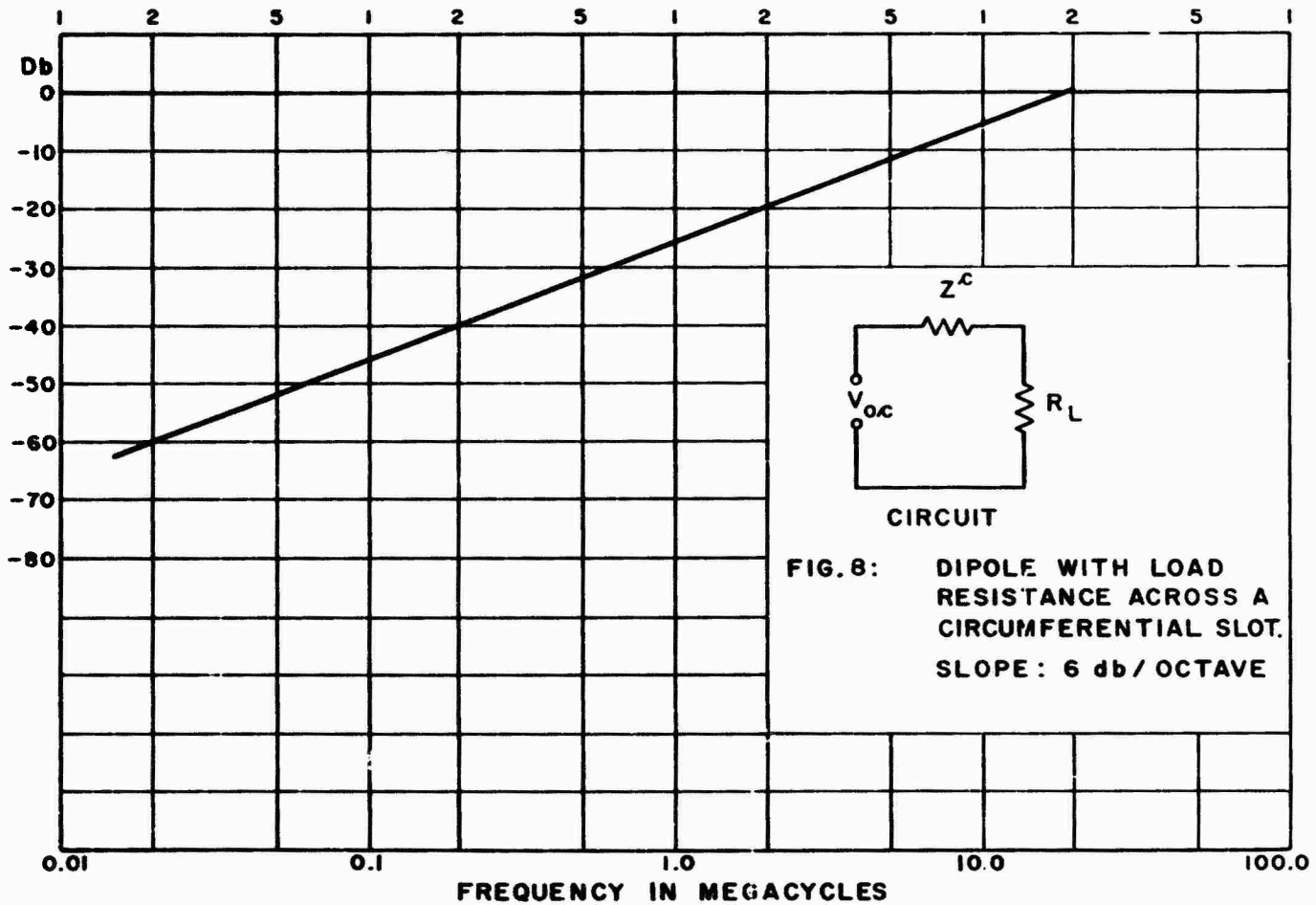

FIG. 8: DIPOLE WITH LOAD RESISTANCE ACROSS A CIRCUMFERENTIAL SLOT.
SLOPE: 6 db/OCTAVE

Radio-Frequency Leakage of a Circumferential Anodized Butt
Located in the Center of a Hollow Cylinder

A section of a hollow cylinder, showing a load Z_L connected across a circumferential anodized butt, is illustrated in Figure 9. The butt capacitance C_s and resistance R_s must be taken into account in the analysis. The equivalent circuit is shown in the cut of Figure 10. Note that C_s, R_s, and R_L are in parallel. $V_{oc} = 2h_e E^{inc}$ as before. The graph shown in Figure 10 was obtained under the following conditions: $E^{inc} = 10$ volts/m, $h^s = 8$ feet, $\Omega = 7$, $R_L = 4$ ohms, $C_s = 10^{-9}$ farads, and $R_s = 0.01$ ohm. Zero-level is $P_L = 50 \times 10^{-3}$ watts. It is thought that the values of C_s and R_s used are representative of those encountered in practical situations. The slope of the transfer characteristic is positive and rises 6 db/octave.

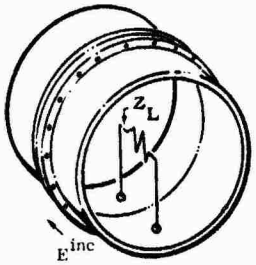

Figure 9. Section of Hollow Cylinder Showing Anodized Butt. The Capacitance of the Butt is C_s and Resistance is R_s.

Radio-Frequency Leakage of an Off-Center Circumferential Anodized Butt

The cut in Figure 10 shows the equivalent circuit of a hollow cylindrical antenna containing a leaky circumferential slot having capacitance, C_s, and leakage resistance, R_s, shunted by a load resistance, R_L. In Section 7 it is shown that the effective length of a cylinder that is short in terms of the wavelength is approximately one-half of its physical length, provided the terminals are not too near either end. Thus, $V_{oc} = 2h_e E^{inc}$ has approximately the same value for an off-center slot as for one located at the middle of the cylinder, provided the cylinder is electrically short, as assumed here.

R_s and C_s remain the same regardless of the slot location. For a fixed load the only property of the circuit that changes with slot location is $Z^c \simeq -jX^c$.

Let Z_t represent the parallel combination of the impedance elements R_s, R_L, and $-j/\omega C_s$. Assume that $|X^c| >> |Z_t|$. The power dissipated in Z_t is proportional to the square of the current through Z^c.

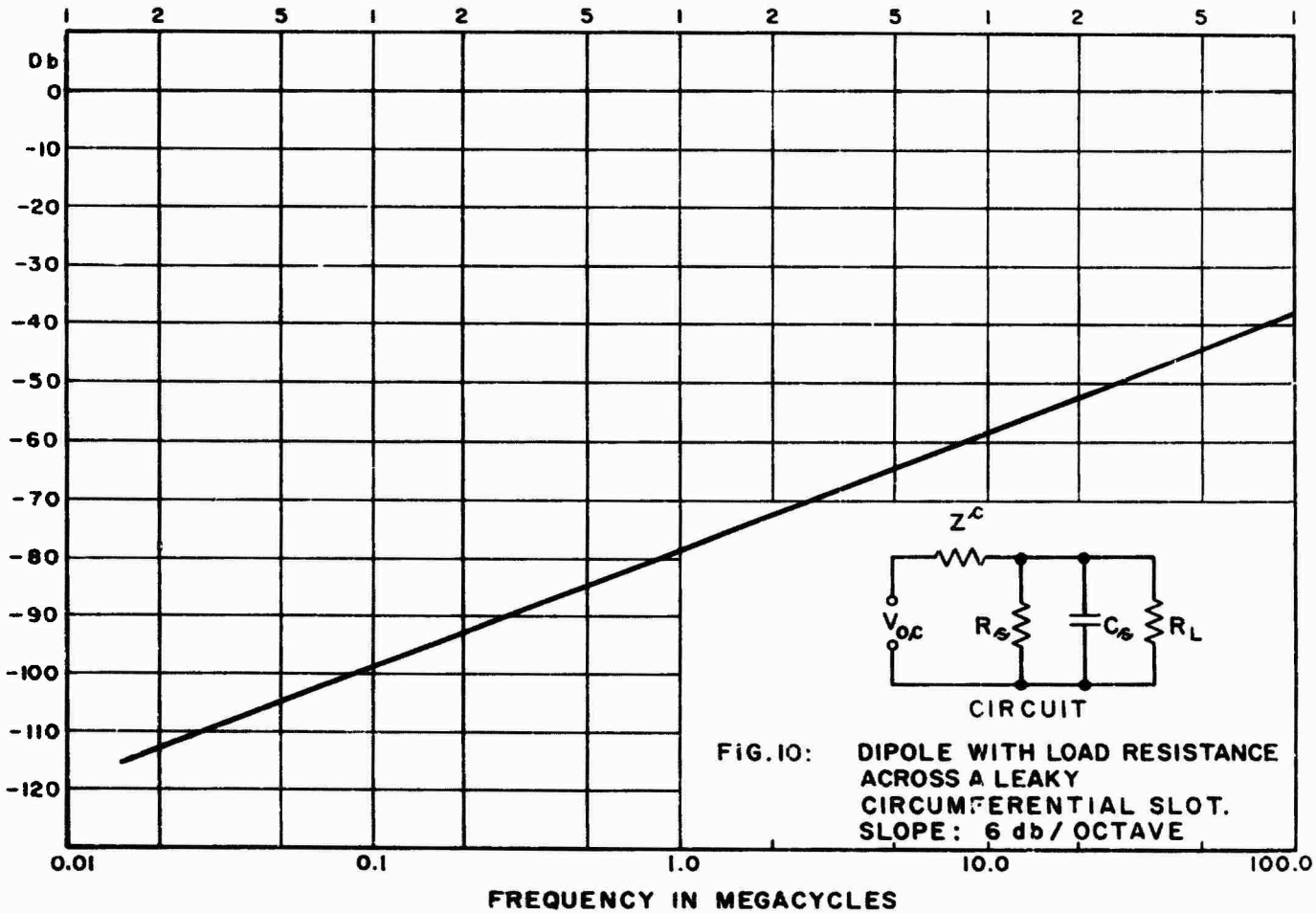

FIG. 10: DIPOLE WITH LOAD RESISTANCE ACROSS A LEAKY CIRCUMFERENTIAL SLOT. SLOPE: 6 db / OCTAVE

It follows that the decibel loss in power in the load caused by moving the slot off-center is given approximately by the relation

$$db = 20 \log_{10} \frac{X^c_{asy}}{X^c} \tag{17}$$

where X^c_{asy} is the reactance of the asymmetrical dipole, and X^c is the reactance of the symmetrical dipole.

As a numerical illustration consider a cylinder for which $2h^c = 2.438$ m (8 feet) and $\Omega^c = 2 \ln 2h^c/a = 10$. Let f = 100 kcs so that $\lambda = 3 \times 10^3$ m. Then, $\beta h^c = 2.554 \times 10^{-3}$ radians. The reactance of the symmetrical structure is[8]

$$X^c = -\frac{\zeta}{2\pi\beta h^c}\left\{\frac{\Omega - 2}{1 + \frac{2 \ln 2}{\Omega - 2}}\right\} \tag{18}$$

so that $X^c = -160.2 \times 10^3$ ohms.

Let the slot now be moved off-center, so that it is 2 feet from one end.

Using King's method of computing the impedance of an asymmetrical dipole,[9] it is found that $\Omega_1 = 10.81$ and $\Omega_2 = 8.614$. Also, $\beta h_1 = 3.83 \times 10^{-3}$ radians, and $\beta h_2 = 1.277 \times 10^{-3}$ radians. The corresponding impedances, from (18), are $X_1 = -119.3 \times 10^3$ ohms and $X_2 = -256.9 \times 10^3$ ohms. Now, $X^c_{asy} = (X_1 + X_2)/2 = -188.12 \times 10^3$ ohms. The db loss resulting from moving the slot off-center by 2 feet is thus $20 \log_{10} 1.174 = 1.4$ db. This additional loss must be added to that given by Figure 10 at 100 kcs.

The loss of power in the load resistance, R_L, rapidly increases as the slot is moved away from the center of the cylinder, because X^c_{asy} increases. Although the problem of the canister with screwed-on lid cannot be treated by methods of antenna analysis, it can be stated with confidence that the pickup of circuitry within a canister with a leaky slot at the end of the container is substantially less than for a canister with a centrally located slot. Since results for the latter case are now available, the pickup of circuitry in a canister with a lid slot is bounded. As before, it is assumed that the load impedance is in shunt with the slot.

Note that a shield is effective only if currents are free to flow in all directions on its surface. Thus, the lid on a canister should be secured with many bolts to reduce R_s and increase C_s as much as possible.

Transfer Characteristic of an Internally Loaded Cylinder with Asymmetrically Located Circumferential Slot

This section presents a method for predicting theoretically the slope of the transfer characteristic of an asymmetric dipole with internal load, and account for the break in this curve at higher frequencies. As defined earlier, the transfer characteristic is that quantity which must be multiplied by the incident field to give the current in the load.

Figure 11 illustrates the slot receiving system under consideration. The cylinder is of radius a^c and length $h_1^c + h_2^c$. Its axis coincides with the z-axis of a cylindrical coordinate system. A circumferential slot is cut at z = 0. The gap voltage is V_c. The incident electric field, E^{inc}, is directed parallel to the cylinder. The internal circuit consists of Z_{L1} and Z_{L2} connected together and grounded to the interior of the cylinder at the ends. This circuit may be generalized in any desired way, as long as a connecting lead to the loads passes through the slot. Normally, Z_{L1} and Z_{L2} are low-impedance elements, and this is assumed in the analysis.

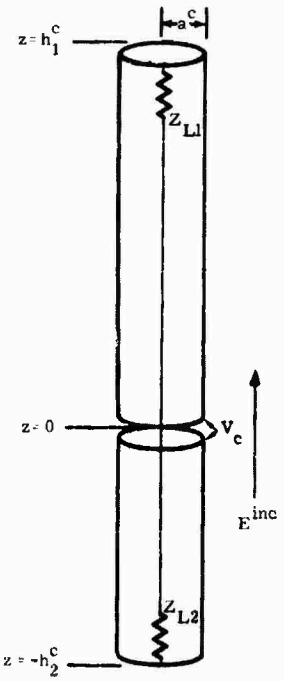

Figure 11. Internally Loaded Hollow Cylindrical Slot Antenna

Let the dimensions of the slot receiving system satisfy the following inequalities.

$$\left.\begin{aligned} &\beta a^c << 1 \\ &\beta h_1^c < 1 \\ &\beta h_2^c < 1 \\ &0.1 < \frac{h_1^c}{h_2^c} < 10 \\ &h_1^c >> a^c \\ &h_2^c >> a^c. \end{aligned}\right\}$$

The cylinder is treated as an asymmetrical dipole receiving antenna. The effective length of the structure can be obtained by taking the Fourier transform of the current existing along the asymmetrical dipole, when used for transmission (driven at the slot). The simple sinusoidal representation of current is assumed adequate for finding the effective length of the cylinder.

$$I_1(z') = \frac{I_o}{\sin \beta h_1^c} \sin \beta\left(h_1^c - z'\right) \tag{20}$$

$$I_2(z') = \frac{I_o}{\sin \beta h_2^c} \sin \beta\left(h_2^c + z'\right). \tag{21}$$

Here I_o is the input current. The effective length is

$$\ell_e = h_{1e} + h_{2e} = \frac{1}{I_o} \int I(z')\, dz'$$

$$= \int_0^{h_1} \frac{\sin \beta\left(h_1^c - z'\right)}{\sin \beta h_1^c} dz' + \int_{-h_2}^{0} \frac{\sin \beta\left(h_2^c + z'\right)}{\sin \beta h_2^c} dz' \tag{22}$$

$$= \frac{1}{\beta}\left[\tan \frac{\beta h_1^c}{2} + \tan \frac{\beta h_2^c}{2}\right] = \frac{\sin \frac{\beta}{2}\left(h_1^c + h_2^c\right)}{\beta \cos \frac{\beta h_1^c}{2} \cos \frac{\beta h_2^c}{2}}.$$

If both βh_1^c and βh_2^c are small, $\cos \beta h_1^c/2 \simeq 1$; $\cos \beta h_2^c/2 \simeq 1$, and $\sin \frac{\beta}{2}\left(h_1^c + h_2^c\right) \simeq \frac{\beta}{2}\left(h_1^c + h_2^c\right)$. Then,

$$\ell_e = \frac{1}{\beta}\left[\frac{\beta}{2}\left(h_1^c + h_2^c\right)\right] = \frac{1}{2}\left(h_1^c + h_2^c\right). \tag{23}$$

The induced voltage in the cylinder, under the assumptions outlined above, is

$$V_{oc} = \ell_e E = \frac{1}{2}\left(h_1^c + h_2^c\right)E . \tag{24}$$

It is important to note that V_{oc} is linearly related to E and is independent of frequency; also that V_{oc} is not the gap voltage, V_c, unless the internal circuit is absent. V_c is smaller than V_{oc} because of the internal impedance of the source. The source impedance is the impedance of the cylinder when used for transmission; i.e., the impedance of an asymmetrical dipole of length $\left(h_1^c + h_2^c\right)$ and radius a^c.

The impedance (reactance) of an electrically short antenna of half-length h and radius a is given by (18), viz:

$$X = -\frac{\zeta}{2\pi\beta h}\left\{\frac{\Omega - 2}{1 + \frac{2 \ln 2}{\Omega - 2}}\right\}.$$

The reactance of the asymmetrical dipole is[9]

$$X_{asy}^c = -\frac{\zeta}{4\pi\beta}\left[\frac{1}{h_1^c}\left(\frac{\Omega_1 - 2}{1 + \frac{2 \ln 2}{\Omega_1 - 2}}\right) + \frac{1}{h_2^c}\left(\frac{\Omega_2 - 2}{1 + \frac{2 \ln 2}{\Omega_2 - 2}}\right)\right] = \frac{K}{f} . \tag{25}$$

In (25), $\Omega_1 = 2 \ln \frac{2h_1^c}{a}$; $\Omega_2 = 2 \ln \frac{2h_2^c}{a}$, $\beta = 2\pi/\lambda = \frac{2\pi f}{v_0}$, where $v_0 = 3 \times 10^8$ m/sec. X_{asy}^c is a good approximation for the source impedance.

It is now necessary to find out how the gap voltage V_c drives the internal circuit. Herein lies the key to the solution of the entire problem. Consider Figure 12. The lower half of the structure is the mirror image of the upper half. Clearly, the voltage $V_c/2$ acts in series with the coaxial transmission line. Accordingly, the voltage V_c in Figure 11 acts in series with the two line sections in series. To solve the problem, one now regards the slot as short-circuited. The voltage V_{oc} drives a circuit consisting of X_{asy}^c, Z_1', and Z_2' in series. Z_1' is the input impedance of the line terminated in Z_{L1}. Since the cylinder is electrically short, Z_1' is approximately equal to Z_{L1}. The same comment applies to Z_2'. Usually, one does not have an electrically long line in an electrically short cylinder. The "line" constants are merely lumped circuit parameters. Z_1' and Z_2' are very small compared to X_{asy}^c at low frequencies. The current in Z_1' and Z_2' is controlled by X_{asy}^c. The desired transfer characteristic, valid at low frequencies, is simply

$$I_L = \frac{V_{oc}}{X_{asy}^c} \simeq \frac{\frac{1}{2}\left(h_1^c + h_2^c\right)Ef}{K} \simeq K'f . \tag{26}$$

Evidently, the db rise in load current per octave is

$$db = 20 \log_{10} \frac{2f}{f} = 20 \log_{10} 2 = 6.02 \text{ db/octave.}$$

At higher frequencies, a break in the curve occurs because X^c_{asy}, a capacitive reactance, no longer dominates the circuit. Hence, the slope in the transfer characteristic must change.

Note that the pickup will increase 6 db/octave at low frequencies no matter what the internal circuit is, as long as it is of low impedance.

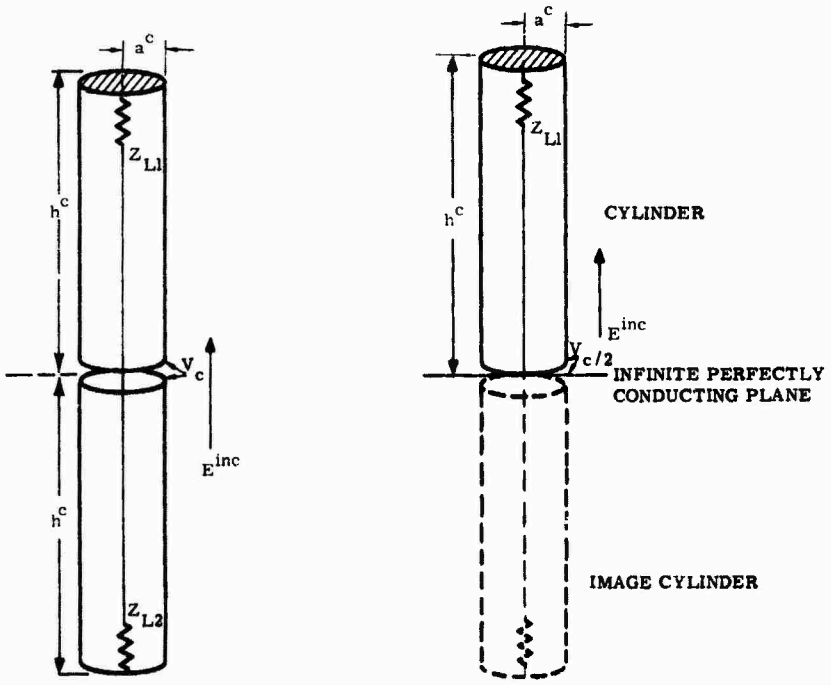

Figure 12. Internally Loaded Hollow Cylindrical Slot Antenna, and Identical Monopole With Image

Conclusions

In this paper a quantitatively correct theory for several slot antenna receiving systems has been presented. In some cases, numerical results were given for a tuned load connected across the slot in the direct field. This insures that an upper bound has been set for the excitation of circuitry within the cylinder, no matter how complicated this circuitry may be, by the propagation of an electromagnetic field through the slot. This is so because only a diffracted field can exist in the cylinder, and this field is much smaller than exists in the window if the cylinder is below cutoff.

LIST OF REFERENCES

1. Harrison, C. W., Jr., Missile with Attached Umbilical Cable as a Receiving Antenna, SCDC-2761, May 17, 1962

2. Harrison, C. W., Jr., Radio Frequency Hazards to Ordnance Materials - Shielding Effect of a Circular Grating of Finite Length, Sandia Corporation Internal Memorandum of July 21, 1961.

3. Harrison, C. W., Jr., "Radio Frequency Shielding of Cables," Journal of the American Society of Naval Engineers, Vol. 73, No. 3, pp 529-533, August 1961.

4. Harrison, C. W., Jr., and King, R. W. P., "Response of a Loaded Electric Dipole in an Imperfectly Conducting Cylinder of Finite Length," Journal of Research of the National Bureau of Standards, Vol. 64D, No. 3, pp 289-293, May-June 1960.

5. King, R. W. P., and Harrison, C. W., Jr., "Cylindrical Shields," IRE Transactions on Antennas and Propagation, Vol. AP-9, No. 2, pp 166-170, March 1961.

6. Harrison, C. W., Jr., and Denton, D. H., Jr., Receiving Characteristics of Quasi-Shielded Antennas, Sandia Corporation Technical Memorandum No. 396-58(14), October 15, 1958.

7. King, R. W. P., The Theory of Linear Antennas, Harvard University Press, 1956, Chapters 2 and 4.

8. King, R. W. P., Theory of Linear Antennas, Harvard University Press, p. 184, Eq. 4b, 1956.

9. Ibid, Section 29, pp 403-407.

LIST OF SUPPLEMENTARY REFERENCES

Booker, H. G., "Slot Aerials and their Relation to Complementary Wire Aerials (Babinet's Principle)," Journal of the Institution of Electrical Engineers, Vol. 93, Part 3A, No. 4, pp 620-626, 1946.

Jordan, E. C., Electromagnetic Waves and Radiating Systems, Prentice-Hall, Inc., Section 15.10 Slot Antennas, pp 587-593, 1950.

Kraus, J. D., Antennas, McGraw-Hill Book Co., Inc., Section 13-5, "The Impedance of Slot Antennas," pp 367-371, 1950.

Owyang, G. H., and King, R. W. P., "Complementarity in the Study of Transmission Lines," IRE Transactions on Microwave Theory and Techniques, Vol. MTT-8, No. 2, pp 172-181, March 1960.

47. A STUDY OF THE SIMULATION OF INSTRUMENTED TO LOADED EED'S[1]

D. Boyd Barker
Richard K. Fry

University of Denver
Denver, Colorado

When the powder is removed from an EED so that thermal instrumentation, such as a thermocouple or thermistor, can be installed, the thermal characteristics of the device are changed. In general, the heat dissipation is decreased and the time constant is increased since the powder surrounding the loaded bridgewire is a better conductor of heat than the air of an instrumented device. Thus the instrumented EED does not react to a power input exactly like a live device: the instrumented bridgewire temperature is, in general, higher than that of the loaded bridgewire. This paper describes theoretical and experimental work done to ascertain the degree of simulation of instrumented EED'S to live devices.

SYSTEM ANALYSIS

The differential equations governing the time response of instrumented and loaded devices to some arbitrary power-input function are

$$C\dot{T}(t) + \gamma T(t) = P(t)$$
$$C'\dot{T}'(t) + \gamma' T'(t) = P(t) \qquad (1)$$

---

1. This work was supported by Sandia Corporation. A more complete discussion may be found in reference 2.

where the superscripts refer to the "instrumented" case, and

T = average bridgewire temperature rise ambient,

γ = dissipation constant of bridgewire,

P = power input into bridgewire

C = heat capacity of bridgewire, and

t = time

Eliminating P(t) and substituting $\gamma = C/\tau$, where τ is the bridgewire time constant yields

$$\dot{T}(t) + \frac{T(t)}{\tau} = \frac{C'}{C}\left\{\dot{T}'(t) + \frac{T'(t)}{\tau'}\right\} \tag{2}$$

whose general solution for t > 0 is

$$T(t) = \left\{\frac{C'}{C}\int_0^t\left(\frac{T'(t)}{\tau'} + \dot{T}'(t)\right)\exp\left(\frac{t}{\tau}\right)dt + T(0)\right\}\exp\left(-\frac{t}{\tau}\right) \tag{3}$$

Integration by parts results in

$$T(t) = \left\{\frac{C'}{C}\left(\frac{1}{\tau'} - \frac{1}{\tau}\right)\int_0^t T'(t)\exp\left(\frac{t}{\tau}\right)dt + T(0) - \frac{C'}{C}T'(0)\right\}\exp\left(-\frac{t}{\tau}\right) + T'(t) \tag{4}$$

Assume that both T(0) and T'(0) are zero (quiescent state) and define the error of temperature simulation as

$$Y(t) = T'(t) - T(t) \tag{5}$$

then from equation (4) we find that

$$Y(t) = \left\{\frac{C'}{C}\left(\frac{1}{\tau} - \frac{1}{\tau'}\right)\int_0^t T'(t)\exp\left(\frac{t}{\tau}\right)dt\right\}\exp\left(-\frac{t}{\tau}\right) \tag{6}$$

Thus it can be seen from these equations that the error of simulation, Y, depends upon time, and more explicitly upon the rate of Joule heating as a function of time. Before the degree of simulation can be completely characterized, the power function must be known; however, some estimates of the degree of simulation can be made for limiting cases and certain conditions without exact solution of equation (6).

Three general areas will be considered since in each the response is of a different character:

A. Steady-state conditions

B. Short pulse transients (duration less than 1% of bridgewire time constant)

C. Transients not covered in B

A. Steady State Simulation.

With a steady, continuous power flow into an EED the bridgewire, after a few time constants, reaches a final steady-state temperature. Under these conditions the rate of change of temperature is zero and equation (2) reduces to

$$T = \frac{C'}{C}\,\frac{\tau}{\tau'}\,T' \tag{7}$$

Thus in the steady-state the average bridgewire temperature of the loaded device is related to the instrumented value through the ratios of the heat capacities and time constants. Since under steady-state conditions $\dot{Y}$ is also equal to zero, the simulation error is maximized and has a value

$$Y_{max} = (T'-T)_{max} = \left(1 - \frac{C'}{C}\frac{\tau}{\tau'}\right) T' \tag{8}$$

B. Simulation in the Case of Short-pulse Transients.

For short-pulse transients it has been shown (ref. 1) that the bridgewire reaches a peak temperature given by

$$T_{max} = E/C$$
$$T'_{max} = E/C' \qquad (9)$$

where E is the pulse energy. Then

$$T_{max} = \frac{C'}{C} T'_{max} \qquad (10)$$

Thus for short-pulse transients the peak bridgewire temperature of the loaded device is related to the instrumented value through the ratio of the heat capacities only.

C. Degree of Simulation for Other than Short-Pulse Transients.

The degree of simulation for transients other than short-pulse transients lies between that for short-pulse transients and steady state.

To completely characterize the degree of simulation for such transients, a detailed knowledge of the power into the bridgewire as a function of time is required, and in general, the ratio of the loaded and instrumented bridgewire temperatures is a function of time. To estimate the degree of simulation for such transients a simple calculation shows that the maximum temperatures achieved by the loaded and instrumented bridgewires, in response to a square pulse of power of duration equal to the instrumented bridgewire's time constant, are related by

$$\frac{T_{max}}{T'_{max}} = \frac{C'}{C}\frac{\tau}{\tau'}\left\{\frac{1-\exp(-\tau'/\tau)}{1-\exp(-1)}\right\} = \frac{x}{y}\left\{\frac{1-\exp(-1/x)}{1-\exp(-1)}\right\} \qquad (11)$$

where

$$y = C/C' \qquad \text{and}$$

$$x = \tau/\tau' \tag{12}$$

A repetition of the calculation for the case of a square pulse of duration τ, instead of τ' as in the above case, results in

$$\frac{T_{max}}{T'_{max}} = \frac{C'\tau}{C\tau'}\left\{\frac{1-\exp(-1)}{1-\exp(-\tau/\tau')}\right\} = \frac{x}{y}\left\{\frac{1-\exp(-1)}{1-\exp(-x)}\right\}$$

Figure 1 compares the degree of simulation for the several modes of bridgewire response as a function of the ratio of the loaded to instrumented bridgewire time constants, x. Notice that the ordinate is the ratio of the loaded to instrumented bridgewire temperatures, T/T', multiplied by the ratio of loaded to instrumented bridgewire heat capacities, y. Thus these normalized curves can be used as universal curves, since the ratio of the temperatures can be found by dividing the ordinate by y, the ratio of the heat capacities. For the three transient curves, T/T' is the ratio of the maximums of T and T', since in general the ratio between T and T' is a function of time. Notice that the curve representing short-pulse transients is not extended to small values of x. This is because the criteria for a short pulse is that its duration be 1% (or less) of the bridgewire time constant (ref. 1). It is possible for a pulse to be considered a short pulse for the instrumented bridgewire and yet be too long to be considered a short pulse for the identical bridgewire when loaded.

VERIFICATION OF MODEL

Two pieces of experimental evidence indicate that the mathematical dependence of the simulation upon the basic thermal parameters, τ and C is

essentially correct. In the first place, it has been verified, within experimental error, that the model predicts the degree of simulation for the steady-state case. This verification involves measuring the relative heat capacities and time constants as well as the resistance changes exhibited by the loaded and instrumented bridgewires when subjected to the same steady-state power input. Secondly, the model is based upon the assumption that the bridgewires behave in both cases as linear systems. This assumption can be verified as a by-product of the way in which the time constants were measured. The time constants were measured by directly comparing the bridgewire's temperature (or more exactly, resistance) decay with that of a true exponential decay. It was found that the decay of both the instrumented and loaded bridgewires were nearly exponential, although the instrumented decay was more truly exponential than the loaded.

EXPERIMENTAL RESULTS

Relative heat capacities of the loaded and instrumented bridgewires were measured by means of the temperature response of bridgewires to short-pulse transients (ref. 1.)

$$\frac{R-R_o}{\alpha R_o} = i = \frac{E}{C} \exp(-t/\tau) \qquad (13)$$

where, in addition to symbols previously used,

R_o is the bridgewire resistance at ambient temperature

R is the bridgewire resistance at temperature T, and

α is the bridgewire's temperature coefficient of resistance.

Pulses of known energy and short duration were introduced into both instrumented and loaded bridgewires. The bridgewire being tested was one arm of an initially balanced wheatstone bridge. The bridge unbalance due to the change in resistance resulting from the short pulse was observed on an oscilliscope. The ratio of pulse energy to peak oscilliscope deflection can be taken as a measured value of the bridgewire's relative heat capacity.

The decay of the bridge unbalance with time was compared on the scope with an exponential generated by an R-C circuit. The decay drove the vertical deflection and the generated exponential drove the horizontal deflection. By this means the time constants were measured and the verification of the exponential decay was obtained.

Table 1 gives the averages of measured values of time constants and relative heat capacities for several devices' bridgewires in the loaded and instrumented conditions. The data represents an average over the values found for 3 of each type in loaded condition and 8 or 9 of each type in the instrumented condition. The spread in values for a given type was less in the loaded condition than in the instrumented condition.

TABLE I

THERMAL PARAMETERS OF LOADED AND INSTRUMENTED BRIDGEWIRES

Device	Time Constant (milliseconds)			Heat Capacity (relative)		
	Loaded	Instru	Ratio = x	Loaded	Instru	Ratio=y
MK-1	5.1	14.6	.35	5.015	4.47	1.12
MC-727	8.1	13.5	.60	3.352	2.00	1.67
MC-749	3.0	7.36	.41	2.445	1.87	1.31
SA-402	3.7	7.66	.48	2.33	1.60	1.46
SA-586	6.3	13.06	.48	3.07	2.56	1.20

The data of table 1 was used with graph 1 to obtain the data of of table 2.

TABLE 2

DEGREE OF SIMULATION

Device	T/T'			
	Case 1	Case 2	Case 3	Case 4
MK-1	.31	.46	.67	.89
MC-727	.36	.46	.50	.60
MC-749	.31	.45	.59	.76
SA-402	.33	.46	.55	.68
SA-586	.40	.56	.67	.83

Graph 2 is a presentation of the information in table 2. These results seem somewhat striking and some explanation of the variations between devices is indicated.

INTERPRETATION OF RESULTS

It is not surprising that there is a spread among the devices in their degree of simulation. Several different explosive powders are used each with a characteristic heat capacity and thermal conductivity. The bridgewires are of various materials (of different thermal conductivities), various lengths and diameters. The effect of a given media upon time constant depends upon the geometry as well as the media, since the resultant time constant is a balance between the effect of heat being conducted down the bridgewire to the binding posts and heat being conducted into the material surrounding the bridgewires.

The results are valid for low frequency rf, i.e., for frequencies low enough that temperature measuring instrument and the plug supporting the bridgewire are not absorbing energy directly from the electromagnetic radiation. Whether case 1, 2, 3 or 4 is realized depends upon the duration of the excitation.

Case 1. Long compared to instrumented bridgewire time constant.

Case 2. About equal to instrumented bridgewire time constant.

Case 3. About equal to loaded bridgewire time constant.

Case 4. Short compared to both loaded and instrumented bridgewire time constants.

With a knowledge of the duration of the excitation and the relative values between loaded and instrumented thermal parameters of the device, fairly meaningful estimates of the temperature of the loaded bridgewire can be made.

REFERENCES

1. Denver Research Institute of the University of Denver, Sandia P. O. No. 73-2582, Task 1 Report, Transient Response of Thermocouple Instrumented EED's, September 1962.
2. Denver Research Institute of the University of Denver, Sandia P. O. No. 73-2582, Task 3 and 4, Report, Study of Degree of EED Simulation, and Increased Thermocouple Sensitivity (contact), to be published.

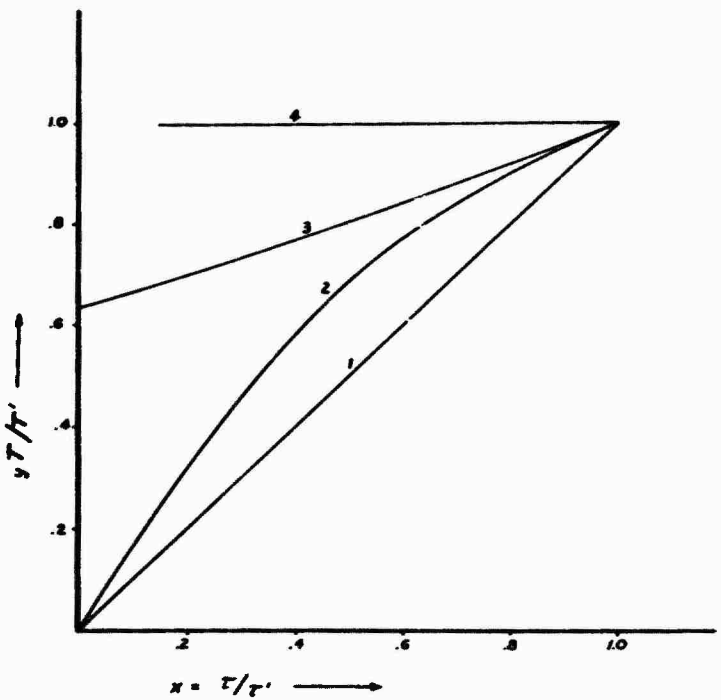

FIG. 1. DEGREE OF SIMULATION AS A FUNCTION OF TIME CONSTANT RATIO

1. steady state
2. square pulse of duration τ'
3. square pulse of duration τ
4. pulse short in duration compared to τ and τ'

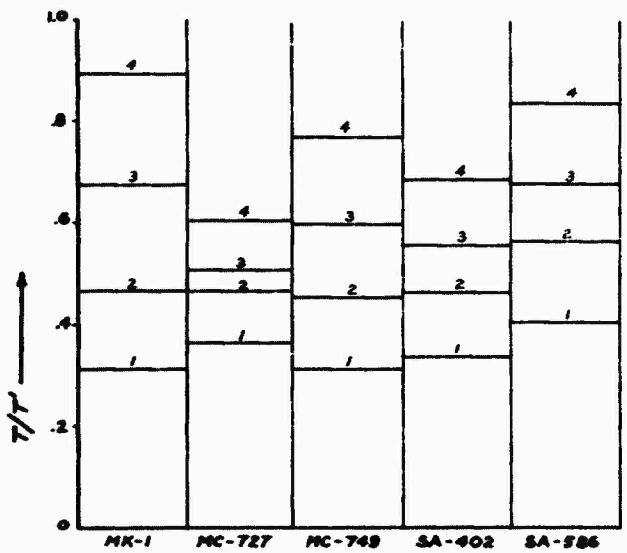

FIG. 2. DEGREE OF SIMULATION FOR SEVERAL DEVICES

1. steady state
2. square pulse of duration τ'
3. square pulse of duration τ
4. pulse short in duration compared to τ and τ'

48. MEASUREMENT OF THE LEAST POSSIBLE (WORST CASE) ATTENUATION OF PROTECTIVE DEVICES FOR EED'S

by Ramie H. Thompson
The Franklin Institute

ABSTRACT

Devices used to protect electroexplosive devices EED's from radio frequency energy (RF) are usually rated in db of attenuation. In many cases the quoted attenuation of a device is actually the measured insertion loss. Since the device may be used in systems where both the load impedance and the equivalent generator impedance are considerably different than those of the system in which the stated attenuation (insertion loss) was measured, a method has been developed for calculating the least possible or "worst case" attenuation from input-output impedance measurements of the device. This worst case attenuation is shown to be the same parameter which we have previously measured in a system employing matching networks on both sides of the sample.

The determination of the least possible, or worst-case, attenuation of a two-port network is analyzed, using non-symmetrical-T network equivalent circuits. The analysis assumes that the two-port network is composed of lumped or distributed elements or combinations thereof, and is passive, bilateral and linear. Formulas for computation of the worst-case attenuation from input-output impedance measurements are presented. This method may be particularly useful at frequencies from 20 Kc to 100 Mc where impedances can easily be measured but matching systems may become lossy.

INTRODUCTION

The effectiveness of a protective device for electroexplosive devices (EED's) is usually stated as being "so many db of attenuation". Prior knowledge of the system in which the particular protective device is to be installed can be used to justify some particular definition of attenuation. Many such definitions have been developed. All of these

definitions imply that attenuation in db is equal to ten times the logarithmic ratio of two values of power, and that these values are measured (or predicted) when the energy source supplies voltage (or current) sinusoidally at a single frequency. The specific type of attenuation defined depends on what values we insert in the ratio and under what conditions power is to be measured. In the case of two-port protective devices, the powers to be measured are in some way associated with an overall system consisting of a power supplying subsystem, the two-port device being evaluated, and a subsystem that receives the output power.

In circuit terminology the system that supplies the input power can be completely described by an equivalent (Thevenin equivalent) voltage generator and series impedance or an equivalent (Norton equivalent) current generator and shunt impedance. The system that receives the output power can be represented as an equivalent load impedance.

By using the above circuit terminology we implicitly make the assumption that the overall system is composed of finite, linear, passive, bilateral elements. The above string of adjectives usually contains the word "lumped". It can be shown that for any one frequency a two-port uniform distributed component system can be represented by an equivalent lumped-component T network. Since we are discussing attenuation, which has a fixed meaningful value only for a single frequency excitation, we may include this type of distributed component network in our lumped constant description.

Commonly given for the value of "attenuation" is the insertion loss of a protective device. All insertion loss definitions put restrictions on <u>both</u> the equivalent generator impedance and the equivalent load impedance. For instance, fifty-ohm insertion loss (in db) equals ten times the logarithm of the ratio of output power to the available generator power when both the equivalent load impedance and the Thevenin equivalent generator impedance are equal to fifty ohms. In general, we may categorize

all types of "attenuation" that put restriction on the equivalent generator impedance as a type of insertion loss.

All other types of attenuation are defined in terms of the input and output powers of the two-port device and put restrictions on the equivalent load impedance only. They are therefore completely independent of the power-supplying subsystem.

We will refer to this type of attenuation as terminated loss (TL), since it depends only on the two-port network and its termination.

A classic example of this type of attenuation is that of "characteristic impedance termination". In this definition no restriction is set on the power supplying system, but a strong restraint is placed on the equivalent load impedance. Characteristic impedance attenuation is defined as ten times the log of the output to input power ratio when the equivalent load impedance is equal to the input characteristic impedance of the device being evaluated. (The input characteristic impedance of a device is equal to that impedance which when applied to the output terminals causes the input impedance of the combination to equal the terminating impedance). This definition of characteristic impedance attenuation can be applied to both symmetrical and dissymmetrical devices. Characteristic impedance attenuation is associated with the voltage propagation constant, ($\gamma = \alpha + \beta$) which is much used in transmission line work. The equivalence of the network propagation constants and transmission line propagation constants is based on an exact electrical equivalence (at one frequency) between a uniform transmission line with propagation constant $\gamma \ell$ and chacteristic impedance Z_o, and a symmetrical T network as shown in Figure 1. (The T network is not necessarily realizable).

In many cases the equivalent load impedance and equivalent generator impedance of the actual system in which the protective device is to be used are not known. Under those conditions none of the types of attenuation mentioned previously will be correct; moreover, any or

all of them may be either greater than or less than the actual effectiveness of the device in the unknown system. The problem of evaluating the effectiveness of a universal protector (one which will provide at least some specified reduction in power between input port and <u>any</u> terminating EED) illustrates this last case perfectly. The solution in the past has been to evaluate the device in a system similar to that diagrammed in Figure 2. In this arrangement, a lossless piece of transmission line is inserted between the supposedly lossless matching systems, and the systems are adjusted for maximum power into the termination; this adjustment will give zero reflected power. The maximum power is noted, and the device to be tested is inserted between the matching systems which are then readjusted so that again the reflected power is zero and the power to the termination is maximum. The logarithm of the ratio of the two powers, multiplied by ten, is the matched attenuation in decibels. If the lossless matching systems are perfect (i.e. are capable of transforming any impedance into any other impedance) the above procedure is seen to be equivalent to holding the input power to the device constant while varying the equivalent termination impedance until the output power is a maximum. From our previous definition of terminated loss it is clear that the matched attenuation is the worst-case (or least) terminated loss and from here on will be referred to as worst-case attenuation (db_{wc}). This quantity is a characteristic of the protective device alone, which, under any impedance condition, will afford this attenuation at the very least. At high frequencies the matching system method can be employed with a small margin of error, since almost perfect matching systems can be constructed of coaxial components*. At lower frequencies lumped components must be employed, and the matching systems become lossy. This not only limits the range of impedance transformation of the network but it also adds a loss associated with the matching systems to the measured

---

*The losses in a matching system are also a function of the internal VSWR. The statements in this paper hold for VSWR's less than a hundred.

loss of the device under test. The net result is that, at low frequencies, the matching method of determining the worst-case attenuation is very uncertain, particularly if the same matching system is used for a wide band of frequencies. This is not meant to imply that the matching method cannot be useful at low frequencies (40 Mc or less) for evaluating some particular device, but that it is extremely difficult to design a matching system that will transform the extremely small impedances encountered in some present protective devices to a common transmission line impedance without excessive losses. The design problem is even more difficult if the system is required to work over a wide range of frequencies and impedances.

Since the worst-case attenuation is a characteristic of the protective device alone, a complete electric description of the protective device must contain the information necessary to calculate the worst-case attenuation.

WORST-CASE ATTENUATION AS A FUNCTION OF THE IMPEDANCES OF A DISSYMMETRICAL T NETWORK

If we represent the electrical behavior of the protective device as a dissymmetrical T network (this is a consistent with our earlier assumptions) and the equivalent load impedance as Z_L, as shown in Figure 3; the expressions for input and load power are:

$$P_{in} = \mathrm{Re}\,\{\bar{V}_{in}\,\bar{I}_{in}^{*}\},\quad P_L = \mathrm{Re}\,\{\bar{V}_L\,\bar{I}_L^{*}\} \tag{1}$$

Where the asterisk indicates the conjugate of the complex quantity or

since $\bar{V}_{in} = Z_{in}\,\bar{I}_{in}$, $\bar{V}_L = Z_L\,\bar{I}_I$, and $\bar{I}_{in}\,\bar{I}_{in}^{*} = |\bar{I}_{in}|^2$, $\bar{I}_L\,\bar{I}_L^{*} = |\bar{I}_L|^2$

$$P_{in} = |\bar{I}_{in}|^2\,\mathrm{Re}\,\{Z_{in}\},\quad P_L = |\bar{I}_L|^2\,\mathrm{Re}\,\{Z_L\} \tag{2}$$

Now, by inspection of Figure 3, $\bar{I}_L = \bar{I}_{in} \frac{Z_2}{Z_2 + Z_3 + Z_L}$ (3)

and the ratio of load to input power, from Equation 2, is therefore

$$\frac{P_L}{P_{in}} = \frac{|\bar{I}_L|^2 \, Re\{Z_L\}}{|I_{in}|^2 \, Re\{Z_{in}\}} \tag{4}$$

If we square the magnitude given by Equation 3 and substitute in Equation 4, we obtain

$$\frac{P_L}{P_{in}} = \frac{|Z_2|^2}{|Z_2 + Z_3 + Z_L|^2} \frac{Re\{Z_L\}}{Re\{Z_{in}\}} \tag{5}$$

The input impedance can be written as

$$Z_{in} = \frac{Z_1 Z_2 + Z_1 Z_3 + Z_2 Z_3 + Z_L (Z_1 + Z_2)}{Z_2 + Z_3 + Z_L} \tag{6}$$

If we substitute this in equation 5 then, with a little manipulation, we obtain

$$\frac{P_L}{P_{in}} = \frac{|Z_2|^2 \, Re\{Z_L\}}{Re\{[Z_1 Z_2 + Z_1 Z_3 + Z_2 Z_3 + Z_L (Z_1 + Z_2)][Z_2 + Z_3 + Z_L]^*\}} \tag{7}$$

The terminated loss expressed in decibels of the dissymmetrical-T network (and therefore of its electrically equivalent protective device) terminated by an impedance Z_L would be given as ten times the logarithm of equation 7, according to our early definition of TL. To obtain an expression for the worst case attenuation we must find the worst case terminated loss, which would be associated with the maximum value of equation 7. If we let $Z_1 = G + j\,H$, $Z_2 = K + j\,L$, $Z_3 = P + j\,Q$, $Z_L = x + j\,y$ and substitute these values in Equation 7 we obtain

$$\frac{P_L}{P_{in}} = \frac{x (K^2 + L^2)}{D} \tag{8}$$

where $D = x^2 [G + K] + y^2 [G + K] + y V + x U + R$

$$V = 2GQ + 2GL + 2KQ \tag{9}$$

$$U = 2GK + 2GP + 2KP + K^2 + L^2$$

$$R = GK^2 + 2GPK + K^2P + GP^2 + KP^2 + PL^2 + 2GQL + GL^2 + GQ^2 + KQ^2$$

Taking the two partial derivatives of equation 8 with respect to x and y, setting them equal to zero, and solving the resulting equations simultaneously, we obtain the load impedance that will maximize the power ratio. We will refer to this impedance as worst case impedance (Z_{wc}).

Thus $Z_{wc} = X_{wc} + j\, y_{wc}$

i.e.

$$X_{wc} = \frac{\sqrt{4R\,(G + K) - V^2}}{2\,(G + K)}$$

$$Y_{wc} = \frac{-V}{2\,(G + K)} \tag{10}$$

where R and V are defined by equation 9. The worst-case attenuation for the dissymmetrical T network is therefore given by ten times the logarithm of equation 7 when Z_{wc} (as defined by equation 9) is substituted for Z_L.

The analysis above was actually carried out after a similar analysis of a symmetrical T network was performed. The solution to this case can of course be had from the above dissymmetrical solution by placing P = G and Q = H. The expression for $x_{wc} = \mathrm{Re}\,\{Z_{wc}\}$ can be factored*, in the symmetrical case, yielding

$$x_{wc} = \mathrm{Re}\,\{Z_{wc}\} = \frac{\sqrt{G(G + 2K)\,([G + K]^2 + L^2)}}{(G + K)^2} \tag{11}$$

A dual purpose computer program was written both to check the analysis and to compute db_{wc} if the open and short circuit input impedances (Z_{oc} and Z_{sc}) are known (for a symmetrical T).

The part of the program for checking the analysis merely computes $\frac{P_L}{P_{in}}$ if Z_L, Z_1, and Z_2 are given (see Figure 4). We make the check by

---

*For this, the author wishes to thank Mr. J.D. LaPlante, Naval Weapons Evaluation Facility, Albuquerque, N. M.

picking particular values for Z_1 and Z_2, calculating Z_{wc} (from the analysis), and then letting the computer evaluate $\frac{P_L}{P_{in}}$ for Z_L equal to Z_{wc}. We then compute the ratio with Z_L very close to not equal to Z_{wc}. If $Z_L = Z_{wc}$ does truly maximize the ratio (that is, if our analysis is correct) then all the values of the ratio associated with Z_L close to Z_{wc} will be less than the ratio evaluated with $Z_L = Z_{wc}$. The results of two checks are presented in Table 1. The results indicate that the analysis is correct. A worst-case analysis using Z_o and γ to describe a uniform transmission line, and Z_L as the independent variable, has been performed by Mr. Charles Stonecypher* and the results check those of the symmetrical T solution. Table 3 shows the results of two such comparisons of results from the separate analyses.

If equation 10 is substituted into equation 7 along with $Z_1 = G + jH$, $Z_2 = K + jL$, $Z_3 = P + jQ$ we obtain the worst-case power ratio as a function of G, K, L, and P**. Note that this worst case power ratio is independent of Q and H, the reactances of the series arms of the dissymmetrical T. This property can be deduced by remembering that the worst case attenuation is, for perfect matching systems, the same attenuation that would be measured by the system indicated in Figure 2. Here it seems obvious that the addition of reactive networks between the device being tested and the matching systems will not change the result of the measurement, because we can always consider these reactive networks as part of the lossless matching systems.

---

*Of the Franklin Institute Laboratories, Applied Physics Lab.

**This conclusion was not actually verified by substituting in the case of the non-symmetrical T, but is valid as will be shown later.

DETERMINATION OF WORST-CASE ATTENUATION FROM THE TERMINAL IMPEDANCES OF THE PROTECTIVE DEVICES

The worst-case attenuation of a known T network can be computed by use of eqs. 7 and 9. A computer program was written to compute the equivalent T network of a protective device from impedance measurements at the terminals of the device and evaluate the worst-case attenuation of the T network by the formulas of preceding sections. There are two sources of errors in the calculated worst-case attenuation: round-off error in the computer, and error in the impedance measurements. The computer round-off errors are estimated to lead to an error of no more than 1% in the calculated attenuation. With the impedance measuring equipment that we are using, worst-case attenuations of more than 20 db are uncertain. Better measuring equipment would improve this figure.

As mentioned earlier a very important property of the worst-case attenuation parameter is that it should not vary if lossless networks are inserted between the measurement points and the device. For instance, we should arrive at the same result for worst-case attenuation (see Figure 5) whether we perform impedance measurements at terminals AA' and BB' or at terminals 11', 22'. We checked this property of the worst-case attenuation parameter by assuming the device shown in Figure 6. We assigned various values to Z_{o1}, $\beta\ell_1$, Z_{o2}, $\beta\ell_2$, then computed what input and output impedances would be measured at terminals 11', and 22' for each selected set of values for the lossless networks. These calculated impedances were used as input data for the computer program. The results are shown in Table 2.

The sixth column of Table 2 indicates whether the equivalent T network (determined by the computer program) between terminals 11', 22' (Figure 6) is realizable or not.

We mentioned earlier that the equivalent T's of networks containing uniform transmission lines were not necessarily physically realizable. We believed that our analysis of the power transfer ratio in T networks

was sufficiently general to include non-realizable elements (we had made no assumption that would exclude them) but we had no easy way to showing this. Fortunately, some of the equivalent T networks of our check in the worst-case attenuation program gave this condition. Since we obtain the same worst-case attenuation with a non-realizable T as with a realizable one (Table 5) we consider the point proved.

The dissymmetrical-T computer program must calculate the equivalent T network between the measurement points, from the measurements of impedances at these points. It can be shown that this is a simple calculation if any three of the following four impedances are known (see Figure 5, in which the measurement points would be terminals 11' and 22', and the computed T would be equivalent electrically to the entire circuit between these terminals).

$$Z_{11'}\Big|_{Z_L=0}\ ,\quad Z_{11'}\Big|_{Z_L=\infty}\ ,\quad Z_{22'}\Big|_{Z_L=0}\ ,\quad Z_{22'}\Big|_{Z_L=\infty}$$

The objection to using three of the above parameters was that at high frequencies the location of an open circuit and an open circuit itself are notoriously difficult to define. We decided to derive the equivalent T network in terms of any three of the following four impedances.

$$Z_{11'}\Big|_{Z_L=0} = \bar{a},\quad Z_{11'}\Big|_{Z_L=Z_T} = \bar{b},\quad Z_{22'}\Big|_{Z_L=0} = \bar{c},\quad Z_{22'}\Big|_{Z_L=Z_T} = \bar{d},$$

where $Z_T = \bar{e}$ is any known impedance. We intended to make Z_T = 50 ohms in the actual measurements since this is a commonly available termination. Appendix A gives the derivation for the equivalent T for two groups of

the above parameters ($\bar{a}$, $\bar{b}$, $\bar{c}$, $\bar{e}$) and ($\bar{a}$, $\bar{b}$, $\bar{d}$, $\bar{e}$). The computer program determines the T networks corresponding to each of the groups and presents them as part of the program output; therefore, the actual measurements are those of $\bar{a}$, $\bar{b}$, $\bar{c}$, and $\bar{d}$ when $\bar{e}$ = 50 ohms. If the two independently derived networks do not agree we immediately know that the impedance measurements are not correct. This affords a built-in check of the measurement procedure. As a check of the solution given in Appendix A, data from each row in Table 2 were substituted into the variables shown in Figure 6; i.e., $\beta\ell$ and Z_o. Each equivalent T network was calculated from the $\bar{a}$, $\bar{b}$, $\bar{c}$, $\bar{d}$ parameters which were obtained by terminating the actual network (Figure 6, with values from a row in Table 2) with $\bar{e}$ equal to 1, 7, 50, 500, 10^3 and 10^9 ohms. This procedure yielded 12 independently derived equivalent T networks for each row of Table 2. The elements of the equivalent T's agreed to at least six significant figures within each row. The $\bar{a}$, $\bar{b}$, $\bar{c}$, $\bar{d}$ parameters for this check were, of course, calculated by another computer program, since hand calculation would have been impractical for the degree of accuracy required.

COMMENTS

An interesting property of the worst-case impedance of a symmetrical network is that it can be defined in much the same way as the characteristic impedance. The characteristic impedance is defined as that impedance which when used as the terminating impedance causes the input impedance to equal the termination impedance. For a symmetrical network, the worst-case impedance is that impedance which, when used as the terminating impedance, causes the input impedance to become the complex conjugate of the termination impedance*. Using equation 5 (and recalling that for the symmetrical case $Z_1 = Z_3$) and the above definition for symmetrical Z_{wc}, the worst-case attenuation expression for a symmetrical network can be

*This can be shown by solving for the impedance which fulfills the above definition and noting that it is the same as symmetrical Z_{wc} as defined by the worst-case analysis.

expressed as

$$db_{wc_{sym}} = 10 \log \frac{|Z_2|^2}{|Z_1 + Z_2 + Z_{wc}|^2} = 20 \log \left| \frac{Z_2}{Z_1 + Z_2 + Z_{wc}} \right| \qquad (12)$$

a considerable simplification. It is possible that equation 12 can be used as the basis of a design equation for uniform distributed networks. An effort has been made to obtain Z_{wc} (for the symmetrical case) as a simple function of various pairs of commonly used network coefficients but we have had no success.

Equation 7, which expressed the terminated power ratio as a function of the load, can be used to develop another method of measuring worst-case attenuation. If the partial differentials of equation 7 in relation to the real and imaginary parts of the load impedance are set equal to zero, the worst-case power ratio is found to be an expression containing four constants. The power ratio itself can be expressed in terms of these four constants and the real and imaginary parts of the load impedance. It turns out that the four constants, and hence the worst-case power ratio, can be uniquely defined if the power ratio is measured four times using a known real terminating impedance for three of these measurements and a known complex terminating impedance for the fourth measurement. We are investigating the feasibility of such a system since the upper limit of the attenuation that can be measured may be very high.

Table 1

RESULTS OF CHECKING PROGRAM
FOR SYMMETRICAL-T ANALYSIS

Case I $Z_1 = 1 + j\,1 = Z_2$

Calculated Z_{wc} (From Analysis)	Value of Z_L Used in Computation	Resulting $\frac{P_L}{P_{in}}$	Resulting $10 \log \frac{P_L}{P_{in}}$ (db)
1.936 - j 1.5	1.936 - j 1.5	.12701	- 8.9613
	1.8 - j 1.4	.1267	- 8.970
	1.8 - j 1.6	.1267	- 8.970
	2.0 - j 1.4	.1269	- 8.965
	2.0 - j 1.6	.1269	- 8.965
Case II $Z_1 = 2 + j\,3; Z_2 = 4 + j\,5$			
5.8214 - 4.6666	5.8214 - j 4.6666	.271780	- 5.6578
	5.72 - j 4.5	.271708	- 5.6589
	5.72 - j 4.75	.271748	- 5.6583
	5.92 - j 4.5	.271712	- 5.6589
	5.92 - j 4.75	.271750	- 5.6583

Table 2

RESULTS OF WORST-CASE ATTENUATION PROGRAM CHECK

Z_{o_1} Ohms	$\beta\ell_1$ Radians	Z_{o_2} Ohms	$\beta\ell_2$ Radians	Calculated db/wc	Equivalent Network Realizable
50	0	50	0	7.40	yes
50	.5	50	.5	7.40	yes
50	1	50	1	7.40	no
50	1.5	50	1.5	7.40	no
2	1.5	2	1.5	7.39	yes
1000	1.5	1000	1.5	7.40	yes
2	1.5	1000	1.5	7.40	yes
50	0	50	1.5	7.40	no
2	1.5	1000	.5	7.40	yes

Table 3

COMPARISON OF T AND DISTRIBUTED NETWORK PREDICTIONS

Network #1	T - Network Prediction	Distributed Network Prediction
$Z_o = 7.68 \angle 54.4°$	$\lvert Z_{wc}\rvert = 7.46$	$\lvert Z_{wc}\rvert = 7.44$
$\gamma = 1.01 + j\ .04$	$\phi_{wc} = 38.7°$	$\phi_{wc} = 38.4°$
Network #2	**T - Network Prediction**	**Distributed Network Prediction**
$Z_o = 7.04 \angle 19.4°$	$\lvert Z_{wc}\rvert = 9.33$	$\lvert Z_{wc}\rvert = 9.37$
$\gamma = 0.258 + j\ 0.549$	$\phi_{wc} = 12.38°$	$\phi_{wc} = 12.27°$

APPENDIX A

DISSYMMETRICAL T NETWORK DETERMINATION

Given the network is shown in Figure A-1. We wish to find x, y, z from either $\bar{a}$, $\bar{b}$, $\bar{c}$, and $\bar{e}$ or from $\bar{a}$, $\bar{b}$, $\bar{d}$, and $\bar{e}$, where these parameters are defined as follows:

$$\left.\begin{aligned} \bar{a} &= Z_{11'}\Big|_{Z_L = 0}, \quad \bar{b} = Z_{11'}\Big|_{Z_L = \bar{e}}, \quad \bar{c} = Z_{22'}\Big|_{Z_L = 0}, \quad \bar{d} = Z_{22'}\Big|_{Z_L = \bar{e}} \end{aligned}\right\} \quad \text{(A-1)}$$

$\bar{e}$ = arbitrary impedance.

From Figure A-1, by inspection

$$\bar{a} = x + \frac{yz}{y+z} \quad \text{(A-2)} \qquad \bar{b} = x + \frac{y(z+\bar{e})}{y+z+\bar{e}} \quad \text{(A-3)}$$

$$\bar{c} = z + \frac{xy}{y+x} \quad \text{(A-4)} \qquad \bar{d} = z + \frac{y(x+\bar{e})}{y+x+\bar{e}} \quad \text{(A-5)}$$

For our first solution we use Equations A-2, A-3, and A-4, which can be rewritten as

$$\bar{a}(y+z) = xy + xz + yz \quad \text{(A-6)}$$

$$\bar{b}(y+z) + \bar{b}\,\bar{e} - \bar{e}(y+x) = xy + xz + yz \quad \text{(A-7)}$$

$$\bar{c}(y+z) = xy + xz + yz \quad \text{(A-8)}$$

If we let

$$\left.\begin{aligned} y + z &= \psi \\ y + x &= \phi \\ xy + xz + yz &= \theta \end{aligned}\right\} \quad \text{(A-9)}$$

then we can rewrite Equations A-6, A-7, A-8 as

$$\left.\begin{aligned} \bar{a}\,\psi \qquad\quad - \theta &= 0 \\ \bar{b}\,\psi - e\,\phi - \theta &= -\bar{b}\,\bar{e} \\ e\,\phi - \theta &= 0 \end{aligned}\right\} \qquad \text{(A-10)}$$

These may be solved by determinants.

$$\left.\begin{aligned} \psi &= \frac{\begin{vmatrix} \bar{b} & \bar{e} & \bar{c} \end{vmatrix}}{|D|}, \quad \phi = \frac{\begin{vmatrix} \bar{a} & \bar{b} & \bar{e} \end{vmatrix}}{|D|}, \quad \theta = \frac{\begin{vmatrix} \bar{a} & \bar{b} & \bar{c} & \bar{e} \end{vmatrix}}{|D|} \\ \text{where} \\ |D| &= \bar{a}\,(\bar{e} + \bar{c}) - \bar{b}\,\bar{c} \end{aligned}\right\} \qquad \text{(A-11)}$$

If we substitute Equations A-11 in Equations A-9, and solve the resulting system by substitution, we obtain

$$\left.\begin{aligned} y &= \frac{\sqrt{\bar{a}\,\bar{b}\,\bar{c}\,\bar{e}\,[\bar{e} + \bar{c}]\,[\bar{b} - \bar{a}]}}{\bar{a}\,(\bar{e} + \bar{c}) - \bar{b}\,\bar{c}} \\ x &= \frac{\begin{vmatrix} \bar{a} & \bar{b} & \bar{e} \end{vmatrix}}{\bar{a}\,(\bar{e} + \bar{c}) - \bar{b}\,\bar{c}} - y \\ z &= \frac{\begin{vmatrix} \bar{b} & \bar{e} & \bar{c} \end{vmatrix}}{\bar{a}\,(\bar{e} + \bar{c}) - \bar{b}\,\bar{c}} - y \end{aligned}\right\} \qquad \text{(A-12)}$$

Equations A-12 are the desired solution for our first parameter group ($\bar{a}$, $\bar{b}$, $\bar{c}$ and $\bar{e}$).

For the second group we use Equations A-5, A-6, and A-7 and make the same change of variable as before (Equations 9). We obtain

$$\left.\begin{aligned} \bar{a}\,\psi \qquad\quad - \theta &= 0 \\ \bar{b}\,\psi - \bar{e}\,\phi - \theta &= -\bar{b}\,\bar{e} \\ \bar{e}\,\psi + \bar{d}\,\phi - \theta &= -\bar{d}\,\bar{e} \end{aligned}\right\} \qquad \text{(A-13)}$$

which when solved, give

$$\left.\begin{aligned} \psi &= \frac{\bar{d}\,\bar{e}\,[\bar{e} + \bar{b}]}{|D|} \\ \phi &= \bar{e}\,\frac{[\overline{ab} - \overline{ad} + \overline{bd} + \overline{eb}]}{|D|} \\ \theta &= \bar{a}\,\bar{d}\,\bar{e}\,\frac{[\bar{e} + \bar{b}]}{|D|} \end{aligned}\right\} \qquad \text{(A-14)}$$

where

$$|D| = \bar{e}\,[\bar{a} + \bar{e}] + \bar{d}\,[\bar{a} - \bar{b}]$$

If Equations A-14 are substituted in Equations 9 and the resulting system solved by substitution, we obtain the solution for the second group ($\bar{a}$, $\bar{b}$, $\bar{d}$ and $\bar{e}$).

This solution is

$$y = \frac{\sqrt{\bar{d}\,\bar{e}\,[\bar{e}+\bar{b}]\,[\bar{b}-\bar{a}]\,[\bar{a}+\bar{e}]\,[\bar{e}+\bar{d}]}}{|D|}$$

$$x = \frac{\bar{e}\,\{\bar{b}\,[\bar{d}+\bar{e}]+\bar{a}\,[\bar{b}-\bar{d}]\}}{|D|} - y \qquad \text{(A-15)}$$

$$z = \frac{\bar{d}\,\bar{e}\,[\bar{e}+\bar{b}]}{|D|} - y$$

where

$$|D| = \bar{e}\,[\bar{a}+\bar{b}] + \bar{d}\,[\bar{a}-\bar{b}]$$

The solutions for both groups were checked by substitution in equations A-2 thru A-5. It should be noted that x, y and z are in general complex, as are $\bar{a}$, $\bar{b}$, $\bar{c}$, $\bar{d}$ and $\bar{e}$.

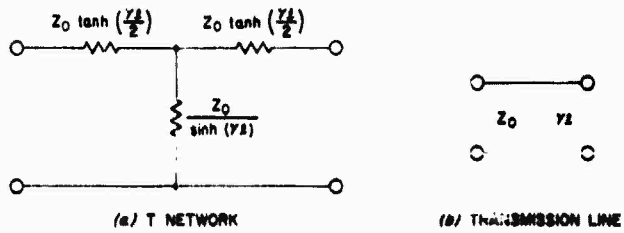

(a) T NETWORK (b) TRANSMISSION LINE

FIG.1 SINGLE FREQUENCY EQUIVALENT CIRCUITS

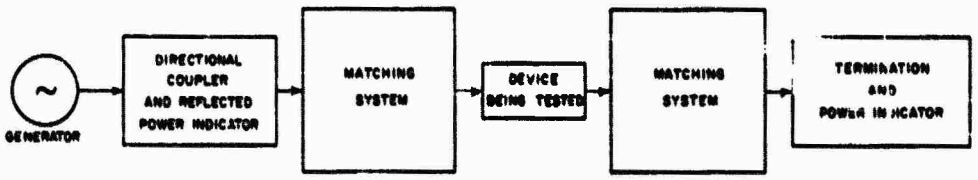

FIG.2 DIAGRAM OF MEASUREMENT SYSTEM USING MATCHING NETWORKS

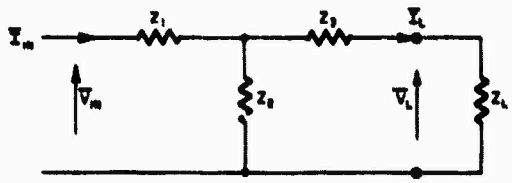

FIG.3 DISSYMMETRICAL T NETWORK AND LOAD

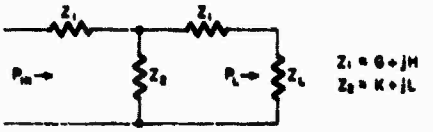

FIG.4 SYMMETRICAL T NETWORK AND LOAD

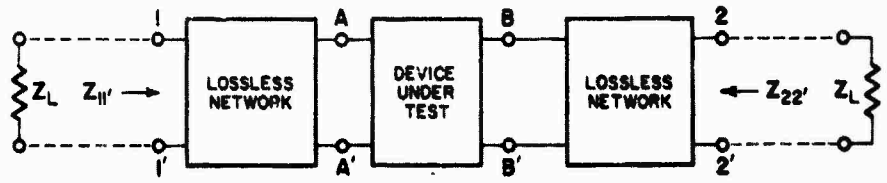

FIG 5. A GENERAL CASE DEVICE

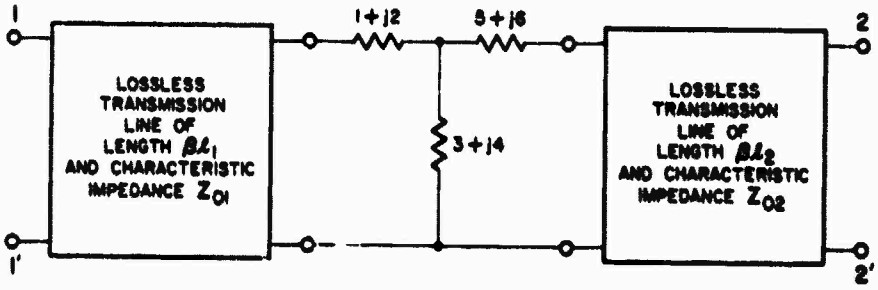

FIG. 6. ASSUMED DEVICE

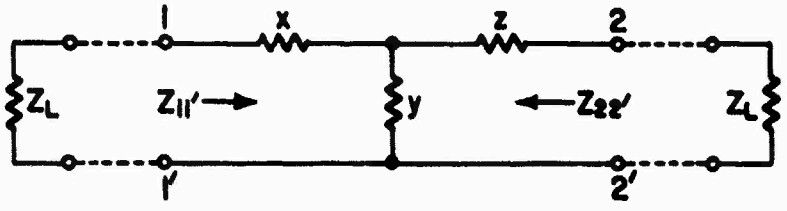

FIG. A-1. THE EQUIVALENT NETWORK

50. Picatinny Arsenal RF Program

Stanley M. Adelman
Picatinny Arsenal, Dover, N. J.

Introduction

Picatinny Arsenal first became actively involved in the HERO program in 1952. For a number of years the funding available for this work was extremely limited and of necessity we conducted a shoe string operation. Most of the effort had to be channelled into an area where it appeared that the returns would be greatest in proportion to the money spent.

The major objective was the development of a solid state attenuator which could be easily incorporated into existing initiator designs and which would not degrade the performance or the stability of the initiators. The development of the powdered iron material and its successful incorporation into a number of initiators has partially fulfilled this objective. It is qualified as a partial solution because this material does not provide as much attenuation for most initiators at the lower frequencies as is necessary.

Picatinny RF Program

During the past few years, more support became available for this program. Consequently, more effort has been expended in areas which were passed by before and which should be included in any well-integrated RF program. The program in which the Arsenal is now engaged may be broken down as follows:

1. Design, development and testing of attenuating materials and devices.

2. Design, development and testing of electroexplosive devices incorporating RF attenuators.

3. Engineering the items developed and manufacturing techniques to qualify these items for mass production.

4. Analysis of vulnerability of warhead sections by mathematical determination.

5. Vulnerability testing of electroexplosive devices and assemblies in the laboratory and in the field.

6. Determination of safety limits for vulnerable munitions.

7. Design, acquisition and installation of equipment and instrumentation for performing RF sensitivity tests and attenuation measurements.

8. Design, acquisition and installation of equipment and instrumentation for determining the probable vulnerability of warhead sections and assemblies.

9. Instrumenting warhead sections for field testing.

Implementation of Programs

Phases 1, 2 and 5 have been actively pursued from the inception of an RF program at Picatinny. Many materials and devices have been tested for attenuation and related properties and RF attenuators have been incorporated into a number of electroexplosive devices. These are now in various stages of the production engineering phase of their development which is Phase 3. An important corollary to Phase 1 is an investigation into the mechanics of

attenuation, in other words, what makes an attenuator attenuate? This study could prove to be far more important in the long run than any other work we are doing since it leads to the development of much more efficient attenuating materials.

Picatinny has also performed several vulnerability analyses of warhead sections and assemblies. These are mathematical determinations based upon known physical configurations of the item of concern. The end result is a listing of frequencies and energy levels to which the item may be vulnerable, if any such exist. These analyses are valuable in pointing out items and conditions for actual testing.

Phase 5 has been an extremely active portion of our program because no RF sensitivity data is available for the great majority of initiators. In the course of planned work and in fulfilling requests for such data from other agencies, a considerable body of data has been amassed in laboratory determinations. Field test data is much more limited in scope with only the M6 Blasting Cap being subjected to a large number of field tests. The T24E1 and XM66E2 Detonators have also been field tested but not as intensively as the M6.

As an adjunct to these studies Picatinny has attempted to set up safety limits for the handling and use of the M6 Blasting Cap in relation to certain transmitters. Continuation of these investigations will enable safety limits to be set up for more items under a wider variety of conditions.

Concurrent with the work described we have been building up a capability for performing RF sensitivity tests of initiators and attenuation measurements in mount. The Arsenal has also been actively engaged in designing, acquiring

and installing equipment for determining the probable vulnerability of warhead sections and assemblies. Fortunately, an existing building has been obtained for housing this equipment and considerable hardware has already been procured.

During the period when this capability has not been available, warhead sections have been instrumented for exposure tests in the field. Since this type of testing does not permit the controlled conditions attainable in our planned setup, it is regarded as an interim procedure.

Conclusion

This outline of Picatinny's activities in the RF program has been presented in order to give you an idea of their scope and their nature. A number of speakers will follow who will give a more detailed insight into specific phases and problems. However, this is the general picture of Picatinny's RF program.

51. INFRARED DETECTOR TECHNIQUES FOR ESTIMATING THE RF POWER IN A HEATED BRIDGE WIRE

By

John P. Warren
The Franklin Institute

When electroexplosive devices are exposed to a source of RF energy, a knowledge of the amount of this energy which actually reaches the bridgewire is extremely desirable. A direct measurement of thie energy would be preferable if at all possible. Such a measurement made at the leads of the device is practical when the source of exposure is a direct current or a low frequency ac generator. We simply measure the power entering the leads of the device and assume that the major portion reaches the bridgewire.

However, as the frequency is raised into the RF region, direct measurement of power at the leads becomes increasingly difficult and the assumption that all of this power reaches the bridgewire becomes invalid. We muet, therefore, make our measurement directly or indirectly at the bridgewire itself. A meaeurement of this type impliee removal of the exploeive material in the EED and eubstitution of a detector in the vicinity of the bridgewire. This detector may be phyeically or electrically attached to the bridgewire. However, physical attachment immediately cauees questions regarding the effect of this attachment on the RF and thermal characteristics of the EED. To avoid thie difficulty we use an indirect method for estimating the thermal effect of the RF power in the bridgewire.

It ehould be emphaeized at thie point, that modification of an EED, in any way at all, ie likely to change the RF characterietice of the device to eome extent. This ie particularly true at very high frequencies euch as 1 to 10 Gc. Therefore, all currently known methode for instrumenting an EED at the bridgewire tend to degrade the device to

the function of a "simulated" version of the unmodified device. Results from our precision firing studies[1] have shown that the use of simulators is valid provided that the loss in the base of the EED is not excessive. One obvious method for estimating the amount of energy in a bridgewire is to compare the heating effect of applied RF energy with that of a known dc power. When the heating effect is the same for both, the two power levels are equal. The principle will be recognized as the "transfer technique" employed for precision ac measurements in standards laboratories.

The transfer technique is valid in principle when applied to the bridgewire of an EED, if we may safely assume that the same amounts of power (RF and dc) produce identical heating effects. If the bridgewire is small in diameter (.002 inch or less) and on the order of several tenths of an inch in length, we have every reason to believe that the above principle holds - at least up to frequencies of 1000 megacycles. We have therefore employed this principle during most of our current RF firing tests. Such a test will be very briefly described in the following paragraphs.

The case of the EED is cut open at the explosive end and the explosive material is removed to expose the bridgewire. The EED is then installed in a specially constructed RF mount. A light-tight housing containing a photo-conductive infrared detector is then placed over the mount to intercept radiation from the bridgewire. The mount and the housing used for tests of the MARK 1 MOD 0 squib are shown in the Figure 1.

The mount and detector assembly is then connected to a source of RF power. RF power sufficient to raise the bridgewire to a temperature roughly corresponding to the 50% RF firing level is then applied. The output of the infrared detector is noted. The mount is then disconnected from the RF system and connected to a variable source of dc. The power is increased until the infrared detector has the same output as it did

for RF, when it is measured accurately using a Leeds and Northrup "K" pot. The transfer technique is fully described in one of our reports[1].

Our methods for comparing the heating effect of RF and dc energies in bridgewires are not unique since similar techniques are employed in various laboratories throughout the country. Thermocouples, bolometers, thermistors and photo-conductive as well as photo-voltaic detectors are utilized in this work. The complexity of the companion instrumentation for these detectors varies according to the sensitivity, stability and accuracy requirements imposed by each particular user.

In our own work, we have chiefly used infrared detectors to determine the amount of RF energy in a bridgewire when it is energized to the 50% firing level. When testing at this level there is no requirement for a highly sensitive detector and ultra-sophisticated instrumentation. Stability and repeatability of results are far more important than sensitivity. Two of the detectors which we have found most satisfactory will be described in this report along with pertinent details of the instrumentation necessary for their use.

While there are many types of photo-conductive detectors available that are responsive to light and infrared radiation, our discussion will be limited to several specific ones which we have used extensively. These detectors are the Clairex CL-404 and the Ektron type N-2 cells.

The CL-404 detector is a cadmium sulfide photo-conductive cell with a spectral response peak at 0.69 microns (6900 Angstroms). However, the response extends past 1 micron and into the near infrared region. This detector requires a minimum amount of instrumentation and is most useful for detecting radiation from a bridgewire whose temperature is near the glow point. The cells and further information regarding their characteristics may be obtained from the Clairex Corporation, 19 West 26th Street, New York 10, New York.

The Ektron N-2 detector is a lead sulfide cell with a peak spectral response at 2 microns. The useful response extends to abcut 3.5 microns. It is therefore useful for detecting radiation from bridgewires heated to temperatures well below the glow-point. However, it requires more elaborate instrumentation than the Clairex cell and is therefore less attractive for purposes which do not require the extra sensitivity. These cells and additional information regarding their characteristics may be obtained from the Eastman Kodak Company - Special Products Sales Section - Rochester 4, New York.

The instrumentation necessary with the Clairex CL-404 cell is relatively simple. This cell is photo-resistive and has a dark resistance on the order of thousands of megohms. The actual dark resistance for a particular cell will depend primarily on the voltage which is applied across the cell. Exposure to a bright light will lower this resistance to thousands of ohms. The resistance is typically around 500 kilohms when mounted above the glowing bridgewire of a MARK 1 MOD 0 squib. It is thus evident that an ordinary ohmmeter may serve as an output indicator for the cell when the bridgewire is at a relatively high temperature. A Triplett Model 630 multimeter has been used for this purpose in our work.

Bruceton tests with the MARK 1 MOD 0 squib and the MARK 2 MOD 0 ignition element indicate that these devices have a 50% firing temperature below that corresponding to a visible glow of the bridgewire. The ordinary ohmmeter proved inadequate for detecting radiation from the bridgewire when its temperature is at the actual firing level. We therefore designed an instrument which would satisfactorily detect the output of the cell at the firing level of the previously mentioned squib and ignition element. A schematic diagram of the instrument is shown in Figure 2. Figure 3 is a photograph of the instrument with a firing mount and photo-cell housing attached. Complete details will be found in Reference 1.

The instrumentation described above is unsuitable for detection of RF energy in bridgewire operated at temperatures very far below the 50% fire level. However, a similar but more sensitive instrument is currently under development for Picatinny Arsenal and preliminary details have already been reported[2]. This is a battery operated instrument intended primarily for field tests with EED's such as the M6 blasting cap, which are instrumented with the Clairex CL-404 detector. We have extended the capabilities of the Clairex cell-ohmmeter combination just about to the limit in this instance. We expect to detect a bridgewire temperature roughly corresponding to the 1% fire level of the M6 cap with this equipment.

A somewhat more intricate system of instrumentation is required with the Kodak-Ektron N-2 cells. These cells are photo-conductive and have a dark resistance which is very low compared with that of the Clairex cell. The resistance of the N-2 cells varies with the dimensions of the exposed sensitive area. Those we use have an exposed area 0.25 x 2.5 mm and have a nominal dark resistance of 60,000 ohms. Optimum results are obtained when a matched pair of the cells are used in a bridge circuit, where the effects of ambient temperature are cancelled. One cell only is then exposed to a source of chopped radiation, and the output of the bridge is amplified by a narrow band amplifier with a center frequency equal to the chopping rate. In our present work, however, a modulated bias is substituted for the chopped radiation.

A schematic diagram of our present system is given in Figure 4. Details of the operation of the system will be found in several of our reports[3]. This system is more sensitive than the one used with the Clairex cell, but it is cumbersome to operate during firing tests. We therefore use the other system for most of our work; there are instances, however, when this system can serve a very useful purpose. An example of this is when a bridgewire glows upon application of power but then

extinguishes, or if an arc occurs instead of bridgewire heating. The response of the Clairex detector with its ohmmeter indicator will not respond to these two conditions. In the Ektron cell system the output is displayed on an oscilloscope and a deflection in these two cases can be measured. We have found this application invaluable in determining why the sensitivity of some devices does not fit a predicted firing level. One word of caution should be spoken at this time. It should not be construed from this discussion that the Ektron cell can be used for evaluation of repetitive pulses applied to the bridgewire. This is not the case. The response of the cell is too slow and will integrate the pulses.

SUMMARY

The methods described in this paper will usually be found adequate for an estimate of the RF power dissipated in a bridgewire. The Clairex cell, with its electronic indicator, was employed for precision sensitivity studies of the MARK 1 MOD 0 squib and the MARK 2 MOD 0, ignition element. In this work, a repeatability of one or two percent was consistently observed. The error of measurement for frequencies up to 1000 Mc was at most ten per cent and was probably closer to 5 per cent. To obtain this type of accuracy, dc calibrations were made immediately following each individual RF measurement.

The more sensitive Ektron cell and bridge circuit was not found suitable for the above precision sensitivity studies. The system was not stable enough to produce consistently repeatable results. This was probably due to the fact that we substituted a 1000 cps modulating bias in place of the radiation chopper which the supplier of the cells recommends. Greater sensitivity, and stability, could no doubt be achieved if the radiation chopper and a narrow band amplifier were employed.

The majority of photosensitive devices are insensitive to the radiation from bridgewires which are heated below their visible emission point. Other types of detectors such as thermocouples and thermistors are sensitive to temperatures just above ambient. Therefore, when extreme sensitivity is required one may resort to detectors of this type. The sensitivity will probably be obtained with some sacrifice in repeatability and accuracy. The photosensitive detectors, however, have been adequate for most of the work at The Franklin Institute and are recommended when employed within their prescribed limitations.

REFERENCES

(1) Q-B1805-1 through 6, Paul F. Mohrbach, Robert F. Wood and John P. Warren, "Precision RF Sensitivity Studies" (Evaluation of MARK 1 MOD 0 Squib and MARK 2 MOD 0 Ignition Element) 1 February 1961 to 1 February 1962, Prepared for U. S. Naval Weapons Laboratory under Contract N178-7830.

(2) P-A2479-21, Paul F. Mohrbach and Melvin R. Smith, "Radio Frequency Studies on Electroexplosive Devices" (U) Contract DA-36-034-501-ORD-3373RD.

(3) P-A2301-21/P-A2479-3, P-A2301-22/P-A2479-4, and P-A2301-23/P-A2479-5, Paul F. Mohrbach and R. F. Wood, "RF Attenuating Materials Studies" (U) (The Franklin Institute, January, February and March 1961) Contract DA-36-034-501-ORD-3117RD.

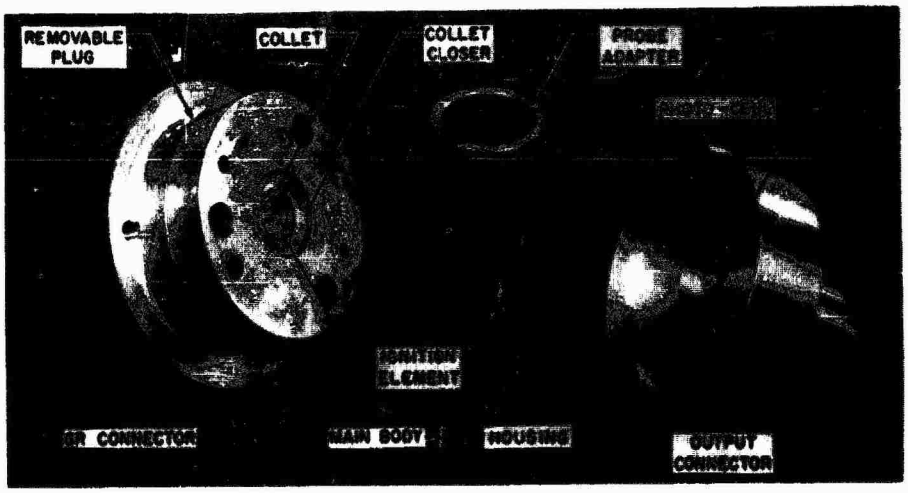

FIG. I. FIRING MOUNT AND PHOTOCELL HOUSING

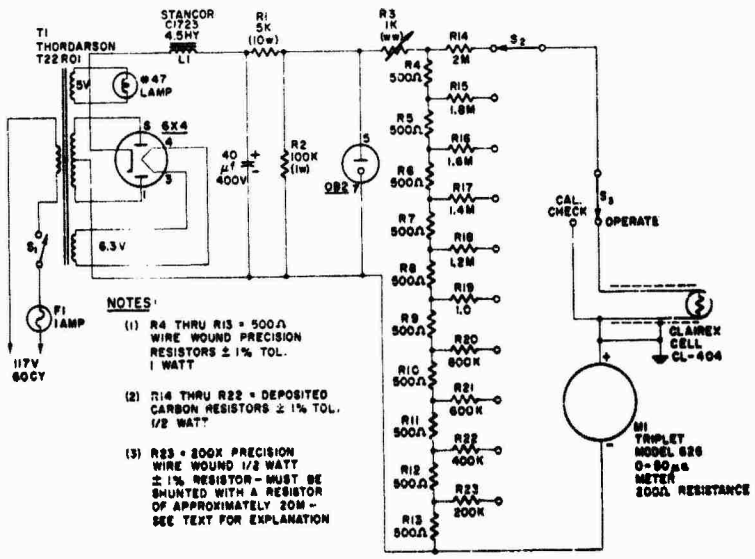

Fig. 2 Schematic Diagram – Clairex Cell Output Indicator And Power Supply

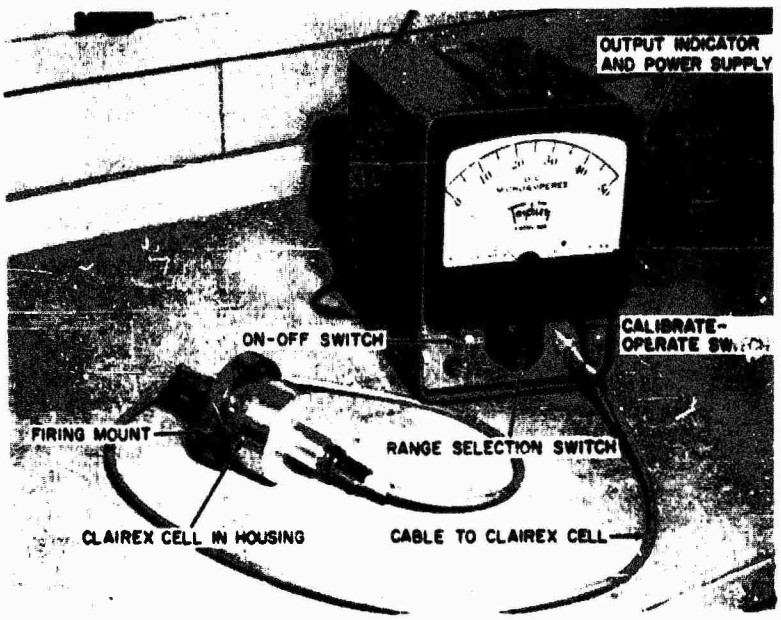

FIG. 3 CLAIREX CELL OUTPUT INDICATOR AND POWER SUPPLY

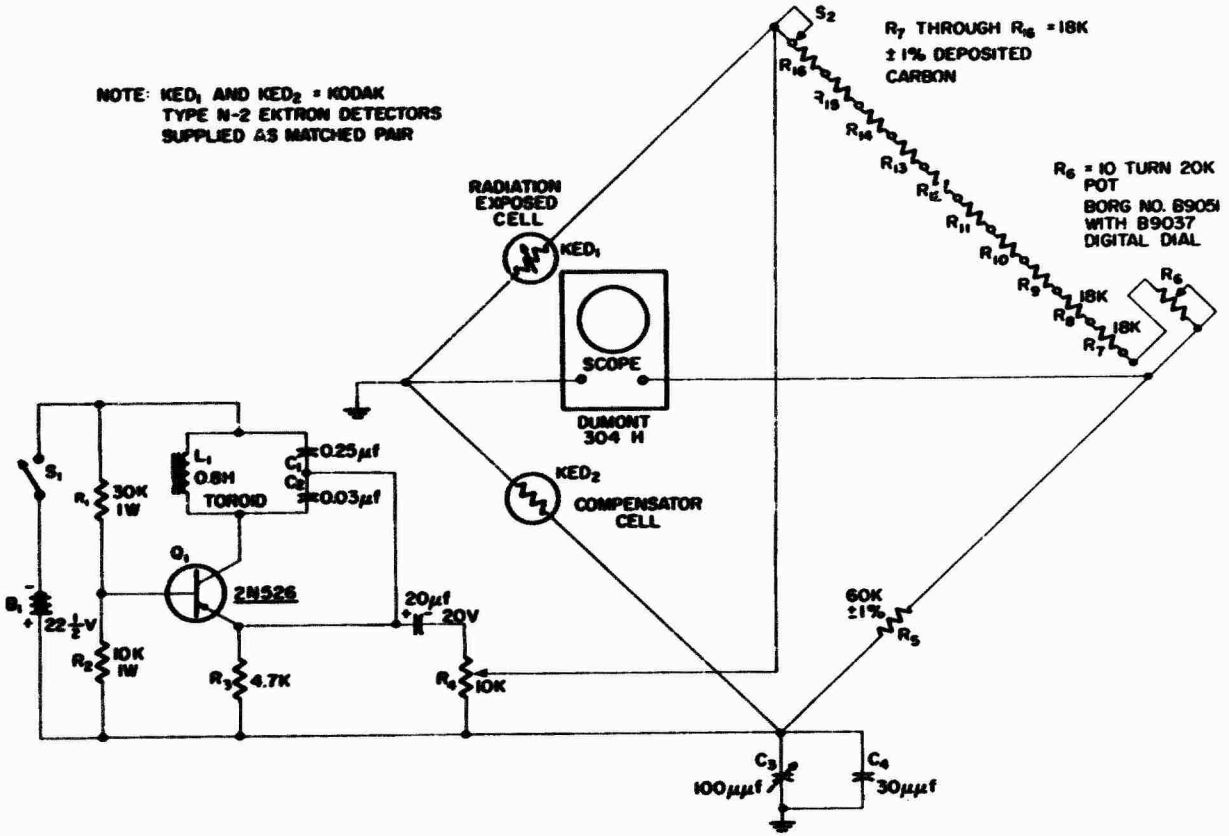

FIG. 4 INFRARED DETECTOR BRIDGE CIRCUIT

52. NON-ELECTRIC STIMULUS TRANSFER SYSTEMS AND THROUGH-BULKHEAD IGNITION

By Robert C. Allen
Product Manager
High Explosive Components and Systems
McCormick Selph Associates, Incorporated

ABSTRACT

Non-electric stimulus transfer systems (NESTS), incorporating completely contained mild or miniature detonating fuse and through-bulkhead detonation or ignition transfer units, can be designed to accomplish any number of one-shot functions from ignition and destruct to the actuation of valves and switches. Properly designed NESTS are completely insensitive to RF, stray currents, and other induced or even deliberately applied electric currents and also eliminate the need for primary explosive compositions, ground check-out equipment, and critical interface tolerances.

DISCUSSION

The purpose of this paper is to merely introduce the reader, by example, to the concept of a relatively unique non-electric stimulus transfer system (NESTS) followed by a more detailed discussion of through bulkhead ignition, a single application suited to the specific NESTS system described. It is hoped

that time will permit the compilation and publication at a later date of additional data concerning NESTS such as alternate systems, history of applications, design flexibility, reliability data, environmental tests, and components among other unclassified information.

Of course, the basic concept of NESTS is not new as evidenced by the percussion fired high pressure gas emergency escape systems used in some aircraft or consider the simple and, by far, the more antiquated rope and pully. We will restrict the present discussion to a NESTS which utilizes only a detonation stimulus. Again the basic concept is not new, for example, commercial detonating fuse, such as "Cordeau" and "Primacord", has been used for years to initiate multiple explosive charges for both Military demolition and commercial blasting applications. The NESTS discussed herein, however, is unique in that the detonating fuse used to transmit the stimulus is completely confined so that no shrapnel or other potentially hazardous, particles are generated when the material detonates.

The subject NESTS is designed to utilize only mild detonating fuse (MDF) type A2 or B2 completely confined. The confined MDF incorporates 2 grains of PETN or RDX high explosive per linear foot contained in a 0.040" diameter flexible metallic tubing. The tube, in turn, is covered by plastic and fabric reinforcing material sufficient in strength to contain all the shrapnel and potentially hazardous products of combustion generated by the detonating high explosive core. The material may be passed through crews quarters or near delicate

instruments and detonated without endangering personnel or damaging equipment. The confined MDF has an outside diameter of approximately 0.3" and a detonating velocity of approximately 23,000 feet per second which is reproducible to ± 1% within a lot. The tensile strength of the confined MDF is in excess of 250 pounds. Also, the confined MDF will reliably propagate a detonation through tight knots or similar kinks, loops, or twists that may be inadvertantly introduced into the assembly during installation.

Figure 1 shows a typical NESTS designed to accomplish three specific functions in a single completely redundant system, or partially redundant dual system. Consider, for example, a dual system, illustrated on Figure 1, involving two large solid propellant booster rocket motors attached to a liquid propellant sustainer motor. The booster motors are to be separated from the sustainer motor at a predetermined time. In such a system functions A, B, and C, referred to in Figure 1, may correspond to thrust neutralization, booster disconnect, and booster separation, respectively. The confined MDF is incorporated into the representative NESTS to multiply and transmit the detonation stimulus generated by a single redundant initiator, such as a conventional safe/arm to accomplish functions A, B, and C, for both booster motors.

The confined MDF is supplied for the representative NESTS as an assembly of the type shown on Figure 2, detail A. Both ends of each assembly will terminate in a standard, interchangeable, quick disconnect end closure. The interchangeable quick disconnect may be connected to, or disconnected from, any mating receptacle by a simple push-and-turn

action similar to that used to operate some standard electrical connectors. Once properly attached to a mating receptacle the confined MDF assembly may be safetied in place to preclude inadvertantly breaking the continuity of the NESTS explosive train. In the event it is desirable to code the connector to the function, the connector size and/or pin location can be varied in a manner similar to that used to code electrical connectors.

The confined MDF assembly for the representative NESTS is designed to be assembled with inert hardware to manifold or initiate multiple lengths of confined MDF from one input. Typical examples of the inert manifold receptacle assembled with confined MDF assemblies are shown on Figure 2. The incoming detonation from any one of the confined MDF assemblies will initiate the remaining assembled MDF assemblies connected to the manifold receptacle.

A pyrotechnic delay manifold, shown on Figure 1 detail, is provided to separate functions A, B, and C with respect to time. Conventional pyrotechnic 100 ms to 200 ms delays are accurate to only approximately ± 20% through a temperature range of -60 to +160°F. It is within the present state-of-the-art, however, to produce 100 to 200 ms delays reproducible to approximately ± 1% through this temperature range. Reproducibility of ± 1/2% already is being realized through this temperature range using previously developed 50 ms pyrotechnic delays. Depending on the accuracy demanded by the application either type pyrotechnic delay can be used.

A variety of previously developed or designed and tested

components and assemblies are available for accomplishing each of the functions mentioned for the representative NESTS. Typical examples are as follows:

Thrust Neutralization

1. MDF initiated explosive bolts or nuts to release thrust neutralization port covers.
2. MDF initiated linear shaped charge systems for severing burst diaphragm port covers, or actually cutting the motor case.
3. MDF fragmented sector used in conjunction with a spring loaded port retainer ring.

Booster Disconnect

1. MDF initiated explosive bolts or nuts to release points of attachment.
2. MDF initiated linear shaped charge systems for severing attachment structures.
3. MDF separation systems involving the impulsive loading of linear piston arrangements retained by shear pins.
4. MDF initiated pin pullers, pistons, or other cartridge actuated device, by application of through bulkhead ignition components (See Appendix "A").

Booster Separation

1. MDF or "Pyrocore" through-nozzle ignition of solid propellant rocket thrust motors.

(Booster Separation, continued)

2. MDF initiated rocket motor or cartridge actuated device by application of through-bulkhead ignition components.

All of the described MDF initiated components and systems, for accomplishing the described functions, except the through-bulkhead components, have previously been developed or designed and tested for various applications in several rockets and missiles including, among others, the Minuteman, Nike Zeus, Eagle, Davy Crockett, Polaris, Skybolt, Saturn, Project Mercury, Samos, Pershing, and many AEC systems.

The feasibility of through-bulkhead ignition components has been proven by tests performed utilizing (1) a shock-transfer type system incorporating a solid steel bulkhead integral with the igniter and (2) a self-sealing type system incorporating a compressed or compressible resilient material to automatically seal the path of the detonating MDF. The details of the through-bulkhead component tests and design approaches are discussed in Appendix "A" to this paper.

Typical NESTS System Performance and Advantages

Referring to Figure 1, the application of a proper "Fire" signal to the armed safe/arm initiator will initiate the safe/arm-to-delay manifold confined MDF assembly. The detonation thus initiated will propagate to and, for function "A", directly through the delay manifold at a velocity of approximately 23,000 feet per second. If the assembled MDF system is properly designed so that all "A" function events are equal in over-all detonation path length from the safe/

arm initiator and this length does not exceed 200 feet, then all twelve (12) "A" events will be initiated with a simultaneity of approximately ± 0.1 millisecond.

Functions "B" and "C" will be delayed approximately 0.1 second 0.2 second respectively before the shorter tolerance delay in each of the two parallel delay cartridges will initiate the remaining confined MDF assemblies. No shrapnel or hazardous blast effects will be generated by the detonating NESTS.

Some of the advantages to be realized by adopting NESTS of the type represented by Figure 1 and 2 and through-bulkhead igniters of the type described in Appendix "A", in place of conventional electroexplosive devices or other "one-shot" electrical systems, include the following:

1. Considering only the integral bulkhead type detonation transfer assembly, Appendix "A", the system, properly applied, can eliminate the need for drilling, tapping, or otherwise disturbing the hermetic seal or unit construction of rocket engine cases, or other pressure vessels to accomplish ignition or stimulus transfer.

2. The complete elimination of ground check-out equipment and procedures, except for simple visual inspection.

3. The complete elimination of primary high explosive and, in turn, associated problems of safety and transportation. In fact, the most temperature and shock insensitive explosive and pyrotechnic compositions known

3. (cont'd)
may be utilized effectively in NESTS.

4. System and component design simplicity unmatched by any previous electroexplosive or electric system or component resulting in a proportionate increase in reliability.

5. This design simplicity also renders the system and components amenable to economic mass production techniques.

6. The developed component designs may be easily standardized and can be utilized for all ignition and detonation applications.

7. The utilization of the rapid and reproducible detonation phenomenon will give extreme ignition reproducibility and, when properly interconnected, simultaneity that cannot be approached by conventional electroexplosive igniters. Only properly designed exploding bridgewire or arc fired igniters can approach the performance of the through-bulkhead igniters at the expense of system weight, volume, and simplicity.

8. The inherent insensitivity of the through-bulkhead transfer components will allow them to be installed and sealed into the missile or booster system during production assembly eliminating the need to disturb hermetic seals in the field.

9. Because the igniters are non-electric, they are

(9. cont'd)

completely insensitive to RF, stray currents, or other induced or even deliberately applied electrical currents.

10. Because the proposed igniters incorporate all activation energy in the form of a potential chemical reaction, no supplementary power or impulse sources and accessories in the form of batteries, generators, capacitors, switches, piezo cells, etc., are required.

11. The system is unaffected by environmental extremes of altitude, humidity, vibration, shock, and low temperature.

12. Electric circuitry and accessories with the attendant problems of improper, corroded, and loose connections, and contacts are completely eliminated.

13. Unlike electroexplosive systems, firing the proposed non-electric system will, in turn, generate no RF or other spurious electrical signals.

14. The performance of the system is dependent on the proper initiation and reaction of a very minimum variety of detonating and deflagrating compositions instead of a complex chain of reactions for each event, i.e., bridgewire, to primer, to booster, to base charge, etc.

APPENDIX "A"

THROUGH-BULKHEAD INITIATORS

McCormick Selph Associates, Inc., recently completed a study program for North American Aviation to determine the feasibility of transmitting a non-electric stimulus generated by contained explosive energy, through a bulkhead and initiate a pyrogen rocket igniter, without jeopardizing the integrity of the bulkhead seal.

Two TBI design approaches were investigated, (1) a detonation shock-wave transfer system incorporating a solid steel bulkhead as an integral part of the igniter assembly as illustrated by Figure 3 and (2) a self-sealing type system incorporating a compressed or compressible resilient material to automatically seal the path of a detonating length of mild detonating fuse (MDF) as illustrated by Figure 4.

Each concept is discussed separately along with the significant test results generated during the referenced feasibility study.

Shock Wave Transfer System

The through-bulkhead transfer assembly shown on Figure 3 is designed to transmit a detonation shock wave through a solid steel bulkhead and initiate a deflagration on the opposite side without perforating the bulkhead or otherwise destroying the integrity of the seal.

Detonation of the MDF and retainer booster charge will initiate, in turn, a small PETN or RDX charge on one side of a metal diaphragm machined into, as an integral part of, the igniter main body.

Sufficient energy will remain in the detonation shock wave, which is transmitted through the metal diaphragm and emerges from the side opposite the booster charge, to initiate the detonation of a PETN pickup charge. For the evaluated design the shock from the pickup charge was attenuated and ignited, in turn, a boron/potassium nitrate ignition pellet.

The feasibility study of the shock wave transfer system involved a total of 23 tests which investigated various parameters affecting the transfer mechanism as well as confined MDF quick disconnect assemblies. The results of all tests are included in Table I.

Although the assembly shown on Figure 5 was the most optimum design evaluated, interface problems introduced in the internal construction of the unit resulted in inconsistant results.

The final evaluated design eliminated all but an absolute minimum explosive-to-metal and metal-to-metal interfaces and the test results indicated that the assembly was functionally reliable. Due to the limited scope of the program only three assemblies having the final functional configuration were tested.

The final test assembly was further designed to attenuate

TABLE I

SHOCK WAVE TRANSFER THROUGH-BULKHEAD DESIGN (FIGURE 3)

Test No	Cumulative Bulkhead Thickness (in.)	Donor Charge	Condition of Bulkhead after firing	Receptor Charge	Output Results
1	0.200	65 mg PETN	Undamaged	Mc/S/A #147 propellant	No deflagration
2	0.200	65 mg PETN	"	Pellet of PETN	No deflagration
3	0.075	65 mg PETN	Ruptured	Mc/S/A #147 propellant	No deflagration
4	0.075	65 mg PETN	"	Pellet of PETN	No deflagration
5	0.103 Maximum	65 mg PETN	Undamaged	X-349 Mild Detonator	Detonation
6	0.103 "	65 mg PETN	Bulged	X-349 (Standoff .050")	Detonation
7	0.128 "	75 mg PETN	Undamaged	X-349 Mild Detonator	Detonation
8	0.128 "	75 mg PETN	"	" " "	Detonation
9	0.148 "	115 mg PETN	"	X-349 + 165 mg Mc/S/A 147	PETN donor failed to detonate.
10	0.148 "	115 mg PETN	"	" " " "	**Detonation to deflagration.
11	0.148 "	X-349 PETN Primer	"	" " " "	** " "
12	0.148 "	" " "	"	" " " "	** " "
13	0.148 "	" " "	"	" " " "	Failed (No output)
14	0.148 "	" " "	"	" " " "	" " "
15*	0.148 "	" " "	"	" " " "	" " "
16	0.148 "	75 mg PETN	"	" " " "	" " "
17	0.148 "	" " "	"	" " " "	" " "
18	0.148 "	" " "	"	" " " "	**Detonation to deflagration.
19	0.148 "	" " "	"	" " " "	Failed (No output)
20	0.148 "	" " "	"	" " " "	" " "
21	0.123+.002"	" " "	"	135 mg PETN + 1015 mg 147	**Detonation to deflagration.
22	0.123+.002"	" " "	"	" " " "	" " "
23	0.123+.002"	" " "	"	" " " "	" " "

NOTE: * shot fired at 250 F.
** X-349 or PETN receptor charge detonated and Mc/S/A 147 deflagrated satisfactorily.

the detonation of the PETN receptor charge and ignite a pressed pellet of boron/potassium nitrate ignition composition. For these specific tests the quick disconnect assembly was not evaluated, instead an X-349 crimped to plain 2 grain per foot PETN core MDF was used to initiate the PETN donor charge. Each unit was fired into a 25 cc closed chamber. The results of this series of tests are as follows: (Also see Table I).

Test No.	*Start of Rise (milliseconds)	**Rise to Peak (milliseconds)	Peak Pressure PSI
21	10.0	40.0	1200
22	11.5	30.5	1275
23	11.5	38.5	1375

* Time from application of current to a standard blasting cap, attached to the MDF, and start of pressure rise within the closed chamber.

** Total time from start of pressure rise to peak pressure.

In all units the shock wave from the detonating donor charge propagated through the bulkhead and initiated the receptor charge the detonation of which, in turn, initiated the deflagration of the boron/potassium nitrate pellet. Attenuation of the detonation is evidenced by the slow pressure rise characteristic of a deflagrating pellet of propellant. Without proper attenuation the shock wave would have pulverized the ignition pellet resulting in a very sharp pressure rise. The fired units later were tested for bulkhead integrity by

applying 3,000 PSI to the output side of each unit. No evidence of leakage was detected.

One of the cross-sectioned fired assemblies is shown on Figure 6. The transfer resulted in no detectable damage to the integral bulkhead. The bulkhead was 0.123" thick.

Self-Sealing Through-Bulkhead System

The concept of the self-sealing through-bulkhead initiator is represented on Figure 4. Detonation of the quick disconnect booster by the confined MDF will, in turn, initiate a short length of .040" diameter plain 2 grain per foot MDF permanently assembled into the main body of the transfer assembly. Previous tests have proven that the output of properly initiated 2 grain MDF will reliably and reproducibly initiate certain deflagrating charges or detonate some other charge such as a second length of MDF. For instance, 2 grain per foot MDF is easily capable of initiating the deflagration of aluminum/potassium perchlorate or boron/potassium nitrate ignition compositions.

A highly compressed resilient packing gland is incorporated into the self-sealing unit so that the perforation left by the detonating MDF will automatically close or collapse immediately following the detonation creating a positive leak-proof barrier.

The feasibility of the self-sealing transfer system was proven by application of the relatively crude test fixture shown on Figure 7. After proving that the assembly would

the detonation of the PETN receptor charge and ignite a pressed pellet of boron/potassium nitrate ignition composition. For these specific tests the quick disconnect assembly was not evaluated, instead an X-349 crimped to plain 2 grain per foot PETN core MDF was used to initiate the PETN donor charge. Each unit was fired into a 25 cc closed chamber. The results of this series of tests are as follows: (Also see Table I).

Test No.	*Start of Rise (milliseconds)	**Rise to Peak (milliseconds)	Peak Pressure PSI
21	10.0	40.0	1200
22	11.5	30.5	1275
23	11.5	38.5	1375

* Time from application of current to a standard blasting cap, attached to the MDF, and start of pressure rise within the closed chamber.

** Total time from start of pressure rise to peak pressure.

In all units the shock wave from the detonating donor charge propagated through the bulkhead and initiated the receptor charge the detonation of which, in turn, initiated the deflagration of the boron/potassium nitrate pellet. Attenuation of the detonation is evidenced by the slow pressure rise characteristic of a deflagrating pellet of propellant. Without proper attenuation the shock wave would have pulverized the ignition pellet resulting in a very sharp pressure rise. The fired units later were tested for bulkhead integrity by

applying 3,000 PSI to the output side of each unit. No evidence of leakage was detected.

One of the cross-sectioned fired assemblies is shown on Figure 6. The transfer resulted in no detectable damage to the integral bulkhead. The bulkhead was 0.123" thick.

Self-Sealing Through-Bulkhead System

The concept of the self-sealing through-bulkhead initiator is represented on Figure 4. Detonation of the quick disconnect booster by the confined MDF will, in turn, initiate a short length of .040" diameter plain 2 grain per foot MDF permanently assembled into the main body of the transfer assembly. Previous tests have proven that the output of properly initiated 2 grain MDF will reliably and reproducibly initiate certain deflagrating charges or detonate some other charge such as a second length of MDF. For instance, 2 grain per foot MDF is easily capable of initiating the deflagration of aluminum/potassium perchlorate or boron/potassium nitrate ignition compositions.

A highly compressed resilient packing gland is incorporated into the self-sealing unit so that the perforation left by the detonating MDF will automatically close or collapse immediately following the detonation creating a positive leak-proof barrier.

The feasibility of the self-sealing transfer system was proven by application of the relatively crude test fixture shown on Figure 7. After proving that the assembly would

seal against 1,700 psi following detonation at ambient conditions similar units were tested using a high temperature, high pressure test fixture of the type shown in Figure 8.

The specific test procedure was as follows, presented in the sequence each function was performed:

1. Calibrate the transducer for the pressure monitoring apparatus.
2. Pressurize chamber and check for any leaks in the system.
3. Record the pressure at 5 minute intervals for 10 minutes.
4. Take a continuous reading of pressure while the part was actually being fired.
5. Turn on induction furnace for 20 minutes.
6. Record the pressure at 5 minute intervals for 20 minutes.

During test No. 7 the MDF failed to initiate due to improper application of the test initiator. The test was re-run as test No. 8. Immediately after firing the MDF pressure losses were noted and the test was discontinued. It is not known if the abortive attempt to initiate the MDF during test No. 7 influenced the results of the re-test No. 8.

Because of the thermal expansion of the confined nitrogen the pressure increased within the chamber during tests No. 4, 5, 6, and 9 when the induction heater was energized. As expected the pressure dropped after the heater was turned off and the test fixture and nitrogen cooled, test No. 6. The results of these tests are shown on Figure 9.

In each test, discounting No. 7 and 8, although the resilient packing was damaged by the long application of intense heat, the test assembly did not leak. It is estimated from the color changes and oxidized condition of the metal surface that the test fixture containing the resilient packing attained temperatures approximating 1,000°F during this extreme 20 minute test. The tungsten rod attained a temperature of approximately 2,000°F.

Considering that the assembly shown on Figure 4, in an actual application, will be exposed to extreme pressures and temperatures for only 20 seconds to 2 minutes maximum duration, these tests prove without a doubt the feasibility of transmitting a detonation through a bulkhead by the proposed self-sealing method. The main advantages of this system include (1) it is not limited to a maximum bulkhead thickness; (2) multiple systems, for redundancy can be incorporated without seriously sacrificing component size; and (3) it requires an absolute minimum total explosive charge to achieve reliable transfer.

It is expected that a number of materials and construction methods can be adapted to successfully accomplish this particular means of detonation transfer.

It is significant to note that both of the final evaluated through-bulkhead NESTS igniters evaluated during this feasibility study are readily adaptable to generating either an ignition or detonation on the sealed side of the bulkhead without destroying the integrity of the bulkhead seal.

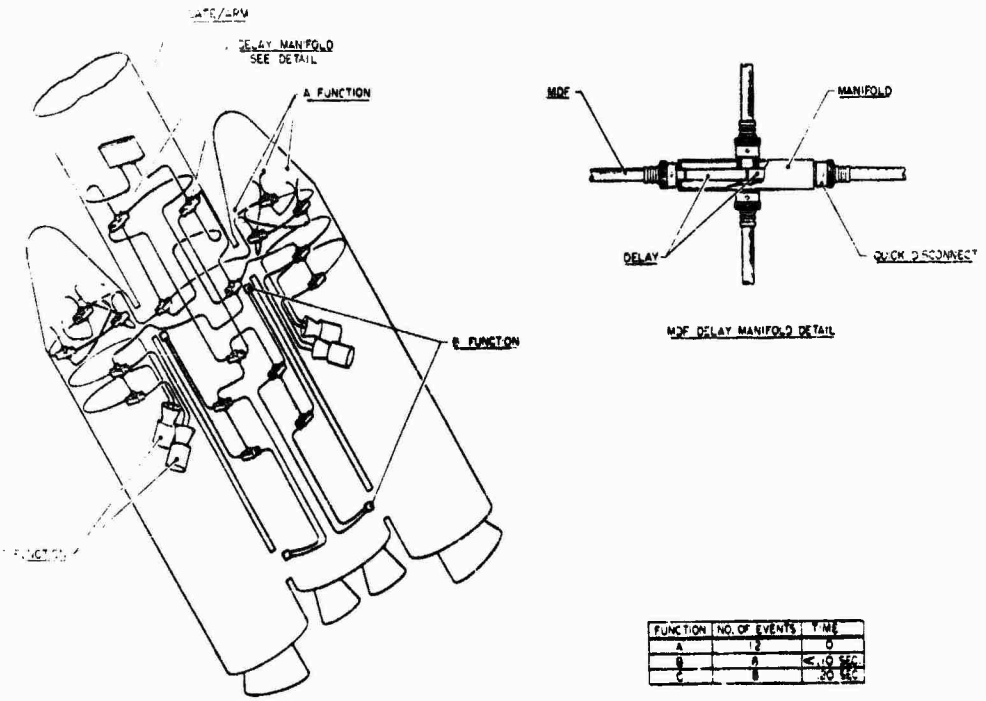

MDF NON ELECTRIC STIMULUS TRANSFER SYSTEM

FIG I

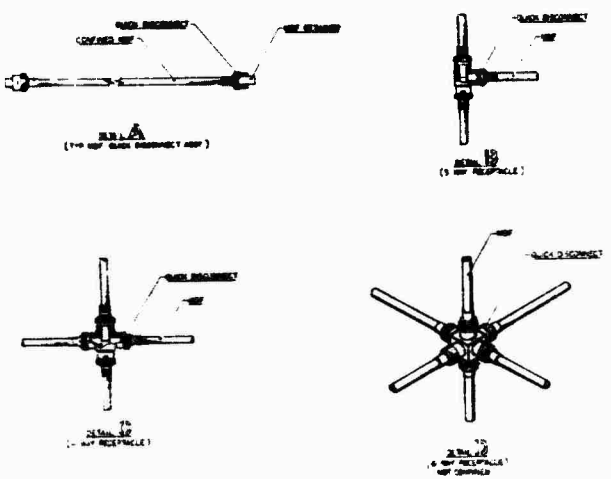

FIG 2

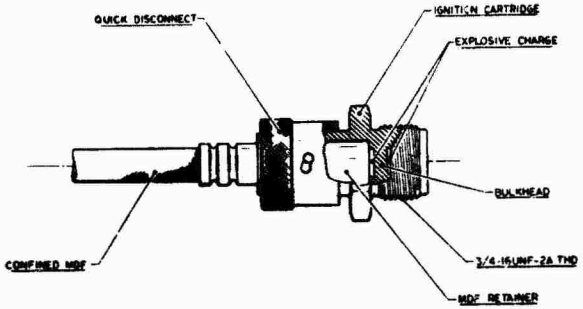

DETONATION / DEFLAGRATION SHOCK TRANSFER SYSTEM

FIG 3

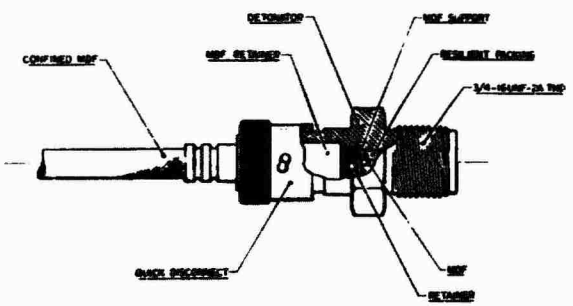

DETONATION TRANSFER ASSY., SELF SEALING (HIGH PRESSURE)

FIG 4

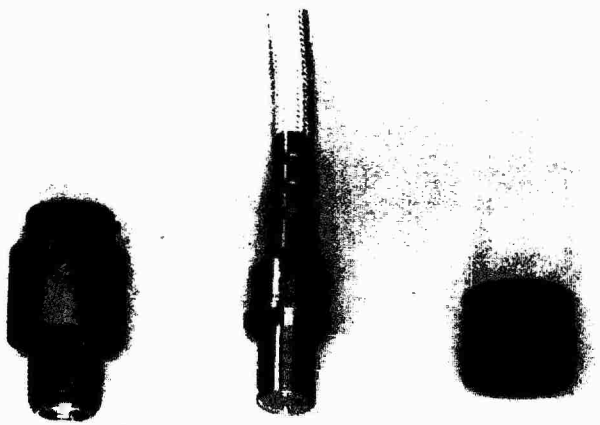

Body Retainer Quick Disconnect

FIG. 5

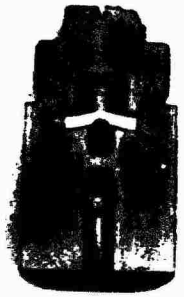

Test No. 22

Enlarged View of the Central Section of a Test Unit Showing Structural Integrity after a Donor Explosive Charge Initiated a Receptor Deflagrating Charge through a Steel Bulkhead

FIG. 6

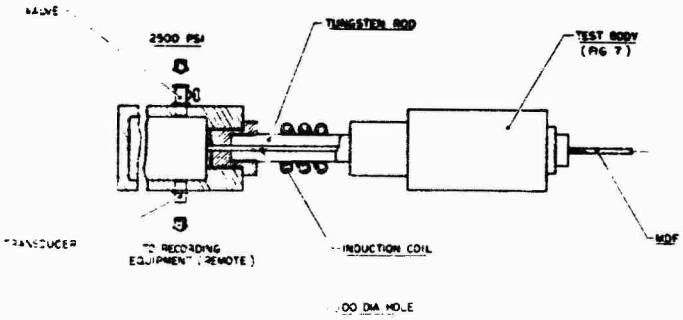

FIG 8

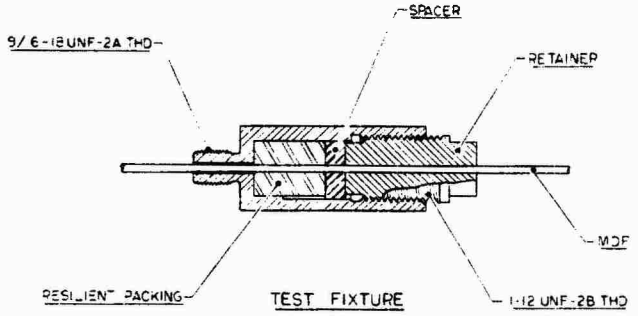

FIG 7

FIGURE 9

DATE: 7 September 1962 TEST NO. B-3297

Test No.	Nitrogen Pressure	After 5 Min.	After 10 Min.	Induction Heat On	After 5 Min.	After 10 Min.	After 15 Min.	After 20 Min.	Induction Heat Off	After 5 Min.
(4)	2200	2200	2200	2200	2350	2455	2700			
(5)	1930	1930	1930	1930	1965	2165	2295	2430	2430	2170
(6)	1840	1840	1840	1840	1915	2040	2190	2315	2315	
(7)*	1700	1700	1700	1700	1700					
(8)**	1700									
(9)	1675	1675	1675	1675	1750	1850	1960	2045	2045	
		(1)		(2)						

NOTES:

1. Bomb pressurized for 10 minutes prior to firing part.
2. Part was fired, and induction heater was turned on. Pressure was read every 5 minutes for 20 minutes.

* MDF failed to initiate due to improper application of end primer.
** Pressure trace lost, leak developed immediately after firing.

54. EMR HAZARDS TO EEDS

by

Lt. Colonel Reuben B. Moody
Directorate of Missile Safety

Concern over electromagnetic radiation hazards to electro-explosive devices (or EEDs) arises from the fact that electrical leads to an EED can, under certain conditions, act as an antenna. There have been incidents, albeit very few, when leads to an EED have abstracted sufficient energy from an electromagnetic field environment to cause inadvertent detonation.[1]*

The equivalent circuit of a receiving antenna is represented by Figure 1.

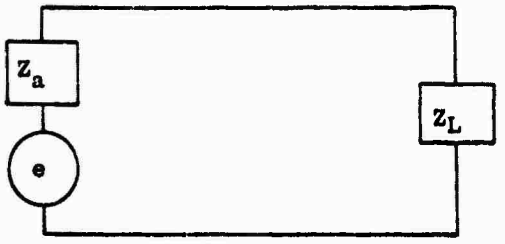

Z_a = Antenna Impedance
Z_L = Load Impedance
e = Induced emf

Figure 1 - Equivalent Circuit of a Receiving Antenna. (2) (3)

When an antenna length precisely accommodates a particular wave length it becomes a resonant circuit, and its impedances become pure resistances. Therefore, the equivalent circuit for a resonant antenna reduces to that indicated by Figure 2.

*Parenthetical numbers refer to the bibliography listed at the end of this paper. Footnote numbers also refer to bibliography.

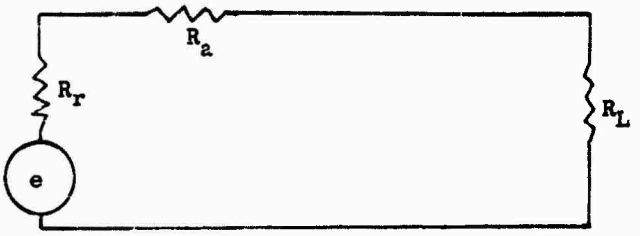

R_r = Radiation resistance
R_a = Antenna Loss resistance
R_L = Load resistance
e = Induced emf

Figure 2. Equivalent Circuit of a Resonant Receiving Antenna

The radiation resistance shown in Figure 2 is a fictitious quantity resistance which indicates the radiation properties of the antenna. It is defined as a resistance which, if inserted in the antenna circuit with current flowing, would dissipate the same energy as is actually radiated by the antenna.(2) (3) The antenna loss resistance is a lumped quantity to account for losses which arise from the presence of earth, the RF ohmic resistance of the antenna wires, dielectrics in the neighborhood, etc. (3)(4)

The total power (P_t) that a receiving antenna abstracts from an electromagnetic field can be determined by the equation:

$$P_t = \frac{(Eh)^2}{R_L + R_r + R_a} \quad \ldots\ldots\ldots\ldots \text{I}$$

where E = field strength (r.m.s. value) of the electromagnetic field in volts per meter;
h is the effective height of the antenna;
R_L, R_r, and R_a are defined by Figure 2. (3).

Of the total power abstracted from the environment a fraction is re-radiated by the antenna. Another fraction is dissipated through the antenna loss resistance, and a third fraction is delivered to the load. This latter or third fraction is represented by the ratio $R_L/(R_L + R_a + R_r)$.

The power delivered to the load (P_L) can therefore be determined by multiplying equation I by this ratio.

$$P_L = \frac{(Eh)^2 R_L}{(R_L + R_a + R_r)^2} \quad \ldots\ldots\ldots\ldots \text{II}$$

It can be shown mathematically that maximum power is transferred to the load resistance when $R_L = R_r + R_a$. In this case the resistances are "matched" and the antenna is operating at maximum efficiency.

Antenna configurations most likely to be assumed by an EED and its leads are a half-wave dipole, a quarter-wave grounded stub, or a short-stub antenna (e.g., where the antenna length is 1/20th the wave length). These possible configurations are shown in Figure 3.

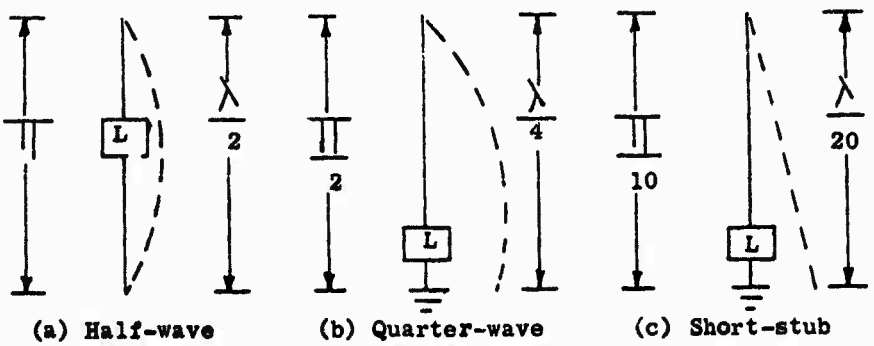

(a) Half-wave (b) Quarter-wave (c) Short-stub

L = Antenna load
λ = Wave length
--- = Current distribution

Figure 3. Antenna Configurations

For a half wave dipole or doublet antenna, the radiation resistance is 73.2 ohms and the effective height (h) is λ/π .(2)(6) The volts per meter field strength can be expressed as a power density (P_d = watts per square meter) by the relationship $E^2 = 120\pi P_d$.(7) Also, the antenna loss resistance can be considered negligible.[4] Substituting these values in equation II yields the power delivered to the load of a resonant dipole antenna.

$$P_L \text{ (dipole)} = \frac{120\, P_d\, \lambda^2\, R_L}{\pi (R_L + R_a + R_r)^2} \quad \ldots\ldots \text{III}$$

The bridgewire resistance of an EED may be considered as the load resistance of an antenna when the leads are configured as a half-wave dipole as indicated in Figure 3. Ordinarily the bridgewire resistance is something less than

one ohm and, consequently, is very much less than the radiation resistance of 73.2 ohms. Equation II can therefore be approximated by the simpler expression:

$$P_L \text{ (dipole)} = (7.2 \times 10^{-3})\, P_d \lambda^2 R_L \quad \ldots\ldots\ldots \text{IV}$$

Also, $P_L = I_L^2 R_L$, so that

$$I \text{ (dipole)} = \sqrt{(7.2 \times 10^{-3})\, P_d \lambda} \quad \ldots\ldots\ldots\ldots \text{V}$$

Similarly, for a quarter-wave grounded antenna with the load located at the grounded end (Figure 3b), the radiation resistance is about 38 ohms and the effective height of the antenna is $\lambda/2\pi$.[3] If, again, the antenna loss resistance is considered negligible and the bridgewire resistance is very much less than the load resistance, then equation II simplifies to:

$$P_L \left(\lambda/4\right) = (6.6 \times 10^{-3}) P_d \lambda^2 R_L \quad \ldots\ldots\ldots\ldots \text{VI}$$

$$\text{and, } I \left(\lambda/4\right) \quad \sqrt{(6.6 \times 10^{-3}) P_d \lambda} \quad \ldots\ldots\ldots \text{VII}$$

Equations IV, V, VI and VII are valid only when R_a is negligible and R_L is very much less than R_r. With these conditions in mind the equations permit the conclusions that (a) the power delivered to the load is directly proportional to the intensity of the electromagnetic field environment, the square of the wave length, and also to the ohmic value of the load resistance; and (b) the current through the load resistance is independent of the value of the load resistance.

For the short-stub grounded antenna (see Figure 3c) the load resistance can no longer be considered as very much less than the radiation resistance. In this case the radiation resistance is only one ohm and the effective height of the antenna is $0.5\,\lambda/20$.[6] If the antenna loss resistance is negligible equation II becomes:

$$P_L \left(\lambda/20\right) = \frac{0.24\, P_d \lambda^2 R_L}{(R_L + 1.0)^2} \quad \ldots\ldots\ldots \text{VIII}$$

$$\text{and, } I \left(\lambda/20\right) = \sqrt{\frac{0.24\, P_d \lambda}{(R_L + 1.0)}} \quad \ldots\ldots\ldots\ldots \text{IX}$$

Equations IV, ~~III~~ VI AND ~~IX~~ VIII are plotted in Figure 4 for the case where the bridgewire resistance is one ohm and

Figure 4. Power delivered by a resonant antenna to a one ohm load; when P_D = 100 watts per square meter, L = antenna length, λ = wave length and f = megacycles.

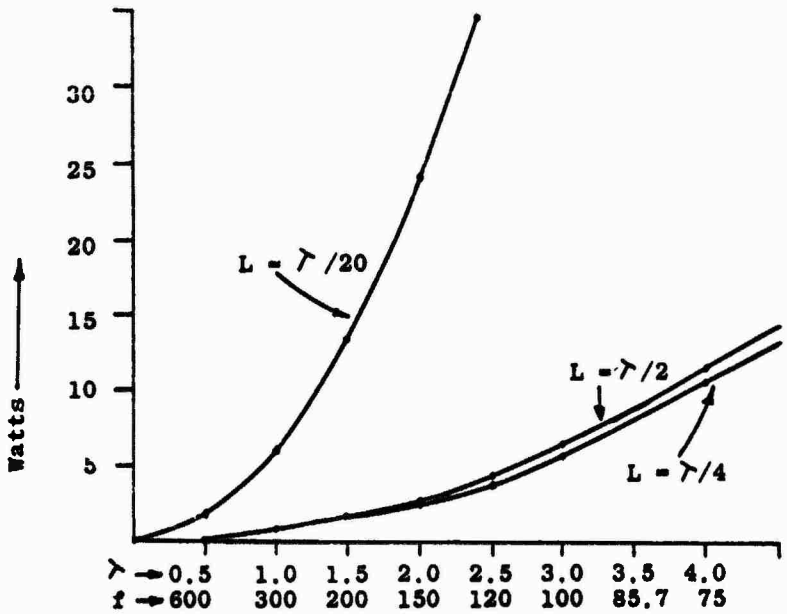

for the 100 watts per square meter considered to be the biological hazard level of an electromagnetic field.[3] Since most EEDs have a power dissipation capability of less than one watt, the power levels indicated by the equations and the graph are quite formidable. However, these power levels represent the worst case predicated upon an ideal antenna and optimum conditions. The validity of these values depend on a most improbable chain of circumstances.

a. The EED must be immersed in a very strong electromagnetic field.

b. The leads to the EED must be exposed and configured as an antenna.

c. The EED itself must be configured as an antenna load.

d. Leads must be of a precise length to provide a resonant circuit for the wave length of the electromagnetic field.

e. Leads must be oriented in a three-dimensional space in order to accommodate the polarization and directivity of the electromagnetic field.

Deviation from any of the above conditions will diminish the magnitude of power transferred to the EED bridgewire. It is extremely improbable the several conditions can be accidentally met to the extent an inadvertent detonation occurs. An extensive research covering more than a decade[1] has revealed only a handful of confirmed incidents wherein EEDs have been accidentally detonated by electromagnetic radiation. More to the point, in 1956 the Institute of Makers of Explosives published a pamphlet[5] which states, in part:

> "From a practical viewpoint, the possibility of premature explosion due to RF energy is extremely remote. This has been demonstrated by numerous tests on representative transmitting equipment, and it is confirmed by many years of experience. The annual consumption of electric blasting caps is well over 100 million, and they are used in every section of the country. Yet there have been only two authenticated cases of a cap being accidentally fired by radio."

Notwithstanding the improbabilities, incidents have occurred and, because of the possibility of catastrophe, protective or safety measures should be taken.

a. The power density of an electromagnetic field decreases as the square of the distance from the radiating source. Therefore, published distance tables (5) (9) should be observed insofar as is operationally possible. This is particularly true for long wave lengths or low frequencies.

b. To decrease the susceptability of EEDs, design criteria should require the largest possible no-fire current that is compatible with the EED application. However, the susceptability is not necessarily decreased by increasing the bridgewire resistance. The equations show that an ideal bridgewire resistance (insofar as protection against electromagnetic radiation is concerned) would have either an infinite or zero value.

c. The electromagnetic radiation hazard to ordnance depends on the probability of EED leads acting as an antenna. This particular hazard can therefore be removed by any technique which destroys the EED antenna characteristics (e.g. shielding, twisting leads).

BIBLIOGRAPHY

1. Investigation of Premature Explosions of Electroexplosive Devices and Systems by Electromagnetic Radiation Energy (U), Final Report - Volume I, April 1962, Midwest Research Institute; Ogden AMA, 2705th Munition Wing, Hill AFB, Utah. (Confidential).

2. Antenna Theory and Design, Volume Two (The Electrical Design of Antennae), H.P. Williams; Sir Issac Pitman and Sons, Ltd; London, 1952.

3. Radio Engineers Handbook, F.E. Terman, McGraw-Hill Book Co., Inc., N.Y., 1943.

4. The Radio Amateur's Handbook, American Radio Relay League, West Hartford, Conn., 29th Edition, 1952.

5. Radio Frequency Energy a Potential Hazard in the Use and Transportation of Electric Blasting Caps, Revised Edition, Pamphlet No. 20, Institute of Makers of Explosives, N.Y., 1956.

6. Antenna Theory and Design, Volume One (Foundations of Antenna Theory), H.P. Williams; Sir Issac Pitman and Sons, Ltd; London, 1950.

7. Reference Data for Radio Engineers, 3rd Edition, Federal Telephone and Radio Corp., N.Y. 1949.

8. Radio Frequency Radiation Hazards, T.O. 31-1-80, USAF, 1958.

9. Explosives Safety Manual, AFM 32-6, USAF, 1961.

56. DISCUSSION HIGHLIGHTS

Charles T. Davey
The Franklin Institute

Terminology A Conflict

One problem emerging from the Congress appeared to be in supplying an adequately comprehensive definition of terms. Such terms as "RF Proof" "RF Safe" "insertion loss," "attenuation" and "RF Protected" were repeatedly questioned. Some of these terms have no standard definition as yet but do deserve a place in the discussion of HERO problems; others are clearly defined. A glossary of HERO terms and definitions may be helpful.

A New Source of Hazards

A primary problem area that was rediscovered in this Congress is that of the sensitivity of electroexplosives in modes other than through the bridgewire. While not all of the problems involved in the bridgewire mode of excitation have been solved, there appears to be an even more difficult problem, that of excitation in the pins-to-case mode. In this mode, results in many cases have indicated that far less power is required for initiation. Apparently many think of this problem as infrequent or insignificant.

Old And New Fixes

Many fixes were discussed that offer excellent chances of resolving the HERO problem over a wide range of frequencies. The carbonyl iron plugs appear to provide an excellent fix for frequencies that are in the tens of megacycles through the radar bands and upward. These devices have been applied to military electroexplosives of both the Army and the Navy. They have been put through MIL Standard tests and have performed satisfactorily. This material is currently being used on newly developed military blasting caps. Production tests are being made. One of the greatest advantages of this material is that it may be made to occupy little or no additional space compared to that of the conventional insulated plug.

Still classified as a problem area is the region that encompasses the lower frequencies of the spectrum. Ferrites appear to offer one of the best chances for a solution in the intermediate regions of frequency. This range extends from 1 Mc to 30 Mc. These materials, like the carbonyl iron, will probably be a replacement for the insulator normally used in the plug of the initiator. It appears to offer the same space-saving advantage.

Ferrites still remain difficult to manufacture and even more difficult to machine and assemble. Solutions to some of these fabrication problems is one of the points that deserves further attention and a powerful approach. The testing and proof of these devices both with respect to conventional firing pulses and to RF are another requirement although this is not considered a technical problem area, but may introduce some problems that are not evident at this point.

For frequencies below that at which the ferrites are effective there are a number of devices that create very high decoupling for RF and yet allow the device to be fired readily by a predetermined signal. Some of these involve magnetic coupling that entirely prevents the electric field from being coupled from the firing line side of the EED system to the EED side of this system. There are unique relays for providing this same function. A single device that operates on atomic radiation was introduced at this Congress that appears to be one of the first "coded pulse" or keyed arming and firing devices. All of these fixes appear to offer solutions to the lower frequencies of the HERO problems. Most of these, in opposition to the iron and ferrite fixes are mounted external to the EED. In some cases this is an advantage, in that it requires no modification to the electroexplosive. In other cases, where handling of the EED and other circuitry is carried out separately, there is a distinct advantage to the internal fix.

A Precaution in Wiring

It was brought out that the United Kingdom insists that electroexplosive initiators use female connectors to avoid extending pins' and lead wires which may act as RF antennas or make accidental contact with charged bodies or power lines.

While the practice has not been introduced as standard procedure in this country, perhaps it should be given some serious thought.

Safety Standards at National Missile Ranges

The most widely discussed and controversial topic was the "Interim Standards to Minimize the Hazards of Electromagnetic Radiation to Electroexplosive Devices," imposed upon users of the National Missile Ranges by the Air Force Systems Command who operates the Atlantic Missile Range. There was such a lively interest and the problems seem so vital

that General Chairman Payne deleted presentation of two papers and scheduled an impromptu discussion period which held the majority of the attendees in the conference hall well after the scheduled adjournment.*

There was discussion both for and against the Interim Standard and many called for clarification and for information regarding methods of testing and of assessing the RF hazards to electroexplosive devices and systems.

The 1-amp 1-watt for five minute dc no-fire requirement was challenged on the basis that dc sensitivity had not been shown to correspond to RF sensitivity particularly in the pin-to-case mode of RF coupling. It was pointed out that 1-amp 1-watt initiators must be considered as new devices and thoroughly evaluated from all aspects before one commits himself to their use. One man commented that the initiator manufacturers in attempting to make 1-amp, 1-watt initiators had to throw away all past knowledge and experience and start all over again. He claimed that lead azide and lead styphnate are now obsolete as ignition mixes. We need to develop design data to help the electroexplosive developers and manufacturers.

Mandatory use of insensitivity devices was also challenged on the basis that it arbitrarily increases the size, weight, and cost of power supplies relays, wiring and so forth, and seriously limits the designer in his choice of components to meet mission requirements.

Test data on 1-amp 1-watt initiators with respect to long time storage, thermal stacking, prepulses and RF sensitivity both through the bridgewire and pin-to-case, and other performance data were called for but appeared to be lacking.

How much safety if any, is gained by going to 1-amp 1-watt initiators appears at this time to be an unanswered question. On the other hand no one seems to have the necessary equipment, know-how, time or funds to determine the RF susceptibility of their systems and their initiators in order to satisfy the Interim Standards. Using 1-amp 1-watt initiators appears to some as the easy way out, but they question whether it is really a solution.

*The text of the Interim Standards appears in these Proceedings, at pp 35-7.

Full scale testing by irradiation in the field of missile systems does not appear to be technically feasible or economically practical. A compromise minimum testing program, which involves determination of the RF sensitivity of the initiators in controlled laboratory tests and analyses of possible antennas in the firing systems and during the transportation, handling, installation and checkout procedures, was described as a method that appears acceptable to the Range Safety people. However, some expressed doubts as to its adequacy and objected to the time and cost required to perform the tests and analyses. RF fixes, 1-amp 1-watt initiators included, were challenged as solutions on the basis that they are not yet readily available, have not been thoroughly evaluated, are expensive, bulky, add weight, and in many instances will require additional power supplies and auxiliary equipment and in some cases will degrade the overall mission performance.

While the discussion centered primarily on the range safety standards and the RF field intensity limits stated therein, it was pointed out that most EED's and systems must also be able to survive in tactical environments, some of which may be many times worse than those at the range.

Good engineering and design practices can go a long way in reducing RF hazards but many feel that they alone can ever be a complete solution to the RF hazard problem. Thus, it appears that the HERO problem remains unsolved. However, some progress seems to have been made especially in making more people aware of the various facets of the overall problem and, in these Proceedings, making available to many people sources of information which can assist them in minimizing RF hazards with respect to their particular systems. Programs that are just beginning to get under way, some of which were mentioned at the Congress, should shed additional light on the RF hazard assessment problem, particularly with respect to the Interim Standards, and will undoubtly lead to modifications of the Standards as time goes on.

Lightning Hazards

Lightning and its effect on missile systems containing EED's was given considerable attention. The theoretical and analytical approaches to the problem face difficulties that are similar to the RF problem. Testing is difficult but what has been done shows good agreement, at least

in two instances. Skin bonding is very important in reducing induced energy. Due to the extensive equipment required for experimental research in lightning, it has been suggested that results of these investigations be given wide circulation. This seems the logical course of action.

Statistical Test Plans

The well established Bruceton sensitivity test plan was challenged on the basis of extensive testing of several electric initiators. It is claimed that these tests show a log-logistic test plan and analytical procedure gives a better fit to the actual distribution curve. The claim was made that, because the Bruceton method concentrates testing data about the mean, large errors can result when attempting to predict the "all-fire" and "no-fire" levels. This is because the Bruceton plan assumes that the response is normally distributed with respect to the stimulus. If this is not true, then the extremes predicted from Bruceton data will be in error. The log-logistic plan requires more initiators to be tested but is claimed to give a more accurate estimate of the "all-fire" and "no-fire" stimuli. It was further claimed that use of small samples in the Bruceton can lead to even greater errors in predicting the extremes. Another challenge to the Bruceton technique was made on the basis that people did not run the test properly or perform the calculations properly thereby leading to errors in the test results. A MIL Standard to assure uniform Bruceton tests was suggested. Exponents of the logistic plan objected to a Bruceton MIL Standard on the basis that the Bruceton should not be used unless the true distribution is normal but presumably have no objection to a MIL Standard for the log-logistics plan. Time did not permit complete discussion. It is hoped to continue it at the Electric Initiator Symposium, to be held October 1 and 2, 1963, at the Franklin Institute, Philadelphia 3, Pa.

A Magic Number

Several requests were made for some magic number such as the personnel hazard limit of 100 watts/sq meter that is clear-cut safe on one side and clear-cut hazardous on the other. There is no such number that can be quoted generally. The hazard to EEDs depends upon the sensitivity of the EED, the ambient power density, the gain or aperture of the "antenna" and the system losses. Most of these parameters are frequency sensitive and vary from system to system. As consequence, no one number is adequately expressive to assure safety.

An attenuation of 60 db is the aim of fixes. This represents a power reduction of one million. An attenuation of 10 db (10 to 1 pow . reduction) is not considered high.

One of the most hazardous conditions has been found to occur during making connections and servicing.

Instrumented EEDs

Several methods of instrumenting EEDs to measure bridgewire heating were discussed. As general rule these devices where thermocouples, photocells, IR cells or resistance thermometers. One exception was the Golay cell that operates by thermal expansion at air. Means of computing transient response were considered and it was pointed out that direct measurement on the input of EEDs excited by RF will probably upset measurements to the point where they are ueeless.

Arcing in EEDs

External arc-over, mentioned in connection with pin-to-case initiation was also considered as a possible protection from RF. While this may work, it is at best a marginal condition. Arcing in EED circuits is a frightening thought.

Effects of Prepulsing

Changes in sensitivity and other characteristics can be caused by RF exposure and by direct current less than the maximum no-fire current. Some experienced ordnance people show great concern over thie problem. Others, while generally wary, have convinced themselves as a result of experiment that exposure to certain levels on certain devices is not harmful.

Fundamental information on prepulse effects is lacking. The need for this information is rapidly becoming apparent in the field. Present testing is limited to one exposure level with subsequent sensitivity testing and comparison of a control lot with an exposed lot. Better means are needed to determine

(1) If there is a sensitivity change with a given device,
(2) At what exposure level thie change occurs.
(3) The mechanisms involved.

Antenna For Maximum Hazard

Arbitrary choice of an antenna that is dubbed a maximum hazard has been described. A half-wave dipole was chosen in one instance. In another case, other investigators found that a rhombic configuration yielded an aperture roughly 8 times that of the half-wave dipole. The choice of a maximum aperture is a matter for conjecture at this point. The antenna is one very important part of the RF hazard. Until many aperture or gain measurements or computations are made, we must consider and check out all of the possible antenna configurations in each case.

A 20-ampere blasting cap was suggested as a solution to protecting them from RF. This suggestion was made because caps are used on the ground. However, weight efficiency is important to the foot soldier just as it is to the missile. Strings of blasting caps are fired from power sources that are of limited weight and output. Further, blasting caps are in need of RF protection because of their inherent long, unshielded, untwisted open-lead construction.

Problems with Dissipative Filters

The problems associated with a dissipative RF protecting device were discussed at intervals throughout the Congress. The ability of the attenuator to withstand heat as a result of power dissipation was questioned as well as the voltage breakdown characteristic of various materials and fixes. The power dissipation for any input can be computed if attenuation is known. From the current and power reported in EED circuits, this value may theoretically approach several hundred watts. Actual experiments have shown that the mounting of the EED can act as a heat sink. Especially in the case of EEDs with integral attenuators, this is all important. Some devices fire within seconds from heat build-up when they are suspended in air, while with metal surroundings they last minutes or even longer. With no size limitation imposed, most attenuators can be built to dissipate a great deal of power as heat.

High Temperature Explosive Devices

The need for high temperature initiator materials was brought forth in two aspects. First, there is a gain in using high temperature explosives along with dissipative attenuators of RF; and second, there is a current need for sterilization of all components that are to be placed into space which calls for exposure to 135°C.

The Effects of Fixes

The effect of filters and attenuator and the normal functioning time characteristics of an EED are important. With the development of most fixes, some effort has been made to obtain information on the effect of the fix on functioning time and sensitivity. This information is lacking, or at the very best, sketchy in many of the newer fixes. Reliability and environmental performance data is also badly needed on those fixes.

HERO CONGRESS, 1963 ATTENDANCE

Aaron, Richard	Picatinny Arsenal, Dover
Abbey, E.K.	USN Electronics Lab, San Diego
Adelmann, Stanley	Picatinny Arsenal, Dover
Ainslie, Robert E.	USNADC, Johnsville
Albanese, Augustino	Aerospace Corp, Los Angeles
Albin, Arnold Leon	Fairchild, Syosset, L.I.
Algeo, Bradley C.	USNADC, Johnsville
Allen, Robert Charles	McCormick Selph Assoc., Inc. Hollister
Altman, P.S.	USN Weapons Lab., Dahlgren
Anthony, Palmer L.Jr.	Naval Ammunition Depot, Macaleater
Ardans, John E.	US Flare Division, Saugus
Ardell, Leroy Lytle	Special Devices, Inc. Newhall
Ashmore, George Hudson	ITT-Industrial Prod. Div., San Fernando
Assante, Romano	Pan American, Patrick AFB
Athey, Howard E.	General Dynamics, Fort Worth
Ashuran, Joe Michael	Martin Marietta Corp., Denver
Atkinson, James Herman	NASA, Wallops Station, Wallops Island
Austin, Claude R.	Aeronautical Systems Div., Wright-Patterson AFB
Ayres, James N.	USN Ordnance Lab, White Oak
Bankston, Weldon S., Jr.	Hi-Shear Corp., Torrance
Barker, Owen C.	Hughes Aircraft Co., Culver City
Barkham, John E.	Lockheed Aircraft, Sunnyvale
Barrett, Col. James E.	Huachuca
Baxter, Edward O'Neill	McCormick Selph Assoc., Inc. Holliater
Bee, Joseph F.	Dept. Of Navy, Bureau Naval Weapons Wash.
Benedict, Anthony G.	Jet Propulsion Lab., Pasadena
Bindas, John Edward	General Electric Co., Phila.
Bird, Harry P.	Vitro Labs, Silver Spring
Blank, Charles B.	Dept. of Navy, Bureau Naval Weapons Wash.
Bliss, George L.	Dept. of Navy, Bureau Naval Weapons Wash.
Bliss, Robert W.	The Magnavox Co. Urbana
Blomdahl, Floyd	Allen-Bradley Co., Milwaukee
Boley, Kenneth N.	Bureau of Naval Weapons, Wash.
Boyd, K.A.	USN Weapons Lab., Dahlgren
Brenner, Morris	US Army Material Command, Wash.
Brown, Joseph G.	Dept. of Navy, Bureau of Naval Weapons Wash.
Bryan, Paul John	DuPont, Wilmington
Burch, William G.	Dept. of Navy, Bureau of Naval Weapons Wash.
Burson, Joe H.	NASA Marshall SFC, Huntsville
Buauttil, Henry L.	Space Tech. Lab., Redondo Beach
Byrd, Cohen B.	Sandia Base Albuquerque,
Campbell, Claude E.	Thiokol Chemical Corp., Bristol
Canale, Salvatore, Jr.	RCA, Camden
Carlson, Richard	Consolidated Control, Inglewood
Caspari, Jacques L.	Olin Mathieson Chemical Corp., East Alton
Cavanaugh, Vincent D.	Dept. of Navy Bureau of Naval Weapons, Wash.
Chesnov, Gilbert F.	CG US Army Munitions Command, Dover
Chloata, N.W.	USN Weapons Lab, Dahlgren
Ciccone, Thomas Q.	US Army Munitions Command, Frankford Arsenal Phila
Clark, Richard R.	Dept. of Navy, Bureau of Naval Weapons, Wash.
Cloud, Joseph M.	Phila. Naval Shipyard, Phila.
Coffee, Tommy L, Jr.	Bureau of Naval Weapons Rep. Sunnyvale
Cohen, Dr. Martin J.	Franklin Systems, Inc. West Palm Beach
Connelly, M.P., Jr.	USN Weapons Lab., Dahlgren
Constant, Paul C.	USN Weapons Lab., Dahlgren
Cook Charles Wayne	Sandia, Albuquerque
Corbin A.M.	US Naval Ordnance Lab., White Oak

Cormack, Charles M., Jr.	Dept. of the Navy, Bureau Naval Weapons Wash.
Correll, F.	Picatinny Arsenal, Dover
Coaby, Adolphus B.	Eureka Williams Co., Bloomington
Cramer, Charles H.	E.I. du Pont de Nemours & Co., Wilmington
Crescas, Charles	AVCOR&D Advanced Development, Wilmington
Crigler, Albert B.	Pacific Missile Range, Point Mugu
Crosby, Robert James	Atlas Chemical Industries, Inc. Wilmington
Curtis, Herbert Elliot	General Electric Co, Cocoa Beach
Davis, Donald M. Maj.	Air Force Systems Command, Washington
Davis, Donald S.	Space Technology Lab, Inc. Redondo Beach
Debuhr, Claude N.	Chief, DASA Washington
De Maris, Elbert E.	General Electric Co. King of Prussia, Pa.
Dietrich, Ray Alvin	Atlas Chemical Industries, Inc. Wilmington
Dignazio. Louis Anthony	Janaky & Bailey, Alexandria
Douglas, H.W.	Headquarters Air Defense Command, Ent. AFB
Drechsler, Robert Jerome	Douglas Aircraft, Santa Monica
Duncan, Richard Henry	New Mexico State Univeraity, University Park
Earnest, John E. Jr.	Jet Propulsion Lab, Pasadena
Edgell, Ross L. Jr.	Astropower, Inc. Newport Beach
Edwards, George D.	Dept of the Navy, Bureau Naval Weapons Wash.
Ehrlich, Sam D.	Hanley Industries, Inc. St. Louis
Ellisen, Arthur R. Capt.	Space Systems Division, Los Angeles
Eneman, Melvin	Bulova R&D Labs, Woodside
Euker, Harold William	Harvey Aluminum, Torrance
Fadeley, C.F.	USN Weapons Lab, Dahlgren
Fairchild, Homer Wayne	Douglas Aircraft Co, Inc. Santa Monica
Fallon, Christopher C.	General Electric Company, Syracuse
Farmer, Robert H.	Naval Weapons Station, Yorktown
Fitzgerald, John Anthony	Minneapolis-Honeywell Regulator Co. Hopkins
Foote, Samuel H.	Aerospace Corp., Los Angeles
Forde, Phillip	General Lab Assoc., Inc. Norwich
Fortner, Commander Herschell	U.S. Atlantic Fleet Cdr 2nd Flt. N.Y.N.Y.
Frantz, Thomas W.	US NADC, Johnsville
Froelich, Richard W.	Aerojet-General Corp. Sacramento
Fry, Richard Kent	University of Denver, Denver
Fukuzawa, Jun	Aerolab Development Co. Pasadena
Fulbo, Mario	NASA, Houston
Fuller, Robert L.	Lockheed Missiles & Space Cor. Santa Cruz Cty
Garawitz, Alfred F.	General Electric Co., Phila.
Garlington, Frank E.	Sprague Electric Co. North Adams
Gay, Benjamin A.	Atlas Chemical Industries, Inc. Tamaqua
Gaylord, Albert	Aerospace Corp., San Bernardino
Gibson, Frank C.	US Dept of the Interior, Pittsburgh
Gieske, Douglas N.	Hughes Aircraft Co., Tucson
Giles, Jack W.	Litton Industries, San Carlos
Gillett, Glenn D.	Lockheed, California
Gjertson, William G.	Chance Vought
Gluckman, Isidore B.	Lockheed Missiles & Space, Sunnyvale
Gould, W.F., Jr.	Gould Labs, Pitman
Gould, W.F., Sr.	Gould Labs, Pitman
Gottier, Thomas	Aerospace Corp. Los Angeles
Gray, David George	GPL Division, Pleasantville
Gray, R.I.	USN Weapons Lab, Dahlgren (British Citizen)
Griffin, Donald Neilson	Pelmec Div. of Quantic Ind. Inc., San Carlos

Grinoch, Abraham	Picatinny Arsenal, Dover
Grom, Richard V.	Federal Aviation Agency, Atlantic City
Gruen, Ernest J.	US Flare Div. Atlantic Research Corp. Saugus
Guinn, Isaac W.	US Naval Ordnance Test Station, China Lake
Haefner, Arthur E.	Conax Corp, Buffalo
Hagenbaugh, James William	Beckman & Whitley, Inc. San Carlos
Hall, David P.	Atlantic Research Corp. West Hanover
Hamilton, Robert M. Lt. Col.	Continental Air Defense Command, Ent AFB
Hampton, Laurence D.	US Naval Ordnance Lab. White Oak
Harrison, Charles W. Jr.	Sandia Corp. Albuquerque
Hart, Albert S.	AF Special Weapons Center, Kirtland AFB
Harvalik, Zabej Y. Dr.	US Army Engineering R&D Labs, Fort Belvoir
Harvey, Edwin Dane	Allegany Ballistics Lab, Cumberland
Hassett, Robert Emmett	Fairchild, Syosset
Hedges, Maurice T.	The Martin Company,Orlando
Heidorn, Raymond William	Elgin National Watch Co., Rolling Meadows
Hendarson, Kenneth A.	The Bendix Corp., Sidney
Hengel, 2/Lt. Raymond J.	Kirtland AFB, New Mexico
Hilbert, William C.	US Army Electronics Research White Sands MR
Hinds, James L.	USNADC,Johnsville
Hinkle, C.J.	US Naval Weapons Lab, Dahlgren
Hitchens, Aaron	North American, Downey
Holinbeck, Dale G.	Bjorksten Res. Lab., Inc. Madison
Holloway, Daniel E.	North American Aviation, Inc. Downey
Holt, David Michael	Mason & Hanger-Silas Mason Co., Inc. Amarillo
Holtman, Richard Fredrick	The Boeing Co., Seattle
Horowitz, Leo	Loral Electronics Corp. New York
Howell, Milton	Grumman Aircraft Engr. Corp. Bethpage L.I.
Huber, John F., Jr.	Unidynamics, St. Louis
Hudgins, Malcolm M.	Army Missile Command, Redstone Arsenal
Hummert,George Thomas	Hercules Powder Co. Ridgeley
Ireland, John Paul	Du Pont, Wilmington, Del.
Jarva, William	Piltron Co., Inc. Flushing
Jones, Clyde M.	Chance Vought Corp., Dallas
Jones, James, Jr.	NASA,Hampton
Jones, Richard W.	US Army, Redstone Arsenal
Kabik, Irving	US Naval Ordnance Lab., White Oak
Kant, Milton	Sperry Gyroscope Co., Great Neck
Katz, Leonard	Rocketdyne, Canoga Park
Kelly, Michael	Hqt GEEIA (ROEMMT) Griffin AFB
Kennedy, William	Canadian Hqts App. 1272
Kesselmann, Warren A.	US Army Research Electronics
Kerstettar, Dale D.	US Naval Ordnance Lab. Silver Spring
Kilpatrick, Lea Vincent	General Dynamics, Pomona
King, Paul V.	NASA,Cocoa Beach,
Klamt, Robert Herman	Douglas Aircraft Co. Inc. Santa Monica
Knippenberg, Edwin	General Electric Co. Phila.
Knudson, Louis	General Laboratory Associates, Norwich
Kochar, William J.	General Electric, Phila.
Kohlheyer, Richard Carl	Douglas Aircraft Co., Inc. Santa Monica
Korb, Monte W.	Hi-Shear Corp. Torrance
Kowalick, James F.	US Army Munitions Command, Phila.
Kraus, Karl	The Bendix Corp. Sidney
Krell, Cdr. P.	US Navy, Flt Cmd, DASA
Kugler, Fred	Ark Electronics, Willow Grove
Kuliberda, Joseph John	Republic Aviation Corp. Farmingdale
Kulik, John J.	NAFEC,Atlantic City

Kurzeja, Stanley	Thiokol Chemical Corp., Denville
Lacy, Howard R.	Dayton T. Brown, Inc. Bohemia, L.I.
LaHaye, Frank W.T., Jr.	McCormick Selph Assoc., Inc. Hollister
Landry, Theodore E.	Lockheed Propulsion Co., Redlands
Lang, Charleton	Dept. of the Navy, Bureau Naval Weapons,Wash.
La Plante, J.D.	US Naval Weapons Evaluation Fac., Albuquerque
Larkin, George Michael, Jr.	Nuclear Weapons Training Center, Norfolk
Larm, Henry A.K.	Raytheon Co., Bedford
Latour, Maximus H.	NASA GSFC,Greenbelt
Lauro, Michael Joseph	Republic Aviation Corp., Farmingdale
Lefort, John V.	Naval Testing Center, Patuxent River
Lemmon, Donald	Canadian Hqts, App. 1272
Lempke, Charles T.	Sprague Electric Co., Wash.
Lewis, R.L.	US Naval Weapons Lab, Dahlgren
Lilly, James Lucius	General Electric Co., King of Prussia
Limbacker, Charles	Magnavox, Urbana
Lockhart, Jess W.	Douglas Aircraft Co., Inc. Long Beach
Lofiego, Louis	Hermite Powder Co., Saugus
Locke, Orville C., Capt	Marine Force Atlantic, Norfolk
Loiler, Roger Dale	ITT-Industrial Products Div., San Fernando
Lurie, William	Dept of Navy, Bureau Naval Weapons,Wash.
Lysher, L.J.	US Naval Weapons Lab, Dahlgren,
Mahler, Leonard H.	Aerospace Corp., Los Angeles
Malaspina, John E.	US Naval Ordnance Plant, Macon
Manabach, Bernard	General Electric Co., Phila.
Martin, Donald F.	Physics International, Inc. Albuquerque
Mashek, William, Jr.	Amphenol Connector Division, Chicago
Masterson, Kleber S. Adm.	Bureau of Naval Weapons, Wash.
McAdams, James H.	TDBR PWS, Redstone Arsenal
McClain, Thomas Chester	Lockheed Missiles & Space Co., Sunnyvale
McClure, R.A.N. Cdr. J.W.	Australian Naval Attache, Wash. App 1614
McCuin, William D.	Interferance Testing & Res. Lab. Havertown
McGirr, Robert	Atlas Chemical Industries, Inc. Wilmington
McKenzie, Robert L.	US Army Electronics R&D Lab, Ft Monmouth
Metcalf, George Edward	Boeing Co., Seattle
Meltzer, Herbert	Republic Aviation Corp., Farmingdale
Merewether, David E.	Sandia Corp., Albuquerque
Meyer, Earl A.	Bjorksten Research Labs, Inc. Madison
Miller, Hugo J. Capt. USAF	Space Systems Div. Los Angeles
Miller, Samuel P.	Hermite Powder Co., Saugus
Mills, Alfred	Convair-Astronautics, Gen. Dynamics, San Diego
Moeller, John Elmer	North American Aviation, Inc. Downey
Mitchell, Burrell	Boston Naval Shipyard, Boston
Moran, Arthur P.	The Bendix Corp., Sidney
Morgan, Gerald C.	US Army Nuclear Weapons Support, Fort Belvoir
Mueller, James H.	Thiokol Chemical Corp,Bristol
Mueller, Roger J.	Amphenol Connector Div., Chicago
Murphy, Merrill O.	Sandia, Albuquerque
Murray, Wendell C.	ITT Federal Laboratories, Nutley
Nagle, F.	US Naval Weapons Lab, Dahlgren
Nalley, Donald W.	US Naval Ordnance Lab, Silver Spring
Nelson, Charles A.	Navy Electronics Lab, San Diego
Noble, Lowell Amon	Eitel McCullough, Inc. San Carlos
Noddin, George A.	E.I. du Pont de Nemours & Co., Gibbstown
Norman, Raymond L.	NASA GSFC,Greenbelt
Norton, Stephen	Grumman Aircraft Engr Corp. Bethpage L.I.
Norton, Thomas W.	The Ensign-Bickford Co., Simsbury
Nuding, J.S.	Convair-Astronautics, San Diego

Nussbaum, Richard D.	USNADC, Johnsville
O'Connor, Albert A.	NASA, Huntsville
Oesterle, Adolph Gustav	Weston Instruments & Electronics, Newark
Olson, Donald L.	US Naval Torpedo Station, Keyport
Ongstad, Orvin C.	Hughes Aircraft Co., Culver City
O'Sullivan, Arthur P.	US Naval Underwater Ordnance Station, New Port
Painter, John, Lcdr	US Atlantic Flt, Norfolk
Parker, Theodore C.	General Precision, Inc. Sunnyvale
Parsons, Frank W.	Small Business Administration, Phila.
Paxson, Larry Leland	General Precision, Wash.
Payne, J.N.	US Naval Weapons Lab, Dahlgren
Peacock, Harry E.	General Electric, Phila.
Perkins, William E.	US Army Munitions Command, Phila.
Pierson, Edward G.	Conax Corp., Buffalo
Popham,	Dept. British Defense Staff App 1432
Potter, R.R.	US Naval Weapons Lab, Dahlgren
Powell, Harold B., Capt.	AFSC Scientific & Tech. Liaison Office, USAF
Price, R.M.	US Naval Weapons Lab, Dahlgren
Pruett, L.S.	US Naval Weapons Lab., Dahlgren
Qualls, Harold Walter	Convair, San Diego
Quatrochi, Philip J.	Picatinny Arsenal, Dover
Queen, Walter G.	US Army Material Command, Wash
Ramer, Edward L.	Hercules Powder Co., Wilmington
Ramsdell, Paul Allen	E.I. duPont de Nemours Co., Wilmington
Rawls, Otis B.	RCA Service Co., Florida
Reid, Albert R.	Air Force Flight Test Center, Edwards AFB, Calif.
Reisberg, M.	Phila. Naval Shipyard, Phila.
Revsin, M.	Loral Electronics Corp., New York
Richardson, William C., Jr.	FAA, Wash.
Rippke, Bruno	USAERDL, Fort Monmouth
Roberts, Albert Lee	Ordnance Association, Inc. South Pasadena
Rosen, Benedict P.	Sprague Electric Co., North Adams
Rosenberg, Gilbert M.	Pentagon, Army Material Command, Wash.
Rosenthal, L.A.	US Naval Ordnance Lab, White Oak
Rosenthal, Morris	Space Tech. Lab., Inc. Redondo Beach
Rucker, Klaus G.	E.I. duPont de Nemours, Gibbstown
Rudikoff, Norman	Griffiss AFB, Rome Hq Geeis (Rommt)
Rung, Robert D.	Westinghouse Electric Co, Sunnyvale
Rush, Stanley H.	Space Tech. Lab., Inc. Redondo Beach
Sacks, Harvey	Ordnance Association, Inc. South Pasadena
Salisbury,	Lawrence Radiation Lab., Calif.
Sanders, Howard E.	US Naval Mine Engrg. Facility, Yorktown
Sanders, Wiley	Unidynamics, St. Louis
Sanford, Richard	Naval Ordnance Lab. White Oak
Sats, Richard G.	Picatinny Arsenal, Dover
Scerrator, Robert C.	Bell Telephone Lab., Inc. Whippany
Schaaf, Herbert L.	DuPont, Wilmington
Scharff, James H., Capt.	Kirtland AFB, New Mexico
Scherrer, George Wilson	Hercules Powder Co., Port Rwen
Schaivi, Ferdinand J.	Dept of Navy, Bureau Naval Weapons, Wash.
Schlachter, D.A.	US Naval Weapons Lab., Dahlgren
Schlesinger, Louis	Bureau of Naval Weapons, Wash.
Schlie, Roland W.	US Naval Ordnance Lab., Silver Spring
Schmidt, Carvel Walter	USAF, Norton AFB, Calif.
Schoeweiler, Karl P.	North American Aviation, Inc., Downey
Schuls, Robert Frank	General Dynamics, Pomona
Scott, Drummond Lee	White Electromagnetics, Bethesda
Segal, Louis H.	Bendix Corp., Sidney

Seibert, Donald J.	Welex Electronics Corp, Wash.
Seifner, John, Jr.	Zenith Radio Corp., Chicago
Sellars, Robert F.	US Naval Weapons Lab, Dahlgren
Senn, James C.	Gensitron, Inc. Los Angeles
Sheng, William T.	Aerospace Corp., Los Angeles
Shrager, Jack J.	FAA, Atlantic City
Silverman, Herbert	North American Aviation, Inc. Downey
Simmons, William H.	NASA,Houston
Simon, Edward Martin	Atlas Chemical Industries, Inc. Wilmington
Simonds, David H.	Sprague Electric Co., North Adams
Simpson, C.E.	Uridynamics, St. Louis, Mo.
Sirmalis, John E.	US Naval Underwater Ordnance Station, Newport
Skelton, Robert T.	US Naval Ordnance Lab, Silver Spring
Smith, Rex L.	US Naval Ordnance Lab, Corona
Smith, William Melbourne	The Ensign-Bickford, Simsbury
Snead, Charles R.	Redstone Arsenal
Snier, Thomas J.	Jet Propulsion Lab, Cape Canaveral
Sowlakis, George Ted	Beckman & Whitley, Inc., San Carlos
Specht, Walter	Long Beach Naval Shipyard, Long Beach
Stecker, Ernest J.	Holex, Inc. Hollister, Calif.
Stegner, Charles	Weston Instruments & Electronics, Newark
Steinmark, Leonard B.	Picatinny Arsenal, Dover
Steptoe, Francis H.	Pacific Missile Range, Point Mugu
Sterrett, David S. Capt	US Atlantic Fleet, Norfolk
Stevens, Franklyn E., Jr.	Pyrofuze Corp., Mt. Vernon,
Stevens, William L.	Sandia Corp., Albuquerque
Stewart, Lt. Col. Ernest	Hqta, 1002 Inspector General Gp Norton AFB Calif
Stinger, Walter E.	US Naval Air Development Center, Johnsville
Stolar, Gerald	Weston Instruments & Electronics, Newark
Strong, Richard	Thiokol Chemical Corp., Brigham City
Sullivan, Robert Raymond	Douglas Aircraft Co., Santa Monica
Svadeba, George	Naval Weapons Station, Yorktown
Sweat, James C.	Pan American World Airways, PAFB,Fla.
Sweton, J.F.	US Naval Weapons Lab., Dahlgren
Swift, Robert	Geniatron, Benseville,
Synder, William	Consolidated Control, Inglewood
Taiani, Angelo J.	NASA, Cocoa Beach
Taylor, George	Thiokol Chemical Corp., Elkton
Terea, Benjamin	General Electric Co., Phila.
Thomas, Fred Max	Hi-Shear Corp., Torrance
Thomas, William Robert	Hercules Powder Co.Port Ewen
Thompson, Claude Ivan	Sprague Electric Co., Los Angeles
Tillery, R.J.	US Naval Weapons Evaluation Facility, Albuquerque
Timmons, Edward A.	NASA,Houston, Texas
Tobin, Henry G.	Armour Res. Fnda., Ill Inst. Tech. Chicago
Trevaskis, William T.	Aerospace Corp., Los Angeles
Trovato, Onofrio C.	USNADC,Johnsville
Tweed, Paul B.	AVCO,Wilmington
Tysenhouse, Edward J.	AF Missile Test Ctr, Patrick AFB
Ungersohn, Harry	Steno-Typist Specialist, N.Y.
Valade, Lt. Cdr. L.G.	Navy Dept.
Vallarino, A.R.	General Precision, Sunnyvale
Vermillion, Raymond K.	Eglin AFB, AF Systems Cmd Fla.
von Breunig, G.A.W.	US Naval Weapons Lab., Dahlgren
Waddington, David	The Martin Co., Denver
Wagner, George	NASA, GSFC, Greenbelt
Walker, Frank	Cannon Electric Co., Santa Ana
Warner, Henry Burt	Douglas Aircraft Co., Santa Monica

Warshall, Theodore	Picatinny Arsenal, Dover
Waxler, Daniel	Picatinny Arsenal, Dover
Wear, Lawrence	Space Flight Center, Huntsville
Weintraub, Herbert S.	AVCO Res. & Advanced Dev. Wilmington
Werner, Allen John	The Martin Company, Denver
White, Alonzo	Frankford Arsenal, Phila.
White, Matthew Judson Jr.	Atlas Chemical Industries, Inc. Wilmington
Whitehurst, Troy N.	General Electric Co., Houston
Wilhelm, Francis A.	Redstone Arsenal, Alabama
Williams, Frank Howlett	Tamar Electronics, Inc. Anaheim
Willis, James F.	Long Beach Naval Shipyard, Long Beach
Wilson, George	General Dynamics, San Diego
Witbeck, Lewis H.	US Naval Ordnance Lab., Corona
Wood, Cecil Kenneth	Hercules Powder Co., Port Ewen
Wood, Donald S.	Physics International Inc., Albuquerque
Wood, William Adkins	Olin Mathieson Chemical Corp., Ill.
Woods, Leslie J.	Eureka Williams Co., Bloomington
Woodward, Lynn P.	Bureau of Naval Weapons, Wash.
Wright, James B.	Redstone Arsenal, Alabama
Yost, George P.	Phila. Naval Shipyard, Phila.
Zeman, Sam, Jr.	Thiokol, Huntsville, Alabama
Zimmerman, George V.	Elgin National Watch Co., Ill.

FRANKLIN INSTITUTE STAFF

Amicone, R.G.	Goldie, V.W.	Mohrbach, P.F.
Campbell, J.B.	Hannum, H.E.	Post, D.L.
Carlson, J.	Heckscher, J.G.R.	Raksnis, R.R.
Cipkins, A.W.	Heffron, J.F.	Roetche, G.C.
Cohn, G.	Kelly, M.J.	Schneck, E.R.
Davey, C.T.	Louie, J.S.	Smith, M.R.
Dunfee, J.D.	Mac Krell, B.R.	Thompson, R.H.
Dunning, R.	Mayer, D.W.	Warren, J.P.
Faunce, N.P.	McKay, G.H.	Wood, R.F.
Fertner, K.S.	McKeaney, P.E.	

DISTRIBUTION LIST

Chief, Naval Operations
Department of the Navy
Washington 25, D.C.
Code: OP-411H (5)
OP-941Q (6)
OP-07T5 (7)
OP-944 (8)

Chief, Bureau of Naval Weapons
Department of the Navy
Washington 25, D.C.
Attn: Adm. K. S. Masterson (9)
Code: C-132 (10)
CB-2 (11)
DLI-31 (12)
FWAE-142 (13)
GTA (14)
GTE (15)
GTR (16)
GTY (17)
FWS-12 (18)
RAAV-1 (19)
RAAV-3421 (20)
RM-3 (21)
RM-15 (22)
RMGA (23)
RMGA-711 (24)
RMLG (25)
RMMO-1 (26)
RMMO-224 (27)
RMMO-235 (28)
RMMO-32 (29)
RMMO-33 (30)
RMMO-4 (31)
RMMO-43 (32)
RMMO-44 (33)
RMMO-5 (34)
RMMO-53 (35)
RMMP-2 (36)
RMMP-4 (37)
RMMP-343 (38)
RMWC-4 (39)
RMWC-22 (40)
RR-12 (41)
RREN-32 (42-43)
RSWI (44)
RU-31 (45)
RUUG (46)
SP-2721 (47)
SP-2733 (48)
SP-43 (49)

Chief, Bureau of Ships
Department of the Navy
Washington 25, D.C.
Code: 452H (50)

Chief, Bureau of Medicine and Surgery
Department of the Navy
Washington 25, D.C.
Code: 74 (51)

Chief, Bureau of Yards and Docks
Department of the Navy
Washington 25, D.C.
Code: C-330 (52)
D-200 (53)

Commander
U.S. Naval Weapons Laboratory
Dahlgren, Virginia
Code: WHR (54-78)

Commander
U.S. Naval Ordnance Laboratory
White Oak, Maryland
Attn: James N. Ayres (79)
Allen M. Corbin (80)
Laurence D. Hampton (81)
Irving Kabik (82)
Dale D. Kerstetter (83)
Donald W. Malley (84)
L. A. Roenthal (85)
Richard Sanford (86)
Roland W. Schlie (87)
Robert T. Skelton (88)
Tech. Info. Section (89)

Commanding Officer
U.S. Naval Ordnance Laboratory
Corona, California
Attn: Rex L. Smith, Code 4521 (90)
Lewis H. Witbeck (91)

Commander
U.S. Naval Ordnance Test Station
China Lake, California
Attn: Mrs. P. A. Griffin,
Code 3040 (92)
Isaac W. Guinn (93)

Commander
U.S. Naval Ordnance Test Station
3202 E. Foothill Blvd.
Pasadena 8, California
Attn: Code P5511 (94)
Pasadena Annex Library (95)

Commanding Officer
U.S. Naval Air Development Center
Johnsville, Pennsylvania
Attn: Robert E. Ainslie (96)
Bradley C. Algee (97)
Thomas W. Frautz (98)
James L. Hinds (99)
Richard D. Nussbaum (100)
Walter E. Stinger (101)
Onofrio C. Trovato (102)

Officer-in-Charge
U.S. Naval Explosive Ordnance Disposal Facility
Indian Head, Maryland
Attn: R. E. Graham (103)

Commanding Officer
U.S. Naval Underwater Ord. Station
Newport, Rhode Island
Attn: Arthur P. O'Sullivan (104)
John E. Sirmalis (105)

Commanding Officer
U.S. Naval Weapons Eval. Facility
Kirtland Air Force Base
Albuquerque, New Mexico
Attn: J. D. LaPlante (106)
R. J. Tillery (107)

Commanding Officer
U.S. Naval Weapons Station
Yorktown, Virginia
Attn: Robert H. Farmer (108)
George Svadeba (109)

Officer-in-Charge
U.S. Naval Mine Engr. Facility
U.S. Naval Weapons Station
Yorktown, Virginia
Attn: Howard E. Sandere (110)

Superintendent
U.S. Naval Weapons Plant
Washington 25, D.C.
Attn: Industrial Health Div. (111)

Commander
Pacific Miseile Range
P.O. Box 8
Point Mugu, California
Attn: Range Safety,
F. H. Steptoe (112)
Albert B. Crigler (113)

Commanding Officer and Director
U.S. Navy Electronics Laboratory
San Diego 52, California
Attn: Library (114)

Commander
U.S. Naval Air Test Center
Patuxent River, Maryland
Attn: John V. Lefort (115)

Commanding Officer
U.S. Naval Ammunition Depot
Crane, Indiana
Code: 34 (116)

Commanding Officer
U.S. Naval Ordnance Plant
Macon, Georgia
Attn: John B. Malaspina (117)
J. L. Partsh, PD270 (118)

Commander
U.S. Naval Torpedo Station
Keyport, Washington
Attn: Donald L. Olson (119)

DISTRIBUTION LIST (Cont.)

Commander
Navy Electronics Laboratory
San Diego, California
Attn: E. R. Abbey (120)
Charles A. Nelson (121)

Commander Naval Air Force
U.S. Pacific Fleet
U.S. Naval Air Station
North Island, Box 1210
San Diego 35, California
Attn: C. T. Faulders,
Jr. 723 (122-123)

Commander Naval Air Force
U.S. Atlantic Fleet
U.S. Naval Air Station
Norfolk 11, Virginia
Code: CNAL 724B (124)

Commander Amphibious Force
U.S. Atlantic Fleet
U.S. Naval Base
Norfolk 11, Virginia
Attn: W. J. Hess (125)

Commander Amphibious Force
U.S. Pacific Fleet
San Diego 32, California (126)

Commander Cruiser-Destroyer Force
U.S. Pacific Fleet
San Diego 32, California
Code: 43 (127)

Commander Cruiser-Destroyer Force
U.S. Atlantic Fleet
Newport, Rhode Island
Attn: Lt. Joseph D. Micelli (128)

Commander Mine Force
U.S. Pacific Fleet
U.S. Naval Station
Long Beach, California
Code: 43 (129)

Commander Mine Force
U.S. Atlantic Fleet Mine Force
Charleston, South Carolina (130)

Commander, Service Force
U.S. Pacific Fleet
c/o Fleet Post Office
San Francisco, California
Code: 25 (131)

Commander Service Force
U.S. Atlantic Fleet
Building 142, U.S. Naval Base
Norfolk 11, Virginia (132)

Commander Submarine Force
U.S. Atlantic Fleet
c/o Fleet Post Office
New York, New York (133)

Commander Submarine Force
U.S. Pacific Fleet
Navy Number 128, c/o FPO
San Francisco, California
Attn: L. G. Yeich (134)

Commander Training Command
U.S. Pacific Fleet
c/o U.S. Fleet Anti-Submarine
Warfare School
San Diego 47, California (135)

Commander Training Command
U.S. Atlantic Fleet
U.S. Naval Base
Norfolk 11, Virginia (136)

Commander-in-Chief
U.S. Pacific Fleet
c/o Fleet Post Office
San Francisco, California
Code: 4 (137)

Commander-in-Chief
U.S. Atlantic Fleet
U.S. Naval Base
Norfolk 11, Virginia
Attn: Capt. David S. Sterrett (138)
Lcdr. John Painter (139)

Commander-in-Chief
U.S. Naval Forces Europe
Navy Number 100, Box 8, FPO
New York, New York
Attn: C. H. Noar (140-142)

Commander First Fleet
c/o Fleet Post Office
San Francisco, California (143)

Commander Second Fleet
c/o Fleet Post Office
New York, New York
Attn: Cdr. Hershell Fortner (144)

Commander Sixth Fleet
c/o Fleet Post Office
New York, New York (145)

Commander Seventh Fleet
c/o Fleet Post Office
San Francisco, California (146)

Commander, Bureau of Naval Weapons
Fleet Readiness Rep. Pacific
Naval Air Station, North Island
San Diego 35, California
Code: FRR-236 (147)

Commander
Operational Test and Eval. Force
Norfolk 11, Virginia (148)

Commander
Nuclear Weapons Training Center
Atlantic
Norfolk 11, Virginia
Attn: George M. Larkin, Jr. (149)

Commander
Boston Naval Shipyard
Boston 29, Massachusetts
Attn: Burrell M. Mitchell (150)

Commander
Puget Sound Naval Shipyard
Bremerton, Washington (151)

Commander
New York Naval Shipyard
Naval Base
Brooklyn 1, New York
Code: 290 (152)

Commander
Charleston Naval Shipyard
U.S. Naval Base
Charleston, South Carolina
Code: 280 (153)
290 (154)

Commander
Long Beach Naval Shipyard
Long Beach 2, California
Attn: Walter A. Specht (155)
James F. Willis (156)

Commander
San Francisco Naval Shipyard
San Francisco 24, California
Attn: Technical Library (157)

Commander
Pearl Harbor Naval Shipyard
Navy Number 128, c/o FPO
San Francisco, California
Code: 246L (158)
280 (159)

Commander
Mare Island Naval Shipyard
Vallejo, California (160)

DISTRIBUTION LIST (Cont.)

Commander
Philadelphia Naval Shipyard
Naval Base
Philadelphia 12, Pennsylvania
Attn: Joseph M. Cloud (161)
M. Reisberg, Code 296 (162)
George P. Yost,
Code 272 (163)

Commander
Portsmouth Naval Shipyard
Portsmouth, New Hampshire (164)

Commander
Norfolk Naval Shipyard
Portsmouth, Virginia
Code: 290 (165)

Commander
Fourth Naval District
Philadelphia 12, Pennsylvania
Attn: Lt. Cdr. L. G. Valade (166)

Commandant, Fourteenth Naval Dist.
Navy Number 128, FPO
San Francisco, California
Attn: G. H. Keyes (166-167)

Commanding Officer
U.S. Naval Ammunition Depot
Navy Number 66, c/o FPO
San Francisco, California (168)

Commander
U.S. Naval Ammunition Depot
Macalester, Oklahoma
Attn: Palmer L. Anthony, Jr. (169)

Director
U.S. Naval Research Laboratory
Washington 25, D.C.
Attn: Rufus W. Wright (170)

Commander
Material Laboratory
New York Naval Shipyard, New York
Code: 930 (171)
746D (172)

Deputy Director
Electromagnetic Compatibility
Analysis Center
U.S. Naval Engr. Exp. Station
Annapolis, Maryland
Attn: A. M. Brouner (173-174)

Office, Secretary of Defense
The Pentagon
Washington 25, D.C.
Attn: Henry Randall (175)

Office of Director of Defense
Research and Engineering
The Pentagon
Washington 25, D.C.
Attn: M. Bell (176)
J. M. Bridges (177)
R. M. Yates (178)

Headquarters
U.S. Army Materiel Command
Washington 25, D.C.
Attn: Gilbert M. Rosenberg (179)
Walter G. Queen (180)

Commanding General
U.S. Army Munitions Command
Dover, New Jersey
Attn: Gilbert F. Chesnov (181)

Commanding Officer
Frankford Arsenal
Philadelphia 37, Pennsylvania
Attn: Thomas Q. Ciccone (182)
James F. Kowalick (183)
William E. Perkins (184)
Marco Petronio, 1336 (185)
Alonzo White (186)
Technical Info. Section (187)

Commanding Officer
Picatinny Arsenal
Dover, New Jersey
Attn: Richard Aaron (188)
Stanley Adelman (189)
Fred Correll (190)
Abraham Grinoch (191)
Philip J. Quatrochi (192)
Richard G. Satz (193)
Leonard B. Steinmark (194)
Theodore Warshall (195)
Daniel Waxler (196)
Technical Info. Section (197)

Commanding General
U.S. Army Missile Command
Redstone Arsenal, Alabama
Attn: Malcolm M. Hudgins (198)
James H. McAndrews,
TDBR-PWS (199)
Charles R. Snead (200)
Francis A. Wilhelm (201)
James B. Wright
Code AMSMI-S (202-203)

Commandant
U.S. Army Ordnance Guided Missile
School
Redstone Arsenal, Alabama
Attn: Richard W. Jones (204)

Headquarters
Army Test and Evaluation Command
Aberdeen Proving Ground, Maryland
Attn: I. R. Obenchain, Jr.,
Col., USA (205)

Director, Ballistic Research
Laboratories
Aberdeen Proving Ground, Maryland
Attn: Harold Zancanta (206)

President
U.S. Army Airborne and Electronics
Board
Fort Bragg, North Carolina (207)

Chief
U.S. Army Nuclear Weapons Support
Group
Fort Belvoir, Virginia
Attn: Gerald C. Morgan (208)

Commanding Officer
U.S. Army Engineer Research
and Development Laboratories
Fort Belvoir, Virginia
Attn: Dr. Z. V. Harvalik (209)

U.S. Army Field Safety Office
P.O. Box 606
Jefferson, Indiana
Attn: R. J. Shirock (210)

Office Chief Signal Officer
Research and Development Division
Washington 25, D.C.
Code: SIGRD-8 (211)

Commanding Officer
U.S. Army Electronics Research and
Development Laboratories
Fort Monmouth, New Jersey
Attn: E. S. Brooks,
SIGRA/EL-PS (212)
Warren A. Kesselman (213)
Robert L. McKenzie (214)
Bruno Rippke (215)

U.S. Army Signal Radio Propulsion
Agency
Fort Monmouth, New Jersey
Attn: Frederick H. Dickson (216)

Commanding Officer
Harry Diamond Laboratories
Washington 25, D.C.
Attn: Morris Brenner (217)

Office, Chief of Engineers
Research and Development Division
Field Engineering Branch
Washington 25, D.C.
Code: ENGRD-F (218)

Commanding General
2nd Region U.S. Army Air Defense Command
621 North Robinson
Oklahoma City 2, Oklahoma (219)

Commanding General
White Sands Missile Range
New Mexico
Attn: Hunter L. Harris (220)

Commanding Officer
U.S. Army Electronics Research
White Sands Missile Range
New Mexico
Attn: William C. Hilbert (221)

Commanding General
U.S. Army Electronics Proving Ground
Fort Huachuca, Arizona
Attn: Technical Library (222)

Director
Office of Special Weapons Devel.
U.S. Continental Army Command
Fort Bliss, Texas
Attn: Capt. Chester I. Peterson(223)

Commanding Officer
Letterkenny Ordnance Depot
Chambersburg, Pennsylvania
Attn: Safety Director (224)

Headquarters
Air Research and Development Command
Andrews Air Force Base
Washington 25, D.C.
Attn: Hyman Ackerman (225)

Headquarters
Air Force Systems Command
Andrews Air Force Base
Washington 25, D.C.
Attn: Maj. Donald M. Davis (226)

AFSC Scientific and Technical Liaison Office
Eastern Contract Management Region
Air Force Systems Command
c/o Department of the Navy
Room 2305, Munition Building
Washington 25, D.C.
Attn: Capt. Harold B. Powell (227)

Commander
Air Force Ballistic Systems Div.
Norton Air Force Base, California
Attn: Lt. Col. C. W. Schmidt (228)

Director
Nuclear Safety Research
Kirtland Air Force Base, New Mexico
Code: AFCNS (229)

Commander
Air Force Missile Test Center
Patrick Air Force Base, Florida
Attn: Edward J. Tyzenhouse, GS-13 (230)

Headquarters
Ogden Air Materiel Area
Hill Air Force Base
Ogden, Utah
Code: OOYSS (231)

Commander
Air Force Missile Devel. Center
Holloman Air Force Base
Alamagordo, New Mexico
Code: MDBG (232)

Commander
Air Force Special Weapons Center
Kirtland Air Force Base
Albuquerque, New Mexico
Attn: Capt. J. Scharff (233)
2/Lt. Raymond J. Hengel (234)
Albert S. Hart (235)

Director
Missile Safety Division
Norton Air Force Base, California
Attn: Maj. P. R. Berry (236)

Commander
Air Force Flight Test Center
Edwards Air Force Base, California
Attn: Albert R. Reid (237)

Hq. Continental Air Defense Cmd.
Ent Air Force Base, Colorado
Attn: Lt. Col. R. M. Hamilton (238)
H. W. Douglas (239)

Commander
Air Force Electronic Systems Div.
Hanscom Air Force Base,
Bedford, Massachusetts
Attn: W. Dix, ESRDV (240)

Commander
Space System Division
Air Force Unit Post Office
Los Angeles 45, California
Attn: Capt. A. R. Ellison (241)
Capt. Hugo J. Miller (242)

Commander
Air Force Aeronautical Systems Div.
Wright-Patterson A. F. Base, Ohio
Attn: Claude R. Austin (243)

Commander
Hanscom Air Force Base, Mass.
Attn: Capt. Long,
AFCCDD/CCSEI-1 (244)

Commander
Strategic Air Command
Offutt Air Force Base. Nebraska
Code: DOSDM (245)

Director Air University Library
Maxwell Air Force Base, Alabama
Code: AUL3T-59-58 (246)

Commander
Headquarters Ground Electronics
Engineering Installation Agency
Griffiss Air Force Base, N.Y.
Attn: Michael Kelly, ROZMWT (247)
Norman Rudikoff, ROZMWT (248)

Commanding Officer
Rome Air Development Center
Griffiss Air Force Base, New York
Code: RCSSL (249)
RCLS (Philip L. Sandler)(250)

Headquarters
Wright Air Development Center
United States Air Force Base
Wright-Patterson AF Base, Ohio (251)

Headquarters
1002 Inspector General Group
Kirtland Air Force Base, N.M.
Attn: Lt. Col. E. Stewart (252)

Armed Serv. Explosives Safety Board
Department of Defense
Rm. 2075, Bldg. T-7, Gravelly Point
Washington 25, D.C. (253)

Commander
Air Force Aeronautical Systems Div.
Eglin Air Force Base, Florida
Attn: Raymond K. Vermillion (254)

Armed Services Tech. Info. Agency
Arlington Hall Station
Arlington, Virginia
Attn: Tech. Info. Section (255-264)

Commandant of the Marine Corps
Washington 25, D.C.
Code: AAE (265)
AO4C (266)

DISTRIBUTION LIST (Cont.)

Marine Corps Headquarters
Washington 25, D.C.
Attn: C. Dey (267)
J. A. Herzog (268)
R. A. Panzo (269)
T. M. Reedy (270)
R. H. Ruesell (271)

Commanding General
Headquarters, Fleet Marine Force, Pacific
c/o Fleet Post Office
San Francisco, California
Attn: Force Communications Electronic Officer (272)

Commanding General
Fleet Marine Force, Atlantic
U.S. Naval Base
Norfolk 11, Virginia
Attn: Capt. O. C. Locke (273)

Commanding General
Air Fleet Marine Force, Pacific
MCAS, El Toro
Santa Ana, California (274)

EOD Officer
Marine Corps Base
29 Palms, California
Attn: J. B. Lemmons, Capt. USMC (275)

U.S. Atomic Energy Commission
Division of Military Application
Washington 25, D.C. (276)

Manager
Albuquerque Operations Office, USAEC
P.O. Box 5400
Albuquerque, New Mexico
Attn: Weapons Systems Safety Branch (277)

Headquarters
2848th Air Base Wing, USAF
Norton Air Force Base, California
Attn: Lt. Col. Carvel W. Schmidt(278)

Headquarters, Defense Atomic Support Agency
Washington 25, D.C.
Attn: Claude N. DeBuhr (279)

Commander, Field Command
Defense Atomic Support Agency
Albuquerque, New Mexico
Attn: Cdr. P. P. Krell (280)

U.S. Atomic Support Agency
Hq. Field Command Defense
Albuquerque, New Mexico
Attn: Lt. Cdr. H.J. Johnson (281)

National Aeronautics and Space Administration
Office of Manned Space Flight
Washington 25, D.C.
Attn. M. J. Krasnican (282)

National Aeronautics and Space Administration
George C. Marshall Space Flight Ctr.
M-PA/E-PS
Huntsville, Alabama
Attn: Joe H. Burson (283)
Albert A. O'Connor (284)
Lawrence D. Wear (285)

National Aeronautics and Space Administration
Goddard Space Flight Center
Greenbelt, Maryland
Attn: Marinus S. Latour (286)
Raymond L. Norman (287)
George W. Wagner (288)

National Aeronautics and Space Administration
Lewis Research Center
Cleveland, Ohio
Attn: Mr. Swasey (289)

National Aeronautics and Space Administration
Cocoa Beach, Florida
Attn: Paul V. King (290)
Angelo J. Taiani (291)

National Aeronautics and Space Administration
Langley Field, Virginia
Attn: James Jones, Jr. (292)

National Aeronautics and Space Administration
Manned Spacecraft Center
Houston 1, Texas
Attn: Mario Falbo (293)
Wm. H. Simmons (294)
E. W. Timmons (295)

National Aeronautics and Space Administration
Wallops Station, Wallops Island
Virginia
Attn: James H. Atkinson (296)

Federal Aviation Agency
Washington 25, D.C.
Attn: Wm. C. Richardson, Jr. (297)

Federal Aviation Agency
Systems R&D Service, NAFEC
Atlantic City, New Jersey
Attn: Richard V. Grom (298)
John J. Kulik (299)
Jack J. Shreger (300)

Bureau of Mines
4800 Forbes Avenue
Pittsburgh 13, Pennsylvania
Attn: F. C. Gibson (301)

Small Business Administration
1015 Chestnut Street
Philadelphia 7, Pennsylvania
Attn: Frank M. Parsons (302)

Bureau of Naval Weapons Rep.
Special Projects Office
Lockheed Missiles & Space Co.
P.O. Box 504
Sunnyvale, California
Attn: Toney L. Coffee, Jr. (303)

Aerojet-General Corporation
11711 Woodruff Avenue
Downey, California
Attn: Dr. H. J. Fisher (304)

Aerojet-General Corp.
P. O. Box 1947
Sacramento, California
Attn: Richard W. Froelich (305)

Aeronab Development Co.
330 W. Holly St.
Pasadena, California
Attn: Jun Fukuzawa (306)

Aerospace Corp.
P. O. Box 95085
Los Angeles 45, California
Attn: Augustino Albanese (307)
I. P. Cohen (308)
Samuel H. Foote (309)
Thomas S. Gottier (310)
Leonard H. Mahler (311)
William T. Sheng (312)
William T. Treveskis (313)
J. R. Wilson (314)
Tech. Library (315)

Aerospace Corp.
P. O. Box 1308
San Bernadino, California
Attn: Albert Gaylord (316)

Allegany Ballistics Lab.
Hercules Powder Co.
P. O. Box 210
Cumberland, Md.
Attn: Edwin D. Harvey (317)

Allegany Ballistics Lab.
Hercules Powder Co.
Ridgeley, West Virginia
Attn: George T. Hummert (318)

Allen-Bradley Co.
Milwaukee, Wisconsin
Attn: Floyd Blomdahl (319)

American Electronics Lab., Inc.
Colmar, Pa.
Attn: Robert H. Sugerman (320)

Amphenol Connector Division
Central Operations
1830 S. 54th Avenue
Chicago 50, Illinois
Attn: William Mashek, Jr. (321)
Roger J. Mueller (322)

Ark Electronics Corp.
624-26 Davisville Rd.
Willow Grove, Pa.
Attn: Fred Kugler (323)

Armour Research Foundation
10 W. 35th St.
Chicago 16, Illinois
Attn: Henry G. Tobin (324)

Astropower, Inc.
2121 Paularino Ave.
P. O. Box 2298
Newport Beach, California
Attn: Rosa L. Edgall, Jr. (325)

Atlee Chemical Industries, Inc.
Reynolds Plant
Tamaqua, Pa.
Attn: Benjamin A. Gay (326)

Atlas Chemical Industries, Inc.
Aerospace Components Division
Wilmington 99, Delaware
Attn: Robert J. Crosby (327)
Ray A. Dietrich (328)
Robert McGirr (329)
Edward M. Simon (330)
Matthew J. White, Jr. (331)

AVCO R&D Advanced Development
201 Lowell St.
Wilmington, Mass.
Attn: Charles Creeces (332)
Paul B. Tweed (333)
Herbert S. Weintraub (334)

Beckman & Whitley, Inc.
993 E. San Carlos Ave.
San Carlos, California
Attn: C. H. Bagley (335)
J. Corcoran (336)
James W. Hagenbeugh (337)
George T. Sowlakis (338)
J. Tim (339)

Bell Telephone Lab., Inc.
Whippany, New Jersey
Attn: Robert C. Scerrator (340)

The Bendix Corp.
Scintille, Division
Sidney, New York
Attn: Kenneth A. Henderson (341)
Karl Kraue (342)
Arthur P. Moran (343)
Louis H. Segal (344)

Bermite Powder Company
22116 W. Soladad Canyon Rd.
Saugus, California
Attn: Louis LoFiego (345)
Samuel P. Miller (346)

Bjorketen Research Labs., Inc.
P. O. Box 265
Madison 1, Wisconsin
Attn: Earl A. Heyer (347)
Dale G. Holinbeck (348)

The Boeing Company
P. O. Box 3707
Seattle 24, Washington
Attn: Richard F. Holtman (349)
George E. Metcalf (350)
R. E. Murakami, Org.2-5472,
Mail Stop 21-31 (351)

Bulova Res. & Devel. Labs.
62-10 Woodside Ave.
Woodside 77, N.Y.
Attn: Melvin Eneman (352)

Cannon Electric Co.
3208 Humboldt St.
Los Angeles, California
Attn: Frank Walker (353)

Chance Vought Corp.
P. O. Box 5907
Dallas 22, Texas
Attn: William G. Gjerteon (354)
Clyde M. Jones (355)

Conax Corp.
2300 Walden Ave.
Buffalo 25, N.Y.
Attn: Arthur E. Heefner (356)
Edward G. Piereon (357)

Consolideted Controls Corp.
750 S. Isis Ave.
Inglewood, California
Attn: Richard G. Carleon (358)
William Snyder (359)

Convair-Astronautics
5001 Kearny Villa Rd.
San Diego 11, California
Attn: Alfred Mills (360)
J. S. Nuding (361)
Herold W. Qualls (362)

Cook Electric Company
6401 Oakton St.
Morton Grove, Illinois
Attn: Mr. W. H. Dunning (363)

Deyetrom, Inc.
Weston Instr. and Electr. Div.
614 Frelinghuysen Avenue
Newark 14, New Jersey
Attn: Mr. C. Stolar (364)

Dayton T. Brown, Inc.
Testing Labs. & Engr. Div.
555 Church Street
Bohemia, L. I., New York
Attn: Howard R. Lacy (365)

Denver Research Institute
University of Denver
University Park
Denver 10, Colorado
Attn: Richard K. Fry (366)

Douglas Aircraft Co., Inc.
Aircraft Division
Long Beach, California
Attn: Jese W. Lockhart (367)

Douglas Aircraft Company, Inc.
Missile & Space Systems Division
Santa Monica, California
Attn: Robert J. Drecnsler (368)
Homer W. Fairchild (369)
Robert H. Klamt (370)
Richard C. Kohlheyer (371)
Robert R. Sullivan (372)
Henry B. Warner (373)

E. I. duPont de Nemours & Co.
Eastern Laboratory
Gibbetown, New Jersey
Attn: George A. Noddin (374)
Klaus G. Ruckar (375)

E. I. duPont de Nemours & Co.
Wilmington 98, Delaware
Attn: Paul J. Bryan (376)
Charles H. Cramer (377)
John P. Ireland, Jr. (378)
Paul A. Ramsdell (379)
Herbert L. Schaaf (380)

Eitel McCullough, Inc.
San Carlos, California
Attn: Lowell A. Noble (381)

Elgin Nation Watch Company
R&D Division, Ind. Group
1200 Hicks Road
Rolling Meadows, Illinois
Attn: Raymond W. Heidorn (382)
George V. Zimmerman (383)

The Ensign-Bickford Co.
660 Hopmeadow St.
P. O. Box 308
Simsbury, Connecticut
Attn: Thomas W. Norton (384)
William M. Smith (385)

Eureka Williams Company
Div. of Nat. Union Electric Corp.
Bloomington, Illinois
Attn: Adolphus R. Cosby (386)
Lealie J. Woods (387)

Fairchild Camera & Instrument Corp.
Robbins Lane
Syosset, L. I., New York
Attn: Arnold L. Albin (388)
Robert E. Hassett (389)

Filtron Company, Inc.
131-15 Fowler Avenue
Flushing 55, N.Y.
Attn: William Jarva (390)

Flare Northern Division
Atlantic Research Corp.
19701 W. Goodvale Rd.
Saugus, California
Attn: John E. Ardsus (391)
Ernest J. Gruen (392)

Flare Northern Division
Atlantic Research Corp.
P.O. Box 175
West Hanover, Mass.
Attn: David P. Hall (393)

Franklin Systems, Inc.
P.O. Box 3250
West Palm Beach, Floride
Attn: Dr. Martin J. Cohen (394)

General Dynamics Corp.
P.O. Box 748
Fort Worth 1, Texas
Attn: Howard E. Athey (395)

General Dynamics Corp.
1675 W. 5th St.
Pomona, California
Attn: Leo V. Kilpatrick (396)
Robert F. Schule (397)

General Dynamics Corp.
San Diego, California
Attn: George Wilson (398)

General Electric Co.
Apollo Support Dept.
P.O. Box 1098
Cocoa Beach, Florida
Attn: Herbert E. Curtis (399)

General Electric Co.
Apollo Support Dept.
7025 Gulf Freeway
Houston 32, Texas
Attn: Troy N. Whitehurst (400)

General Electric Co.
Advanced Space Project Dept.
King of Prussia, Pa.
Attn: Elbert E. deMaris (401)
James L. Lilly (402)

General Electric Co.
Re-Entry Systems Dept.
3198 Chestnut St.
Philadelphia, Penna.
Attn: Alfred F. Garawitz (403)
William Kocher (404)
Bernard Mansbach (405)
Harry E. Peacock (406)
Benjamin Teres (407)

General Electric Co.
Re-Entry Systems Dept.
Spring Garden St.
Philadelphia, Penna.
Attn: John E. Bindis (408)
Edwin Knippenberg (409)

General Electric Co.
Lakeside Avenue
Burlington, Vt.
Attn: S. Benson, M.E.E. (410)

General Electric Co.
Room 35, Bldg. 3
Court Street
Syracuse, N.Y.
Attn: Christopher C. Fallon(411)

General Laboratory Assoc., Inc.
Norwich, New York
Attn: Phillip Forde (412)
Louis Knudson (413)

General Precision, Inc.
808 17th St. N.W.
Washington, D.C.
Attn: Larry L. Paxson (414)

General Precision, Inc.
Librascope Division
670 Arques Avenue
Sunnyvale, California
Attn: Theodore C. Parker (415)
James A. Rummel (416)
A. R. Vallarino (417)

General Precision, Inc.
GPL Division
63 Bedford Rd.
Pleasantville, N.Y.
Attn: David G. Gray (418)

Genistron, Inc.
111 Gateway Rd.
Bensenville, Illinois
Attn: Robert Swift (419)

Genistron, Inc.
6320 W. Arizona Circle
Los Angeles 45, California
Attn: James C. Senn (420)

Gould Laboratories
Melman, New Jersey
Attn: W. F. Gould, Jr. (421)
W. F. Gould, Sr. (422)

Grumman Aircraft Engr. Corp.
Bethpage, L.I., New York
Attn: Milton Howell (423)
Stephen Norton (424)

Hanley Industries Inc.
4575 N. Goodfellow Blvd.
St. Louis 20, Mo.
Attn: Sam D. Ehrlich (425)

Harvey Aluminum
Torrance, California
Attn: Harold W. Euker (426)

Hercules Powder Company
Port Ewen, N.Y.
Attn: George H. Scherrer (427)
William R. Thomas (428)
Cecil K. Wood (429)

Hercules Powder Company
Hercules Tower
910 Market St.
Wilmington 99, Delaware
Attn: Edward L. Remer (430)

Hi-Shear Corporation
2600 W. 247th St.
Torranos, California
Attn: Weldon S. Bankston, Jr.(431)
Monte W. Korb (432)
Fred M. Thomas (433)

Holex, Inc.
2751 San Juan Rd.
Hollister, Calif.
Attn: Ernest J. Stecker (434)

Hughes Aircraft Company
Florence Avenue at Teale
Culver City, California
Attn: Security General Office, for
Owen C. Barker (435)
Orvin C. Ongsted (436)

Hughes Aircraft Company
P.O. Box 11337
Tucson, Arizona
Attn: Plant Security, for
Douglas W. Gieske (437)

Interference Testing & Res. Lab.
P.O. Box 776
Havertown, Pa.
Attn: William D. McGuin (438)

ITT - Federal Laborstories
500 Washington Avenue
Nutley 10, New Jersey
Attn: Wendell C. Murray (439)

ITT - Industrial Products Division
13191 Bledsoe St.
San Fernando, California
Attn: George H. Ashmore, Jr.(440)
Roger D. Loiler (441)

Jansky & Bailey
Shirley Highway & Edsall Rd.
Alexandria, Va.
Attn: Louis A. Dignazio (442)

Jet Propulsion Laboratory
P.O. Box 147
Cape Canaveral, Florida
Attn: Thomas J. Snier (443)

Jet Propulsion Laboratory
California Institute of Technology
4800 Oak Grove Drive
Pasadena, California
Attn: Anthony G. Benedict (444)
John E. Earnest, Jr. (445)

The Johns Hopkins University
Applied Physics Lab.
8621 Georgia Ave.
Silver Spring, Md.
Attn: P.O. Orury, Jr. (446)

Lawrence Radiation Lab.
University of California
Livermore, Calif.
Attn: Mr. Salisbury (447)

Librascope Division
General Precision, Inc.
670 Arques Ave.
Sunnyvale, Calif.
Attn: Staff Engr.
J. A. Rummell, (448)

Litton Industries
Electron Tube Division
960 Industrial Rd.
San Carlos, California
Attn: Jack W. Gilas (449)

Lockheed Missiles & Space Co.
Empire Grade
Santa Cruz County, California
Attn: Robert L. Fullar (450)

Lockheed Missiles & Space Co.
1111 Lockheed Way
Sunnyvale, Calif.
Attn: Glen O. Gillett (451)
John E. Barkham (452)
Isidore B. Gluckman (453)
Thomas C. McClain (454)

Lockheed Propulsion Co.
Redlands, California
Attn: Theodore E. Landry (455)

Loral Electronics Corp.
New York, New York
Attn: Leo Horowitz (456)
M. Revzin (457)

McCormick-Selph Assoc. Inc.
Hollister Airport
Hollister, California
Attn: Robert C. Allen (458)
Edward O. Baxter (459)
Frank W.T. LaHaye, Jr.(460)

The Magnavox Co.
Urbana, Illinois
Attn: Robert W. Bliss (461)
Charles Limbacker (462)

The Martin Company
P.O. Box 179
Denver 1, Colorado
Attn: Joe M. Ashuran (463)
David Waddington (464)
Allen J. Werner (465)

The Martin Company
P.O. Box 5837
Orlando, Florida
Attn: Maurice T. Hedges (466)

Mason & Hanger
Silas Mason Co., Inc.
P.O. Box 647
Amarillo, Texas
Attn: David M. Holt (467)

Metavac, Inc.
45-68 162nd St.
Flushing 58, N.Y.
Attn: Mr. H. Fadel (468)

Midwest Research Institute
425 Volkar Blvd.
Kansas City, Mo.
Attn: James J. Downs (469)
Howard W. Christie (470)
Paul C. Constant (471)

Minneapolis-Honeywell Regulator Co.
600 Second Street North
Hopkins, Minnesota
Attn: John A. Fitzgerald (472)

New Mexico State University
Physical Science Laboratory
University Park, New Mexico
Attn: Richard H. Duncan (473)

North American Aviation, Inc.
Space & Info. Systems Div.
12214 Lakewood Blvd.
Downey, California
Attn: Aaron Hitshens (474)
Daniel E. Holloway (475)
John E. Moeller (476)
Earl F. Schoueller (477)
Herbert Silverman (478)

Olin Mathieson Chemical Corp.
East Alton, Illinois
Attn: Jacquas L. Caspari (479)
William A. Wood (480)

Ordnance Associates, Inc.
855 El Centro St.
South Pasadena, California
Attn: Albert L. Roberts (481)
Harvey Sacks (482)

Pan American World Airways, Inc.
Guided Missiles Range Div.
Patrick AFB, Florida
Attn: Romano V. Assante (483)
James C. Sweat (484)

Palmer Division
Quantic Industries, Inc.
1011 Commercial Street
San Carlos, California
Attn: Donald N. Griffin (485)

Physics International, Inc.
Albuquerque, New Mexico
Attn: Donald F. Martin (486)
Donald S. Wood (487)

Pyrofuze Corp.
121 S. Columbus Avenue
Mount Vernon, New York
Attn: Franklyn E. Stevens, Jr.(488)

Radio Corp. of America
Camden, New Jersey
Attn: Salvatore Canale, Jr. (489)

RAMCOR Incorporated
190 Duffy Avenue
Hicksville, L. I., N. Y.
Attn: Mr. W. D. Marshall (490)

Raytheon Company
Hartwell Rd.
Bedford, Mass.
Attn: Henry A. K. Larm (491)

RCA Service Co.
Missile Test Project
Patrick Air Force Base, Fla.
Attn: Otis B. Rawle (492)

Republic Aviation Corp.
Farmingdale, L. I. New York
Attn: Joseph J. Kuliberda (493)
Michael J. Lauro (494)
Herbert Meltzer (495)

Rocketdyne
6633 Canoga Avenue
Canoga Park, California
Attn: Leonard Katz (496)

Sandia Corp.
Albuquerque, New Mexico
Attn: Cohen B. Eyrd (497)
Charles W. Cook (498)
Charles W. Harrison, Jr. (499)
David E. Merewether (500)
Merrill O. Murphy (501)
William L. Stevens (502)

E. H. Smith & Co., Inc.
Suite 201, 901 Pershing Dr.
Silver Spring, Md.
Attn: E. H. Smith (503)

Space Ordnance Systems, Inc.
133 Penn St.
El Segundo, Calif.
Attn: W. R. Oickie (504)

Space Technology Labs., Inc.
One Space Park
Redondo Beach, California
Attn: Henry L. Busuttil (505)
Donald S. Davis (506)
Morris Rosenthal (507)
Stanley H. Rush (508)

Special Devices, Inc.
16830 W. Placerita Canyon Rd.
Newhall, California
Attn: Leroy L. Ardell (509)

Sperry Gyroscope Company
Great Neck, N.Y.
Attn: Milton Kant (510)

Sprague Electric Company
12870 Panama Street
Los Angeles 66, California
Attn: Claude I. Thompson (511)

Sprague Electric Company
North Adams, Massachusetts
Attn: Frank E. Garlington (512)
Benedict P. Roman (513)
David H. Simonds (514)

Sprague Electric Company
2321 Wisconsin Avenue N.W.
Washington 7, D.C.
Attn: P. Sheridan, Security Officer,
for Charles T. Lempke (515)

Tamar Electronics, Inc.
1360 S. Los Angeles St.
P.O. Box Q-3
Anaheim, California
Attn: Frank H. Williams (516)

Thiokol Chemical Corp.
Brigham City, Utah
Attn: Richard Strong (517)

Thiokol Chemical Corp.
P.O. Box 27
Bristol, Pa.
Attn: Claude E. Campbell '518)
James H. Mueller (517)

Thiokol Chemical Corp.
Reaction Motors Division
Denville, N.J.
Attn: Stanley Kurseja (520)

Thiokol Chemical Corp.
P.O. Box 241
Elkton, Maryland
Attn: George Taylor (521)

Thiokol Chemical Corp.
Huntsville, Alabama
Attn: Sam Zeman, Jr. (522)

Unidynamics
472 Paul Ave.
St. Louis 35, Missouri
Attn: John P. Huber, Jr. (523)
Wiley Sanders (524)
C. E. Simpson (525)

Vitro Laboratories
Silver Spring Laboratory
14000 Georgia Ave.
Silver Spring, Md.
Attn: Harry P. Bird (526)

Welex Electronics Corporation
Selar Bldg. Suite 201
16th & K Streets, N.W.
Washington, D.C.
Attn: Donald J. Seibert (527)

Westinghouse Electric Corp.
Mendy Ave.
Sunnyvale, Calif.
Attn: Robert D. Rung (528)

White Electromagnetics, Inc.
4903 Auburn Ave.
Bethesda, Md.
Attn: Drummond L. Scott (529)

Zenith Radio Corp.
6001 W. Dickens Avenue
Chicago 39, Illinois
Attn: John Seifner, Jr. (530)

AD- Div. 22 Unclassified

The Franklin Institute, Laboratories for Res. and Dev.
Philadelphia 3, Pennsylvania

PROCEEDINGS OF HERO CONGRESS-1963- ON HAZARDS OF ELECTROMAGNETIC RADIATION TO ORDNANCE, held at The Franklin Institute on 30 April, 1,2 May 1963.
706 p. incl illus, tables (Rept. no. F-B1982)
Contract N178-8083 Unclassified Report

Descriptors: (Electromagnetic Fields, Hazard)* Explosive Initiators,* Symposia,* Attenuators, Attenuation

Identifiers: HERO

The Second HERO Congress, of 392 representatives from government and industry, comprised 52 papers, continuing the work of the First HERO Congress of 1961 (Proceedings, AD-326-263). The papers gave broad coverage of the Hazards of Electromagnetic Radiation to Ordnance. The opening session was for statements of approaches and programs; this was followed by nine papers on theoretical analysis and field studies of vulnerability, and on methods of measuring radio frequency power, and determining sensitivity of initiators to RF. There were 16 papers on fixes, including filters and absorptive attenuators; relays, transformers, and magnetic coupling; inherent protection by initiator design; and protective shielding. Nine papers were devoted to special aspects, such as the effects of lightning, RF field distribution over a carrier deck, statistical studies, new attenuating materials, and thermal analyses. Twelve additional papers, in the same general areas mentioned, are printed in the Proceedings although they were not presented at the Congress.

The report contains abstracts of the individual papers, and a summary of the discussions. Twelve papers were classified; they are bound separately in a 174 page supplement (Report No. F-B1982 Supplement; AD-)